

**University of Strathclyde**  
**Faculty of Engineering**  
**Department of Civil and Environmental Engineering**



**Development of Prediction and Design Models for Wide  
Concrete Beams with Various Load and Support Widths**

**BY**

**AYED EID ALLUQMANI, *B.Sc. (Eng.), M.Sc., MSCE and MSSCE***

A Thesis Presented to the University of Strathclyde in Fulfillment of the  
Requirements for the Degree of  
**Doctor of Philosophy (Ph.D) in Civil Engineering**

**March 2014**

**Glasgow, UK**

# DECLARATION

‘The author declares that, except for commonly understood and accepted ideas, or where specific reference is made to the work of other authors, the contents of this Thesis has been composed by the author, except where stated. This Thesis has not been submitted to any University or institution for any degree’.

‘The copyright of this Thesis belongs to the author under the terms of the United Kingdom Copyrights Acts as qualified by University of Strathclyde Regulation 3.50. Due acknowledgement must always be made of the use of any material contained in, or derived from this Thesis’.

**Signed:**

**Date:**

**Ayed Eid H. ALLUQMANI**

**March 2014**

*A Lecturer in the department of Civil Engineering at Umm Al-Qura University, UQU, KSA (4280535).*

A member of **ACI** (01227956); **ASCE** (9923373, **SEI**); **IStructE** (088387123); **IET** (1100352217); **ICE** (68320689); **SCE** (8797) and **SSCE** (30-3-0538).

Student ID: 201282036 (Strathclyde-University)

Saudi ID: 1010183729. Saudi Passport ID: M237939

**Email:** [eng.ayed@hotmail.com](mailto:eng.ayed@hotmail.com), [aeluqmani@uqu.edu.sa](mailto:aeluqmani@uqu.edu.sa) and [alluqmani-ayed-eid-h@strath.ac.uk](mailto:alluqmani-ayed-eid-h@strath.ac.uk)  
[ayedalloqmani.jeeran.com](http://ayedalloqmani.jeeran.com)

**Facebook & ResearchGate:** [Ayed Eid Alluqmani](#). **LinkedIn:** [Ayed Alluqmani](#).

**Twitter:** [@Dr\\_Ayed\\_CE](#) ([https://twitter.com/Dr\\_Ayed\\_CE](https://twitter.com/Dr_Ayed_CE)).

**Correspondence Address:**

Civil Engineering Department, College Of Engineering, Umm Al-Qura University, P.O. Box 5555, Makkah 21955, Saudi Arabia.

**In the Name of Allah (God), the Beneficent, the Merciful**

بِسْمِ اللَّهِ الرَّحْمَنِ الرَّحِيمِ



## DEDICATION

I would like to dedicate this work to my parents (*Eid and Huwamedah*), my wife (*Rasha*), and my sons (*Suhayb and Jiyad*).

## ACKNOWLEDGEMENTS

Firstly, all thanks, blessing, praise and glory are to ALLAH, my God, for granting me the physical and mental ability to undertake this work. Then, my thanks and acknowledgements are to my family (parents, wife, sons, brothers and sisters). Thank is approaching to my mother who spent all her days and nights in prayers to God seeking His help and protection for me always.

My warm thanks are to all the people, who have supported me during my study, either in the Kingdom of Saudi Arabia (my home) or in the United Kingdom. All their continual kindness and encouragement during the journey to complete my PhD are gratefully acknowledged. I thank all people who helped me during my work and research at Heriot-Watt University submitted in the 23<sup>rd</sup> of August 2010 and in the 19<sup>th</sup> of April 2012. Thank is also sent to those people in the University of Strathclyde who helped and encouraged me during the theoretical and experimental studies. Special thank is to Dr. Binsheng (Ben) Zhang from Edinburgh Napier University in 2012 (Glasgow Caledonian University in 2014) for all his advices on this research through years 2012 and 2014. I would also like to thank Dr. Ben Zhang and the Mathematic's PhD Student, Omar Alharbi, for their help with Mathematic issues after the period of my PhD-Viva held on 31<sup>st</sup> March 2014. I also very grateful thank to Prof. Samir Ashour from The University of King Abdulaziz in Saudi Arabia for all his advices through the initial stage of this study.

I send a special thanks to both my academic supervisors, Dr. M. Saafi and Dr. Y. Xu. Oh' Dr. Saafi, all your helps, encouragements to publish my work, comments, feedback, and corrections on the manuscripts and reports are gratefully acknowledged, and I will not forget all your helps.

My indebtedness is to the Ministry of Higher Education and my employer, Umm Al-Qura University, in Saudi Arabia for providing me the support and the finance to pursue my postgraduate studies. I would also like to thank all the people in the Saudi Cultural Bureau in London for their great support and encouragement.

# LIST OF AUTHOR'S CONTRIBUTIONS

**The author's contributions shown below have been undertaken in reviews, debates, corrections and revisions:**

## **1. Technical and Published Works**

1. Alluqmani, A. E. 2013a. "Flexural and Shear Behaviour of Wide RC Beams". The Civil Engineering PhD Conference, University of Strathclyde, Glasgow, Scotland-UK. 30 October 2013.

2. Alluqmani, A. E. 2013b. "Development of Detailing and Design Models for Wide Concrete Beams". The Engineering RPD Conference, University of Strathclyde, Glasgow, Scotland-UK. 27 June 2013.

3. Alluqmani, A. E.; and Saafi, M. B. 2014a. "Structural Reinforced Concrete Beams in Shear". The 2014 SSC-07 Conference, University of Edinburgh, Edinburgh, Scotland-UK. Paper No. ENG 506. 1-2 February 2014.

4. Alluqmani, A. E.; and Saafi, M. B. 2014b. "The Effect of Bearing Plate Widths on Wide Concrete Member Capacities". The 2014 SSC-07 Conference, University of Edinburgh, Edinburgh, Scotland-UK. Paper No. ENG 507. 1-2 February 2014. *This Paper got a Prize of 1000 Sterling Pound and a travel grant.*

5. Alluqmani, A. E.; and Saafi, M. B. 2014c. "New Detailing-Approach and Design-Model for Wide RC Beams". The 16<sup>th</sup> Young Structural Researchers' Conference 2014 (YRC), the Institution of Structural Engineers, London, England-UK. 5 March 2014. *This Paper got a travel grant.*

6. Alluqmani, A. E. 2014. "Design and Behaviour of R.C. Beams to ACI318-and-SBC304; and EC2 Codes When Subjected To Asymmetric Loading". *Journal of Engineering, Design and Technology (JEDT)*, Vol. 12, Issue 2, April-May 2014. pp.158 – 176.

7. Alluqmani, A. E.; and Haldane, D. 2011a. "Design of Reinforced Concrete Beams to ACI318-and-SBC304; and EC2 Codes". COBRA-2011 (RICS) Conference, University of Salford, Manchester, England-UK. Paper No.2150. 12-13 September 2011. pp 459-468.

8. Alluqmani, A. E.; and Haldane, D. 2011b. "Structural Design of Reinforced Concrete Beams: Comparison In Accordance With ACI318-and-SBC304; and EC2 Codes". The 5<sup>th</sup> SSIC-2011 Conference, University of Warwick, Coventry, England-UK. Paper No.21. 23-26 June 2011. *This Paper was awarded the second best paper in Engineering, and got an iPad and a Prize of 945 Sterling Pound.*

9. Alluqmani, A. E.; and Haldane, D. 2011c. "Structural Behaviour of Reinforced Concrete Beams: Comparison In Accordance With ACI318-and-SBC304; and EC2 Codes". The 5<sup>th</sup> SSIC-2011 Conference, University of Warwick, Coventry, England-UK. Paper No.22. 23-26 June 2011.

10. Alluqmani, A. E. 2010. "Reinforced Concrete Beams Design: Comparison In Accordance With Saudi Building Code (SBC304) and Eurocode (EC2) Subjected To Asymmetric Loading". *MSc Dissertation*, Heriot-Watt University, UK. 23 August 2010. 111pp.

## **2. Oral Presentations in Conferences**

Presentation 1: "Structural Reinforced Concrete Beams in Shear". The 2014 SSC-07 Conference, University of Edinburgh, Edinburgh, Scotland-UK. 1-2 February 2014.

Presentation 2: "The Effect of Bearing Plate Widths on Wide Concrete Member Capacities". The 2014 SSC-07 Conference, University of Edinburgh, Edinburgh, Scotland-UK. 1-2 February 2014.

Presentation 3: "Flexural and Shear Behaviour of Wide RC Beams". The Civil Engineering PhD Conference, University of Strathclyde, Glasgow, Scotland-UK. 30 October 2013.

Presentation 4: "Development of Detailing and Design Models for Wide Concrete Beams". The Engineering RPD Conference, University of Strathclyde, Glasgow, Scotland-UK. 27 June 2013.

Presentation 5: "Design of Reinforced Concrete Beams to ACI318-and-SBC304; and EC2 Codes". COBRA-2011 (RICS) Conference, University of Salford, Manchester, England-UK. 12-13 September 2011.

Presentation 6: "Structural Design of Reinforced Concrete Beams: Comparison In Accordance With ACI318-and-SBC304; and EC2 Codes". The 5<sup>th</sup> SSIC-2011 Conference, University of Warwick, Coventry, England-UK. 23-26 June 2011.

Presentation 7: "Structural Behaviour of Reinforced Concrete Beams: Comparison In Accordance With ACI318-and-SBC304; and EC2 Codes". The 5<sup>th</sup> SSIC-2011 Conference, University of Warwick, Coventry, England-UK. 23-26 June 2011.

## **3. Posters in Conferences**

1. Alluqmani, A. E. 2014. "A New Prediction-Model for Wide Concrete Members". The University Research Day (URD) Conference, University of Strathclyde, Glasgow-UK, 19 June 2014.

2. Alluqmani, A. E. 2011. "Structural Design and Behaviour of R.C. Beams Accordance With the Combined of American and Saudi Building Codes (ACI318-and-SBC304) and EuroCode (EC2)". The Joint Research Institute of Civil & Environmental Engineering Review Visit Conference (JRI-CEE REVIEW VISIT), Heriot-Watt University, Edinburgh-UK, 27-29 June 2011.

#### **4. Technical Reports on PhD Research Area**

**The following technical reports have been undertaken in reviews, debates, corrections and revisions:**

1. Alluqmani, A. E. "New Models for Design and Prediction the Wide Concrete Beams with Various Loads and Supports". *Annual Research Report (3<sup>rd</sup> PhD-Year Report)*, University of Strathclyde, Glasgow-UK, November **2013**, 214 pp.

2. Alluqmani, A. E. "Structural Design and Behaviour of Wide RC Beams". *Annual Research Report (2<sup>nd</sup> PhD-Year Report)*, University of Strathclyde, Glasgow-UK, March **2013**, 77 pp.

3. Alluqmani, A. E. "Structural Design and Behaviour of Wide Structural Concrete Members". *Annual Research Report (1<sup>st</sup> PhD-Year Report)*, University of Strathclyde, Glasgow-UK, June **2012**, 109 pp.

4. Alluqmani, A. E. "Structural Wide Reinforced Concrete Members". *Research Report*, Heriot-Watt University, UK, December **2011**, 75 pp.

# TABLE OF CONTENTS

<b>DECLARATION</b> .....	<b>i</b>
<b>DEDICATION</b> .....	<b>ii</b>
<b>ACKNOWLEDGEMENTS</b> .....	<b>iii</b>
<b>LIST OF AUTHOR'S CONTRIBUTIONS</b> .....	<b>iv</b>
<b>TABLE OF CONTENTS</b> .....	<b>vii</b>
<b>LIST OF TABLES</b> .....	<b>xv</b>
<b>LIST OF FIGURES</b> .....	<b>xix</b>
<b>LIST OF APPENDICES</b> .....	<b>xxv</b>
<b>ABSTRACT</b> .....	<b>xxvi</b>
<b>CHAPTER 1: INTRODUCTION</b> .....	<b>1</b>
<b>1.1 Introduction</b> .....	<b>1</b>
<b>1.2 Wide Reinforced Concrete Beams</b> .....	<b>2</b>
<b>1.3 The Nature of The Problem</b> .....	<b>4</b>
<b>1.4 Contributions to Knowledge</b> .....	<b>6</b>
<b>1.5 Aims and Objectives of the Research</b> .....	<b>6</b>
<b>1.6 The Programme of Research</b> .....	<b>7</b>
<b>1.7 Outline of Thesis</b> .....	<b>9</b>
<b>CHAPTER 2: GENERAL LITERATURE REVIEW FOR REINFORCED CONCRETE MEMBERS</b> .....	<b>11</b>
<b>2.1 Introduction</b> .....	<b>11</b>
<b>2.2 Beam Classification</b> .....	<b>11</b>
2.2.1 Type I Beams (Long Beams) .....	<b>12</b>
2.2.2 Type II Beams (Normal Beams of Intermediate Length) .....	<b>12</b>



2.2.3 Type III Beams (Short Beams) -----	12
2.2.4 Type IV Beams (Deep Beams) -----	12
<b>2.3 Beams Classification Based on the Geometry -----</b>	<b>12</b>
<b>2.4 Failure Modes of Beams -----</b>	<b>14</b>
2.4.1 Flexural Failure -----	15
2.4.2 Diagonal Shear Failure -----	15
2.4.3 Deep-Beam Failure -----	20
2.4.4 Conclusion -----	22
<b>2.5 Structural Concrete Beams in Flexure -----</b>	<b>22</b>
2.5.1 General -----	22
2.5.2 Multiaxial Stress Behaviour -----	23
2.5.3 Conclusion -----	25
<b>2.6 Structural Concrete Beams in Shear -----</b>	<b>25</b>
2.6.1 Shear Strength of Beams without Shear Reinforcement -----	25
2.6.2 Shear Strength of Beams with Shear Reinforcement -----	26
2.6.2.1 Introduction -----	26
2.6.2.2 Truss Analogy -----	27
2.6.2.3 Strut-and-Tie Models -----	29
2.6.2.4 Diagonal Compression Field Theory -----	31
2.6.2.5 Modified Compression Field Theory -----	32
2.6.2.6 Plasticity Theory Model -----	33
2.6.2.7 Equilibrium Analysis -----	35
2.6.2.8 Arch Action Theory -----	35
2.6.2.9 Compressive Force Path (CFP) Concept -----	35
<b>2.7 Behaviour of Beams under the Combined Action of Shear Force and Bending Moment -</b>	<b>38</b>
-----	38
2.7.1 Mechanisms of Shear Transfer -----	38
2.7.1.1 Shear Transfer by Concrete Stress -----	39
2.7.1.2 Interface Shear Transfer (Aggregate Interlock) -----	40
2.7.1.3 Dowel Action -----	41
2.7.1.4 Beam and Arch Actions -----	42
2.7.1.5 Shear Reinforcement -----	44
2.7.2 Contribution of Shear Transfer Mechanisms to Shear Resistance -----	44
2.7.3 Conclusion -----	47

<b>2.8 General Conclusion</b> .....	47
<b>CHAPTER 3: LITERATURE REVIEW FOR WIDE REINFORCED CONCRETE MEMBERS</b> .....	<b>49</b>
<b>3.1 Introduction</b> .....	49
<b>3.2 Wide Concrete Beams in Shear [Without and With Shear Reinforcement]</b> .....	51
<b>3.3 Punching Shear on Wide Members</b> .....	52
<b>3.4 Previous Research on Wide Reinforced Concrete members</b> .....	54
<b>3.5 Factors Influencing the Wide Member Strengths</b> .....	57
<b>3.6 Influence of Transverse Stirrup Spacing</b> .....	58
<b>3.7 Influence of Support and/or Load Width</b> .....	66
<b>3.8 Cases of Support and Load Width Conditions</b> .....	73
3.8.1 Case 1: Full-Width Load and Full-Width Support .....	73
3.8.2 Case 2: Narrow-Width Load and Narrow-Width Support (Both equal) .....	74
3.8.3 Case 3: Narrow-Width Load and Full-Width Support .....	75
3.8.4 Case 4: Full-Width Load and Narrow-Width Support .....	75
3.8.5 Case 5: Narrow-Width Load and Narrow-Width Support (support wider than load) --	76
3.8.6 Case 6: Narrow-Width Load and Narrow-Width Support (Load wider than support) -	77
<b>3.9 Effect of Flexural Reinforcement Ratios on Wide RC Beam Capacities</b> .....	77
<b>3.10 Conclusion</b> .....	81
<b>CHAPTER 4: DESIGN AND PREDICTION METHODS FOR WIDE BEAMS IN FLEXURE &amp; SHEAR TO THE EXISTING CODES AND MODELS</b> .....	<b>82</b>
<b>4.1 Introduction</b> .....	82
<b>4.2 Wide Structural Concrete Members</b> .....	82
<b>4.3 Wide RC Beams in Flexure and Shear</b> .....	84
<b>4.4 Provisions of Structural Design of Wide RC Beams to ACI318-and-SBC304 and EC2-90</b>	
4.4.1 Design Methods (Ultimate Capacity and Serviceability) .....	90
4.4.2 Load Factors .....	91
4.4.3 Reduction Design Strength Factors .....	92
4.4.4 Concrete Strengths .....	92
4.4.5 Steel Strengths .....	93
<b>4.5 Design Method</b> .....	94

4.5.1 Flexural Capacity on RC Beams: Moment Resistance -----	96
4.5.2 Shear Capacity on RC Beams: Shear Resistance -----	98
4.5.3 Serviceability: Deflections and Crack Widths -----	110
<b>4.6 Prediction Method -----</b>	<b>113</b>
4.6.1 Flexural Strength Method to ACI318, SBC304 and EC2 -----	114
4.6.2 Shear Strength Method to ACI318, SBC304 and EC2 -----	115
4.6.3 Shear Strength Model Developed by Lubell et al (2008) -----	115
4.6.4 Shear Strength Model Developed by Serna-Ros et al (2002) -----	116
4.6.5 Shear Strength Model Developed by Shuraim (2012) -----	117
4.6.6 Comments on the Prediction Methods -----	117
<b>4.7 Conclusion -----</b>	<b>139</b>
 <b>CHAPTER 5: WIDE RC BEAMS SPECIALLY DETAILED FOR SHEAR: SERIES (A) --</b>	 <b>----- 141</b>
 <b>5.1 Introduction -----</b>	 <b>141</b>
<b>5.2 Description of Test Specimens -----</b>	<b>142</b>
<b>5.3 Design and Configurations of Test Specimens -----</b>	<b>144</b>
<b>5.4 Materials Information -----</b>	<b>147</b>
5.4.1 Concrete -----	147
5.4.2 Reinforcement -----	148
<b>5.5 Manufacture of Test Specimens -----</b>	<b>149</b>
5.5.1 Steel Cages -----	149
5.5.2 Shutters -----	150
5.5.3 Casting -----	151
5.5.4 Curing -----	152
5.5.5 Preparing the Test Specimens for Testing -----	152
<b>5.6 Testing Arrangements and Instrumentation -----</b>	<b>153</b>
5.6.1 Testing Machine -----	153
5.6.2 Loading Arrangement -----	154
5.6.3 Loading Procedures and Steps -----	154
5.6.4 Instrumentation Arrangements -----	155
5.6.5 Marking of Cracks -----	155
<b>5.7 Test Programme and Procedure -----</b>	<b>155</b>
<b>5.8 Measurements -----</b>	<b>156</b>

5.8.1 Total Applied Load -----	156
5.8.2 Deflection -----	156
5.8.3 Concrete Strain -----	157
5.8.4 Cracking -----	157
5.8.5 Beam Testing Results -----	157
<b>5.9 Material Test-Results and Prediction of Beam-Results -----</b>	<b>158</b>
<b>5.10 Test Results of Beams -----</b>	<b>159</b>
<b>5.11 Discussion of Test Results -----</b>	<b>165</b>
5.11.1 Failure Modes -----	165
5.11.2 Behaviour of the Beams in Series (A) -----	166
<b>5.12 Conclusions -----</b>	<b>168</b>
<b>CHAPTER 6: A NEW PREDICTION-MODEL FOR SHEAR AND FLEXURE OF WIDE RC BEAMS -----</b>	<b>170</b>
<b>6.1 Introduction -----</b>	<b>170</b>
<b>6.2 Shear Strength of Concrete Beams -----</b>	<b>171</b>
<b>6.3 A Proposed Prediction Model -----</b>	<b>173</b>
<b>6.4 Validation of the Proposed Prediction-Model -----</b>	<b>192</b>
6.4.1 The Ultimate Shear Capacity ( $V_u = V_c + V_s$ ) -----	193
6.4.2 The Shear Capacity Resisted by Concrete ( $V_c$ ) -----	193
6.4.3 The Shear Capacity Resisted by Stirrups ( $V_s$ ) -----	193
6.4.4 The Ultimate Flexural Capacity ( $M_u$ ) -----	194
6.4.5 Validation on Series (A) Results -----	194
<b>6.5 The Suitable Load and Support Widths for Wide RC Beams -----</b>	<b>209</b>
<b>6.6 Conclusion -----</b>	<b>210</b>
<b>CHAPTER 7: BEHAVIOUR OF WIDE RC BEAMS DESIGNED TO THE EC2 CODE: SERIES (1) -----</b>	<b>212</b>
<b>7.1 Introduction -----</b>	<b>212</b>
<b>7.2 Description of Test Specimens -----</b>	<b>212</b>
<b>7.3 Design and Configurations of Test Specimens -----</b>	<b>215</b>
<b>7.4 Materials Information -----</b>	<b>219</b>
7.4.1 Concrete -----	220
7.4.2 Reinforcement -----	221

<b>7.5 Manufacture of Test Specimens</b>	222
7.5.1 Steel Cages	222
7.5.2 Shutters	223
7.5.3 Casting	223
7.5.4 Curing	225
7.5.5 Preparing the Test Specimens for Testing	225
<b>7.6 Testing Arrangements and Instrumentation</b>	226
7.6.1 Testing Machine	226
7.6.2 Loading Arrangement	227
7.6.3 Loading Procedures and Steps	227
7.6.4 Instrumentation Arrangements	228
7.6.5 Marking of Cracks	228
<b>7.7 Test Programme and Procedure</b>	228
<b>7.8 Measurements</b>	229
7.8.1 Total Applied Load	229
7.7.2 Deflection	229
7.8.3 Cracking	229
7.8.4 Beam Testing Results	229
<b>7.9 Material Test-Results and Prediction of Beam-Results</b>	230
<b>7.10 Test Results of Beams</b>	231
<b>7.11 Discussion of Test Results</b>	246
7.11.1 Failure Modes	247
7.11.2 Effect of $b_s$ and $b_p$	247
7.11.3 Effect of $S_L$ and $S_w$	249
7.11.4 Validation of $K_{cd,act.}$ and $K_{cd,act.,Prop.}$ on Series (1)	252
7.11.5 Validation of $K_{sd,act.}$ and $K_{sd,act.,Prop.}$ on Series (1)	252
7.11.6 Behaviour of the Beams in Series (1)	253
<b>7.12 Conclusions</b>	256
<b>CHAPTER 8: NEW DETAILING-APPROACH AND DESIGN-MODEL FOR WIDE RC BEAMS</b>	<b>259</b>
<b>8.1 Introduction</b>	259
<b>8.2 Series (1) Summary on the Effect of <math>k_s</math> and <math>k_p</math></b>	259
<b>8.3 A Proposed Detailing-Approach</b>	261

<b>8.4 Series (1) Summary on the Effect of SL and S<sub>w</sub></b>	267
<b>8.5 A Proposed Design-Model</b>	270
<b>8.6 Conclusion</b>	281
<b>CHAPTER 9: BEHAVIOUR OF WIDE RC BEAMS DESIGNED TO THE PROPOSED MODELS: SERIES (2)</b>	<b>283</b>
<b>9.1 Introduction</b>	283
<b>9.2 Description of Test Specimens</b>	283
<b>9.3 Design and Configurations of Test Specimens</b>	287
<b>9.4 Materials Information</b>	291
9.4.1 Concrete	291
9.4.2 Reinforcement	292
<b>9.5 Manufacture of Test Specimens</b>	293
9.5.1 Steel Cages	293
9.5.2 Shutters	294
9.5.3 Casting	295
9.5.4 Curing	296
9.5.5 Preparing the Test Specimens for Testing	297
<b>9.6 Testing Arrangements and Instrumentation</b>	297
9.6.1 Testing Machine	297
9.6.2 Loading Arrangement	298
9.6.3 Loading Procedures and Steps	299
9.6.4 Instrumentation Arrangements	299
9.6.5 Marking of Cracks	299
<b>9.7 Test Programme and Procedure</b>	299
<b>9.8 Measurements</b>	300
9.8.1 Total Applied Load	300
9.8.2 Deflection	300
9.8.3 Cracking	301
9.8.4 Beam Testing Results	301
<b>9.9 Material Test-Results and Prediction of Beam-Results</b>	301
<b>9.10 Test Results of Beams</b>	304
<b>9.11 Discussion of Test Results</b>	314
9.11.1 Failure Modes	315

9.11.2 Effect of $b_s$ and $b_p$ on the flexural and shear Strengths -----	316
9.11.3 Effect of $S_L$ and $S_w$ on the Beam Behaviours -----	318
9.11.4 Validation of $K_{cd,Vc,act.}$ and $K_{cd,Mu,act.}$ on Series (2) -----	319
9.11.5 Behaviour of the Beams in Series (2) -----	320
<b>9.12 Conclusions -----</b>	<b>324</b>
<b>CHAPTER 10: CONCLUSIONS AND RECCOMENDATIONS -----</b>	<b>326</b>
<b>10.1 Conclusions -----</b>	<b>326</b>
10.1.1 Wide RC Beams -----	327
10.1.2 Current Provisions of Design and Prediction -----	327
10.1.3 The Initial Stage of This Study -----	328
10.1.4 The Current Programme of Research -----	329
10.1.4.1 The Proposed Models -----	329
10.1.4.2 Summary of This Study -----	330
<b>10.2 Recommendations -----</b>	<b>332</b>
<b>APPENDICES -----</b>	<b>334</b>
<b>BIBLIOGRAPHY -----</b>	<b>377</b>

## LIST OF TABLES

Table 2.1: Percentage Contributions to Shear Resistance. -----	46
Table 3.1: Properties and Test Results for Lubell et al. (2008) Specimens with Full-Width (AX) and Narrow-Width (AW) Bearing Plates. -----	70
Table 3.2: Four Wide RC Members without Stirrups Tested by Lubell et al. (2009b) with Variation in Reinforcement Ratio. -----	79
Table 4.1: Comparison of the Load Factors to EC2, ACI318 and SBC304 Codes. -----	91
Table 4.2: Comparison of Design Reduction Factors to EC2, ACI318 and SBC304 Codes. ----	92
Table 4.3: Details and Summary of the Results of Wide RC Beams Previously Tested -----	120
Table 4.4a: Test Results obtained by Serna-Ros et al. (2002) Investigation on EC2 Code. ----	123
Table 4.4b: Test Results obtained by Serna-Ros et al. (2002) Investigation on ACI Code. ----	123
Table 4.5: Test Results obtained by Shuraim (2012) Investigation. -----	124
Table 4.6: Test Results obtained by Hanafy et al. (2012) Investigation. -----	124
Table 4.7: Test Results obtained by Al.Dywany (2010) Investigation. -----	125
Table 4.8: Test Results obtained by Lubell et al. (2008, 2009) Investigation. -----	125
Table 4.9: Test Results obtained by McAllister (2011) Investigation. -----	126
Table 4.10: Test Results obtained by Al-Harithy (2002) Investigation. -----	126
Table 5.1: Test-Series "A" to Adopt a New Prediction-Model for Shear and Flexure of Wide RC Beams. -----	142
Table 5.2: Design Details of Wide Beams in Test-Series "A". -----	145
Table 5.3: Properties of Wide Beam Specimens in Test-Series "A". -----	146
Table 5.4: Material Properties used to Design the Beam Specimens in Series "A". -----	148
Table 5.5: Concrete Mix Proportions used to cast for the Beams in Series "A". -----	148
Table 5.6: Actual Concrete Strengths for Test-Series "A". -----	158
Table 5.7: Material Properties used to Predict and Analyze the Beams in Series "A". -----	159
Table 5.8: Re-calculation of the Maximum Design Load and Prediction of Failure Load for the Beams in Series "A". -----	159
Table 5.9: Comparison of the Predictions of Flexural and Shear Failure Loads with the Test Results obtained from Series "A". -----	160
Table 5.10: Predicted and Measured Capacities for the Beams in Series "A". -----	161
Table 5.11: Test Summary of Mid-Span Deflection and Crack Width Measurements at Different Load Levels for the Beams in Series "A". -----	161



Table 5.12: Test Summary of Strain and Stress Measurements in Concrete at Different Load Levels for the Beams in Series "A". -----	163
Table 5.13: Total Load versus Crack Widths for the Beams in Series "A". -----	164
Table 5.14: Total Load versus Mid-Span Deflections for the Beams in Series "A". -----	164
Table 6.1: Details and Summary of the Test Results of Wide Beams Previously Tested. -----	177
Table 6.2: Details and Summary of the Test Results of Wide Beams Previously Tested Based on New Parameters to the Proposed Prediction-Model. -----	184
Table 6.3a: Validation of the Proposed Prediction Model on the Test Results obtained by Serna-Ros et al. (2002) Investigation on EC2 Code. -----	195
Table 6.3b: Validation of the Proposed Prediction Model on the Test Results obtained by Serna-Ros et al. (2002) Investigation on ACI Code. -----	195
Table 6.4: Validation of the Proposed Prediction Model on the Test Results obtained by Shuraim (2012) Investigation. -----	196
Table 6.5: Validation of the Proposed Prediction Model on the Test Results obtained by Hanafy et al. (2012) Investigation. -----	196
Table 6.6: Validation of the Proposed Prediction Model on the Test Results obtained by Al.Dywany (2010) Investigation. -----	197
Table 6.7: Validation of the Proposed Prediction Model on the Test Results obtained by Lubell et al. (2008, 2009) Investigation. -----	197
Table 6.8: Validation of the Proposed Prediction Model on the Test Results obtained by McAllister (2011) Investigation. -----	198
Table 6.9: Validation of the Proposed Prediction-Model on the Test Results obtained by Test-Series (A) Investigation in Chapter 5. -----	198
Table 6.10: Validation of the Proposed Prediction Model on the Test Results obtained by Al-Harithy (2002) Investigation. -----	198
Table 6.11: Average Strengths of all Wide RC Beams Validated by the Proposed Prediction-Model. -----	199
Table 7.1: Test Series "1" to Study the Effect of $S_L$ , $S_w$ , $k_s$ and $k_p$ on Wide Beam Strengths and to Verify the Proposed Prediction Model. -----	213
Table 7.2: Design Details of the Wide Beams in Test-Series "1". -----	217
Table 7.3: Properties of the Wide Beam Specimens in Test-Series "1". -----	218
Table 7.4: Material Properties used to Design the Beam Specimens in Series "1". -----	220
Table 7.5: Mix Proportions of Concrete used to cast the Beams in Series "1". -----	221
Table 7.6: Actual Concrete Strengths for Test-Series "1". -----	231

Table 7.7: Material Properties used to Predict and Analyze the Beams in Series "1". -----	231
Table 7.8: Prediction of Flexural and Shear Failure Loads for the Beams in Test-Series "1". -	232
Table 7.9: Re-calculation of the Maximum Design Load and Prediction of the Failure Load based on the Proposed Prediction Model. -----	233
Table 7.10: Validation of the Proposed Prediction Model on the Test Results obtained from Test-Series "1". -----	234
Table 7.11: Summary of the Crack Widths at Different Load Levels for the Beams in Test-Series "1". -----	235
Table 7.12: Total Load versus Mid-Span Deflections for Beams-Type (A) in Series (1). -----	242
Table 7.13: Total Load versus Mid-Span Deflections for Beams-Type (B) in Series (1). -----	242
Table 7.14: Total Load versus Mid-Span Deflections for Beams-Type (C) in Series (1). -----	243
Table 7.15: Total Load versus Mid-Span Deflections for Beams-Type (D) in Series (1). -----	243
Table 7.16: Total Load versus Crack Widths for Beams-Type (A) in Series (1). -----	244
Table 7.17: Total Load versus Crack Widths for Beams-Type (B) in Series (1). -----	244
Table 7.18: Total Load versus Crack Widths for Beams-Type (C) in Series (1). -----	245
Table 7.19: Total Load versus Crack Widths for Beams-Type (D) in Series (1). -----	245
Table 8.1: Prediction of Flexural & Shear Failure Loads for Traditional and Proposed Wide Beams (TB & PB) with Wide and Narrow Bearing Plates Compared with EC2 Code. -----	278
Table 8.2: Prediction of Flexural & Shear Failure Loads for Traditional & Proposed Wide Beams (TB & PB) with Wide & Narrow Bearing Plates Compared with Beam ECC2 in Series (A). -	281
Table 9.1: Test-Series "2" to Validate of the Proposed Detailing/Design Models and to Verify the Proposed Prediction Model. -----	284
Table 9.2: Design Details of the Wide Beams in Test-Series "2". -----	288
Table 9.3: Properties of the Wide Beam Specimens in Test-Series "2". -----	290
Table 9.4: Material Properties used to Dsign the Beam Specimens in Series "2". -----	292
Table 9.5: Mix Proportions of Concrete Used to Cast the Beams in Series "2". -----	292
Table 9.6: Actual Concrete Strengths for Test-Series "2". -----	302
Table 9.7: Material Properties used to Predict and Analyze the Beams in Series "2". -----	303
Table 9.8: Prediction of Flexural and Shear Failure Loads for Beams in Test-Series "2". -----	303
Table 9.9: Re-calculation of the Maximum Design Load and Prediction of the Failure Load based on the Proposed Prediction Model. -----	305
Table 9.10: Validation of the Proposed Prediction Model on the Test Results obtained from Test-Series "2". -----	305

Table 9.11: Summary of the Crack Widths at Different Load Levels for the Beams in Test-Series "2".	306
Table 9.12: Total Load versus Mid-Span Deflections for Beams-Type (A) in Series (2).	310
Table 9.13: Total Load versus Mid-Span Deflections for Beams-Type (B) in Series (2).	311
Table 9.14: Total Load versus Mid-Span Deflections for Beams-Type (C) in Series (2).	311
Table 9.15: Total Load versus Mid-Span Deflections for Beams-Type (D) in Series (2).	312
Table 9.16: Total Load versus Crack Widths for Beams-Type (A) in Series (2).	312
Table 9.17: Total Load versus Crack Widths for Beams-Type (B) in Series (2).	313
Table 9.18: Total Load versus Crack Widths for Beams-Type (C) in Series (2).	313
Table 9.19: Total Load versus Crack Widths for Beams-Type (D) in Series (2).	314
Table A.1: Flexural Reinforcement for the Beams in Series "A".	357
Table A.2: Beam-Shear (One-Way) Reinforcement & Spacing for the Beams in Series "A".	357
Table A.3: Punching-Shear (Two-Way) Check for the Beams in Series "A".	357
Table A.4: Calculations of Deflections for the Beams in Series "A" at $P_d = 600$ kN.	357
Table A.5: Calculations of Crack Widths for the Beams in Series "A" at $P_d = 600$ kN.	357
Table A.6: Bar Bending Schedule for Beam ECC2 in Series "A".	358
Table A.7: Bar Bending Schedule for Beam ECC3 in Series "A".	359
Table A.8: Concrete Quantities of the Beams in Test-Series "A".	360
Table A.9: Flexural and Shear Reinforcement Quantities of the Beams in Test-Series "A".	361
Table A.10: Actual Concrete Strengths for Series "A".	361
Table A.11: Material Properties used to Predict and Analyze the Beams in Series "A".	361
Table A.12: Results of Indirect Tensile Stress Test For Reinforcing Steel Bars in Series "A".	362
Table A.13: Tensile Strength and Strain of Reinforcing Steel Bars in Series "A".	362

## LIST OF FIGURES

Figure 1.1: Comparison of Wide & Narrow Beams, and Parameters investigated in this Study. - 3	
Figure 2.1: Classification of Beams Based on Kani's Valley. -----	11
Figure 2.2: Types and Classification of Beams Based on Their Shapes and Geometries. -----	13
Figure 2.3: Flexural Failure Mode. -----	15
Figure 2.4: a) Types of Inclined (Diagonal) Cracking and b) Modes of Shear Failures. -----	16
Figure 2.5: Types of Diagonal Failure and Crack. -----	17
Figure 2.6: Shear Compression Failure. -----	20
Figure 2.7: Splitting Shear Failure. -----	20
Figure 2.8: Deep-Beam Failures: a) Arch Action, and b) Types of Failures. -----	21
Figure 2.9: Strain Profiles at the Flexural Strength of a Section. -----	22
Figure 2.10: Uniaxial Stress-Strain Relationship: a) Typical Curves, b) Effects of Boundary Restraints. -----	24
Figure 2.11: Longitudinal-Strain and Transverse-Strain Relationships for a Uniaxial Compression Test for Flexure. -----	24
Figure 2.12: Superposition of Concrete and Stirrup Contributions Using 45 degree Truss Analogy. -----	29
Figure 2.13: Refined Strut-and-Tie Models Proposed by Al-Nahlawi and Wight, 1992. -----	29
Figure 2.14: Effects of $a/d$ on Shear Strength. -----	30
Figure 2.15: Compression Field Theory: a) Free-Body Diagram of a Beam Section, and b) Compatibility Condition for Average Strains in Concrete. -----	31
Figure 2.16: Mechanisms of Failure Based on the Theory of Plasticity. -----	34
Figure 2.17: Influence of $a/d$ on Shear Strength According to Theory of Plasticity. -----	34
Figure 2.18: a) Compressive Force Path, b) Effect of Bond Failure, and c) Equilibrium Conditions at Force Changing Directions. -----	36
Figure 2.19: Internal Forces in a Cracked Beam: a) with Stirrups, and b) without Stirrups. -----	38
Figure 2.20: Mechanism of Aggregate Interlock. -----	40
Figure 2.21: Shear in Beam without Shear Reinforcement. -----	43
Figure 2.22: a) Beam Action, and b) Arch Action. -----	43
Figure 2.23: Bond between Reinforcing Steel-Bar and Concrete. -----	43
Figure 2.24: Traditional Concepts of Shear Strength. -----	45
Figure 2.25: Kani's Tooth Model. -----	45

Figure 3.1: Wide Beams (Hidden Beams) in a Ribbed Slab System, and Cross-Section Details of Wide and Narrow Beams. -----	50
Figures 3.2: Punching Shear Failure. -----	54
Figure 3.3: Force Flow Analogy in Diagonal Strut Toward Shear Reinforcement Legs. -----	60
Figure 3.4: Wide Beams Tested by Hanafy et al (2012), they may be considered as T-Sectioned Wide Beams. -----	65
Figure 3.5: $V_{s,exp}$ . versus $S_L/d$ . -----	65
Figure 3.6: $V_{s,exp}$ . versus $S_w/d$ . -----	65
Figure 3.7: Failures of Typical Wide RC Beams Tested by Al.Dywany (2010) with Full-Width Loads and Narrow-Width Supports. -----	67
Figure 3.8: Configuration of Lubell et al. (2008) Specimens with Full-Width (AX) and Narrow-Width (AW) Bearing Plates. -----	70
Figure 3.9: Crack Patterns after Failure for Lubell et al. (2008) Specimens. -----	71
Figure 3.10: $V_{c,exp}$ . versus $k_s$ . -----	71
Figure 3.11: $V_{c,exp}$ . versus $k_p$ . -----	71
Figure 3.12: $V_{c,exp}$ . versus $k$ . -----	71
Figure 3.13: $M_{u,exp}$ . versus $k_s$ . -----	72
Figure 3.14: $M_{u,exp}$ . versus $k_p$ . -----	72
Figure 3.15: $M_{u,exp}$ . versus $k$ . -----	72
Figure 3.16: $V_{s,exp}$ . versus $k_s$ . -----	72
Figure 3.17: Failure Mode of Wide Concrete Beams for Case 1 of Support and Load Widths. -	73
Figure 3.18: Failure Mode of Wide Concrete Beams for Case 2 of Support and Load Widths. -	74
Figure 3.19: Failure Mode of Wide Concrete Beams for Case 3 of Support and Load Widths. -	75
Figure 3.20: Failure Mode of Wide Concrete Beams for Case 4 of Support and Load Widths. -	76
Figure 3.21: $V_{c,exp}$ . versus $\rho_s$ . -----	80
Figure 3.22: $V_{c,exp}$ . versus $\rho_s'$ . -----	80
Figure 3.23: $M_{u,exp}$ . versus $\rho_s$ . -----	80
Figure 3.24: $M_{u,exp}$ . versus $\rho_s'$ . -----	81
Figure 4.1: Types of Cracking in RC Beams. -----	85
Figure 4.2: A Typical RC Beam Containing Shear Reinforcement. -----	86
Figure 4.3: Inclined Shear Cracks, and Forces in a RC Beam. -----	88
Figure 4.4: Ultimate Shear Stress ( $v_u$ ) at which Stirrups are required to ACI318 and SBC304 Codes. -----	90
Figure 4.5: Stress-Strain Relationship of Concrete to ACI318-and-SBC304, and EC2 Codes. -	93

Figure 4.6: Stress-Strain Relationship of Steel to ACI318-and-SBC304, and EC2 Codes. -----	94
Figure 4.7: Stresses and Strains Distribution on a Wide Beam Section used in the Design Equations. -----	95
Figure 4.8: Equivalent Stresses and Strains Distribution on a Wide Beam Section Compared to ACI318-and-SBC304 and EC2 Codes. -----	96
Figure 4.9: Longitudinal & Shear Reinforcements in a Beam to ACI318 & SBC304 Codes. ---	99
Figure 4.10: Longitudinal and Shear Reinforcements in a Beam to EC2 Code, and which are designed in accordance with EC2, ACI318 and SBC304 Codes. -----	99
Figure 4.11: Sectional Model for Transfer at Flexural-Shear Cracks. -----	100
Figure 4.12: Punching Shear Failure Surfaces of Wide Concrete Members. -----	104
Figure 4.13: Typical Punching Shear Failure and Crack Patterns on Wide Members. -----	105
Figure 4.14: Types of Shear Failure Surfaces in a Wide Member. -----	107
Figure 4.15: Flexural & Shear Cracks due to Applied Shear Forces & Stresses on a Beam. ---	110
Figure 4.16: Tension & Compression Stresses cause the Diagonal Tension Cracks. -----	111
Figure 4.17: $k_s$ versus $V_{u,exp}/V_{u,Pred.}$ . -----	127
Figure 4.18: $k_s$ versus $V_{c,exp}/V_{c,Pred.}$ . -----	128
Figure 4.19: $k_s$ versus $V_{s,exp}/V_{s,Pred.}$ . -----	129
Figure 4.20: $k_s$ versus $M_{u,exp}/M_{u,Pred.}$ . -----	129
Figure 4.21: $k_p$ versus $V_{u,exp}/V_{u,Pred.}$ . -----	130
Figure 4.22: $k_p$ versus $V_{c,exp}/V_{c,Pred.}$ . -----	131
Figure 4.23: $k_p$ versus $M_{u,exp}/M_{u,Pred.}$ . -----	131
Figure 4.24: $k$ versus $V_{u,exp}/V_{u,Pred.}$ . -----	132
Figure 4.25: $k$ versus $V_{c,exp}/V_{c,Pred.}$ . -----	133
Figure 4.26: $k$ versus $M_{u,exp}/M_{u,Pred.}$ . -----	133
Figure 4.27: $SL/d$ versus $V_{u,exp}/V_{u,Pred.}$ . -----	134
Figure 4.28: $SL/d$ versus $V_{s,exp}/V_{s,Pred.}$ . -----	135
Figure 4.29: $S_w/d$ versus $V_{u,exp}/V_{u,Pred.}$ . -----	136
Figure 4.30: $S_w/d$ versus $V_{s,exp}/V_{s,Pred.}$ . -----	137
Figure 4.31: $SL/S_w$ versus $V_{u,exp}/V_{u,Pred.}$ . -----	138
Figure 4.32: $SL/S_w$ versus $V_{s,exp}/V_{s,Pred.}$ . -----	138
Figure 5.1: Details of Wide Beam Specimens in Test-Series "A". -----	143
Figure 5.2: Design of Wide Beam Specimens in Test-Series "A". -----	144
Figure 5.3: Difference Sizes of Steel Plates for Load & Support Conditions in Series "A". ---	146
Figure 5.4: Steel Cages of the Beams in Test-Series "A". -----	150

Figure 5.5: Steel Shutters used for the Beam Specimens in Test-Series "A".	151
Figure 5.6: Beams in Series "A" together with own Control Samples.	152
Figure 5.7: The Curing Process of the Beams in Series "A" after Removing the Shutters.	153
Figure 5.8: Testing Instrumentation and Equipment used in the Tests of Series "A".	154
Figure 5.9: Failure Modes and Crack Patterns at Failure for the Beams in Test-Series "A".	161
Figure 5.10: Photos of the Failure Modes, Crack Patterns and Deformed Shapes after Failure for the Beams in Series "A".	162
Figure 5.11: Total Applied Load versus Mid-Span Deflection for the Beams in Series "A".	162
Figure 6.1: a) Ritter's Truss Model, and b) Mörsh's Truss Analogy.	172
Figure 6.2: a) Flow of the Diagonal Compressive Force in Wide Beam Cross-Sections, and b) Distribution of Principal Stresses.	173
Figure 6.3: $V_{c,exp}$ versus $\rho_s$ .	180
Figure 6.4: $V_{c,exp}$ versus $\rho_s'$ .	180
Figure 6.5: $V_{c,exp}$ versus $k_s$ .	180
Figure 6.6: $V_{c,exp}$ versus $k_p$ .	180
Figure 6.7: $V_{c,exp}$ versus $k$ .	181
Figure 6.8: $M_{u,exp}$ versus $\rho_s$ .	181
Figure 6.9: $M_{u,exp}$ versus $\rho_s'$ .	181
Figure 6.10: $M_{u,exp}$ versus $k_s$ .	181
Figure 6.11: $M_{u,exp}$ versus $k_p$ .	182
Figure 6.12: $M_{u,exp}$ versus $k$ .	182
Figure 6.13: $V_{s,exp}$ versus $S_L/d$ .	182
Figure 6.14: $V_{s,exp}$ versus $S_w/d$ .	182
Figure 6.15: $V_{s,exp}$ versus $k_s$ .	183
Figure 6.16: $V_{c,exp}$ versus $ \rho_s - \rho_s' $ .	187
Figure 6.17: $M_{u,exp}$ versus $ \rho_s - \rho_s' $ .	187
Figure 6.18: $V_{c,exp}$ versus $k^{(h/b_w)}$ .	187
Figure 6.19: $M_{u,exp}$ versus $k^{(h/b_w)}$ .	188
Figure 6.20: $V_{s,exp}$ versus $S_L/S_w$ .	188
Figure 6.21: $V_{s,exp}$ versus $k_s^{(1-k_s)}$ .	188
Figure 6.22: $k_s$ versus $V_{u,exp}/V_{u,Pred.}$ .	199
Figure 6.23: $k_s$ versus $V_{c,exp}/V_{c,Pred.}$ .	200
Figure 6.24: $k_s$ versus $V_{s,exp}/V_{s,Pred.}$ .	200
Figure 6.25: $k_s$ versus $M_{u,exp}/M_{u,Pred.}$ .	201

Figure 6.26: $k_p$ versus $V_{u,exp.}/V_{u,Pred.}$ .....	201
Figure 6.27: $k_p$ versus $V_{c,exp.}/V_{c,Pred.}$ .....	202
Figure 6.28: $k_p$ versus $M_{u,exp.}/M_{u,Pred.}$ .....	202
Figure 6.29: $k$ versus $V_{u,exp.}/V_{u,Pred.}$ .....	203
Figure 6.30: $k$ versus $V_{c,exp.}/V_{c,Pred.}$ .....	204
Figure 6.31: $k$ versus $M_{u,exp.}/M_{u,Pred.}$ .....	204
Figure 6.32: $SL/d$ versus $V_{u,exp.}/V_{u,Pred.}$ .....	205
Figure 6.33: $SL/d$ versus $V_{s,exp.}/V_{s,Pred.}$ .....	206
Figure 6.34: $S_w/d$ versus $V_{u,exp.}/V_{u,Pred.}$ .....	206
Figure 6.35: $S_w/d$ versus $V_{s,exp.}/V_{s,Pred.}$ .....	207
Figure 6.36: $SL/S_w$ versus $V_{u,exp.}/V_{u,Pred.}$ .....	208
Figure 6.37: $SL/S_w$ versus $V_{s,exp.}/V_{s,Pred.}$ .....	208
Figure 7.1: Details of Wide Beam Specimens in Test-Series "1". .....	214
Figure 7.2: Design of Wide Beam Specimens in Test-Series "1". .....	215
Figure 7.3: Difference Sizes of Steel Plates for Load and Support Conditions in Series "1". --	218
Figure 7.4: Typical Steel Cages for the Beams in Test-Series "1". .....	223
Figure 7.5: Typical Steel Shutters used for the Beam Specimens in Test-Series "1". .....	224
Figure 7.6: Typical Beams for Series "1" together with own Control Samples. ....	225
Figure 7.7: The Curing Process of Typical Beams in Series "1". .....	225
Figure 7.8: Testing Instrumentation and Equipment used in the Tests of Series "1". .....	226
Figure 7.9: Critical Failure Modes and Crack Patterns for the Beams in Test-Series "1". .....	235
Figure 7.10: Failure Modes and Crack Patterns after Failure for the Beams in Series "1". .....	239
Figure 7.11: Total Load versus Mid-Span Deflection for the Beams in Type (A), Series "1". -	240
Figure 7.12: Total Load versus Mid-Span Deflection for the Beams in Type (B), Series "1". -	240
Figure 7.13: Total Load versus Mid-Span Deflection for the Beams in Type (C), Series "1". -	241
Figure 7.14: Total Load versus Mid-Span Deflection for the Beams in Type (D), Series "1". -	241
Figure 8.1: Application of Equations 8.1.a&b and 8.2.a&b on Wide Beams with Narrow-Width Load and Support Conditions. ....	266
Figure 8.2: Effect of the Loading Width on Shear Stress Distributions of a Narrow Supported Wide Beam. ....	266
Figure 8.3: The Effect of Narrow Support on a Wide RC Beam. ....	277
Figure 9.1: Details of Wide Beam Specimens in Test-Series "2". .....	285
Figure 9.2: Design of Wide Beam Specimens in Test-Series "2". .....	287
Figure 9.3: Difference Sizes of Steel Plates for Load and Support Conditions in Series "2". --	290



Figure 9.4: Typical Steel Cages for the Beams in Test-Series "2".	294
Figure 9.5: Typical Steel Shutters used for the Beam Specimens in Test-Series "2".	295
Figure 9.6: Typical Beams for Series "2" together with own Control Samples.	296
Figure 9.7: The Curing Process of Typical Beams in Series "2".	297
Figure 9.8: Testing Instrumentation and Equipment used in the Tests of Series "2".	298
Figure 9.9: Critical Failure Modes and Crack Patterns for the Beams in Test-Series "2".	306
Figure 9.10: Failure Modes and Crack Patterns after Failure for the Beams in Series "2".	308
Figure 9.11: Total Load versus Mid-Span Deflection for the Beams in Type (A), Series "2".	309
Figure 9.12: Total Load versus Mid-Span Deflection for the Beams in Type (B), Series "2".	309
Figure 9.13: Total Load versus Mid-Span Deflection for the Beams in Type (C), Series "2".	309
Figure 9.14: Total Load versus Mid-Span Deflection for the Beams in Type (D), Series "2".	310
Figure A.1: Equivalent Stresses and Strains Distributions on a Section for Single Flexural Reinforcement.	336
Figure A.2: Equivalent Stresses and Strains Distributions on a Section for Double Flexural Reinforcement.	338
Figure A.3: Truss Model.	339
Figure A.4: Longitudinal and Shear Reinforcements in a Beam to EC2, ACI318 and SBC304 Codes.	339
Figure A.5: Strut Inclination Method.	341
Figure A.6: Type of Shear Failure Surfaces in a Wide Member.	346
Figure A.7: SFD and BMD Diagrams for the Beams in Test-Series "A".	356
Figure A.8: Design Details and Reinforcement Drawing of Beam ECC2 in Series "A".	358
Figure A.9: Design Details and Reinforcement Drawing of Beam ECC3 in Series "A".	359
Figure A.10: Shape Codes of the Reinforcing Steel Bars.	359
Figure A.11: Typical Stress-Strain Curves for Steel Reinforcement Bars in Series "A".	362

## LIST OF APPENDICES

<b>APPENDIX (A): Design and Prediction Calculations</b> .....	<b>334</b>
<b>A.1: Design Procedure of Wide Beams</b> .....	<b>334</b>
1. Flexural Reinforcement .....	335
2. Shear Reinforcement .....	339
3. Serviceability Check .....	349
<b>A.2: Prediction Procedure of Wide Beams</b> .....	<b>351</b>
1. Predicted Flexural Failure Load .....	351
2. Predicted One-Way Shear Failure Load .....	352
3. Check of Two-Way Shear (Punching-Shear) Stress .....	352
4. Final Predicted Failure Load and Mode .....	354
<b>A.3: Analysis and Design of Wide Beams [Beam ECC2 and ECC3]</b> .....	<b>354</b>
1. Beam Analysis .....	355
2. Beam Design .....	356
3. Material Quantities .....	360
4. Compression and Tensile Tests of Concrete .....	361
5. Tensile Tests of Steel .....	362
<b>A.4: Prediction of Wide Beams [Beam ECC2 and ECC3]</b> .....	<b>363</b>
1. Beam ECC2 .....	363
2. Beam ECC3 .....	365
3. Check of Two-Way Shear (Punching-Shear) Stress .....	367
<b>APPENDIX (B): Experimental Work Activities</b> .....	<b>368</b>
<b>B.1: Activities to Manufacture the Steel Cages</b> .....	<b>368</b>
<b>B.2: Activities to Cast the Concrete</b> .....	<b>368</b>
<b>B.3: Activities to Test the Beams</b> .....	<b>369</b>
<b>APPENDIX (C): Author's Contributions</b> .....	<b>371</b>
<b>C.1: Technical and Published Works</b> .....	<b>371</b>
<b>C.2: Oral Presentations in Conferences</b> .....	<b>372</b>
<b>C.3: Posters in Conferences</b> .....	<b>373</b>
<b>C.4: Technical Reports on PhD Research Area</b> .....	<b>373</b>
<b>C.5: Attendance and Participation in Conferences, Workshops, and Training Courses</b> -	<b>374</b>

## ABSTRACT

In reinforced concrete (RC) structures, wide RC beams are used as primary structural members to support floor loads and to transfer forces from the floor to the vertical elements which are below them, e.g. columns and walls. In these cases, wide concrete beams may be loaded and supported by wide columns or walls (full-width loads and supports) and/or by narrow columns (partial-width loads and supports). In both cases of support and load conditions, the one-way (beam) and two-way (punching) shear capacities should be checked for wide RC members. For both wide and narrow load/support configurations, the provisions of current design Codes require that one-way shear capacity is assessed for a cross-section involving the full width of the beam, and the contribution of shear strength resisted by stirrups is assessed according to the longitudinal stirrup-legs spacing where the transverse stirrup-legs spacing is neglected. Moreover, the current design Codes neglect the load and support widths to predict the flexural strength. The main concern is whether the requirements of current design Codes may lead to poor predictions of flexural and shear strengths of wide concrete beams, especially for narrow-supported wide beams, because they ignore the support width, load width, longitudinal and transverse spacing of stirrup-legs.

The objective of this study is to develop new Prediction, Detailing and Design Models for wide reinforced concrete beams to be used in Practice. The results of 26 tests on wide RC beam specimens are reported in this study.

The models were developed to account for the missed parameters mentioned above which showed an actual influence on the flexural and shear strengths of wide RC beams with full- and narrow- width loads and supports (wide- and narrow- supported wide RC beams). They take into the consideration the load- and support- widths (or at best, the ratios of load- and support- width to the beam-width). Comprehensive verifications and evaluations of the proposed models were conducted for comparing them with the existing design Codes and other proposed models. It is shown that the proposed models perform the best among the existing Codes and models. It is shown that the flexural and shear strengths decrease as the ratio of the load- and/or support-width to the beam-width decreases, while the shear strength resisted by stirrups contribution decreases as the transverse stirrup legs spacing increases. These influences occur for members with and without shear reinforcement.

Based on the proposed design model, the longitudinal and transversal stirrup legs spacing are reduced as the ratio of the load- and/or support- width to the beam-width decreases, and then this will enhance to increase the shear strength; therefore, the failure mode will change from brittle to ductile manner. These influences occur for members with shear-reinforcement. For the members without shear-reinforcement, the proposed detailing approach will enhance the flexural reinforcements (tensile and compressive bars) when they are distributed according to their portions of concentrations within the effective-widths of supports and loads.

For wide RC beams with and without shear-reinforcement, test results showed that the shear strength decreased as the support-width and/or load-width was reduced. In addition, for wide RC beams with shear-reinforcement, tests results showed that the shear strength decreased as the longitudinal or transverse spacing of stirrup-legs increased. The tests results also showed that the flexural strength of wide RC beams with stirrups decreased as the support-width and/or load-width was reduced.

**Author keywords:** Wide Beams; Existing Codes and Models; Stirrup Leg Spacings; Load and Support; Proposed Prediction, Detailing and Design Models.

# CHAPTER 1

## INTRODUCTION

### 1.1 Introduction

Reinforced concrete (RC) beams are classified, in general, according to the geometry and shape of their cross-sections (Al.Dywany, 2010; Alluqmani, 2014; Alluqmani and Haldane, 2011a, 2011b). Constraints are placed upon the selection of their geometries by both structural and architectural requirements. In these RC members, the concrete resists the shear forces and its failure is sudden and evident with diagonal cracks; while the steel resists the bending moments and its failure happens with a deflection. The load caused by concrete or shear failure should be higher than that load caused by steel or flexural (bending-moment) failure; but if otherwise, the design and dimensions of the structural RC member should be changed (Alluqmani, 2010; Alluqmani and Haldane, 2011c).

Even through the rectangular solid beams variation in the length, width, and depth are possible, where shallow, deep and conventional beams are considered rectangular in shape and the difference is only by their behaviour, which finally affect the design procedures and requirements (Al.Dywany, 2010). In the design of buildings, contemporary architectural constraints and conditions are pushing design engineers to provide longer clear spans at reasonable costs. Simultaneously, minimising the overall structural depth may be needed which can be achieved by using of wide beams or thick structural slabs. The cross-section shape of the beam, shear reinforcement (stirrups) and the main tensile reinforcing ratio can have an effect on the beam design for shear and flexure capacities (Grant, 2003). In rectangular slender beams (either shallow and/or deep beams, or narrow and/or wide beams), the increase of beam width ( $b_w$ ) leads to increase shear and flexural strengths of beams (Diaz de Cossio, 1962; Leonhardt and Walther, 1961). Consequently, in the construction industry there is an advantage in using wide RC beam where its width is larger than its depth.

A reinforced concrete beam can be strengthened for flexure or shear or both types of resistance. Strengthening a beam for either of these mechanisms has different effects on the beam itself. If a concrete beam is strengthened for shear it will make the beam more ductile while strengthening the beam for flexure will stiffen the beam; meaning there will be large forces present at the ends

of the beam, causing the beam to fail in shear. Strengthening a beam for flexure may mean the beam will fail prematurely in shear, meaning although the beam has been strengthened for flexure it cannot actually carry any greater load as it will fail prematurely in shear.

## 1.2 Wide Reinforced Concrete Beams

Wide RC beams are the beams which have obvious width to height ( $b_w/h$ ) ratio in comparison to the narrow beams (Figure 1.1), and they are designed as conventional RC beams (Al.Dywany, 2010; Sherwood et al., 2006). For these wide beams, the  $b_w/h$  ratio exceeds 2.0 (Al.Dywany, 2010; Sherwood et al., 2006), where this ratio was taken equal to 2.0 for all examined wide RC beams throughout this programme of research. For wide RC beams, the shear-span to effective-depth ( $a/d$ ) ratio is more than 1.0 (Teck FU, 2009). Structural wide RC beams are used in buildings to reduce reinforcement congestion and floor heights for the required headroom. Wide beams are most often used as transfer elements where the total structural depth ( $h$ ) must be kept to a minimum (Alluqmani, 2014; Alluqmani and Haldane, 2011a, 2011b, 2011c). In addition, these members provide large cross-sectional areas of concrete to resist shear demands. In most of these cases, the beam is either equal to or wider than that of the supporting columns or loads. Consequently, their shear capacity might be affected and differ from that of conventional beams. In this study, test specimens were designed and examined with either full-width or narrow-width load and support conditions.

In reinforced concrete structures, like buildings and bridges, wide beams are used as primary structural members to support floor loads and to transfer forces from the floor to the vertical elements which are below them, e.g. columns and walls. In these cases, wide beams may be loaded and supported by wide columns or walls (full-width loads and supports) and/or by narrow columns (partial-width loads and supports). In the both cases of support and load conditions, the one-way (beam) and two-way (punching) shear capacities should be checked for wide RC members (Alluqmani, 2013a). For both wide and narrow load/support configurations, the provisions of current design Codes require that one-way shear capacity is assessed for a cross-section involving the full width of the beam, and the contribution of shear strength resisted by stirrups is assessed according to the longitudinal stirrup legs spacing where the transverse stirrup legs spacing is neglected (Alluqmani and Saafi, 2014a). Moreover, the current design Codes neglect the load and support widths to predict the flexural and shear strengths of these wide beams (Alluqmani, 2013a; Alluqmani and Saafi, 2014b). For wide members, design Codes do not provide guidance on appropriate limits for spacing of the shear reinforcement legs across the

member width (transverse stirrup spacing,  $S_w$ ) (Alluqmani, 2014; Alluqmani and Haldane, 2011a, 2011b).

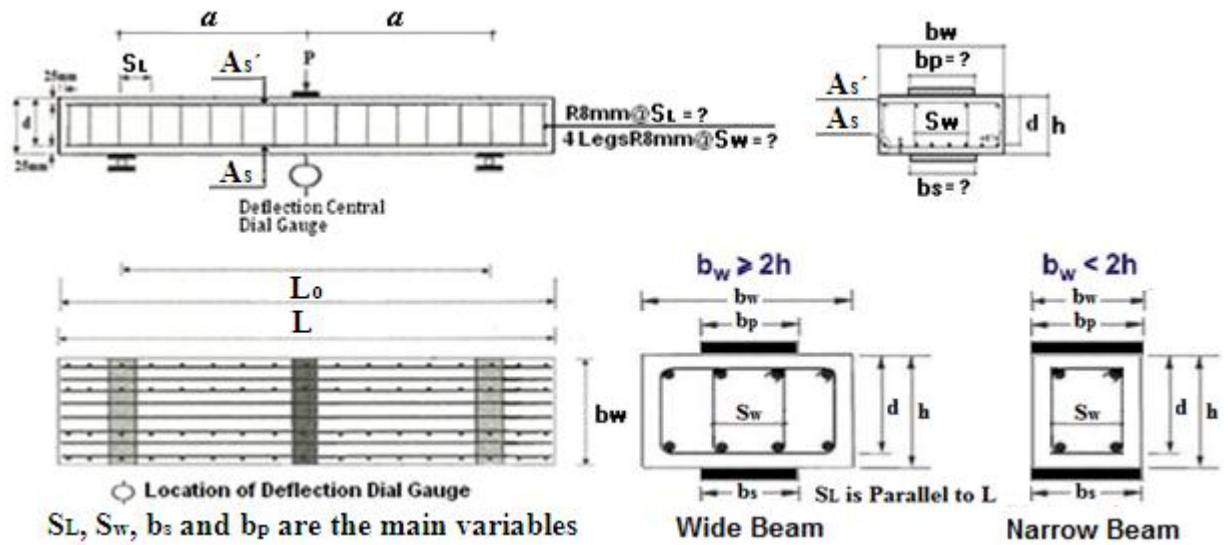


**Figure 1.1:** Comparison of Wide and Narrow Beams, and Parameters investigated in this Study.

Design of wide structural concrete members should follow a logical approach (Alluqmani, 2013a, 2013b). None of the current design approaches take into their design considerations the design provisions of shear for wide RC beams, where these approaches are widely admitted as being inadequate to design these beams. A number of analytical and design models, and many theories have been put forward in an attempt to explain and discuss the shear mechanism and also to predict the shear strength of structural concrete members in general. Therefore, many design approaches have been developed to prevent the diagonal (shear) failures in structural beams. All of these approaches were attempts. The lack of understanding of the diagonal shear failure mechanism of wide beams is still prevalent up to date (Alluqmani, 2013a, 2013b). In the design of wide RC beams, these methods neglect principal factors affecting both shear and flexural strengths of these beams.

Currently, some research programmes (Lubell et al., 2008; Lubell et al., 2009a; Lubell et al., 2009b; Lubell et al., 2004; Lubell, 2006; Al.Dywany, 2010) have attempted to investigate the behaviour of wide structural concrete members under shear loading conditions. Despite the availability of some theoretical and experimental research studies, the prediction of wide RC beams behaviour subject to transverse loading conditions is still a challenging task. It is possible with any degree of accuracy to determine the ultimate capacity and deformation of structural beams under shear force and bending moment which are applied to design beams in practice. Most of the analytical models have been proposed for structural beams subject to such loadings.

In practical and realistic applications of design procedures, there is an evident view from applied theories; consequently there is still a need to find a suitable model to predict the load capacity of wide structural beams under the effect of transverse loadings.

However, there is a deficiency of understanding of the shear strength and the diagonal shear failure mechanism of wide concrete members. This deficiency has contributed to find logical design model and detailing approach for structural concrete wide beams (Alluqmani, 2013a, 2013b; Alluqmani and Saafi, 2014c), as well as to find a logical prediction model (Alluqmani, 2013a), which are based on the actual parameters affecting the flexural and shear strengths of these wide beams.

The enhancing influence of confinement on the flexural behaviour of beams is widely acknowledged, however, little attempt has been made to utilise this enhancement in the design of beams under static loading conditions. To utilise the enhancing influence of the confining stirrups, a proposed design model was developed to account for determining the stirrup legs spacing in both length and width directions. The brittle compression failures which are characteristic of over-reinforced beams can be prevented by confining the compression concrete with closed stirrups.

### **1.3 The Nature of The Problem**

The main concern of the current research conducted in this study is whether the requirements of current design Codes and existing models may lead to poor predictions of the flexural and shear strengths of wide concrete beams, especially for narrow-supported wide beams. This is because the existing Codes neglect the main factors affecting wide RC beam strengths and behaviour. Accordingly, a proposed Prediction-Model was developed based on the main missed parameters unconsidered in the current Codes which showed an actual influence on the flexural and shear strengths of both wide- and narrow- supported wide RC beams (Alluqmani, 2013a). The proposed prediction model takes into the consideration the load- and support- widths to predict the flexural and shear strengths, as well as takes into the consideration the longitudinal and transverse stirrup-legs spacing to predict the shear strength resisted by stirrups. Moreover, proposed Detailing-Approach and Design-Model were developed to detail and design the wide RC beams for the interaction between shear and flexural stresses for estimating the flexural reinforcing bars that should be concentrated and distributed within the effective widths of supports and loads, and for estimating the longitudinal and transversal stirrup-legs spacing,



respectively (Alluqmani, 2013a; Alluqmani and Saafi, 2014c). It was found that the proposed models developed in this study perform better than the existing Codes and models (Alluqmani, 2013a, 2013b).

The proposed models (prediction, detailing and design models) developed in this study are based on an exhaustive intelligence of the actual structural behaviour of wide RC beams and the actual effect of bearing-plate (load and support) widths and stirrup-legs spacing. In addition, they take into consideration the interaction between shear and flexure, and the effect of one behavioural mechanism which is within the beam structure subjected to applied loadings.

In the literature, the enhancing effect of confining closed stirrups (hoop stirrups) and open stirrups (U-shaped stirrups), the stirrup legs spacing along the member length ( $S_L$ ) and across the member width ( $S_w$ ), and the influence of support width ( $b_s$ ) and loading width ( $b_p$ ) on the strengths and ductility of structural wide RC members have been highlighted. There have been attempts to adopt this enhancement in the design of wide RC beams under the conditions of static loadings. Therefore, this programme of research describes an effort to adopt confinement stirrups and their spacing ( $S_L$  and  $S_w$ ) based on the ratios of support- and/or load- width to the beam-width for the prevention of diagonal shear failure in wide beams and lead to enhance their flexural strength and behaviour. The main variables considered in this research, which are  $S_L$ ,  $S_w$ ,  $b_s$  and  $b_p$ , are shown in Figure 1.1.

Traditional design methods used for reinforced concrete design, such as EC2, ACI318 and SBC304, treat the wide beams like narrow beams, where the factors mentioned above are not taken in the consideration. The support width, load width and transverse spacing of stirrup-legs are not assumed at any point throughout the design procedure. However, research showed there was an influence for these parameters on the shear and flexural strengths of wide RC beams. The models developed in this study recognize these factors affecting the design and behaviour of wide RC beams. The proposed design model determines the longitudinal and transverse spacing of stirrup legs based on the ratios of support- and load- widths to the beam-width to prevent premature shear failure and hence to achieve a higher shear capacity and make the beams behave in a flexural manner (Alluqmani and Saafi, 2014c). The proposed detailing approach contributes in distributing a portion of the flexural -tensile and -compressive reinforcing bars with the support and load regions to enhance the high stresses in these regions and shear strength, and hence to ensure that the beams behave in a ductile-flexural manner (Alluqmani and Saafi, 2014c).

## **1.4 Contributions to Knowledge**

Structures, that have wide RC beams such as building and bridges, have indicated that wide concrete beams have different design, manufacturing and behaviour in comparison with those narrow beams. Previous researches showed that the support and load widths and the longitudinal and transverse spacing of stirrup legs have influence on the design and strengths of wide RC beams. These factors have been put forward to develop proposed Prediction, Detailing and Design models to be investigated throughout this study. The proposed design model determines the longitudinal and transverse spacing of stirrup legs based on the ratios of support- and load-widths to the beam-width to prevent shear failure and to ensure that the beams behave in a flexural manner. The proposed detailing approach contributes in distribution portion of the flexural -tensile and -compressive reinforcing bars within the support and load regions to enhance the high stresses and shear strengths in these regions, and hence to ensure that the beams behave in a ductile-flexural manner.

This study has resulted in a significant simplification of the prediction, detailing and designing of wide RC members. It is shown that the simplified proposed models developed in this study are capable of predicting and designing the flexural and shear strengths of wide RC members with various load and support conditions (various bearing plate widths). The expressions developed in this Thesis can form the basis of simple, general, and accurate flexural and shear prediction/design methods for wide RC members. The author believes that this study, which is detailed and described in this Thesis, is carried out for the first time and will be very useful to concrete technology.

## **1.5 Aims and Objectives of the Research**

The principal aim of this programme of research has been directed towards the development of simple analytical models for the detailing, designing and prediction of the structural wide concrete beams under static loadings either with full-width or narrow-width load and support conditions.

**The principal objectives of this study are summarized as follows:**

1. To review the previous work conducted on the reinforced concrete (RC) beams in general and in wide RC beams In particular.
2. To review the existing approaches and models developed for reinforced concrete, as well as to review the design and prediction methods for both shear and flexure used in the current Codes and models.
3. To investigate the effect of shear reinforcement and its spacing on the shear and flexural behaviours and strengths of wide RC beams to be used with those data of wide RC beams tested previously in order to develop a proposed Prediction-Model.
4. To develop a new Prediction-Model in order to determine the flexural and shear strengths of wide RC beams with various support and load widths either without stirrups or with stirrups and various stirrup-legs spacing along the beam length and across its width.
5. To investigate various parameters experimentally which have influence on the wide RC beam strengths, such as the support width, load width, longitudinal and transverse spacing of stirrup legs, effecting of the transverse stirrup legs spacing, as well as to verify the proposed Prediction-Model developed in this study.
6. To develop new Detailing-Approach and Design-Model based on the effect of various parameters investigated in this study.
7. To validate experimentally the proposed Detailing-Approach and Design-Model developed in this study.
8. To summarize and conclude the findings of this study.

## **1.6 The Programme of Research**

**The present programme of research includes the following component parts:**

1. A general review of the design and behaviour of reinforced concrete members and beams was included and discussed.

2. A specific review of the behaviour of wide RC beams was included and discussed.
3. The basis of theoretical design (ultimate strength design and serviceability check) of structural RC beams was discussed according to the provisions of EC2, ACI318 and SBC304 Codes as well as to the prediction methods used in these Codes were compared with the existing prediction models developed by Lubell et al (2008), Serna-Ros et al (2002) and Shuraim (2012).
4. The structural behaviour of wide RC beams (totally two beams specially detailed for shear, Test-Series "A") was investigated and discussed experimentally.
5. The theoretical basis of the proposed Prediction-Model for the prediction of failure loads and modes (shear and flexural strengths) have been developed with reference to the actual structural behaviour of wide RC beams previously tested. The proposed Prediction-Model was discussed and verified experimentally.
6. The structural behaviour of wide RC beams (totally sixteen beams with various support and load widths and various longitudinal and transverse stirrup-legs spacings, Test-Series "1") was investigated and discussed experimentally to verify the proposed Prediction-Model and to study the influence of the support and load widths and the longitudinal and transverse spacings of stirrup legs.
7. The theoretical basis of the proposed Detailing-Approach and Design-Model for the prevention of diagonal shear failures have been developed with reference to the actual structural behaviour of wide RC beams. The theoretical basis of the proposed Detailing and Design models was confined to account for the factors which were believed to influence diagonal failures in wide beams e.g. the support-width to beam-width ratio ( $k_s$ ), the load-width to beam-width ratio ( $k_p$ ), the longitudinal stirrup legs spacing ( $S_L$ ) and the transverse stirrup legs spacing ( $S_w$ ). The proposed Detailing and Design models were discussed and validated experimentally.
8. The structural behaviour of wide RC beams (totally eight beams with various support and load widths correspondingly to those beams in Series (1) and various longitudinal and transverse spacing of stirrup-legs determined based on the proposed design model, Test-Series "2") was investigated and discussed experimentally to validate the proposed Detailing-Approach and Design-Model.

## 1.7 Outline of Thesis

**This Thesis consists of ten Chapters as follows:**

- **Chapter 1:** An Introduction to the reinforced concrete structures and wide RC beams was included. In addition, the main objectives and the programme of the present study were outlined in this Chapter.
- **Chapter 2:** A general literature review on the reinforced concrete beams was discussed. The classification and failure modes of beams were included. The behaviour of beams in flexure and shear (with and without shear-reinforcement) were also discussed and explained in this Chapter. Moreover, emphasis has been placed on shear transfer and the resulting failure mechanisms, and on the recently developed techniques which aim to solve the shear problem.
- **Chapter 3:** A specific literature review of the wide reinforced concrete beams was discussed. Previous researches, which have been conducted previously on wide RC members, were also discussed and concluded. Conclusions relating to the influence of previous work on the present investigation have been outlined in this Chapter.
- **Chapter 4:** The design and prediction methods of flexural and shear of reinforced concrete beams in accordance with the existing Codes (such as EC2, ACI318 and SBC304) and the existing developed models (Lubell's model, 2008; Serna-Ros's model, 2002; Shuraim model, 2012) were explained and discussed. Conclusions relating to the present study were made in this Chapter.
- **Chapter 5:** Two wide RC beams specially detailed for shear were investigated in this Chapter for studying the flexural and shear strengths and behaviours of these beams to be used together with the wide RC beams tested previously in the literature in order to develop a proposed Prediction-Model.
- **Chapter 6:** A new proposed Prediction-Model for determining the shear and flexural strengths of wide RC beams was developed and discussed in this Chapter.
- **Chapter 7:** Verification on the proposed Prediction-Model developed in this study, and studying the influence of the support width, load width, longitudinal and transverse spacing of stirrups legs were conducted and discussed on the wide RC beams included in Test-Series "1".

- **Chapter 8:** New Detailing-Approach and Design-Model for wide RC beams were developed and discussed in this Chapter.

- **Chapter 9:** Validation on the proposed Detailing and Design models developed in this study was conducted and discussed on the wide RC beams included in Test-Series "2".

- **Chapter 10:** Conclusions and recommendations relating to the present study were summarized and outlined in this Chapter.

**Appendices:** The design and prediction calculations, the experimental work activities, and the author's contributions are included in Appendices A, B and C, respectively.

**Bibliography:** All references, books, journals and resources used, which were referred to in this Thesis, are attached to the end of Thesis.

## CHAPTER 2

# GENERAL LITERATURE REVIEW FOR REINFORCED CONCRETE MEMBERS

### 2.1 Introduction

The emphasis in this Chapter has been placed on the beams classification, failure modes of beams, and beams in flexure and shear. The approaches which have been used for the prevention of diagonal shear failures in reinforced concrete beams have been discussed. In addition, the flexural behaviour of beams in general is briefly examined in this Chapter. The conclusions relating to the impact of previous work are also outlined.

### 2.2 Beam Classification

The results of experimental investigations of diagonal failures for tested rectangular beams have indicated that both the ultimate flexural capacity ( $M_u$ ) and the mode of failure depend on the shear-span to effective-depth ratio ( $a/d$ ). The results from such investigations are shown in Figure 2.1. The relationship is commonly referred to as Kani's Valley (Kani, 1964; Kani, 1966). It can be noted from Figure 2.1 that the longitudinal reinforcement ratio ( $\rho$ ) only affects the transition point from one type of behaviour to another. A reduction in the value of  $\rho$  tends to increase the relative flexural capacity ( $M_u/M_f$ ) and to either decrease or increase the  $a/d$  ratio which marks the transition points for the different types of beams.

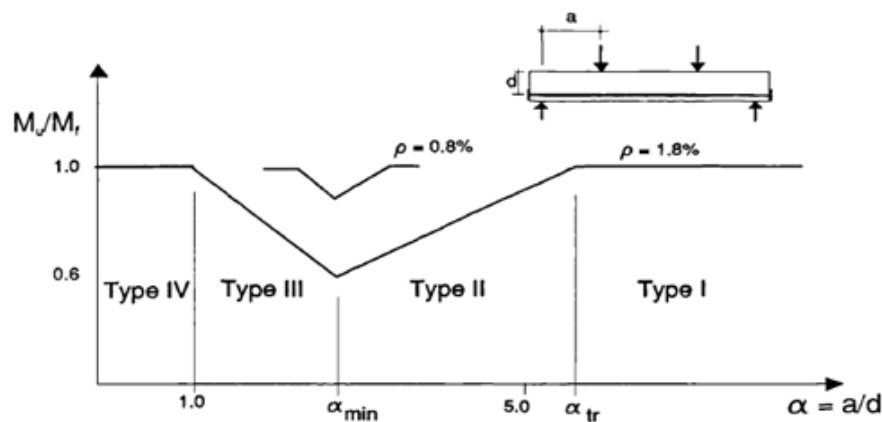


**Figure 2.1:** Classification of Beams Based on Kani's Valley (Kani, 1964; Kani, 1966).

The beams are divided into four groups (Kotsovos, 1988; Kani, 1964; Wange and Salmon, 1979) depending on their failure mode (Figure 2.1), as discussed below:

### **2.2.1 Type I Beams (Long Beams)**

Type I beams achieve their full flexural capacity ( $M_f$ ) where  $M_u = M_f$ , and fail in flexure. Long beams, in which  $a/d > 6.0$  and the value of  $\rho \approx 1.8\%$ , have a shear strength higher than their full flexural capacity.

### **2.2.2 Type II Beams (Normal Beams of Intermediate Length)**

Type II beams do not reach their full flexural capacity ( $M_f$ ). Their ultimate flexural capacity ( $M_u$ ) is equal to the diagonal cracking capacity. In normal beams when  $2.5 < a/d \leq 6.0$  and  $\rho \approx 1.8\%$ , the  $M_u/M_f$  ratio decreases as the  $a/d$  ratio decreases to a minimum value which is dependent on the value of  $\rho$ . This value is the lowest point in Kani's Valley.

Type II Beams are used in this study for all investigated wide RC beams (Alluqmani, 2013a).

### **2.2.3 Type III Beams (Short Beams)**

Type III beams do not reach their full flexural capacity ( $M_f$ ). Short beams, in which  $1.0 < a/d \leq 2.5$  and the value of  $\rho \approx 1.8\%$ , have an ultimate shear capacity higher than the inclined cracking capacity. The  $M_u/M_f$  ratio increases as the  $a/d$  ratio decreases until it reaches unity (i.e.  $M_u=M_f$ ).

Beams of types II & III are commonly provided with shear reinforcement in order to ensure that they achieve their full flexural capacity.

### **2.2.4 Type IV Beams (Deep Beams)**

Deep beams, in which  $a/d \leq 1.0$  and the value of  $\rho \approx 1.8\%$ , have an ultimate shear capacity higher than their full flexural capacity.

## **2.3 Beams Classification Based on the Geometry**

Traditionally, reinforced concrete (RC) beams are classified, in general, by the shape and geometry of their cross-sections (width ( $b_w$ ), height ( $h$ ), and length ( $L$ )), as shown in Figure 2.2



[Al.Dywany, 2010]. The structural designers may classify the beams as follows (Alluqmani, 2014, Alluqmani and Haldane, 2011a, 2011b):

1. When  $b_w \neq h$ , the beam is a rectangular beam, and it is divided as following:
  - a) When  $b_w < h$ , the beam is a drop beam in the vertical position, and it is:
    - I) When  $h \leq 5b_w$ , the beam is a shallow, slender, or narrow beam,
    - II) When  $h > 5b_w$ , the beam is a deep beam.
  - b) When  $b_w > h$ , the beam is a wide beam in the horizontal position (usually when,  $b_w \geq 2h$ ), where this beam is the scope of this programme of research.
2. When  $b_w = h$ , the beam is a square beam.
3. When  $b_w = h = D$ , the beam is a circular beam where  $D$  is the diameter of the beam.

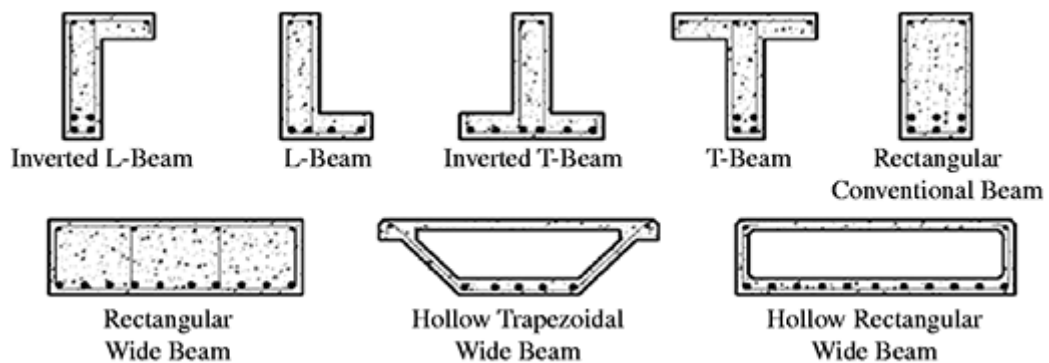


**Figure 2.2:** Types and Classification of Beams Based on Their Shapes and Geometries.

The main purpose of the beams is to transfer the load from the floor to the vertical elements which are below them, e.g. columns and walls. The selections of their geometries (cross sections) are constrained by both structural and architectural requirements. In these RC members, the concrete resists the shear stresses and its failure is sudden with diagonal cracks; while the steel (flexural reinforcement) resists the bending moments and its failure happens with a deflection. The load caused by concrete or shear failure should be higher than that load caused by steel or flexural failure; otherwise, the design of the structural member should be altered (Alluqmani, 2010; Alluqmani and Haldane, 2011c).

The shallow and the conventional RC beams are widely used in all types of concrete structures. They are normally carried by either solid slabs or wide beams, or both. The length to the overall depth ( $L/h$ ) ratio of these members usually exceeds 5.0. Therefore, they are designed as slender beams, where the section is first designed to resist the flexural stresses by providing adequate reinforcement, then, the section is checked for shear and deflection.

In addition, the design procedures are the same for both the shallow and the conventional beams, and they are provided in all the practical design Codes in a simple manner, based on experimental and theoretical investigations. When the conventional beam has obvious width comparing with its depth, shallow beam section forms as a result, and since the shallow term usually refers to the slab, a wide reinforced concrete beam term is given to such geometry change. These wide beams are frequently used as primary structural members in buildings, especially in the Middle East countries which are used in the ribbed slab systems, supporting the slab and transferring the load from the slab to the columns or walls.

The flanged concrete beams, such as T-beam and L-beam, are wide beams in their flange and are narrow beams in their web. These flanged concrete beams have economical advantages by reducing the required concrete quantity, based on the design assumption, the tensile resistance of concrete at the tension face assumed negligible, in addition, the top sides of these beams are enlarged, additional flexural resistance is provided by the top flange in continuous beams situation at the support. The requirements in design of such beams according to ACI318 (2008) are taking place by limiting the flange width, where for T-beam, the effective flange width which use in design should not exceeds the (span length/4), (web thickness + 16 times flange thickness) or (centre to centre of the next beam); while for inverted L-beam, the effective flange width should not exceeds the (span length/12), (6 times the flange thickness) or (half the clear distance to the next beam). In addition, since the web thickness of these beams is quite small comparing with the conventional beam width, hence, the concrete shear strength is always less than conventional beams if the depth is fixed among them (Al.Dywany, 2010).

The other beams geometries such the L-beams and inverted T-beams are commonly used in pre-cast concrete structures, where the enlargement in the bottom flange is mainly to provide support bearing to the pre-cast slab. Moreover, the box shape or trapezoidal beams are rarely used in structural buildings, and its application is limited in pre-stress highway or pedestrian bridges.

## **2.4 Failure Modes of Beams**

In wide beams, there are two types of failure, which can occur, called flexural failure (longitudinal-flexural cracks) and shear failure (diagonal-shear cracks). Wide beams are designed to resist shear failure resulting from various combinations of ultimate loads. The shear reinforcement is provided to resist diagonal shear failure. While the flexural reinforcements are designed to resist flexural failure or longitudinal cracks which may occur parallel to the member

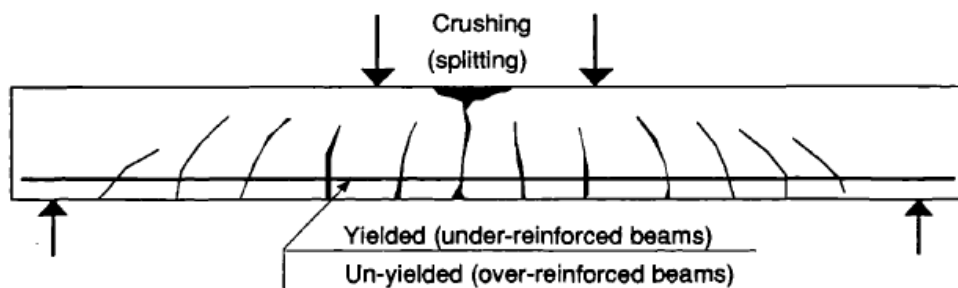
span due to transverse tensile stresses. Transverse tensile stresses occur on the top of wide beam in transverse direction. The failure happens, by the longitudinal splitting of concrete, parallel to the span on top of wide beam. Thus, the arrangement of shear reinforcements (either along the member length or across the member width) affects the resistance to transverse tensile stresses (Engineering Investigation, 2005; Teck FU, 2009). The different types of beam failure are described as follows:

### 2.4.1 Flexural Failure

In long beams (type I), almost vertical cracks develop in the region of the maximum bending moments. Eventually, these cracks cause failure of the beams as shown in Figure 2.3. The failure is due to either of the following:

- a) Excessive yielding of the longitudinal reinforcement, followed by crushing (splitting) of the compression concrete resulting in a ductile failure (under-reinforced beams);
- b) Crushing (splitting) of the compression concrete above the flexural crack before yielding of the longitudinal reinforcement which is termed a brittle failure (over-reinforced beams).

These modes of failure are collectively referred to as a "Flexural Failure".



In under-reinforced beams, the steel will yield

Figure 2.3: Flexural Failure Mode.

### 2.4.2 Diagonal Shear Failure

Shear distress and diagonal failure have been reported in almost all types of structural concrete members. These include beams, corbels, shear walls, slabs, columns, beam-column junctions, construction and expansion joints, foundations, etc. It is recognised that the cracking pattern and the failure mode may be different for each type of member, but, it is believed that the actual mechanisms by which shear is transferred within members are similar regardless of their

structural use. Unlike flexural failures, shear failures in reinforced concrete structures are brittle and sudden. When shear failures occur, they typically do so with little or no warning.

In general, a diagonal failure occurs under a combination of shearing force and bending moment. Axial load, torsion, or a combination of both may also be present and contribute to failure. Diagonal cracks in webs of either non-pestressed (reinforced) or prestressed concrete beams may develop regardless of the existence of flexural cracks in their vicinity. Diagonal cracks which occur in beam webs and were previously un-cracked due to flexural stresses are referred to as "Web-Shear Cracks" (Figure 2.4a). An inclined crack originating from the tip of a flexural crack and effectively becoming an extension of this crack is referred to as a "Flexural-Shear Crack" and the flexural crack is as an "Initiating Crack" (Figure 2.4a). In addition to the two primary inclined cracks (the web-shear and the flexural-shear cracks), other cracks caused by either splitting stresses between the longitudinal reinforcement and the concrete, or by dowel action forces in the longitudinal bars, are referred to as "Secondary Cracks" (Wange and Salmon, 1979; Sozen and Hawkins, 1962). The different types of inclined (diagonal) cracks and modes of shear (diagonal) failures are shown in Figure 2.4.

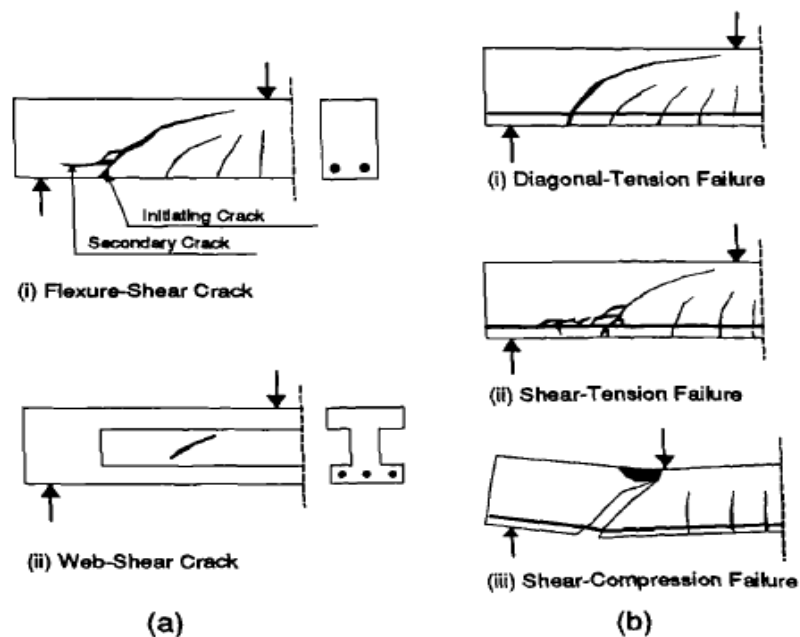


**Figure 2.4:** a) Types of Inclined (Diagonal) Cracking, and b) Modes of Shear (Diagonal) Failures.

Depending on the beam configurations, support condition and load distribution, the inclined crack (shear crack or diagonal crack) is classified into two categories, namely; web-shear and flexural-shear cracks, as shown in Figure 2.5 (Al.Dywany, 2010).

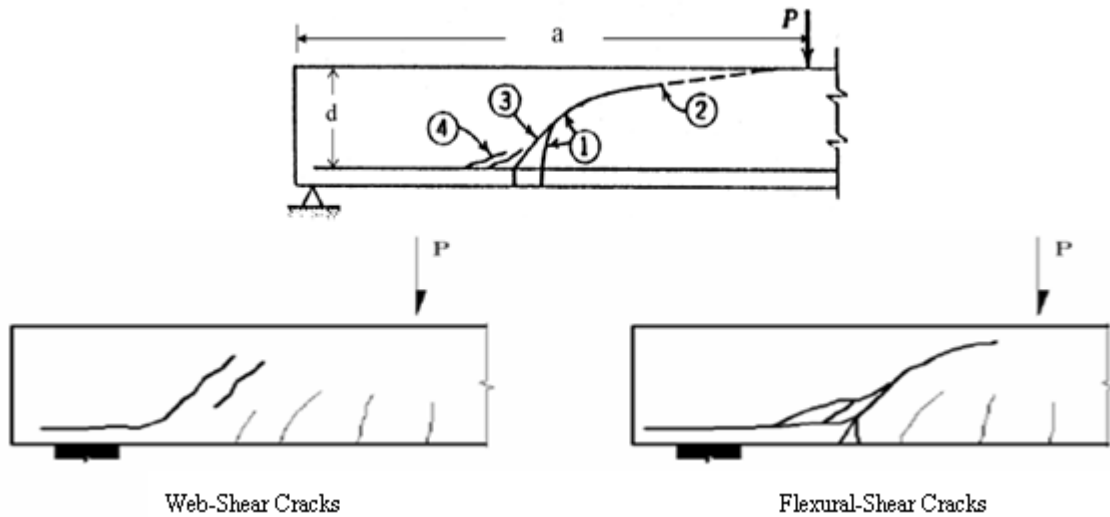


**Figure 2.5:** Types of Diagonal Failure and Crack.

The shear failure always occurs in the shear span ( $a$ ) when the  $a/d$  ratio is above 2.0. Diagonal cracking begins from the last flexural crack and turns gradually into a crack which becomes further inclined under the shear loading as noted in Figure 2.5. When such a crack appears it may not result in immediate failure, although in some longer shear spans this can be the case or an entirely new and flatter diagonal crack suddenly causes failure. More typically, the diagonal crack encounters resistance as it moves up into the zone of compression becomes flatter and stops at some point such as that marked 1 in Figure 2.5. With further load, the tension crack extends and widens gradually at a very flat slope until finally sudden (abrupt) failure occurs, possibly from point 2 shown in Figure 2.5. Shortly before reaching the critical failure point at 2 the more inclined lower crack 3 will open back at least to the steel level and usually cracks marked 4 will develop.

Web-shear cracks are only common in thin-web I-shaped prestressed beams with relatively large flanges (Wange and Salmon, 1979), Figure 2.4a. Web-Shear cracks may also be found near a point of inflection and at bar cut-off points in reinforced concrete continuous beams subjected to axial tension.

Flexural-shear cracks are common in both non-prestressed (reinforced) and prestressed concrete beams (Campbell et al., 1979). In reinforced concrete beams, almost vertical flexural cracks are expected to develop under service loads. These cracks cause no distress to the beams until a critical combination of flexural and shear stresses develop near the internal extremity of one of the cracks. At this point the inclined crack forms. The rate of transformation of the initiating crack into a flexural-shear crack depends on the growth and height of the flexural cracks as well

as on the magnitude of the shear stresses near the tips of the flexural cracks. The resulting failure modes are described below.

The shear failure (Figure 2.4b) in reinforced concrete beam depends mainly on the member geometry and load location. It is classified into four categories, namely; diagonal-tension, shear-tension, shear-compression, and splitting or true shear failures, which describe the manner in which the compression-zone concrete fails, as described below (Stratford and Burgoyne, 2003; Al.Dywany, 2010):

- Diagonal-tension failure (type II beams),
- Shear-tension failure (type III beams),
- Shear-compression failure (type III beams), and
- Splitting or true shear failure (type IV beams).

#### **a) Diagonal-Tension Failure**

Following the formation of flexural cracks in the normal beams (type II beams), one of the diagonal cracks which developed in the shear span continues to propagate through the beam until it becomes unstable. Eventually, the beam collapses as a result of splitting of the compression concrete at the tip of the crack as shown in Figure 2.4b. This mode of failure is referred to as a "Diagonal-Tension Failure" (ASCE-ACI Committee 426, 1973; Bresler and MacGregor, 1967).

The diagonal-tension failure mode usually occurs in slender beams, where the combination of shear stresses and the bending stresses effect the formation of the diagonal crack, such beams widely used in structures; thereby, investigation the wide reinforced concrete beams in such failure mode will provide practical and safe guide.

#### **b) Shear-Tension Failure**

In short beams (type III beams), a curved diagonal crack forms in regions subjected to combined shear and bending moment actions which may also lead to the initiation of additional secondary cracks. The secondary cracks may propagate backwards along the longitudinal reinforcement resulting in a loss of bond and anchorage failure as shown in Figure 2.4b. Eventually, the beam collapses as a result of splitting of the compression concrete. This mode of failure is referred to as a "Shear-Tension Failure" (Laupa et al., 1955), [from reference (ASCE-ACI Committee 426, 1973)].

### c) Shear-Compression Failure

Alternatively, a short beam (type III beams) may collapse as a result of splitting of the compression concrete above the tip of the diagonal crack but there is no accompanying anchorage failure as shown in Figure 2.4b. This mode of failure is referred to as a "Shear-Compression Failure".

The integrity of the compression-zone concrete relies upon triaxial confinement. If this confinement is lost, the concrete can dilate, and micro cracks form and appear in the compression-zone concrete, parallel to the top-fibre of the beam (Kotsovos and Pavlovic', 1999). These micro cracks coalesce and result in shear-compression failure of the compression-zone concrete, which is often described as "crushing".

In the case when the concrete immediately in front of a crack, the concrete is subjected to a tension field that causes the crack to propagate diagonally into the beam. If shear-compression failure is avoided, the crack propagates along the shear-span of the beam towards the point at which load is applied. Load cannot be transferred between flexural reinforcement across the crack and the compression zone concrete, so that beam action is not possible. An unstable diagonal-tension failure follows, which in turn splits the beam into two pieces (Kotsovos and Pavlovic', 1999).

The degree of confinement, and hence the strain-capacity of the compression-zone, depends upon the triaxial stress-state within the compression-zone. However, the triaxial stress-state is difficult to model as found (Stratford and Burgoyne, 2002; Kotsovos and Pavlovic', 1999). Confinement in the compression-zone is increased by the presence of shear reinforcement and under a point of load application, where it is reduced by shear action.

In short shear spans, a large shear may initiate approximately a 45 degree crack, called a web-shear crack, across the neutral axis before a flexural crack appears. Such a crack crowds the shear resistance into a smaller depth and thereby increasing the stresses, tends to be self-propagating until stopped by the load or reaction. A compression failure finally occurs and appears adjacent to the load. This type of failure is designated as a shear-compression failure. This is because the shaded area in Figure 2.6 carries most of the shear and the failure is caused by the combination. This failure occurs at a range of  $a/d$  ratio between 1.0 and 2.5 (type III beams). The ultimate load is sometimes more than twice at diagonal cracking (Kumar and Tech, N.D.).

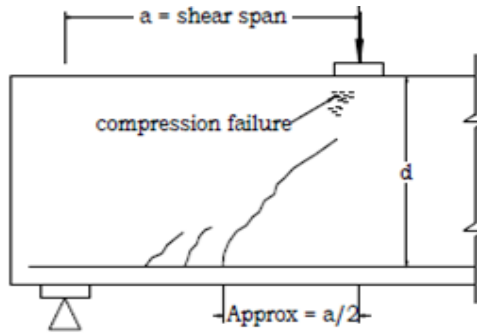


**Figure 2.6:** Shear Compression Failure.

#### d) Splitting or True Shear Failure:

When the shear-span ( $a$ ) is less than the effective-depth ( $d$ ), such type IV beams, the shear crack is carried as an inclined between load and reaction that almost eliminates ordinary diagonal tension concepts. In such cases, shear strength is much higher. As shown in Figure 2.7, the final failure becomes a splitting failure or it may fail in compression at the reaction. The study of such an end section closely relates to the analysis of a deep beam (type IV beams), where this failure occurs when  $a/d$  is less than unity ( $a/d < 1.0$ ) (Kumar and Tech, N.D.).

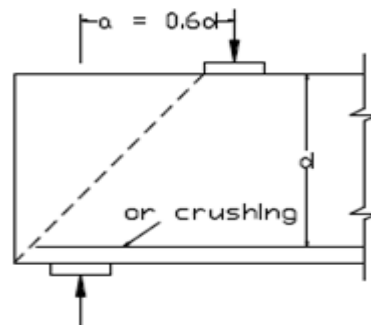


**Figure 2.7:** Splitting Shear Failure.

### 2.4.3 Deep-Beam Failure

In deep beams (type IV beams), after the occurrence of inclined cracking, it has been suggested that these beams behave as a tied-arch as shown in Figure 2.8a. Five possible modes of failure have been suggested (Crist, 1975; Manual, 1974; Taylor, 1972) as shown in Figure 2.8b and described below (Ziara, 1993):



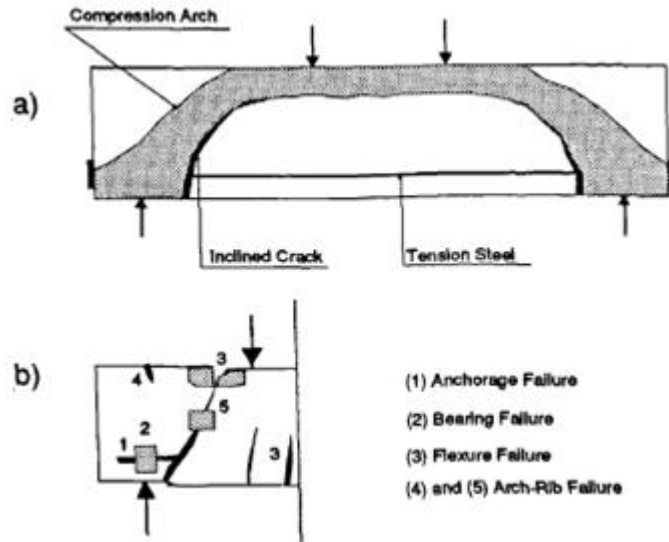


Figure 2.8: Deep-Beam Failures: a) Arch Action, and b) Types of Failures.

### 1) Anchorage Failure

Anchorage failure occurs near the support, and may be linked to splitting of the concrete due to dowel action.

### 2) Bearing Failure

Bearing failure occurs at the supports, when the bearing stresses exceed the bearing capacity of the concrete.

### 3) Flexural Failure

Flexural failure occurs due to either yielding of the steel reinforcement or fracture of the concrete near the top of the arch.

### 4) Arch-Rib Failure Over the Support

Arch-rib failure occurs due to the presence of tension cracks over the support.

### 5) Arch-Rib Failure Along the Diagonal Crack

Arch-rib failure may also occur due to cracking of the concrete along the diagonal cracks bordering the underside of the rib of the arch.

The structural behaviour of deep beams can be studied in isolation (Kotsovos, 1988; Mau and Hsu, 1987; Mau and Hsu, 1989) as a special case.

## 2.4.4 Conclusion

The final collapse of beams occurs as a result of splitting of the compression concrete in spite of all the attempts to identify individual modes of failure many of which centre on the development of either diagonal cracks or bond failure.

## 2.5 Structural Concrete Beams in Flexure

### 2.5.1 General

The currently accepted theory for evaluating the flexural capacity, equilibrium, and compatibility requirements of beams is based on the assumption that plane sections remain plane after bending. Concrete compressive and longitudinal-reinforcement tensile stresses are found by considering the uniaxial stress-strain relationships for the two materials. Transverse stresses in the concrete are assumed not to influence the behaviour of the beams and are therefore ignored, where they play a role in the compression-zone and transverse-direction of wide RC beams. Figure 2.9 shows the strain profiles used to determine the flexural strength at a section in a beam. The longitudinal reinforcement ratio ( $\rho$ ) is used to determine the type of failure. When  $\rho < \rho_b$  (at the balanced-failure condition),  $\varepsilon_s > \varepsilon_y$  and hence the longitudinal steel yields and a Tension-Failure occurs. When  $\rho > \rho_b$ ,  $\varepsilon_s < \varepsilon_y$  and a Compression-Failure (brittle failure) occurs in the concrete compression region without yielding of the longitudinal reinforcement.

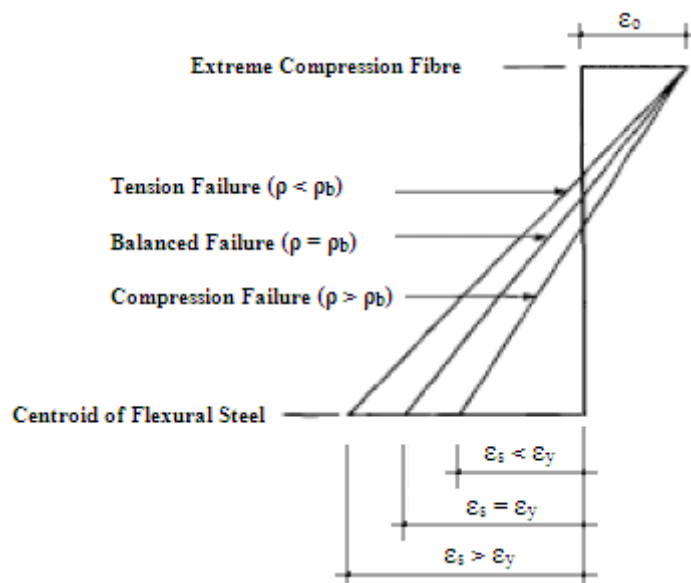


**Figure 2.9:** Strain Profiles at the Flexural Strength of a Section.

## 2.5.2 Multiaxial Stress Behaviour

The stress-strain relationships for concrete under uniaxial loading are shown in Figure 2.10a (Kotsovos, 1987). Figure 2.10a shows the ascending and descending parts of the curves for the longitudinal strains developed. The transverse strains show an abrupt increase in value just before the load reaches its peak level. The volumetric strain ( $\varepsilon_v = \Delta V/V$ ) relationship indicates that the peak load is reached when the volume reaches its minimum level at which point an abrupt increase in transverse strain is initiated.

To investigate the validity of using the uniaxial stress-strain relationship to describe the actual behaviour of concrete in the design of beams, the longitudinal and the transverse strains were measured in the region of the beams subjected to maximum bending (Kotsovos, 1982). The results from these measurements are shown in Figure 2.11. Figure 2.11 indicates that while the first part corresponding to the ascending portion of the curve is correct, the other part corresponding to the descending portion is totally different.

It was concluded, from the above test results, that in the case of the uniaxial concrete compression tests, the descending portion of the longitudinal strain relationship does not exist. The appearance of this part was attributed to secondary effects resulting from the test machine i.e. due to the restraint between the specimen and the loading platens of the test machine. Kotsovos and Cheong (1984) tested prisms under different boundary conditions. In order to minimise the friction between the specimens and the loading platens of the test machine, the axial load was applied through loading plates smaller than the cross section of the specimen. The results from the tests confirmed that the true stress-strain relationship consists of only the ascending portion of the curve as shown in Figure 2.10b.

It can be concluded from the above discussion that the uniaxial stress-strain characteristics cannot describe the post ultimate behaviour of the compression concrete in beams under bending action i.e. the descending portion does not exist. The ascending portion of the curve only partially describes the response of the specimens because it ignores the multiaxial state of stress which develops during the later stages of loading at about 90% of the failure load. Test results have indicated increases of up to 75% in the uniaxial concrete compressive strength in the compressive stresses in beams (Kotsovos, 1982).

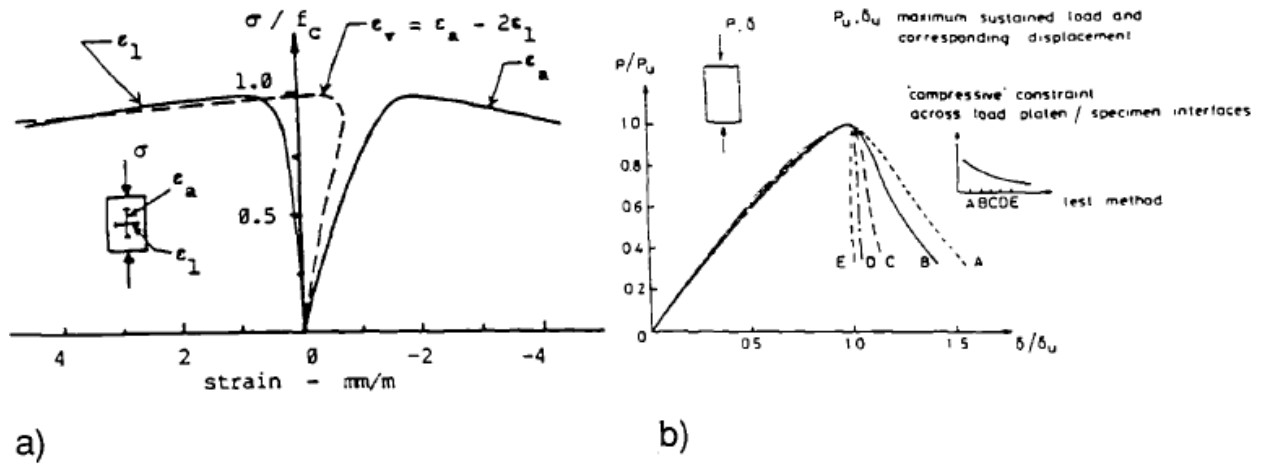


**Figure 2.10:** Uniaxial Stress-Strain Relationship. A) Typical Curves, b) Effects of Boundary Restraints. (after Kotsovos, 1987).

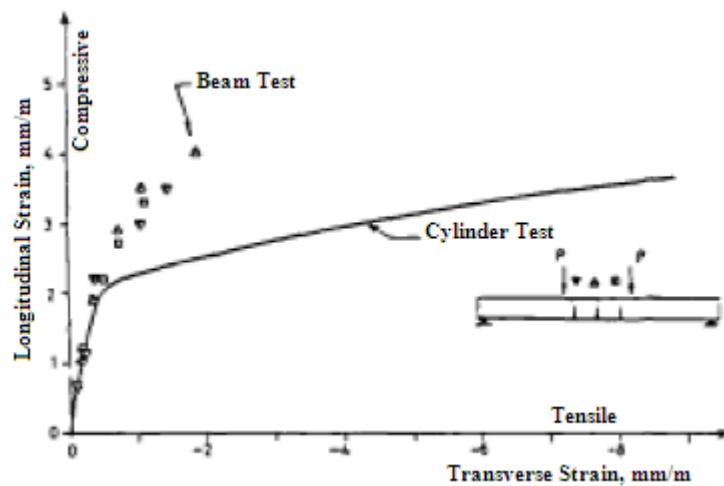


**Figure 2.11:** Longitudinal-Strain and Transverse-Strain Relationships for a Uniaxial Compression Test for Flexure. (after Kotsovos, 1982).

In cases where there are no stirrups, a flexural failure may be related to the development of a multiaxial state of stress resulting from dilation of the concrete in a localised region within the compression zone. This region coincides with the position of a deep flexural crack. The localised transverse expansion of the concrete is restrained by the concrete in the adjoining regions. This may be considered to have the same effect as confinement. At the same time, this restraint induces tensile stresses in the adjacent areas of concrete. These tensile stresses reduce significantly the compressive strength of the concrete and eventually initiate failure by splitting of the compression zone in the region between two flexural cracks. The crushing of the compression concrete appears to be a post-failure phenomenon which occurs as a result of the loss of the restraint in the adjacent concrete regions.

### **2.5.3 Conclusion**

The evaluation of the multiaxial stress conditions, which develop within the compression zone or within the transverse direction along the member width as the ultimate load is approached, is difficult. In accordance with the approach to structural concrete, which is based on simplicity rather than misleading precision, it is considered sufficient for practical purposes to assess the flexural capacity on the basis of the rectangular stress block as specified by current Codes of Practice.

It should be noted, however, that despite the presence of a multiaxial state of stress in concrete compression regions, Codes of Practice do not always insist on providing these regions with transverse reinforcement (e.g. stirrups) in order to restrain the development of the tensile stresses which significantly reduces the concrete compressive strength. The provision of transverse reinforcement in columns implies that compression concrete requires such reinforcement. In the case of a beam, this requirement depends mainly on whether or not shear stresses are present. This inconsistency in Codes of Practice appears to have originated from the adoption of design principles based on a uniaxial state of stress. The introduction of confining stirrups in the compression zone and in the transverse direction along the width in the beam structure will enhance the strength and ductility of the concrete which in turn prevents brittle failures which are characteristic of the behaviour of over-reinforced beams.

## **2.6 Structural Concrete Beams in Shear**

### **2.6.1 Shear Strength of Beams without Shear Reinforcement**

The shear failure of structural RC beams without shear-reinforcement (stirrups) is a distinctive case of failure which depends on various parameters such as shear-span to effective-depth ratio ( $a/d$ ), longitudinal tensile reinforcement ratio ( $\rho_s$ ), aggregate type, strength of concrete ( $f_c$ ), type of loading, support and load conditions ( $k_s$  and  $k_p$ ), and etc.

It is believed that the shear failure of reinforced concrete members without stirrups initiates when the principal tensile stress within the shear span exceeds the tensile strength of concrete. This results in initiation of diagonal crack which later propagates through the beam web. In other words, the diagonal cracking strength of reinforced concrete members depends on the tensile strength of concrete, which in turn is related to its compressive strength.

There is a considerable difference of opinions among researchers regarding the diagonal failure mechanism of beams without shear (web) reinforcement as described below;

- In the models which were based on the concrete-tooth action, the failure was assumed to be associated with the stress condition below the neutral axis. In the original model (Kani, 1964), the failure was assumed to occur when the tensile strength at the root of the concrete cantilever was reached (Kani's hypothesis). In the modified models (Hamadi and Regan, 1980; Reineck, 1991a; Reineck, 1991b), failure was assumed to be governed by aggregate interlock, dowel action, and concrete tensile strength. Krefeld and Thurston (1966) and Chana (1987), however, have suggested that dowel action at the level of the longitudinal reinforcement initiates the failure of the beams.
- In the strut and tie models, failure was assumed to occur when the concrete compressive strength was reached (Regan and Placas, 1970; Nielsen and Braestrup, 1976; Marti, 1991).
- Theorems based on fracture mechanics (Bazant and Oh, 1983; Hillerborg, 1981) are solely concerned with the instability of the diagonal crack and do not consider a crushing failure or splitting due to dowel action.
- Bobrowski (1982) and Kotsovos (1983) have deduced that failure takes place in the compression zone as a result of the development of a state of stress in which tensile stresses initiate failure of the beams.

It is believed that the nominal shear strength of beams is not a good indicator of the load carrying capacity of beams at diagonal failure since it is not an indicator of the actual state of stress which exists and results in the failure of beams. However, in order to develop the required analytical model to evaluate the requirements of beam strengths, it was necessary to review all the principal published models.

## **2.6.2 Shear Strength of Beams with Shear Reinforcement**

### **2.6.2.1 Introduction**

Traditionally, in order to minimise the risk of having undesirable brittle diagonal failures, shear reinforcement (stirrups) is introduced into regions subjected to high shearing stresses, e.g. the region of the effective support width in wide RC beams. The basic philosophy of the current

Codes of Practice is to ensure that stirrups restrain the growth of inclined cracking, increase ductility, and give adequate warning in situations in which diagonal cracking may result in a failure.

In the last 30 years, extensive research has been conducted on the analytical shear models and progress has been made. A number of numerical analyses based on truss analogy, strut-and-tie models, plasticity theory model, equilibrium analysis, arch action theory, compatibility-aided truss models (such as the compression field theory (CFT), modified compression field theory (MCFT), and the fixed-angle softened truss model (FA-STM)), and compressive force path (CFP) concept, were developed to predict the shear strength of reinforced concrete membrane elements subjected to shear and normal stresses. The current approaches and models do not have a well prediction of the shear strength of wide concrete beams; where there are other factors affect the wide RC beam strengths which are unconsidered in the current Codes and models. These factors are discussed in detail in the next Chapter.

Therefore, it was necessary to develop a theoretical prediction model to evaluate the shear strength of wide beams without and with shear-reinforcement which is one of the main objectives of this programme of research. Thus, in order to develop the required analytical model to evaluate the shear strength of wide RC beams, it was necessary to review all the principal published models and researches. Where the shear strength of the beam without shear-reinforcement is the concrete contribution ( $V_c$ ) of the beam with shear-reinforcement for the same characteristics.

This section critically reviews some of the assumed shear mechanisms and the solution techniques for beams with web shear reinforcement which have been put forward in an attempt to clarify the shear problem.

### **2.6.2.2 Truss Analogy**

The truss analogy provides a rational tool for the design of reinforced concrete beams in flexure, shear and torsion.

The 45° truss model allows designers to calculate tensile stresses in longitudinal steel and stirrups and to calculate compressive stresses in the un-cracked compression zone and inclined struts. To produce the expression shown in Equation (2.1) for the shear strength of a concrete section ( $v$ ), it was assumed in the model that shear cracks form at a strut angle ( $\theta$ ) of 45°:

$$v = \frac{V}{b_w \cdot jd} = \frac{A_v \cdot f_{yv}}{b_w \cdot S_L} \quad (2.1)$$

Where:

V = shear force at a section,

A<sub>v</sub> = area of shear reinforcement (stirrups),

b<sub>w</sub> = web width of beam,

f<sub>yv</sub> = yield tensile stress of stirrups,

jd = flexural lever arm, and

S<sub>L</sub> = stirrups spacing along the beam length (so called longitudinal stirrup-legs spacing).

The 45° truss model enters in various design methods and still forms the basis for the ACI expression for the shear resistance provided by stirrups (The current ACI and SBC expressions have simplified the Equation by replacing the term jd with d, where d is the member effective-depth). As its use became more widespread, however, it was criticized for being overly conservative. In particular, the model assumes that only transverse reinforcement is effective at carrying shear, thereby predicting that a section without bent-up bars or stirrups will have no shear strength whatever. Clearly, this is not the case. Extensive research efforts were undertaken in order to ascertain the so-called “concrete contribution” to shear resistance, which was eventually set at an empirically derived safe working shear stress (*v<sub>c</sub>*) as illustrated in Equation (2.2).

$$v_c = \frac{V_c}{b_w \cdot d} = 0.03f'_c \quad (2.2)$$

For the first time, the shear resistance of a reinforced concrete section (V) was (is) divided up into two components: a concrete contribution (V<sub>c</sub>) and a web (shear) reinforcement contribution (V<sub>s</sub>) predicted by the 45° truss model, as illustrated in Equation (2.3) and Figure 2.12:

$$V = V_c + V_s \quad (2.3)$$

MacGregor (1967) agreed with Kani’s basic finding that the shear strength decreases as the depth increases. While in the use of wide beam, the depth should be minimized, therefore, there is a benefit to use the wide RC beams to ensure that the shear strength will increase and the beam can behave in a ductile flexural-manner. However, despite the shortcomings and limitations in the



current design provisions, the truss analogy is still to date the only basis for designing reinforced concrete structures in many Codes of Practice.

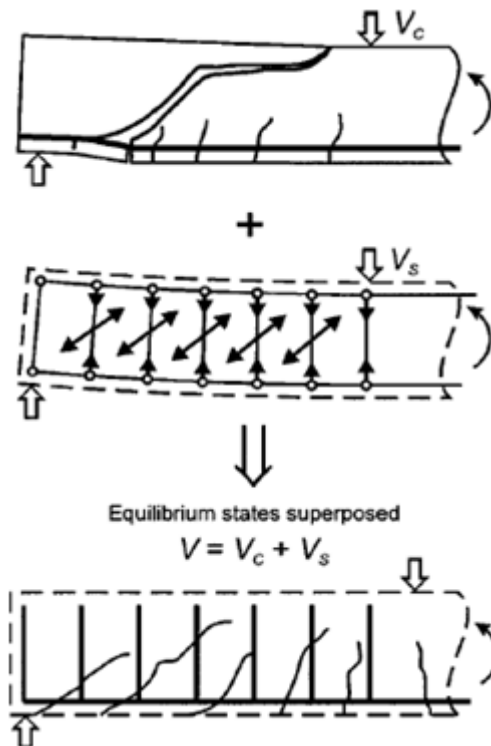


**Figure 2.12:** Superposition of Concrete and Stirrup Contributions Using 45 degree Truss Analogy.

### 2.6.2.3 Strut-and-Tie Models

The standard truss model was found not to be applicable to all types of members, particularly at static and geometric discontinuities. In these cases, approaches based on available test results, rules of thumb, and past experience were usually applied.

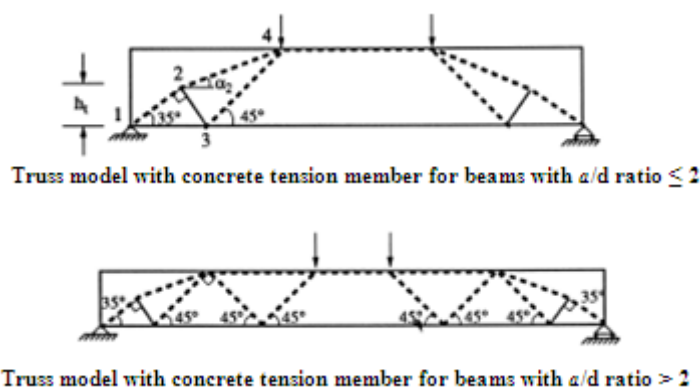


**Figure 2.13:** Refined Strut-and-Tie Models Proposed by Al-Nahlawi and Wight, 1992.

In order to apply a design concept to all parts of any structure a generalised form of the truss analogy was proposed in form of strut-and-tie-models (Schlaich et al., 1987; Schlaich and Schafer, 1991), as shown in Figure 2.13.

At the turn of the century, Ritter (1899) and Mörsh (1909) pioneered the use of a truss concept to simulate the action of a structural RC beam subjected to shear and bending. They viewed a structural RC member as an assembly of two types of linear elements: the tensile steel ties and the compressive concrete struts. Even though the ties and struts are idealized as lines without cross sectional dimensions, the forces in these linear elements are obliged to satisfy the equilibrium condition at the joints (points of intersection). This model with linear elements was frequently found to overestimate the shear and torsional strengths of structural RC members.

Considerably higher loads can be reached in members where secondary strut action can occur. This is generally observed in beams where the shear-span to effective-depth ratio,  $a/d$ , is less than about 2.5. In members with  $a/d < 2.5$ , strut-and-tie methods may be applied to determine the expected shear capacity, but this is beyond the scope of this thesis. Figure 2.14 is adapted from Collins et al. (2007), and it can be seen that taking the higher of the shear strengths predicted by 2004 CSA Code strut-and-tie provisions and sectional models accurately predicts the variation in  $V_c$  in beams with varying  $a/d$ .

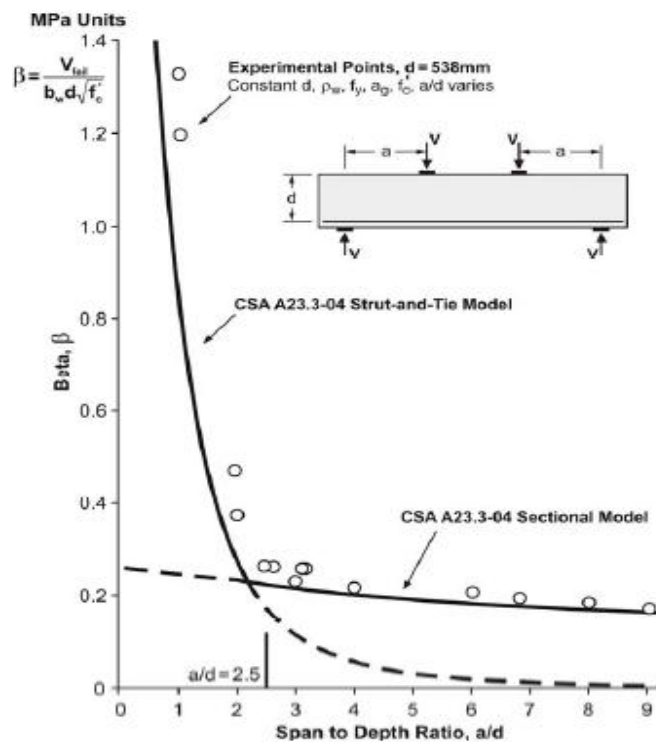


Figure 2.14: Effects of  $a/d$  on Shear Strength (Adapted from Collins et al., 2007).

### 2.6.2.4 Diagonal Compression Field Theory

A few numerical analyses based on compatibility-aided truss models, such as the fixed-angle softened truss model (FA-STM) (Pang, and Hsu, 1996), the compression field theory (CFT) (Collins, 1978), and the modified compression field theory (MCFT) (Vecchio and Collins, 1986), were developed to predict the deformation and shear strength of structural RC membrane elements subjected to shear and normal stresses.

In 1929, Wanger (Collins, 1978) proposed a theory to predict the post-buckling shear resistance of thin metal beams. He assumed that after buckling, metal would not resist compression and that shear would be carried by a diagonal tensile field. In 1978, Collins investigated the applicability of this theory to structural concrete. Collins assumed that after cracking, concrete cannot resist tension, and that shear would be carried by a diagonal compression field. The ultimate shear capacity of a member was assumed to be reached either when the longitudinal or the transverse steel reached yield, or when the average concrete compressive stress reached its limiting value.

The theory was first developed for rectangular sections with symmetrical arrangements of longitudinal reinforcement. The stirrups were assumed to be perpendicular to the beam longitudinal axis and it was also assumed that the crack widths would be controlled. The effect of bending moment, local disturbances and the presence of tensile stresses were neglected. The average stresses and strains were considered in the approach, Figure 2.15a.

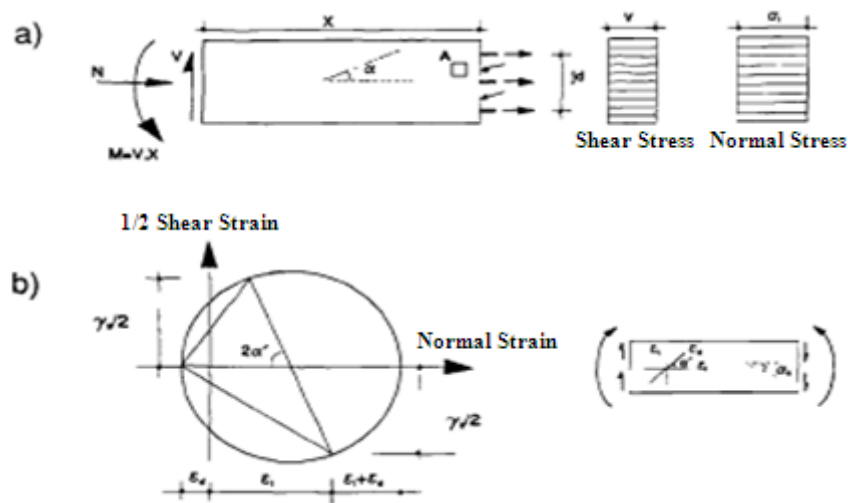


**Figure 2.15:** Compression Field Theory: a) Free-Body Diagram of a Beam Section, and b) Compatibility Condition for Average Strains in Concrete.

The compression field theory attempted to outline a framework for developing a rational theory for evaluating not only the shear strength of all types of structural concrete elements, but also their overall load-deformation response. However, because of the ideal conditions considered, which rarely exist in practice, and because of the large number of assumptions required to develop this theory, it was very difficult for it to be adopted as a rational approach for the solution of the shear problem.

#### **2.6.2.5 Modified Compression Field Theory**

Vecchio and Collins (1986; 1982) proposed the modified compression field theory (MCFT) because of the perceived limitations in the original compression field theory. The modified theory studied the plane state of stress which influences the concrete compressive strength as well as the presence of the tensile stresses between cracks which had been ignored in the original approach.

The concept of MCFT can be applied to the beam design (Collins et al., 1996) as well as the analysis of load-deformation response of structural RC beams subjected to shear, moment, and axial load (Vecchio and Collins, 1988; Bentz et al., 2006). Besides, in relation to the fixed-angle softened truss model (FA-STM), a new algorithm was proposed to be able to predict the shear response of structural RC beams (Lee and Mansour, 2006). The preceding methods (Lee and Mansour, 2006; Bentz et al., 2006; Vecchio and Collins, 1988) can predict the load-deformation response of structural RC beams very well; although, the calculation procedures are too complex (Vecchio and Collins, 1988) and the iteration for solution is inevitable (Lee and Mansour, 2006; Bentz et al., 2006; Vecchio and Collins, 1988). Nevertheless, these models have made great contributions to the other application on torsion and to the prediction of shear behaviour of structural RC beams (Jeng and Hsu, 2009). However, an analytical model with physical significance and simple calculations to predict the shear behaviour of wide RC beams in particular and structural RC beams in general is still needed.

In the MCFT, it was assumed that the strain in the concrete was equal to that in the steel. The principal stress axes were assumed to coincide with the principal strain axes in the concrete. The relationships between the principal stresses and principal strains were evaluated for both tension and compression stresses using Mohr's circle, Figure 2.15b. The principal compressive stress ( $f_{c2}$ ) was given as a function of the compressive strain ( $\epsilon_2$ ) and the corresponding tensile strain ( $\epsilon_1$ ).

In another attempt to simplify the design approach and to generalise the theoretical approach in order to make it applicable to any shape of cross section, Vecchio and Collins (1988) proposed dividing the cross section into layers and treating the concrete and steel layers separately. The principle of plane sections remaining plane after bending was assumed. The equilibrium conditions included:

1. Balancing of vertical shear, moment, and normal forces.
2. Balancing of the horizontal shear.

The compression field theory can be considered to be an attempt to promote a rational theory for solving the shear problem. It is based on equilibrium and compatibility considerations as well as material characteristics.

On the other hand, this theory is suited to conditions, where stress trajectories are parallel and the shear distribution is uniform. The traditional truss analogy, however, offers a simpler and an adequate solution to these conditions. The theory was not applied, to static and geometric discontinuities (D-regions). Instead the Canadian Code of Practice adopted strut-and-tie models. In addition, the design was based on the concept of critical sections for shear (sectional design) rather than considering the overall behaviour of the beam under load (member design).

The enhancing influence of stirrup confinement on the strength and the ductility of concrete was also not considered. The modified compression field theory cannot therefore be considered as a rigorous and straightforward approach which could be followed for the solution of different shear problems in a similar manner.

#### **2.6.2.6 Plasticity Theory Model**

The mathematical theory of plasticity (Nielsen and Braestrup, 1976; Thfilimann, 1979) was applied to beams with web reinforcement (Figure 2.16). In this approach, the shear resistance was obtained by equating the internal and the external work done in a beam under the assumed deformation pattern shown in Figure 2.16c.

The application of the theory of plasticity to members subjected to shear was initially investigated by Drucker (1961) who proposed several stress fields in which the load is carried directly by inclined struts or arches. According to this model, the strength of a beam is governed

by the yielding of the flexural reinforcement. The stress fields proposed by Drucker (1961) were not found suitable for reinforced concrete beams, however, leading to unsafe designs.

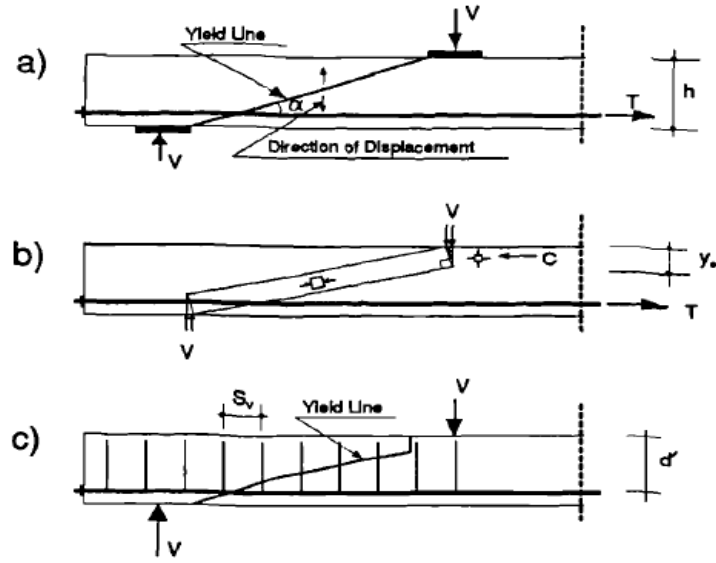


**Figure 2.16:** Mechanisms of Failure Based on the Theory of Plasticity: a) Upper-Bound Solution, b) Lower-Bound Solution, and c) Beam with Web Reinforcement.

The development of cracks through the inclined compression strut of a beam and its influence in the member's shear strength shows a strong dependency on the  $a/d$ , a phenomenon known as Kani's valley (Kani et al., 1979). Figure 2.17 presents several tests performed by Leonhardt and Walther (1962) where  $a/d$  was varied from 1.5 to 8.0. For small values of  $a/d$ , the cracks practically do not develop through the inclined strut and thus the flexural strength can be reached (Test B2). For larger values of  $a/d$ , cracks develop through the inclined struts, consequently decreasing the shear strength of the member (Tests B4 and B6). This phenomenon is less significant for very large values of  $a/d$  where the flexural strength is again reached before the critical crack can develop (Beam B10/1).

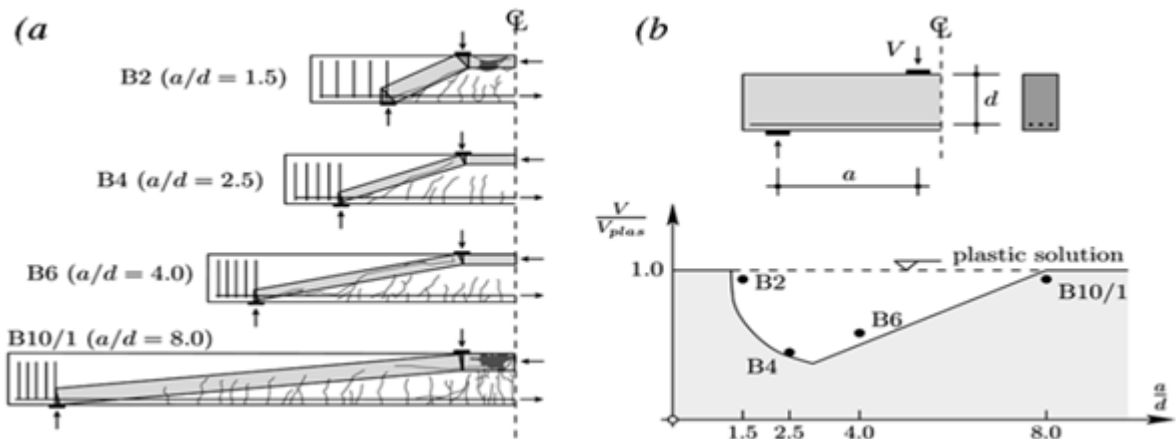


**Figure 2.17:** Influence of  $a/d$  on Shear Strength According to Theory of Plasticity: a) Tests B2, B4, B6, and BP10/1 by Leonhardt and Walther (1962), Cracking Pattern and Theoretical Strut Position; and b) Kani's Valley (Kani et al., 1979), Comparing Actual Strength with Failure Load.

Campbell et al. (1980) showed that the rigid plastic theory over-estimates the amount of reinforcement required for a balanced section when the elastic deformation was considered. It also over-estimates the shear capacity of a section which is over-reinforced in shear.

#### **2.6.2.7 Equilibrium Analysis**

It was suggested that the provision of shear reinforcement be based on the shear compression theory (ASCE-ACI Committee 426, 1973) for short beams (type III beams) failing in shear-compression. In the analogy, equilibrium was satisfied by summing moments about a point in the compression zone above the tip of the inclined crack.

Regan (1969) assumed that failure was caused by normal tensile stresses in the compression zone of the beam. These stresses were obtained using equilibrium and approximate compatibility Equations. Regan admitted that the resulting Equation for the ultimate shear strength was too complex, and recommended the use of graphical or other related types of solutions.

#### **2.6.2.8 Arch Action Theory**

The remaining tied arch theory which was developed by Kani (1964) for beams without web reinforcement was extended to beams with web reinforcement. The transverse loading was assumed to be carried by arch action. Kani (1969) postulated that after cracking a beam was transformed into a number of tied arches hanging into the compression zone by stirrups. Only the outer arch was supported directly at the supports. The purpose of stirrups, based on this theory, was to provide reactions for the internal concrete arches which support the compression zone, and not to carry the shear force as widely accepted and adopted in Codes of Practice. This theory was intended to be regarded as a rational approach; however, it is a qualitative and impractical theory (Bobrowski, 1982).

#### **2.6.2.9 Compressive Force Path (CFP) Concept**

##### **a) Introduction**

The aim of the Compressive Force Path (CFP) concept was to promote a better understanding of the behaviour of reinforced concrete beams under transverse loading and to produce a more

realistic explanation of the causes of diagonal failure. In this concept, the applied loads were assumed to be carried to the supports along a CFP.

Kotsovos (1988) developed a model for shear behaviour termed the Compressive Force Path (CFP) Concept (Figure 2.18). The model assumes shear failure occurs by excessive tensile stresses perpendicular to the compressive path. These can occur due to changes in the direction of the force path requiring a tensile resultant ( $T$  in Figure 2.18a), high tensile stresses at the tip of cracks ( $t_2$ ), and dilation in the vertical direction due to varying intensity of the compressive stress field ( $t_1$ ). It should be noted that  $T$  represents a tensile force that must be developed by unrealistically high tensile stresses in cracked concrete. Furthermore, the assumed stress conditions in the compression zone indicate that all of the shear is carried above the neutral axis.

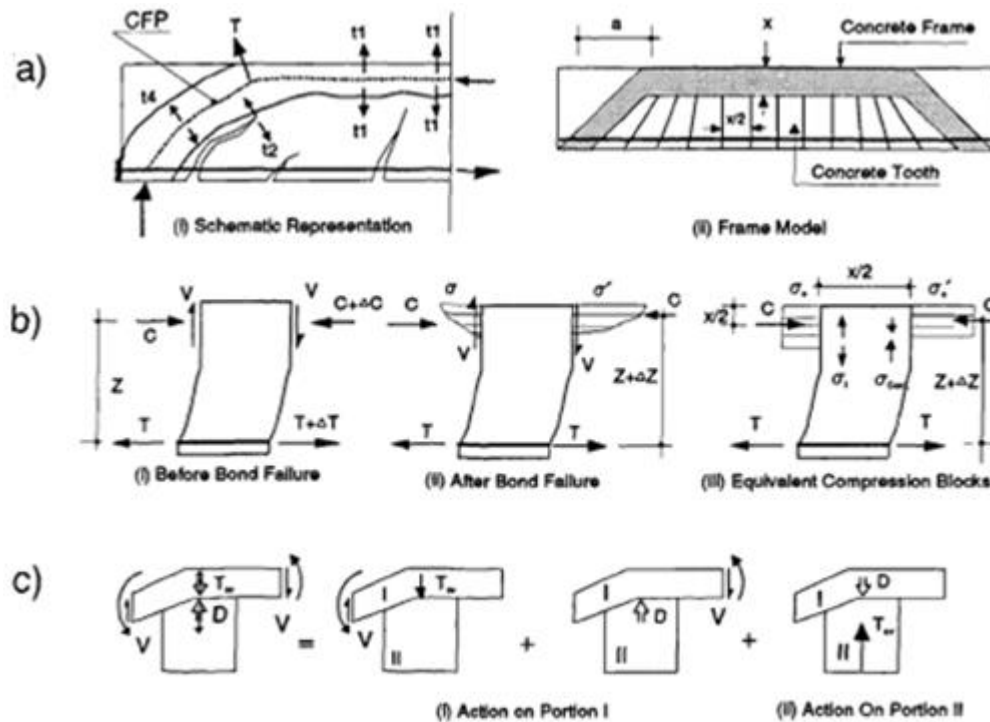


**Figure 2.18:** a) Compressive Force Path, b) Effect of Bond Failure, and c) Equilibrium Conditions at Force Changing Directions.

### b) Shape of the CFP

The shape of the CFP as shown in Figure 2.18a is based on the diagonal failure mode. The failure mode characterising type II (normal beams) behaviour, is represented by a curved path comprising two intersecting and almost linear portions connected by a smooth transitional curve. The failure mode, characterising type III (short beams) behaviour, is represented by an almost linear path connecting the load point to the support.



The CFP can be visualized as a flow of compressive stresses with varying cross sections perpendicular to the path. The compressive force represents the resultant of the stresses at each section (Kotsovos, 1988). In the case of a simple beam at the ultimate limit state, the shape of the path was considered to be bi-linear (horizontal and inclined legs) as shown in Figure 2.18a. The horizontal projection of the inclined leg is approximately equal to  $2d$  ( $d$  is the member effective depth) in the case of two point loading with  $a/d > 2.0$ , and also equal to  $2d$  in the case of uniformly distributed loads with span to effective-depth ratios ( $L/d$ ) greater than 6.0. For smaller  $a/d$  or  $L/d$  ratios, the point at which the force direction changes was assumed to coincide with the load points. In the case of uniformly distributed loads, it was assumed that the load can be replaced by an equivalent two-point loading positioned at the third points along the span.

### c) Causes of Failure

In the CFP approach, the failure was related to the development of transverse-tensile stresses in the region of the path along which the loads were transmitted to the supports.

Some of the reasons for the development of the tensile stresses, Figure 2.18a, are detailed below:

1. The change in the path direction produces a tensile force ( $T$ ). This is to satisfy the equilibrium requirements at that location.
2. The variation in the intensity of the compressive stresses along the horizontal leg of the CFP results in the development of tensile stresses ( $t_1$ ). The highest stress intensity exists at the point where the cross section of the compression zone is smallest. The adjacent concrete provides restraint (confinement) at this section. A critical level of stress intensity would be reached before the stresses in the adjacent sections reach similar intensities. This critical stress level marks an abrupt and large dilation in the concrete which induces transverse tensile stresses in the surrounding concrete.
3. Large tensile stresses ( $t_2$ ) develop perpendicular to the compressive stress trajectories in the region of the crack tip (Kotsovos, 1979; Kotsovos and Newman, 1981; Kotsovos, 1984).
4. Bond failure between the longitudinal reinforcement and the concrete results in changes in the compressive stress distribution in the zone between two consecutive flexural cracks, as shown in Figure 2.18b. The rise of the neutral axis at the right-hand side of the crack, which is required to maintain equilibrium after loss of bond, can be noted from Figure 2.18b. The change in the

intensity of the compressive stress produces tensile stresses in the adjacent concrete region in a similar way to that discussed previously ( $t_1$ ).

## 2.7 Behaviour of Beams under the Combined Action of Shear Force and Bending Moment

### 2.7.1 Mechanisms of Shear Transfer

Traditionally, it is assumed that the behaviour and failure modes of beams subjected to shear loading are dependent on the method by which shear is transmitted from one plane to another. The majority of the Codes of Practice assume that shear is transferred through a beam by means of shear stress, interface shear transfer (often called 'aggregate interlock' or 'crack friction'), dowel action, arch action, and shear reinforcement (ASCE-ACI Committee 445, 1998; ASCE-ACI Committee 426, 1973).

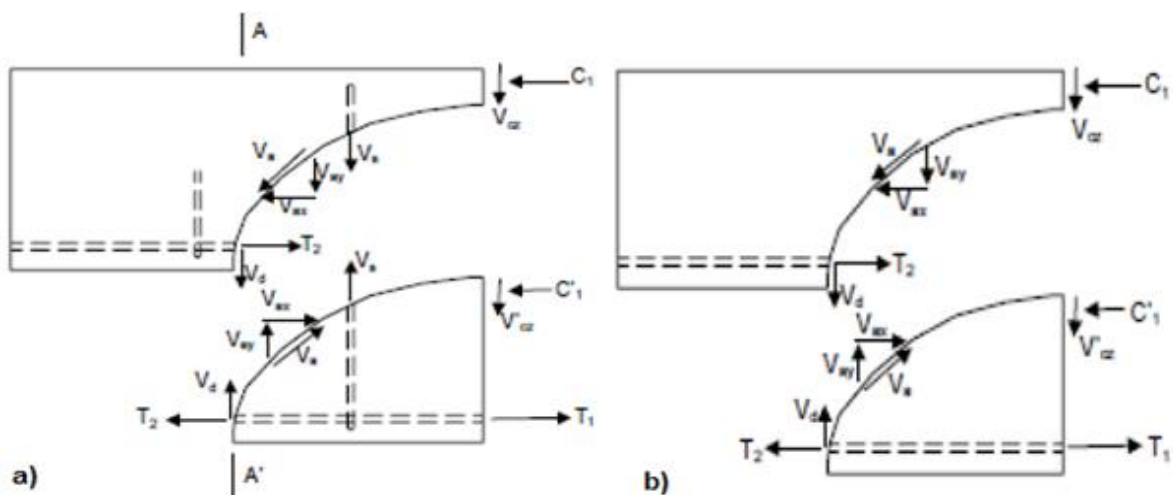


**Figure 2.19:** Internal Forces in a Cracked Beam: a) with Stirrups, and b) without Stirrups.

The 1998 ASCE-ACI Committee 445 Report highlights a new mechanism, residual tensile stresses, which are transmitted directly across cracks. Opinions vary about the relative importance of each mechanism in the total shear resistance, resulting in different models for members without transverse (shear) reinforcement. The forces transferring shear across an inclined crack in a beam with and without stirrups are illustrated in Figure 2.19 (ASCE-ACI Committee 445, 1998).

The different mechanisms of shear transfer which have been assumed are briefly discussed below:

### 2.7.1.1 Shear Transfer by Concrete Stress

Assuming concrete possesses no tensile strength in flexure, the maximum shear stress ( $v$ ) at the neutral axis in a beam subjected to a shear force ( $V$ ) is given by Equation (2.4).

$$v = \frac{V}{b_w \cdot jd} \quad (2.4)$$

Where  $b_w$  is the beam web width, and  $jd$  is the lever arm of the internal couple.

Equation (2.4), which was developed by Mörsh (1909) at the turn of this century, has been widely used to date as a convenient "index" to measure diagonal tension stress even for cracked beams (Park and Paulay, 1975). The shear stress at failure in most beams is considerably less than the direct shear strength of the concrete. The real concern is with diagonal tension stress, resulting from the combination of shear and longitudinal flexural stresses (Nilson and Winter, 1991).

At a point below the neutral axis which is subjected to shear stress ( $v$ ) and normal tensile stress ( $f_t$ ), the maximum principal tensile stress ( $f_{t,max.}$ ) occurs on a diagonal plane and can be determined from Equation (2.5).

$$f_{t,max.} = \frac{1}{2}f_t + \sqrt{\left(\frac{f_t}{2}\right)^2 + v^2} \quad (2.5)$$

The direction of the maximum principal tensile stress ( $\alpha$ ) is found from Equation (2.6).

$$\alpha = \frac{1}{2} \tan^{-1} \frac{v}{\frac{1}{2}f_t} \quad (2.6)$$

Where  $\alpha$  is approximately equal to 45 degrees assuming  $f_t$  is very small.

The maximum principal tensile stress ( $f_{t,max.}$ ) was linked to the inclined cracking of concrete. When the tensile stresses become excessive, diagonal cracks develop at approximately right angles ( $90^\circ$ ) to the compressive principal stress trajectories.

### 2.7.1.2 Interface Shear Transfer (Aggregate Interlock)

Interface shear, aggregate interlock, shear roughness, shear friction, or tangential shear transfer are different expressions which have been used by researchers to describe the transfer of shear forces along diagonal cracks.

If the shear plane is an existing crack, failure is assumed to involve slippage along the crack as well as movement at right angles ( $90^\circ$ ) to the direction of the crack (Bass et al., 1989). In this case, shear can be transferred only if either lateral reinforcement or lateral restraint is provided as shown in Figure 2.20a. This type of shear transfer is referred to as the "shear-friction hypothesis" (ACI318-85, 1985). Experimental studies on concrete push-off specimens (Bass et al., 1989; Etebar, 1987) have shown that shear stiffness and strength increase with increasing reinforcement strength ( $\rho_s \cdot f_y = (A_s \cdot f_y) / (b_w \cdot d)$ ).

If the shear plane is located in monolithic concrete, diagonal cracks normally form across that plane. In this case, it is assumed that failure involves truss action as shown in Figure 2.20b.

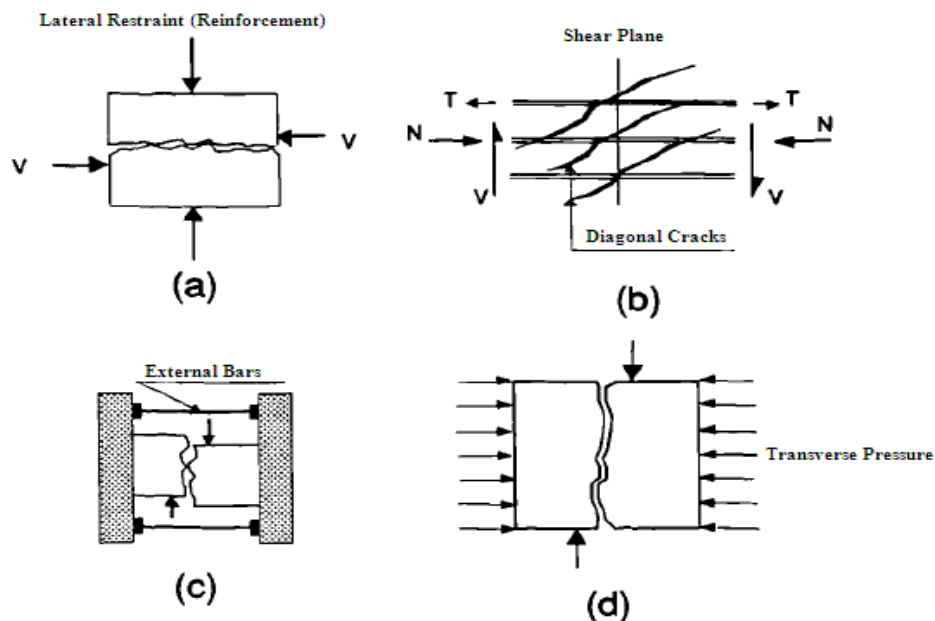


**Figure 2.20:** Mechanism of Aggregate Interlock: a) Shear-Friction Hypothesis; b) Formation of Truss Action; c) Partial Lateral Restraint; and d) Full Lateral Restraint.

Shear is resisted in beams through the combined contributions of the compression zone at the head of the shear crack, aggregate interlock, dowel action and stirrups if present. The contribution of each mechanism has been keenly debated since pioneering work by Taylor (1970) and others showed that aggregate interlock contributes up to 50% of the shear strength of

beams without stirrups (Sagaseta and Vollum, 2011). The ability of concrete to transmit stresses across cracks is termed 'aggregate interlock'. Aggregate interlock is particularly important in connections of precast concrete segments and in plane stress situations if the principal stress directions change during the loading process. Much theoretical and experimental work have been done in order to establish aggregate interlock relationships between the crack displacements ( $\delta_n$  and  $\delta_s$ ) and the normal and shear stresses ( $\sigma_n$  and  $\tau_{tn}$ ) acting on the crack surface.

As shear research progressed in the 1960's, it was gradually realized that aggregate interlock did play a significant role in shear behaviour (Moe, 1962; Fenwick and Paulay, 1964, 1968; MacGregor, 1964; Taylor, 1970; MacGregor and Walters, 1967; Kani et. al., 1979). In order for the stress in the longitudinal tensile steel to change along the span, these researchers realized that shear stresses had to be transferred across cracks by aggregate interlock action. Two of these early references are discussions of Kani (1964), in which he outlined his solution to the riddle of shear failure, which, while a useful tool to conceptualize shear failure, does not consider aggregate interlock.

It was concluded, based on test results (Millard and Johenson, 1985), that the shear stiffness and strength provided by aggregate interlock increase with increasing concrete compressive strength and the size of the aggregate in the matrix, and with decreasing crack width.

### **2.7.1.3 Dowel Action**

When longitudinal reinforcement crosses a crack, part of the shear force is resisted by dowel action. As a sequence of dowel action splitting cracks running along the bars may occur as a result of increasing tension in the surrounding concrete combined with the wedging action due to the deformation of the bars. The occurrence of splitting cracks decreases the stiffness of concrete around the bar and decreases the shear strength which in turn reduces the possible contribution from actual dowel action.

Dowel action is not very significant in members without transverse reinforcement, as the maximum shear in a dowel is limited by the tensile strength of the concrete cover supporting the dowel. Nevertheless, it may be significant in members with large amount of longitudinal reinforcement, particularly when the longitudinal reinforcement is distributed in more than one layer.

#### 2.7.1.4 Beam and Arch Actions

It has been argued that a load on a beam is transmitted to the supports through arch and beam actions (Kani, 1964). The full strength of the two actions cannot be combined because of the assumed incompatibility of the deformation associated with the two mechanisms. It is assumed that there is a transition in the behaviour from beam to arch action (Kani, 1964). Nevertheless, some of the recently developed models for the evaluation of shear strength are based on the assumption that both mechanisms take place simultaneously (Russo et al., 1991). Kotsovos (1983) has suggested that loads are transmitted to the supports along a compressive force path i.e. at the ultimate limit state, beam action is insignificant.

Compatibility in the shear-span is dominated by the growth of inclined cracks through the concrete (Kotsovos and Pavlovic', 1999). The cracks determine how the beam and arch mechanisms carry shear load, and are a fundamental part of shear failure. Figure 2.21 shows the shear mechanisms resulting from beam and arch actions in a beam without shear reinforcement (Stratford and Burgoyne, 2003). Crack propagation must be considered in conjunction with compatibility of each of the components of a beam.

Beam action, Figure 2.22a, describes shear transfer by changes in the magnitude of the compression-zone concrete and flexural reinforcement actions with a constant lever-arm. Beam action requires load-transfer between the two forces resulting from concrete and steel (Kotsovos and Pavlovic', 1999). In a cracked beam, load-transfer from the flexural reinforcement to the compression-zone occurs through the 'teeth' of concrete between cracks. Also, it requires bond between the concrete and reinforcing steel, Figure 2.23. Bending and failure of this concrete is studied by tooth models (Regan, 1993).

Arch action, Figure 2.22b, occurs in the un-cracked concrete near the end of a beam where load is carried from the compression-zone to the support by a compressive strut. The vertical component of this strut transfers shear to the support while the constant horizontal component is reacted by the tensile flexural reinforcement.

Both beam action and arch action can act in the same region. Equilibrium and compatibility near the end of a beam and across a single shear crack are studied by shear-compression theories.

Beam action, which is dominant at large  $a/d$  values when the load cannot be transferred to the supports by the arch supporting mechanism, is generally considered to result from the resistance

offered by the longitudinal reinforcement (dowel action), the un-cracked concrete and the aggregate interlock mechanisms. While arch action, which is dominant at low  $a/d$  values, generally results in the direct transfer of shear load from the point of application to the supports. As the support is approached by the load, the depth of the compression zone increases and thus the mechanism is facilitated, the horizontal resistance to the opening of the arch being provided by the longitudinal reinforcement.

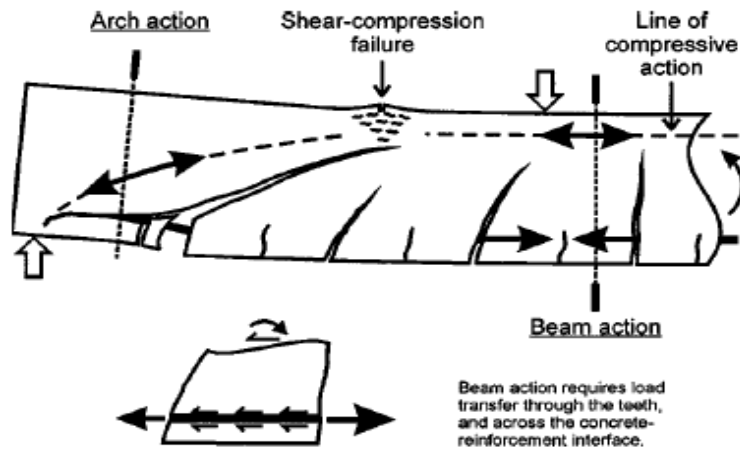


Figure 2.21: Shear in Beam without Shear Reinforcement.

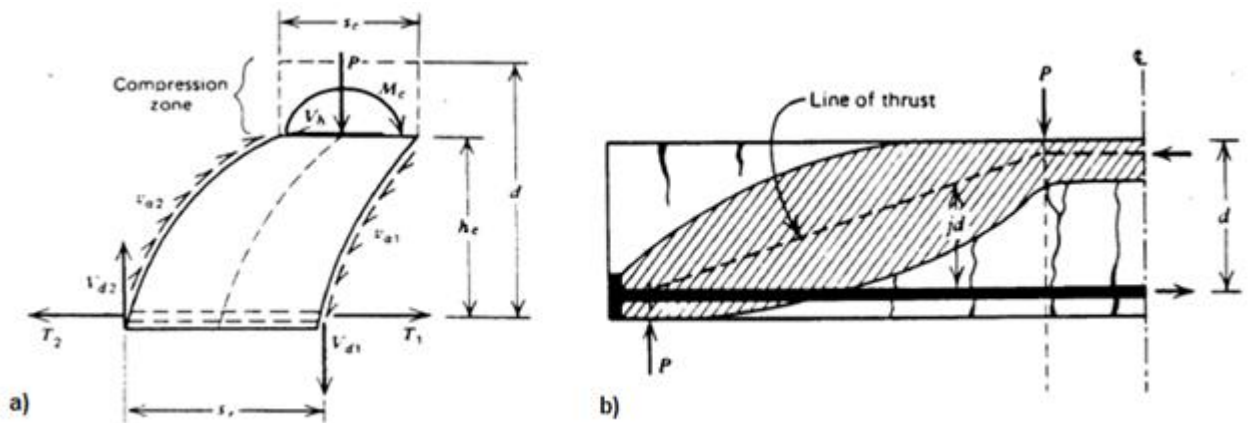


Figure 2.22: a) Beam Action (Tooth-Model), and b) Arch Action.

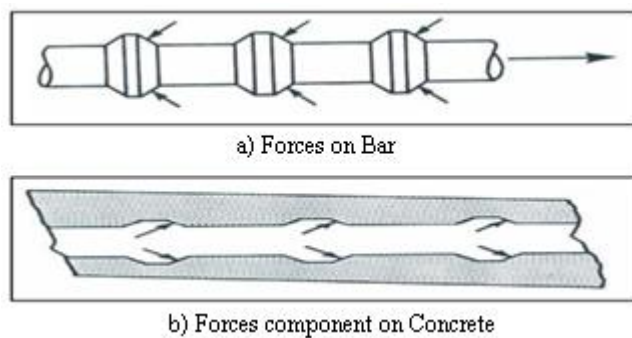


Figure 2.23: Bond between Reinforcing Steel-Bar and Concrete.

### 2.7.1.5 Shear Reinforcement

Traditionally, shear reinforcement is viewed as tension members in a conventional truss analogy. Although this analogy is helpful in simplifying the design concept, it was considered to oversimplify the solution because it does not consider the influence of web reinforcement on the other shear transfer mechanisms. Test results (Bresler and Scordelis, 1963; Haddadin et al., 1971; Mphonde and Frantz, 1985; Palaskas et al., 1981) have shown that shear strengths can be up to 80% higher than that predicted by the truss analogy because of the presence of stirrups. The role of shear reinforcement has been very controversial among researchers. It was considered that in addition to their direct resistance to shear, they restrict the widening of cracks, maintain aggregate interlock, and increase dowel action (ASCE-ACI Committee 426, 1974). Mphonde (1989) argued that the increase in shear resistance was due among other things to the role of the stirrups in enhancing the concrete compressive strength resulting from confinement.

### 2.7.2 Contribution of Shear Transfer Mechanisms to Shear Resistance

In the design methods adopted by Codes of Practice, it is postulated that all the types of shear transfer mechanism occur to widely varying extents in structural concrete members. The shear force ( $V$ ) is assumed to be carried by the mechanisms shown in Figure 2.24 and are related in Equation (2.7) below.

$$V = V_s + V_c = V_s + V_{cz} + V_{ay} + V_d \quad (2.7)$$

Where:

$V_s$  is the shear resistance due to web (shear) reinforcement,

$V_c$  is the shear resistance due to other actions (excluding the web reinforcement),

$V_{cz}$  is the shear resistance due to compression concrete,

$V_{ay}$  is the shear resistance due to aggregate interface action, and

$V_d$  is the shear resistance due to dowel action.

Kani (1964) attempted a more realistic approach by addressing the problem of the bending of the 'teeth' of the concrete between flexural cracks. The concrete between two adjacent flexural cracks was considered to be analogous to a tooth in a comb. The concrete teeth were assumed to be free cantilevers fixed in the compression zone of the beams and loaded by the horizontal shear



from bonded reinforcement, Figure 2.25. Although this theory did not cover most of the shear transfer mechanisms, it was probably the start of more rational approaches. Working with 'tooth' models, Fenwick and Paulay (1968) pointed out the significance of the forces transferred across cracks in normal beams by crack friction.

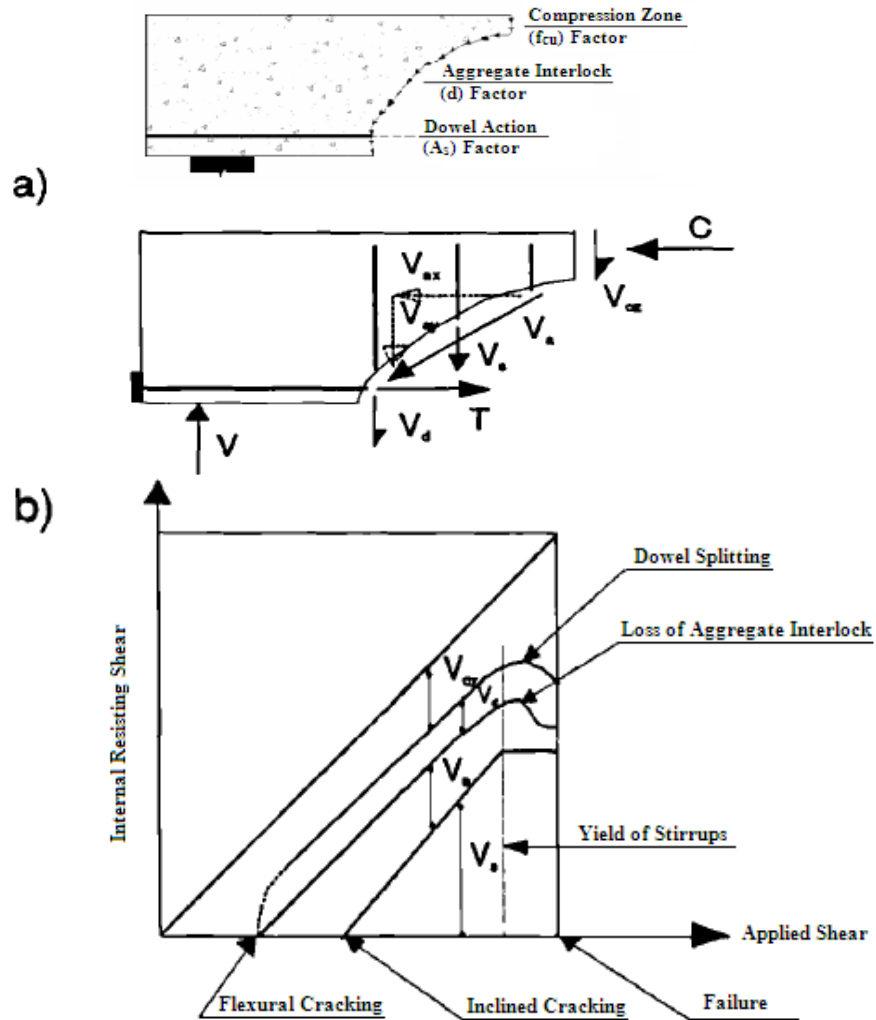


**Figure 2.24:** Traditional Concepts of Shear Strength: a) Mechanism of Shear Transfer, and b) Effect of Web Reinforcement on Shear Strength.

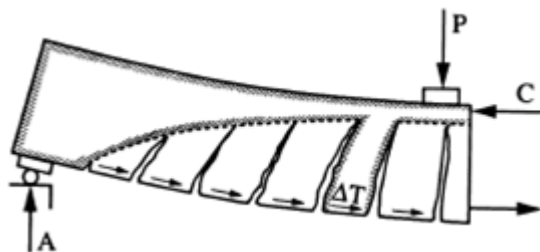


**Figure 2.25:** Kani's Tooth Model (Kani, 1964).

A number of experimental investigations (Fenwick, 1966; Fenwick and Paulay, 1968; Mattock and Hawkins, 1972; Taylor, 1970; Taylor, 1974; Gergely, 1969; ASCE-ACI Committee 445, 2000) have been carried out on beams without shear reinforcement in order to assess the

contribution from each of the above mechanisms related in Equation (2.7). It was concluded from these investigations, evaluating Kani's model, that between 20-40% of shear is carried in the compression zone ( $V_{cz}$ ), 33-50% due to aggregate interlock ( $V_{ay}$ ), and 15-25% by dowel action ( $V_d$ ). Krefeld and Thurston (1966) found a similar proportion of the shear to be carried by dowel action, and ASCE-ACI Committee 426 (1973) quote Parmelee (1961) and Baumann (1968) as also finding a similar proportion of the shear to be carried by dowel action. Etebar (1987) proposed the relative contributions shown in Table 2.1.

The contribution from all of the internal mechanisms of shear transfer for beams with web (shear) reinforcement is assumed (ASCE-ACI Committee 426, 1973) to be as shown in Figure 2.24b. Figure 2.24b indicates that before flexural cracking all the shear is carried by the concrete. After flexural cracking but before diagonal cracking has appeared, the shear is resisted by  $V_{cz}$ ,  $V_{ay}$ , and  $V_d$ . After the occurrence of inclined cracking, the shear reinforcement contributes to the resistance of a section ( $V_s$ ). When the stirrups have yielded, any additional shear force is assumed to be carried by the other shear transfer mechanisms. As the inclined cracks widen,  $V_{ay}$  is reduced and the contributions from  $V_d$  and  $V_{cz}$  have to increase until failure occurs.

**Table 2.1:** Percentage Contributions to Shear Resistance.

Contributions to Shear Resistance		Parameters Investigated		
		$f_c$	a/d	$\rho$
Long Beams	Aggregate Interlock	8-48%	25-40%	25-50%
	Dowel Action	22-42%	40-60%	32-55%
	Compression Zone	10-62%	0-35%	20-32%
Deep Beams	Aggregate Interlock	7-12%	5-42%	7-13%
	Dowel Action	31-43%	30-50%	33-42%
	Compression Zone	45-65%	2-65%	45-60%

Most ultimate load design procedures, which are based on these shear transfer mechanisms, divide the applied shear into two components. One component is assumed to be carried by the web (shear) reinforcement ( $V_s$ ) and the second component is carried by the other transfer mechanisms, collectively referred to as the concrete shear strength ( $V_c$ ). Empirical relationships and/or tabulated values estimating the shear strength of concrete ( $V_c$ ) are incorporated in the different Codes of Practice.

### **2.7.3 Conclusion**

It is widely accepted that the main contributor to shear resistance in beams is aggregate interlock (Fenwick and Paulay, 1968; Regan, 1969; Taylor, 1968; Belarbi and Hsu, 1990). The concept of aggregate interlock forms the basis of current Code provisions for shear design. Sliding along the crack interface must take place in order to mobilise this action. This concept is, however, incompatible with the observed behaviour of beams which have failed by diagonal cracking. In this case, a crack propagates in the direction of the principal compressive stress and opens in an orthogonal direction (Kotsovos, 1979; Kotsovos and Newman, 1981). Kotsovos (1988) has argued that if there was a significant sliding movement along the crack interfaces, localised cracks would branch out in all directions along the crack. The occurrence of such crack branching was not reported. Bobrowski (1982) stated that aggregate interlock and dowel action are only secondary mechanisms in beams. He emphasised that the principal aspect of a diagonal failure in beams is associated with the stress conditions in the compression zone.

### **2.8 General Conclusion**

The following general conclusions with regard to the behaviour of beams under transverse loadings have emerged from the literature review:

1. The currently accepted theory for evaluating the flexural capacity, equilibrium, and compatibility requirements of beams is based on the assumption that plane sections remain plane after bending. Transverse stresses in the concrete are assumed not to influence the behaviour of the beams and are therefore ignored, where they play a role in the compression-zone and transverse-direction of wide RC beams. The flexural failure of beams occurs as a result of the development of a multiaxial state of stress resulting from the dilation of the concrete in a localised region within the compression zone. The evaluation of the multiaxial stress conditions, which develop within the compression zone or within the transverse direction along the member width as the ultimate load is approached, is difficult. In accordance with the approach to structural concrete, which is based on simplicity rather than misleading precision, it is considered sufficient for practical purposes to assess the flexural capacity on the basis of the rectangular stress block as specified by current Codes of Practice.

2. The truss analogy provides a rational tool for the design of reinforced concrete beams in flexure, shear and torsion. The 45° truss model allows designers to calculate tensile stresses in

longitudinal steel and stirrups and to calculate compressive stresses in the un-cracked compression zone and inclined struts. It was suggested that the provision of shear reinforcement be based on the shear compression theory. Traditionally, it is assumed that the behaviour and failure modes of beams subjected to shear loading are dependent on the method by which shear is transmitted from one plane to another. The majority of the Codes of Practice assume that shear is transferred through a beam by means of shear stress, aggregate interlock, dowel action, arch action, and shear reinforcement.

3. Test results (Base and Read, 1965) have indicated that confining the compression concrete with closed stirrups improves the ductility of beams. Furthermore, based on the possibility to make over-reinforced beams fail in a ductile manner, it is concluded that the limitations on the longitudinal reinforcement ratio ( $\rho_s$ ) imposed by Codes of Practice are too restrictive when the compression concrete is confined with closed stirrups (Ziara, 1993).

4. Traditional design models for shear consider the nominal ultimate shear strength ( $v_u = V/b_w.d$ ) as an indicator of the load carrying capacity of beams at diagonal failure. The evaluation of  $v_u$  as given by Codes of Practice is based on results obtained from a large number of tests. The variation in  $v_u$  may reach 150% depending on the value of flexural reinforcement ratio ( $\rho_s$ ) and the shear-span to effective-depth ( $a/d$ ) ratio (Kani, 1964). The relative flexural capacity of beams ( $M_u/M_f$ ) represents a more realistic indicator of the load carrying capacity of beams at diagonal cracking. The results from tests on beams have shown that all the values of ultimate flexural capacity ( $M_u$ ) range between 50% to 100% of full flexural capacity ( $M_f$ ) (Kani, 1964).

## CHAPTER 3

# LITERATURE REVIEW FOR WIDE REINFORCED CONCRETE MEMBERS

This Chapter discusses the previous works conducted on wide reinforced concrete beams. It highlights the main factors affecting the behaviour of wide concrete beams. The conclusions relating to the impact of previous work on the scope of this programme of research are also outlined. This Chapter reviews the investigations conducted on wide RC beams and factors affecting their shear and flexural strengths.

### 3.1 Introduction

The rectangular RC beam which has a width ( $b_w$ ) larger than its depth ( $d$ ) and has obvious ( $b_w/d$ ) ratio in comparison to the narrow beam is called a *wide RC beam* (Figure 3.1) and is designed as a conventional RC beam (Al.Dywany, 2010; Sherwood et al., 2006). A wide beam must have a width to height ( $b_w/h$ ) ratio exceeding 2.0 (Al.Dywany, 2010; Sherwood et al., 2006), while slabs typically have much larger ratios. A  $b_w/h$  ratio of 2.0 was used throughout this programme of research based on laboratory work for all examined wide RC beams. Moreover, for structural RC wide beams, the ratio of shear-span to effective-depth ( $a/d$ ) is greater than 1.0 (Teck FU, 2009). Structural RC Wide beams are used in buildings to reduce reinforcement congestion and floor heights for the required headroom. Wide beams are frequently used as transfer elements where the total structural depth ( $h$ ) must be kept to a minimum (Alluqmani, 2014; Alluqmani and Haldane, 2011a, 2011b, 2011c). Therefore, these wide members provide large cross-sectional areas of concrete to resist shear demands. In most of these cases, the beam is either equal to or wider than that of the supporting loads or columns (Figure 3.1). Consequently, their shear capacity might be effected and differ from that of conventional beams. Adopting a wide beam system for the design scheme provides many advantages. They include reducing the amount of formwork required, providing simplicity for repetition and thus decreases the story height. All of these would eventually result in a faster construction at a reduced cost. In this study, wide RC beam specimens were designed and examined with either full-width or narrow-width load and support conditions.

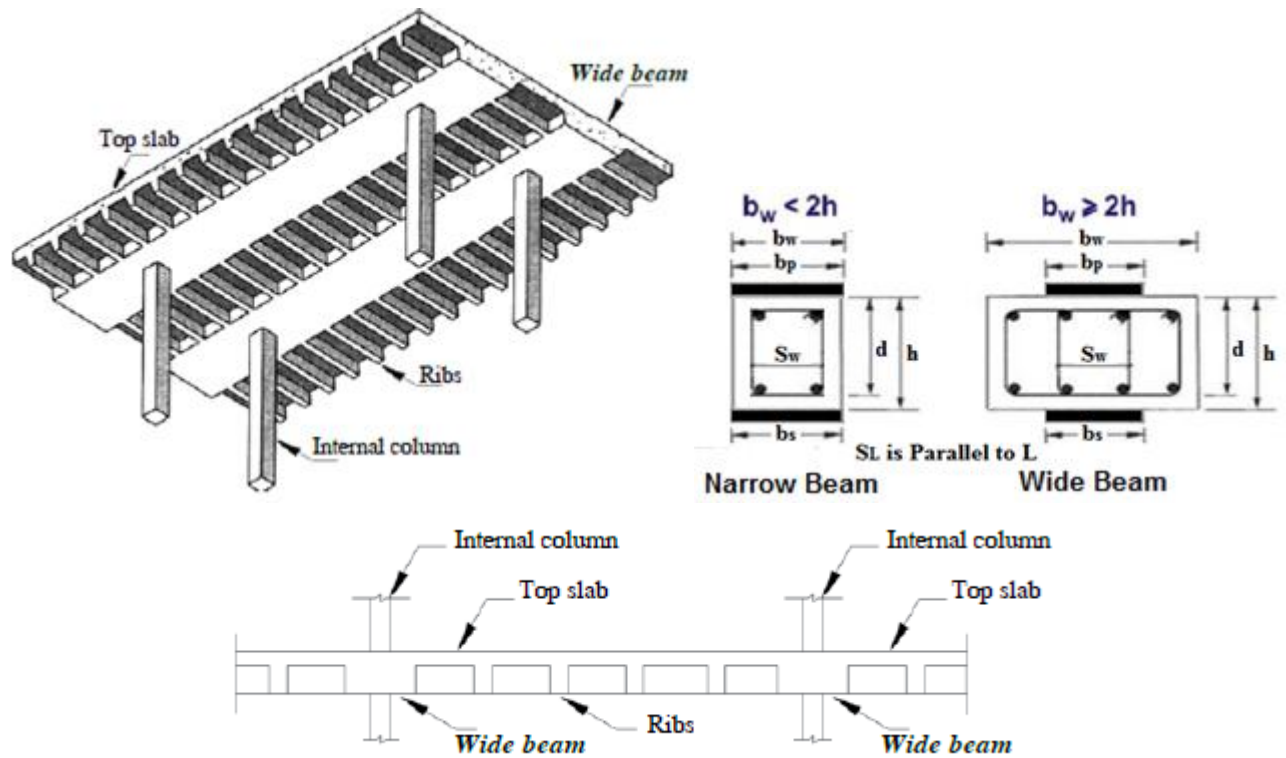


**Figure 3.1:** Wide Beams (Hidden Beams) in a Ribbed Slab System, and Cross-Section Details of Wide and Narrow Beams.

In Middle East countries, like Saudi Arabia, wide RC beams are common used in the ribbed (hollow-bricked) slab structure systems. Wide RC beams are commonly used as primary structural members in buildings and bridges, to support floor loads and to transfer forces from discontinuous walls or columns above. In addition, wide RC beams and thick slabs are commonly used as economical transfer elements. Wide beams systems supply large cross-sections to resist shear forces. Many structural schemes provide the wide members to carry direct forces, or to serve as primary transfer elements. However, some Codes of Practice, such as Eurocode2 Code (EC2), American building Code (ACI318) and Saudi building Code (SBC304), are not consistent in their treatment of shear in wide beams as compared to narrow beams.

Some structural designers consider one-way slab is a wide beam, where solid slab is designed as a one-metre wide strip which is as a wide beam. They also consider the footings and strip foundations are wide beams. The Footing can fail in bending (flexural failure) and shear (shear failure) as a wide beam. On the other hand, if wide and slender concrete beams support the slab, they are called band beams floor system.

### **3.2 Wide Concrete Beams in Shear [Without and With Shear Reinforcement]**

Recent researches concerning shear capacity of structural RC members concentrated on studying of shear failure mechanisms and specially on modelling the shear failure (Collins et al., 2008; Jensen and Hoang, 2009; Lee and Kim, 2008). The shear failure mechanism is a very complex phenomenon. Some experimental studies reveal that unlike flexural failures, reinforced concrete shear failures may be relatively brittle and for members without shear-reinforcement (stirrups) it can occur without warning (Collins et al., 2008). Nevertheless, the most recent formulated design models for shear in structural RC beams assume plastic effects in concrete and steel.

The shear design method in EC2 Code is based on the Inclined Strut method while the shear design method in ACI318 and SBC304 Codes is based on the Strut-Tie method. Ensuring sufficient ductility in structures is one of the prime objectives in the design philosophy of reinforced concrete. The provision of ductility gives sufficient warning before failure. To fulfil the requirements of ductility, several methods such as provision of reinforcement and confinement by stirrups were in use. However, the confinement provided by stirrups is limited due to the spacing limits. Also it is established in the literature (Rao and Reddy, 1981; Paulay and Priestley, 1992), that the stirrup reinforcement provided beyond what is required for resisting the shear failure will only provide confinement. Hence with the practical minimum spacing that can be provided at the critical sections, there is a limitation to the quantity of confinement, which can be provided by the stirrups. Thus it may not be possible to sufficiently confine the structure and thereby achieving required ductility by providing the laterals alone.

The purpose of the shear reinforcement is to ensure that shear failure does not occur and that the full flexural capacity can be used. As the strain in the stirrups is equal to the corresponding strain in the concrete prior to inclined cracking, the stress in the stirrups will be small. Thus, Stirrups do not prevent inclined cracks from forming as they come into play only after cracks have formed.

Open stirrups are provided principally to resist shear stresses and forces in concrete beams and they are applied in locations in which the effect of torsion is insignificant. U-shaped stirrups are placed in the tension side of concrete beams in which shear cracks would occur. However, when concrete beams are designed to resist a substantial amount of shear and torsion, closed stirrups should be used instead of other shapes of stirrups.

It was found that at the same stirrup strain, the closed-stirrups configuration shows smaller shear crack width as result of the slip of stirrup end which affect the slip at the end of vertical leg of stirrup as proved in some previous studies (Hassan and Ueda, 1987; Zakaria et al., 2009).

Although there are great research efforts, however, there is still not a simple, albeit analytically derived formula to predict quickly and accurately the shear strength of slender, narrow and wide beams. In addition, many of the factors that influence the determination of the required minimum amount of shear reinforcement are not yet known. As a consequence, the current provisions for shear in standard Codes of Practice, such as EC2, ACI318 and SBC304 Codes, are still based on traditional empirical or semi empirical considerations. As such, there are considerable differences in various aspects of the respective shear design methods. These differences include how each Code accounts for the effects of: a) maximum aggregate size, b) member depth, c) web width, d) flexural reinforcement ratio, e) minimum stirrups, and f) crack control steel.

### **3.3 Punching Shear on Wide Members**

In wide structural members when the support or the load is concentrated on these members, a new mechanism of shear might occur and is called punching shear. Punching shear stresses should be checked for two types of reinforced concrete members which are classified as wide structural members. These types of structural members are flat slabs (for all types: normal flat slab, flat slab with drop panel, flat slab with column head, and flat slab with drop panel -and-column head), and footings (for all types: shallow and pad footings (isolated and combined foundations), and deep footings (raft and pile cap foundations)). For these types of structural members, there are limits for punching shear stresses depended on the compressive strength of concrete, but if these stresses are out of these limits, the depth of a structural member should be changed. Moreover, punching shear reinforcement may be required as per the check, and it is placed around the support (or column) from a distance as a percentage of  $d$  (effective depth of member) as a perimeter surrounded the support for cone or pyramid shape.

On the other hand, punching shear stresses may need to check on wide RC beams but their reinforcement is not required. The case of a wide beam is like to the case of a flat slab with drop panel, because the wide beam is here considered as the drop panel that is connected between the column (or support) and the flat slab; and also a wide beam is like to the case of isolated footing (strip or pad foundation) and raft footing, because the wide beam is here considered as the footing that is connected between the column (or support) and the soil.



Consider a column delivering a downward load on a slab, or a footing, or may be a wide beam of concrete, the load from the column will want to punch through these members, pushing some concrete along with it into the air, or soil, or whatever lies below. Since concrete shears at 45° angles (diagonal tension), the 45° angle thing will manifest itself as a three dimensional (3D) pyramid or cone shape piece of concrete wanting to punch through.

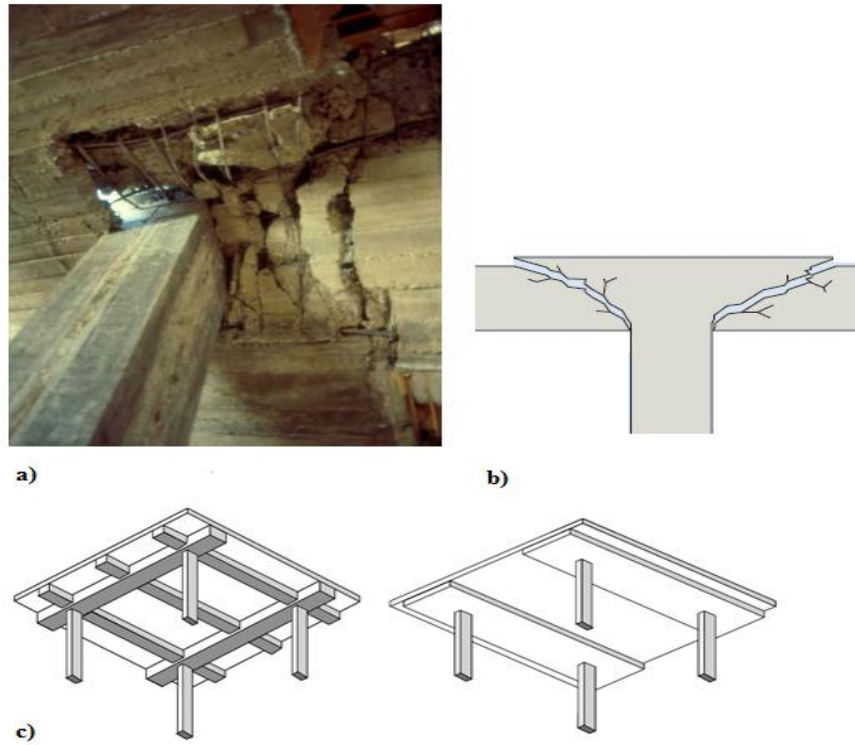
Punching shear arises in wide concrete members when a concentrated load is applied to a small area of a member (like a slab) or, most commonly, the reaction of a column against a slab (or a wide member), as shown in Figure 3.2a. The resulting stresses are verified along defined control perimeters around the loaded area.

The weight of a slab (or a wide member) supported on a column induces shear stresses in the slab (or the wide member). These stresses, if sufficient and where additional reinforcement has not been provided, would result in the column ‘punching’ through the slab (or the wide member), as shown in Figure 3.2b. This punching shear is similarly induced in the footing (or in the wide member) on which the column bears.

Despite punching shear can be relieved by localised thickening of the concrete with enlarged column heads and down-stand beams, the construction of flat slabs, as wide members, offers many advantages. A consistent head space can reduce the overall height of a building and provide material savings and significant time.

Figure 3.2c shows wide beams are connected between the columns and slabs where they are used to prevent the punching shear failure. If wide and narrow concrete beams support the slab, it is called a band beam floor system which has a simple formwork and is economical with labour.

A flat slab usually does not have girders or beams, but is supported by column capitals or drop panels directly, or both, which are considered as wide beams. All loads are transferred to the supporting column, with punching shear resisted by drop panels. Therefore, punching shear reinforcement is increasingly used in flat slabs because of the significant improvements introduced both in terms of strength and ductility.



**Figures 3.2:** Punching Shear Failure, and Using the Wide Beams to be Connected Between the Columns and Slabs to Prevent the Punching Shear Failure.

### 3.4 Previous Research on Wide Reinforced Concrete members

Recent researches (Lubell et al., 2008; Lubell et al., 2009a; Lubell et al., 2009b; Lubell et al., 2004; Lubell, 2006; Al.Dywany, 2010; Serna-Ros et al., 2002; Shuraim, 2012; Hanafy et al., 2012; Al-Harithy, 2002; Collins and Kuchma, 1999) have been conducted to investigate the behaviour of wide RC members with and without shear reinforcement. Some of these researches (Lubell et al., 2004; Lubell, 2006; Collins and Kuchma, 1999) have highlighted the difficulty of accurately assessing the shear capacity for large, lightly reinforced concrete wide members without shear reinforcement using ACI318 Code, due to size effects in shear.

A limited number of studies (Sherwood, 2008; Sherwood et al., 2006; Shioya, 1989; Collins and Kuchma, 1999; Kani, 1967) on relatively narrow beams without stirrups, reported that the shear stress at failure decreases as the effective-depth of a member increases. This has been called the 'size effect' in shear (Kani, 1967; Collins and Kuchma, 1999). The tests in the AT-2 and AT-3 series presented in the study of Sherwood et al. (2006) and the test of the AT-1 series reported in the study of Lubell et al. (2004), demonstrated that the failure shear-stresses of slabs, wide beams, and narrow beams are all very similar, if the members have the same depth, the same concrete, the same loading ratios, and the same percentage of longitudinal reinforcement. Thus,

it has been recommended that stirrups be included in all large members to mitigate size effect in shear and to enhance the member's ductility (Lubell et al., 2004). In other design situations, architectural limitations may require shallower structural depths, thus requiring web reinforcement to cope with the shear demands on the reduced cross section. While shear reinforcement spacing limits measured along the member length ( $S_L$ ) are provided in design Codes such as EC2, ACI318 and SBC304, few guidelines exist for appropriate limits on the spacing of stirrup legs across the member width ( $S_w$ ).

It was concluded (Sherwood, 2008; Sherwood et al., 2006) that the shear stress causing failure decreases as the beam depth increases. The size-effect can be explained by reduced aggregate interlock capacity in members with widely spaced cracks. Various methods to eliminate the size effect in shear are explored, including the use of stirrups or longitudinal reinforcement distributed over the beam height. Beam/slab width is shown to have no effect on failure shear stress (Sherwood, 2008; Sherwood et al., 2006). The size effect in shear is a phenomenon exhibited by slender reinforced concrete members constructed without shear reinforcement in which the failure shear stress decreases as the effective depth increases (Sherwood, 2008).

The development of the 1963 ACI shear provisions is explained in a report by ASCE-ACI Committee 326 entitled "Shear and Diagonal Tension" (ASCE-ACI Committee 326, 1962). As part of the discussion of this report, Diaz de Cossio (1962) offered new data from 57 tests investigating width effects on the one-way shear capacity of beams. Diaz de Cossio's specimens can be characterized as being heavily reinforced in flexure (approximately 2% reinforcement) and rather shallow, with effective depths ( $d$ ) typically less than 170mm. From these tests, Diaz de Cossio (1962) asserted that the width to effective-depth ( $b_w/d$ ) ratio was a significant parameter in predicting shear capacity. By modifying the basic ACI318 shear expression with this ratio, he obtained better test-to-predicted-strength ratios for the data set. In light of current knowledge concerning the size effect in shear, where the shear stress at failure decreases as the member depth increases, Lubell et al. (2009a) recommended that a re-examination of Diaz de Cossio's data is warranted.

From the investigation of Diaz de Cossio (1962), typical results from Specimens A8.5-34A & A8.5-34B and A34-8.5A & A34-8.5B, for example, suggest a very different relationship than that proposed by Diaz de Cossio. The Specimen A8.5 beams had dimensions of  $b_w = 85\text{mm}$  and  $d = 340\text{mm}$ , while the Specimen A34 beams had  $b_w \approx 340\text{ mm}$  and  $d \approx 85\text{ mm}$ . Thus, the two sets of beams had essentially identical values of shear area,  $b_w \cdot d$ , but  $b_w$  and  $d$  were

interchanged. The narrower (and deeper) specimens, specimen A8.5 beams, failed at the lowest shear stress ( $v = A_v.f_{yv}/b_w.SL$ ) of all of Diaz de Cossio's beam results at approximately 0.187 MPa, while the wider (and shallower) companions, specimen A34 beams, failed in flexure and carried over twice the shear stress. Furthermore, the specimen A8.5 beams have the lowest value of test-to-predicted results using Diaz de Cossio's modified Equation at approximately 0.76 MPa, indicating that his proposed model was ill-suited to deeper members. Overall, Lubell et al. (2009a) concluded that Diaz de Cossio's results cannot justify the claim that  $b_w/d$  directly affects the shear capacity of a wide member, when the more relevant influence of the absolute value of  $d$  has not been fully considered.

The influence of member width on the shear stress at failure was investigated by Kani (1967). His test series compared the capacities of wide beams 610mm wide by 305mm deep with companion narrow beams 162mm wide by 305mm deep, at shear-span to effective-depth ratios ( $a/d$ ) of 3.0, 4.0, 5.0, and 6.0. The failure shear stresses in the wide beams were within 10% of the failure shear stresses of the corresponding narrow beams. Thus, in contrast to Diaz de Cossio (1962), Kani (1967) concluded that the width to effective-depth ratio ( $b_w/d$ ) had no significant influence on the shear stress at failure.

Sherwood et al. (2006) found that the member width does not significantly affect the shear stress at failure. They concluded that ACI 318-05's provisions, which dictate different levels of useable shear capacity for slabs, wide beams and narrow beams, are not appropriate. They found that the narrow design strips have been shown to behave in shear in a similar manner to wider members. Accordingly, they concluded that the well-established size effect of decreasing shear stress at failure as the member depth increases, and also also applies to wide beams and thick one-way slabs. Sherwood et al. (2006) recommended that a reformulation of ACI 318-05's basic expression for shear strength be developed to better predict the shear capacity of members regardless of depth or classification.

Early investigation based on experimental tests was conducted in 2008 by Sherwood concerning influence of the width of wide members on their shear capacity. Various beam widths were used in the comparison, with fixing both depth ( $d$ ) and longitudinal reinforcement percentage ( $\rho_s$ ). His experiments showed that the width of the wide beam ( $b_w$ ) has no affect on the shear capacity of the member.

It is well established in both British and American design Codes (BS8110, 1997; ACI318, 2008) that the failure mode of rectangular RC beams without shear reinforcement is strongly dependent on the shear-span to effective-depth ( $a/d$ ) ratio, and:

- a) For  $a/d > 6.0$ , failure usually occurs in bending (long beams – type I beams),
- b) For  $6.0 > a/d > 2.5$ , the development of a flexural crack into an inclined flexure-shear crack results in diagonal tension failure (normal beams – type II beams),
- c) For  $2.5 > a/d > 1.0$ , a diagonal crack forms independently but the beam remains stable until shear-compression failure occurs (short beams – type III beams), and
- d) For  $a/d < 1.0$ , the behaviour approaches that of deep beams (deep beams – type IV beams).

Most of the researchers, who conducted experiments, concluded that failure mode strongly depends on the shear-span to effective-depth ( $a/d$ ) ratios. Berg (1962), Taylor (1960), Ferguson (1956) and Gunneswara-Rao (2006) observed that the shear capacity of structural RC beams varied with  $a/d$  ratio. Ahmad and Lue (1987) also found an increase in shear capacity due to decrease in  $a/d$  ratio. The flexural strength and mode of failure were also observed to be dependent on the  $a/d$  ratio (Bukhari and Ahmad, 2007). At constant  $a/d$  ratio, the tests made by Bukhari and Ahmad (2007) showed that the failure load increased with increasing in longitudinal (flexural) steel ratio ( $\rho_s$ ). Fewer but wider cracks were observed in beams with lower longitudinal reinforcement ratios. At constant longitudinal reinforcement ratio ( $\rho_s$ ), their tests also showed that shear strength and failure load decreased and deflection of the beam increased with increasing in  $a/d$  ratio. In addition to the shear-span to effective-depth ( $a/d$ ) ratio, the contribution of the concrete to the shear strength ( $V_c$ ) is dependent on a number of other factors including the concrete compressive strength ( $f_c$ ), the beam size ( $b_w \cdot d$ ) and the main tension reinforcement ratio ( $\rho_s$ ). These factors are represented in the ACI318 (2008), SBC304 (2007), and BS18110 (1997) design formulae for  $V_c$ .

### **3.5 Factors Influencing the Wide Member Strengths**

Various parameters have been recently studied to investigate their influence on the wide RC beam strengths (Lubell et al., 2009a; Lubell et al., 2009b; Lubell et al., 2008; Lubell, 2006; Lubell et al., 2004; Shuraim, 2012; Hanafy et al., 2012; Al-Dywan, 2010; Sherwood, 2008; Serna-Ros et al., 2002; Al-Harithy, 2002; Collins and Kuchma, 1999), such as stirrup configurations and spacing in both longitudinal direction ( $S_L$ ) and transverse direction ( $S_w$ ), support and load width ( $b_s$  and  $b_p$ ) condition (full-width and/or narrow-width conditions,  $k_s$  and  $k_p$ ), flexural reinforcement ratios ( $\rho_s$  and  $\rho_s'$ ), type of loading, and etc.

The main parameters which have exhibited effects on the wide concrete beam strengths and have been considered in the present study are the bearing plate widths in the locations of support and load (the dimension of the plate that is parallel to the beam width) and the stirrup-legs spacing in the longitudinal and transverse directions (the spacing of the legs that is parallel to the beam length and width, respectively). Therefore, this programme of research focuses on the effect of these four factors to evaluate and predict the wide beam strengths, as well as to develop proposed models to predict, detail and design these wide beams. The load width ( $b_p$ ), support width ( $b_s$ ), stirrup legs spacing along the member length ( $S_L$ ) and across the member width ( $S_w$ ) are taken as main considered variables, keeping all other parameters constant.

A small number of studies have directly examined the behaviour of wide concrete beams. The main objectives of these investigations were either to study the influence of stirrup legs spacing across the member width ( $S_w$ ) of wide beams, or to study the influence of support and/or load conditions (support width ( $b_s$ ) and/or load width ( $b_p$ )) to the width of wide beams ( $b_w$ ), as described in Sections 3.6 and 3.7, respectively.

### **3.6 Influence of Transverse Stirrup Spacing**

It is believed for RC beams when the stirrup legs are distributed along the member length that the RC beam strengths decrease as the the longitudinal spacing of stirrup legs (stirrup legs spacing along the member length) increases; but in the case of wide RC beams, the stirrup legs are also distributed and spaced across the member width and have influence on the wide beam strengths. The influence of the transverse spacing of stirrup legs (stirrup legs spacing across the member width) has been studied by several researchers (Lubell et al., 2009a; Shuraim, 2012; Hanafy et al., 2012; Lubell, 2006; Serna-Ros et al., 2002; Anderson and Ramirez, 1989; Zheng, 1989; Hsiung and Frantz, 1985; Leonhardt and Walther, 1964) and methods to account for its influence in capacity model have been provided (Serna-Ros et al., 2002; Shuraim, 2012).

In wide RC members, shear-reinforcement (stirrups) legs for one-way shear must be appropriately spaced along the member length and across the member width. EC2 (2004, 2008) suggests stirrup-legs spacing limits of  $0.75d$  or  $600\text{mm}$  in both the longitudinal and transversal directions. ACI318 (2008, 2011), SBC304 (2007), CSA-A23.3 (2004), and AASHTO-LRFD (2004) limit the stirrup-legs spacing in the longitudinal direction to  $0.50d$ ,  $0.50d$ ,  $0.63d$ , and  $0.72d$  respectively, but none of these Codes provide stirrup-legs spacing limits across the

member width. The CEB-FIP (1990) suggests that the maximum transverse spacing of the stirrup-legs should be limited to the smaller of  $2/3(d)$  or 80mm, where  $d$  is the effective-depth of the member. However, requirements for the stirrup-legs spacing are given in BS8110 (1997), Clause 3.4.5.5; where in the longitudinal direction along the span length, the stirrup-legs spacing should not exceed  $0.75d$ , and in the transverse direction across the width (the perpendicular direction to the beam span), the stirrup-legs spacing should be such that no longitudinal tension bar is more than 150mm from a vertical stirrup-leg; this spacing should in any case not exceed the effective-depth of the member. On the other hand, Serna-Ros et al (2002) concluded that the maximum distance in the transverse direction between stirrup-legs should be limited to  $d$ . In addition, based on previous and current experimental investigations conducted on wide RC beams, Lubell et al (2009a) summarized that the transverse stirrup-legs spacing should be the lesser of  $d$  or 600mm; but it should be halved when the nominal shear force ( $V_n$ ) exceeds  $(0.42\sqrt{f_c'})*b_w*d$  (N and mm Units), where  $f_c'$  is the specified concrete strength in MPa ( $\text{N}/\text{mm}^2$ ),  $b_w$  is the web width of the beam in mm and  $d$  is the effective-depth of the beam in mm.

A number of studies have directly examined the influence of stirrup-legs spacing across the member width on the shear strength of wide RC members.

Leonhardt and Walther (1964) suggested that the transverse spacing of stirrup legs (stirrup-legs spacing across the member width) should be minimized to adequately anchor and suspend the diagonal compression struts associated with the truss model used for shear reinforcement (stirrups) design. The diagonal compression force must flow toward the stirrup legs as shown in Figure 3.3a (Leonhardt and Walther, 1964). Anderson and Ramirez (1989) likened this to considering a series of effective truss planes oriented in the longitudinal direction and centred on each line of stirrup legs. An effective width of this plane was not defined (Anderson and Ramirez, 1989), but detailing rules for strut-and-tie- models in the AASHTO-LRFD Code (2004), shown in Figure 3.3b, can serve as a guide. These rules suggest that it may no longer be appropriate to consider the shear-reinforcement as uniformly smeared over the cross section, for members where the legs of the stirrups are spaced further apart than 12 times the bar diameter of the longitudinal reinforcement ( $d_b$ ).

Without specific experimental validation presented, Leonhardt and Walther (1964) suggested a shear-reinforcement (stirrups) spacing limit in the transverse direction of  $d$  for low shear stresses, a stirrup-legs spacing of 200mm for high shear stresses ( $v > 1.59\sqrt{f_c}$ , N and mm Units) was proposed and 400mm otherwise. They also recommended stirrup-legs spacing limits of  $0.6d$  or

300mm in the longitudinal direction, with the limits decreased by 50% for shear stresses ( $v = A_v \cdot f_{yv} / b_w \cdot S_L$ ) exceeding approximately  $0.135f_c'$ .

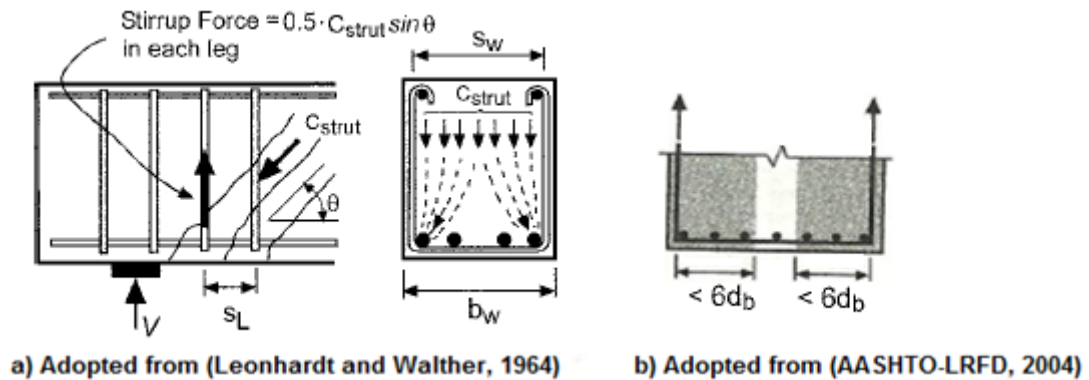


**Figure 3.3:** Force Flow Analogy in Diagonal Strut Toward Shear Reinforcement Legs: a) Spreading Model; and b) Effective Strut Anchorage Width for Truss Modelling.

Hsiung and Frantz (1985) performed tests on members up to 457mm in width using different stirrup configurations and having shear reinforcement ratios approximately 60% higher than the ACI318 minimum limit (shear stress,  $v = A_v \cdot f_{yv} / b_w \cdot S_L \approx 0.62$  MPa). Specimens had width to overall-depth ( $b_w/h$ ) ratios from 0.33 to 1.0. Higher web reinforcement strains in interior stirrup-legs were reported, but the transverse stirrup-legs spacing across the width, ranging from  $d/4$  to  $d$ , did not result in discernible changes in ultimate shear capacity or differences in crack widths measured across the specimen width. Hsiung and Frantz (1985) reported that shear strength does not affect by the transverse stirrup-legs spacing.

Anderson and Ramirez (1989) tested members 406mm deep, with  $b_w/h$  ratio of 1.0 and sectional shear stresses of approximately 60% of ACI318 maximum limits ( $v = A_v \cdot f_{yv} / b_w \cdot S_L \approx 2.14$  MPa). They found in their experimental work that shear strength depends on transversal spacing of stirrup legs, and explained the Hsiung and Frantz (1985)'s results because of the low level of shear stresses in their tests. They also explained that the stirrup-legs spacing limits proposed in the study of Leonhardt and Walther (1964) were appropriate for members subject to high shear stresses. In addition, they concluded that transversal stirrup-legs spacing is important for high level of shear stresses (which often occur in the interim region between the interior stirrups, especially for narrow-supported width wide beams), as Leonhardt and Walther (1964) reported before them. Anderson and Ramirez (1989) found that the beam shear strength was improved when the shear reinforcement was more uniformly distributed across the member width, or when the longitudinal stirrup legs spacing was decreased.



Tests conducted by Zheng (1989) on reinforced concrete shells with rectilinear patterns of shear reinforcement showed that the shear capacity decreased as the stirrup-legs spacing across the member width increased for constant shear-reinforcement ratios. A staggered pattern of web reinforcement of shear studs was found to improve the performance of cyclically loaded shells with superimposed in-plan tension and compression by preventing excessive transverse splitting along the longitudinal reinforcement and by improving the confinement of the concrete core (Monteleone, 1993).

Serna-Ros et al. (2002) tested beams 750mm wide and 250mm high ( $b_w/h = 3.0$ ), with different shear-reinforcement configurations (shear stress,  $v = A_v.f_{yv}/b_w.S_L \approx 0.76$  MPa). They concluded that capacity predictions using the ACI318 model could be improved by adjusting the shear reinforcement fraction,  $V_s$ , of the total one-way shear capacity,  $V_n$ , by the ratios  $\sqrt{(d/S_L)}$  and  $\sqrt{(d/S_w)}$ , where  $S_L$  and  $S_w$  represent the longitudinal and transversal spacing of stirrups-legs, respectively. In addition, they concluded that the use of two stirrup legs across the member width should be banned in wide RC beams. They found that the shear capacity decreased as the transverse stirrup-legs spacing increased and as the longitudinal stirrup-legs spacing increased. Serna-Ros et al. (2002) developed a shear strength model to account for the effect of longitudinal and transverse stirrup-legs spacing on the one-way shear strength of wide beams. Their model is described in the next Chapter and compared with the proposed Prediction-Model developed in the present study. Further, the effect of longitudinal and transverse spacing of stirrup legs is taken into the consideration in the present study for developing a proposed Prediction-Model (see Chapter 6) (Alluqmani, 2013a).

In 2006, Lubell conducted experimental investigations on reinforced concrete wide members. His test results showed that member width or the inclusion of temperature reinforcement did not influence the shear stress at failure for members without web reinforcement. He concluded that the shear stress at failure decreased as the member depth increased and as a measure of the member axial strain increased. He found that when shear reinforcement was well-distributed across the width of a wide member, the shear stress at failure was in good agreement with the shear capacity models. In contrast with Hsiung and Frantz (1985), Lubell (2006) concluded that the shear capacity decreases as the transverse spacing of stirrup legs increases, as Serna-Ros et al. (2002) and Zheng (1989) concluded before. On the study of Lubell (2006), a limit on the spacing over the width was proposed as the lowest of  $d$  (effective-depth), every 4th longitudinal reinforcing bar in a layer, or 600mm. He also found that the shear capacity of members with and without web reinforcement decreased as the partial-to-full width ratio decreased.

Early investigation conducted on wide RC members was in 2009 by Lubell et al. (2009a), which explained the behaviour of wide beams on shear and was described in this review. Their study was designed to examine the relationship between one-way shear capacity and transverse stirrup-legs spacing across the member width. Their primary objective was to establish appropriate spacing limits for which the existing ACI318 modified truss model for sectional one-way shear would produce safe predictions of member capacity. The research focused on members with shear reinforcement ratios close to the ACI318 minimum requirements, consistent with the relatively low levels of shear stress that would typically be encountered in wide members within building-type structures.

Lubell et al. (2009a) tested 13 reinforced concrete, wide beams, and slab strips under a three-point loading system. Experiments were conducted as part of larger study on shear in wide RC members which was related to the reference of Lubell (2006). The specimens were divided into two different Series (AW and AX). In this investigation, shear reinforcement spacing was a primary test variable. The AW series included seven specimens while the AX series included six specimens. The specimens were contained web reinforcement ratios consistent with the relatively low levels of shear stress. All specimens had the same shear-span to effective-depth ( $a/d$ ) ratio of 3.65. The seven specimens in the AW series were loaded and supported with either narrow or full width plates. Four of these seven specimens were loaded and supported with narrow supports via 305 x 305 mm steel plates. The other three specimens were loaded and supported with wide supports by full-width plates. Five specimens were with shear reinforcement, had stirrups spaced at 300mm along the member length ( $SL = 0.59d$ ), and contained four stirrup legs across the member width (two legs were near the specimen edges and two legs were concentrated within a central column-strip); while two specimens were without shear reinforcement. The arrangement with four stirrup legs across the width resulted in a stirrup clamping stress parameter, ( $v = A_v.f_{yv}/b_w.SL$ ), only 69% as great as that produced by the two-stirrup-leg arrangements. The seven specimens were constructed to nominal dimensions of 1170mm width, 590mm total height, and 4880mm total length. All seven specimens had the same longitudinal reinforcement, resulting in a  $\rho_s$  ratio of 1.68%. The six specimens in the AX series were all loaded and supported with full width plates. Five specimens were with shear reinforcement, had stirrups spaced at 175mm along the member length ( $SL = 0.61d$ ) and contained either two, or three, or four stirrup legs across the member width; while one specimen was without shear reinforcement. The six specimens were constructed to nominal dimensions of 700mm width, 335mm total height, and 2800mm total length. The study showed that the trends of decreased stirrup

efficiency and decreased  $V_{test}/V_n$  for increased  $S_w/d$  in their recent test programme were similar, regardless of the load or support condition. The study proposed new guidelines for the maximum transverse spacing of shear reinforcement to ensure adequate safety of wide members designed using the ACI318 truss model for one-way shear. The following conclusions were the main outcomes concluded from the investigation of Lubell et al. (2009a) on the influence of shear strength from shear reinforcement configurations in wide RC members:

1. The effectiveness of the shear reinforcement decreases as the transverse stirrup-legs spacing increases.
2. The use of few shear (transverse) reinforcement legs (two stirrup-legs), even when widely spaced up to a distance of approximately  $2d$ , has been shown to decrease the brittleness of the failure mode comparing with a geometrically similar member without shear reinforcement.
3. The distribution of strains in the flexural (longitudinal) reinforcement varies across the width of a simply-supported wide member with a central concentrated load. Moreover, this distribution changes from that of typically higher strains in the outer bars at mid-span to higher strains in the middle bars near the supports, where the pattern may be influenced by the support geometry; and
4. To ensure that the shear capacity of all members with shear reinforcement are adequate when designed according to ACI 318-08, the transverse stirrup-legs spacing should be limited to the lesser of a) the effective member depth,  $d$ ; and b) 600mm. Lubell et al. (2009a) recommended that these limits should be reduced by 1/2 when the nominal shear stress ( $v_n$ ) exceeds  $0.42\sqrt{f_c}$  MPa.

Early investigation on wide reinforced concrete beams was conducted in 2012 by Shuraim. He tested 16 continuous wide, shallow, RC beams 700mm wide and 180mm high ( $b_w/h = 3.88$ ), with different web reinforcement configurations (shear stress,  $v = A_v.f_{yv}/b_w.S_L \approx 1.07$  MPa to 1.77 MPa). The main variable of the tests was to study the influence of transverse stirrup configurations on the shear strength of wide beams. His results showed that the stirrup efficiency and shear strength of four stirrup legs is better than that efficiency and strength of two stirrup legs at the same amount of stirrups, as well that the shear strength of closed stirrups is better than that strength of partially closed stirrups and then it is better than the shear strength of open stirrups. Shuraim (2012) concluded that the transverse stirrup-legs spacing ( $S_w$ ) should be taken into the consideration to determine the shear strength resisted by stirrups ( $V_s$ ); where his results showed that the shear capacity decreased as the transverse stirrup-legs spacing ( $S_w$ ) increased and as the longitudinal stirrup-legs spacing ( $S_L$ ) increased. He also concluded that shear capacity predictions using the ACI318 model could be improved by adjusting the shear reinforcement

fraction ( $V_s$ ) of the total one-way shear capacity by replacing a new equivalent stirrup spacing ( $S_{eq}$ ) instead of the longitudinal stirrup-legs spacing ( $S_L$ ) for computing purposes only, where  $S_{eq}$  depends on the ratios of  $(S_L/d)^{0.25}$  and  $\sqrt{(S_L*S_w)}$ , where  $S_L$  and  $S_w$  represent the spacing of the web reinforcement legs in the longitudinal and transverse directions, respectively. Shuraim (2012) developed a shear strength model to account for the effect of longitudinal and transverse stirrup-legs spacing on the one-way shear strength of wide beams. His model is described in the next Chapter and compared with the proposed Prediction-Model developed in the present study. Further, the effect of longitudinal and transverse spacing of stirrup legs is taken into the consideration in the present study for developing a proposed Prediction-Model (see Chapter 6) (Alluqmani, 2013a). In addition, Shuraim (2012) suggested a proposed Equation to determine the transverse stirrup-legs spacing ( $S_w$ ). This Equation is discussed later in Chapter 8 when the proposed Design-Model is being developed.

A recent experimental investigation on shallow wide reinforced concrete beams was conducted by Hanafy et al. (2012). The main objective of the tests was to study the influence of transverse shear reinforcement on the shear strength of shallow wide beams. The concrete compressive strengths (with  $f_{cu}$  of 40 MPa and 90 MPa) and the amount, configuration and spacing of shear reinforcement were the main parameters considered in their study. They tested 12 simply-supported reinforced concrete wide beams under a four point-loading system. The specimens had 500mm wide and 250mm high ( $b_w/h = 2.0$ ), with different web reinforcement configurations (shear stress,  $v = A_v.f_{yv}/b_w.S_L \approx 0.50$  MPa to 1.93 MPa). The beams tested in this investigation may be considered as T-Sectioned wide beams (Figure 3.4). All wide beams failed in shear. Their results showed that the shear reinforcement significantly improved the shear capacity and the ductility of the shallow wide beams. The shear strength of wide beam specimens increased as the stirrup legs spacing decreased. This observation, concluded by Hanafy et al (2012)'s tests, is linked with the conclusions made by Lubell et al. (2009a), Lubell (2006), Serna-Ros et al. (2002), Shuraim (2012), Anderson and Ramirez (1989) and Zheng (1989), and is contradictory with the conclusions made by Hsiung and Frantz (1985), and Leonhardt and Walther (1964). They concluded that the contribution of shear strength resisted by stirrups cannot be ignored in wide RC beams. The results also showed that the shear strength of wide beams increases as the concrete compressive strength increases. Hanafy et al. (2012) compared the experimental results with five design Codes. All Codes compared in their study appeared their deficiencies to predict the strengths of wide RC beams. It can be concluded that all current design Codes do not treat, and are not safe, with wide RC beams.

Finally, it can be concluded based on the investigations conducted in regards to study the effect of stirrup legs spacing on the strengths of wide beams as discussed in Section 3.6 that the strengths of wide RC beams decrease as the stirrup legs spacing increase (Figures 3.5 and 3.6) (Alluqmani, 2013a).



**Figure 3.4:** Wide Beams Tested by Hanafy et al. (2012), they may be considered as T-Sectioned Wide Beams.

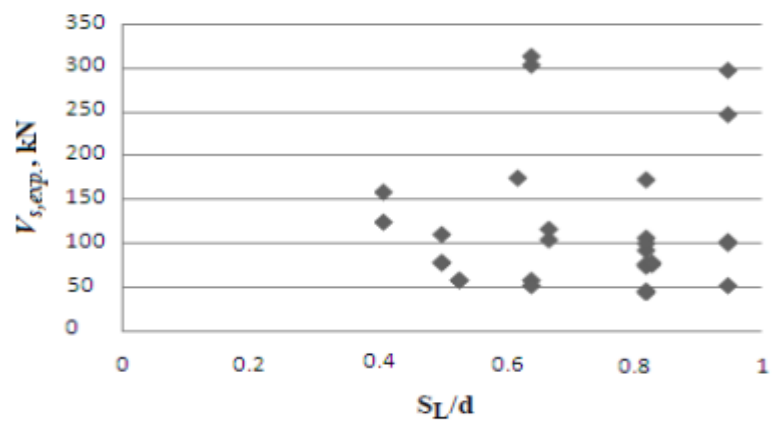


**Figure 3.5:**  $V_{s,exp.}$  versus  $S_L/d$ .

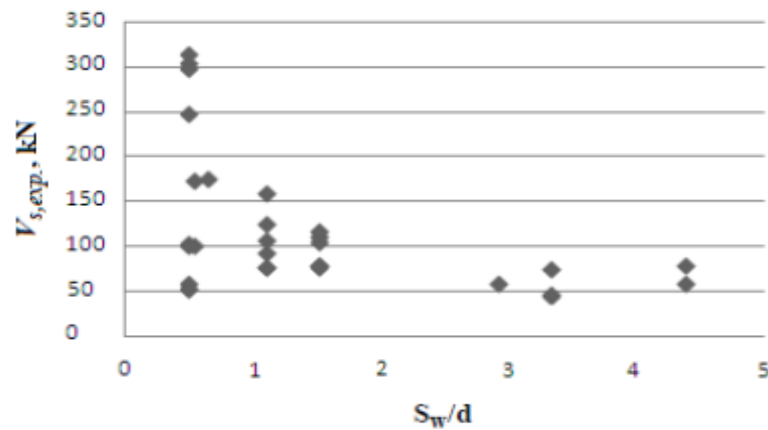


**Figure 3.6:**  $V_{s,exp.}$  versus  $S_W/d$ .

### 3.7 Influence of Support and/or Load Width

The influence of load and support widths (bearing plate widths) has been studied by several researchers (Lubell et al., 2008; Lubell et al., 2009a; Lubell, 2006; Serna-Ros et al., 2002; Al.Dywany, 2010; Regan and Rezai-Jorabi, 1989; Leonhardt and Walther, 1964; Diaz de Cossio, 1962) and methods to account for their influence in capacity models have been provided (Lubell et al., 2008; Serna-Ros et al., 2002).

A number of studies have directly examined the influence of support and load widths to the overall width of wide members on the shear strength of wide RC members.

Current research based on experimental tests was conducted on the behaviour of wide RC beams in 2010 by Al.Dywany, which explained behaviour of wide beams on shear and was described in this review. He tested ten wide beam specimens under four-point loading system with full-width loads and various support widths in two groups (Groups A and B). All specimens had the same dimensions of 2400mm long (with clear span of 2200mm), 750mm width, 250mm height ( $b_w/h = 3.0$ ), and effective depth ( $d$ ) of 210mm; the same flexural reinforcement ratio ( $\rho_s$ ) of 1.293%; the same shear span ( $a$ ) of 630mm; and the same shear span to effective-depth ( $a/d$ ) ratio of 3.0. Group A had five specimens without shear-reinforcement, while group B had five specimens with shear-reinforcement. The main objective of the tests was to study the effect of the support width ( $b_s$ ) on the shear strength of wide RC beams, where  $b_s$  was equal to the quarter (0.25), the half (0.50), or the full (1.00) width of the beam width. It should be noted that all specimens with shear-reinforcement in Group B were reinforced with stirrups in the both shear spans only, where the mid-span of the beams between the two concentrated loads did not contain stirrups. Two beams with narrow-width supports in each group (RA1/2 and RA1/4, and RB1/2 and RB1/4) were detailed with concentrating of portions of their flexural reinforcing bars to be distributed within the effective support widths. Al.Dywany (2010) used Equations (3.1) and (3.2) to estimate the concentrating flexural reinforcing bars distributed within the effective support width ( $\rho_s$ ) and the effective support width ( $w_s$ ), respectively; where  $A_s$  is the total amount of flexural tensile reinforcement,  $b_s$  is support width,  $b_w$  is beam width,  $h$  is the overall-depth of the beam and  $d$  is the effective-depth of the beam.

$$\rho_s = A_s * \sqrt{\left(\frac{b_s}{b_w}\right)} \quad (3.1)$$

$$w_s = \left[ \frac{(h - d) * (b_w - b_s)}{h} \right] + b_s \quad (3.2)$$

Finally, all specimens tested by Al.Dywany (2010) failed in shear with diagonal cracks occurred in the left shear span of the beams and reached to the compression concrete region, where for specimens supported with narrow-width supports (Figure 3.7), additional cracks also occurred on the centre of the beam width, reached to the top face of the beam and were stopped by the loading plate. Al.Dywany (2010) reported the following conclusions from his investigation on the behaviour of wide concrete beams:

- 1) The support width had no effect on the shear strength of wide RC beams without shear-reinforcement.
- 2) The narrow support width reduced the efficiency of the shear stirrups by 80% for those wide RC beams included shear-reinforcement.
- 3) Concentrating the flexural reinforcement within the effective support width ( $\rho_s$ ) using Equations (3.1 and 3.2) had no significant effect in increasing the shear strength of wide RC beams without shear-reinforcement; while in wide RC beams with shear-reinforcement, concentrating the flexural reinforcement within the effective support width ( $\rho_s$ ) using Equations (3.1 and 3.2) increased the efficiency of the shear stirrups to 100%.

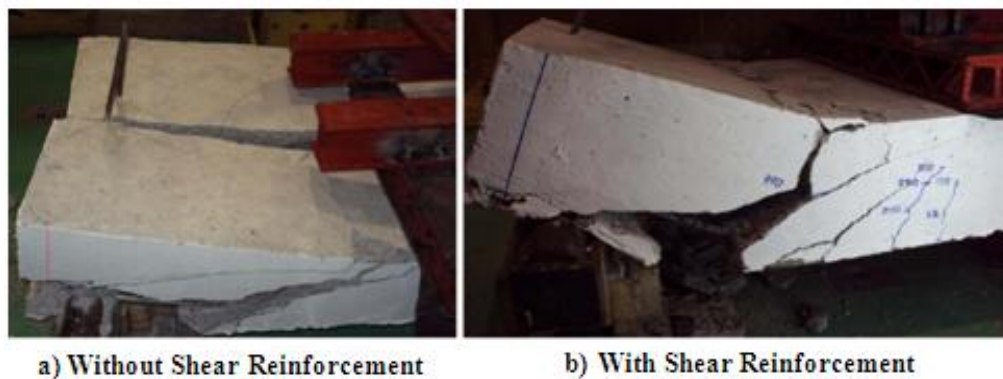


**Figure 3.7:** Failures of Typical Wide RC Beams Tested by Al.Dywany (2010) with Full-Width Loads and Narrow-Width Supports.

Equations (3.1) and (3.2) were undertaken to evaluation in the present study and were studied in Chapter 8 in accordance with the proposed Detailing-Approach (Alluqmani, 2013a). Equation (3.1) was investigated in Chapter 9 for  $N_{w_s}$  which is the concentrating flexural-tensile reinforcing bars distributed within the effective-width of support, where  $w_s$  is the effective-width of support. While Equation (3.2) was developed in Chapter 8 to be suitable for all cases of wide

RC members for estimating the effective-width of support ( $w_s$ ). Similar to  $N_{w_s}$  and  $w_s$ , two Equations were developed in the present study in Chapter 8 related to the proposed Detailing-Approach for estimating  $N_{w_p}$  and  $w_p$ , which are the concentrating flexural-compression reinforcing bars distributed within the effective-width of load and the effective-width of load, respectively (Alluqmani, 2013a).  $N_{w_s}$  and  $w_s$ , and  $N_{w_p}$  and  $w_p$  have been adopted and investigated in the present study in accordance with the proposed Detailing-Approach (see Chapters 8 and 9).

Leonhardt and Walther (1964) tested a series of slab strips under four-point loading, using full-width support conditions. One of the loading plates on the top face of each specimen was equal to the member width (full-width load condition), while the other loading plate was approximately 15% of the member width (narrow-width load condition). Seven out of nine specimens reported to have failed in shear did so on the side with the narrow loading plate. Leonhardt and Walther (1964)'s results showed that the influence of load width was not much greater than typical experimental scatter for the geometries studied.

Serna-Ros et al. (2002) reported on tests of shallow, wide members that did not contain shear reinforcement, in which three specimens had full-width load and support conditions (full-width loads and supports) and one specimen had full-width loads but support widths were each 40% of the member width (full-width loads and narrow-width supports). The specimen with the narrow support conditions had a shear capacity ranging from 85% to 105% of the three companion specimens with full-width conditions, after normalizing the results by the square root of the concrete strength. While in the study of Sherwood et al. (2006), reducing the width of the support to 15% of the member width for specimen AT-2/1000B, reduced the failure load by approximately 5% when compared with specimen AT-2/1000A, which had full-width supports. Serna-Ros et al. (2002) concluded that the support width has influence on the shear strength of wide RC beams, where the shear capacity decreased as the support width was reduced. Serna-Ros et al. (2002) developed a shear strength model to account for the effect of support width on the one-way shear strength of wide beams. Their model is described in the next Chapter and compared with the proposed Prediction-Model developed in the present study. Further, the effect of support and load widths is taken into the consideration in the present study for developing a proposed Prediction-Model (see Chapter 6) (Alluqmani, 2013a), as well as for developing proposed Detailing-Approach and Design-Model (see Chapter 8) (Alluqmani, 2013a; Alluqmani and Saafi, 2014c).



The study of Lubell et al. (2009a), which was discussed in Section 3.6, has also examined the load and support width conditions; where the support or load width, relative to the member width ( $k_s = b_s/b_w$  or  $k_p = b_p/b_w$ , respectively), was one of the variables related to the present study. Lubell et al. (2009a) concluded that the use of narrow bearing plate sizes at the load and support locations reduced the comparable test-to-model predictions ( $V_{test}/V_n$ ).

Lubell et al. (2008) conducted an experimental investigation on the effect of narrow-width supports and loads on the shear capacity of wide beams. Two groups with a total of eight large scale reinforced concrete beams were used. The details of beam specimens are related to the AW and AX specimens tested by Lubell et al (2009a) which were conducted as part of larger study on shear in wide RC members to the reference of Lubell (2006) as mentioned in Section 3.6. In this investigation, the support or load width, relative to the member width ( $k_s = b_s/b_w$  or  $k_p = b_p/b_w$ ), was a primary test variable. The properties and the experimental shear capacities resulted from each specimen are summarized in Table 3.1. The reinforcement and test configurations for each specimen are illustrated in Figure 3.8. All wide beam specimens failed in shear. The test results showed that the shear strength for members without shear reinforcement reduced due decreasing in k value, where k is the lesser of  $k_s = b_s/b_w$  or  $k_p = b_p/b_w$  (where,  $b_s$  is support width,  $b_p$  is load width and  $b_w$  is beam width). For members with shear reinforcement, a reduction in shear strength was due k value, but only for those members had adequate stirrups in which the spacing between the vertical legs does not exceeds the effective-depth of the beam (d), i.e., specimens AW5 and AW7 shown in Table 3.1 and Figure 3.8. On the other hand, in case of specimens AW2 and AW6, with large transverse spacing of the stirrup legs, the peak capacity was only about 2% higher than the corresponding load to cause significant diagonal cracking. Lubell et al. (2008) concluded that the one-way shear strength was moderately decreased as the support and load widths to beam width ( $k_s = b_s/b_w$  and  $k_p = b_p/b_w$ ) ratios were reduced, for both members, without shear reinforcement and with a moderate shear reinforcement ratio. This conclusion is linked with the conclusions made by Lubell et al (2009a) and Serna-Ros et al (2002), and is in contrast with the conclusions made by Al.Dywany (2010) and Leonhardt and Walther (1964). Lubell et al. (2008) developed a shear strength model to account for the effect of support and load widths on the one-way shear strength of wide beams. Their model is described in the next Chapter and compared with the proposed Prediction-Model developed in the present study. Further, the effect of support and load widths is taken into the consideration in the present study for developing a proposed Prediction-Model (see Chapter 6) (Alluqmani, 2013a), as well as for developing proposed Detailing-Approach and Design-Model (see Chapter 8) (Alluqmani, 2013a; Alluqmani and Saafi, 2014c).

**Table 3.1:** Properties and Test Results for Lubell et al. (2008) Specimens with Full-Width (AX) and Narrow-Width (AW) Bearing Plates.

Specimen	$b_w$	$d$	$a/d$	$f'_c$	$\rho$	$\frac{A_s f_y}{b_w s}$	$\kappa$	$V_{test}$	$\frac{V_{test}}{b_w d \sqrt{f'_c}}$
	(mm)	(mm)		(MPa)	(%)	(MPa)		(kN)	
AW4	1168	506	3.66	39.9	1.69	-	0.26	725	0.194
AW8	1169	507	3.65	39.4	1.69	-	1.00	800	0.215
AX8	705	289	3.60	41.0	1.72	-	0.22	274	0.210
AX6	703	288	3.61	41.0	1.73	-	1.00	283	0.218
AW5	1170	511	3.62	34.8	1.67	0.355	0.26	963	0.273
AW7	1170	512	3.61	35.8	1.67	0.355	1.00	1074	0.300
AW2	1172	507	3.65	39.3	1.68	0.514	0.26	818	0.220
AW6	1169	509	3.63	43.7	1.68	0.516	1.00	841	0.213

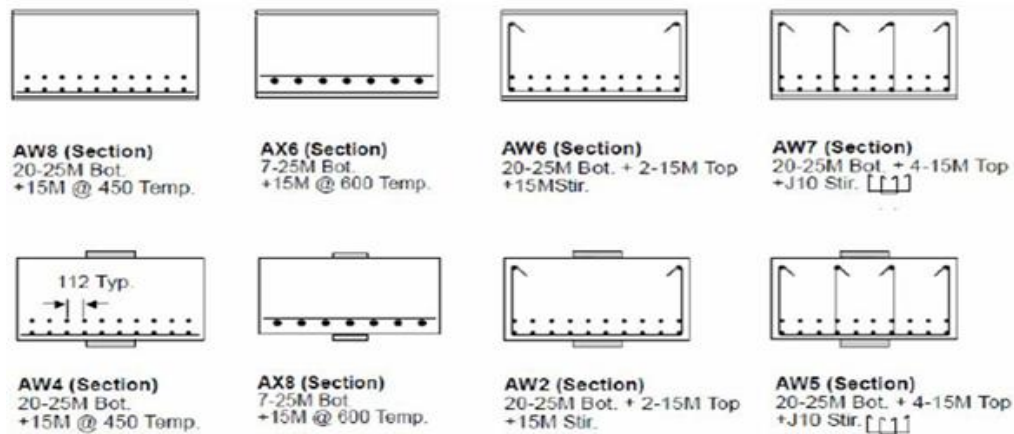


**Figure 3.8:** Configuration of Lubell et al. (2008) Specimens with Full-Width (AX) and Narrow-Width (AW) Bearing Plates.

In the investigation of Lubell et al. (2008), the tops of the diagonal shear cracks extended to pass through the beam mid span when the load plate was partial-width, and stopped at the face of the loading plate at failure when the load was full-width, as shown in Figure 3.9. No significant differences observed in the force required to cause flexural cracking due to the decrease in  $k$  value. A significant difference in performance was related to the crack pattern on the side faces of the members. For specimens when a wide loading plate was used, the diagonal shear cracks ended at the edge of the loading plate; but, when a narrow loading plate was used, the top of the flexure-shear crack extended past the centreline of the specimen (Figure 3.9). In some cases, this extended crack joined to the flexure-shear crack propagating from the adjacent shear span, where the difference in crack extent is explained by the lack of confining pressure in the latter case (case of narrow-width load), which allows tensile splitting cracks to form.

Finally, it can be concluded based on the investigations conducted in regards to study the effect of support and loads widths on the strengths of wide beams as discussed in Section 3.7 that the

strengths of wide RC beams decrease as the support- and/or load- widths are reduced (Figures 3.10 to 3.16) (Alluqmani, 2013a)

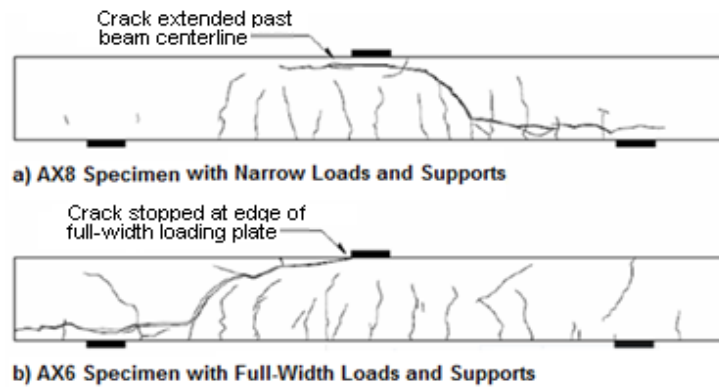


**Figure 3.9:** Crack Patterns after Failure for Lubell et al. (2008) Specimens: a) AX8 Specimen with Narrow-Width Bearing Plates; and b) AX6 Specimen with Full-Width Bearing Plates.

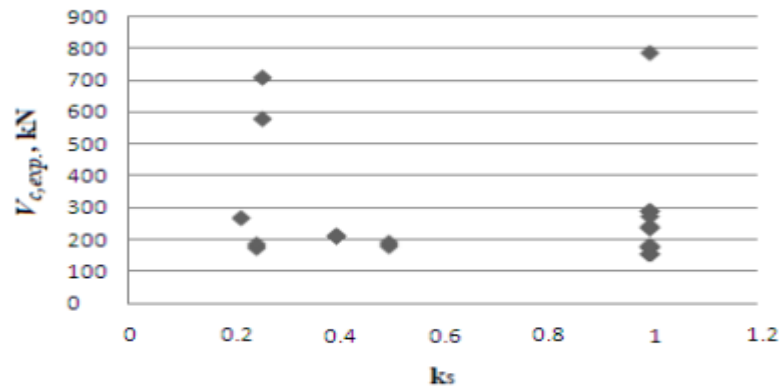


**Figure 3.10:**  $V_{c,exp.}$  versus  $k_s$ .

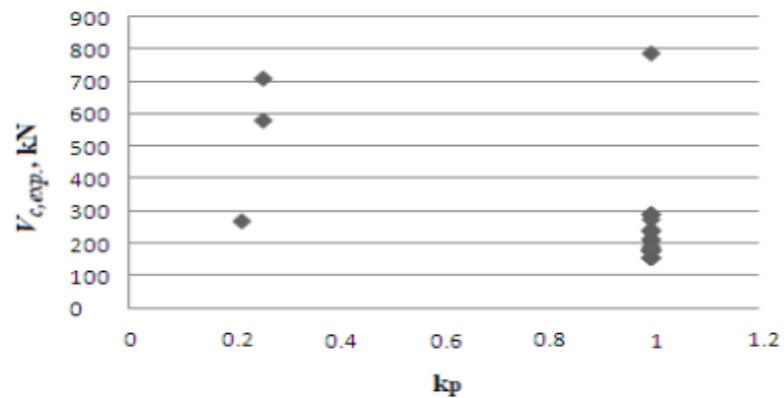


**Figure 3.11:**  $V_{c,exp.}$  versus  $k_p$ .

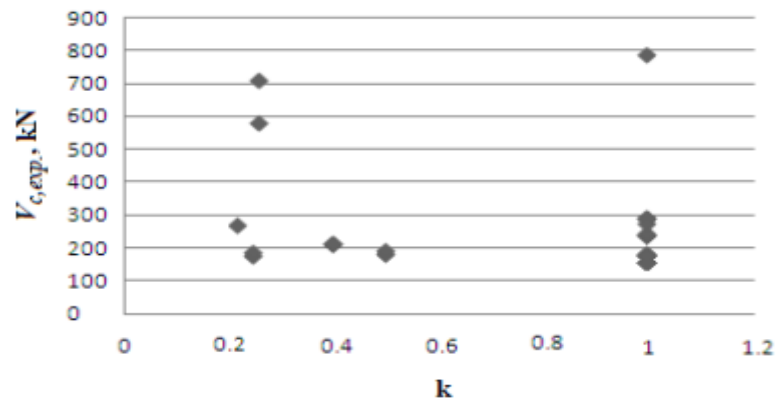


**Figure 3.12:**  $V_{c,exp.}$  versus  $k$ .

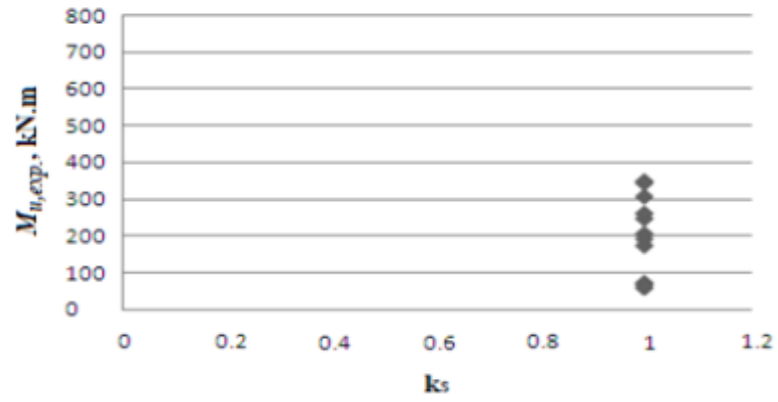


Figure 3.13:  $M_{n,exp.}$  versus  $k_s$ .

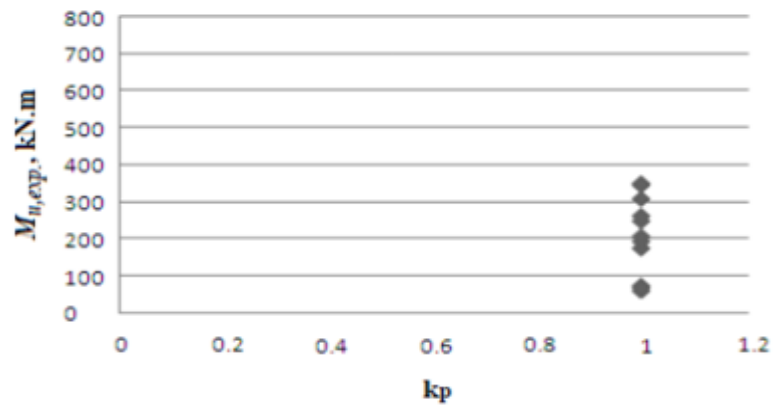


Figure 3.14:  $M_{n,exp.}$  versus  $k_p$ .

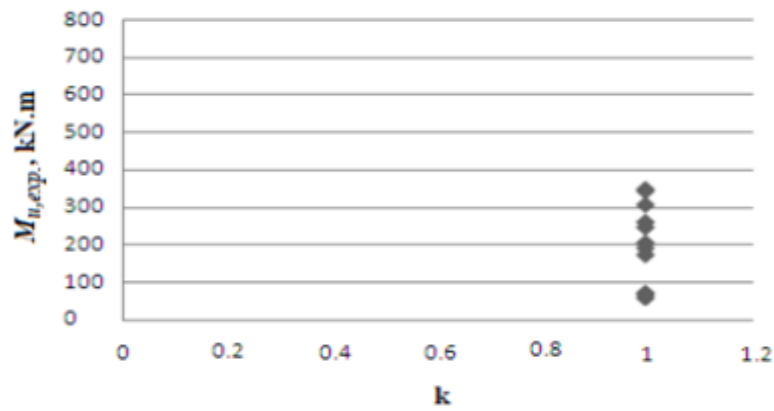


Figure 3.15:  $M_{n,exp.}$  versus  $k$ .

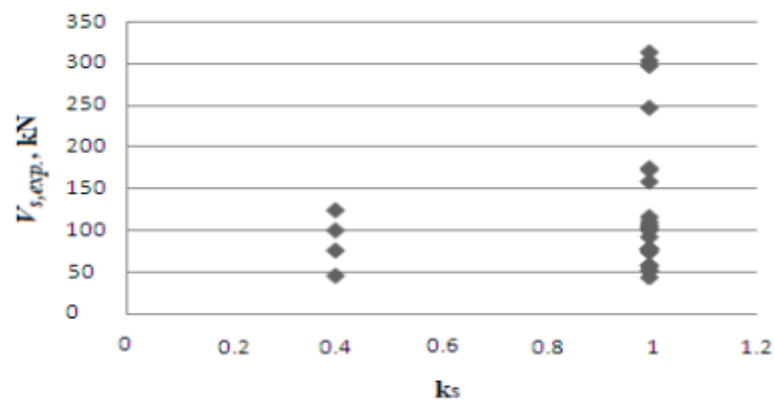


Figure 3.16:  $V_{s,exp.}$  versus  $k_s$ .

### 3.8 Cases of Support and Load Width Conditions

There are six cases relating to the influence of the load and support width conditions to the behaviour of wide concrete beams. Four types of these cases were previously investigated on the behaviour of wide RC beams. On the other hand, two types of these cases were not investigated; where they are considered as important cases affecting the behaviour of wide RC beams especially take into the consideration the effect of punching shear. Differences in the crack patterns after failure were observed among the wide beam specimens previously tested with different ratios of load and support widths to wide-beam width. The cases related to the effect of the load and support width conditions on the behaviour of wide concrete beams are summarised in Sections 3.8.1 to 3.8.6 as follows (Alluqmani and Saafi, 2014b):

#### 3.8.1 Case 1: Full-Width Load and Full-Width Support [ $b_p/b_w = b_s/b_w = 1.00$ ]:

This case was investigated for wide concrete beams with and without shear reinforcement either under three-pint loading system in some previous published researches (Lubell et al., 2008; Lubell et al., 2009a; Lubell et al., 2009b) using  $b_w/h$  ratio of 2.0, or under four-point loading system in one previous published research (Serna-Ros et al., 2002) using  $b_w/h$  ratio of 3.0, and in one previous unpublished research (Al.Dywany, 2010) using  $b_w/h$  ratio of 3.0. In these investigations, the beams failed in shear, the possibility of occurring the punching shear failure was not studied.

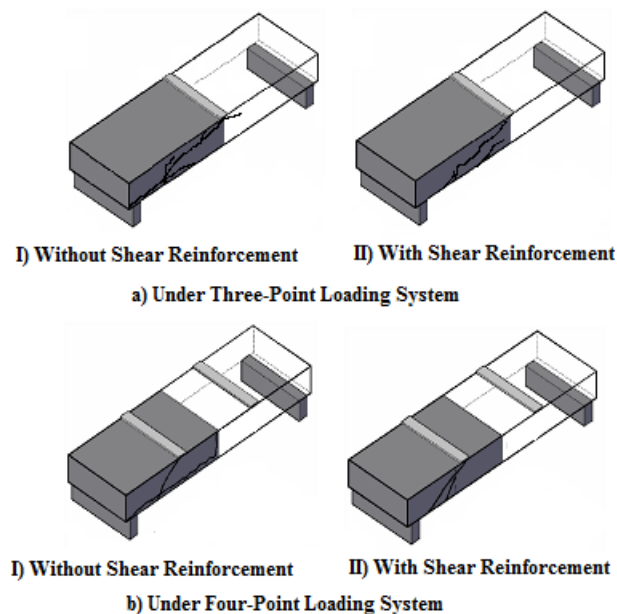


**Figure 3.17:** Failure Mode of Wide Concrete Beams for Case 1 of Support and Load Widths.

Figure 3.17 shows a summary of the failure mode occurred for this type of the load and support case. This case is investigated in the present study based on laboratory work for the beams in Type (A).

**3.8.2 Case 2: Narrow-Width Load and Narrow-Width Support (Both are equal) [ $b_p/b_w = b_s/b_w < 1.00$ ]:**

This case was investigated for wide concrete beams with and without shear reinforcement under three-point loading system only in some previous published researches (Lubell et al., 2008; Lubell et al., 2009a; Lubell et al., 2009b) using  $b_w/h$  ratio of 2.0, and  $b_s/b_w$  ratio =  $b_p/b_w$  ratio of either 0.22 or 0.26. In these investigations, the beams failed in diagonal shear, the possibility of occurring the punching shear failure was not studied where it is very important in this type of load and support case. The well-distributed and concentrating of the flexural tensile steel bars and transverse stirrup legs within the support width were not studied in these investigations, where it is considered an important details affecting the shear behaviour of wide concrete beams. On the other hand, the concentrating of flexural compressive (hanger) steel bars within the load width was not studied in these investigations. Figure 3.18 shows a summary of the failure mode occurred for this type of the load and support case. It should be emphasised that all investigations, which were conducted for this type of load and support width case, were tested with load widths are equal to the support widths, where it is important to change the both widths to check the behaviour of wide concrete beams under punching shear. This type of load and support case may need to further investigations in regards to the behaviour of wide RC beams under a four point-loading system. This case is investigated in the present study based on laboratory work for the beams in Type (B) at  $b_p/b_w = b_s/b_w = 0.50$ .

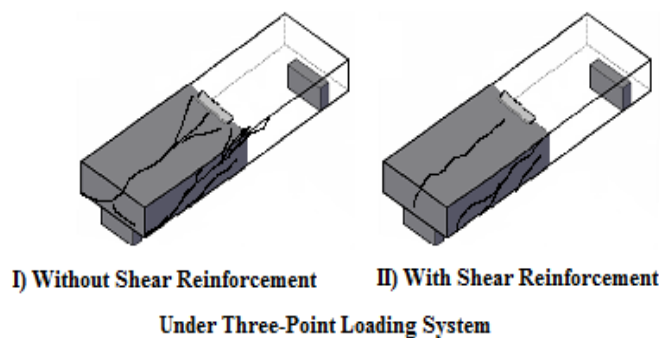


**Figure 3.18:** Failure Mode of Wide Concrete Beams for Case 2 of Support and Load Widths.

### 3.8.3 Case 3: Narrow-Width Load and Full-Width Support [ $b_p/b_w < 1.00$ , $b_s/b_w = 1.00$ ]:

This case was not investigated for wide concrete members, but it was investigated for slab strips under four-point loading system only in one previous published research (Leonhardt and Walther, 1964) using  $b_p/b_w$  ratio of 0.15 for one load plate, where the other load plate was with full-width condition. In this investigation, the beams failed in diagonal shear on the side with the narrow loading plate, the possibility of occurring the punching shear failure was not studied where it may be important in this type of load and support case. The concentrating flexural compressive (hanger) steel bars within the load width was not studied in this investigation. Figure 3.19 shows a summary of the failure mode occurred for this type of the load and support case. It should be emphasised that in this investigation, which was conducted with narrow-width loads and full-width supports, the beams did not fail under punching shear. This type of load and support case may need further investigations in regards to the behaviour of wide RC beams under a three point-loading system.

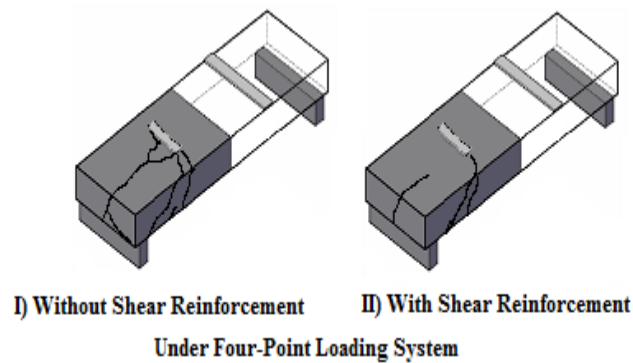
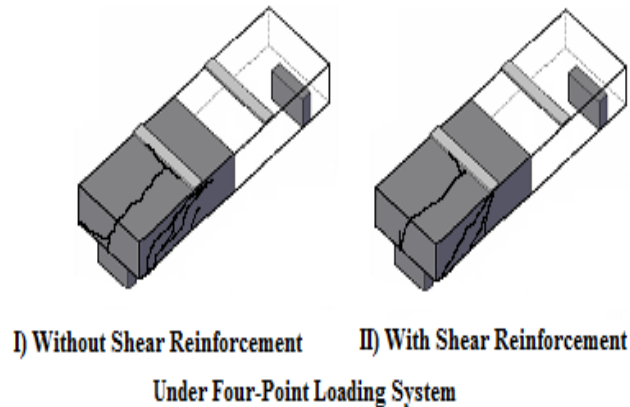


Figure 3.19: Failure Mode of Wide Concrete Beams for Case 3 of Support and Load Widths.

### 3.8.4 Case 4: Full-Width Load and Narrow-Width Support [ $b_p/b_w = 1.00$ , $b_s/b_w < 1.00$ ]:

This case was investigated for wide concrete beams with and without shear reinforcement under four-point loading system only in one previous published research (Serna-Ros et al., 2002) using  $b_w/h$  ratio of 3.0, and  $b_s/b_w$  ratio of 0.40, and in one previous unpublished research (Al.Dywany, 2010) using  $b_w/h$  ratio of 3.0, and  $b_s/b_w$  ratio of 0.25, or 0.50. In these investigations, the beams failed in diagonal shear, the possibility of occurring the punching shear failure was not studied where it is very important in this type of load and support case. The well-distributed and concentrating of the flexural tensile steel bars and transverse stirrup legs within the support width were studied in the investigation of Al.Dywany for two beams only. Figure 3.20 shows a summary of the failure mode occurred for this type of the load and support case. It should be

emphasised that in this investigation, which was conducted with full-width loads and narrow-width supports, the beams did not fail under punching shear. The stirrups distributed along the member lengths were concentrated in the both shear spans only, where in the distance between the two loads the stirrups were not provided. Also, the stirrups distributed across the member widths were two separated closed stirrups connected with Z-legs (the same configuration for all specimens). This type of load and support case may need further investigations in regards to the behaviour of wide RC beams under a three point-loading system.



**Figure 3.20:** Failure Mode of Wide Concrete Beams for Case 4 of Support and Load Widths.

### 3.8.5 Case 5: Narrow-Width Load and Narrow-Width Support (Support is wider than load) [ $b_p/b_w < 1.00$ , $b_s/b_w < 1.00$ , but $b_s > b_p$ ]:

This case was not investigated for wide concrete beams. In this case, the possibility of occurring the punching shear failure should be studied where it is important in this type of load and support case. This type of load and support case needs to be investigated in regards to the behaviour of wide RC beams under either three or four point-loading system, or both. Therefore, it is necessary to investigate this case of load and support condition for the wide RC beams included in this programme of research. The well-distributed and concentrating of the flexural tensile steel bars and transverse stirrup legs within the effective support width should be studied in this investigation. On the other hand, the concentrating of flexural compressive (hanger) steel bars within the effective load width should be also studied in this investigation. This case is investigated in the present study based on laboratory work for the beams in Type (C) at  $b_p/b_w = 0.25$  and  $b_s/b_w = 0.50$ .



### **3.8.6 Case 6: Narrow-Width Load and Narrow-Width Support (Load is wider than support) [ $b_p/b_w < 1.00$ , $b_s/b_w < 1.00$ , but $b_p > b_s$ ]:**

This case was not investigated for wide concrete beams. In this case, the possibility of occurring the punching shear failure should be studied where it is important in this type of load and support case. This type of load and support case needs to be investigated in regards to the behaviour of wide RC beams under either three or four point-loading system, or both. Therefore, it is necessary to investigate this case of load and support condition for the wide RC beams included in this programme of research. The well-distributed and concentrating of the flexural tensile steel bars and transverse stirrup legs within the effective support width should be studied in this investigation. On the other hand, the concentrating of flexural compressive (hanger) steel bars within the effective load width should be also studied in this investigation. This case is investigated in the present study based on laboratory work for the beams in Type (D) at  $b_p/b_w = 0.50$  and  $b_s/b_w = 0.25$ .

### **3.9 Effect of Flexural Reinforcement Ratios on Wide RC Beam Capacities**

The influence of flexural reinforcement ratios has been studied by several researchers (Lubell et al., 2009b; Lubell, 2006; Al-Harithy, 2002).

A small number of studies have directly examined the influence of flexural reinforcement ratios on the flexural and shear strengths of wide RC members.

It is believed that the both shear and flexural strengths of a beam increase with increasing in longitudinal flexural reinforcement ratio. It was concluded (Bukhari and Ahmad, 2007) that the beam strengths increase with increasing of the longitudinal reinforcement ratio; however, the relative flexural strength decreases. The flexural strength and mode of failure were also observed to be dependent on longitudinal flexural reinforcement ratio. The tests made by Bukhari and Ahmad (2007) showed that, at constant  $a/d$  ratio, the failure load increased with increasing in longitudinal flexural reinforcement ratio. Batchelor (1981) confirmed a strong relationship between longitudinal steel ratio and cracking shear in lightly reinforced concrete beams having main steel ratio ( $\rho_s$ )  $< 0.015$ . Berg (1962) found a highly significant correlation between the nominal shear strength ( $v_n$ ) and the tension reinforcement ratio ( $\rho_s$ ). Ahmad and Lue (1987) carried out a research and found that for very low reinforcement ratios, the flexural capacity is smaller than shear capacity, and that for constant shear-span to effective-depth ( $a/d$ ) ratio, the

relative flexural strength ( $M_u/M_f$ ) increases as the tensile reinforcement ratio ( $\rho_s$ ) decreases. Taylor (1960) found increase in diagonal cracking load for a beam with increase in the amount of longitudinal reinforcement. In other research work (Bukhari and Ahmad, 2007; Mathey and Watstein, 1963), it was observed that reduction in tensile steel ratio in comparable beams, resulted in lower shear strength and higher steel stresses.

Al-Harithy (2002) tested 12 wide RC beams with 800mm wide and 200mm high ( $b_w/h = 4.0$ ), with the same shear reinforcement configurations (shear stress,  $v = A_v.f_{yv}/b_w.SL \approx 1.27$  MPa). The main variable of the tests was to study the influence of flexural (tensile and compression) reinforcement ratios ( $\rho_s$  and  $\rho_s'$ ) and concrete compressive strength ( $f_c$ ) on the flexural strength and deflection of wide RC beams. His results showed that the  $f_c$  had more influence on the cracking moment than the flexural reinforcement ratios; and that the flexural reinforcement ratios had an obvious influence on the yielding and ultimate moments of wide beams. Moreover, test results showed that the  $f_c$  had little effects on the deflection of wide beams, even though many mechanical properties were enhanced such as modulus of elasticity, modulus of rupture and split tensile strength of concrete. However, it was noted that an unfavorable characteristic of concrete, which was "brittleness", increased as  $f_c$  increased. In addition, the displacement ductility ( $\mu_d = \Delta_u/\Delta_y$ ) increased with increasing of  $f_c$  up to a certain limit, after which it decreased with increasing of  $f_c$ . On the other hand, his test results showed that the flexural reinforcement ratios had a significant influence on the mid-span deflection due to the relationship between the flexural rigidity ( $EI$ ) and the amount of reinforcement ( $A_s$  and  $A_s'$ ). For low reinforcement ratio, the top steel exhibited tensile strain at or near the yield moment for all beams regardless of their  $f_c$  values. The displacement ductility decreased as the flexural reinforcement ratios increased. In the scope of the present study, the results obtained by Al-Harithy (2002) investigation showed that the ultimate flexural strength ( $M_u$ ) of wide RC beams decreased as the flexural (tensile and compression) reinforcement ratios ( $\rho_s$  and  $\rho_s'$ ) decreased.

Early study based on experimental tests was conducted in 2009 by Lubell et al. (2009b). Their study was carried out on slender shear-critical wide RC members with variation in flexural reinforcement ratio ( $\rho_s$ ). The details of beam specimens are related to the AW and AX specimens tested by Lubell et al. (2009a) which were conducted as part of larger study on shear in wide RC members to the reference of Lubell (2006) as mentioned in Section 3.6. All wide beam specimens failed in shear. The results of four experimental tests on wide RC members (without stirrups) with variation in reinforcement ratio are illustrated in Table 3.2 to study the effect of flexural reinforcement ratio on the shear capacity of members without shear reinforcements.

From their results shown in Table 3.2, a significant increasing in the shear capacity was noted as the flexural reinforcement ratio increased, even through specimens with narrow-width or full-width supports, due increasing in dowel action. The experiment observed that as the flexural reinforcement ratio decreased, the flexural cracking load was observed to decrease slightly, where after the flexural cracking, the members with lower reinforcement ratios exhibited lower flexural stiffness and increased deflection at failure, and hence, the member with smaller flexural reinforcement ratio had a lower magnitude of shear stress at failure. Comparison with related published data were arranged by Lubell et al. (2009b) in a graph, showing the shear capacity of members without shear reinforcements is influenced by both the member depth ( $d$ ) and the flexural reinforcement ratio ( $\rho_s$ ). It is clear from the investigation conducted by Lubell et al. (2009b) that the wide beam strength decreased as the flexural reinforcement ratio decreased.

**Table 3.2:** Four Wide RC Members without Stirrups Tested by Lubell et al. (2009b) with Variation in Steel Ratio.

Specimen	$b_w$ (mm)	$d$ (mm)	$h$ (mm)	$L$ (mm)	$a/d$	$\rho$ (%)	$f'_c$ (MPa)	$\kappa$	$V_u$ (kN)
AX7	704	287	335	2,080	3.62	1.04	41.0	1.00	249
AX6	703	288	338	2,080	3.61	1.73	41.0	1.00	281
AW1	1,170	538	590	3,700	3.44	0.79	36.9	0.26	585
AW4	1,168	506	590	3,700	3.66	1.69	39.9	0.26	716

Finally, it can be concluded based on the investigations conducted in regards to study the effect of flexural reinforcement ratios on the strengths of wide beams as discussed in Section 3.9 that the flexural reinforcement ratios have influence on the ultimate flexural strength ( $M_u$ ) of wide RC beams, and also have influence on the ultimate shear strength ( $V_u$ ), or at best, on the shear strength resisted by concrete contribution ( $V_c$ ) of wide RC beams (Figures 3.21 to 3.24) (Alluqmani, 2013a). Both flexural and shear strengths of wide RC beams have exhibited to decrease as the flexural reinforcement ratios decrease at the same characteristics.

The arrangement of flexural reinforcement in beams are limited for two purposes, improving the compaction of concrete during casting, and minimizing the flexural cracks width at service loading. Where as stated previously, the shear capacity of beams is a function of flexural reinforcement ratio, and since the wide beams have obvious width, therefore, arranging of flexural reinforcement in these beams to enhance or increase the shear strength is possible to serve both the practical and the design requirements, then hence that the beam behaves in a ductile flexural manner. None of the current researchers took into the consideration the effect of flexural reinforcement ratio on the strengths of wide beam when they have developed their

models. The effect of flexural (tensile and compression) reinforcement ratios ( $\rho_s$  and  $\rho_s'$ ) on the strengths of wide RC beams is taken into the consideration in the present study for developing a proposed Prediction-Model (see Chapter 6) (Alluqmani, 2013a), as well for developing a proposed Detailing-Approach (see Chapter 8) (Alluqmani, 2013a; Alluqmani and Saafi, 2014c). Both  $\rho_s$  and  $\rho_s'$  ratios are taken into the consideration to predict the ultimate flexural strength ( $M_u$ ) and the shear strength resisted by concrete contribution ( $V_c$ ).

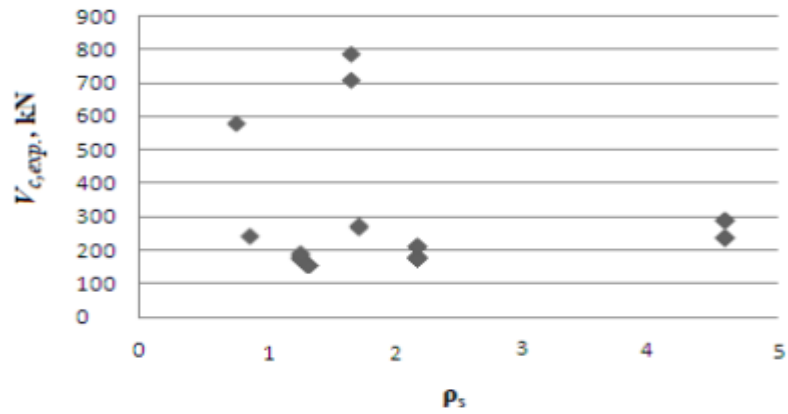


Figure 3.21:  $V_{c,exp.}$  versus  $\rho_s$ .

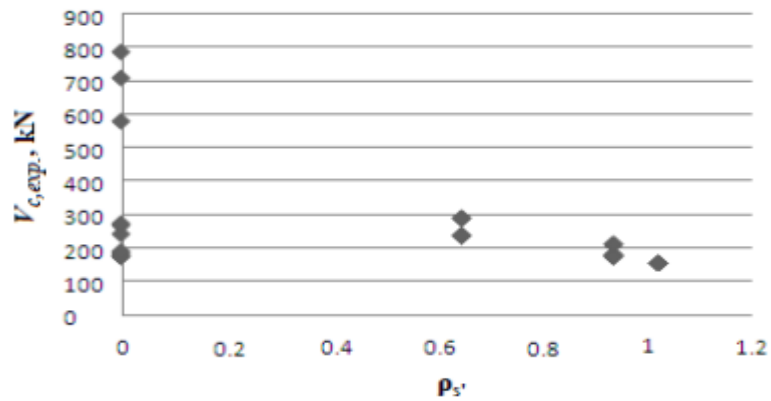


Figure 3.22:  $V_{c,exp.}$  versus  $\rho_s'$ .

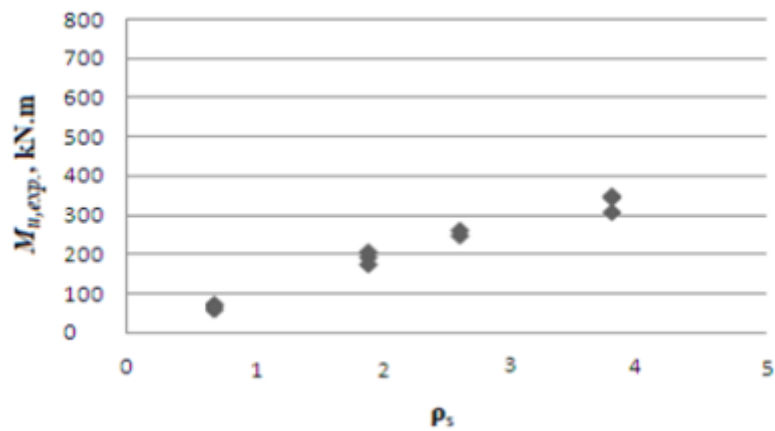
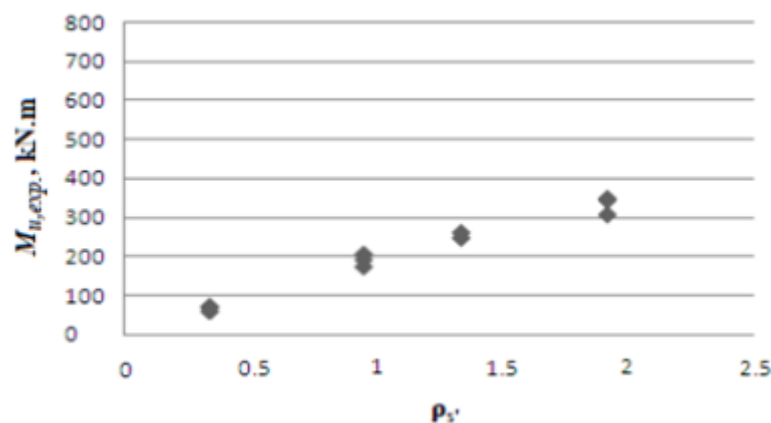


Figure 3.23:  $M_{u,exp.}$  versus  $\rho_s$ .



**Figure 3.24:**  $M_{u,exp.}$  versus  $\rho_s'$ .

### 3.10 Conclusion

The previous investigations conducted on wide RC beams have been discussed in this Chapter. The investigations and discussions showed the effect of support width, load width, longitudinal and transverse spacing of stirrup legs, and flexural -tensile and -compression reinforcement ratios on the strengths of wide RC beams. These factors must be taken into the consideration to develop rational models to predict, detail and design the wide RC beams.

The influence of both support and load widths ( $b_s$  and  $b_p$ ), or at best both ratios of support and load widths to wide beam width ( $k_s = b_s/b_w$  and  $k_p = b_p/b_w$ ), on the ultimate flexural and shear strengths ( $M_u$  and  $V_u$ ) of wide RC beams was clear. In addition, the influence of both longitudinal and transverse spacing of stirrup legs ( $S_L$  and  $S_w$ ) on the ultimate shear strength of wide RC beams ( $V_u$ ) was also clear. This influence had obvious observation on the shear strength resisted by stirrup contribution ( $V_s$ ). On the other hand, the influence of flexural reinforcement ratios ( $\rho_s$  and  $\rho_s'$ ) on the ultimate flexural strength ( $M_u$ ) of wide RC beams, as well on the ultimate shear strength ( $V_u$ ), or at best, on the shear strength resisted by concrete contribution ( $V_c$ ) of wide RC beams, was also clear. All these observations are taken into the account to develop the rational models proposed in this study.

## CHAPTER 4

# DESIGN AND PREDICTION METHODS FOR WIDE BEAMS IN FLEXURE & SHEAR TO THE EXISTING CODES AND MODELS

### 4.1 Introduction

The emphasis in this Chapter has been placed on the methods of determination the shear and flexural strengths assumed by the existing Codes of Practice, such as EC2, ACI318 and SBC304 Codes. The existing prediction Models for prediction the wide RC beam strengths are also discussed in this Chapter. The shortcoming of the existing design Codes and models on the design and prediction of wide RC beams are identified and discussed. All definitions of the parameters and notations used in the provisions of ACI318-and-SBC304 and EC2 Codes are illustrated in this Chapter, and are also included in details in Appendix A.

### 4.2 Wide Structural Concrete Members

Wide RC members are designed as shallow rectangular RC members in terms of flexure and shear, but they have differences in the design of shear (transverse) reinforcement. The basic expressions for flexure and shear design, and serviceability checks (mid-span deflection and flexural crack width) in the provisions of EC2, ACI318 and SBC304 Codes are the same for narrow beams, wide beams, and slabs (Sherwood et al., 2006; Al.Dywany, 2010). However, there is concern that the current provisions can be unconservative when applied to wide beams. As discussed in the literature (Chapter 3), the behaviour of wide RC members fails in shear; therefore, wide beams should be designed for shear to prevent the shear failure and to behave in a ductile manner. Wide beams should have stirrup legs along the length and across the width, which must be more than two legs across the width (Serna-Ros et al., 2002). In wide RC beams, the stirrup-legs spacing along the beam length ( $S_L$ ) may be designed as per the provisions of the current Codes of Practice, but the stirrup-legs spacing across the beam width ( $S_w$ ) should be designed to a logical guide where it is one of the main variables in the present study. According to EC2 Code,  $S_w$  should not exceed  $0.75d$ , while according to Lubell et al. (2009a),  $S_w$  should not exceed  $d$  ( $d$  is the effective-depth of the member). In addition, the ratios of the bearing plate width to the wide beam width should be taken into the consideration to estimate  $S_L$  and  $S_w$ . In

the scope of the present study, the main variables which affect the strengths of wide RC beams with shear reinforcement, are the longitudinal and transverse stirrup-legs spacings ( $S_L$  and  $S_w$ ), and the support and load widths ( $b_s$  and  $b_p$ ) or at the best the ratios of support- and load- width to the beam-width ( $k_s$  and  $k_p$ ). While for the wide RC beams without shear reinforcement, the main variables are the ratios of support- and load- width to the beam-width ( $k_s$  and  $k_p$ ).

In the past, the design was carried out regarding predominantly two major stages of the structure's performance: the Ultimate Limit State (ULS) and the Serviceability Limit State (SLS). Basically, the ULS was checked for static loading. For the control of the SLS, two aspects were controlled: deflection and crack width. Experiences with damage have learned that there has not been sufficient attention for a number of design criteria.

In each instance, the design consists of one or more of the following checks (ACI318-08 Concrete Floor Systems, 2009):

1. Bending of section
2. Minimum reinforcement
3. Beam shear (one-way shear) or two-dimensional problem
4. Punching shear (two-way shear) or three-dimensional problem.

There are actions that contribute to total shear resisting force on cracked wide beam without any shear reinforcement. These actions are summarised as follows:

1. Concrete shear stress in compression zone ( $V_{cz}$ ),
2. Force resulting from aggregate interlock at crack ( $V_{ay}$ ), and
3. Dowel shear from longitudinal flexural reinforcement ( $V_d$ ).

Shear reinforcement allows for maximum utility of tension steel (section capacity is not limited by shear) and ductile failure mode (shear failure is not ductile, it is sudden and dangerous). The configuration of shear reinforcement in wide RC members may be vertical stirrups (also called "ties" or "hoops"), inclined stirrups, or bend up bars. Where the effect of stirrups is as the following cases:

1. Before shear cracking - no effect (web steel is free of stress)
2. After shear cracking, the effect is due to:
  - Resist shear across crack;
  - Reduce shear cracking propagation;

- Confine longitudinal steel - resist steel bond loss, splitting along steel, increase dowel actions;
- Increase aggregate interlock by keeping cracks small.

3. Behaviour of members with shear reinforcement is somewhat unpredictable - Current design procedures are based on:

- Rational analysis;
- Test results;
- Success with previous designs.

#### **4.3 Wide RC Beams in Flexure and Shear**

It is a common design practice to first design a reinforced concrete beam for flexural capacity and then to ensure that any type of failure, other than flexural which would occur when the flexural capacity is attained, is prevented. The flexural capacity is assessed on the basis of the plane sections theory which not only is generally considered to describe realistically the deformational response of the beams, but is also formulated so that it provides a design tool noted for both its effectiveness and simplicity.

It is believed that concrete is a brittle material while reinforcement steel is a ductile material. Therefore, flexural failure (ductile failure), which causes from the reinforcement, should be rather than shear failure (brittle failure) which causes from the concrete. Thus, structural RC elements are designed to fail in a ductile manner by emphasizing on the detailing requirements due to the brittle nature of concrete.

It is common to use reinforcing steel to carry tensile forces and concrete to carry compressive forces in flexural design of structural RC beams. This idea was further developed into the concept of a truss analogy utilizing reinforcing bars as tension ties to carry tensile force and concrete blocks as compression struts to resist compressive forces.

Flexural design provisions are based on the rational assumption that plane sections remain plane, and this assumption has proven to be accurate over a wide range of reinforced concrete flexural elements.

The flexural reinforcement is used in concrete to resist tensile stresses near the tension face, and it does not reinforce the concrete against the diagonal tension stresses that occur elsewhere,



caused by shear alone or by combined effect of shear and flexure; therefore, these stresses attain sufficient magnitudes to open additional tension cracks in the direction perpendicular to the local tension stress, a diagonal shear crack will form in which the failure of beam immediately follows.

The shear design method in EC2 Code is based on the Inclined Strut method which is a method using the theory of plasticity. While the shear design method in ACI318 and SBC304 Codes is based on the Strut-Tie method. Shear in wide RC members, such as wide beams or one-way slabs, subjected to a concentrated load is typically checked in two ways: by calculating the beam shear capacity (one-way shear) over a certain effective width of the support, and by checking the punching shear capacity (two-way shear) on a perimeter around the load.

The philosophy in most current design approaches to shear imposes an artificial separation between the shear and the flexural resistances of beams. The design procedures adopted by Codes of Practice do not relate a given level of moment capacity to a given amount of shear reinforcement. This artificial separation could result in a design that prevents the development of the full moment capacity of a beam. It would therefore be better to determine the optimum amount of shear reinforcement which will ensure attainment of the full moment capacity of a member.

Since shear reinforcement is ineffective in the uncracked beam, the magnitude of the shear force or stress that causes cracking to occur is the same as in a beam without shear reinforcement, hence, each stirrup resists the crack growth by their strength as  $(A_v * f_{yv})$  on a given portion of the beam, and failure will be imminent when stirrups start yielding. Figure 4.1 shows types of cracks in reinforced concrete beams which depend on the magnitude of bending moment ( $M$ ) and shear force ( $V$ ).

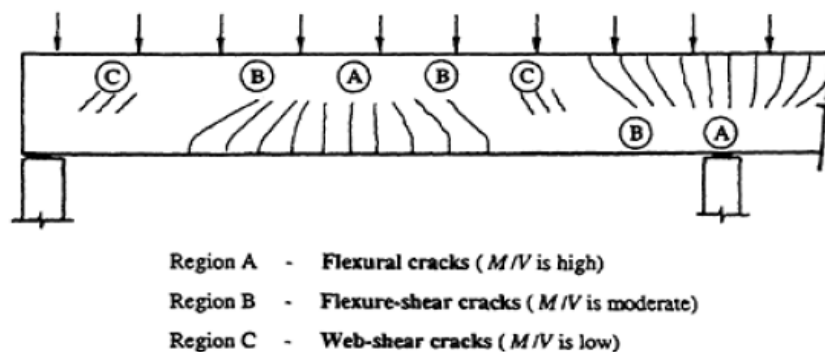


**Figure 4.1:** Types of Cracking in RC Beams, ( $M$  = Bending Moment, and  $V$  = Shear Force).

Ideally, the purpose of the web reinforcement is to increase the strength of the beam, and also, of course, to ensure that shear failure does not occur and that the full flexural capacity can be used. Prior to inclined cracking, the strain in the stirrups is equal to the corresponding strain in the concrete; therefore, the stress in the stirrups prior to inclined cracking will be relatively small. Subsequently, stirrups do not prevent inclined cracks from forming as they come into play only after cracks have formed (Figure 4.2a).

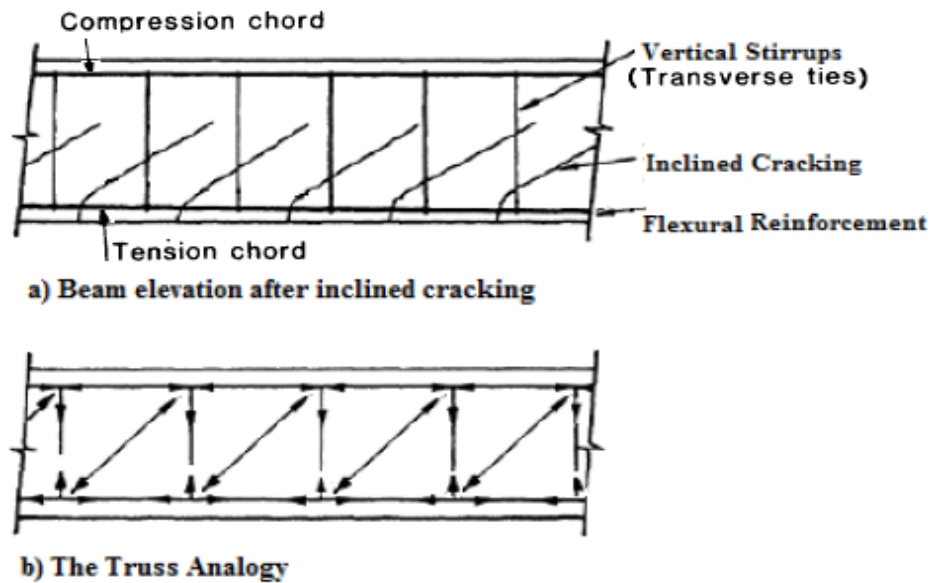


Figure 4.2: A Typical RC Beam Containing Shear Reinforcement.

The truss analogy (Figure 4.2b), which is based on relevant experimental evidence, assumes that inclined cracks form in RC beams at failure. The concrete stress blocks between adjacent cracks would carry the inclined compressive forces and act as diagonal compression struts. This led to the realization that a truss-like action could be achieved through longitudinal reinforcement representing the tensile chord of the truss while the concrete represents the compressive chord on either side of the beam, and then stirrups to provide vertical tension ties joining the adjacent longitudinal chords. Such a truss model analogy has greatly influenced the shear design procedure for determining ultimate shear capacities of structural RC beams throughout the years. Moreover, its visible nature allows it to represent the shear failure mechanism, through which many analytical models have been developed. These models aid in the analysis of deformation and stiffness of structural RC elements. Significant contributions have been made by many researchers to the development of truss models of structural RC beams subjected to flexure and shear.

The absence of shear reinforcement would make the beams very susceptible to accidental large overloads, which would result in catastrophic failures without notice; therefore, it is good practical to provide a minimum amount of shear reinforcement even if calculation does not require, thereby increasing ductility and providing warning in advance of actual failure.

In beams with shear reinforcement, usually, two types of shear reinforcement are used in reinforced concrete beams, namely; web and bent-up reinforcement. The bent-up reinforcement is provided by bending up a part of the flexural reinforcement where it is no longer needed to resist flexural tension. The web reinforcement is widely used and preferred in beams, provided in the form of vertical stirrups, spaced at varying intervals along the axis of the beam depending on the requirements, where in the situation of wide RC beams, these vertical stirrups must be also spaced across the member width.

It was concluded that the diagonal failure of beams occurs primarily as a result of the development of transverse secondary tensile stresses in the concrete compression region of the beam structure (Ziara, 1993). Where ideally, design methods to prevent diagonal failure must be based on the evaluation of the magnitude of the tensile stresses. Unfortunately, the determination of the magnitude of the tensile stresses is difficult (Kotsovos, 1984). Also, there is disagreement between researchers on the significance of transverse tensile stresses on the concrete compressive strength (Kotsovos and Newman, 1977; Gerstle et. al., 1976; Linhua et al., 1991).

When the tension cracks form in the concrete beam, the flexural tension strength is carried by the reinforcement, and higher loads can be carried, hence, shear stresses increase proportionally to the loads. This will lead to that intensive diagonal tension stresses are created in regions of high shear forces, and particularly close to the supports as resulted from the wide beams previously tested.

Web reinforcement has no noticeable effect prior to the formation of diagonal cracks. In fact, the web steel leg of shear reinforcement is practically free stress prior to crack formation. As mentioned before, prior to an inclined cracking, strains in the vertical stirrups are equal to strains in concrete; therefore the stresses in stirrup legs are relatively small. Consequently, the stirrups cannot prevent the shear zone against an inclined crack appearance. While, after inclined cracks occur, stirrups come into play in this region. In a flexural member with stirrups, these cracks will be noted as flexure-shear cracks. The forces in a flexure-shear crack in a beam with stirrups are presented in Figure 4.3 (after MacGregor and Wight, 2005).

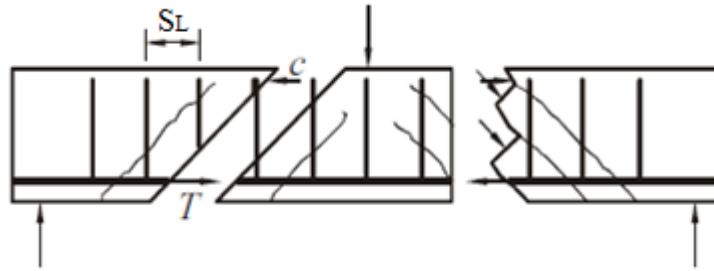


**Figure 4.3:** Inclined Shear Cracks, and Forces in a RC Beam (after MacGregor and Wight, 2005).

After the diagonal cracks have developed, shear reinforcement enhances the shear resistance of beams in four separate ways (Al.Dywany, 2010):

- 1) Part of the shear force is resisted by the bars that traverse a particular crack,
- 2) The presence of these bars restricts the growth of diagonal cracks and reduces their penetration into the compression zone,
- 3) The stirrups also counteract the widening of the cracks, so that the two crack faces stay in close contact, and
- 4) The stirrups are arranged so that they tie the longitudinal reinforcement into the main bulk of the concrete, where this provides some measure of restraint against the splitting of concrete along the longitudinal reinforcement, and increase the share of the shear force resisted by dowel action.

Accordingly, it is important to consider the effect of stirrup legs spacing across the width of wide beams at estimating the ultimate strength of a structural concrete wide member. For all types of loading conditions, the trend is that the strength of a wide member tends to decrease when the stirrup legs spacing across the member width ( $S_w$ ) increase regardless of the load and support widths (Lubell et al, 2008; Lubell et al, 2009a; Shuraim, 2012; Serna-Ros et al, 2002). It is also essential to evaluate the effect of well-distributed flexural reinforcement on the flexural compressive strength of a wide beam. The current experimental data on wide RC members is still insufficient.

In 1989, Anderson and Ramirez noted that although all the stirrups crossing a discontinuity were activated, only those that the discontinuity passed through near their centre were effective in resisting shear. They also showed the benefit of interior stirrup legs for wide beams with multiple longitudinal bars per layer, as the outside longitudinal bars had reduced strains in specimens containing interior stirrup legs, and these specimens exhibited higher shear capacity. In 1998, the

Concrete Society TR49 proposed the following Equation (Equation 4.1) for the minimum amount of stirrups ( $A_{v,min.}$ ) to be placed in a concrete beam:

$$A_{v,min.} \geq 0.40 * \left( \frac{f_{cu}}{40} \right)^{\frac{2}{3}} * \left[ \frac{(b_w * S_L)}{f_{yv}} \right] \quad (4.1)$$

Where,  $f_{cu}$  is the cubic compressive strength of concrete,  $b_w$  is the beam width,  $f_{yv}$  is the tensile strength of shear reinforcing steels and  $S_L$  is the shear reinforcement spacing in the longitudinal direction.

Since design consists of a complicated and heavy rebar cages, the structural engineers and designers may modify the beam width in order to both reduce flexural reinforcement requirements and reduce, or possibly exclude, the use of stirrups. The structural engineers may also modify the beam depth, but architectural and sightline restrictions may prevent this. The structural design engineers in general, and in Saudi Arabia in particular, may have chosen to use an exception to the requirements for minimum shear reinforcement according to the ACI-318 and SBC-304 concrete Codes. Both Codes exempt beams with widths ( $b_w$ ) greater than twice their thickness ( $h$ ) from the requirement that a minimum quantity of stirrups specified by Equation (4.2) be provided where  $V_u$  exceeds  $0.5\Phi V_c$ . The same exemption applies to slabs (Sherwood, 2008).

$$v_s = \frac{(A_{v,min.} * f_{yv})}{(b_w * S_L)} = 0.062 * \sqrt{f'_c} \quad (4.2)$$

$$\text{Where, } A_{v,min.} = 0.062 * \sqrt{f'_c} * \left[ \frac{(b_w * S_L)}{f_{yv}} \right]$$

Where,  $v_s$  is the factored shear stress in shear reinforcement (stirrups),  $A_{v,min.}$  is the minimum area of shear reinforcement (stirrups) in the width,  $f'_c$  is the nominal (specified) compressive strength of concrete,  $b_w$  is the beam width,  $f_{yv}$  is the tensile strength of shear reinforcing steels and  $S_L$  is the shear reinforcement spacing in the longitudinal direction.

The advantage of using this exemption is that, in structural RC wide beams, the full value of  $\Phi V_c$  may be bestowed in resisting the factored shear force ( $V_u$ ) before stirrups are required (Sherwood, 2008). This is in contrast to structural RC narrow beams, in which both Codes require minimum stirrups for narrow beams where  $v_u > 0.5\Phi v_c$  ( $v_c = V_c/b_w.d$ ). Thus, a possible alternate beam design is shown in Figure 4.4 [reference: (Sherwood, 2008)], in which  $V_u$  is 98%

of  $\Phi V_c$ ; where for structural RC wide beams and slabs,  $v_u > \Phi v_c$ . The structural Codes have remained essentially unchanged; the commentary made clear that wide beam exemption is applied to shallow narrow beams. No guidance is provided, however, on what exactly differentiates a shallow beam from a thick or a deep beam.

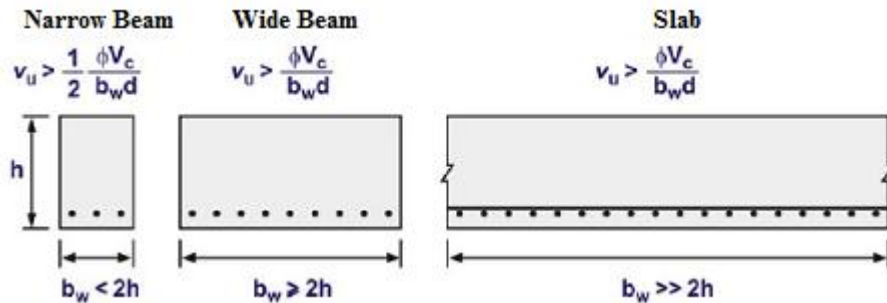


Figure 4.4: Ultimate Shear Stress ( $v_u$ ) at which Stirrups are required to ACI318 and SBC304 Codes.

#### 4.4 Provisions of Structural Design of Wide RC Beams to ACI318-and-SBC304 and EC2

##### 4.4.1 Design Methods (Ultimate Capacity and Serviceability)

To design the reinforced concrete members for the ultimate capacity (section capacity) of both flexure and shear capacities, ACI318 (2008) and SBC304 (2007) deal with the Ultimate Strength Design Method while EC2 (2004) deals with the Limit State Design Method (Alluqmani and Haldane, 2011a, 2011b; Alluqmani, 2010). There are not many differences between the design criteria in ACI318-and-SBC304 Codes and EC2 Code, where they are similar in many points. However, the differences are related to the notations, and the design equations and factors used in these Codes; where the design fundamentals are also similar (Alluqmani, 2010; Alluqmani and Haldane, 2011a, 2011b).

In the serviceability (mid-span deflection and flexural crack width) check, the three Codes deal with the Serviceability Limit State Design Approach (Alluqmani and Haldane, 2011a, 2011b; Alluqmani, 2010).

The main requirement for the design of section strength used in both ACI318 and SBC304 Codes is expressed as follows:

Design Strength  $\geq$  Required Strength [ $\Phi(\text{Nominal Strength}) \geq U$ ]

$$\Phi P_n \geq P_u, \quad \Phi M_n \geq M_u, \quad \Phi V_n \geq V_u, \quad \Phi T_n \geq T_u$$

Where, P is the axial load, M is the bending moment, V is the shear force, T is the torsion moment, and  $\Phi$  is the reduction strength factor.

All notations with (u), i.e.  $P_u$ ,  $M_u$ , and  $V_u$ , refer to the required strength values, while the design strength values are denoted by ( $\Phi$ \*nominal strength), i.e.  $\Phi P_n$ ,  $\Phi M_n$  and  $\Phi V_n$ .

The main requirement for the design of section strength used in the EC2 Code is expressed as follows:

$$\text{Design Strength} = \text{Characteristic Strength} / \text{Partial factor of safety} [R_d = R_k/\gamma_m]$$

The design resistance is equal to the characteristic resistance divided by the partial factor of safety for structural material.

To determine the shear reinforcement (stirrups), ACI318 and SBC304 Codes deal with the Strut-and-Tie Method while EC2 Code deals with the Variable Strut Inclination Method. Both methods are represented by tensile reinforcement at the bottom of the member section for tensile members, and represented by vertical stirrups at the top of the section for compression member.

#### 4.4.2 Load Factors

The three design Codes deal with a load factor ( $\lambda$ ) for their load combination (Table 4.1). ACI318 and SBC304 are applied with 1.20 for dead load (D.L), 1.60 for live load (L.L) and 1.60 for wind load (W.L). While EC2 uses 1.35 for permanent action ( $G_k$ ), 1.50 for variable action ( $Q_k$ ) and 1.15 for wind action ( $W_k$ ).

**Table 4.1:** Comparison of the Load Factors to EC2, ACI318 and SBC304 Codes.

ACI318-and-SBC304 Load Factors ( $\lambda$ )		EC1 / EC2 Load Factors ( $\lambda$ )	
Dead Load, D.L (1.40, old)	<b>1.20</b>	Permanent Action, $G_k$	<b>1.35</b>
Live Load, L.L (1.70, old)	<b>1.60</b>	Variable Action, $Q_k$	<b>1.50</b>
Wind Load, W.L	<b>1.60</b>	--	--

For ACI318 and SBC304 Codes:

The load combination for dead and live loads: 1.20 D.L + 1.60 L.L

The load combination for dead and wind loads: 1.20 D.L + 1.60 W.L.

For EC2 Code:

The load combination for permanent and variable actions:  $1.35 G_k + 1.50 Q_k$

The load combination for permanent and wind actions:  $1.35 G_k + 1.15 W_k$ .

#### 4.4.3 Reduction Design Strength Factors

The three design Codes also deal with design reduction factors for the reinforcement, flexural concrete and shear concrete (Table 4.2). ACI318 and SBC304 are applied with the reduction design strength factor ( $\Phi$ ) which is taken as 0.90 ( $\Phi_F$ ) for flexure concrete and reinforcement, and taken as 0.75 ( $\Phi_S$ ) for shear concrete. While EC2 is applied with the reduction material strength factor ( $1/\gamma_m$ ) which is taken as  $1/1.15$  ( $1/\gamma_s = 0.87$ ) for reinforcement, and taken as  $1/1.50$  ( $1/\gamma_c = 0.67$ ) for flexure and shear concrete.

**Table 4.2:** Comparison of the Design Reduction Factors to EC2, ACI318 and SBC304 Codes.

ACI318-and-SBC304		EC2	
Reduction Strength Factor ( $\Phi$ )		Reduction Material Factors ( $1/\gamma_m$ )	
Reinforcement ( $\Phi_F$ )	<b>0.90</b>	Reinforcement ( $1/\gamma_s$ )	$1/1.15 = \mathbf{0.87}$
Flexural Concrete ( $\Phi_F$ )	<b>0.90</b>	Flexural Concrete ( $1/\gamma_c$ )	$1/1.50 = \mathbf{0.67}$
Shear Concrete ( $\Phi_S$ )	<b>0.75</b>	Shear Concrete ( $1/\gamma_c$ )	$1/1.50 = \mathbf{0.67}$

#### 4.4.4 Concrete Strengths

In the three design Codes, the concrete test sample used to determine the compressive strength is the characteristic of a cylinder sample of concrete, typically with a diameter of 150mm and a height of 300mm but its values are different. The cylinder compressive strength of concrete is approximately equal to 0.80 of the cubic compressive strength. The tensile strength of concrete is approximately 15% of its compressive strength (McCormac, 2001).

ACI318 and SBC304 refer to the ultimate strength of concrete by ( $f_c$ ) but EC2 refers to it by characteristic concrete strength ( $f_{ck}$ ). In the design concrete strength, ACI318 and SBC304 deal with the specified concrete strength ( $f_c'$ ) which is  $\Phi f_c$  ( $0.9f_c$ ), but EC2 deals with the specified concrete strength ( $f_c$ ) which is  $f_{ck}/\gamma_c$  ( $f_{ck}/1.50 = 0.67f_{ck}$ ). In the present study, the design concrete strength was assumed  $40 \text{ N/mm}^2$ .



Figure 4.5 shows the comparison of stress-strain relationship for concrete that is assumed in the design process. The Elastic modulus of concrete ( $E_c$ ) is the concrete stress divided by its strain,  $E_c = \sigma/\epsilon$  (N/mm<sup>2</sup>). It is also obtained and taken as  $4700\sqrt{f'_c}$  to ACI318 and SBC304 Codes or taken as  $5500\sqrt{f_c}$  to EC2 Code, where the density of normal weight concrete is approximately 2500 kg/m<sup>3</sup> (i.e. the unit weight is 25 kN/m<sup>3</sup>). The concrete strain ( $\epsilon_c$ ) is 0.0030mm/mm to ACI318 and SBC304 Codes and is 0.0035mm/mm to EC2 Code.

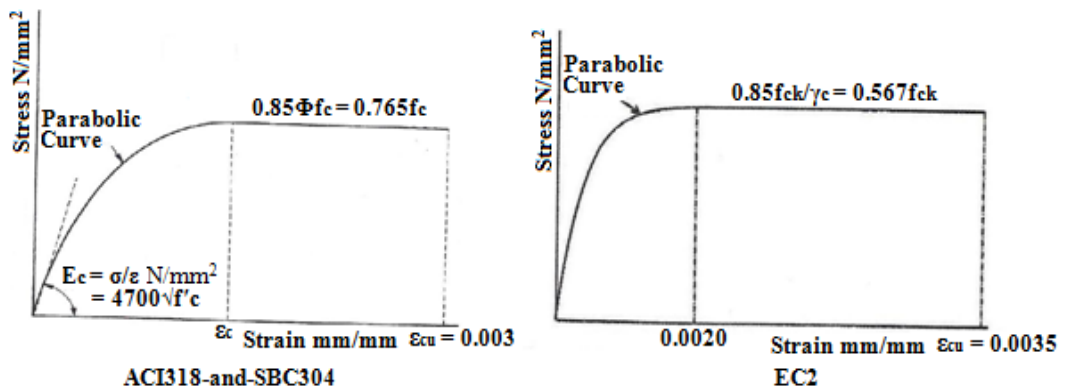


Figure 4.5: Stress-Strain Relationship of Concrete to ACI318-and-SBC304, and EC2 Codes.

#### 4.4.5 Steel Strengths

In the three design Codes, the steel strength refers to either hot rolled or cold worked high yield steel but the values are different. Whereas, it is believed that when the yield strength of the steel increases, the required area of reinforcement will decrease, thus saving the construction costs.

There are small differences in the steel strength between these Codes. ACI318 and SBC304 apply to the ultimate strength of reinforcement by ( $f_y$ ) which is 420 N/mm<sup>2</sup> in order to avoid excessive crack width, but EC2 refers to it by characteristic strength of reinforcement ( $f_{yk}$ ) which is 500 N/mm<sup>2</sup>. In terms of the design reinforcement strength, ACI318 and SBC304 use the specified reinforcement strength ( $f_s$ ) which is  $\Phi f_y$  ( $0.9f_y = 378$  N/mm<sup>2</sup>) but EC2 uses the specified steel strength ( $f_y$ ) which is  $f_{yk}/\gamma_s$  ( $f_{yk}/1.15 = 0.87f_{yk} = 435$  N/mm<sup>2</sup>). In the present study, the design strengths of flexural and shear reinforcements were assumed 500 N/mm<sup>2</sup>, where both flexural and shear reinforcing bars were supplied as high-strength deformed bars.

Figure 4.6 shows the comparison of stress-strain relationship for steel that is assumed in the design process. The Elastic modulus of steel ( $E_s$ ) is the steel stress divided by its strain,  $E_s = f_y/\epsilon_s$  (N/mm<sup>2</sup>). For the three Codes,  $E_s$  is obtained and taken as 200,000 N/mm<sup>2</sup> where the steel strain ( $\epsilon_s$ ) is 0.0025 mm/mm and the maximum steel concrete strain ( $\epsilon_{max.}$ ) is 0.0050 mm/mm.

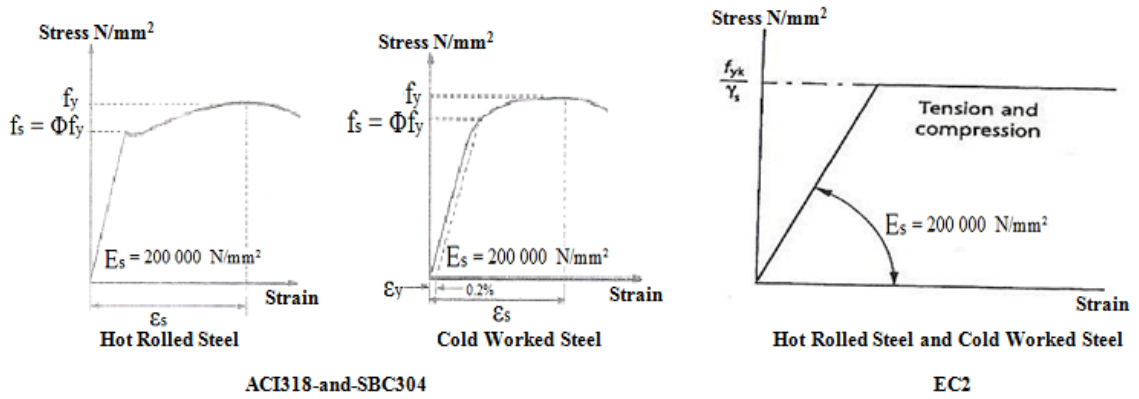


**Figure 4.6:** Stress-Strain Relationship of Steel to ACI318-and-SBC304, and EC2 Codes.

## 4.5 Design Method

There are three types of stress distributions: triangular, parabolic (actual), and rectangular (equivalent) stress distributions, as shown in Figures 4.7. The rectangular or equivalent stress-strain distribution is used in the design Equations. Figure 4.8 shows the rectangular or equivalent stress and strain distributions used for the design Equations at the ultimate capacity case on a wide beam section. While, the triangular stress block is used for the deflection calculations at the serviceability limit state. The design differences refer to the diagrams of the stress distributions (Figures 4.7 and 4.8), and are as follows:

### A. Ultimate (Specified) Concrete Strength Differences:

ACI318-and-SBC-304:

$$f_c' = \Phi_F \cdot f_c = 0.90 \cdot f_c$$

$$\text{Also, } 0.85f_c' = 0.85\Phi_F \cdot f_c = 0.85 \cdot 0.90 \cdot f_c = 0.765f_c = 0.765 \cdot (0.8 \cdot f_{cu}) = 0.612f_{cu}$$

Where,  $f_c$  and  $f_{cu}$  are the concrete compressive strength of cylinder and cube samples, respectively.

EC2:

$$f_c = f_{ck} / \gamma_c = f_{ck} / 1.50 = 0.67 \cdot f_{ck}$$

$$\text{Also, } 0.85f_c = 0.85f_{ck} / \gamma_c = 0.85 \cdot 0.67 \cdot f_{ck} = 0.567f_{ck} = 0.567 \cdot (0.8 \cdot f_{cu}) = 0.454f_{cu}$$

Where,  $f_{ck}$  and  $f_{cu}$  are the concrete compressive strength of cylinder and cube samples, respectively.

**B. Ultimate (Specified) Steel Strength Differences:**

1. For Flexural Reinforcement:

ACI318-and-SBC304:

$$f_s = \Phi_F \cdot f_y = 0.90 \cdot f_y$$

EC2:

$$f_y = f_{yk} / \gamma_s = f_{yk} / 1.15 = 0.87 \cdot f_{yk}$$

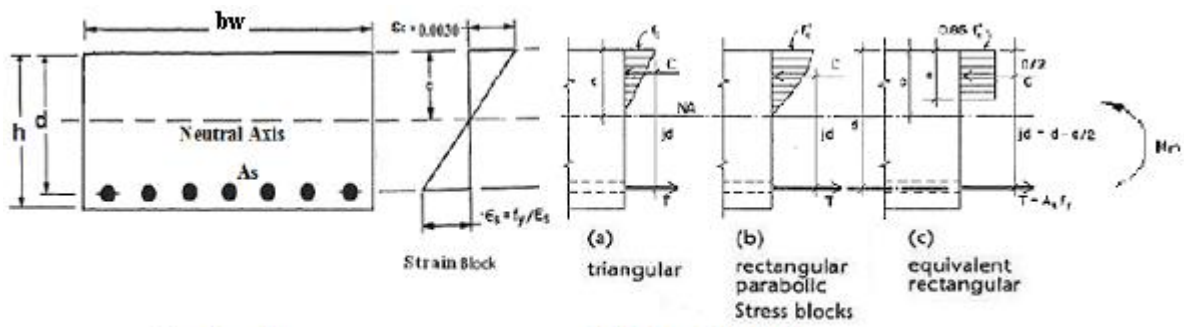
1. For Shear Reinforcement (Stirrups):

ACI318-and-SBC304:

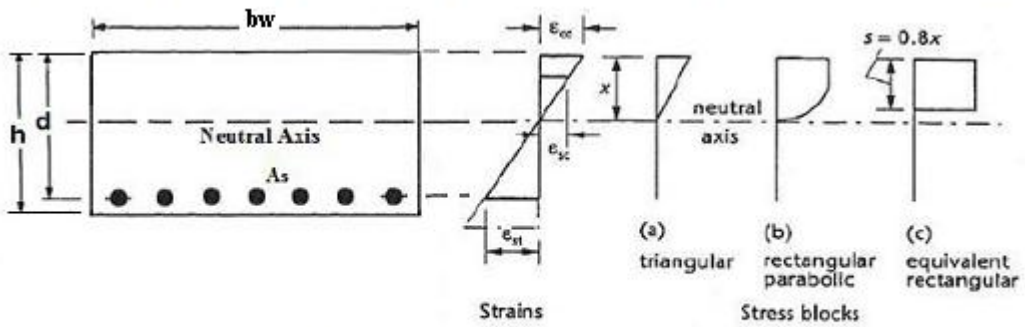
$$f_{yv} = \Phi_s \cdot f_{ys} = 0.75 \cdot f_{ys}$$

EC2:

$$f_{yv} = f_{yvk} / \gamma_s = f_{yvk} / 1.15 = 0.87 \cdot f_{yvk}$$



**Cross Section** **ACI-318 and SBC-304**  
 a) Stresses and Strains Distribution on a Section to ACI318 and SBC304 Codes.



**Cross Section** **EC-2**  
 b) Stresses and Strains Distribution on a Section to EC2 Code.

**Figure 4.7:** Stresses and Strains Distribution on a Wide Beam Section.

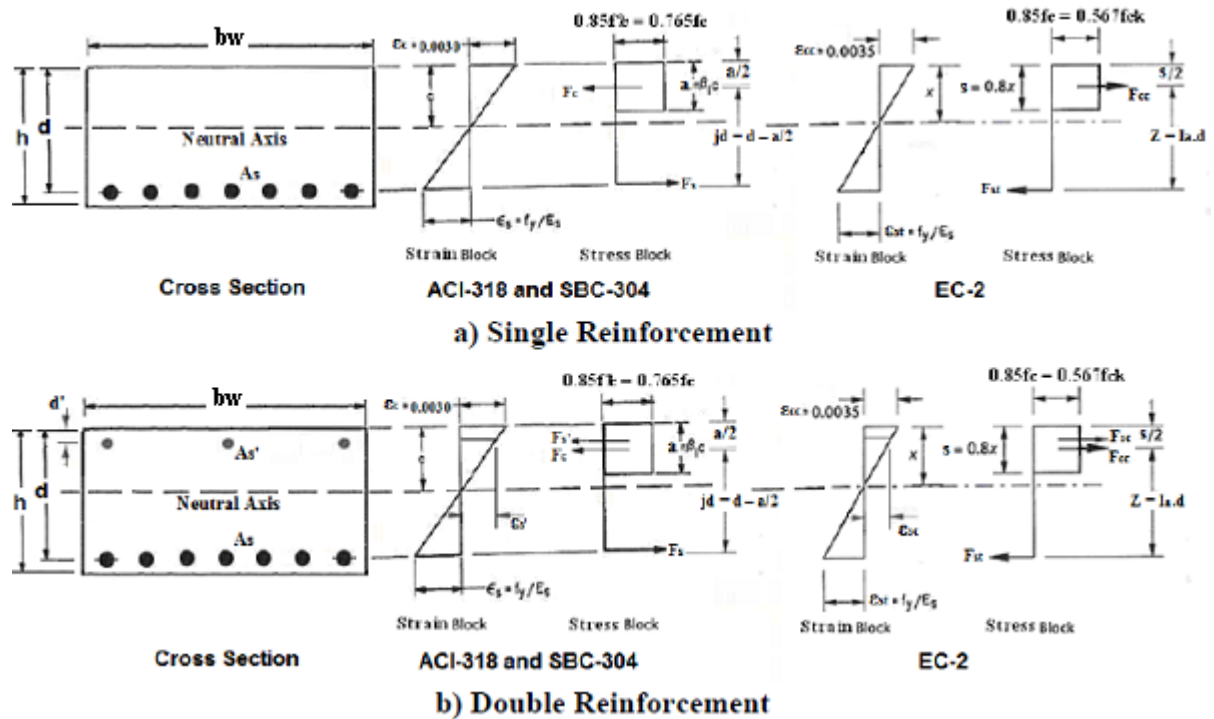


Figure 4.8: Equivalent Stresses and Strains Distribution on a Wide Beam Section Compared to ACI318-and-SBC304 and EC2 Codes.

The design section capacities are different and summarized in Sections 4.5.1, 4.5.2 and 4.5.3, as discussed below:

#### 4.5.1 Flexural Capacity on RC Beams: Moment Resistance

It is believed that flexural behaviour dominates in long beams (type I beams) while shear behaviour becomes more important in short beams (type III beams) (White et al, 1974). Thus, flexural strength is the ability of a beam to resist failure in bending, where flexural reinforcement is designed to carry tensile forces. In ACI318 and SBC304 Codes, flexural strength is applied with the nominal design strength which is multiplied by the reduction design strength factor and must be less than or equal to the ultimate required strength.

The structural design Equations of the flexural capacity on a beam section according to ACI318-and-SBC304 and EC2 Codes are illustrated as follows:

ACI318-and-SBC-304:

$$K_n = \frac{M_n}{f_c * b_w * d^2} = \frac{M}{0.90 * f_c * b_w * d^2} \quad (4.3a)$$

Where,  $M_n = M/\Phi_F = M/0.90$ .

If  $K_n > K_n' = 0.297$ , hence the compression reinforcement is required.

EC2:

$$K = \frac{M}{f_{ck} * b_w * d^2} \quad (4.3b)$$

If  $K > K' = 0.167$ , hence the compression reinforcement is required.

Required area of flexural tensile reinforcement:

ACI318-and-SBC-304:

$$A_{s,req.} = \frac{M}{(0.90 * f_y * jd)} \quad (4.4a)$$

EC2:

$$A_{s,req.} = \frac{M}{(0.87 * f_{yk} * Z)} \quad (4.4b)$$

Lever arm:

ACI318-and-SBC-304:

$$jd = d - \left(\frac{a}{2}\right) = \left(\frac{2}{3}\right) * h < 0.875d \quad (4.5a)$$

$$\text{Where, } a = \beta_1 * c = \frac{A_s * f_y}{0.85 * f_c * b_w}$$

$$\beta_1 = 0.85 \text{ for } f'_c \leq 28\text{N/mm}^2; \beta_1 = 0.85 - \left[0.05 \left(\frac{(f'_c - 28)}{7}\right)\right] \geq 0.65 \text{ for } f'_c > 28\text{N/mm}^2$$

$$c = \left[\frac{\epsilon_c}{\epsilon_c + \epsilon_s}\right] * d$$

Where,  $\epsilon_{cu} = \epsilon_c = 0.0030$ ,  $\epsilon_{max.} = 0.0050$ ,  $\epsilon_s = f_s/E_s = 0.90 * f_y/E_s < \epsilon_{max.}$ , and  $\epsilon_y = [(d-c)/c] * \epsilon_{cu} < \epsilon_{max.}$ .

EC2:

$$Z = d - \frac{s}{2} = d * I_a = d * \left\{0.5 + \sqrt{\left[0.25 - \left(\frac{K}{1.134}\right)\right]}\right\} < 0.95d \quad (4.5b)$$

Where,  $s = \lambda * x$

$$\lambda = 0.8 \text{ for } f_{ck} \leq 50\text{N/mm}^2; \lambda = 0.8 - \left[\frac{(f_{ck} - 50)}{400}\right] \text{ for } 50\text{N/mm}^2 < f_{ck} \leq 90\text{N/mm}^2$$

$$x = \left[\frac{\epsilon_c}{\epsilon_c + \epsilon_s}\right] * d$$

Where,  $\epsilon_{cu} = \epsilon_c = 0.0035$ ,  $\epsilon_{max.} = 0.0050$ ,  $\epsilon_s = f_y/E_s = (1/1.15) * f_{yk}/E_s < \epsilon_{max.}$ ,  $\epsilon_y = [(d-x)/x] * \epsilon_{cu} < \epsilon_{max.}$ .

In the three Codes, the minimum reinforcement ratio ( $\rho_{s,min.}$ ) is equal to  $A_s/b_w*d$ . In reinforced concrete members, the maximum clear horizontal and vertical spacing between individual parallel bars should be equal to the minimum of: the main bar diameter, maximum size of aggregate (plus 5mm to EC2), or 25mm (to ACI318 and SBC304) or 20mm (to EC2). The laps at any section are arranged symmetrically. The arrangement of lapped bars must not be greater than  $(4\phi_s)$  or 50mm, where  $\phi_s$  is the diameter of main flexural reinforcing bar.

The beam may be designed for a single reinforcement, if the section capacity is sufficient for this; but there are reasons for providing compression reinforcement which are to (McCormac, 2001; White et al, 1974):

1. Reduce sustained load deflection,
2. Increase the flexural capacity of beams,
3. Increase the ductility of beams,
4. Maintain the positioning of stirrups during concrete casting, and
5. Change the failure mode of beams from compression to tension.

In the present study, the wide beam specimens were subjected to be designed for single reinforcement only (for  $A_s$ ) as required by the design. However, the compression reinforcement was used in the design of the beams as hanger bars and it was assumed to be a portion of the main longitudinal tensile reinforcement, as  $A_s' = 12\%*A_s$  (Alluqmani, 2013a). The design procedure of flexural reinforcement is summarized in Appendix A.1.

#### **4.5.2 Shear Capacity on RC Beams: Shear Resistance**

There are two types of shear in wide structural RC members. The first one is two-dimensional problem of shear which is called one-way shear (so called wide-beam shear, or beam-type shear); while the other one is three-dimensional problem of shear which is called two-way shear (so called slab shear, or punching shear).

##### **A. One-Way Shear (Beam-Shear) Capacity**

The one-way shear reinforcement consists of vertical stirrups to resist the shear forces and diagonal tension. In ACI318 and SBC304, the stirrups are inclined at angle of  $45^\circ$  to the member axis as shown in Figure 4.9; while EC2 applies with the same angle which is between  $21.8^\circ$  and

45°. The shear strength is based on an average shear stress on the full effective cross section,  $b_w d$ , where  $b_w$  is the section web-width and  $d$  is the section effective-depth. Moreover, ACI318 and SBC304 use the shear reinforcement strength ( $f_{ys}$ ) that is equal to 280 N/mm<sup>2</sup>, but EC2 uses the characteristic shear reinforcement strength ( $f_{yk}$ ) that is equal to 250 N/mm<sup>2</sup> where it also uses 500 N/mm<sup>2</sup> for high yield strength stirrups. For the purpose of shear design, ACI318 and SBC304 assume 10mm diameter of stirrup legs, while EC2 applies with 8mm diameter of stirrup legs. In the present study, the shear reinforcement strength was assumed 500 N/mm<sup>2</sup> and the stirrups diameter was taken 8mm.

The shear reinforcement spacing along the beam length ( $S_L$ ), so called the longitudinal stirrup-legs spacing, is located perpendicular to the axis of the member length and it is not allowed to exceed  $0.5d$  according to ACI318 and SBC304 Codes or  $0.75d$  according to EC2 Code. While the shear reinforcement spacing across the beam width ( $S_w$ ), so called the transverse stirrup-legs spacing, is located perpendicular to the axis of the member width and depends on the configuration and pattern of the stirrup legs. Current Codes of Practice do not give limits for the transverse stirrup legs spacing, except the EC2 Code. Figure 4.10 shows the flexural (longitudinal) and shear (transverse) reinforcements, and shear stirrups spacing in a wide RC beam; where the longitudinal tensile bars are made bent in the end quarter of the span near the supports to resist shear forces (White et al, 1974).

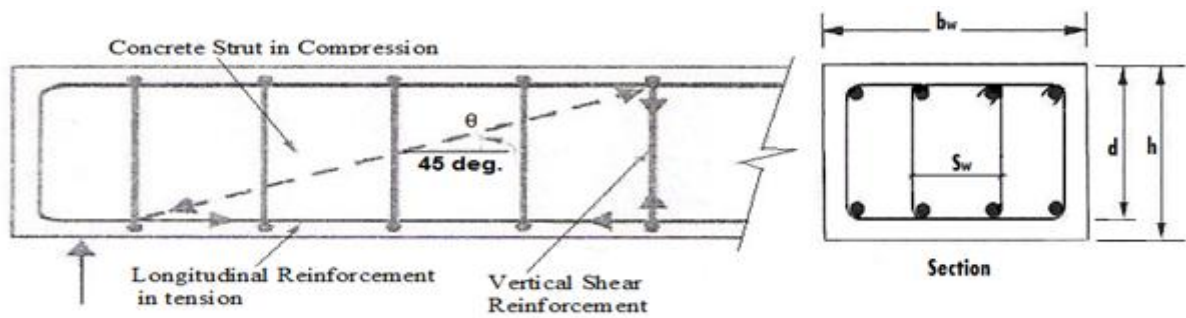


Figure 4.9: Longitudinal and Shear Reinforcements in a Beam to ACI318 and SBC304 Codes.

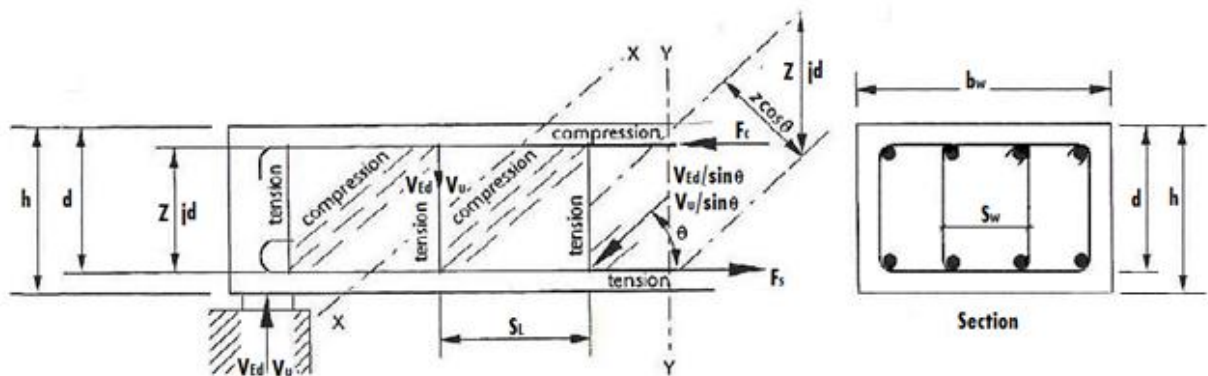
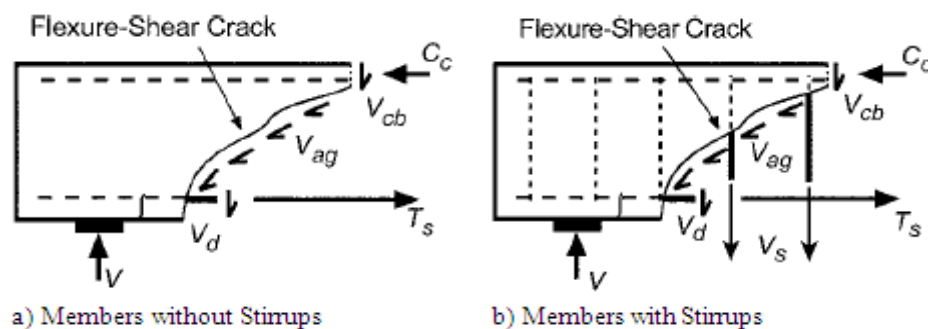


Figure 4.10: Longitudinal and Shear Reinforcements in a Beam to EC2 Code, and which are designed in accordance with EC2, ACI318 and SBC304 Codes.

In a slender diagonally cracked member without shear-reinforcement (Figure 4.11a), resistance to shear is provided by the un-cracked compression block ( $V_{cb}$ ); aggregate interlock along the crack surface ( $V_{ag}$ ); and dowel action from the longitudinal reinforcement ( $V_d$ ), (ASCE-ACI Committee 426, 1973; ASCE-ACI Committee 326, 1962). Most design Code models for shear (ACI318, 2008; SBC304, 2007; CSA, 2004; AASHTO, 2004) do not attempt to isolate each mechanism, but instead provide a strength term to estimate the equivalent combined action of all three modes ( $V_{cb}$ ,  $V_{ag}$ , and  $V_d$ ). Indeed, ACI318 (2008) and SBC304 (2007) design provisions use an empirical estimate of the force to cause significant diagonal cracking as a proxy to the mechanisms described previously. The commonly used ACI318 and SBC304 expressions for one-way shear capacity of a member without shear reinforcement ( $V_c$ ), which is subject to flexure and shear and is the contribution from concrete only, is given in Equation (4.6). EC2 Code deals with Equation (4.9) to determine  $V_c$ .

When web shear reinforcement is introduced to the beams (Figure 4.11b), the behaviour after the formation of a principal diagonal crack is considerably more ductile. Based on truss models originally developed by Ritter (1899) and Mörsh (1909), the ACI318 and SBC304 models estimate the shear resisted by the shear reinforcement ( $V_s$ ) using a 45° truss analogy as given in Equation (4.7). Equation (4.7) assumes that all shear reinforcement within an averaged distance of  $\pm 0.5d$  of the critical section for shear will have reached the yield strength at the time of shear failure. For members designed for vertical shear reinforcement according to EC2 Code, their design is based on the truss model and the shear resistance ( $V_{Rd,s}$ ) is given in Equation (4.10), where the recommended limiting values for  $\cot\theta$  are  $1.0 \leq \cot\theta \leq 2.5$ .



**Figure 4.11:** Sectional Model for Transfer at Flexural-Shear Cracks: a) Members without Stirrups; and b) Members with Stirrups.



The structural design Equations of the shear capacity on a beam section according to ACI318-and-SBC304 and EC2 Codes are illustrated as follows:

**The design shear strengths are:**

ACI318-and-SBC304:

$$V_c = [0.166 * (\sqrt{f'_c})] * b_w * d \quad (4.6)$$

$$V_s = \frac{[A_v * f_{yv} * \cot(\theta)]}{S_L} = \frac{[V - \Phi_s * V_c]}{\Phi_s} \quad (4.7)$$

$$V_n = V_c + V_s \quad (4.8)$$

Where,  $\Phi_s * V_n = 0.75 * V_n \geq V$

EC2:

$$V_c = V_{Rd,c} = \left[ \left( \frac{0.18}{\gamma_c} \right) * \left( 1 + \sqrt{\frac{200}{d}} \right) * (100\rho_s * f_{ck})^{\frac{1}{3}} + 0.15\sigma_{cp} \right] * b_w * 0.9d \quad (4.9)$$

$$V_{Rd,c} \geq \left[ \left( 0.035 * \left( 1 + \sqrt{\frac{200}{d}} \right)^{\frac{3}{2}} * (f_{ck})^{\frac{1}{2}} \right) + 0.15\sigma_{cp} \right] * b_w * 0.9d \quad (4.9a)$$

$$V_s = V_{Rd,s} = \frac{[A_v * f_{yv} * 0.9d * \cot(\theta)]}{S_L} \geq V \quad (4.10)$$

$$V_{Rd,max} = \left[ \frac{\left\{ 0.6 \left( 1 - \left( \frac{f_{ck}}{250} \right) \right) * f_{cd} \right\}}{(\cot(\theta) + \tan(\theta))} \right] * b_w * 0.9d \geq V \quad (4.11)$$

$$V_u = V_{Rd,d} = V_{Rd,c} + V_{Rd,s} = V_c + V_s \geq V \quad (4.12)$$

Where,

$A_v$  is the shear reinforcement (stirrups) area,

$\rho_s$  is the flexural-tensile reinforcement ratio,

$V$  is the design shear strength of a member section,

$V_u$  is the ultimate one-way shear strength, and

The other parameters are defined in Section 4.4.

Where for ACI318 and SBC304,  $\Phi_s$  is taken as 0.75 for shear,  $\theta$  is taken as 45 degree and hence  $\cot(\theta)$  is 1.0. While for EC2,  $\gamma_c$  is taken as 1.50 for concrete, and  $\sigma_{cp}$  is taken zero for no axial

load. Contrary to the ACI 318 and SBC304 Codes, EC2 Code enables us to compute the shear strength with a variable angle  $\theta$  of compression diagonal in truss analogy. In EC2 Code, the limits of  $\theta$  are between 21.8 and 45 degrees such that  $\cot \theta$  is greater than or equal to 1.0 and it is less than or equal to 2.5; but if the angle is not 45 degree, the concrete contribution is cancelled out. The designer should choose an appropriate angle  $\theta$  to use in the model. Equation (4.12) is proposed to investigate in this programme of research as a general form for the ultimate shear strength, where EC2 Code does not assume the contribution of concrete to estimate the shear strength. Through this programme of research,  $\theta$  is taken as 45 degree and  $\cot(\theta)$  is equal to 1.0. The shear strength of a beam without stirrups is equal to the concrete contribution ( $V_c$ ) of a beam with stirrups for the same characteristics. The check procedure of one-way shear strength is summarized in Appendix A.1.

The minimum effective cross sectional area of the design shear stirrups is calculated as:

ACI318-and-SBC304:

$$A_{v,min.} = \left[ \frac{V_s * S_L}{\Phi_S * f_{yv} * d} \right] = N_L * A_{str.} \geq (0.062 * \sqrt{f'_c}) * \left( \frac{b_w * S_L}{\Phi_S * f_{yv}} \right) \quad (4.13)$$

EC2:

$$A_{v,min.} = (0.08 * \sqrt{f_{ck}}) * \left( \frac{b_w * S_L}{\gamma_c * f_{yv}} \right) * \sin \alpha = N_L * A_{str.} \quad (4.14)$$

From Equations (4.13) and (4.14), the number of stirrup legs ( $N_L$ ) to be distributed across the member width can be provided as per the Code of Practice that be applied.  $A_{str.}$  is the cross-section area of one-leg of stirrups.

The maximum stirrup-legs spacing along the member length ( $S_L$ ):

ACI318-and-SBC304:

$$S_L = 0.50 * d \leq 380 \left( \frac{f_{yv}}{f_s} \right) - (2.5 * C_c) \leq 300 * \left( \frac{f_{yv}}{f_y} \right) \quad (4.15a)$$

EC2:

$$S_L = 0.75 * d \leq \frac{[A_v * f_{yv}]}{[(0.08 * \sqrt{f_{ck}}) * b_w * \sin \alpha]} \quad (4.15b)$$

The maximum stirrup-legs spacing across the member width ( $S_w$ ):

ACI318-and-SBC304:

No Limit for  $S_w$

EC2:

Suggests,  $S_w = 0.75*d$  (4.16)

## **B. Two-Way Shear (Punching-Shear) Capacity**

Generally, there are two types of reinforced concrete shear on wide structural members. The first one is two-dimensional problem of shear which is called one-way shear (so called wide-beam shear, or beam-type shear); while the other one is three-dimensional problem of shear which is called two-way shear (so called slab shear, or punching shear). However, the failure which occurs for flats slabs and footings is a punching shear failure (two-way shear failure), while that failure which occurs for wide beams is a beam-shear failure (one-way shear failure) (Lantsoght et al., 2011; Zhang, 2002; Menetrey, 2002). Moreover, the punching shear stresses are required to check for all wide reinforced concrete members (e.g. flat slabs, footings, and maybe wide beams), especially the structural concrete members that have narrow-width supports and loads. The shape of punching shear failure is cone if the member is loaded and supported via narrow-width columns, while it is pyramid if the member is loaded and supported via full-width columns.

### **B.1 Mechanisms and Patterns of Punching Shear Failure**

Punching shear failure is a local phenomenon which generally occurs in a brittle manner (a shear failure) for the concrete, at concentrated load or column support regions. This type of failure is catastrophic because no external, visible signs are shown prior to the occurrence of the failure. Punching shear failure disasters have occurred several times in the last two decades. It normally occurs around a column or a concentrated load on a slab or on wide concrete members in general. It is associated with a particular collapse mechanism in which a conical plug of concrete suddenly perforates the slab above the column (Menetrey, 2002). Punching shear may result from a concentrated load or reaction acting on a relatively small area, called the "loaded area", of a slab, of a foundation, or in general of a wide concrete member.

Reinforced concrete slabs and footings can fail in bending (flexural failure) or in shear (shear failure) as a wide member, and also they can fail in a third way, by punching shear (punching shear failure). Punching shear is a type of failure of slabs and footings subjected to high localized forces. In flat slab and wide member elements, this occurs at column support points. The failure is due to shear.

Punching shear failure is a three-dimensional problem due to the high shear stress in concrete. The punching crack is generated at different inclinations:  $30^\circ$ ,  $45^\circ$ ,  $60^\circ$  and  $90^\circ$  to the middle plane of the slab (Alexander and Simmonds, 1987; Menetrey, 2002), or wide concrete members. The punching crack is initiated by coalescence of micro-cracks at the top of the slab. Those micro-cracks are formed across the slab thickness before failure occurs. At failure, the punching crack has reached the corner of the slab-column intersection (Moe, 1961; Regan, 1983; Chana, 1991, Menetrey, 2002).

A typical flat plate, wide member punching shear failure is characterized by the punching of a column through a portion of the surrounding member. Figure 4.12 shows an example of a punching shear failure and surfaces of wide concrete members. This type of failure is one of the most critical considerations when determining the thickness of flat plates at the column-slab intersection (Zhang, 2002), or the thickness of wide beam at the intersection of narrow column to the beam itself.

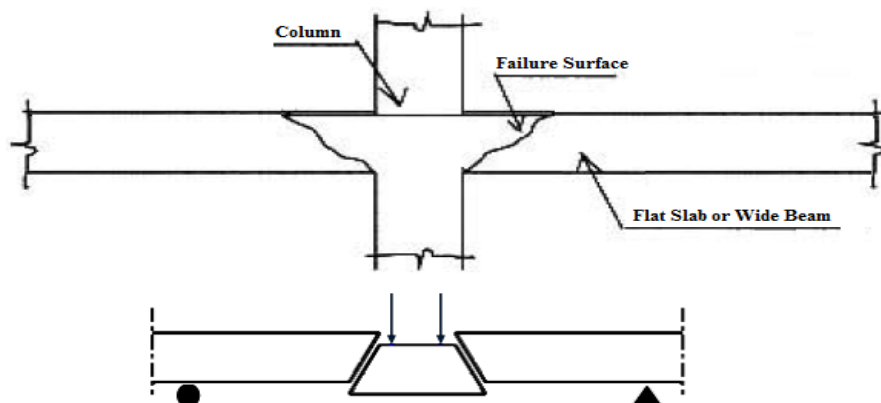


**Figure 4.12:** Punching Shear Failure Surfaces of Wide Concrete Members.

Three typical punching shear failures, as shown in Figure 4.13, may occur to wide structural concrete members. When the structure is under symmetric loads, the inclined punching shear failure surface takes place in the shape of a truncated cone surrounding the column (Figure 4.13a). In contrast, a combination of flexural failure and punching shear failure would occur once the unbalanced load exists (Figure 4.13b). The punched region is confined to the area near

the more heavily loaded face of the column. The regions around the two adjacent sides show extensive torsional cracking while the area near the opposite face shows little or no distress (Alexander and Simmonds, 1987; Zhang, 2002; Guan, 1996).

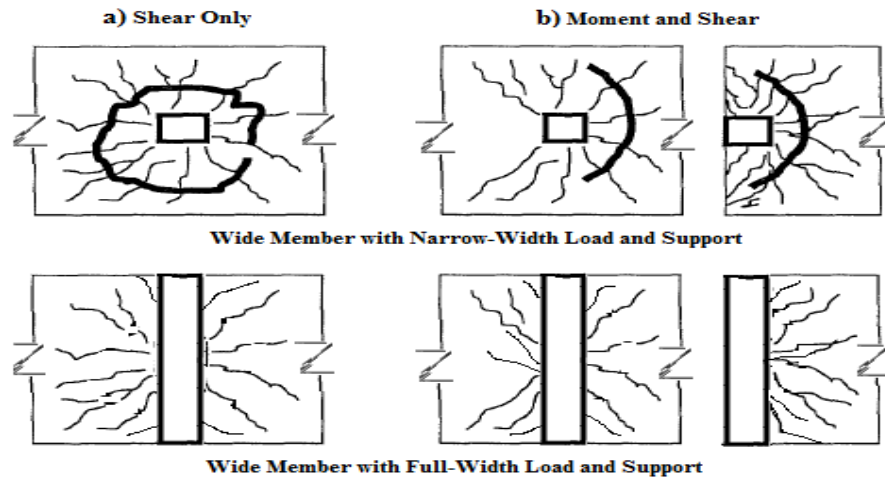


**Figure 4.13:** Typical Punching Shear Failure and Crack Patterns on Wide Members.

There are various factors influencing the punching shear strength ( $v_p$ ), such as concrete strength, ratio and arrangement of reinforcing steel, shear reinforcement, size effect, and boundary restraint (Zhang, 2002). Size effect is one of the salient aspects of fracture mechanics. The adoption of large scale model structures would help to eliminate the problem of size effects (Falamaki, 1990). By assuming a constant fracture energy, Bazant (1984) derived a size-effect law which was shown by Bazant and Cao (1987) to describe the size effect in punching failure. This law was adopted by Menetrey et al. (1997) in the numerical analysis of four slabs of different thicknesses. It was concluded that the nominal shear stress decreases with increasing thickness of the slab.

Most Codes of Practice present formulae, where the design punching load is a product of the design nominal shear strength and the area of a chosen control surface. Depending on the method used, the critical section for checking punching shear in slabs is usually situated between  $d/2$  to  $2d$  ( $d$  is the effective-depth of member) from the edge of the load or the reaction. Influences of slab depth, reinforcement, and other parameters are customarily governed by the application of different modification factors. The methods do not reflect the physical reality of the punching phenomenon, but when properly calibrated, can lead to reasonable predictions (CEB-FIP, 1990). In principle the design for punching shear in EC2 and BS8110 is similar, where both ACI318 and SBC304 have independent design for punching shear. The main variable for designing the punching shear in EC2, ACI318 and SBC304 Codes is the effective critical area of punching shear section.

**The design to prevent punching shear failure proceeds as:**

1. Check if the concrete is strong enough alone;
2. If not, check if the amount of reinforcement is reasonable;
3. Design reinforcement if reasonable; if not, change form of structure.

Changing the form of structure includes making the column larger, deepening the slab, introducing flared column heads or drop panels, or maybe using wide beams that may be hidden within the slab depth. There is also the possibility to adapt foreign approaches or Codes of Practice which are in reality more liberal!

In the design of slabs and footings, strength in shear frequently controls the thickness of the structural member, particularly in the vicinity of concentrated column or load. When the pad footing shown in Figure 4.14 is considered, shear failure may occur on one of two critical sections (beam shear or punching shear failure).

The footing (or the wide member) may act basically as a wide beam and shear failure may occur across the entire width of the member, as shown in Figure 4.14a. This is beam-type shear (or one-way shear) and the shear strength of the critical section is calculated as for a beam. The critical section for this type of shear failure is usually assumed to be located at a distance  $d$  (to ACI318 and SBC304) or  $1.5d$  (to EC2) from the face of the column (the support) or concentrated load (Figure 4.14a). Beam-type shear is often critical for footings and wide structural members but will rarely cause concern in the design of floor slabs. The design one-way (wide-beam) shear stresses at the critical wide-beam shear section ( $v$ ) are calculated as follows:

ACI318-and-SBC304:

$$v = \frac{V}{(l * d)} \quad (4.17a)$$

EC2:

$$v = \frac{V}{(l * 1.5d)} \quad (4.17b)$$

Where  $V$  is the corresponding shear force at the critical shear section,  $l$  is equal to the smaller of  $l_1$  or  $l_2$  (usually it is taken equal to the member width,  $b_w$ ) and  $d$  is the effective-depth of the member.

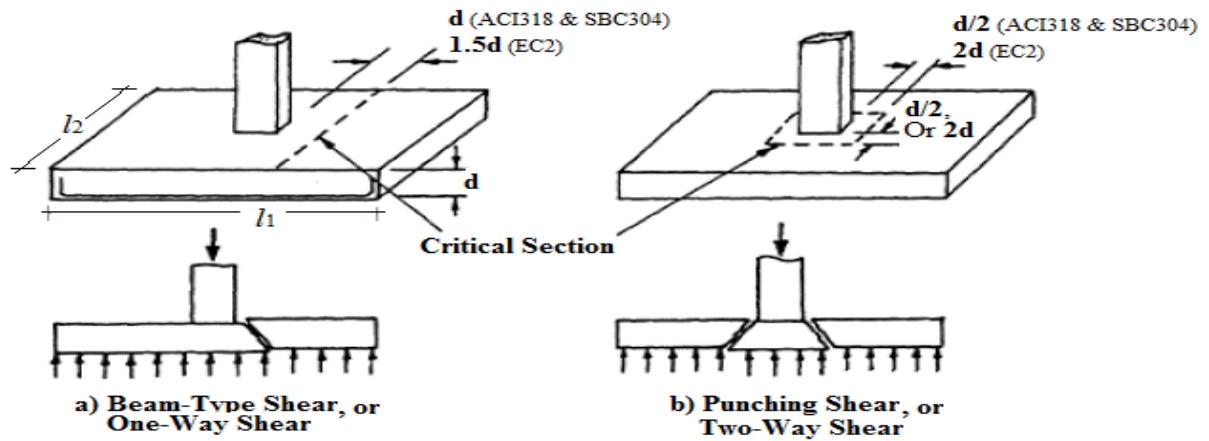


**Figure 4.14:** Types of Shear Failure Surfaces in a Wide Member (i.e. a Slab, a footing, or maybe a wide beam).

There is an alternative type of shear failure which may occur in the vicinity of a concentrated column or load as shown in Figure 4.14b. Failure may occur on a surface that forms a truncated cone or pyramid around the loaded area, (Figure 4.14b). This is known as punching shear failure (or two-way shear failure) and usually is more critical than one-way shear in wide members or slab systems supported directly on columns. Two-way shear or punching shear is often a critical consideration when determining the thickness of pad footings and flat slabs at the slab-column intersection. The critical section for failure cone of punching shear is approximated as a prism with vertical sides and is usually taken to be geometrically similar to the loaded area and located at a distance  $d/2$  (to ACI318 and SBC304) or  $2d$  (to EC2) from the face of the loaded area to the four edges or corners of columns; concentrated loads; reaction areas for narrow-width columns and loads, or to the two longitudinal edges for full-width columns and loads. For prevention the punching shear failure, the structural designers may increase the slabs thickness, or provide columns capitals (column heads) or drop panels in flat slabs; or they may provide wide beams (hidden beams) to be connected between the slabs and columns.

## B.2 Punching Shear Stresses

Punching shear stresses should be checked for two types of reinforced concrete members which are classified as wide structural members. These types of structural members are flat slabs (for all types: normal flat slab, flat slab with drop panel, flat slab with column head, and flat slab with drop panel -and- column head), and footings (for all types: shallow and pad footings (isolated and combined foundations), and deep footings (raft and pile cap foundations)). For these types of structural members, there are limits for punching shear stresses depended on the compressive strength of concrete, but if these stresses are out of the limits, the depth of a structural member

should be changed. Moreover, punching shear reinforcement may be required as per the check, and it affects around the support (or column) from a distance as a percentage of d (effective depth of member) to be as a surrounded perimeter around this support for cone or pyramid shape.

The critical section (or surface) of the punching shear is assumed to be perpendicular to the plane of the wide members, i.e. footings or slabs, Figure 4.14. For reinforced concrete (non-prestressed) wide members, footings or flat slabs, of normal-weight concrete, the design two-way (punching) shear stresses at the critical punching shear section ( $v_p$ ) are calculated as follows:

**a) According to ACI318 and SBC304**

$$v_p = \frac{V}{u * d} \leq \Phi_s * v_c \quad (4.18a)$$

$u$  = Critical perimeter =  $2(x+d) + 2(y+d)$ , where  $x$  and  $y$  are the plan dimensions of a rectangular load area. The sides of the critical section for failure cone of punching shear are taken to be geometrically similar to the loaded area and located at a distance  $d/2$ .

$v_c$  is the smallest of:

1.  $v_c \leq \Phi_s * \left( 0.166 + \left[ \frac{0.33}{\beta} \right] \right) * \sqrt{f'_c} = \Phi_s * 0.166 * \left[ 1 + \left( \frac{2}{\beta_c} \right) \right] * \sqrt{f'_c}$
2.  $v_c \leq \Phi_s * \left[ 0.166 + \left( \alpha_s * \left( \frac{d}{u} \right) \right) \right] * \sqrt{f'_c} = \Phi_s * 0.083 * \left[ 2.0 + \left( \alpha_s * \left( \frac{d}{u} \right) \right) \right] * \sqrt{f'_c}$
3.  $v_c \leq \Phi_s * (0.33) * \sqrt{f'_c}$

If  $v_p \leq \Phi_s.v_c$ : hence the punching shear reinforcement is not required.

If  $v_p > \Phi_s.v_n$ : hence the member section should be changed.

If  $\Phi_s.v_n > v_p \leq \Phi_s.v_c$ : hence the punching shear reinforcement is required.

For stirrups,  $\Phi_s.v_n = \Phi_s * 0.50 * \sqrt{f'_c}$ .

For Studs,  $\Phi_s.v_n = \Phi_s * 0.66 * \sqrt{f'_c}$ .

$$A_v = \frac{[(v_p - \Phi_s * v_c) * u * S]}{[\Phi_s * f_{yv} * \sin(\alpha)]} \geq A_{v,min} = \left( \frac{2.0 * \sqrt{f'_c} * u * S}{f_{yv}} \right)$$

Where  $v_p$  is the design factored punching shear stress at the critical punching shear section (it will usually be the support reaction at the ultimate strength state),  $v_c = 0.166 * \sqrt{f'_c}$  for stirrup and  $v_c = 0.25 * \sqrt{f'_c}$  for studs,  $\beta_c = l_1/l_2$  ( $l_1$  is greater than  $l_2$ , where  $l_1 = L$  and  $l_2 = b_w$ ),  $\alpha_s$  is equal 40 for



interior column case; 30 for edge column case; and 20 for corner column case,  $\alpha$  is angle of shear reinforcement (take as  $\theta$ ),  $S$  is shear reinforcement spacing (taken as  $d/2$  according to ACI318 and SBC304 Codes),  $\Phi_F = 0.90$ ,  $\Phi_S = 0.75$ ,  $f_c' = \Phi_F * f_c$ , and all other variables are defined in Section 4.5.2 related to the one-way shear.

**b) According to EC2**

$$v_p = \beta * \frac{V}{(u * d)} \leq v_{Rd,c} \quad (4.18b)$$

$u$  = Critical perimeter =  $(2*dx)+(2*dy) = 2(x+4d) + 2(y+4d)$ , where  $x$  and  $y$  are the plan dimensions of a rectangular load area. The sides of the critical section for failure cone of punching shear are taken to be geometrically similar to the loaded area and located at a distance  $2d$ .

If  $v_p \leq v_{Rd,c}$ : hence the punching shear reinforcement is not required

If  $v_p > v_{Rd}$ : hence the member section should be changed

If  $v_p > v_{Rd,c}$ : hence the punching shear reinforcement is required.

$$v_{Rd} = 0.30 * \left(\frac{f_{ck}}{\gamma_c}\right) * \left[1.0 - \left(\frac{f_{ck}}{250}\right)\right]$$

$$v_{Rd,c} = C_{Rd,c} * k * (100\rho_1 * f_{ck})^{\frac{1}{3}}$$

$$C_{Rd,c} = \frac{0.18}{\gamma_c} = \frac{0.18}{1.50} = 0.12$$

$$k = 1.0 + \sqrt{\left(\frac{200}{d}\right)} < 2.0$$

$$\rho_1 = \sqrt{\left[\left(\frac{A_{sx}}{(b_w * d_x)}\right) * \left(\frac{A_{sy}}{(b_w * d_y)}\right)\right]}, \text{ where } A_{sx} \approx A_{sy}, d_x = x + 4d, d_y = y + 4d$$

$$f_{ywd,ef} = 250 + 0.25d \leq f_{ywd} = \frac{f_{yk}}{\gamma_s} = 0.87f_{yk}$$

$$A_v = \frac{[(v_p - 0.75 * v_{Rd,c}) * u * S]}{[(1.5 * f_{ywd,ef}) * n]}$$

Where  $v_p$  is the design punching shear stress at the critical punching shear section (it will usually be the support reaction at the ultimate limit state),  $S$  is shear reinforcement spacing (taken as  $2d$  according to EC2 Code),  $\beta$  is equal 1.15 for interior column case; 1.40 for edge column case; and 1.50 for corner column case, and all other variables are defined in Section 4.5.2 related to the

one-way shear. The check procedure of the two-way shear (punching-shear) strength is summarized in Appendix A.1.

#### 4.5.3 Serviceability: Deflections and Crack Widths

The performance of the structure under its service life is considered in the design where the magnitudes of deflections and crack widths indicate the behaviour of the structure. It is believed that to reduce the deflection, the depth of the structural member should be increased (McCormac, 2001). There are some factors which affect the beam deflection; these include tensile strength, modulus of elasticity, creep, cracking and shrinkage curvature (Bond et al, 2006). On the other hand, structural cracking is dependent on bending, shear, torsion or tension resulting.

The three design Codes use the Serviceability Limit State Approach to estimate the mid-span deflection and maximum flexural crack widths, but they differ in their calculations. The serviceability limit states discuss and include stress limitation, crack control, and deflection control of the structural members. Moreover, deflection control gives an indication of the serviceability of the structure through its life (Mosley et al., 2007, 2008). In addition, the three design Codes assume that the maximum flexural cracks width should not be greater than 0.40 mm.

The shear forces and diagonal tension cause vertical flexural cracks or diagonal shear cracks or both. Figure 4.15 shows three types of cracks, namely called, flexural cracks, flexural-shear cracks, and web-shear cracks which develop due to applied shear forces and diagonal tension stresses. While Figure 4.16 shows the tension and compression stresses which cause the diagonal tension cracks in a beam.

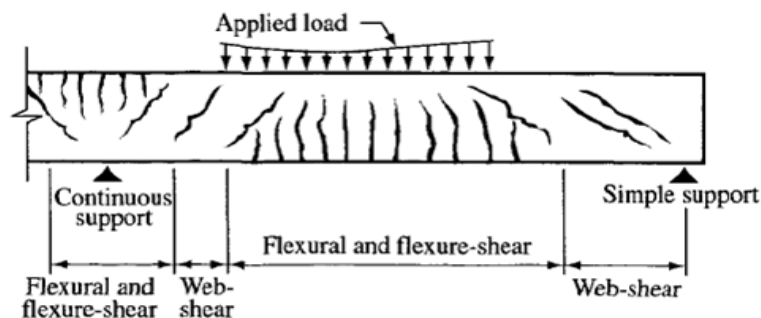


**Figure 4.15:** Flexural and Shear Cracks due to Applied Shear Forces and Stresses on a Beam.

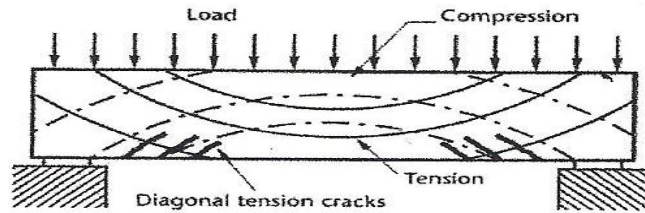


**Figure 4.16:** Tension and Compression Stresses cause the Diagonal Tension Cracks in a Beam.

The check procedures of mid-span deflection and flexural crack width are summarized in Appendix A.1. The procedures used to estimate the maximum mid-span deflection and flexural crack width for a beam according to ACI318-and-SBC304 and EC2 Codes are illustrated as follows:

### A. Mid-Span Deflection

The maximum mid-span deflection is calculated as follows:

ACI318-and-SBC304:

For concentrated load case:

$$\delta = \frac{P * (L_o)^3}{48 * E_c * I} < \frac{L}{360} \quad (4.19a)$$

For uniform distributed load case:

$$\delta = \frac{5w * (L_o)^4}{384 * E_c * I} < \frac{L}{360} \quad (4.19b)$$

Where, P = applied concentrated load, w = applied uniform distributed load,  $L_o$  = clear span length of the beam, L = overall span length of the beam,  $E_c$  = concrete modulus of elasticity =  $4700 * \sqrt{f_c}$ , and I = section moment of inertia =  $b_w * h^3 / 12$  for a rectangular section.

EC2:

For all cases of load:

$$a = k * (L_o)^2 * \left(\frac{1}{r_b}\right) < \frac{L}{d} \text{ or } \frac{L}{250} \quad (4.19c)$$

$$\text{Where, } k = 0.125 - \left[\frac{a^2}{6}\right], a = 0.025, \text{ and } \left(\frac{1}{r_b}\right) = \frac{M}{E_c * I}$$

Where,  $L_o$  = clear span length of the beam, L = overall span length of the beam, M = section bending moment,  $E_c$  = concrete modulus of elasticity =  $5500 * \sqrt{f_c}$ , and I = section moment of inertia =  $b_w * h^3 / 12$  for a rectangular section.

## B. Flexural Crack Width

The maximum flexural crack width is calculated as follows:

ACI318-and-SBC304:

$$z = \frac{0.03f_s * (d_c * A)^{\frac{1}{3}}}{1000} < 0.40\text{mm} \quad (4.20a)$$

Where

$$f_s = 0.6f_y$$

$$A = \frac{b_w * 2d_c}{N_s}$$

$$d_c = C_c + \emptyset_{str.} + \frac{\emptyset_s}{2}$$

Where,  $z$  = flexural crack width,  $f_s$  = specified flexural reinforcing steel strength,  $f_y$  = characteristic flexural reinforcing steel strength,  $N_s$  = total numbers of flexural tensile reinforcing bars,  $C_c$  = concrete cover,  $\emptyset_s$  = diameter of the main tensile reinforcing bar,  $\emptyset_{str.}$  = diameter of the stirrups leg, and  $b_w$  = member web-width.

EC2:

$$w_{,k} = S_{r,max.} * (\varepsilon_{sm} - \varepsilon_{cm}) < 0.40\text{mm} \quad (4.20b)$$

Where

$$S_{r,max.} = 3.4C + \left[ \frac{(0.42 * k_1 * k_2 * \emptyset_s)}{\rho_{p,eff.}} \right]$$

$$\varepsilon_{sm} - \varepsilon_{cm} = 0.6 * \varepsilon_s = 0.6 * \left( \frac{f_y}{E_s} \right)$$

$$\rho_{p,eff.} = \frac{A_s}{b_w * d}$$

Where,  $w_{,k}$  = flexural crack width,  $S_{r,max.}$  = maximum spacing of cracks,  $(\varepsilon_{sm}-\varepsilon_{cm})$  = change in the flexural steel and concrete strains,  $k_1 = 0.70$ ,  $k_2 = 0.40$ ,  $C$  = concrete cover,  $\emptyset_s$  = diameter of the main tensile reinforcing bar,  $f_y$  = specified flexural reinforcing steel strength =  $0.87 * f_{yk}$ ,  $f_{yk}$  = characteristic flexural reinforcing steel strength,  $\varepsilon_s$  = flexural steel bar strain,  $E_s$  = modulus of elasticity of flexural steel,  $\rho_{p,eff.}$  = effective flexural tensile reinforcement ratio,  $A_s$  = total area of flexural tensile reinforcing bars,  $b_w$  = member web-width, and  $d$  = member effective-depth.

## 4.6 Prediction Method

To predict the flexural and shear strengths, the total provided area of flexural and shear reinforcing steel bars as built, the actual material strengths obtained from the tests (i.e actual concrete and steel strengths), and the actual dimensions of the beam cross-sections must be taken into the estimations. It should be emphasized that all factors of safety must be assumed equal to a unity in order to predict the flexural and shear strengths. This means that  $\Phi_F$ ,  $\Phi_s$ ,  $\gamma_c$ ,  $\gamma_s$ , and etc must be taken as 1.0; these must be also taken 1.0 at estimating the concrete and steel strains ( $\epsilon_c$  and  $\epsilon_s$ ), the depth of the equivalent rectangular stress block ( $a$  and  $s$ ) and the distance from extreme compression fibre to neutral axis ( $c$  and  $x$ ).

The predicted failure load is obtained from the lesser predicted load given by the ultimate shear and flexural strengths. In addition, the predicted failure mode is the mode which corresponds to the lesser predicted load accounted for the predicted failure load; e.g. if the lesser predicted load is obtained by the ultimate shear strength, this means that the failure mode is a shear failure mode. The predicted load obtained from the reinforcement steels data is a flexural load; while the predicted load obtained from the concrete data is a shear load. As an example for a beam has a three-point loading system loaded at the mid-span point for a design load ( $P_d$ ) of 600 kN with a shear span ( $a$ ) of 1400mm, this gives a maximum flexural capacity (bending moment,  $M$ ) of 420 kN.m and a maximum shear capacity (shear force,  $V$ ) of 300 kN; but based on the actual tested material strengths, actual dimensions and actual total provided area of flexural reinforcing steel bars, if the beam as an example had an ultimate predicted flexural strength ( $M_u$ ) of 500 kN.m and an ultimate predicted shear strength ( $V_u = V_c + V_s$ ) of 250+150 = 400 kN; this means that the predicted flexural failure load ( $P_{M,pred.}$ ) is 715 kN [ $2 * M_u / a = 2 * (500 / 1.4)$ ] and the predicted shear failure load ( $P_{V,pred.}$ ) is 800 kN [ $2 * V_u = 2 * 400$ ]. Based on this example [Alluqmani, 2013a, 2013b], the assumed beam has a predicted failure load ( $P_{f,pred.}$ ) of 715 kN which refers to the lesser predicted load according to the predicted flexural failure load; therefore, the failure mode for this beam is a flexural failure mode.

The wide RC beams tested by previous researches, which have been reviewed in the literature (Chapter 3), were used in this Section to predict their shear or flexural strengths according to the correspondingly actual experimental strengths obtained from their tests. The predicted and tested shear and flexural strengths of wide RC beams examined previously are summarized in Tables 4.3 to 4.10 and Figures 4.17 to 4.32. The prediction procedures of flexural and shear strengths are summarized in Appendix A.2. The methods used for the prediction of flexural and shear strengths are illustrated as follows:

#### 4.6.1 Flexural Strength Method to ACI318, SBC304 and EC2

The prediction differences refer to the diagrams of the stress distributions (Figures 4.7 and 4.8), and are as follows:

The predicted flexural strengths are:

ACI318-and-SBC-304:

$$M_{u,flexure}(\text{from steel}) = A_{s,prov.} * f_{y,act.} * jd \quad (4.21a)$$

Where,  $jd = \text{Lever arm} = d - (a/2)$

$$a = \beta_1 * c$$

$$\beta_1 = 0.85 \text{ for } f_{c,act.} \leq 28 \text{ N/mm}^2. \beta_1 = 0.85 - [0.05((f_c - 28)/7)] \geq 0.65 \text{ for } f_{c,act.} > 28 \text{ N/mm}^2.$$

$$c = [\varepsilon_c / (\varepsilon_c + \varepsilon_s)] * d$$

Where,  $\varepsilon_{cu} = \varepsilon_c = 0.0030$ ,  $\varepsilon_{max.} = 0.0050$ ,  $\varepsilon_s = f_{y,act.} / E_s < \varepsilon_{max.}$ , and  $\varepsilon_y = [(d-c)/c] * \varepsilon_{cu} < \varepsilon_{max.}$ .

$$M_{u,shear}(\text{from concrete}) = (f_{c,act.} * b_w * d^2) * K \quad (4.21b)$$

$$\text{Where, } K = \omega * [1.0 - 0.59\omega], \text{ and } \omega = \rho_{s,prov.} * \left( \frac{f_{y,act.}}{f_{c,act.}} \right)$$

$M_{u,pred.} = \text{the lesser of } (M_{u,flexure} \text{ or } M_{u,shear})$

EC2:

$$M_{u,flexure}(\text{from steel}) = A_{s,prov.} * f_{y,act.} * Z \quad (4.22a)$$

$$\text{Where, } Z = jd = \text{Lever arm} = d - \left( \frac{s}{2} \right) = d * I_a = d * \left\{ 0.5 + \sqrt{\left[ 0.25 - \left( \frac{K}{1.134} \right) \right]} \right\}$$

$$s = \lambda * x$$

$$\lambda = 0.8 \text{ for } f_{c,act.} \leq 50 \text{ N/mm}^2. \lambda = 0.8 - [(f_c - 50)/400] \text{ for } 50 \text{ N/mm}^2 < f_{c,act.} \leq 90 \text{ N/mm}^2.$$

$$x = [\varepsilon_c / (\varepsilon_c + \varepsilon_s)] * d$$

Where,  $\varepsilon_{cu} = \varepsilon_c = 0.0035$ ,  $\varepsilon_{max.} = 0.0050$ ,  $\varepsilon_s = f_{y,act.} / E_s < \varepsilon_{max.}$ , and  $\varepsilon_y = [(d-x)/x] * \varepsilon_{cu} < \varepsilon_{max.}$ .

$$M_{u,shear}(\text{from concrete}) = (f_{c,act.} * b_w * d^2) * K \quad (4.22b)$$

$$\text{Where, } K = -1.134 * \left( \frac{Z}{d} \right)^2 + 1.134 * \left( \frac{Z}{d} \right)$$

$M_{u,pred.} = \text{the lesser of } (M_{u,flexure} \text{ or } M_{u,shear})$

#### 4.6.2 Shear Strength Method to ACI318, SBC304 and EC2

The predicted shear strengths are:

ACI318-and-SBC304:

$$V_c = [0.166 * \sqrt{f_{c,act.}}] * b_w * d \quad (4.23)$$

$$V_s = \frac{[A_{v,prov.} * f_{yv,act.} * d]}{S_l} \quad (4.24)$$

$$V_u = V_c + V_s \quad (4.25)$$

EC2:

$$V_c = \left[ (0.18) * \left( 1 + \sqrt{\frac{200}{d}} \right) * (100\rho_{s,prov.} * f_{c,act.})^{\frac{1}{3}} + 0.15\sigma_{cp} \right] * b_w * 0.9d \quad (4.26)$$

Where,  $\sigma_{cp}$  is taken zero for no axial load.

$$V_s = \frac{[A_{v,prov.} * f_{yv,act.} * 0.9d]}{S_l} \quad (4.27)$$

$$V_u = V_c + V_s \quad (4.28)$$

For the prediction purpose, the ultimate shear strength of a beam without shear reinforcement ( $V_{u0}$ ) is equal to the concrete contribution ( $V_c$ ) of a beam with stirrups for the same characteristics. For the analysis purpose of test results, the shear strength resisted by concrete of a beam with shear reinforcement ( $V_c$ ) is equal to the ultimate shear strength of the beam without shear reinforcement ( $V_{u0}$ ) for the same characteristics.

As mentioned early, Equation (4.28) is proposed to investigate in this programme of research as a general form to predict the ultimate shear strength according to EC2 Code. In addition, through this programme of research,  $\theta$  is taken as 45 degrees and  $\cot(\theta)$  is equal to 1.0.

#### 4.6.3 Shear Strength Model Developed by Lubell et al (2008)

Lubell, Bentz, and Collins (2008) proposed a model to predict the one-way shear strength of wide RC beam, as shown in Equation (4.29). Their model represents the effect of narrow support on the total shear strength and assumes that the total shear strength should be corrected by a

proposed reduction factor ( $\beta_L$ ), where  $\beta_L$  depends on the smaller ratio of the support- or load-width to the beam-width ( $k$  ratio) recommended in shear design equal to  $(0.7+0.3k)$  for both members with and without shear reinforcement. According to their model shown in Equation (4.29), the Equation ignores the influence of the load and support widths, as independent variables, on the total shear strength and ignores the effect of the transverse stirrup legs spacing and/or the longitudinal stirrup legs spacing on the shear strength resisted by stirrups (Alluqmani, 2013a). Consequently, Equation (4.29) seems to predict the total shear strength for those wide RC beams with the smallest widths of bearing plates only. Hence, for example, the total shear strength will be the same for six wide RC beams have the same load width, equals to quarter the beam width ( $0.25*b_w$ ), and have various support widths greater than  $0.25*b_w$  (i.e.  $0.30*b_w$ ,  $0.40*b_w$ ,  $0.50*b_w$ ,  $0.75*b_w$ ,  $0.85*b_w$  and  $1.0*b_w$ ) at the same characteristics. On the other wise, this hence, the total shear strength will be the same for the same six wide RC beams if the load and support locations are interchanged; i.e. if the beams have the same support width, equals to quarter the beam width ( $0.25*b_w$ ), and have various load widths greater than  $0.25*b_w$  (i.e.  $0.30*b_w$ ,  $0.40*b_w$ ,  $0.50*b_w$ ,  $0.75*b_w$ ,  $0.85*b_w$  and  $1.0*b_w$ ). Finally, Equation (4.29) will give the same total shear strength for the 12 wide RC beams mentioned above. Therefore, it can be concluded that the both load and support widths have influences on the total shear strength.

$$V_{n'} = \beta_L * [V_c + V_s] = (0.7 + 0.3k) * [V_c + V_s] \quad (4.29)$$

#### 4.6.4 Shear Strength Model Developed by Serna-Ros et al (2002)

Serna-Ros, Fernandez-Prada, Miguel-Sosa and Debb (2002) proposed a model to predict the one-way shear strength of wide RC beam, as shown in Equation (4.30). Their model assumes that the shear strength resisted by stirrups should be corrected by a proposed factor ( $\Phi_s$ ), where  $\Phi_s$  depends on the ratio of the support width to beam width and the ratio of the effective-depth to the square root of the longitudinal and transverse stirrup-legs spacing. Equation (4.30) ignores the influence of the load width on the total shear strength and ignores the effect of the load and/or support width on the shear strength resisted by concrete (Alluqmani, 2013a). Equation (4.30) seems to predict the shear strength resisted by stirrups contribution only for those wide RC beams with various support widths only.

$$V_u = V_c + \Phi_s \cdot V_s = V_c + \left[ \left( \frac{b_s}{b_w} \right)^{0.41} * \left( \frac{d}{\sqrt{S_L * S_w}} \right) \right] * V_s \quad (4.30)$$



#### 4.6.5 Shear Strength Model Developed by Shuraim (2012)

Shuraim (2012) proposed a model to predict the one-way shear strength of wide RC beams, as shown in Equation (4.31). His model assumes that the shear strength resisted by stirrups should be determined based on the equivalent stirrup spacing ( $S_{eq}$ ) shown in Equation (4.32).  $S_{eq}$  is a function of  $S_w$ , and must be greater than or equal to  $S_L$ ; otherwise,  $S_{eq}$  is taken equal to  $S_L$ . This means that  $S_{eq}$  is compared with  $S_L$ , and the greater one is taken for  $S_{eq}$ . Equation (4.31) ignores the influence of the load and support widths on the total shear strength and the effect of the load and/or support width on the shear strength resisted by concrete and/or by stirrups (Alluqmani, 2013a). Therefore, this Equation seems to predict the shear strength resisted by stirrups only. In addition, based on Equation (4.32), Shuraim (2012) found a relationship between the transverse and longitudinal spacing of stirrup legs by equating  $S_{eq}$  to  $S_L$  in Equation (4.32) and solving for the transverse spacing ( $S_w$ ). This is discussed in Chapter 8 regarding to developing a proposed design model to be suitable for all cases of wide RC beams.

$$V_u = V_c + V_{seq} = V_c + \left[ \frac{(A_v * f_{yv} * d)}{S_{eq}} \right] \quad (4.31)$$

$$S_{eq} = \left( \frac{S_L}{d} \right)^{0.25} * \sqrt{S_L * S_w} \geq S_L \quad (4.32)$$

#### 4.6.6 Comments on the Prediction Methods

The current Codes of Practice ignore the influence of the load and support widths ( $b_p$  and  $b_s$ ), or at best the ratios of load-width and support-width to beam-width ( $k_p$  and  $k_s$ ), as independent variables, on the total flexural and shear strengths, as well they ignore the effect of the transverse stirrup legs spacing ( $S_w$ ) and/or the longitudinal stirrup legs spacing on the shear strength resisted by stirrups (Alluqmani, 2013a). Consequently, these Equations seem that the ultimate flexural and shear strengths will be the same for all wide RC beams even if they are loaded and/or supported by full- and/or narrow- width load and support conditions at the same characteristics. On the other wise, this hence that the ultimate flexural and shear strengths will be the same for all these wide RC beams if the load and support locations are interchanged. While as metioned in the literature, both load and support widths have influence on the wide RC beams strengths, where their strengths decrease as the load and/or support widths are reduced. Moreover, based on the comparison between predictions of flexural and shear strengths and the actual test strengths shown in Tables 4.3 to 4.10 and Figures 4.17 to 4.32, it can be concluded

(Alluqmani, 2013a) that the both load and support widths ( $b_p$  and  $b_s$ ) should be taken into the considerations to predict the ultimate flexural and shear strengths of wide RC beams, and that the both longitudinal and transverse stirrup-legs spacing ( $S_L$  and  $S_w$ ) should be taken into the considerations to predict the shear strength of wide RC beams. Therefore, it can be also concluded that the prediction methods used in the current Codes of Practice need to be reformulated with taking into the consideration the effect of  $k_s$ ,  $k_p$ ,  $S_L$  and  $S_w$ .

Based on the predictions shown in Tables 4.3 to 4.10 and Figures 4.17 to 4.32, it is clear that the load and support widths ( $b_p$  and  $b_s$ ), or at best the ratios of load-width and support-width to beam-width ( $k_p$  and  $k_s$ ) have influence on the ultimate flexural strength and the shear strength resisted by concrete contribution; while that the support width ( $b_s$ ), or at best the ratio of support-width to beam-width ( $k_s$ ) and the longitudinal and transverse stirrup-legs spacing ( $S_L$  and  $S_w$ ) have influence on the shear strength resisted by stirrups contribution. These factors, concluded in the above conclusion, must be used to develop a rational proposed prediction model in order to predict both flexural and shear strengths of wide RC beams. In addition, testing of two wide RC beams with narrow bearing plates to be one fails in shear and the other one fails in flexure is required in order to develop the proposed prediction model.

The model developed by Lubell et al. (2008) is only applied for the shear strength of wide RC beams with narrow load and support conditions (Alluqmani, 2013a, 2013b). Their model ignores the effect of the transverse stirrup legs spacing on the shear strength resisted by stirrups. As mentioned in Section 4.6.3, their model estimates the total shear strength for those wide RC beams with the smallest widths of bearing plates only, where the total shear strength will be the same for the 12 wide RC beams mentioned above. While as mentioned in the literature, the transverse stirrup legs spacing has influence on the shear strength of wide RC beams, where the shear strength decreases as the transverse stirrup-legs spacing increases. Moreover, based on the comparison between predictions of shear strengths and the actual test strengths shown in Tables 4.4 to 4.9 and Figures 4.17 to 4.32 (except, Figures 4.20, 4.23 and 4.26 for  $M_u$  predictions), it can be concluded (Alluqmani, 2013a) that the both longitudinal and transverse stirrup-legs spacing ( $S_L$  and  $S_w$ ) should be taken into the consideration to predict the shear strength resisted by stirrups contribution for wide RC beams. Therefore, it is also concluded that the prediction method of shear strength used by Lubell et al. (2008) model is not sufficient for prediction the shear strength of wide RC beams as shown in Tables 4.4 to 4.9.

The model developed by Serna-Ros et al. (2002) is only applied for the shear strength resisted by stirrups contribution for wide RC beams with full and narrow support conditions only

(Alluqmani, 2013a, 2013b), where the load width is not considered at all in their model. Their model ignores the influence of the load width on the total shear strength and the effect of the load and/or support width on the shear strength resisted by concrete. As mentioned in Section 4.6.4, their model estimates the shear strength resisted by stirrups contribution only for those wide RC beams with various support widths only, where the shear strength resisted by concrete contribution will be the same strength given by the applied Code. While as mentioned in the literature, the load width has influence on the shear strength of wide RC beams, where the shear strength decreases as the load width is reduced. Moreover, based on the comparison between predictions of shear strengths and the actual test strengths shown in Tables 4.4 to 4.9 and Figures 4.17 to 4.32 (except, Figures 4.20, 4.23 and 4.26 for  $M_u$  predictions), it can be concluded (Alluqmani, 2013a) that the load width ( $b_p$ ) should be taken into the consideration to predict the shear strength resisted by concrete contribution for wide RC beams. Therefore, it is also concluded that the prediction method of shear strength used by Serna-Ros et al. (2002) model is not sufficient for prediction the shear strength of wide RC beams as shown in Tables 4.4 to 4.9.

The model developed by Shuraim (2012) is only applied for the shear strength resisted by stirrups contribution for wide RC beams regardless the load and support width conditions (Alluqmani, 2013a, 2013b), where both load and support widths are not considered at all in his model. His model ignores the influence of the load and support widths on the total shear strength, and the effect of the load and/or support width on the shear strength resisted by concrete. As mentioned in Section 4.6.5, his model estimates the shear strength resisted by stirrups contribution only for those wide RC beams with ignoring the load and support widths, where the shear strength resisted by concrete contribution will be the same strength given by the Code applied. While as mentioned in the literature, the load and support widths have influence on the shear strength of wide RC beams, where the shear strength decreases as the load width and/or support width is reduced. Moreover, based on the comparison between predictions of shear strengths and the actual test strengths shown in Tables 4.4 to 4.9 and Figures 4.17 to 4.32 (except, Figures 4.20, 4.23 and 4.26 for  $M_u$  predictions), it can be concluded (Alluqmani, 2013a) that the load and support widths ( $b_p$  and  $b_s$ ) should be taken into the consideration to predict the shear strength resisted by concrete contribution for wide RC beams; while that the support width ( $b_s$ ) should be taken into the consideration to predict the shear strength resisted by stirrups contribution for wide RC beams. Therefore, it is concluded that the prediction method of shear strength used by Shuraim (2012) model is not sufficient for prediction the shear strength of wide RC beams as shown in Tables 4.4 to 4.9.

**Table 4.3:** Details and Summary of the Results of Wide RC Beams Previously Tested.

Beams	bw	h	d	$\rho_s$	$\rho_s'$	S <sub>L</sub>	S <sub>w</sub>	S <sub>L</sub> /S <sub>w</sub>	k <sub>p</sub>	k <sub>s</sub>	k	Test Strengths, kN - m				ACI318 & SBC304			EC2 Code		
												V <sub>c,ex</sub>	V <sub>s,ex</sub>	V <sub>u,ex</sub>	M <sub>u,ex</sub>	V <sub>c</sub>	V <sub>s</sub>	M <sub>u</sub>	V <sub>c</sub>	V <sub>s</sub>	M <sub>u</sub>
Reference: Serna-Ros et al (2002)																					
R0	750	250	206	2.20	0.94	-	-	-	1.00	1.00	1.00	244	-	244	-	139	-	-	173	-	-
R1	750	250	206	2.20	0.94	170	690	0.25	1.00	1.00	1.00	244	22	266	-	139	87	-	173	79	-
A0	750	250	206	2.20	0.94	-	-	-	1.00	1.00	1.00	187	-	187	-	128	-	-	147	-	-
A1	750	250	206	2.20	0.94	170	230	0.74	1.00	1.00	1.00	187	78	265	-	128	92	-	147	82	-
A2	750	250	206	2.20	0.94	170	690	0.25	1.00	1.00	1.00	187	47	234	-	128	97	-	147	88	-
A3	750	250	206	2.20	0.94	170	230	0.74	1.00	1.00	1.00	187	95	282	-	128	113	-	147	102	-
C0	750	250	206	2.20	0.94	-	-	-	1.00	1.00	1.00	182	-	182	-	130	-	-	151	-	-
C1	750	250	206	2.20	0.94	170	690	0.25	1.00	1.00	1.00	182	76	258	-	130	122	-	151	110	-
C2	750	250	206	2.20	0.94	170	230	0.74	1.00	1.00	1.00	182	109	291	-	130	109	-	151	98	-
C3	750	250	206	2.20	0.94	170	115	1.48	1.00	1.00	1.00	182	176	358	-	130	123	-	151	111	-
C4	750	250	206	2.20	0.94	127.5	138	0.92	1.00	1.00	1.00	182	178	360	-	130	164	-	151	147	-
C5	750	250	206	2.20	0.94	85	230	0.37	1.00	1.00	1.00	182	161	343	-	130	246	-	151	221	-
D0	750	250	206	2.20	0.94	-	-	-	1.00	0.40	0.40	218	-	218	-	148	-	-	171	-	-
D1	750	250	206	2.20	0.94	170	690	0.25	1.00	0.40	0.40	218	48	266	-	148	121	-	171	108	-
D2	750	250	206	2.20	0.94	170	230	0.74	1.00	0.40	0.40	218	78	296	-	148	105	-	171	94	-
D3	750	250	206	2.20	0.94	170	115	1.48	1.00	0.40	0.40	218	102	320	-	148	118	-	171	106	-
D5	750	250	206	2.20	0.94	85	230	0.37	1.00	0.40	0.40	218	127	345	-	148	237	-	171	213	-
Reference: Shuraim (2012)																					
S0	700	180	150	1.34	1.026	-	-	-	1.00	1.00	1.00	161	-	161	-	94	-	-	124	-	-
S1-80	700	180	150	1.34	1.026	80	660	0.12	1.00	1.00	1.00	161	60	221	-	94	142	-	124	128	-
S2-80	700	180	150	1.34	1.026	80	440	0.18	1.00	1.00	1.00	161	61	222	-	94	142	-	124	128	-
S3-80	700	180	150	1.34	1.026	80	230	0.35	1.00	1.00	1.00	161	71	232	-	94	142	-	124	128	-
S0-1	700	180	150	1.34	1.026	-	-	-	1.00	1.00	1.00	162	-	162	-	94	-	-	124	-	-
S1-75-1A	700	180	150	1.34	1.026	75	660	0.11	1.00	1.00	1.00	162	0	162	-	94	188	-	124	169	-
S3-75-1	700	180	150	1.34	1.026	75	230	0.33	1.00	1.00	1.00	162	58	220	-	94	144	-	124	130	-
S13-75-1A	700	180	150	1.34	1.026	75	230	0.33	1.00	1.00	1.00	162	112	274	-	94	188	-	124	169	-
S13-100-1	700	180	150	1.34	1.026	100	230	0.43	1.00	1.00	1.00	162	106	268	-	94	143	-	124	129	-
S13-125-1	700	180	150	1.34	1.026	125	230	0.54	1.00	1.00	1.00	162	79	241	-	94	110	-	124	99	-
S0-2	700	180	150	1.34	1.026	-	-	-	1.00	1.00	1.00	160	-	160	-	94	-	-	124	-	-
S1-75-2	700	180	150	1.34	1.026	75	660	0.11	1.00	1.00	1.00	160	81	241	-	94	188	-	124	169	-
S3-75-2	700	180	150	1.34	1.026	75	230	0.33	1.00	1.00	1.00	160	81	241	-	94	144	-	124	130	-
S13-75-2	700	180	150	1.34	1.026	75	230	0.33	1.00	1.00	1.00	160	146	306	-	94	188	-	124	169	-

Beams	bw	h	d	$\rho_s$	$\rho_s'$	S <sub>L</sub>	S <sub>w</sub>	S <sub>L</sub> /S <sub>w</sub>	k <sub>p</sub>	k <sub>s</sub>	k	Test Strengths, kN - m				ACI318 & SBC304			EC2 Code		
												V <sub>c,ex</sub>	V <sub>s,ex</sub>	V <sub>u,ex</sub>	M <sub>u,ex</sub>	V <sub>c</sub>	V <sub>s</sub>	M <sub>u</sub>	V <sub>c</sub>	V <sub>s</sub>	M <sub>u</sub>
-	mm	mm	mm	%	%	mm	mm	-	-	-	-	V <sub>c,ex</sub>	V <sub>s,ex</sub>	V <sub>u,ex</sub>	M <sub>u,ex</sub>	V <sub>c</sub>	V <sub>s</sub>	M <sub>u</sub>	V <sub>c</sub>	V <sub>s</sub>	M <sub>u</sub>
S13-100-2	700	180	150	1.34	1.026	100	230	0.43	1.00	1.00	1.00	160	118	278	-	94	143	-	124	129	-
S13-125-2	700	180	150	1.34	1.026	125	230	0.54	1.00	1.00	1.00	160	81	241	-	94	110	-	124	99	-
Reference: Hanafy et al (2012)																					
NB1	500	250	210	4.61	0.65	-	-	-	1.00	1.00	1.00	245	-	245	-	110	-	-	191	-	-
NB2	500	250	210	4.61	0.65	200	110	1.82	1.00	1.00	1.00	245	105	350	-	110	67	-	191	60	-
NB3	500	250	210	4.61	0.65	200	110	1.82	1.00	1.00	1.00	245	55	300	-	110	40	-	191	36	-
NB4	500	250	210	4.61	0.65	135	110	1.23	1.00	1.00	1.00	245	61	306	-	110	49	-	191	44	-
NB5	500	250	210	4.61	0.65	200	110	1.82	1.00	1.00	1.00	245	250	495	-	110	201	-	191	181	-
NB6	500	250	210	4.61	0.65	135	110	1.23	1.00	1.00	1.00	245	305	550	-	110	230	-	191	207	-
HB1	500	250	210	4.61	0.65	-	-	-	1.00	1.00	1.00	295	-	295	-	165	-	-	250	-	-
HB2	500	250	210	4.61	0.65	200	110	1.82	1.00	1.00	1.00	295	103	398	-	165	67	-	250	60	-
HB3	500	250	210	4.61	0.65	200	110	1.82	1.00	1.00	1.00	295	45	340	-	165	40	-	250	36	-
HB4	500	250	210	4.61	0.65	135	110	1.23	1.00	1.00	1.00	295	55	350	-	165	49	-	250	44	-
HB5	500	250	210	4.61	0.65	200	110	1.82	1.00	1.00	1.00	295	300	595	-	165	201	-	250	181	-
HB6	500	250	210	4.61	0.65	135	110	1.23	1.00	1.00	1.00	295	315	610	-	165	230	-	250	207	-
Reference: AlDywany (2010)																					
A1	750	250	210	1.29	0.0	-	-	-	1.00	1.00	1.00	179	-	179	-	166	-	-	168	-	-
A1/2	750	250	210	1.29	0.0	-	-	-	1.00	0.50	0.50	188	-	188	-	166	-	-	168	-	-
A1/4	750	250	210	1.29	0.0	-	-	-	1.00	0.25	0.25	178	-	178	-	166	-	-	168	-	-
RA1/2	750	250	210	1.29	0.0	-	-	-	1.00	0.50	0.50	194	-	194	-	166	-	-	168	-	-
RA1/4	750	250	210	1.29	0.0	-	-	-	1.00	0.25	0.25	191	-	191	-	166	-	-	168	-	-
B1	750	250	210	1.29	0.036	110	160	0.69	1.00	1.00	1.00	-	-	241	-	166	67	-	168	61	-
B1/2	750	250	210	1.29	0.036	110	160	0.69	1.00	0.50	0.50	-	-	195	-	166	67	-	168	61	-
B1/4	750	250	210	1.29	0.036	110	130	0.85	1.00	0.25	0.25	-	-	198	-	166	67	-	168	61	-
RB1/2	750	250	210	1.29	0.036	110	135	0.81	1.00	0.50	0.50	-	-	251	-	166	67	-	168	61	-
RB1/4	750	250	210	1.29	0.036	110	135	0.81	1.00	0.25	0.25	-	-	237	-	166	67	-	168	61	-
Reference: Lubell et al (2008, 2009)																					
AX8	700	340	286	1.75	0.0	-	-	-	0.22	0.22	0.22	272	-	272	-	200	-	-	237	-	-
AX7	700	340	286	0.89	0.0	-	-	-	1.00	1.00	1.00	249	-	249	-	200	-	-	189	-	-
AX6	700	340	286	1.75	0.0	-	-	-	1.00	1.00	1.00	281	-	281	-	217	-	-	250	-	-
AX1	700	340	286	1.75	0.20	175	625	0.28	1.00	1.00	1.00	-	-	458	-	217	105	-	250	95	-
AX2	700	340	286	1.75	0.20	175	625	0.28	1.00	1.00	1.00	-	-	338	-	200	101	-	237	91	-
AX3	700	340	286	1.75	0.30	175	350	0.50	1.00	1.00	1.00	-	-	450	-	217	119	-	250	107	-
AX4	700	340	286	1.75	0.40	175	235	0.74	1.00	1.00	1.00	-	-	415	-	217	109	-	250	98	-

Beams	bw	h	d	$\rho_s$	$\rho_s'$	SL	S <sub>w</sub>	SL/S <sub>w</sub>	k <sub>p</sub>	k <sub>s</sub>	k	Test Strengths, kN - m				ACI318 & SBC304			EC2 Code		
												V <sub>c,ex</sub>	V <sub>s,ex</sub>	V <sub>u,ex</sub>	M <sub>u,ex</sub>	V <sub>c</sub>	V <sub>s</sub>	M <sub>u</sub>	V <sub>c</sub>	V <sub>s</sub>	M <sub>u</sub>
-	mm	mm	mm	%	%	mm	mm	-	-	-	-	V <sub>c,ex</sub>	V <sub>s,ex</sub>	V <sub>u,ex</sub>	M <sub>u,ex</sub>	V <sub>c</sub>	V <sub>s</sub>	M <sub>u</sub>	V <sub>c</sub>	V <sub>s</sub>	M <sub>u</sub>
AX5	700	340	286	1.75	0.40	175	470	0.37	1.00	1.00	1.00	-	-	359	-	217	105	-	250	95	-
AW8	1170	585	509	1.68	0.0	-	-	-	1.00	1.00	1.00	789	-	789	-	648	-	-	653	-	-
AW6	1170	585	509	1.68	0.07	300	1080	0.28	1.00	1.00	1.00	-	-	826	-	648	301	-	653	271	-
AW7	1170	585	509	1.68	0.14	300	370	0.81	1.00	1.00	1.00	-	-	1062	-	580	215	-	606	194	-
AW1	1170	585	538	0.79	0.0	-	-	-	0.26	0.26	0.26	585	-	585	-	625	-	-	500	-	-
AW4	1170	585	509	1.68	0.0	-	-	-	0.26	0.26	0.26	716	-	716	-	580	-	-	606	-	-
AW2	1170	585	509	1.68	0.07	300	1080	0.28	0.26	0.26	0.26	-	-	809	-	580	301	-	606	271	-
AW3	1170	585	509	1.68	0.07	300	800	0.38	0.26	0.26	0.26	-	-	828	-	580	301	-	606	271	-
AW5	1170	585	509	1.68	0.14	300	375	0.80	0.26	0.26	0.26	-	-	953	-	580	215	-	606	194	-
Reference: McAllister (2011)																					
B1 (ACI)	703	339	295	0.76	0.075	134	600	0.22	1.00	1.00	1.00	-	-	285	-	171	173	-	163	156	-
B2 (EC2)	703	339	295	1.65	0.075	184	600	0.31	1.00	1.00	1.00	-	-	330	-	171	125	-	210	113	-
Reference: Al-Harithy (2002)																					
B1-25	800	200	165	3.81	1.93	82	370	0.22	1.00	1.00	1.00	-	-	-	311	-	-	257.1	-	-	257.1
B1-65	800	200	165	3.81	1.93	82	370	0.22	1.00	1.00	1.00	-	-	-	351	-	-	277.5	-	-	261.5
B1-95	800	200	165	3.81	1.93	82	370	0.22	1.00	1.00	1.00	-	-	-	348	-	-	277.5	-	-	267.9
B2-25	800	200	165	2.62	1.35	82	370	0.22	1.00	1.00	1.00	-	-	-	215	-	-	176.8	-	-	176.8
B2-65	800	200	165	2.62	1.35	82	370	0.22	1.00	1.00	1.00	-	-	-	253	-	-	190.8	-	-	179.8
B2-95	800	200	165	2.62	1.35	82	370	0.22	1.00	1.00	1.00	-	-	-	263	-	-	190.8	-	-	184.2
B3-25	800	200	165	1.90	0.96	82	370	0.22	1.00	1.00	1.00	-	-	-	176	-	-	128.2	-	-	128.2
B3-65	800	200	165	1.90	0.96	82	370	0.22	1.00	1.00	1.00	-	-	-	195	-	-	138.4	-	-	130.4
B3-95	800	200	165	1.90	0.96	82	370	0.22	1.00	1.00	1.00	-	-	-	211	-	-	138.4	-	-	133.6
B4-25	800	200	165	0.70	0.35	82	370	0.22	1.00	1.00	1.00	-	-	-	64	-	-	47.2	-	-	47.2
B4-65	800	200	165	0.70	0.35	82	370	0.22	1.00	1.00	1.00	-	-	-	74	-	-	51.0	-	-	48.0
B4-95	800	200	165	0.70	0.35	82	370	0.22	1.00	1.00	1.00	-	-	-	73	-	-	51.0	-	-	49.2

1 mm = 0.0394 in, 1 kN = 1000 N = 0.225 kip, 1 MPa = 145 psi, 1 kN.m = 0.738 kip.ft = 8.858 kip.in.

k<sub>p</sub> = b<sub>p</sub>/b<sub>w</sub>, k<sub>s</sub> = b<sub>s</sub>/b<sub>w</sub>, and k = the lesser of (k<sub>p</sub> or k<sub>s</sub>).

**Table 4.4a:** Test Results obtained by Serna-Ros et al. (2002) Investigation on EC2 Code.

	Code Stren.,kN			Lubell Stren.,kN			Serna-Ros Stren.,kN			Shuraim Stren.,kN			Test Stren., kN		
	Vc	Vs	Vu	Vc	Vs	Vu	Vc	Vs	Vu	Vc	Vs	Vu	Vc,ex	Vs,ex	Vu,ex
	EC2 Code														
R0	173	-	173	173	-	173	173	-	173	173	-	173	244	-	244
R1	173	79	252	173	79	252	173	48	221	173	45	218	244	22	266
A0	147	-	147	147	-	147	147	-	147	147	-	147	187	-	187
A1	147	82	229	147	82	229	147	85	232	147	82	229	187	78	265
A2	147	88	235	147	88	235	147	53	200	147	50	197	187	47	234
A3	147	102	249	147	102	249	147	106	253	147	102	249	187	95	282
C0	151	-	151	151	-	151	151	-	151	151	-	151	182	-	182
C1	151	110	261	151	110	261	151	66	217	151	64	215	182	76	258
C2	151	98	249	151	98	249	151	102	253	151	98	249	182	109	291
C3	151	111	262	151	111	262	151	164	315	151	158	309	182	176	358
C4	151	147	298	151	147	298	151	228	379	151	177	328	182	178	360
C5	151	221	372	151	221	372	151	326	477	151	186	337	182	161	343
D0	171	-	171	140	-	140	171	-	171	171	-	171	218	-	218
D1	171	108	279	140	89	229	171	45	216	171	63	234	218	48	266
D2	171	94	265	140	77	217	171	67	238	171	95	266	218	78	296
D3	171	106	277	140	87	227	171	107	278	171	150	321	218	102	320
D5	171	213	384	140	175	315	171	216	387	171	180	351	218	127	345

**NOTE:** bw = 750mm, h = 250mm, d = 206mm,  $\rho_s = 2.2\%$ ,  $\rho_{s'} = 0.94\%$ ,  $\rho_v = 0.089\%$  (Beams R1, A1),  $\rho_v = 0.123\%$  (All other beams),  $f_c = 24.5\text{-}32.6$  MPa,  $f_{yv} = 512\text{-}670$  MPa,  $k_p = 1.0$  ( $b_p = b_w = 750\text{mm}$ ) for all Beams,  $k_s = 0.4$  ( $b_s = 300\text{mm}$ ) for Beams in Series D,  $k_s = 1.0$  ( $b_s = b_w = 750\text{mm}$ ) for Beams in other Series,  $S_L = 85\text{mm}$  (Beams C5 and D5),  $S_L = 127.5\text{mm}$  (Beam C4),  $S_L = 170\text{mm}$  (all other Beams),  $S_w = 115\text{mm}$  (Beams C3 and D3),  $S_w = 138\text{mm}$  (Beam C4),  $S_w = 230\text{mm}$  (Beams A1, A3, C2, C5, D2, and D5),  $S_w = 690\text{mm}$  (Beams R1, A2, C1, and D1).

1 mm = 0.0394 in, 1 kN = 1000 N = 0.225 kip, 1 MPa = 145 psi, 1 kN.m = 0.738 kip.ft = 8.858 kip.in.

**Table 4.4b:** Test Results obtained by Serna-Ros et al. (2002) Investigation on ACI318 Code.

	Code Stren.,kN			Lubell Stren.,kN			Serna-Ros Stren.,kN			Shuraim Stren.,kN			Test Stren., kN		
	Vc	Vs	Vu	Vc	Vs	Vu	Vc	Vs	Vu	Vc	Vs	Vu	Vc,ex	Vs,ex	Vu,ex
	ACI318 & SBC304														
R0	139	-	139	139	-	139	139	-	139	139	-	139	244	-	244
R1	139	87	226	139	87	226	139	52	191	139	45	184	244	22	266
A0	128	-	128	128	-	128	128	-	128	128	-	128	187	-	187
A1	128	92	220	128	92	220	128	96	224	128	82	210	187	78	265
A2	128	97	225	128	97	225	128	58	186	128	50	178	187	47	234
A3	128	113	241	128	113	241	128	118	246	128	102	230	187	95	282
C0	130	-	130	130	-	130	130	-	130	130	-	130	182	-	182
C1	130	122	252	130	122	252	130	73	203	130	64	194	182	76	258
C2	130	109	239	130	109	239	130	114	244	130	98	228	182	109	291
C3	130	123	253	130	123	253	130	181	311	130	158	288	182	176	358
C4	130	164	294	130	164	294	130	255	385	130	177	307	182	178	360
C5	130	246	376	130	246	376	130	362	492	130	186	316	182	161	343
D0	148	-	148	121	-	121	148	-	148	148	-	148	218	-	218
D1	148	121	269	121	99	220	148	50	198	148	63	211	218	48	266
D2	148	105	253	121	86	207	148	75	223	148	95	243	218	78	296
D3	148	118	266	121	97	218	148	119	267	148	150	298	218	102	320
D5	148	237	385	121	194	315	148	240	388	148	180	328	218	127	345

**NOTE:** bw = 750mm, h = 250mm, d = 206mm,  $\rho_s = 2.2\%$ ,  $\rho_{s'} = 0.94\%$ ,  $\rho_v = 0.089\%$  (Beams R1, A1),  $\rho_v = 0.123\%$  (All other beams),  $f_c = 24.5\text{-}32.6$  MPa,  $f_{yv} = 512\text{-}670$  MPa,  $k_p = 1.0$  ( $b_p = b_w = 750\text{mm}$ ) for all Beams,  $k_s = 0.4$  ( $b_s = 300\text{mm}$ ) for Beams in Series D,  $k_s = 1.0$  ( $b_s = b_w = 750\text{mm}$ ) for Beams in other Series,  $S_L = 85\text{mm}$  (Beams C5 and D5),  $S_L = 127.5\text{mm}$  (Beam C4),  $S_L = 170\text{mm}$  (all other Beams),  $S_w = 115\text{mm}$  (Beams C3 and D3),  $S_w = 138\text{mm}$  (Beam C4),  $S_w = 230\text{mm}$  (Beams A1, A3, C2, C5, D2, and D5),  $S_w = 690\text{mm}$  (Beams R1, A2, C1, and D1).

1 mm = 0.0394 in, 1 kN = 1000 N = 0.225 kip, 1 MPa = 145 psi, 1 kN.m = 0.738 kip.ft = 8.858 kip.in.

**Table 4.5:** Test Results obtained by Shuraim (2012) Investigation.

	Code Stren.,kN			Lubell Stren.,kN			Serna-Ros Stren.,kN			Shuraim Stren.,kN			Test Stren., kN		
	Vc	Vs	Vu	Vc	Vs	Vu	Vc	Vs	Vu	Vc	Vs	Vu	Vc,ex	Vs,ex	Vu,ex
	ACI318 & SBC304														
S0	140	-	140	140	-	140	140	-	140	140	-	140	161	-	161
S1-80	140	142	282	140	142	282	140	93	233	140	59	199	161	60	221
S2-80	140	142	282	140	142	282	140	114	254	140	71	211	161	61	222
S3-80	140	142	282	140	142	282	140	157	297	140	98	238	161	71	232
S0-1	140	-	140	140	-	140	140	-	140	140	-	140	162	-	162
S1-75-1A	140	188	328	140	188	328	140	127	267	140	74	214	162	0	162
S3-75-1	140	144	284	140	144	284	140	164	304	140	74	214	162	58	220
S13-75-1A	140	188	328	140	188	328	140	215	355	140	126	266	162	112	274
S13-100-1	140	143	283	140	143	283	140	141	281	140	101	241	162	106	268
S13-125-1	140	110	250	140	110	250	140	97	237	140	86	226	162	79	241
S0-2	140	-	140	140	-	140	140	-	140	140	-	140	160	-	160
S1-75-2	140	188	328	140	188	328	140	127	267	140	74	214	160	81	241
S3-75-2	140	144	284	140	144	284	140	164	304	140	74	214	160	81	241
S13-75-2	140	188	328	140	188	328	140	215	355	140	126	266	160	146	306
S13-100-2	140	143	283	140	143	283	140	141	281	140	101	241	160	118	278
S13-125-2	140	110	250	140	110	250	140	97	237	140	86	226	160	81	241

**NOTE:** bw = 700mm, h = 180mm, d = 150mm,  $\rho_s = 1.34\%$  and  $\rho_s' = 1.026\%$  (for all beams),  $A_v = 157\text{mm}^2$  and  $201\text{mm}^2$ ,  $\rho_v = 0.28\%$ ,  $0.38\%$  and  $0.23\%$ ,  $f_{c,av} = 29\text{ MPa}$ ,  $f_{yv} = 483\text{ MPa}$  and  $465\text{ MPa}$ .  $S_L = 80, 75, 100$  and  $125\text{mm}$ .  $S_w = 660\text{mm}$  (for beams S1-80, S1-75-1A and S1-75-2),  $S_w = 440\text{mm}$  (for beam S2-80), and  $S_w = 230\text{mm}$  (for all other beams).  $k = 1.0$  ( $b_s = b_p = b_w = 700\text{mm}$ ) for all beams.

These Beams are continuous wide RC beams.

1 mm = 0.0394 in, 1 kN = 1000 N= 0.225 kip, 1 MPa = 145 psi, 1 kN.m = 0.738 kip.ft = 8.858 kip.in.

**Table 4.6:** Test Results obtained by Hanafy et al. (2012) Investigation.

	Code Stren.,kN			Lubell Stren.,kN			Serna-Ros Stren.,kN			Shuraim Stren.,kN			Test Stren., kN		
	Vc	Vs	Vu	Vc	Vs	Vu	Vc	Vs	Vu	Vc	Vs	Vu	Vc,ex	Vs,ex	Vu,ex
	Av. Various Codes														
NB1	102	-	102	102	-	102	102	-	102	102	-	102	245	-	245
NB2	102	67	169	102	67	169	102	95	197	102	73	175	245	105	350
NB3	102	40	142	102	40	142	102	57	159	102	68	170	245	55	300
NB4	102	49	151	102	49	151	102	84	186	102	65	167	245	61	306
NB5	102	201	303	102	201	303	102	285	387	102	284	386	245	250	495
NB6	102	230	332	102	230	332	102	396	498	102	254	356	245	305	550
HB1	129	-	129	129	-	129	129	-	129	129	-	129	295	-	295
HB2	129	67	196	129	67	196	129	95	224	129	73	202	295	103	398
HB3	129	40	169	129	40	169	129	57	186	129	68	197	295	45	340
HB4	129	49	178	129	49	178	129	84	213	129	65	194	295	55	350
HB5	129	201	330	129	201	330	129	285	414	129	284	413	295	300	595
HB6	129	230	359	129	230	359	129	396	525	129	254	383	295	315	610

**NOTE:** bw = 500mm, h = 250mm, d = 210mm,  $\rho_s = 4.61\%$ ,  $\rho_s' = 0.65\%$ ,  $\rho_v = 0.16\%$  -0.47%,  $f_{c,av} = 40\text{ MPa}$  (for all beams in Series NB),  $f_{c,av} = 90\text{ MPa}$  (for all beams in Series HB),  $f_y = 420\text{ MPa}$ ,  $f_{yv} = 300\text{ MPa}$  (for beams NB2, NB3, NB4, HB2, HB3 and HB4),  $f_{yv} = 420\text{ MPa}$  (for beams NB5, NB6, HB5 and HB6).  $S_L = 200\text{mm}$  (Beams NB2, NB3, NB5, HB2, HB3 and HB5),  $S_L = 135\text{mm}$  (Beams NB4, NB6, HB4 and HB6).  $S_w = 110\text{mm}$  (for all beams with stirrups).  $k = k_s = k_p = 1.0$  ( $b_s = b_p = b_w = 500\text{mm}$ ) for all beams.

These Beams may be considered beams with T-Sections.

1 mm = 0.0394 in, 1 kN = 1000 N= 0.225 kip, 1 MPa = 145 psi, 1 kN.m = 0.738 kip.ft = 8.858 kip.in.



**Table 4.7:** Test Results obtained by Al.Dywany (2010) Investigation.

	Code Stren.,kN			Lubell Stren.,kN			Serna-Ros Stren.,kN			Shuraim Stren.,kN			Test Stren., kN		
	Vc	Vs	Vu	Vc	Vs	Vu	Vc	Vs	Vu	Vc	Vs	Vu	Vc,ex	Vs,ex	Vu,ex
	BS8110 Code														
A1	137	-	137	137	-	137	137	-	137	137	-	137	179	-	179
A1/2	137	-	137	116	-	116	137	-	137	137	-	137	188	-	188
A1/4	137	-	137	106	-	106	137	-	137	137	-	137	178	-	178
RA1/2	137	-	137	116	-	116	137	-	137	137	-	137	194	-	194
RA1/4	137	-	137	106	-	106	137	-	137	137	-	137	191	-	191
B1	137	68	205	137	68	205	137	108	245	137	66	203	-	-	241
B1/2	137	68	205	116	58	174	137	81	218	137	66	203	-	-	195
B1/4	137	68	205	106	53	159	137	68	205	137	73	210	-	-	198
RB1/2	137	68	205	116	58	174	137	88	225	137	72	209	-	-	251
RB1/4	137	68	205	106	53	159	137	66	203	137	72	209	-	-	237

**NOTE:** bw = 750mm, h = 250mm, d = 210mm,  $\rho_s = 1.29\%$ ,  $f_{c,av} = 28.5$  MPa,  $f_{yv} = 250$  MPa for all beams ( $\rho_s = 0.036\%$ ,  $\rho_v = 0.17\%$  for all beams in Series B).  $k_p = 1.0$  ( $b_p = b_w = 750$ mm) for all Beams.  $k_s = 0.25$  ( $b_s = 190$ mm) for Beams A1/4, RA1/4, B1/4, and RB1/4.  $k_s = 0.50$  ( $b_s = 375$ mm) for Beams A1/2, RA1/2, B1/2, and RB1/2.  $k_s = 1.0$  ( $b_s = 750$ mm) for Beams A1 and B1.  $S_L = 110$ mm (for all Beams in Series B).  $S_w = 160$ mm (for Beams B1 and B1/2),  $S_w = 130$ mm (for Beam B1/4),  $S_w = 135$ mm (for Beams RB1/2 and RB1/4).

Beams without stirrups (in series A) are not references for beams with stirrups (in series B), because they did not have top flexural bars for  $\rho_s$  and ( $V_{c,ex}$ ) verifications. 1 mm = 0.0394 in, 1 kN = 1000 N = 0.225 kip, 1 MPa = 145 psi, 1 kN.m = 0.738 kip.ft = 8.858 kip.in.

**Table 4.8:** Test Results obtained by Lubell et al. (2008, 2009) Investigation.

	Code Stren.,kN			Lubell Stren.,kN			Serna-Ros Stren.,kN			Shuraim Stren.,kN			Test Stren., kN		
	Vc	Vs	Vu	Vc	Vs	Vu	Vc	Vs	Vu	Vc	Vs	Vu	Vc,ex	Vs,ex	Vu,ex
	ACI318 & SBC304														
AX8	200	-	200	153	-	153	200	-	200	200	-	200	272	-	272
AX7	200	-	200	200	-	200	200	-	200	200	-	200	249	-	249
AX6	217	-	200	200	-	200	200	-	200	200	-	200	281	-	281
AX1	217	105	322	217	105	322	217	91	308	217	63	280	-	-	458
AX2	200	101	301	200	101	301	200	87	287	200	60	260	-	-	338
AX3	217	119	336	217	119	336	217	138	355	217	95	312	-	-	450
AX4	217	109	326	217	109	326	217	154	371	217	106	323	-	-	415
AX5	217	105	322	217	105	322	217	105	322	217	72	289	-	-	359
AW8	648	-	621	621	-	621	621	-	621	621	-	621	789	-	789
AW6	648	301	922	621	301	922	621	269	890	621	181	802	-	-	826
AW7	580	215	795	580	215	795	580	328	908	580	221	801	-	-	1062
AW1	625	-	625	486	-	486	625	-	625	625	-	625	585	-	585
AW4	580	-	580	451	-	451	580	-	580	580	-	580	716	-	716
AW2	580	301	881	451	234	685	580	155	735	580	181	761	-	-	809
AW3	580	301	881	451	234	685	580	180	760	580	210	790	-	-	828
AW5	580	215	795	451	167	618	580	188	768	580	219	799	-	-	953

**NOTE:** For Beams in Series AX: bw = 700mm, h = 340mm, d = 286mm,  $\rho_s = 1.75\%$  ( $\rho_s = 0.89\%$  for beam AX7),  $\rho_s = 0.20\%$  (for beams AX1 & AX2),  $\rho_s = 0.30\%$  (for beam AX3),  $\rho_s = 0.40\%$  (for beams AX4 & AX5),  $\rho_v = 0.08\% - 0.11\%$ . For Beams in Series AW: bw = 1170mm, h = 585mm, d = 509mm (d = 538mm for beam AW1),  $\rho_s = 1.68\%$  ( $\rho_s = 0.79\%$  for beam AW1),  $\rho_s = 0.07\%$  (for beams AW2, AW3 & AW6),  $\rho_s = 0.14\%$  (for beams AW5 & AW7),  $\rho_v = 0.08\% - 0.11\%$ . For all:  $f_{c,av} = 36-43$  MPa,  $f_{yv} = 458-625$  MPa.  $S_L = 175$ mm (all Beams in Series AX),  $S_L = 300$ mm (all Beams in Series AW).  $S_w = 625, 625, 350, 235$  and  $470$ mm (for Beams in Series AX),  $S_w = 1080, 800, 375, 1080$  and  $370$ mm (for Beams in Series AW).  $k = k_s = k_p = 0.26$  ( $b_s = b_p = 305$ mm) for beams AW1, AW2, AW3, AW4 and AW5.  $k = k_s = k_p = 0.22$  ( $b_s = b_p = 152$ mm) for beam AX8.  $k_s = k_p = 1.0$  for all other Beams.

Beams without stirrups are not references for beams with stirrups, because they did not have top flexural bars for  $\rho_s$  and ( $V_{c,exp}$ ) verifications. 1 mm = 0.0394 in, 1 kN = 1000 N = 0.225 kip, 1 MPa = 145 psi, 1 kN.m = 0.738 kip.ft = 8.858 kip.in.

**Table 4.9:** Test Results obtained by McAllister (2011) Investigation.

	Code Stren.,kN			Lubell Stren.,kN			Serna-Ros Stren.,kN			Shuraim Stren.,kN			Test Stren., kN		
	Vc	Vs	Vu	Vc	Vs	Vu	Vc	Vs	Vu	Vc	Vs	Vu	Vc,ex	Vs,ex	Vu,ex
	Various Codes														
<b>B1 (ACI318 &amp; SBC304)</b>	172	173	345	172	173	345	172	180	352	172	99	271	-	-	285
<b>B2 (EC2)</b>	172	113	285	172	113	285	172	100	272	172	78	250	-	-	330

**NOTE:** bw = 703mm, h = 339mm, d = 295mm,  $f_{c,av.} = 24.8$  MPa,  $f_{yv} = 500$  MPa, k=1.0 ( $b_s = b_p = b_w = 703$ mm) for both Beams. Beam B1:  $\rho_s = 0.76\%$ ,  $\rho_s' = 0.075\%$ ,  $\rho_v = 0.167\%$ . Beam B2:  $\rho_s = 1.65\%$ ,  $\rho_s' = 0.075\%$ ,  $\rho_v = 0.121\%$ .  $S_L = 134$ mm (Beam B1) and  $S_L = 184$ mm (Beam B2).  $S_w = 600$ mm for both Beams.  
 1 mm = 0.0394 in, 1 kN = 1000 N = 0.225 kip, 1 MPa = 145 psi, 1 kN.m = 0.738 kip.ft = 8.858 kip.in.

**Table 4.10:** Test Results obtained by Al-Harithy (2002) Investigation.

	Code Stren., kN.m	Test Stren., kN.m
	Mu	Mu,exp
	ACI318 & SBC304	
B1-25	276	311
B1-65	276	351
B1-95	276	348
B2-25	190	215
B2-65	190	253
B2-95	190	263
B3-25	138	176
B3-65	138	195
B3-95	138	211
B4-25	51	64
B4-65	51	74
B4-95	51	73

**NOTE:** bw = 800mm, h = 200mm, d = 165mm, jd= 123.5-133.3mm (ACI Code), jd= 123.5-125.6-128.7mm (EC2 Code), and  $\rho_v = 0.15\%$  (for all beams),  $\rho_s = 3.81\%$  and  $\rho_s' = 1.93\%$  (beam-type B1),  $\rho_s = 2.62\%$  and  $\rho_s' = 1.35\%$  (beam-type B2),  $\rho_s = 1.90\%$  and  $\rho_s' = 0.96\%$  (beam-type B3),  $\rho_s = 0.70\%$  and  $\rho_s' = 0.35\%$  (beam-type B4),  $f_{c,av.} = 25, 65$  and  $95$  MPa,  $f_y = 414$  MPa, k = 1.0 ( $b_s = b_p = b_w = 800$ mm) for all Beams.  $S_L = 82$ mm and  $S_w = 370$ mm for all beams.

1 mm = 0.0394 in, 1 kN = 1000 N = 0.225 kip, 1 MPa = 145 psi, 1 kN.m = 0.738 kip.ft = 8.858 kip.in.

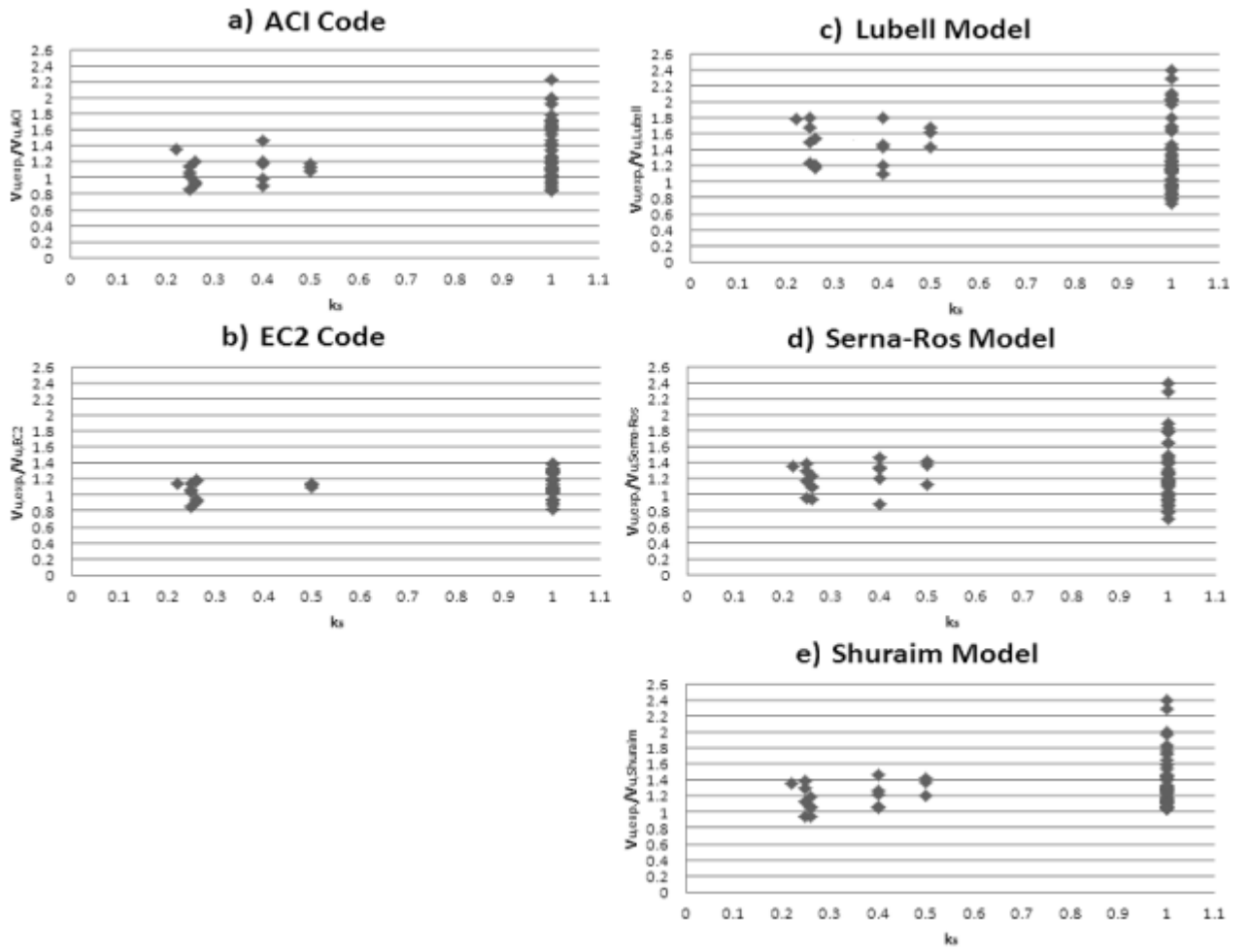


Figure 4.17:  $k_s$  versus  $V_{u,exp}/V_{u,Pred.}$ .

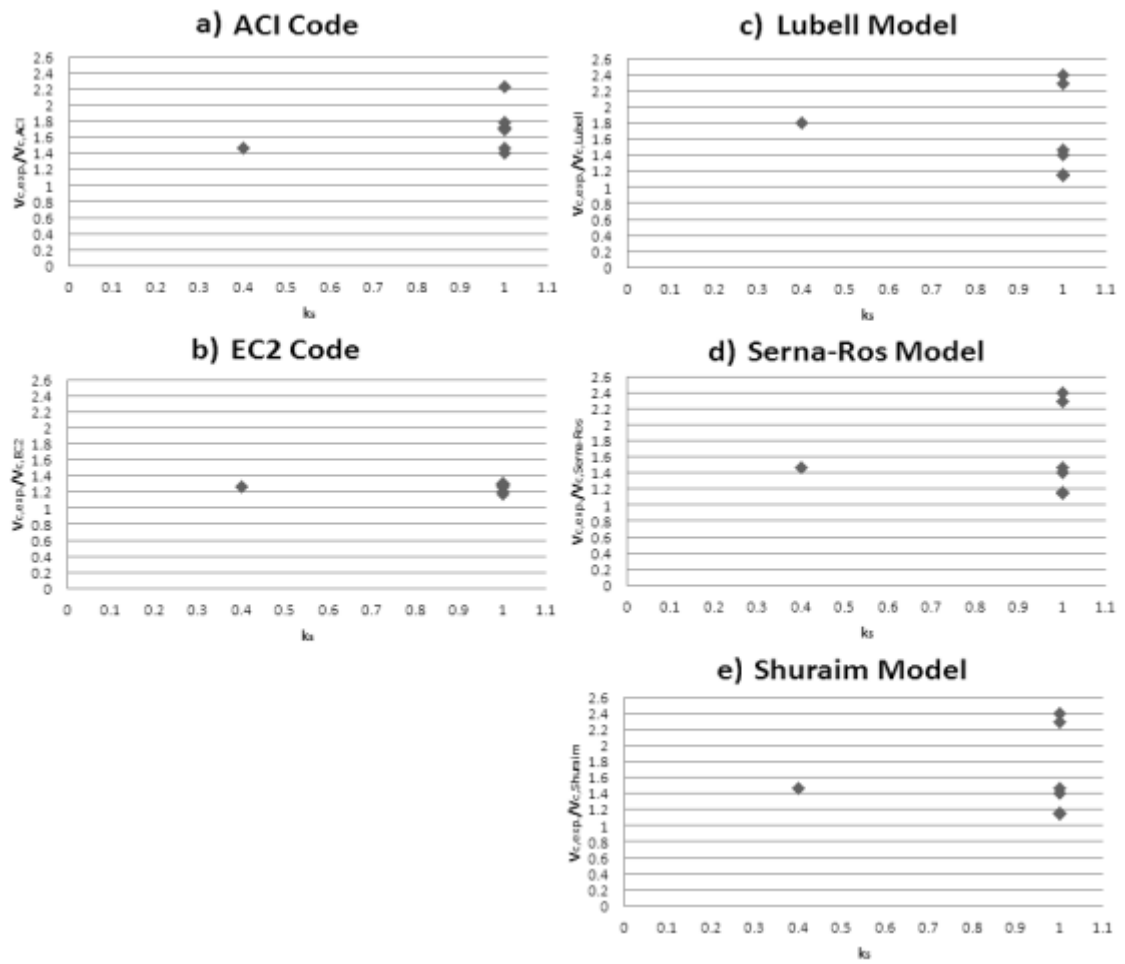


Figure 4.18:  $k_s$  versus  $V_{c,exp}/V_{c,Pred.}$ .

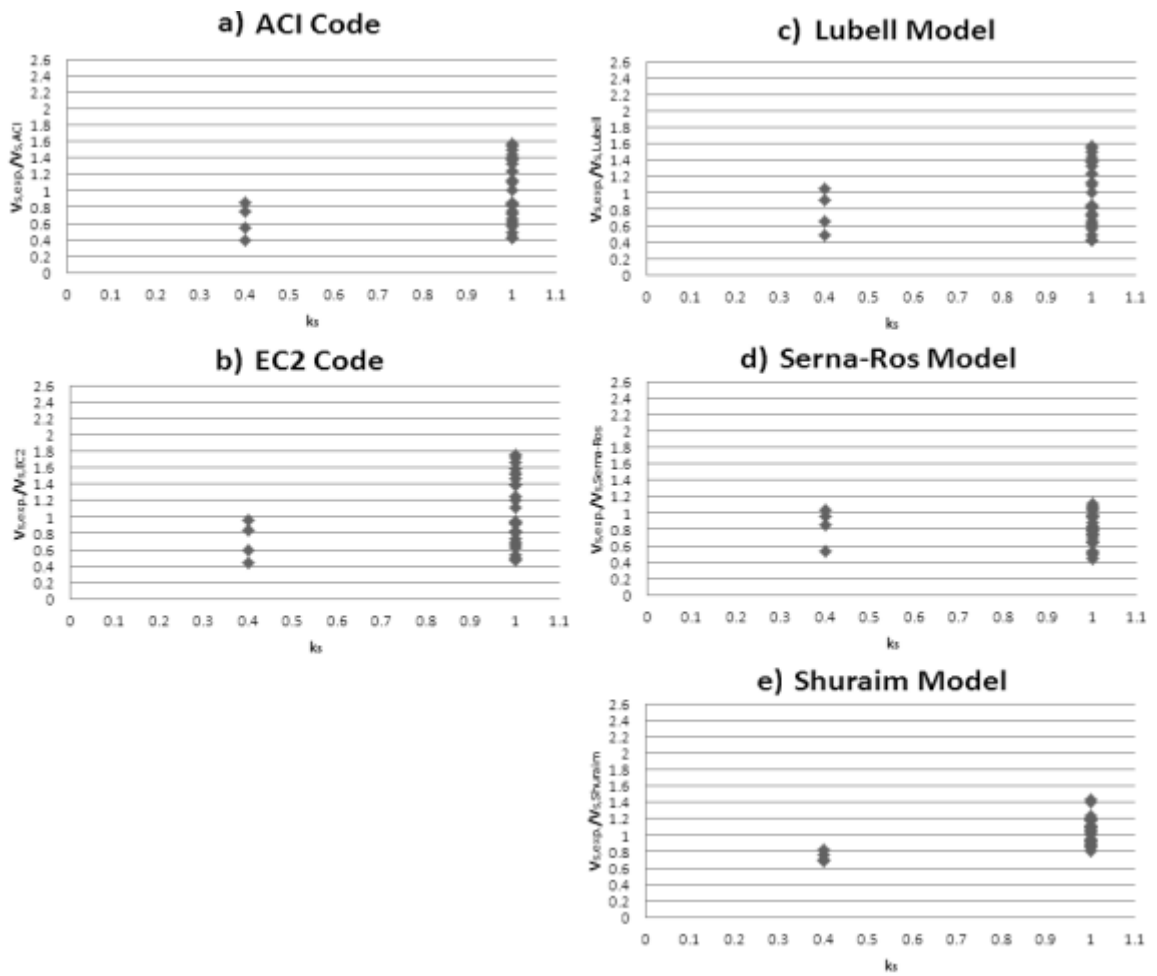


Figure 4.19:  $k_s$  versus  $V_{s,exp}/V_{s,Pred.}$ .

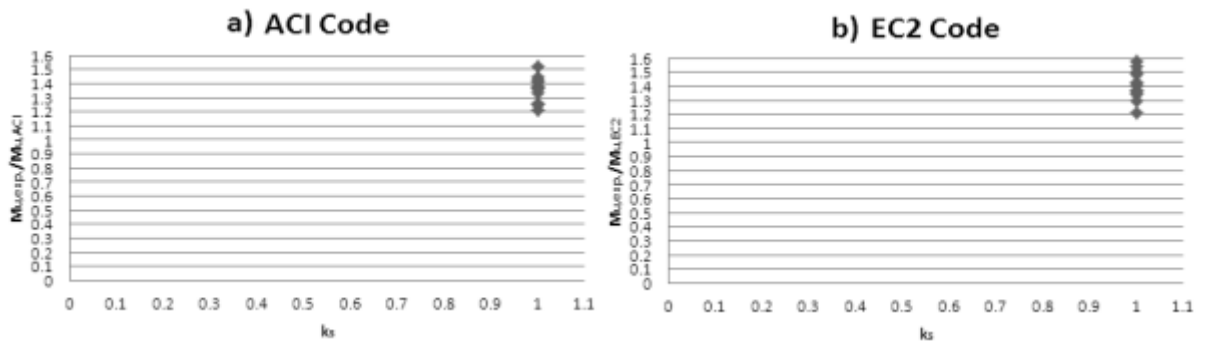


Figure 4.20:  $k_s$  versus  $M_{u,exp}/M_{u,Pred.}$ .

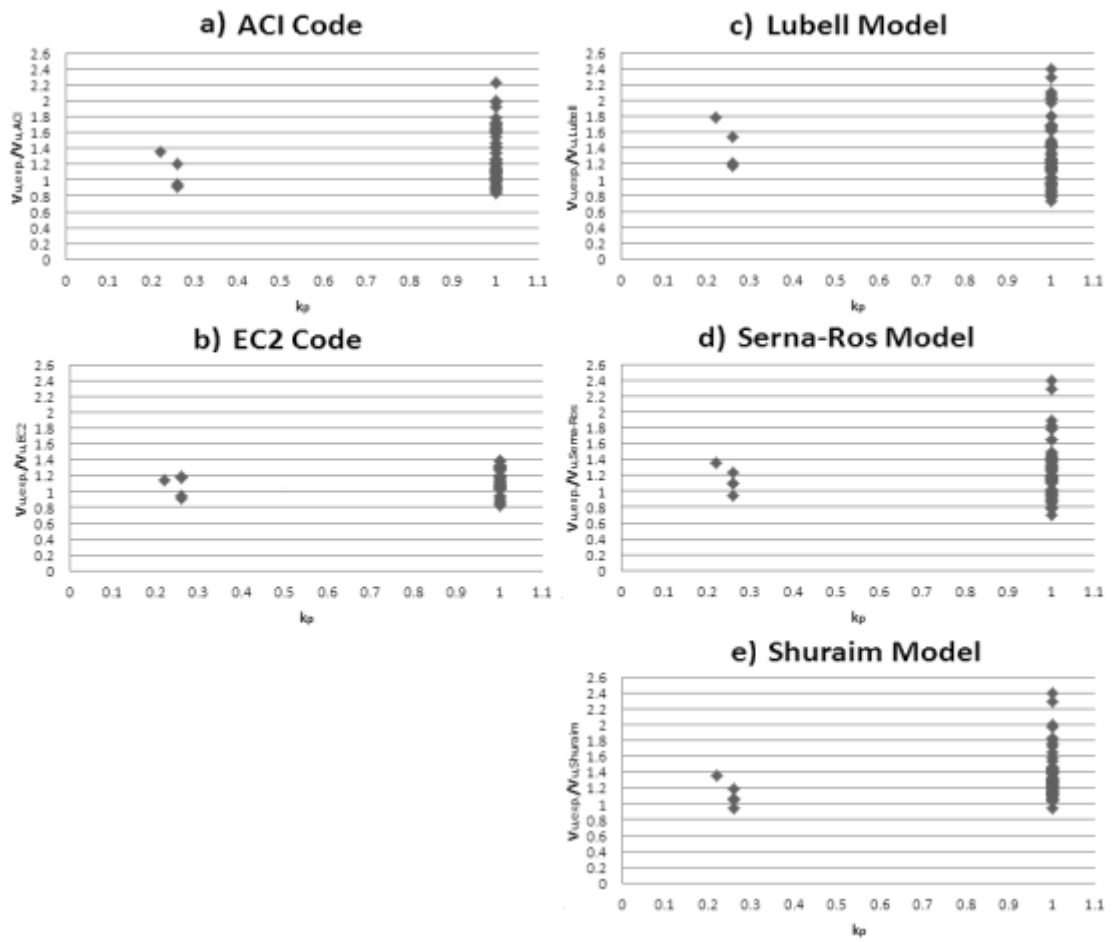


Figure 4.21:  $k_p$  versus  $V_{u,exp}/V_{u,Pred.}$ .

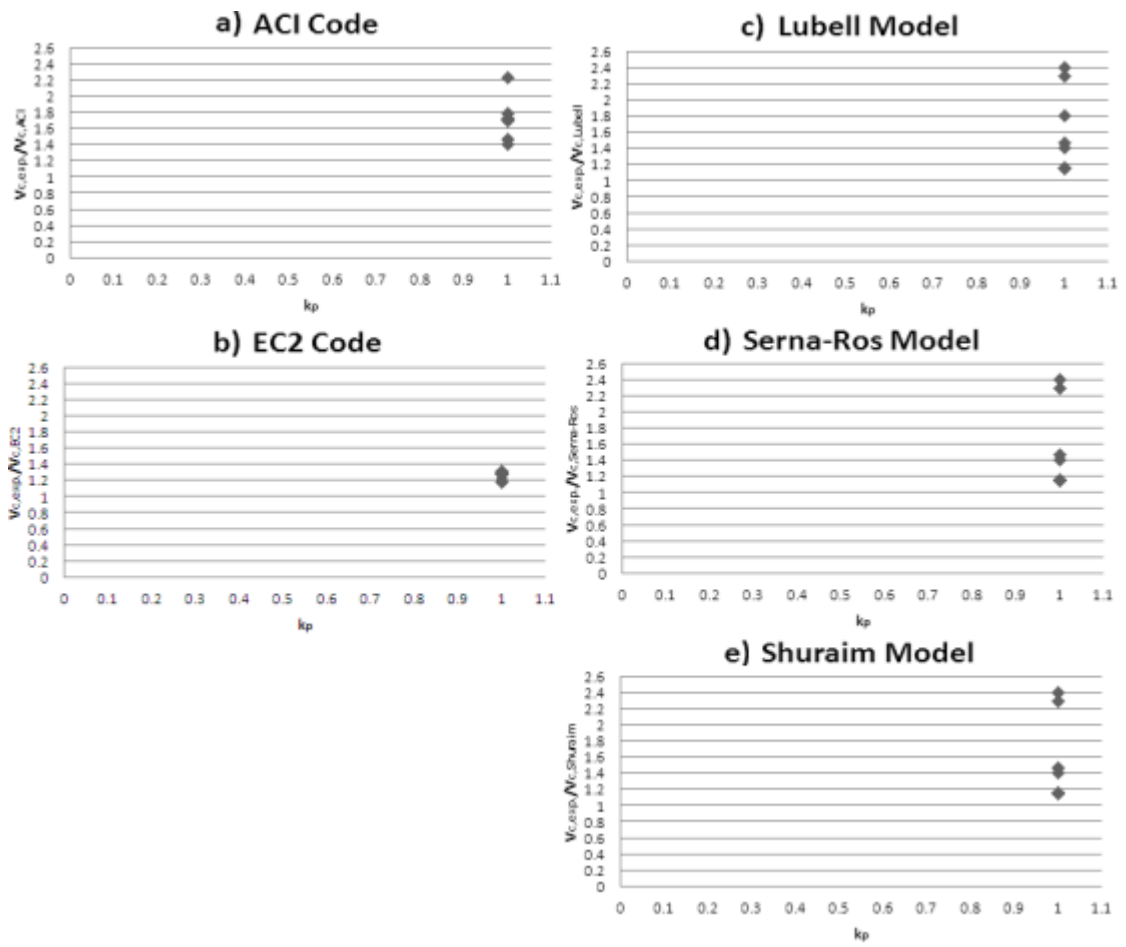


Figure 4.22:  $k_p$  versus  $V_{c,exp}/V_{c,Pred.}$ .

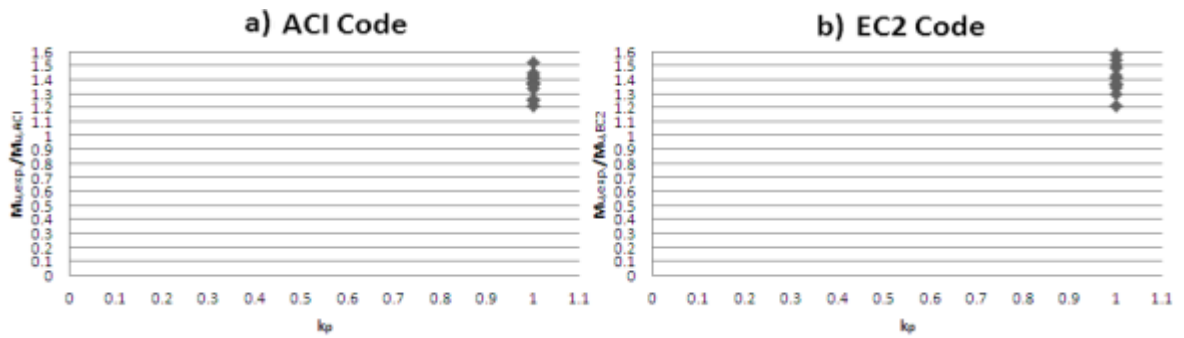


Figure 4.23:  $k_p$  versus  $\mu_{u,exp}/\mu_{u,Pred.}$ .

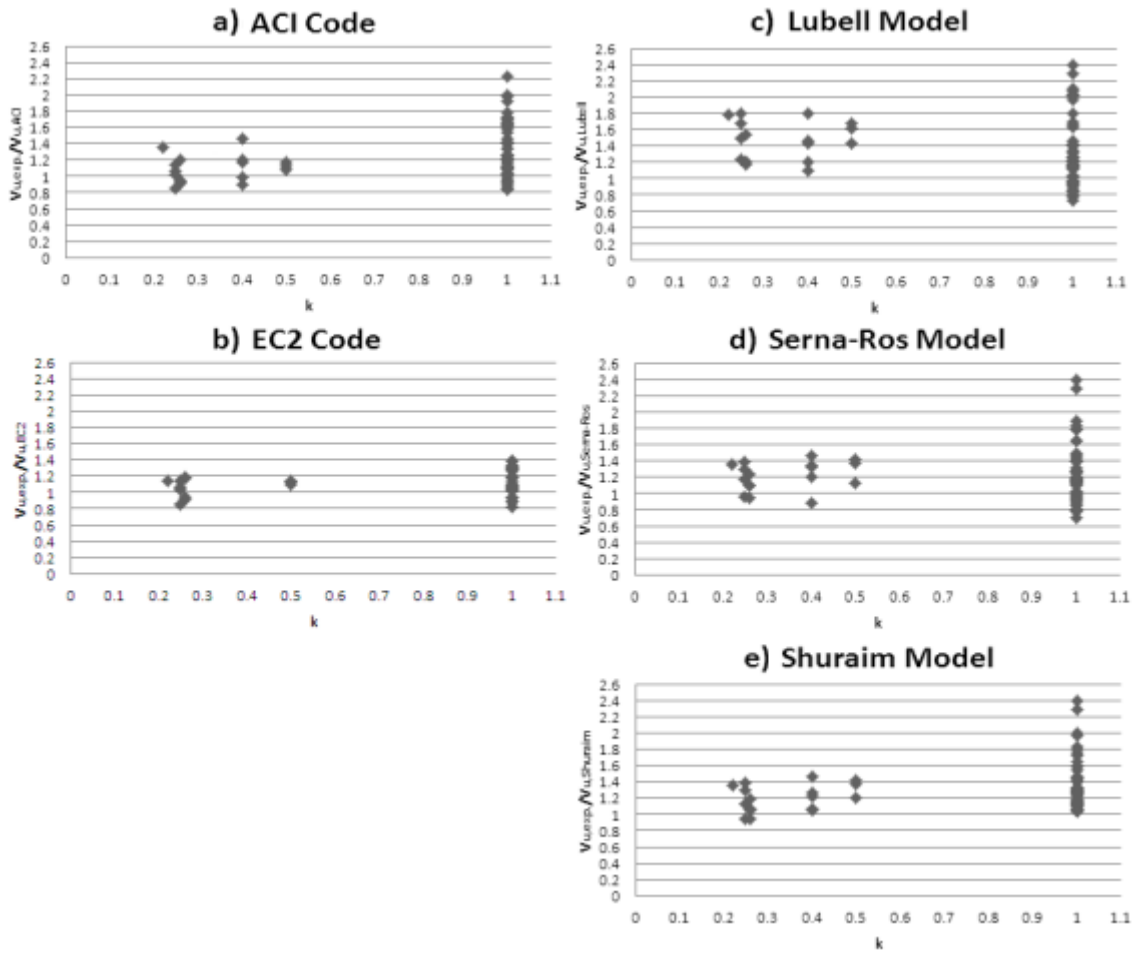


Figure 4.24:  $k$  versus  $V_{u,exp}/V_{u,Pred.}$ .



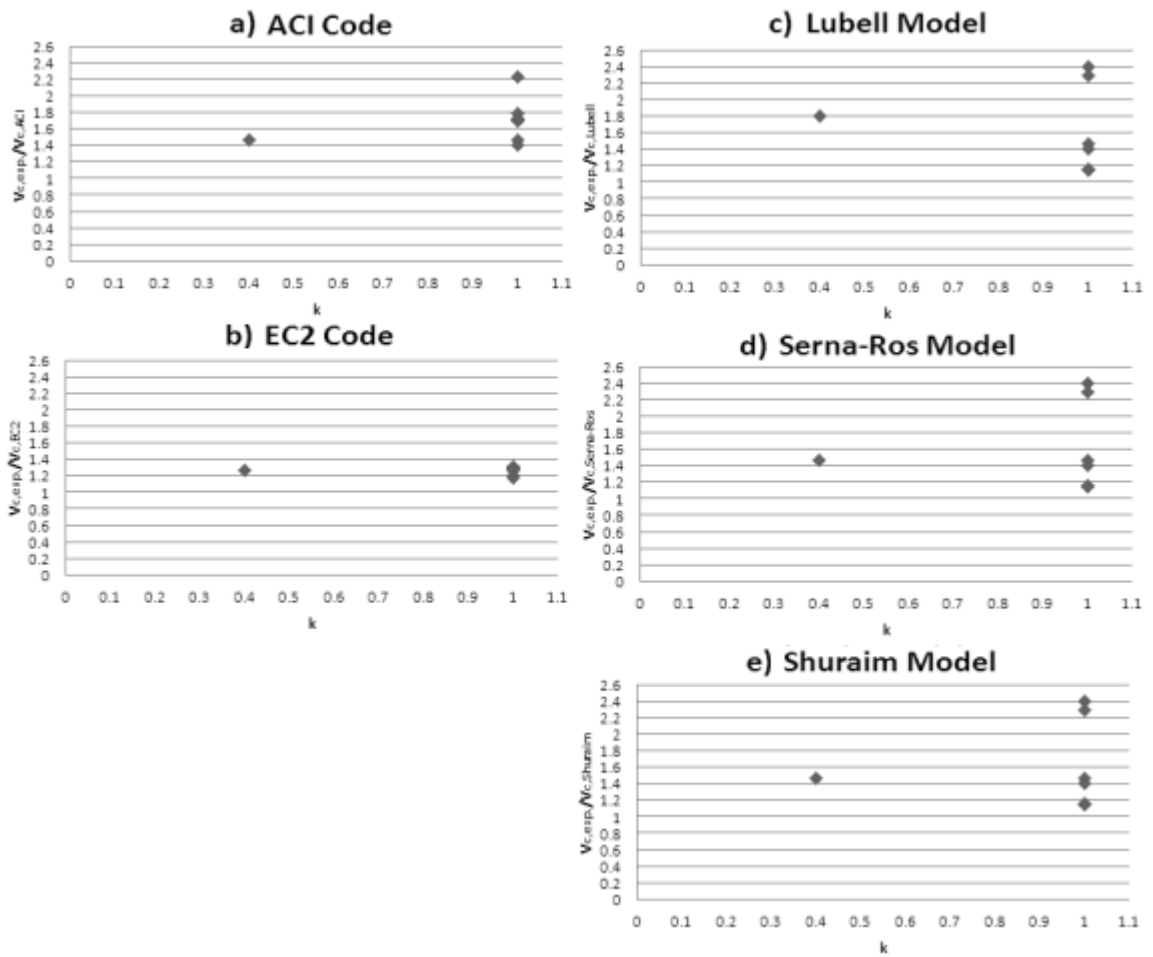


Figure 4.25:  $k$  versus  $V_{c,exp}/V_{c,Pred.}$ .

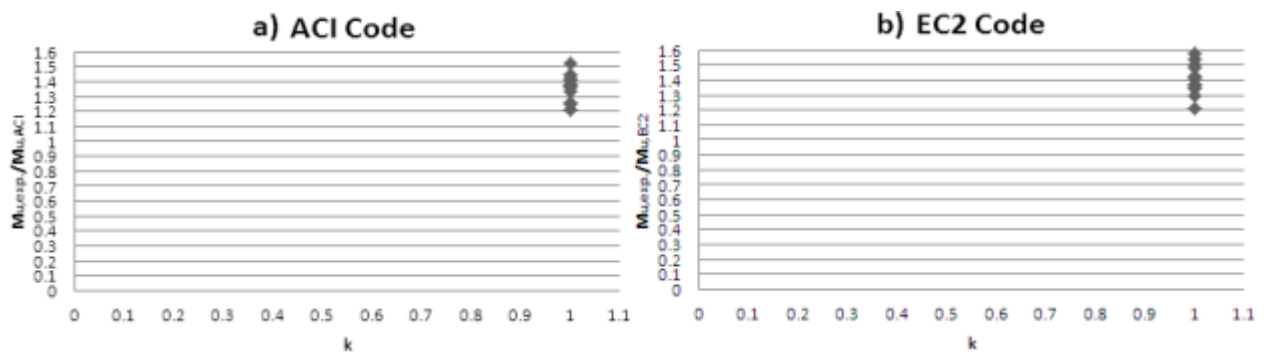


Figure 4.26:  $k$  versus  $\mu_{u,exp}/\mu_{u,Pred.}$ .

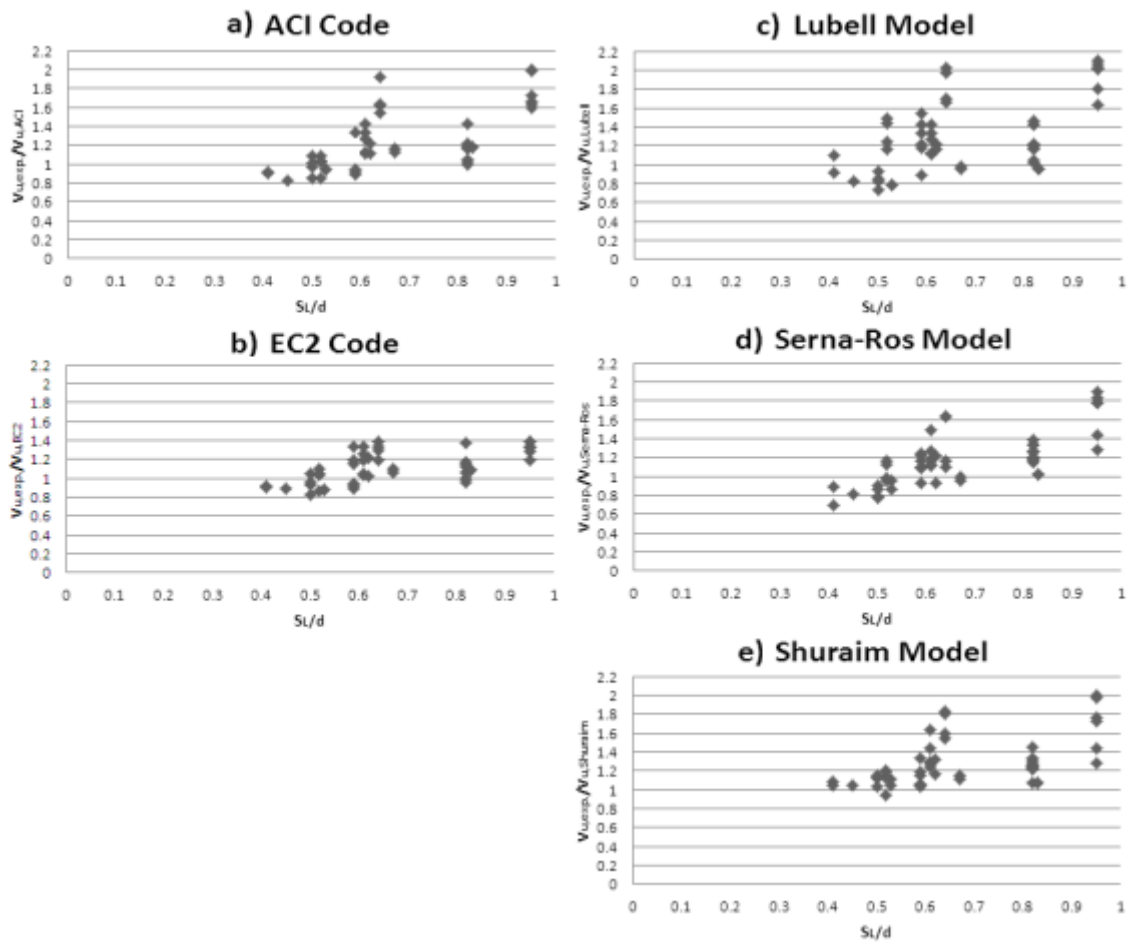


Figure 4.27:  $Sl/d$  versus  $V_{u,exp}/V_{u,Pred.}$ .

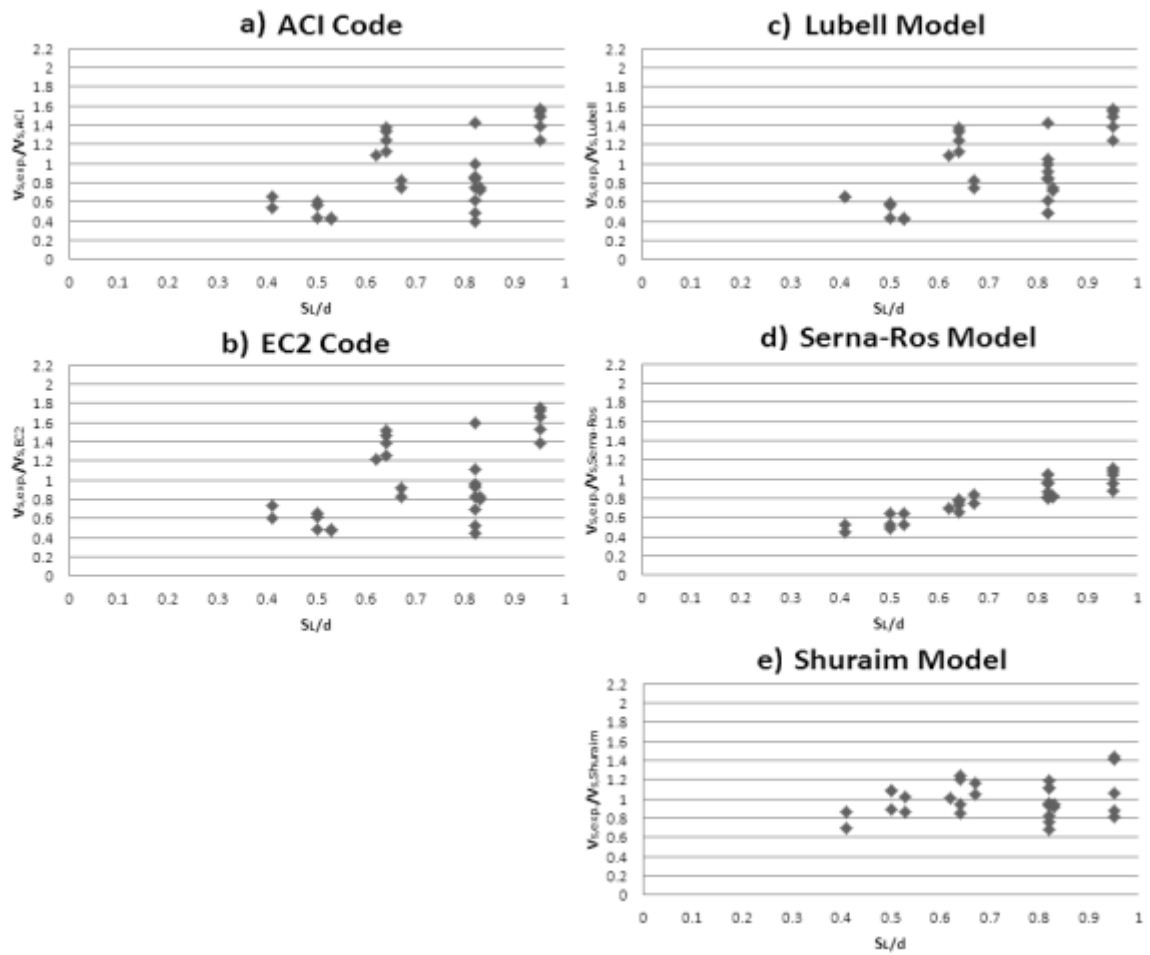


Figure 4.28:  $Sl/d$  versus  $V_{s,exp.}/V_{s,Pred.}$ .

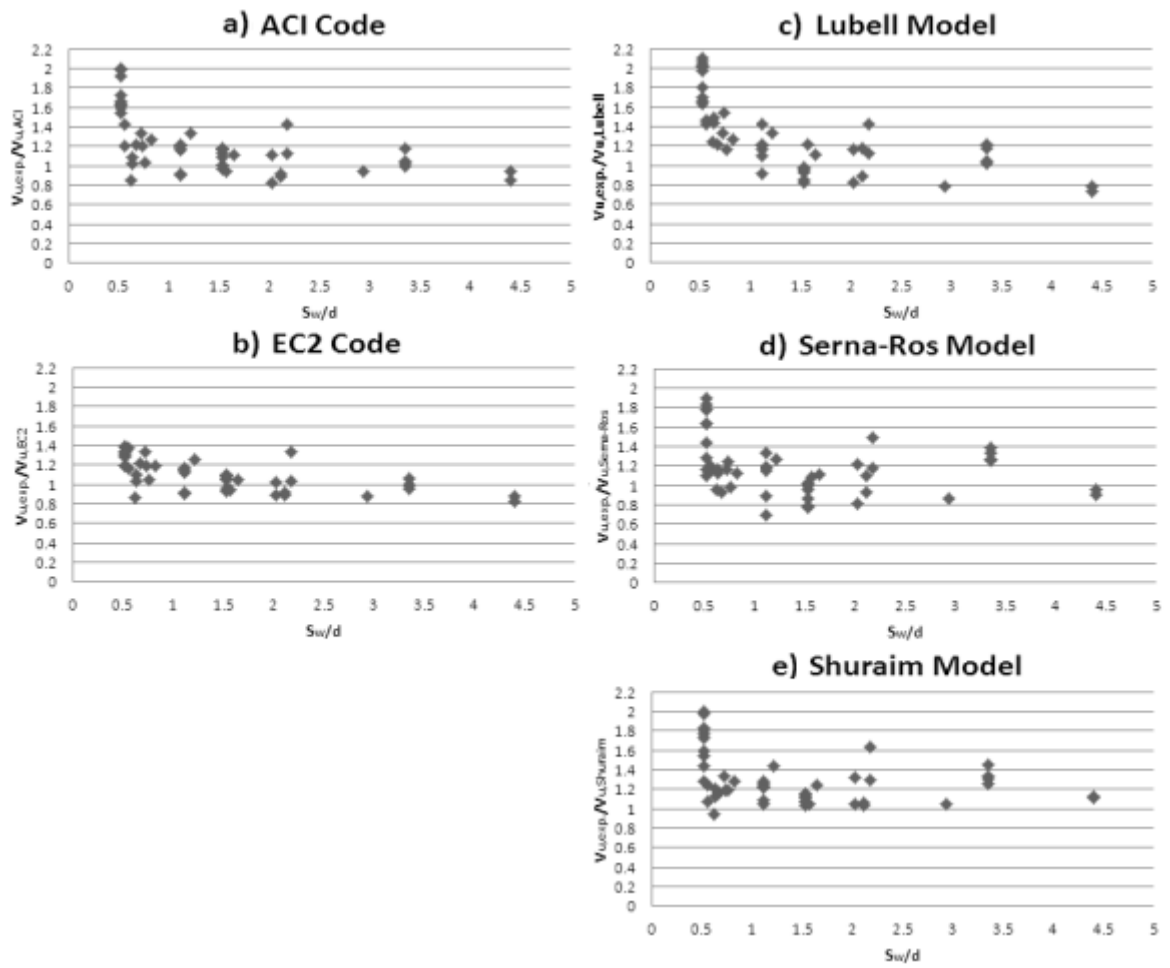


Figure 4.29:  $S_w/d$  versus  $V_{u,exp}/V_{u,Pred.}$ .

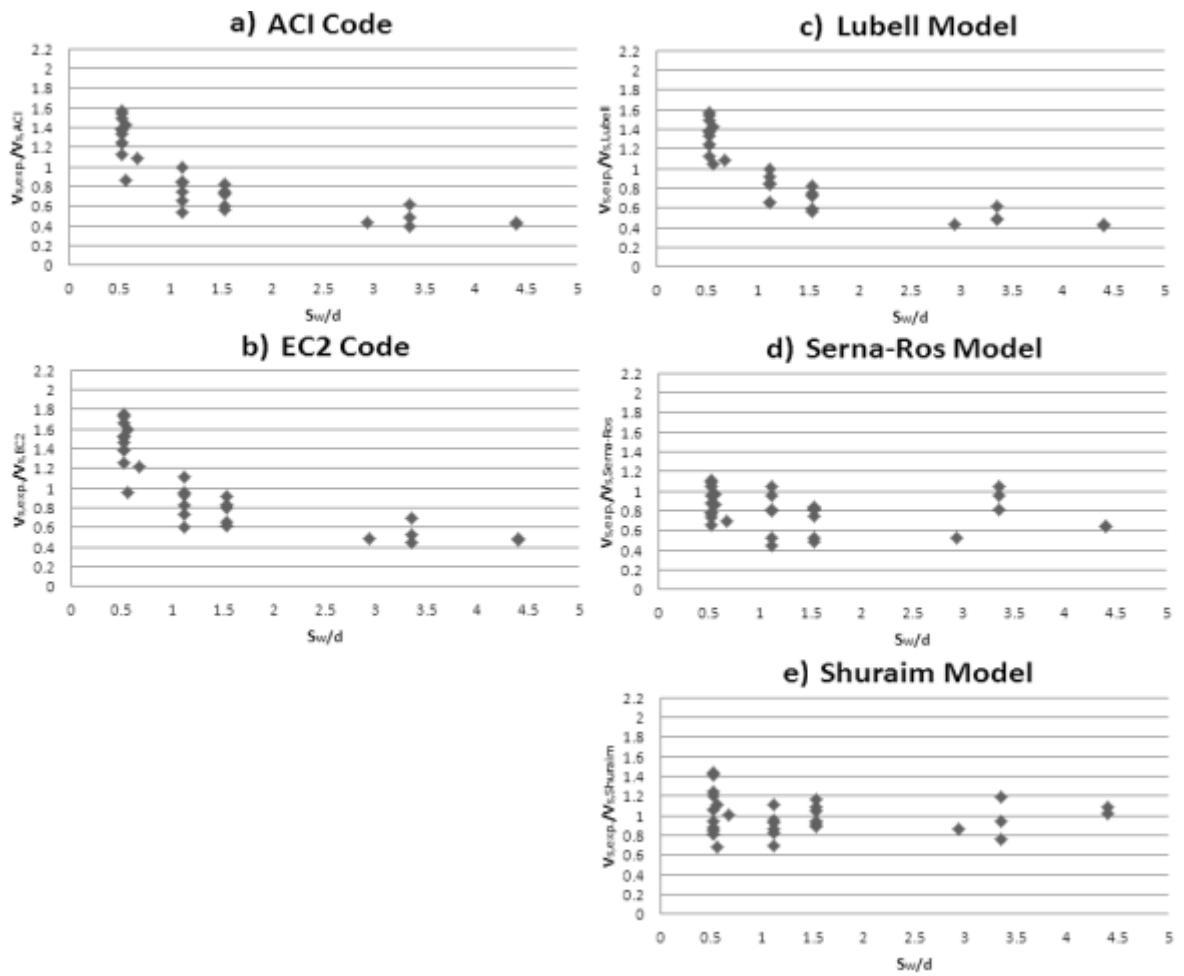


Figure 4.30:  $S_w/d$  versus  $V_{s,exp.}/V_{s,Pred.}$ .

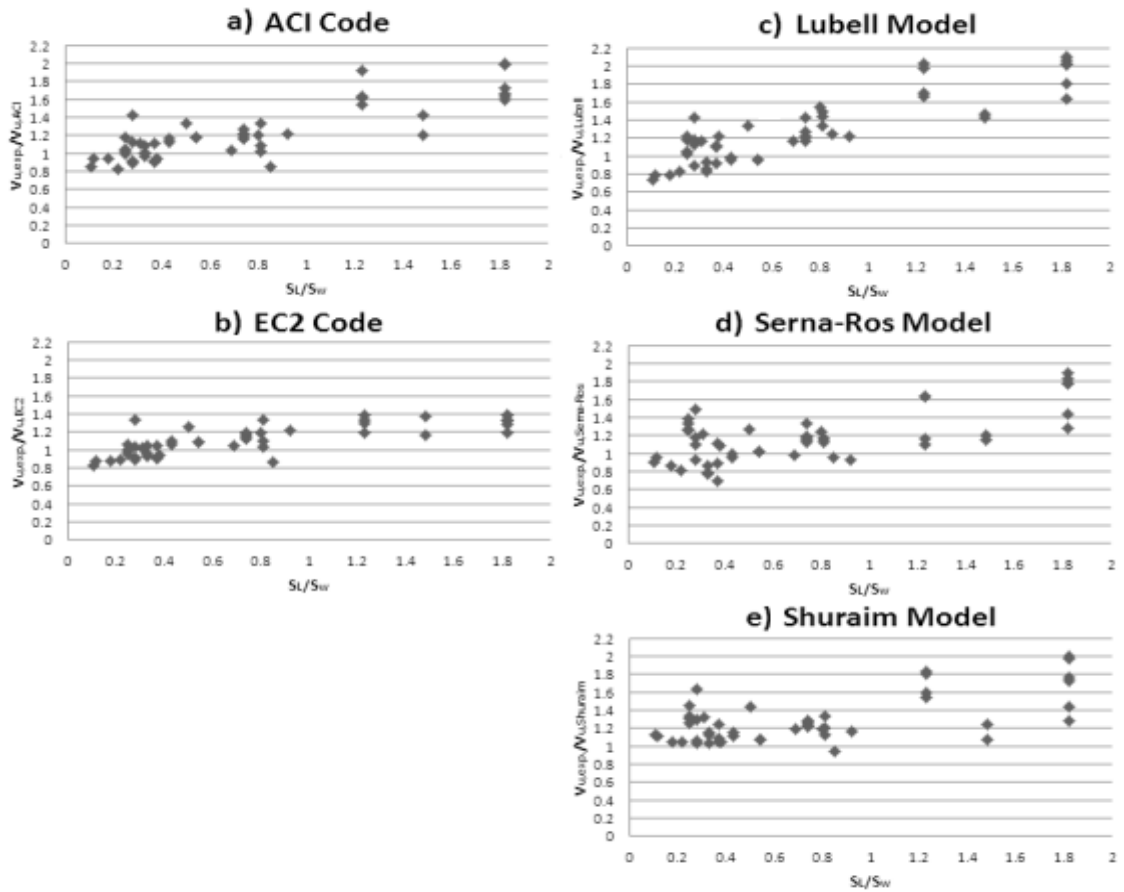


Figure 4.31:  $SL/S_w$  versus  $V_{u,exp}/V_{u,Pred.}$ .

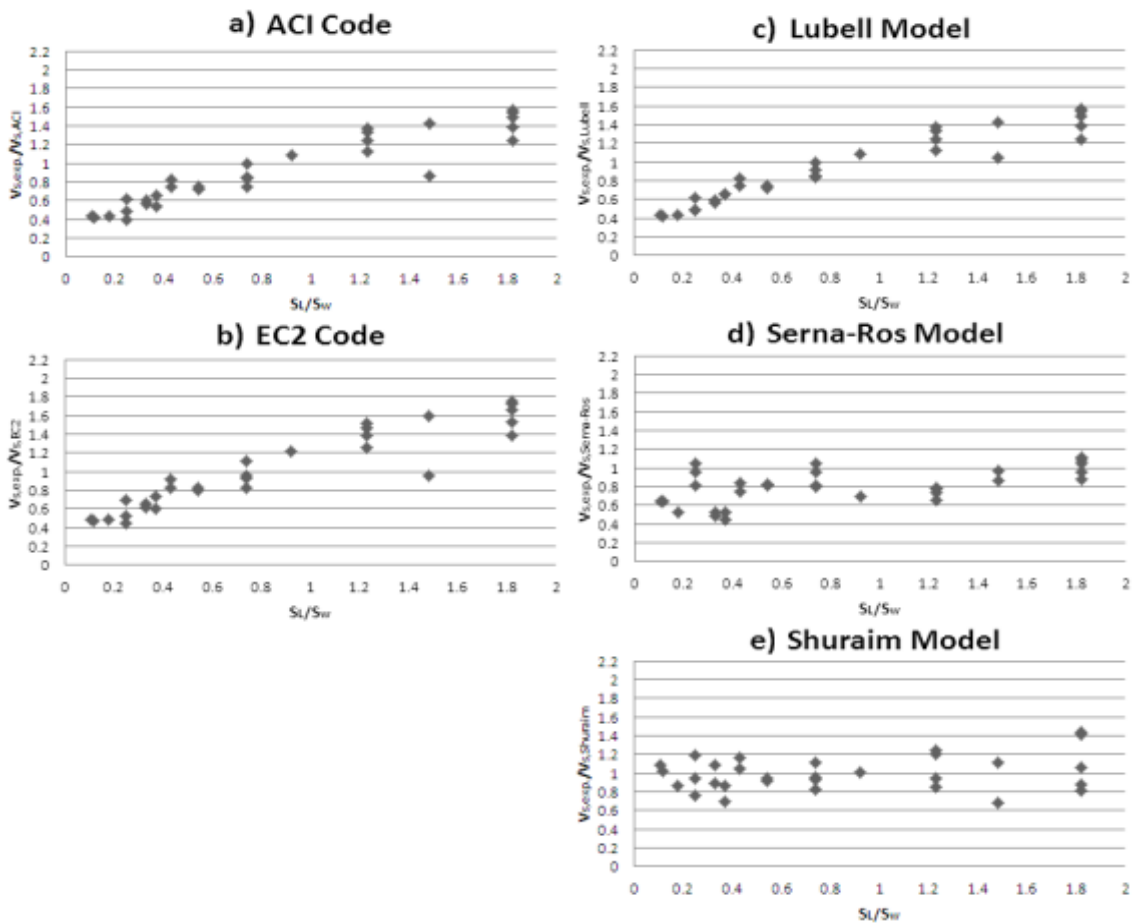


Figure 4.32:  $SL/S_w$  versus  $V_{s,exp}/V_{s,Pred.}$ .

## 4.7 Conclusion

The current provisions of design and prediction the flexural and shear strengths were discussed in this Chapter. The existing shear models developed by previous researches were also included. The experimental results of shear and flexural strengths obtained from the current investigations data were compared with the existing Codes and models. The discussions showed the effect of support width, load width, longitudinal and transverse spacing of stirrup legs on the strengths of wide RC beams. These factors must be taken into the consideration to develop rational models to predict, detail and design the wide RC beams (Alluqmani, 2013a, 2013b). When the rational models are being developed, the general formulae used by the current Codes of Practice are taken into the consideration (Alluqmani, 2013a, 2013b).

This Chapter has highlighted the inadequacy of current design approaches for wide structural concrete beams subjected to the actions of shear force or bending moment. The design approaches do not treat under their design considerations the flexural and shear design of wide concrete members, especially in the transverse direction which is parallel to the width of these members, i.e. the effect of support width, load width and transverse spacing of stirrup legs (Alluqmani, 2013a, 2013b). A wide beam is first designed for flexure using the moment envelope and then it is designed for shear using the shear envelope (this is section design). In the design for shear, these models ignore the stirrup-legs spacing in the transverse direction of wide concrete beams, or at best deal them as narrow beams for two stirrup legs across the width and for full-width load and support conditions (Alluqmani, 2013a, 2013b). It is believed that in the design for shear, these models assume that part of the shear is carried by the concrete ( $V_c$ ) by beam and/or arch actions. The stirrups are assumed to carry the shear ( $V_s$ ) in excess of the concrete capacity through truss action. In addition,  $V_c$  is normally related to the strength of the cracked concrete below the level of the neutral axis through the so called aggregate interlock action which, if indeed it exists, is to be regarded as only a secondary mechanism (Bobrowski, 1982; Kotsovos, 1983). The design methods adopted by the different Codes of Practice do not relate the failure of beams to the actual state of stress which exists in the transverse direction which shear stresses are distributed across the beam width.

Based on the discussion and the relationships demonstrated in Tables 4.3 to 4.10 and Figures 4.17 to 4.32 (Alluqmani, 2013a, 2013b), the influence of the support and load widths ( $b_s$  and  $b_p$ ), or at best the ratios of support and load widths to wide beam width ( $k_s = b_s/b_w$  and  $k_p = b_p/b_w$ ),

and the longitudinal and transverse spacing of stirrup legs ( $S_L$  and  $S_w$ ) on the ultimate flexural and shear strengths ( $M_u$  and  $V_u$ ) of wide RC beams was clear. The deficiency of the current Codes of Practice and the existing shear strength models to predict the strengths of wide RC beams is also clear.

Current Codes of Practice ignore these factors in their design provisions. However, even if there were attempts to develop shear strength models by Lubell et al (2008), Serna-Ros et al (2002) and Shuraim (2012), these existing shear strength models are confined for some factors and do not cover all requirements (Alluqmani, 2013a, 2013b). This is, for example, the model developed by Lubell et al (2008) does not include the effect of the longitudinal and transverse spacing of stirrup legs ( $S_L$  and  $S_w$ ) on the ultimate shear strength ( $V_u$ ), or at best the shear strength resisted by stirrups ( $V_s$ ), of wide RC beams. Furthermore, the model developed by Serna-Ros et al (2002) does not include the effect of the support and load widths ( $b_s$  and  $b_p$ ) on the shear strength resisted by concrete ( $V_c$ ). In addition, the model developed by Shuraim (2012) does not include the effect of the support and load widths ( $b_s$  and  $b_p$ ) on the shear strength resisted by concrete ( $V_c$ ) or by stirrups ( $V_s$ ). Otherwise, the effect of flexural reinforcement ratios on the flexural and shear strengths of wide beams was not taken into the consideration in the existing models neither for estimating the ultimate flexural strength ( $M_u$ ) nor for estimating the shear strength resisted by concrete ( $V_c$ ) (Alluqmani, 2013a).

The current experimental data may not be sufficient for well evaluation, especially for the evaluation of ultimate flexural strength ( $M_u$ ) where the previous data for this evaluation was obtained by one previous research referred to "Al-Harithy (2002)" with full-width support and load condition (Alluqmani, 2013a). Therefore, it is necessary to test a beam with narrow-width support and load condition to fail in flexure. This is one of the main objectives to investigate Test-Series "A" in the next Chapter as an initial stage of the present study. The evaluation of both full- and narrow- width support and load conditions, among other variables such as the longitudinal and transverse spacing of stirrup legs, on both ultimate flexural strength ( $M_u$ ) and ultimate shear strength ( $V_u$ ) is also considered to be investigated, discussed and concluded in the present study (see Chapters 6 to 9) in order to develop and validate the proposed models adopted in this study (i.e. the proposed Prediction-Model, Detailing-Approach and Design-Model) (Alluqmani, 2013a, 2013b; Alluqmani and Saafi, 2014b, 2014c).



## CHAPTER 5

### WIDE RC BEAMS SPECIALLY DETAILED FOR SHEAR: SERIES (A)

#### 5.1 Introduction

A new prediction model to predict the shear and flexural strengths of wide RC beams should be developed based on the experimental results obtained from the previous researches reviewed in the literature (Chapter 3) on the structural behaviour of wide RC beams in shear and flexure. Accordingly, it was necessary that an initial stage of this programme of research is made to be experimentally investigated and compared for the both shear and flexural strengths of wide RC beams with those results previously investigated in the literature (Alluqmani, 2013a). It was clear that the support and load widths ( $b_s$  and  $b_p$ ) have influence on the capacities of wide RC beams as concluded. It was suggested to start from wide beams with narrow-width loads and supports. It is recognised that the longitudinal spacing of stirrup legs (SL) has an influence on the strength of reinforced concrete beams. Therefore, a new factor has been recently found to have an influence on the strength of wide RC beams, which is the transversal spacing of stirrup legs ( $S_w$ ). Consequently, two wide RC beams reinforced with stirrups were suggested to be investigated in Test-Series (A) included in this Chapter.

Test-Series (A) included two simply supported wide RC beams with concentrated load for a three point-loading system (beams ECC2 and ECC3). The two beams in Series (A) are used to investigate the influence of transverse stirrup-legs spacing ( $S_w$ ) on the shear and flexural behaviours of wide RC beams with narrow-width loads and supports. Where the load- and support- widths ( $b_p$  and  $b_s$ ) are lesser than the beam width. The two beams in Series (A) are also used together with those beams tested previously in the literature to develop a proposed Prediction-Mode (Alluqmani, 2013a). Both specimens were detailed and designed for flexure and shear, and checked for the serviceability (mid-span deflection and flexural crack width) according to the design provisions (requirements) of the current Codes of Practice, such as EC2 Code approach (EC2, 2004), except the shear reinforcement (stirrups) spacing. The total required area of shear reinforcement ( $A_{v,req.}$ ) for both beams is  $279 \text{ mm}^2$ , but the aim is to make one beam fails in shear while the other one fails in flexure. Beam ECC2 was designed to fail in shear, while beam ECC3 was designed to fail in flexure. The only main variable of both beams was the area of shear reinforcement, leading to have a different stirrup-legs spacing across the width of both

beams. The experimental test programme, the material properties, beam manufacture, test arrangements and procedures, and experimental methodology for Test-Series (A) specimens are described and discussed in this Chapter. Moreover, this Chapter discusses the experimental works in general for those wide RC beams tested and investigated in Test-Series (A).

## 5.2 Description of Test Specimens

Test-Series (A) included two wide RC beam specimens made with normal-strength concrete and high-strength reinforcement. The specimens were designed, constructed and examined at Heriot-Watt University, Edinburgh-UK. The beam specimens to be experimentally investigated were simply supported beams using a three point-loading system. The specimens were detailed and designed for flexure and shear using the methods in current Codes of Practice, such as EC2 Code, except  $S_w$ . The scope of this programme of research for the beams in Test-Series (A) focuses on the flexural and shear behaviours of wide concrete beams, with constant cross section and constant flexural (longitudinal) reinforcement along the beam length. The shear (transverse) reinforcement made up exclusively by closed vertical stirrups with 4-legs 8mm diameter legs distributed along the beam length and across the beam width. The main concern is to analyse the influence of the transversal stirrup-legs spacing ( $S_w$ ) on the flexural and shear behaviours of wide RC beams, as well to use the results with those experimental results obtained by previous researches in order to develop a rational Prediction-Model.

**Table 5.1#:** Test-Series "A" to Adopt a New Prediction-Model for Shear and Flexure of Wide RC Beams.

		Beam-Type (ECC)
		$k_p = 0.50, k_s = 0.34$
		$k = 0.34$
<b>Test-Series (A):</b> $bw/h = 2.0$ $d = 304\text{mm}$ <u>Developing a New Prediction-Model</u> $(SL \approx 0.6d)^{*1}$	<b>Beam Group</b> Effect of $S_w$ on Shear and Flexural Strengths of Narrow Supported Wide-Beams	
	<b>ECC2<sup>*2</sup></b> <b>Beam ECC2</b> $(SL = 0.6d = 180)$ $(S_w \approx d = 1.67SL = 300)$	
	<b>ECC3<sup>*3</sup></b> <b>Beam ECC3</b> $(SL = 0.6d = 180)$ $(S_w \approx 0.40d = 0.68SL = 122)$	

# This Test Series is aimed to 1. Investigate the influence of  $S_w$  on shear and flexural strengths of wide RC beams with narrow-width supports and loads, and 2. Be used together with those beams tested previously in the literature to develop a *Proposed Prediction-Model*.

\*1  $SL \approx 0.6d = 180\text{mm}$  for both beams. SL was arranged and distributed along the beam length.

\*2  $S_w \approx d = 300\text{mm}$  for Beam ECC2.  $S_w$  was arranged within the center of beam width.

\*3  $S_w \approx 0.40d = 122\text{mm}$  for Beam ECC3.  $S_w$  was arranged within the center of beam width.

- Both beams had the same  $bw/h$  ratio equal to 2.0 ( $bw = 700\text{mm}$ ,  $h = 350\text{mm}$ ,  $d = 304\text{mm}$ ), the same  $\rho_s$  ratio greater than 1.0% (equal to 1.84%,  $8\Phi 25\text{mm}$ ), the same  $\rho_s'$  ratio less than 1.0% (equal to 0.22%,  $6\Phi 10\text{mm}$ ). They had different  $A_v$ .

The results to be analysed were obtained from the test to failure carried out on two wide beams (Table 5.1). The analysis will also focus on the comparison between the strengths actually reached in the tests and those values that would be obtained applying the calculation formulae included in the Codes, such as EC2 Code, as well as with those values obtained from the existing models. Several improvements to the Codes are proposed in order to take such effects into account. Some design recommendations about spacing of stirrups to optimise the vertical shear reinforcement effectiveness are included in this study to make the wide beam behaves in a ductile flexural manner and then to prevent premature shear failures.

Table 5.1 shows the beams in Test-Series (A) used to investigate the shear and flexural behaviours of wide RC beams, and to contribute for developing a prediction model. Figures 5.1 and 5.2 show description of the details and design of wide RC beam specimens, respectively, used in Test-Series (A).

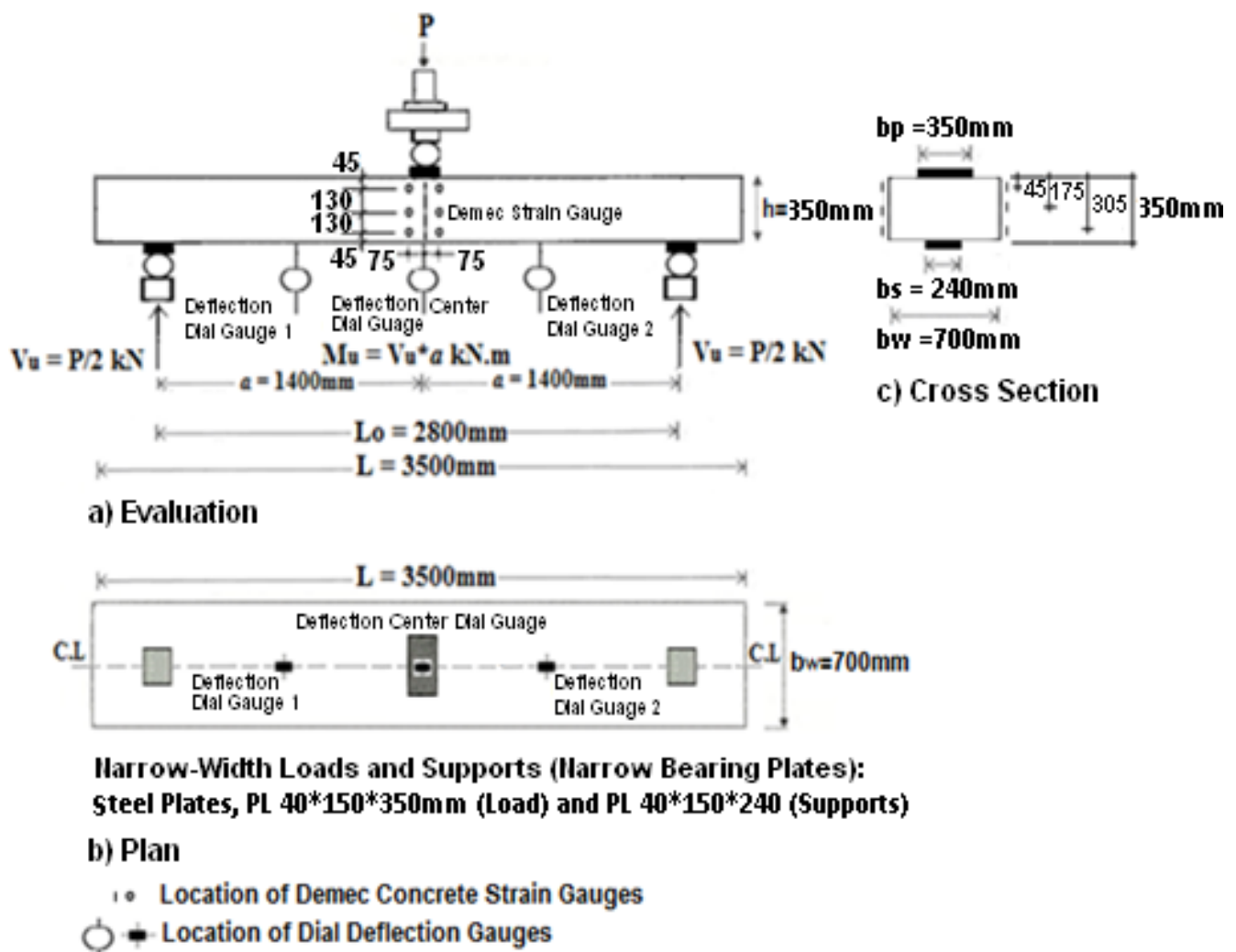


Figure 5.1: Details of Wide Beam Specimens in Test-Series "A".

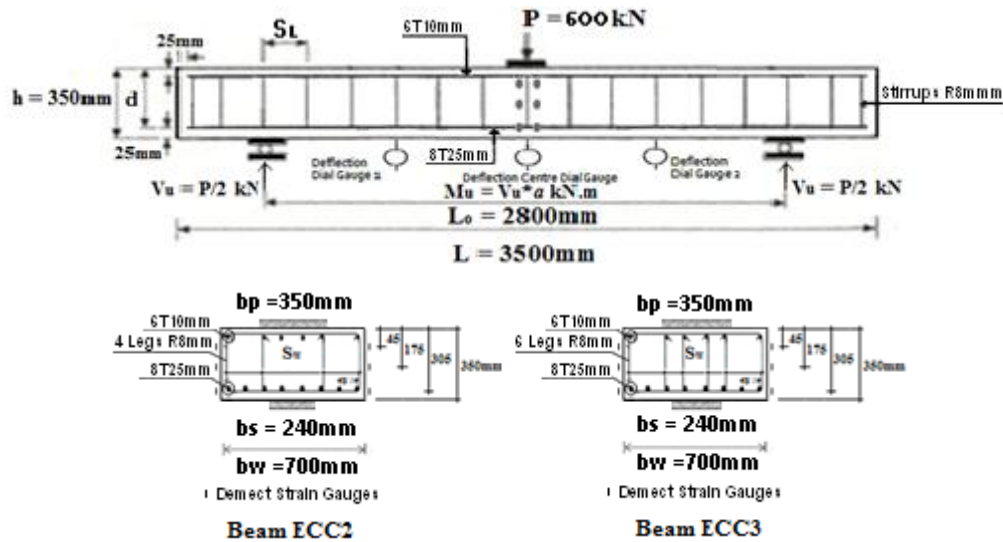


Figure 5.2: Design of Wide Beam Specimens in Test-Series "A".

### 5.3 Design and Configurations of Test Specimens

Both beam specimens were designed for their reinforcements according to the current Codes of Practice, such as EC2 Code. The beams had 700mm wide, 350mm height, 3500mm overall length, 2800mm effective span, 25mm diameter of tension flexural bars, 10mm diameter of compression flexural (hanger) bars, 8mm diameter of stirrups, a longitudinal reinforcement ratio ( $\rho_s$ ) of 1.84%, a shear-span to effective-depth ratio ( $a/d$ ) of 4.60 (type II beams), a three point-loading arrangement, and a narrow-width load and support condition where  $b_p > b_s$ . The stirrup legs spacing along the beam length ( $S_L$ ) was taken as  $0.6d$  ( $= 180\text{mm}$ ) for both beams to be distributed along the beam length. The stirrup legs spacing across the beam width ( $S_w$ ) was chosen approximately as  $d$  ( $= 300\text{mm}$ ) and  $0.4d$  ( $= 122\text{mm}$ ) for beams ECC2 and ECC3, respectively, to be arranged within the center of beam width. The number of bars in the tension and compression zones was the same in both test specimens, where  $\rho_s = 1.84\%$  and  $\rho_s' = 0.22\%$ . The design process used for the beams in Series "A" is summarized in Appendix A.3.

The specimens, which were described in Figures 5.1 and 5.2, and Table 5.2, were constructed to nominal dimensions of 700mm width, 350mm total height (304mm effective depth,  $d$ ), and 3500mm total length (2800mm clear span). The specimens were analyzed, designed and tested under three-point loading with a central span ( $L_o$ ) of 2800mm and shear span ( $a$ ) of 1400mm, giving a shear-span to effective-depth ratio ( $a/d$ ) of 4.60. They were designed to carry a concentrated design load ( $P_d$ ) in the mid-span point of 600 kN. The specimens were loaded and supported with narrow steel-plates by 40x150x350mm for loads and by 40x150x240mm for supports (partial-width bearing-plates).

**Table 5.2:** Design Details of Wide Beams in Test-Series "A".

Beam Type	Cross-Section Dimensions	Tensile Reinforcement	Compressive Reinforcement	Shear Reinforcement Along the Length, C/C	Shear Reinforcement Across the Width, C/C
Beam ECC2	700*350mm $A_c = 245000\text{mm}^2$	8T25mm $A_s = 3928\text{mm}^2$	6T10mm $A_s' = 472\text{mm}^2$	20 Stirrups R8mm@180mm	4 Stirrup Legs-R8mm @ <b>300</b> -642mm
Beam ECC3	700*350mm $A_c = 245000\text{mm}^2$	8T25mm $A_s = 3928\text{mm}^2$	6T10mm $A_s' = 472\text{mm}^2$	20 Stirrups R8mm@180mm	6 Stirrup Legs-R8mm @ <b>122</b> -300-642mm

Both beams were with web (shear) reinforcement and their longitudinal and transverse spacing ( $S_L$  and  $S_w$ ) were taken as a percentage of the effective-depth of the beam ( $d$ ). Web reinforcement patterns included four and six stirrup-legs across the width in beam ECC2 and ECC3, respectively. Two legs were near the specimen edges (external legs) and the other legs were concentrated between edge and central beam-width (internal legs), which are measured from the centre line of the beam width ( $b_w$ ). The total required area of shear reinforcement ( $A_{v,req.}$ ) for both beams was  $279\text{ mm}^2$ , but the aim of this test was to make beam ECC2 fails in shear while beam ECC3 fails in flexure. The only main variable of both beams was the area of shear reinforcement, leading to have different stirrup legs and a different spacing across the width of both beams. The provided area of shear reinforcement ( $A_{v,prov.}$ ) was  $201\text{ mm}^2$  for beam ECC2 and  $302\text{ mm}^2$  for beam ECC3. Both specimens had the same main longitudinal reinforcement ( $8\text{Ø}25\text{mm}$ ), resulting in a  $\rho_s$  ratio of 1.84%. Top longitudinal (hanger) bars ( $6\text{Ø}10\text{mm}$ ) were used to anchor the stirrups, but would have minimal influence on overall member response.  $S_L$  should be distributed along the member length, and  $S_w$  should be arranged and distributed across the member width. The total number of the flexural -tensile and -compressive reinforcing bars was distributed within the beam width, where it was the same for both beams.

Both beams had shear reinforcement and narrow bearing plates. Flexural and shear reinforcements were determined based on the provisions of the current Codes, such as EC2 Code, except  $S_w$  for beam ECC2 which was chosen as a maximum value equal to  $d$ , Tables 5.1, 5.2 and 5.3. The longitudinal legs spacing ( $S_L$ ) used for both beams was chosen to be equal to  $0.6d$  ( $S_L \approx 180\text{mm}$ ) and to be in the limits of most of current design Codes. The transversal legs spacing ( $S_w$ ) and the configuration of the stirrups across the beams width were based on a logical understanding of the transverse shear stresses which are high within the bearing-plate widths.  $S_w$  was chosen to be either  $0.4d$  ( $\approx 0.68*S_L$ ) for beam ECC3, or  $d$  ( $\approx 1.67*S_L$ ) for beam ECC2 where this spacing was chosen as an ultimate value for  $S_w$ . The designed  $S_w$  was 300mm (for

interior legs) and 642mm (for external legs) for beam ECC2, and was 122mm, 300mm (for interior legs) and 642mm (for external legs) for beam ECC3. Spacing, which was chosen to be approximately equal to 0.4d or d, is because it seemed likely that members where the longitudinal spacing of the stirrups was close to the maximum permitted by EC2 Code would be more sensitive to any detrimental effects of wide spacing across the width of the member on the failure load and mode. This is also because a proposed prediction model to account for the shear and flexural strengths of wide RC beams must be developed. Details of the reinforcements are shown in Figure 5.2.

The design details of the test specimens in Test-Series (A) are shown in Table 5.2. The characteristics and properties of the test specimens are shown in Table 5.3. Figure 5.3 shows the steel plates used in both cases of load and support conditions.

**Table 5.3:** Properties of Wide Beam Specimens in Test-Series "A".

Beams	b <sub>s</sub> mm	k <sub>s</sub> -	b <sub>p</sub> mm	k <sub>p</sub> -	k -	S <sub>L</sub> mm	S <sub>w</sub> mm	ρ <sub>v</sub> %
Beam ECC2	240	0.34	350	0.50	0.34	180	300	0.16
Beam ECC3	240	0.34	350	0.50	0.34	180	122	0.24

**NOTE:** b<sub>w</sub> = 700mm, h = 350mm, d = 304mm, ρ<sub>s</sub> = 1.84% (8Φ25mm), ρ<sub>s'</sub> = 0.22% (6Φ10mm), A<sub>v</sub> = 201mm<sup>2</sup> (4-LegsΦ8mm) beam ECC2, =302mm<sup>2</sup> (6-LegsΦ8mm) beam ECC3.

-----

A<sub>v,req.</sub> = [(V<sub>s</sub>\*S<sub>L</sub>)/(Φ<sub>s</sub>\*f<sub>yv</sub>\*d)] = 279 mm<sup>2</sup>. V = 300 kN. V<sub>c</sub> = 223 kN. V<sub>s</sub> = [(V-(Φ<sub>s</sub>\*V<sub>c</sub>))/Φ<sub>s</sub>] = 177 kN. f<sub>c</sub> = 40 MPa f<sub>yv</sub> = 500 MPa. S<sub>L</sub> = 180mm. d = 304mm. Φ<sub>s</sub> = 0.75 (shear). Φ<sub>F</sub> = 0.90 (flexure). [A<sub>v,prov.</sub> = 201 mm<sup>2</sup> (ECC2) = 302 mm<sup>2</sup> (ECC3)].



**Figure 5.3:** Difference Sizes of Steel Plates Used for Load and Support Conditions in Series "A".

**The main features of the experimental programme of Series (A) are:**

- 1) Cross section of beams: 700mm wide x 350mm height, and b<sub>w</sub>/h ratio of 2.0.
- 2) Support and load system: simple supported beams with a 3500mm total span and 2800mm free span. The load is applied at mid-span point (Figures 5.1 and 5.2) and the ratio of shear-span to effective-depth (a/d) is equal to 4.60.

- 3) The longitudinal reinforcement is kept constant along the beam and is eight 25mm diameter ( $\rho_s = 1.84\%$ ). Compression reinforcement is used as hanger bars and is six 10mm diameter ( $\rho_{s'} = 0.22\%$ ). The effective depth ( $d$ ) is 304mm for both beams.
- 4) The reinforcement is designed according to the current Code specifications, such as EC2 Code, except for the transversal spacing of stirrup legs, which is considered the main variable in this investigation.
- 5) The number of stirrup legs across the beam-width ( $N_L$ ) used in beams ECC2 and ECC3 was 4 and 6 stirrup-legs, respectively, where the stirrup legs were used for the shear reinforcement arrangement. Diameter of stirrups ( $\Phi_{str.}$ ) was 8mm. The area of shear reinforcement ( $A_v$ ) was  $201\text{mm}^2$  for beam ECC2 and  $302\text{mm}^2$  for beam ECC3.
- 6) Support width ( $b_s$ ): both beams are supported with narrow bearing plates where  $b_s$  is equal to 240mm ( $k_s = b_s/b_w = 0.34$ ).
- 7) Load width ( $b_p$ ): both beams are loaded with narrow bearing plates where  $b_p$  is equal to 350mm ( $k_p = b_p/b_w = 0.50$ ).

## 5.4 Materials Information

The performance and quality of concrete member depend to a large extent on the proportions and characteristics of its constituent materials (Ziara, 1993; Alluqmani, 2010; Alluqmani, 2014; Alluqmani and Haldane, 2011c). Therefore, it was important that the quality of the material remained consistent during this programme of research. The information relating to the materials used to design the beam specimens and cast the concrete were the same as assumed in the design calculations, Tables 5.4.

**A brief detail and description of the materials used for test specimens are as follows:**

### 5.4.1 Concrete

For both test specimens, a 40 MPa cylinder compressive strength (50 MPa cubic compressive strength) was used in the design calculations, which was used in this programme of research as it is being applied according to the design provisions of EC2 approach, as shown in Table 5.4.

Both beam specimens with their own control samples (cubes and cylinders) were made simultaneously with concrete from the same mixture at the same time. Ready mixed concrete was used to cast the beam specimens and control samples, contained 10-20mm (3/8-3/4 in.) coarse aggregate, 4mm (3/16 in.) fine aggregate, 350 kg cement content per cubic metre of

concrete, and 0.42 design water/cement (w/c) ratios to give a workability of 60-80mm slump. The aggregate was crushed limestone for both test specimens. The cube samples used in the laboratory tests had dimensions of 150x150x150 mm, where the cylinder samples had dimensions of 300mm height x150mm diameter. The nominal specified strength of the concrete used to cast the specimens was as that used for the design purpose for class C40, which was 40 MPa for concrete cylinder strength or 50 MPa for concrete cubic strength (Table 5.4). Table 5.4 shows the material properties used to design the beam specimens. The mix proportions of concrete used to cast the beams are shown in Table 5.5. The concrete mixes used in the experimental investigation were designed to give an average cubic compressive strength at 28 days ( $f_{cu}$ ) equal to the specified strength, this means, the target mean strength was taken to be equal to the characteristic strength.

**Table 5.4:** Material Properties used to Design the Beam Specimens in Series "A".

	<b>Properties</b>	<b>Series (A)</b>
<b>Concrete</b>	Cylinder Compressive Strength ( $f_c$ ), MPa	40
	Cube Compressive Strength ( $f_{cu}$ ), MPa	50
	Young's Modulus ( $E_c$ ), MPa	28000
<b>Flexural Reinforcement</b>	Yield Strength for $\Phi 25$ mm ( $f_y$ ), MPa	500
	Yield Strength for $\Phi 10$ mm ( $f_y$ ), MPa	500
	Young's Modulus ( $E_s$ ), MPa	200000
<b>Shear Reinforcement</b>	Yield Strength for $\Phi 8$ mm ( $f_{yv}$ ), MPa	500
	Young's Modulus ( $E_s$ ), MPa	200000

**Table 5.5:** Concrete Mix Proportions used to cast for the Beams in Series "A".

<b>Properties</b>	<b>Test-Series (A)</b>
Cement Type	Ordinary Portland Cement
Coarse Aggregate Size (Gravel)	10 to 20mm (3/8 to 3/4 in.)
Fine Aggregate Size (Sand)	<4.75mm Sieve No.4 (3/16 in.)
Slump for Concrete	60-80mm
Coarse Aggregate Content	1175 kg/m <sup>3</sup>
Fine Aggregate Content	830 kg/m <sup>3</sup>
Cement Content	350 kg/m <sup>3</sup>
Water/Cement (w/c) Ratio	0.42
Free-Water Content	147 litre/m <sup>3</sup>

## 5.4.2 Reinforcement

In both test specimens, high deformed yield steel bars were used in the design of the flexural (longitudinal) and shear (transverse) reinforcements. The sizes of steel bars used to fabricate the beam specimens are as follows:



**25mm** high strength deformed yield steel bars were used for tensile flexural (main) reinforcement for both test beams.

**10mm** high strength deformed yield steel bars were used for compressive flexural (hanger) reinforcement for both test beams.

**8mm** high strength deformed yield steel bars were used for transverse shear reinforcement (stirrups) for both test beams.

For both test specimens, a 500 MPa high yield steel strength was used in the design calculations for both flexural and shear reinforcements, which was used in this programme of research as it is being applied according to the design provisions of EC2 approach, as shown in Table 5.4.

The beams in Series (A) were made simultaneously with concrete from the same mixture. The actual average cube and cylinder concrete compressive strengths were  $f_{cu,act} = 56.0$  MPa and  $f_{cy,act} = 45.0$  MPa, respectively. Eight 25mm nominal diameter high-strength deformed steel bars were used for the longitudinal tensile reinforcement ( $A_s = 490.9$  mm<sup>2</sup> and  $f_y = 525$  MPa) for both beams. Six 10mm nominal diameter high-strength deformed steel bars were used for the longitudinal compressive (hanger) reinforcement ( $A_s = 78.6$  mm<sup>2</sup> and  $f_y = 517$  MPa) for both beams in order to prevent accidental failure of the beam during the handling operations. It should be noted that these beams were designed for singly reinforcement only as required. The stirrups were fabricated from 8mm nominal diameter high-strength deformed steel bars ( $A_s = 50.3$  mm<sup>2</sup> and  $f_y = 512$  MPa) for both beams. Typical details of the test beams in Series (A) are shown in Figure 5.2 and Table 5.2. Based on the actual dimensions of the beams, the actual ratios of flexural -tensile and -compression reinforcements used for the analysis process are  $\rho_{s,act} = 1.82\%$  and  $\rho_{s',act} = 0.221\%$ , respectively.

## **5.5 Manufacture of Test Specimens**

### **5.5.1 Steel Cages**

The reinforcing steel bars were supplied as Take-Loose rebars, instead of the Prefab steel cages, from a local steel production company. Both steel cages of beam specimens were made in the Concrete/Structures Laboratory at the Heriot-Watt University.

To produce the steel cages of both beam specimens, the main reinforcement bars were put straight through two Workbenches (Trestles); then the positions of the stirrups were marked out

in the main bars according to the stirrups spacing along the beam length ( $S_L$ ) and across the beam width ( $S_w$ ). After that, the stirrups were tied to the main bars at each position. Also, the compression (hanger) reinforcement bars were put straight at the inside corners of the top face of the stirrups (in the compression concrete region), to prevent any movement during concrete pouring and compaction and also to assist in the assembly of the reinforcement cage and not to contribute to the flexural capacity of the beams (because these beams were designed for single reinforcement, as required). The steel bars were cleaned to remove any traces of oil, paint, or loose scale, i.e. surface rust, in order not to weaken the bond with the concrete.

The concrete covers were made using plastic spacers and were fixed on either the main bars or on the stirrups to ensure that the required cover distances were maintained and to avoid any movement of the reinforcement cage during compaction of the concrete, where 25mm thick spacers were attached to the stirrups (8mm diameter) and 33mm thick spacers were attached to the main bars (25mm diameter) for both beam specimens. The steel cages and spacers were well fixed prior to the concrete pouring and compaction. In addition, four lifting points were placed in the ends of beams (two hangers at each end) for lifting purpose. The steel cages of both beam specimens investigated in this study are shown in Figure 5.4.



**Figure 5.4:** Steel Cages of the Beams in Test-Series "A"; From Left: Beams ECC2 and ECC3.

### 5.5.2 Shutters

Structural steel channel sections were used in the manufacture of the shutters. The shutters were cleaned and coated with oil to prevent the concrete from adhering to the shutters during the concrete casting and curing; also, the steel cages were placed in the shutters and the plastic spacers were used to maintain the required cover distance.

For both beam specimens, the shutters had inside dimensions of 700\*350mm with overall length of 3500 mm. The steel shutters were manufactured and supplied by a local steel formwork

(moulds) company. The shutters were fixed firmly during the concrete pouring and compaction (or vibration) to prevent the shutters from moving. Steel shutters used for the casting purposes are shown in Figure 5.5.



**Figure 5.5:** Steel Shutters used for the Beam Specimens in Test-Series "A".

### 5.5.3 Casting

Both beam specimens with their own control samples (cubes and cylinders) were made simultaneously with concrete from the same mixture at the same time to ensure the concrete's consistency. A total of two beam specimens, six cubes and four cylinders were cast in steel shutters and moulds in the Concrete/Structures Laboratory at Heriot-Watt University. The volume of each beam, cube and cylinder was known, and then the total required volume of concrete was calculated. The concrete mixture was supplied from a local ready mixed concrete company. One lorry was brought to cast both beams and their control specimens. Both beams and their control specimens were cast from the same mixture. The concrete workability depends on the water/cement (w/c) ratio to control the strength and consistency (slump) of the concrete; therefore, the w/c ratio was taken 0.42 to give a workability of 60-80mm slump for all specimens (Table 5.5).

The casting process was initiated from the tension zone of the beam at the bottom surface of the shutter through two layers, and it was stopped at the outside face of the compression zone of the beam at the top surface of the shutter. This was to ensure that any bleeding of the concrete did not occur in the concrete compression region (Ziara, 1993). Also during the concrete casting of each layer, beam specimens were compacted using a poker vibrator and vibrated using a vibrator and rods to ensure quality, a strong consistent concrete mix, to increase concrete strength, and to reduce the air voids. The vibration was terminated when air bubbles stopped appearing at the top surface of the concrete (Ziara, 1993). The control specimens were compacted using a standard electrically operated vibrating table for a period of approximately 90 seconds. Figure 5.6 shows

both beams together with their own set of control cube and cylinder samples after finishing the concrete casting and after the polishing.



**Figure 5.6:** Beams in Series "A" together with own Control Samples after Concrete Casting.

#### **5.5.4 Curing**

After the concrete casting of both test specimens and control samples, they were stored in their moulds under ambient conditions inside the laboratory. To ensure that beams, cubes and cylinders were treated, damp sheets of hessian were placed over the beams and control samples. In the following days after casting, beam specimens and control samples were treated by spraying water over all surfaces of beams, control samples and hessian. The beams and control specimens were cured, inside their moulds, under moist burlap and plastic for 9 days.

#### **5.5.5 Preparing the Test Specimens for Testing**

The beams and control specimens were removed from the moulds after about 14 days. Test beam specimens were whitewashed to enable the early identification of cracks development under loading. A 70mmx70mm grid consisting of horizontal and vertical lines was drawn on each surface of each test beam to act as a reference for the cracks. At this stage, test beam specimens and control samples were already prepared for the laboratory test programme. Figure 5.7 shows the curing process of both beams after removing the shutters.

Specimens' age at the test was approximately around 140 days. The control specimens were made at the same time as the beams, were cured like the beams and were tested in crushing on the same day as the beams. The average values of actual dimensions for both beams were 708mm wide, 353mm height and 3513mm overall span. These resulted in  $\rho_{s,act} = 1.82\%$  and  $\rho_{s',act} = 0.221\%$ .



**Figure 5.7:** The Curing Process of the Beams in Series "A" after Removing the Shutters.

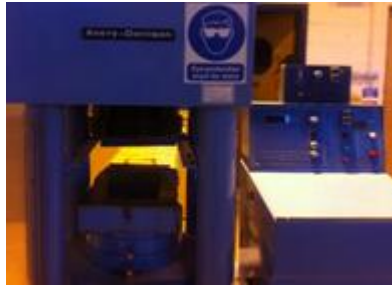
## **5.6 Testing Arrangements and Instrumentation**

### **5.6.1 Testing Machine**

Figure 5.8 shows the testing instrumentation and equipment that were used in the tests. Both test specimens were loaded using a servo-controlled universal test machine (Figure 5.8a) which has a vertical load capacity of up to 2500 kN with a resolution of 1 kN, where the applied force was controlled through manual operation of the hydraulic valve at the loading piston. The total load applied was displayed on a digital indicator on the control panel of the test machine. Each specimen was loaded in 50 kN load increments to failure. A Tonipact 3000 crushing machine (Figure 5.8b), which has a minimum vertical load capacity of 3000 kN with a resolution of 1 kN, was used to test the control samples (cubes and cylinders). The control specimens were tested in crushing on the same day as the beams. Continuous recordings of the applied load, concrete strains and deflections were provided throughout each test. The cracks were marked, photographed and measured with a microscope (Figure 5.8c). Two electrically operated overhead cranes were used to move the beams in the laboratory.



a) Beams Testing Machine



b) Control Specimens Testing Machine



c) Test Instrumentation

**Test Instrumentation:** From Left, Deflection Dial Gauge, Strain Demec Gauge, and Crack Width Microscope.

**Figure 5.8:** Testing Instrumentation and Equipment used in the Tests of Series "A".

**The details of testing arrangements are discussed below:**

### 5.6.2 Loading Arrangement

Both test beams were loaded using a three-point loading arrangement. The load was concentrated from the hydraulic jack of testing machine to the loading plate of test beam specimens. According to the system of loading points for both test specimens, the beams were supported at three ends (for a three point-loading system) on an assembly consisting of roller or hinge bearing sandwiched between two steel plates. The length of the loading and support plates ( $C_p$  and  $C_s$ ), which was in contact with the beam parallel to its length, was 150mm in order to prevent bearing failures in the concrete. The thickness of the loading and support plates ( $t_p$  and  $t_s$ ) was 40mm. Moreover, according to the case of the load and support conditions, both loads and supports in both beams were applied with narrow-width plates (narrow-width load and support case) to the centreline of the overall beam width ( $b_w$ ). The width of the loading plate ( $b_p$ ), which was parallel to the beam width, was larger than the support width ( $b_p > b_s$ ) for both beams. The load-width to beam-width ( $k_p = b_p/b_w$ ) ratio was 0.50 for both beams. While the support-width to beam-width ( $k_s = b_s/b_w$ ) ratio was 0.34 for both beams. The loading arrangements and testing machine used to test the beams are shown in Figures 5.1 and Figure 5.8a, respectively.

### 5.6.3 Loading Procedures and Steps

Both beams were tested under loading control at a rate of 10 kN/minute. The data generated during each test (i.e. total applied loads, concrete strains, deflections, crack widths, etc.) was recorded after each 50 kN increments of loading. The loading steps for both test specimens were similar. The loading step started from zero and then increased incrementally of 50 kN until the collapse (failure) load of the beam reached.

The test sequences were continued until the beams failed. The time required to record a complete set of readings at each load stage varied between 15 to 20 minutes. The overall testing time of a beam varied from 5 to 6 hours.

#### **5.6.4 Instrumentation Arrangements**

Instrumentation for each specimen was designed to capture the load-deflection response, strains in the concrete and crack development. Vertical displacement measurements, at the mid-span of beam length and at the middle of both shear spans, were recorded from Linear Variable Displacement Transformers (LVDTs). Three deflection dial gauges were placed on each test specimen prior to testing. These were placed at the mid-point of the beam width for three locations: under loading point (central dial gauge), and at the middle of both shear spans (dial gauge 1 and dial gauge 2). Also, three Demec strain gauges were placed at the mid-span of each beam length to measure the change in beam concrete strain. They were placed at the bottom, top and middle of the beam height. A crack width microscope was used to measure crack widths. Figure 5.1 shows a typical arrangement for the Demec buttons used for concrete strain measurements and the linear variable differential transducers (LVDT's) used for the deflection dial gauge measurements for the beams in Series (A).

#### **5.6.5 Marking of Cracks**

A 70mmx70mm grid was drawn on the surfaces of the beam specimens to show the development of the crack patterns as the load increases. The surfaces of both beam specimens were marked with different coloured Pens to follow the development of the cracks. The crack width microscope was used for both test specimens to measure the crack width during the test at each increment of the loading.

### **5.7 Test Programme and Procedure**

The procedure of the experimental test programme used for testing the specimens is summarized as follows (Alluqmani, 2010)

Step.1: Both beams were painted white to show of cracks.

Before testing, the sides of both beams were painted white, which has the benefit to show the cracks during the testing of the beams.

Step.2: Marking grids on both sides of the test specimens (Grids of 70\*70mm).

A 70\*70mm grid was drawn and marked on both sides of the specimens to assist in referencing and measuring widths and lengths of the cracks.

Step.3: Assembling of test arrangement.

The areas between the surfaces of each test specimen and the load and support plates were coated with a layer of gypsum plaster to ensure the load is applied to a smooth level surface.

Step.4: Position the beam in the test arrangement and position loading and support plates at appropriate points.

Step.5: Concentration the center of hydraulic jack of testing machine on top of the center of loading plate.

A gypsum plaster was placed at points between the beam specimen and loading points, and also at points between the beam specimen and both supports, to ensure load is applied on a level surface.

Step.6: First beam specimen, three cubes and two cylinders were tested.

Step.7: the other beam and control samples were also tested.

Before starting the test, all necessary Personal Protective Equipments (PPE), e.g. Overalls, safety Shoes, Gloves, Glasses and etc, were made available in the laboratory (Alluqmani, 2010). Figure 5.8 shows the instrumentation and testing equipments used in the tests.

The experimental work activities for manufacturing the steel cages, casting the concrete, and testing the specimens are included in Appendix B.

## **5.8 Measurements**

### **5.8.1 Total Applied Load**

The total load (P) applied to each test specimen was continuously displayed on the control unit of the test machine. The accuracy of the load readings was checked and found to be correct using a load cell which had been calibrated using a reference test machine.

### **5.8.2 Deflection**

Three Linear Variable Differential Transducers (LVDT's) were used to measure the deflections at the loading point (the mid-span of each beam) and at both mid shear-spans for the mid-point of each beam width. The dial gauges had a resolution of 0.01mm.



### **5.8.3 Concrete Strain**

The strains in the concrete were measured at predetermined positions in both beams. The strain in the concrete was measured using a Demec gauge and an arrangement of Demec buttons bonded to the external surfaces of the beams using an epoxy adhesive. Strain gauges with gauge lengths of 100mm were used to measure the strain in the concrete. A typical arrangement for the positions of the Demec buttons on the surfaces of the beams is shown in Figure 5.1.

### **5.8.4 Cracking**

After each load increment, the beams were inspected for cracks. Two crack width microscopes were used in the investigation to measure the crack widths with a resolution of 0.1mm.

The cracks were marked on each face of the test specimens with the corresponding applied load level at each load level. The development of each crack was recorded on the beam surfaces with the corresponding applied load level. The crack patterns were photographed and hard copy sketches were also made.

### **5.8.5 Beam Testing Results**

At each load stage, the following recordings were made:

1. The total applied load (P) in kN.
2. The deflection dial gauge readings which were shown in millimetres on the display panel on the control unit of the test machine.
3. The concrete strain readings on the Demec gauges in millimetres.
4. The flexural and the shear (diagonal) crack widths in millimetres.
5. Comments on the physical state of each beam.

On completion of each increment of loading, the beams were inspected for cracks which were then measured using a crack micrometer. Cracks were marked on the beam surfaces. The magnitudes of the applied loads, concrete strains, deflections, and crack widths were also recorded at each stage. On the completion of each test, the beam was photographed to record the final deflected shape and the crack pattern developments.

All test results were finally recorded. The control samples (cubes and cylinders) were also tested, and the concrete compressive strengths were recorded at the time of the corresponding beam test.

## 5.9 Material Test-Results and Prediction of Beam-Results

Based on the results of material strengths obtained by the tests as shown in Tables 5.6 and 5.7, both flexural and shear capacities of both specimens were predicted by EC2 Code provisions (Table 5.8). It was predicted that both beams will fail in flexure at 690 kN, as shown in Table 5.8.

The concrete compressive strengths obtained from the control samples of cubes and cylinders are shown in Table 5.6. The actual average cube and cylinder concrete compressive strengths were  $f_{cu,act} = 56.0$  MPa and  $f_{cy,act} = 45.0$  MPa, respectively. The actual material strengths used to predict and analyze the test specimens for the compressive strength of concrete ( $f_c$ ), the yield tensile strength of the longitudinal reinforcing bars ( $f_y$ ), and the yield tensile strength of the stirrups ( $f_{yv}$ ) were determined and the results are given in Table 5.7. The value of  $f_c$  used for the analysis, reported in Table 5.7, represents the average strength of cylinders tested on the same day as the specimen, after having been cured under similar laboratory conditions. Table 5.8 shows the prediction of flexural and shear failure loads according to the EC2 Code for both beams in Test-Series (A) based on the actual strengths of materials. It should be emphasised that no partial safety factors were included in the structural calculations for the prediction of failure load. The prediction procedure used for the beams in Series "A" is summarized in Appendix A.4.

**Table 5.6:** Actual Concrete Strengths for Test-Series "A".

Control Sample	Dimensions, mm*mm*mm	Weight, kg	Density, kg/m <sup>3</sup>	Load, kN	Correct. Load, kN	Strength, $f_c$ , N/mm <sup>2</sup>
<b>Actual Concrete Cube Compressive Strengths at 140 days, <math>f_{cu}</math></b>						
1	101*100*102	2.46	2388	590.4	560.7	56.07
2	99*103*101	2.39	2320	582.3	552.9	54.22
3	100*101*100	2.43	2406	581.1	551.8	54.63
4	100*102*99	2.42	2396	577.2	548.1	53.74
5	100*100*102	2.39	2343	615.1	584.2	58.42
6	101*99*101	2.39	2366	621.4	590.6	59.06
<b>Average</b>	--	--	<b>2371</b>	--	--	<b>56.0</b>
<b>Actual Concrete Cylinder Compressive Strengths at 140 days, <math>f_c</math></b>						
1	150*301	12.77	2400	727.2	799.92	45.27
2	152*303	13.28	2414	740.8	814.88	44.91
<b>Average</b>	--	--	<b>2407</b>	--	--	<b>45.0</b>
<b>Actual Concrete Cylinder Split Strengths, <math>f_{ct}</math>, L = 300mm</b>						
1	151*302	13.26	2451	201.6	221.75	3.10
2	150*300	12.71	2397	237.4	261.15	3.70
<b>Average</b>	--	--	<b>2424</b>	--	--	<b>3.40</b>

**Test-Series (A): Date of Casting:** 24 November 2011, **Date of Testing:** 11 April 2012.

$f_{ct} = 2P/(3.142*d*L) = 0.637*P/(d*L)$ . D is the cylinder diameter and L is the cylinder height.

**Table 5.7:** Material Properties used to Predict and Analyze the Beams in Series "A".

	Properties	Series (A)
<b>Concrete</b>	Cylinder Compressive Strength ( $f_c$ ), MPa	45
	Cube Compressive Strength ( $f_{cu}$ ), MPa	56
	Cylinder Split Tensile Strength ( $f_t$ ), MPa	3.40
	Young's Modulus ( $E_c$ ), MPa	31000
<b>Flexural Reinforcement</b>	Yield Strength for $\Phi 25$ mm ( $f_y$ ), MPa	525
	Yield Strength for $\Phi 10$ mm ( $f_y$ ), MPa	517
	Young's Modulus ( $E_s$ ), MPa	200000
<b>Shear Reinforcement</b>	Yield Strength for $\Phi 8$ mm ( $f_{yv}$ ), MPa	512
	Young's Modulus ( $E_s$ ), MPa	200000

**Table 5.8:** Re-calculation of the Maximum Design Load and Prediction of Failure Load for the Beams in Series "A".

Beam Type	Max. Original Design Load, kN	Max. Original Flexural Capacity, kN.m	Max. Re-Calculated (Actual) Flexural Capacity, kN.m	Max. Re-Calculated (Actual) Design Load, kN	Actual Exp. Failure Load, kN (F. Mode)
	$P_d$	$M_d$	$M_u = M_{d,act}$	$P_{d,act}$	$P_{f,exp}$
<b>ECC2</b>	600	420	483	690 (Flexure)	<b>985</b> (Shear)
<b>ECC3</b>	600	420	483	690 (Flexure)	<b>1000</b> (Flexure)

$P_d = 600$  kN,  $V = 300$  kN,  $M = 420$  kN.m,  $a = 1400$ mm,  $A_{s,prov.} = 3927$  mm<sup>2</sup>,  $f_{y,act.} = 525$  MPa,  $f_{c,act.} = 45$  MPa.

$P_{d,act.} =$  Actual design load =  $2(M_{d,act.}/a)$ , and  $M_{d,act.} = M_{u,code} = M_{small} = 483$  kN.m (from Steel).

$M_{u,code, Flexure}$  (from Steel) =  $A_{s,prov.} * f_{y,act.} * Z = 483$  kN.m. Where,  $Z = d - (s/2) = 234.3$  mm.

$s = 0.8x = 139$ mm,  $x = d * [\epsilon_c / (\epsilon_c + \epsilon_s)] = 173.7$ mm, where,  $\epsilon_s = f_{y,act.} / E_s = 0.002625$ ,  $\epsilon_c = 0.0035$ ,  $E_s = 200000$  MPa.

$M_{u,code, Shear}$  (from Concrete) =  $(f_{c,act.} * b_w * d^2) * K = 582.2$  kN.m. Where,  $K = -1.134 * (Z/d)^2 + 1.134 * (Z/d) = 0.20$  and  $Z = d - (s/2) = 234.3$  mm.

No factors of safety are used neither in calculation of  $Z$  nor in calculation of  $M_{u,code}$ .

## 5.10 Test Results of Beams

In order to characterise the materials used in the beam manufacture, the compression strength of concrete is determined by cylindrical and cubic specimens. The actual reinforcement properties and strengths, the concrete strengths, and the actual beam dimensions were used to re-calculate the original design load as well as to predict the failure load of each beam. Table 5.8 shows the re-calculation of the maximum design loads and predicted failure loads according to the actual results of material strengths, as well shows the experimental failure loads and capacities for the test specimens in Series (A).

Table 5.9 shows the test results obtained from Test-Series (A), as well shows a comparison of the failure loads and modes predicted by EC2, ACI318 and SBC304 Codes with those values either obtained from the tests or predicted by the existing models, such as Lubell et al model (2008), Sernar-Ros et al model (2002) and Shuraim model (2012). All prediction models showed that both beams will fail in flexure at 690 kN according to EC2 or at 721 kN according to ACI318

and SBC304. The actual experimental failure loads (failure modes) of beams ECC2 and ECC3 were 985 kN (shear) and 1000 kN (flexure), respectively. Based on the experimental results, the deficiency of the current design models and Codes to predict the capacity of wide RC beams is clear. This confirms that a rational Prediction-Model should be proposed and developed based on the main variables which affect on the shear and flexural strengths of wide RC beams as mentioned in the literature.

**Table 5.9:** Comparison of the Predictions of Flexural and Shear Failure Loads with the Test Results obtained from Series "A".

Beam Type	Code			Code Pred.		Lubell Pred.		Serna-Ros Pred.		Shuraim Pred.		Test Strength, kN		Deflec., mm	Crack Width, mm	
	V <sub>c</sub>	V <sub>s</sub>	M <sub>u</sub>	P <sub>V,d</sub>	P <sub>M,d</sub>	P <sub>V</sub>	P <sub>M</sub>	P <sub>V</sub>	P <sub>M</sub>	P <sub>V</sub>	P <sub>M</sub>	P <sub>V,exp.</sub>	P <sub>M,exp.</sub>	Δu	Flex.	Diag.
<b>According to EC2</b>																
ECC2	274	156	483	860	690	690	690	810	690	854	690	985	-	6.63	1.45	2.40
ECC3	274	235	483	1018	690	816	690	1167	690	1070	690	-	1000	16.24	1.52	1.10
<b>According to ACI318 and SBC304</b>																
ECC2	240	174	505	828	721	664	721	772	721	786	721	985	-	6.63	1.45	2.40
ECC3	240	261	505	1002	721	804	721	1168	721	1002	721	-	1000	16.24	1.52	1.10

**NOTE:**  $b_w = 708\text{mm}$ ,  $h = 353\text{mm}$ ,  $d = 304\text{mm}$ ,  $a = 1400\text{mm}$ ,  $Z = 234.3\text{mm}$  (EC2),  $jd = Z = 244.8\text{mm}$  (ACI318-and-SBC304),  $\epsilon_c = 0.0035$  (EC2),  $\epsilon_c = 0.003$  (ACI318-and-SBC304),  $E_c = 31000\text{ MPa}$ ,  $E_s = 200000\text{ MPa}$ ,  $\rho_s = 1.82\%$ ,  $\rho_s' = 0.221\%$ ,  $f_{c,y,d} = 45\text{ MPa}$ ,  $f_{y,d} = 525\text{ MPa}$ ,  $f_{y,v,d} = 512\text{ MPa}$ .  $P_d = 600\text{ kN}$ ,  $V = 300\text{ kN}$ , and  $M = 420\text{ kN.m}$ .  $A_v = 201\text{mm}^2$  (4-Legs $\Phi 8\text{mm}$ ) for Beam ECC2,  $A_v = 302\text{mm}^2$  (6-Legs $\Phi 8\text{mm}$ ) for Beam ECC3.  $S_L = 180\text{mm}$  for Beams ECC2 and ECC3.  $S_w = 300\text{mm}$  for Beam ECC2,  $S_w = 122\text{mm}$  for Beam ECC3.  $k_p = 0.50$  ( $b_p = 350\text{mm}$ ) for both Beams,  $k_s = 0.34$  ( $b_s = 240\text{mm}$ ) for both Beams. Hence  $k = 0.34$ .

$P_d = 600\text{ kN}$ ,  $V = 300\text{ kN}$ ,  $M = 420\text{ kN.m}$ ,  $a = 1400\text{mm}$ ,  $A_{s,prov.} = 3927\text{ mm}^2$ ,  $f_{y,act.} = 525\text{ MPa}$ ,  $f_{c,act.} = 45\text{ MPa}$ .

$P_{d,act.} = \text{Actual design load} = 2(M_{d,act.}/a)$ , and  $M_{d,act.} = M_{u,code} = M_{small}$ .

#### **EC2:**

$M_{u,code, Flexure}$  (from Steel) =  $A_{s,prov.} * f_{y,act.} * Z = 483\text{ kN.m}$ . Where,  $Z = d - (s/2) = 234.3\text{ mm}$ .

$s = 0.8x = 139\text{mm}$ ,  $x = d * [\epsilon_c / (\epsilon_c + \epsilon_s)] = 173.7\text{mm}$ , where,  $\epsilon_s = f_{y,act.} / E_s = 0.002625$ ,  $\epsilon_c = 0.0035$ ,  $E_s = 200000\text{ MPa}$ .

$M_{u,code, Shear}$  (from Concrete) =  $(f_{c,act.} * b_w * d^2) * K = 582.2\text{ kN.m}$ . Where,  $K = -1.134 * (Z/d)^2 + 1.134 * (Z/d) = 0.20$  and  $Z = d - (s/2) = 234.3\text{ mm}$ .

$M_{u,code}$  (EC2) =  $M_{small} = 483\text{ kN.m}$  (from Steel).

#### **ACI318-and-SBC304:**

$M_{u,code, Flexure}$  (from Steel) =  $A_{s,prov.} * f_{y,act.} * jd = 505\text{ kN.m}$ . Where,  $jd = Z = d - (a/2) = 244.8\text{ mm}$ .

$a = \beta_1 * c = 118.3\text{mm}$ ,  $c = d * [\epsilon_c / (\epsilon_c + \epsilon_s)] = 162.1\text{mm}$ ,  $\beta_1 = 0.85$  for  $f_c' \leq 28\text{ N/mm}^2$ ,  $\beta_1 = 0.85 - [0.05 * ((f_c' - 28) / 7)] \geq 0.65$  for  $f_c' > 28\text{ N/mm}^2$  (Hence:  $\beta_1 = 0.73$ ), where,  $\epsilon_s = f_{y,act.} / E_s = 0.002625$ ,  $\epsilon_c = 0.003$ ,  $E_s = 200000\text{ MPa}$ .

$M_{u,code, Shear}$  (from Concrete) =  $(f_{c,act.} * b_w * d^2) * K = 544.7\text{ kN.m}$ . Where  $K = \omega * [1.0 - 0.59 * \omega] = 0.185$ , and  $\omega = \rho_{s,prov.} * (f_{y,act.} / f_{c,act.}) = 0.212$ , and  $jd = Z = d - (a/2) = 244.8\text{ mm}$ .

$M_{u,code}$  (ACI318-and-SBC304) =  $M_{small} = 505\text{ kN.m}$  (from Steel).

No factors of safety are used neither in calculation of  $Z$  nor in calculation of  $M_{u,code}$ .

$P_V = \text{Predicted shear failure load} = 2V_{u,d}$  and  $P_M = \text{Predicted flexural failure load} = 2(M_{u,d}/a)$ .

$P_{f,pred.}$  = the smallest of ( $P_V$  or  $P_M$ ) and the predicted failure mode is the failure mode corresponding to  $P_{f,pred.}$ .

No factors of safety are used neither in this prediction  $V_c$  and  $V_s$  nor in calculation of  $P_V$  and  $P_M$ .

Table 5.10 shows a summary of the predicted, measured and analyzed capacities for the beams in Series (A). Table 5.11 summarizes the mid-span deflection and crack width measurements at different load levels for the beams in Series (A). Table 5.12 summarizes the strain and stress measurements in concrete at different load levels for the beams in Series (A).

Failure modes and crack patterns at failure for the beams in Series (A) are shown in Figure 5.9. Figure 5.10 shows photos of the failure modes and deformed shapes after failure for the beams in Series (A). The response of total applied load versus mid-span deflection for the beams in Series (A) is shown in Figure 5.11. Tables 5.13 and 5.14 show the total applied load versus the crack widths and mid-span deflections, respectively, for the beams in Series (A).

**Table 5.10:** Predicted and Measured Capacities for the Beams in Series "A".

	Beam ECC2	Beam ECC3
Design Load ( $P_d$ ), kN	600	600
Actual Design Load ( $P_{d,act.}$ ), kN	690	690
Predicted Failure Load ( $P_{f,pred.}$ ), kN	690 (Flexure)	690 (Flexure)
Load at 1 <sup>st</sup> Flex. Crack Formation, kN	200	200
Load at 1 <sup>st</sup> Diag. Crack Formation, kN	450	250
Working (Service) Load ( $P_w$ ), kN	500	750
Actual Failure Load ( $P_{f,exp.}$ ), kN	985 (Shear)	1000 (Flexure)
$V_{u,exp.} = P_{f,exp.}/2$ , kN	493	-
$M_{u,exp.} = (P_{f,exp.}/2)*a$ , kN.m	-	700
$\tau = V_{exp.} / bw*d$ , N/mm <sup>2</sup>	2.31	-
$\sigma = (M_{exp.}/a) / bw*d$ , N/mm <sup>2</sup>	-	2.35
$(P_{f,exp.} / P_d)$	1.64	1.67
$(P_{f,exp.} / P_{d,act.})$	1.43	1.45
$(P_{f,exp.} / P_{f,pred.})$	1.43	1.45

**Table 5.11:** Test Summary of Mid-Span Deflection and Crack Width Measurements at Different Load Levels for the Beams in Series "A".

Beam Type	At Service (Working) Load*				At Ultimate (Design) Load				Prior to Failure (Maximum) Load			
	Load ( $P_w$ ), kN	Deflec. ( $\delta$ ), mm	Crack Width, mm		Load ( $P_d$ ), kN	Deflec. ( $\delta$ ), mm	Crack Width, mm		Load ( $P_T$ ), kN	Deflec. ( $\delta$ ), mm	Crack Width, mm	
			Flex.	Diag.			Flex.	Diag.			Flex.	Diag.
ECC2	500	2.61	0.41	0.21	600	3.14	0.50	0.38	950	6.63	1.45	2.40
ECC3	750	12.50	0.40	0.61	600	9.44	0.27	0.16	950	16.24	1.52	1.10

Date of Casting: 24/11/2011, Date of Testing: 11/4/2012.

Locations of Deflection Dial Gauges refer to Figure 5.1.

\* Service (working) load is the total applied load when the maximum flexural crack width reaches to the limit per the applied Code of Practice, which is 0.40mm for EC2, ACI318 and SBC304.



a) Beam ECC2, Failure at  $P = 985$  kN



b) Beam ECC3, Failure at  $P = 1000$  kN

**NOTE:** these Figures are enlarged to show Crack Patterns

**Figure 5.9:** Failure Modes and Crack Patterns at Failure for the Beams in Test-Series "A".



a) Beam ECC2



b) Beam ECC3

**Figure 5.10:** Photos of the Failure Modes, Crack Patterns and Deformed Shapes after Failure for the Beams in Test-Series "A".

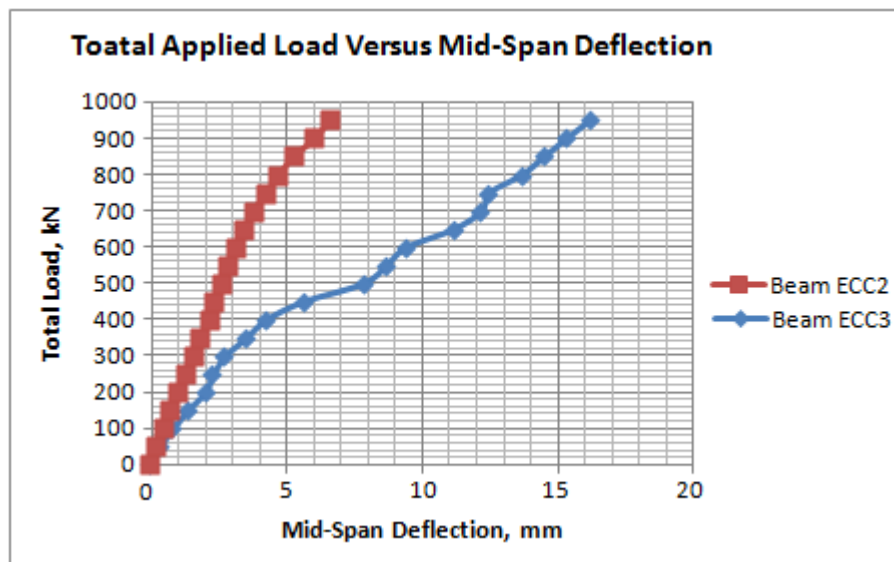


**Figure 5.11:** Total Applied Load versus Mid-Span Deflection for the Beams in Test Series "A".

**Table 5.12:** Test Summary of Strain & Stress Measurements in Concrete at different Loads for the Beams in Series "A".

Total Applied Load, P, kN	Strains and Stresses in Concrete of Beam <b>ECC2</b>					
	Top Gauge Increment, $\Delta$ , mm	Strain, $\epsilon_c = \Delta/L$ , mm/mm $\times 10^{-3}$	Middle Gauge Increment, $\Delta$ , mm	Strain, $\epsilon_c = \Delta/L$ , mm/mm $\times 10^{-3}$	Bottom Gauge Increment, $\Delta$ , mm	Strain, $\epsilon_c = \Delta/L$ , mm/mm $\times 10^{-3}$
	Front Face Back Face (Average)	Front Face Back Face (Average)	Front Face Back Face (Average)	Front Face Back Face (Average)	Front Face Back Face (Average)	Front Face Back Face (Average)
500 <sup>*1</sup>	-1.01 -0.91 (-0.96)	(-6.4)	0.30 0.20 (0.25)	(1.7)	2.01 2.11 (2.06)	(13.7)
600 <sup>*2</sup>	-1.14 -1.00 (-1.07)	(-7.1)	0.33 0.10 (0.22)	(1.5)	2.49 2.44 (2.47)	(16.5)
950 <sup>*3</sup>	-1.70 -1.63 (-1.55)	(-10.3)	0.83 0.79 (0.81)	(5.4)	3.76 3.43 (3.60)	(24.0)
Total Applied Load, P, kN	Strains and Stresses in Concrete of Beam <b>ECC3</b>					
	Top Gauge Increment, $\Delta$ , mm	Strain, $\epsilon_c = \Delta/L$ , mm/mm $\times 10^{-3}$	Middle Gauge Increment, $\Delta$ , mm	Strain, $\epsilon_c = \Delta/L$ , mm/mm $\times 10^{-3}$	Bottom Gauge Increment, $\Delta$ , mm	Strain, $\epsilon_c = \Delta/L$ , mm/mm $\times 10^{-3}$
	Front Face Back Face (Average)	Front Face Back Face (Average)	Front Face Back Face (Average)	Front Face Back Face (Average)	Front Face Back Face (Average)	Front Face Back Face (Average)
750 <sup>*1</sup>	-0.70 -1.29 (-1.00)	(-6.7)	0.08 -0.09 (0.00)	(0)	2.19 1.90 (2.05)	(13.7)
600 <sup>*2</sup>	-0.01 -0.93 (-0.47)	(-3.1)	-0.11 -0.27 (-0.19)	(-1.3)	1.88 1.57 (1.73)	(11.5)
950 <sup>*3</sup>	-0.64 -1.57 (-1.11)	(-7.4)	0.51 0.41 (0.46)	(3.1)	2.34 2.47 (2.41)	(16.1)

$L = L_{D,B} = 150\text{mm}$ ,  $E_c = 31000 \text{ N/mm}^2$ . Stress ( $\sigma$ ) =  $E_c \cdot \epsilon_c$  (N/mm<sup>2</sup>).

Date of Casting: 24 November 2011. Date of Testing: 11 April 2012.

\*1 At Service (Working) Load. \*2 At Ultimate (Design) Load. \*3 Prior to Failure Load.

\* Locations of Concrete Demec Strain Gauges refer to Figure 5.1.

Average Reference Readings at P = 0 kN for Beam ECC2 – Top = 8.705, Middle = 8.640, Bottom = 8.560.

Average Reference Readings at P = 0 kN for Beam ECC3 – Top = 8.210, Middle = 8.575, Bottom = 8.635.

**Table 5.13:** Total Applied Load versus Crack Widths for the Beams in Series "A".

Load, kN	Beam ECC2 Crack Width, mm		Beam ECC3 Crack Width, mm	
	Flexural	Diagonal	Flexural	Diagonal
0	-	-	-	-
50	-	-	-	-
100	-	-	-	-
150	Too Fine	-	Too Fine	-
200	<u>0.09</u>	-	<u>0.10</u>	Too Fine
250	0.10	-	0.12	<u>0.08</u>
300	0.12	-	0.13	0.10
350	0.16	-	0.16	0.10
400	0.18	Too Fine	0.16	0.12
450	0.21	<u>0.10</u>	0.19	0.12
500	<u>0.41</u>	0.21	0.21	0.14
550	0.47	0.32	0.24	0.16
600	0.50	0.38	0.27	0.16
650	0.55	0.56	0.30	0.32
700	0.62	0.66	0.36	0.48
750	0.74	0.78	<u>0.40</u>	0.61
800	0.82	0.86	0.55	0.76
850	0.91	0.96	0.86	0.82
900	1.2	1.45	1.12	0.94
950	<b>1.45</b>	<b>2.40</b>	<b>1.52</b>	<b>1.10</b>

Date of Casting: 24/11/2011, Date of Testing: 11/4/2012.

**Table 5.14:** Total Applied Load versus Mid-Span Deflections for the Beams in Series "A".

Applied Load, kN	Centre Dial Reading, mm	Centre Dial Increment, $\Delta$ , mm	Centre Dial Reading, mm	Centre Dial Increment, $\Delta$ , mm
	Beam ECC2		Beam ECC3	
0	<u>2.80</u>	0	<u>7.60</u>	0
50	3.02	0.22	7.93	0.33
100	3.27	0.47	8.42	0.82
150	3.53	0.73	8.95	1.35
200	3.82	<u>1.02</u>	9.61	<u>2.01</u>
250	4.10	1.30	9.90	<u>2.30</u>
300	4.38	1.58	10.34	2.74
350	4.64	1.84	11.12	3.52
400	4.99	2.19	11.86	4.26
450	5.16	<u>2.36</u>	13.24	5.64
500	5.41	<u>2.61</u>	15.46	7.86
550	5.67	2.87	16.30	8.70
600	5.94	<u>3.14</u>	17.04	<u>9.44</u>
650	6.25	3.45	18.80	11.20
700	6.60	<u>3.80</u>	19.82	<u>12.22</u>
750	7.06	4.26	20.10	<u>12.50</u>
800	7.54	4.74	21.32	13.72
850	8.07	5.27	22.14	14.54
900	8.86	6.06	22.97	15.37
950	9.43	<b><u>6.63</u></b>	23.84	<b><u>16.24</u></b>

Date of Casting: 24/11/2011, Date of Testing: 11/4/2012.

Locations of Deflection Dial Gauges refer to Figure 5.1.



## 5.11 Discussion of Test Results

All results, discussions and conclusions on the behaviour of the wide RC beams tested in Series (A) are described in the following Sections (Alluqmani, 2013a):

The two wide RC beams tested in Test-Series (A) were predicted by the existing Codes and Models to fail in flexure at 690 kN to EC2 or at 721 kN to ACI318 and SBC304 (Table 5.9). Beam ECC2 had a predicted shear failure load ( $P_{f,pred.} = P_{V,d}$ ) between 664 kN and 860 kN and a predicted flexural failure load ( $P_{f,pred.} = P_{M,d}$ ) of 690 kN to EC2 or 721 kN to ACI318 and SBC304 (Table 5.9), where the beam failed in shear at a total failure load of 985 kN. Beam ECC3 had a predicted shear failure load ( $P_{f,pred.} = P_{V,d}$ ) between 804 kN and 1168 kN and a predicted flexural failure load ( $P_{f,pred.} = P_{M,d}$ ) of 690 kN to EC2 or 721 kN to ACI318 and SBC304 (Table 5.9), where the beam failed in flexure at a total failure load of 1000 kN.

Both beams investigated in Test-Series (A), included shear span ( $a$ ) of 1400mm, effective depth ( $d$ ) of 304mm and  $a/d$  ratio of 4.60, were designed and detailed by EC2 Code. Beam ECC2 was designed with longitudinal and transversal stirrup-legs spacing of  $S_L \approx 0.6d = 180\text{mm}$  and  $S_w \approx d = 300\text{mm}$ , respectively, and failed in shear by diagonal cracking in the shear-span region at 985 kN. Beam ECC3 was designed with longitudinal and transversal stirrup-legs spacing of  $S_L \approx 0.6d = 180\text{mm}$  and  $S_w \approx 0.4d = 122\text{mm}$ , respectively, and failed in flexure by flexural deformation and cracking at 1000 kN.

### 5.11.1 Failure Modes

The failure mode was different for the both beams. Beam ECC2 failed in shear by diagonal cracking in the shear-span region; while beam ECC3 failed in flexure by flexural deformation and cracking, as shown in Figures 5.9 and 5.10. In all beams, hair-line flexural cracks developed in the lower part of the beams and extended vertically towards the neutral axis before the appearance of diagonal cracks. As loading was continued, the flexural cracks proliferated and widened; and diagonal cracks appeared in the both shear spans.

All current Codes and Models gave that both beams will fail in flexure (failure mode) at a load between 690 kN and 721 kN (failure load), however, beam ECC2 failed in shear at 985 kN. Moreover, even if beam ECC3 failed in a flexural mode as predicted, but it failed at 1000 kN where the predicted failure load was either 690 kN to EC2 or 721 kN to ACI318 and SBC304

( $P_{f,exp.} / P_{f,pred.} = 1.45$  to EC2 and 1.39 to ACI318 and SBC304, more conservative), Table 5.9. This confirms that current Codes and models do not give a prediction for either the failure load or even the failure mode of wide RC beams. Based on the results obtained from the two beams tested in this Series and based on the results of previous researches reviewed in the literature, development of a proposed Prediction-Model to account for both shear and flexural strengths of wide RC beams is significantly needed. The proposed prediction model should take into the account the main variables mentioned in the literature that affect the shear and flexural strengths of wide RC beams. The prediction model must also predict the failure load and mode of wide RC beams based on the general methods used in the current Codes, but with taking into the considerations the effect of  $k_s$ ,  $k_p$ ,  $S_L$  and  $S_w$ .

### **5.11.2 Behaviour of the Beams in Series (A)**

The crack development was similar on both elevation side faces (front and back faces) for each beam, and did not appear neither on both cross-section side faces (right and left faces) nor on both plan side faces (top and bottom faces) for both beam specimens. The flexural and diagonal cracks developed and widened under increasing loads. For both specimens, the flexural cracks developed before the diagonal cracks. Spoiling of the compression concrete under the loading occurred at failure.

Flexural cracks developed in the lower part of the both beams. For both beams, the flexural cracks developed at a load level approximately of 33.3% of the ultimate (design) load (600 kN), Table 5.13. Diagonal cracks appeared in the shear span regions of both beams. For beam ECC2, the diagonal cracks appeared at a load level approximately of 75.0% of the ultimate (design) load (600 kN). While for beam ECC3, the diagonal cracks appeared at a load level approximately of 41.7% of the ultimate (design) load (600 kN).

For both beams, the flexural cracks were wider than the diagonal cracks up to the ultimate (design) load (600 kN). For beam ECC3, the flexural cracks were again wider than the diagonal cracks from a load level equal to 1.42 times the ultimate (design) load (at  $P = 850$  kN) up to failure, Table 5.13. For both beams, diagonal cracks developed in the shear spans as an extension of existing flexural cracks. The diagonal cracks extended towards the loading plate, passed the neutral axis of the beam, and reached to the concrete compression region.

Additional flexural and diagonal cracks appeared and widened under increasing loads. For beam ECC2, the width of the flexural crack at the design load (600 kN), was 0.50mm; the corresponding width of the diagonal crack at the same load was 0.38mm. While for beam ECC3, the widths of the flexural cracks at the design load (600 kN), was 0.27mm; the corresponding widths of the diagonal cracks at the same load was 0.16mm.

Based on the test results, the concentrating flexural- and shear- reinforcements within the widths of supports and loads succeeded in preventing the appearance of punching-shear failure for both beams in those regions (regions of supports and loads) which have high shear stresses; and have also succeeded in preventing the appearance of shear failure for beam ECC3. It should be noted that the presence of proportion of the flexural and shear reinforcements arranged and distributed within the support and load widths has succeeded to prevent the propagation of the diagonal cracks into the compression zone in those regions, thus resulting in an increase in the load carrying capacity for both beams.

The widths of the flexural and diagonal cracks were similar for both beams (0.20mm and 0.11mm respectively) at a load level of 450 kN, which was approximately 45% of the maximum (failure) load, 1000 kN, (75% of the ultimate (design) load, 600 kN). At the maximum load level (950 kN), which was prior to the failure load, the flexural crack widths were approximately similar for both beams (about an average of 1.48mm). However, the diagonal crack width at the maximum load level for beam ECC3 (1.10mm) was smaller than half of the corresponding value for beam ECC2 (2.40mm). Beam ECC3 had wider flexural crack widths (about 1.52mm) comparing with their diagonal crack widths (about 1.10mm) under the maximum loading.

To analyze the behaviour of the beams, the widths of the diagonal cracks at the service (working) load levels and at the maximum load levels should be discussed. As per the provisions of the EC2, ACI318 and SBC304 Code approaches, the service (working) load is the load level when the maximum width of the flexural crack exceeds to 0.40mm.

For beam ECC2, the width of the diagonal crack at the service (working) load level, which was approximately 83.3% of the design load (600 kN), was 0.21mm. While for beam ECC3, the width of the diagonal crack at the service (working) load level, which was approximately 125.0% of the design load (600 kN), was 0.61mm, Tables 5.11 and 5.13. For beams ECC2 and ECC3, the widths of the diagonal crack at the maximum load level (950 kN), which was 158.3% of the design load (600 kN) for both beams, were 2.40mm and 1.10mm, respectively.

The mid-span deflections were recorded at each step of the loading increment (Table 5.14). For beams ECC2 and ECC3, the mid-span deflections at the maximum load level (950 kN) were 6.63mm and 16.24mm, respectively.

The width of the diagonal cracks at the maximum load level (950 kN, one step prior to failure) for beam ECC2 (2.40mm) was wider than that obtained from beam ECC3 (1.10mm). It seems that the wide transverse spacing of stirrup legs ( $S_w = 300\text{mm} \approx d \approx 1.67 \cdot S_L$ ) within the support width ( $b_s = 240\text{mm}$ ) in beam ECC2 resulted in wider diagonal crack widths. The width of the crack in this beam just at one step before the maximum load level (at 900 kN), supports this conclusion (Table 5.13). At failure of beam ECC2, the widest critical diagonal crack bypassed the loading point and entered the concrete compression region adjacent to the loading point where spoiling of the compression concrete had occurred. This type of behaviour resulted from the transverse stirrup-legs spacing ( $S_w = 300\text{mm}$ ) of beam ECC2 which was greater than the support width ( $b_s = 240\text{mm}$ ). This type of behaviour did not prevent the beam from achieving its full capacity. Nevertheless, the arrangement of the inner stirrup legs within the support width for a distance equal to  $S_w$  (transverse spacing of stirrup legs) to be less than  $d$  (the effective-depth of the beam) is recommended for all wide beams, and a design model should be developed for designing  $S_w$  of wide RC beams.

Confining the regions of the effective widths of bearing plates resulted in enhancement in the load carrying capacity of the beams. It is concluded that for beams with narrow-width bearing plates ( $k < 1.0$ ), confinement of the regions of bearing plates has an effect on the load carrying capacity of beams and helps to prevent the punching shear failure (two-way shear failure).

It is concluded that the shear strength of wide beams decreases as the transverse spacing of the stirrup legs ( $S_w$ ) increases, as Lubell et al (2009a) and Serna-Ros et al (2002) concluded. Thus as result, beam ECC2 had a  $S_w$  of 300mm, which was approximately equal to  $d$ , and failed in shear; accordingly, the design value of  $S_w$  to be smaller than  $d$  (the effective-width) is recommended.

## **5.12 Conclusions**

Two beams were tested in order to investigate the shear and flexural behaviours of wide RC beams as well as to be used with those beams tested previously in the literature for developing a proposed Prediction-Model. The main objective from testing the two beams in Series (A) was to

investigate the failure load and mode of each beam to be compared with those predictions obtained by the existing Codes and Models. The failure mode of both beams was different, where beam ECC2 failed in shear and beam ECC3 failed in flexure. All current models gave a prediction that both beams will fail in flexure. Based on the results and discussion, the development of a rational Prediction-Model is necessary needed. All factors which affect the shear and flexural strengths of wide RC beams must be taken into the account when the prediction model is being developed.

The observations described above, which were obtained from the initial stage of this programme of research, explain the following conclusions:

1. The shear strength of wide beams decreases as the transverse spacing of their stirrup legs ( $S_w$ ) increases, and it is recommended that  $S_w$  should be smaller than  $d$  (effective depth). Development of a design model to account for the stirrup-legs spacing of wide RC beams is suggested.

2. The shear and flexural strengths of wide RC beams cannot be determined using the provisions of the current Codes and Models. The general formulae for the design and prediction methods applied in the current Codes of Practice should be used as guideline to develop a new Prediction-Model. The formulae should be also corrected by factors depend on the real parameters which affect the wide concrete beam strengths. These parameters are the ratios of support- and load-widths to the wide-beam width ( $k_s$  and  $k_p$ ), and the longitudinal and transverse spacing of stirrup legs ( $S_L$  and  $S_w$ ).

3. The presence of portions of the flexural -tensile and -compressive reinforcing bars within the support- and load- widths, respectively, has succeeded to prevent the punching shear failure (two-way failure) for both beams. Therefore, it is recommended that a detailing approach to account for detailing, arranging and distribution the reinforcements of wide RC beams within the support and load widths should be developed.

## CHAPTER 6

# A NEW PREDICTION-MODEL FOR SHEAR AND FLEXURE OF WIDE RC BEAMS

### 6.1 Introduction

The two wide RC beams tested in Test-Series (A), Chapter 5, were predicted by the existing Codes and models. All current Codes and models gave that both beams will fail in flexure (failure mode) at a load between 690 kN and 721 kN (failure load); however, beam ECC2 failed in shear at 985 kN (Tables 5.9, Chapter 5). Moreover, even if beam ECC3 failed in a flexural mode as predicted, but it failed at 1000 kN where the predicted failure load was either 690 kN to EC2 or 721 kN to ACI318 and SBC304 ( $P_{f,exp.} / P_{f,pred.} = 1.45$  to EC2 and 1.39 to ACI318 and SBC304, more conservative).

This confirms that current Codes and models do not give a prediction for either the failure load or even the failure mode of wide RC beams. Based on the discussions and results obtained from the two beams tested in Series (A) and based on the results of previous researches reviewed in the literature, development of a proposed Prediction-Model to account for both shear and flexural strengths of wide RC beams is significantly needed. The proposed Prediction-Model must be developed and adopted based on the conclusions obtained from testing the beams in Series (A) and based on a well understanding of the flexural and shear behaviours of wide RC beams to ensure that the shear and flexural capacities of all wide concrete members are adequate when they are designed according to the current Codes of Practice. When the prediction model is being developed, the main factors mentioned in the literature which affect the shear and flexural strengths of wide RC beams should be taken into the account. These factors are: 1) the widths of supports and loads ( $b_s$  and  $b_p$ ), 2) the ratios of the support- and load- widths to beam-width ( $k_s$  and  $k_p$ ), and 3) the longitudinal and transverse stirrup-legs spacing ( $S_L$  and  $S_w$ ). The prediction model must predict the failure load and failure mode of wide RC beams based on the general methods used in the current Codes, with taking into the considerations the effect of  $k_s$ ,  $k_p$ ,  $S_L$  and  $S_w$ .

The flexural behaviour of RC members has been well understood for narrow concrete members (drop beams) such that their flexural strengths are predicted with reasonable accuracy over a

wide range of cases; while for wide concrete members, the effect of the bearing plate widths at the load and support locations should be taken into the consideration in order to predict their flexural and shear capacities (Alluqmani, 2013a, 2013b, Alluqmani and Saafi, 2014b). By contrast, it is difficult to predict the shear strengths of RC members accurately due to the uncertainties in the shear transfer mechanism, especially after cracks are initiated. For more accurate prediction of the shear strengths, many sophisticated approaches have been proposed based on mechanical or physical models of structural behaviour/failure, fracture mechanics, and nonlinear finite element analyses.

Many deterministic models have been developed in order to predict the shear strengths of RC beams, which are based on rules of mechanics and on experimental test results. While the constant and variable angle truss models are known to provide reliable bases and to give reasonable predictions for the shear strengths of RC members. In the case of wide concrete members, these models may show lack of accuracy or lead to fairly different predictions. Since there is yet no agreement on such approaches among researchers, prediction of shear strengths of RC beams is still considered an active open research field with important recent publications.

Therefore, in order to predict the flexural and shear strengths of wide RC beams with full- and/or narrow- width load and support conditions, a proposed prediction model should be developed to predict the shear and flexural strengths of wide RC beams with and without shear reinforcement based on influential parameters and recent experimental test results reported in the literature (Chapter 3). The proposed prediction model, which is needed for prediction the flexural and shear strengths of wide RC beams, must take into the account the effect of the ratios of bearing-plate widths to beam width and the effect of stirrup legs spacing along the length and across the width (Alluqmani, 2013a, 2013b).

## **6.2 Shear Strength on Concrete Beams**

In the early 20<sup>th</sup> century, truss models were used as conceptual tools in the analysis and design of reinforced concrete beams. Ritter (1899) and Morsch (1909) postulated independently that after a reinforced concrete beam cracks due to diagonal tension stresses, it can ideally be thought of as a parallel chord truss with compression diagonals inclined at 45° with respect to the longitudinal axis of the beam. Several years later, Morsch (1920, 1922) introduced the use of truss models for torsion. In these truss models (Figure 6.1), in which the contribution of the concrete in tension is neglected, the diagonal compressive concrete stresses ( $v_c$ ) push apart the top and bottom faces of

the beam, while the tensile stresses in the stirrups ( $v_s$ ) pull them together. Equilibrium requires these two effects to be equal. According to the 45° truss model, the shear capacity is reached when the stirrups yield and will correspond to a shear stress ( $\tau = v_s$ ) as given in Equation (6.1).

$$\tau = v = \frac{A_v * f_{yv}}{b_w * S_L} = \rho_v * f_{yv} \quad (6.1)$$

Where

$A_v$  is the area of the shear (transverse) reinforcement (or stirrups);

$f_{yv}$  is the yield tensile stress of stirrups;

$b_w$  is the web width;

$S_L$  is the spacing of the transverse reinforcement along the member length; and

$\rho_v$  is the shear reinforcement ratio ( $A_v/b_w.S_L$ ).

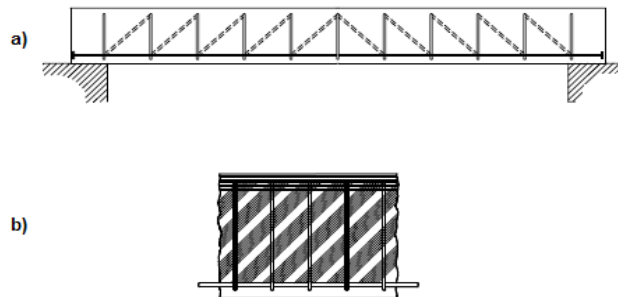


**Figure 6.1:** a) Ritter's Truss Model, and b) Morsch's Truss Analogy.

The studies, on the shear behaviour of wide RC beams, investigated by Leonhardt and Walther (1964); Anderson and Ramirez (1989); and Lubell et al. (2009a) have shown that locating the stirrups solely around the perimeter of the beam core is not efficient in beams under high shear demand. This means that in a wide beam with stirrups around the perimeter, the diagonal compressive stresses in the web tend to be supported by the longitudinal bars in the corners, as shown in Figure 6.2a. When viewed as a truss, the internal diagonal compressive struts need to be equilibrated at the internal truss joints. This requires a vertical stirrup leg in close proximity to an internal longitudinal bar used to resist flexure. Therefore, the situation is improved if there are more than two stirrup legs. Accordingly, it is important to consider the effect of stirrup legs spacing across the width of wide beams when estimating the ultimate shear strength of a wide RC member. It is also essential to evaluate the effect of well-distributed flexural reinforcement on the both ultimate flexural and shear strengths of a wide RC beam.



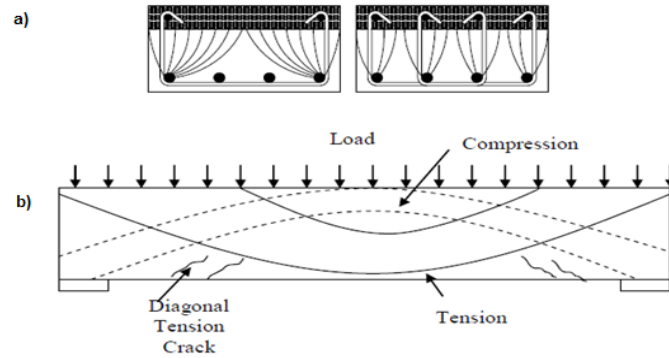


**Figure 6.2:** a) Flow of the Diagonal Compressive Force in Wide Beam Cross-Sections, and b) Distribution of Principal Stresses.

Transverse stress (Figure 6.2b) is an important parameter to be determined in wide beam design. This is to ensure that the transverse (shear) reinforcement in the form of shear link arrangement can take the transverse stresses. From the finite element analysis modelling, it is indicated that transverse tensile stresses are present at the top of wide beam especially at the point near to the concentrated loading (Teck FU, 2009). This failure often results in longitudinal splitting of concrete at the top surface of the crosshead. The direction of failure is parallel to the span of wide beam. The bearings, which rest on the wide beam, cause additional stress on the beam which in turn produces the transverse tensile stress. The location of the bearings relative to the wide beam makes it very likely to cause transverse tensile stress when loading is applied (Engineering Investigation, 2005).

Ultimate shear strength of concrete members ( $V_u$ ) consists of two terms of capacities as applied in most current Codes of Practice. The first capacity is the shear strength resisted by concrete ( $V_c$ ), while the other one is the shear strength resisted by stirrups ( $V_s$ ). The shear strength resisted by concrete ( $V_c$ ) of a beam with stirrups is equal to the ultimate shear strength ( $V_u$ ) of a beam without stirrups for the same characteristics.

### 6.3 A Proposed Prediction Model

The proposed prediction model shall be developed to predict the wide RC beam strengths with improved accuracy taking into the consideration logical influence factors unconsidered in the design provisions of most of the current Codes of Practice which have real effect on the shear and flexural strengths of wide beams.

Using the general method of shear design, the truss analogy forms the basis of most design methods for shear. Traditionally the shear resistance is assumed to be given by  $V_u = V_c + V_s$ , where  $V_c$  is the shear resisted by a beam without stirrups (or the concrete contribution) and  $V_s$  is the shear resisted by stirrups (stirrups contribution) calculated using a truss system with struts inclined at  $45^\circ$ . The concrete term “ $V_c$ ” was introduced to improve the correlation between test results and strengths predicted with Mörsh’s truss (Figure 6.1b). This term is estimated using empirical rules first appended in Codes.

As a result, most design Code provisions use empirical models developed based on simplified rules of mechanics and/or regression analyses of experimental data. The number of experimental observations used then for developing such models was often limited especially for narrow concrete members (i.e. drop beams). These deterministic models exhibit uncertain biases and errors that prevent accurate predictions over a wide range of input parameter values. This uncertainty may be due to imperfect descriptions of shear transfer mechanism, missing parameters, and insufficient amount of the test data.

The proposed prediction model, which will be adopted in this study, shall be developed based on logical parameters for practical uses, and is validated using previous experimental data. The model is developed to be used to predict the shear and flexural strengths of wide RC beams, and based on existing shear strength models and roles of various parameters on shear strengths and experimental observations.

In some countries, it is common practice to use wide beams in building work, like Saudi Arabia and the Middle-East Countries. This kind of beam has two special features that influence the wide RC beam strengths, which are: 1) support and load widths (or at best, the ratios of support- and load- width to beam-width) and 2) longitudinal and transversal spacing of stirrup legs. Although some researchers have studied these effects before, however, Codes are still not considering them in their design and prediction provisions on the flexural and shear strengths of wide concrete beams.

Hsiung and Frantz (1985) tested several beams with different width/depth ratios, and considered that there was no influence of transversal spacing of stirrup legs on shear strength. However, Anderson and Ramirez (1989) found in their experimental work that shear strength depends on transversal spacing of stirrup legs, and explained the Hsiung-and-Frantz’s results because of the low level of shear stresses in their tests. In addition, they concluded that transversal spacing of

stirrup legs is important for high level of shear stresses (which often occur in the interim region between the interior stirrups, especially for narrow-supported width wide beams), as Leonhardt and Walther (1964) reported before them. Leonhardt and Walther (1964) recommended a distance between two consecutive stirrup legs less than 200mm for high shear stresses ( $v > 1.59\sqrt{f_c}$ , N and mm Units) and 400mm otherwise. Moreover in contrast with Hsiung and Frantz (1985), recent published researches (Lubell et al., 2009a; Lubell, 2006; Serna-Ros et al., 2002; Zheng, 1989) showed that the shear capacity of wide RC beams decreases as the transverse stirrup-legs spacing across the member width increases.

Al.Dywany (2010), Leonhardt and Walther (1964) and Regan and Rezai-Jorabi (1989) studied the possible decrease in the shear resistance with changing in the bearing-plate (support and load) width, and showed, from their experimental tests, that the bearing plate width has little influence. Contrary, Lubell et al. (2009a, 2008) and Serna-Ros et al. (2002) concluded that the bearing plate width has influence on the shear strength of wide RC beams, where the shear strength decreases as the width of bearing plates reduced.

From the previous experiments, a clear influence of the arrangement of longitudinal and transversal spacing of stirrup legs, and the support and load widths on the wide RC beam strengths is found.

As wide concrete members have a width-to-height ( $b_w/h$ ) ratio is larger than 1.0 (typically, equals to 2.0) comparing with narrow concrete members which have the same ratio is lesser than 1.0; therefore, these wide members should have transverse stirrup legs to be distributed across their widths to resist the transverse shear stresses. Accordingly, it was concluded that the transverse spacing of the stirrup legs has an effect on the behaviour of wide concrete members. Consequently, the transverse stirrup-legs spacing should be taken into the consideration to predict the shear strength of wide RC beams, especially for the shear strength provided by stirrups (Alluqmani, 2013a, 2013b).

According to previous researches conducted on wide concrete members, the longitudinal and transverse stirrup-legs spacing and the support and load (bearing plate) widths have a significant influence on the behaviour of wide concrete beams. Current Codes of Practice do not provide these factors in their design provisions. Therefore, it is necessary to develop a prediction model based on the conclusions made early and on a well understanding of the influence of the stirrup legs spacing and the bearing plate widths on the strengths of wide concrete beams.

Based on the results of previous researches conducted on wide RC beams which were reviewed in the literature (Chapter 3), and based on Tables 4.3 to 4.10, and based on Table 6.1, Figures 6.3 to 6.12 show the real effect of the flexural -tensile and -compressive reinforcement ratios ( $\rho_s$  and  $\rho_s'$ ) and the ratios of support and load widths to the beam-width ( $k_s$ ,  $k_p$  and  $k$ ) on the shear strength resisted by concrete ( $V_c$ ) and on the ultimate flexural strength ( $M_u$ ), where  $k$  is the lesser of  $k_s$  or  $k_p$ ; while Figures 6.13 to 6.15 show the real effect of the ratios of longitudinal- and transverse- spacing of stirrups-legs ( $S_L/d$  and  $S_w/d$ ) and the ratio of support-width to beam-width ( $k_s$ ) on the shear strength resisted by stirrups ( $V_s$ ). Thus, it can be concluded that  $\rho_s$ ,  $\rho_s'$ ,  $k_s$ ,  $k_p$  and  $k$  have a significant influence on the shear strength of wide RC beams without stirrups (or the shear strength resisted by concrete,  $V_c$ ) and the ultimate flexural strength ( $M_u$ ); while that  $S_L$ ,  $S_w$  and  $k_s$  have a significant influence on the shear strength, of wide RC beams, resisted by stirrups (or stirrups contribution to the shear strength,  $V_s$ ) (Alluqmani, 2013a, 2013b).

**Table 6.1:** Details and Summary of the Test Results of Wide RC Beams Previously Tested.

Beams	bw	h	d	$\rho_s$	$\rho_s'$	$S_L$	$S_L/d$	$S_w$	$S_w/d$	bp	kp	bs	ks	k	$V_{c,ex}$	$V_{s,ex}$	$V_{u,ex}$	$M_{u,ex}$
-	mm	mm	mm	%	%	mm	-	mm	-	mm	-	mm	-	-	kN	kN	kN	kN.m
<b>Reference: Serna-Ros et al (2002)</b>																		
R0	750	250	206	2.20	0.94	-	-	-	-	750	1.00	750	1.00	1.00	244	-	244	-
R1	750	250	206	2.20	0.94	170	0.82	690	3.35	750	1.00	750	1.00	1.00	244	22	266	-
A0	750	250	206	2.20	0.94	-	-	-	-	750	1.00	750	1.00	1.00	187	-	187	-
A1	750	250	206	2.20	0.94	170	0.82	230	1.12	750	1.00	750	1.00	1.00	187	78	265	-
A2	750	250	206	2.20	0.94	170	0.82	690	3.35	750	1.00	750	1.00	1.00	187	47	234	-
A3	750	250	206	2.20	0.94	170	0.82	230	1.12	750	1.00	750	1.00	1.00	187	95	282	-
C0	750	250	206	2.20	0.94	-	-	-	-	750	1.00	750	1.00	1.00	182	-	182	-
C1	750	250	206	2.20	0.94	170	0.82	690	3.35	750	1.00	750	1.00	1.00	182	76	258	-
C2	750	250	206	2.20	0.94	170	0.82	230	1.12	750	1.00	750	1.00	1.00	182	109	291	-
C3	750	250	206	2.20	0.94	170	0.82	115	0.56	750	1.00	750	1.00	1.00	182	176	358	-
C4	750	250	206	2.20	0.94	127.5	0.62	138	0.67	750	1.00	750	1.00	1.00	182	178	360	-
C5	750	250	206	2.20	0.94	85	0.41	230	1.12	750	1.00	750	1.00	1.00	182	161	343	-
D0	750	250	206	2.20	0.94	-	-	-	-	750	1.00	300	0.40	0.40	218	-	218	-
D1	750	250	206	2.20	0.94	170	0.82	690	3.35	750	1.00	300	0.40	0.40	218	48	266	-
D2	750	250	206	2.20	0.94	170	0.82	230	1.12	750	1.00	300	0.40	0.40	218	78	296	-
D3	750	250	206	2.20	0.94	170	0.82	115	0.56	750	1.00	300	0.40	0.40	218	102	320	-
D5	750	250	206	2.20	0.94	85	0.41	230	1.12	750	1.00	300	0.40	0.40	218	127	345	-
<b>Reference: Shuraim (2012)</b>																		
S0	700	180	150	1.34	1.026	-	-	-	-	700	1.00	700	1.00	1.00	161	-	161	-
S1-80	700	180	150	1.34	1.026	80	0.53	660	4.40	700	1.00	700	1.00	1.00	161	60	221	-
S2-80	700	180	150	1.34	1.026	80	0.53	440	2.93	700	1.00	700	1.00	1.00	161	61	222	-
S3-80	700	180	150	1.34	1.026	80	0.53	230	1.53	700	1.00	700	1.00	1.00	161	71	232	-
S0-1	700	180	150	1.34	1.026	-	-	-	-	700	1.00	700	1.00	1.00	162	-	162	-
S1-75-1A	700	180	150	1.34	1.026	75	0.50	660	4.40	700	1.00	700	1.00	1.00	162	0	162	-
S3-75-1	700	180	150	1.34	1.026	75	0.50	230	1.53	700	1.00	700	1.00	1.00	162	58	220	-
S13-75-1A	700	180	150	1.34	1.026	75	0.50	230	1.53	700	1.00	700	1.00	1.00	162	112	274	-
S13-100-1	700	180	150	1.34	1.026	100	0.67	230	1.53	700	1.00	700	1.00	1.00	162	106	268	-
S13-125-1	700	180	150	1.34	1.026	125	0.83	230	1.53	700	1.00	700	1.00	1.00	162	79	241	-
S0-2	700	180	150	1.34	1.026	-	-	-	-	700	1.00	700	1.00	1.00	160	-	160	-
S1-75-2	700	180	150	1.34	1.026	75	0.50	660	4.40	700	1.00	700	1.00	1.00	160	81	241	-
S3-75-2	700	180	150	1.34	1.026	75	0.50	230	1.53	700	1.00	700	1.00	1.00	160	81	241	-

Beams	bw	h	d	$\rho_s$	$\rho_s'$	$S_L$	$S_L/d$	$S_w$	$S_w/d$	bp	kp	bs	ks	k	$V_{c,ex}$	$V_{s,ex}$	$V_{u,ex}$	$M_{u,ex}$
-	mm	mm	mm	%	%	mm	-	mm	-	mm	-	mm	-	-	kN	kN	kN	kN.m
S13-75-2	700	180	150	1.34	1.026	75	0.50	230	1.53	700	1.00	700	1.00	1.00	160	146	306	-
S13-100-2	700	180	150	1.34	1.026	100	0.67	230	1.53	700	1.00	700	1.00	1.00	160	118	278	-
S13-125-2	700	180	150	1.34	1.026	125	0.83	230	1.53	700	1.00	700	1.00	1.00	160	81	241	-
<b>Reference: Hanafy et al (2012)</b>																		
NB1	500	250	210	4.61	0.65	-	-	-	-	500	1.00	500	1.00	1.00	245	-	245	-
NB2	500	250	210	4.61	0.65	200	0.95	110	0.52	500	1.00	500	1.00	1.00	245	105	350	-
NB3	500	250	210	4.61	0.65	200	0.95	110	0.52	500	1.00	500	1.00	1.00	245	55	300	-
NB4	500	250	210	4.61	0.65	135	0.64	110	0.52	500	1.00	500	1.00	1.00	245	61	306	-
NB5	500	250	210	4.61	0.65	200	0.95	110	0.52	500	1.00	500	1.00	1.00	245	250	495	-
NB6	500	250	210	4.61	0.65	135	0.64	110	0.52	500	1.00	500	1.00	1.00	245	305	550	-
HB1	500	250	210	4.61	0.65	-	-	-	-	500	1.00	500	1.00	1.00	295	-	295	-
HB2	500	250	210	4.61	0.65	200	0.95	110	0.52	500	1.00	500	1.00	1.00	295	103	398	-
HB3	500	250	210	4.61	0.65	200	0.95	110	0.52	500	1.00	500	1.00	1.00	295	45	340	-
HB4	500	250	210	4.61	0.65	135	0.64	110	0.52	500	1.00	500	1.00	1.00	295	55	350	-
HB5	500	250	210	4.61	0.65	200	0.95	110	0.52	500	1.00	500	1.00	1.00	295	300	595	-
HB6	500	250	210	4.61	0.65	135	0.64	110	0.52	500	1.00	500	1.00	1.00	295	315	610	-
<b>Reference: AlDywanly (2010)</b>																		
A1	750	250	210	1.29	0.0	-	-	-	-	750	1.00	750	1.00	1.00	179	-	179	-
A1/2	750	250	210	1.29	0.0	-	-	-	-	750	1.00	375	0.50	0.50	188	-	188	-
A1/4	750	250	210	1.29	0.0	-	-	-	-	750	1.00	190	0.25	0.25	178	-	178	-
RA1/2	750	250	210	1.29	0.0	-	-	-	-	750	1.00	375	0.50	0.50	194	-	194	-
RA1/4	750	250	210	1.29	0.0	-	-	-	-	750	1.00	190	0.25	0.25	191	-	191	-
B1	750	250	210	1.29	0.036	110	0.52	160	0.76	750	1.00	750	1.00	1.00	-	-	241	-
B1/2	750	250	210	1.29	0.036	110	0.52	160	0.76	750	1.00	375	0.50	0.50	-	-	195	-
B1/4	750	250	210	1.29	0.036	110	0.52	130	0.62	750	1.00	190	0.25	0.25	-	-	198	-
RB1/2	750	250	210	1.29	0.036	110	0.52	135	0.64	750	1.00	375	0.50	0.50	-	-	251	-
RB1/4	750	250	210	1.29	0.036	110	0.52	135	0.64	750	1.00	190	0.25	0.25	-	-	237	-
<b>Reference: Lubell et al (2008, 2009)</b>																		
AX8	700	340	286	1.75	0.0	-	-	-	-	152	0.22	152	0.22	0.22	272	-	272	-
AX7	700	340	286	0.89	0.0	-	-	-	-	700	1.00	700	1.00	1.00	249	-	249	-
AX6	700	340	286	1.75	0.0	-	-	-	-	700	1.00	700	1.00	1.00	281	-	281	-
AX1	700	340	286	1.75	0.20	175	0.61	625	2.18	700	1.00	700	1.00	1.00	-	-	458	-
AX2	700	340	286	1.75	0.20	175	0.61	625	2.18	700	1.00	700	1.00	1.00	-	-	338	-

Beams	bw	h	d	$\rho_s$	$\rho_s'$	$S_L$	$S_L/d$	$S_w$	$S_w/d$	bp	kp	bs	ks	k	$V_{c,ex}$	$V_{s,ex}$	$V_{u,ex}$	$M_{u,ex}$
-	mm	mm	mm	%	%	mm	-	mm	-	mm	-	mm	-	-	kN	kN	kN	kN.m
AX3	700	340	286	1.75	0.30	175	0.61	350	1.22	700	1.00	700	1.00	1.00	-	-	450	-
AX4	700	340	286	1.75	0.40	175	0.61	235	0.82	700	1.00	700	1.00	1.00	-	-	415	-
AX5	700	340	286	1.75	0.40	175	0.61	470	1.64	700	1.00	700	1.00	1.00	-	-	359	-
AW8	1170	585	509	1.68	0.0	-	-	-	-	1170	1.00	1170	1.00	1.00	789	-	789	-
AW6	1170	585	509	1.68	0.07	300	0.59	1080	2.12	1170	1.00	1170	1.00	1.00	-	-	826	-
AW7	1170	585	509	1.68	0.14	300	0.59	370	0.73	1170	1.00	1170	1.00	1.00	-	-	1062	-
AW1	1170	585	538	0.79	0.0	-	-	-	-	305	0.26	305	0.26	0.26	585	-	585	-
AW4	1170	585	509	1.68	0.0	-	-	-	-	305	0.26	305	0.26	0.26	716	-	716	-
AW2	1170	585	509	1.68	0.07	300	0.59	1080	2.12	305	0.26	305	0.26	0.26	-	-	809	-
AW3	1170	585	509	1.68	0.07	300	0.59	800	1.57	305	0.26	305	0.26	0.26	-	-	828	-
AW5	1170	585	509	1.68	0.14	300	0.59	375	0.74	305	0.26	305	0.26	0.26	-	-	953	-
Reference: McAllister (2011)																		
B1 (ACI)	703	339	295	0.76	0.075	134	0.45	600	2.03	703	1.00	703	1.00	1.00	-	-	285	-
B2 (EC2)	703	339	295	1.65	0.075	184	0.62	600	2.03	703	1.00	703	1.00	1.00	-	-	330	-
Reference: Author's Series (A) [Chapter 5]																		
ECC2	708	353	304	1.82	0.221	180	0.59	300	0.99	350	0.50	240	0.34	0.34	-	-	492	-
ECC3	708	353	304	1.82	0.221	180	0.59	122	0.40	350	0.50	240	0.34	0.34	-	-	-	700
Reference: Al-Harithy (2002)																		
B1-25	800	200	165	3.81	1.93	82	0.50	370	2.24	800	1.00	800	1.00	1.00	-	-	-	311
B1-65	800	200	165	3.81	1.93	82	0.50	370	2.24	800	1.00	800	1.00	1.00	-	-	-	351
B1-95	800	200	165	3.81	1.93	82	0.50	370	2.24	800	1.00	800	1.00	1.00	-	-	-	348
B2-25	800	200	165	2.62	1.35	82	0.50	370	2.24	800	1.00	800	1.00	1.00	-	-	-	215
B2-65	800	200	165	2.62	1.35	82	0.50	370	2.24	800	1.00	800	1.00	1.00	-	-	-	253
B2-95	800	200	165	2.62	1.35	82	0.50	370	2.24	800	1.00	800	1.00	1.00	-	-	-	263
B3-25	800	200	165	1.90	0.96	82	0.50	370	2.24	800	1.00	800	1.00	1.00	-	-	-	176
B3-65	800	200	165	1.90	0.96	82	0.50	370	2.24	800	1.00	800	1.00	1.00	-	-	-	195
B3-95	800	200	165	1.90	0.96	82	0.50	370	2.24	800	1.00	800	1.00	1.00	-	-	-	211
B4-25	800	200	165	0.70	0.35	82	0.50	370	2.24	800	1.00	800	1.00	1.00	-	-	-	64
B4-65	800	200	165	0.70	0.35	82	0.50	370	2.24	800	1.00	800	1.00	1.00	-	-	-	74
B4-95	800	200	165	0.70	0.35	82	0.50	370	2.24	800	1.00	800	1.00	1.00	-	-	-	73

1 mm = 0.0394 in, 1 kN = 1000 N = 0.225 kip, 1 MPa = 145 psi, 1 kN.m = 0.738 kip.ft = 8.858 kip.in.

$k_p = b_p/b_w$ ,  $k_s = b_s/b_w$ , and  $k =$  the lesser of ( $k_p$  or  $k_s$ ).

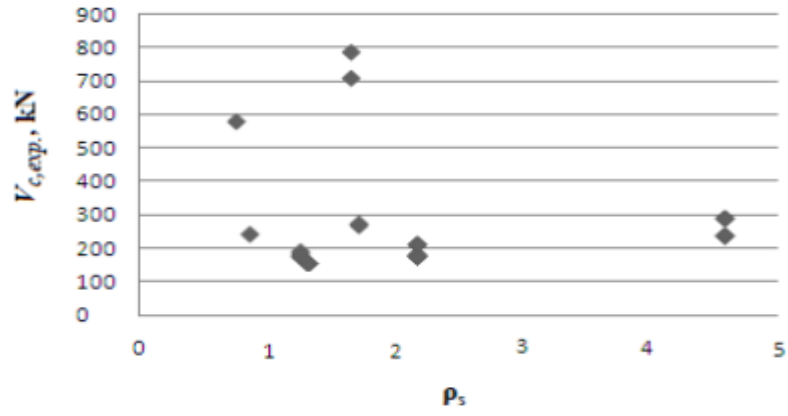


Figure 6.3:  $V_{c,exp.}$  versus  $\rho_s$ .

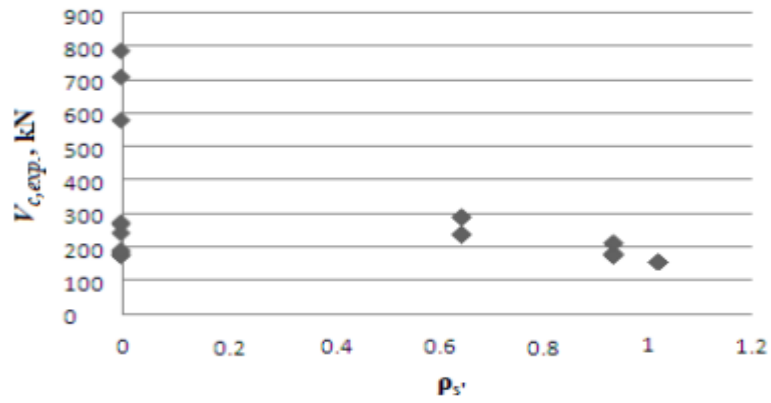


Figure 6.4:  $V_{c,exp.}$  versus  $\rho_s'$ .

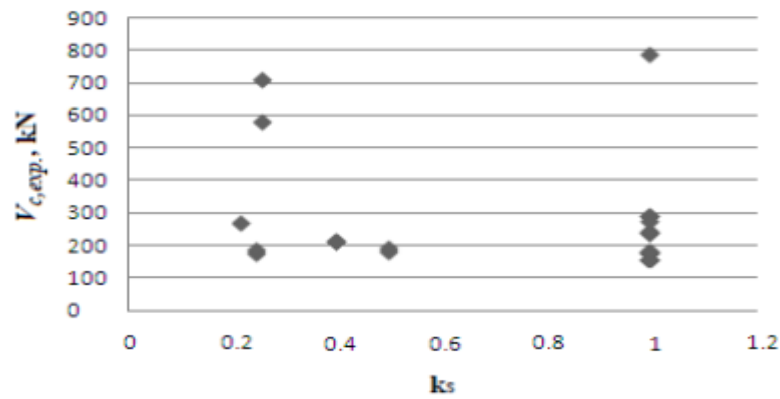


Figure 6.5:  $V_{c,exp.}$  versus  $k_s$ .

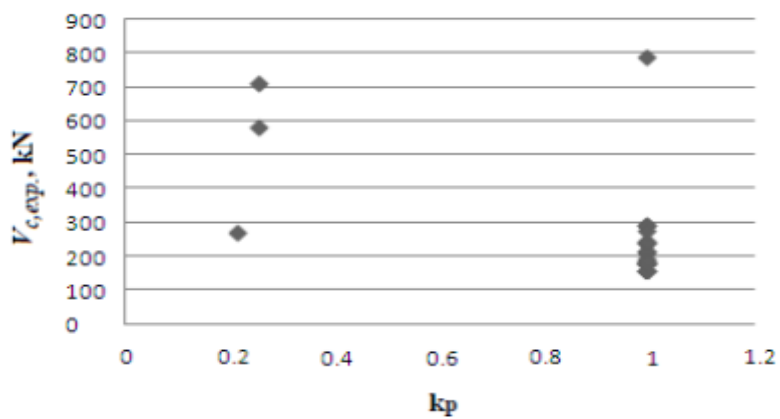


Figure 6.6:  $V_{c,exp.}$  versus  $k_p$ .



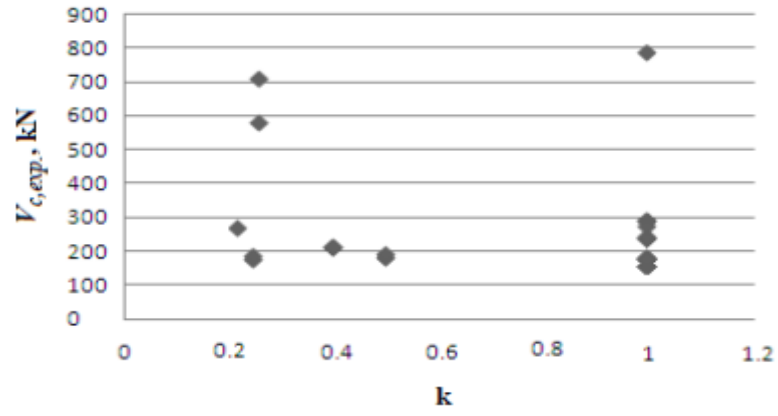


Figure 6.7:  $V_{c,exp.}$  versus  $k$ .

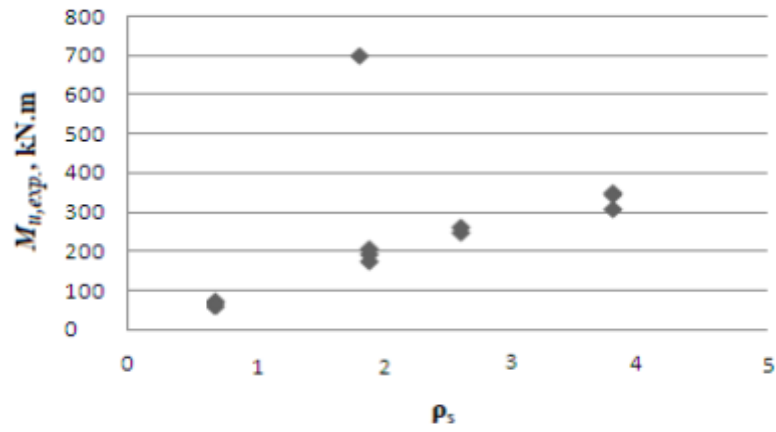


Figure 6.8:  $M_{u,exp.}$  versus  $\rho_s$ .

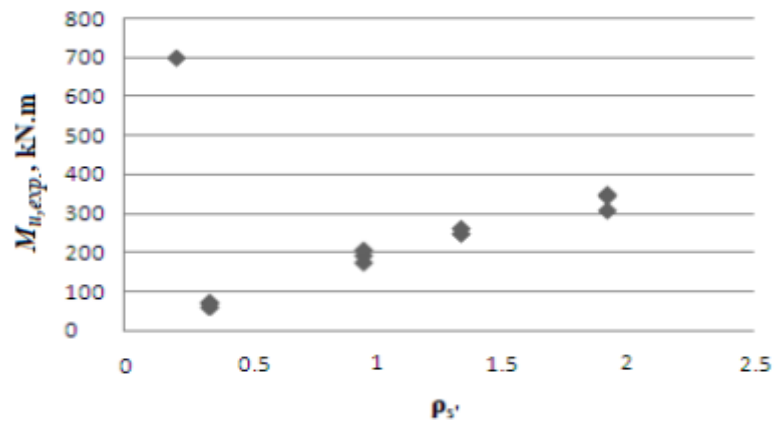


Figure 6.9:  $M_{u,exp.}$  versus  $\rho_{s'}$ .

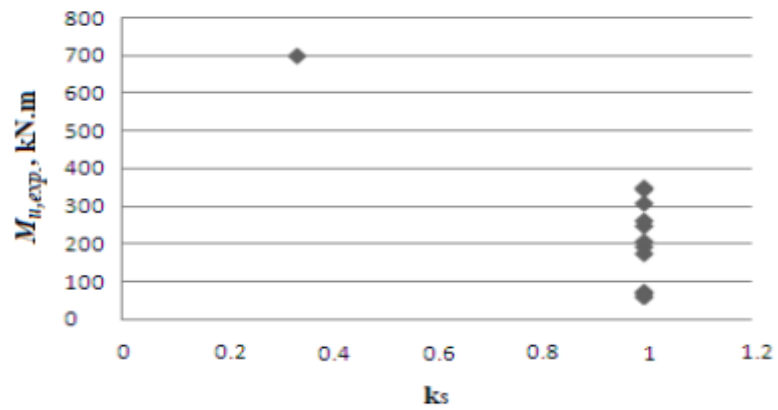


Figure 6.10:  $M_{u,exp.}$  versus  $k_s$ .

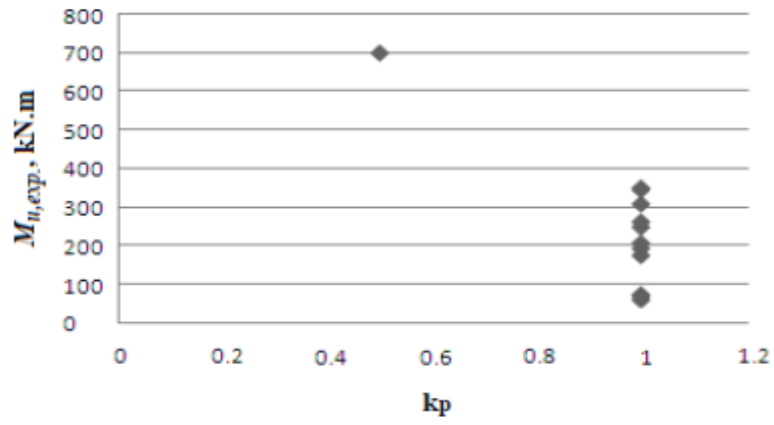


Figure 6.11:  $M_{u,exp.}$  versus  $k_p$ .

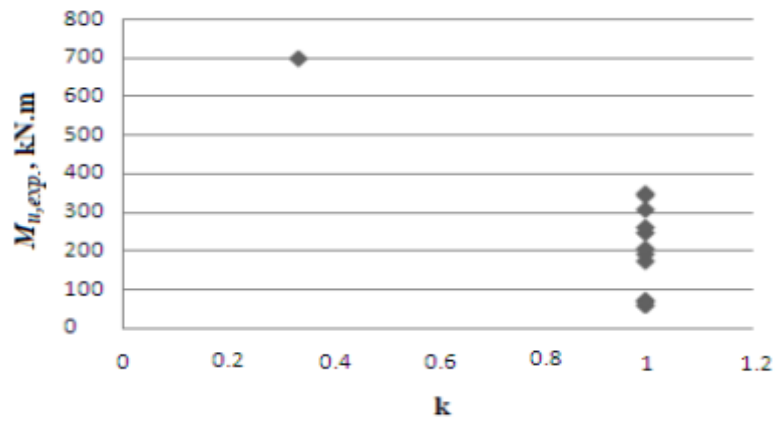


Figure 6.12:  $M_{u,exp.}$  versus  $k$ .

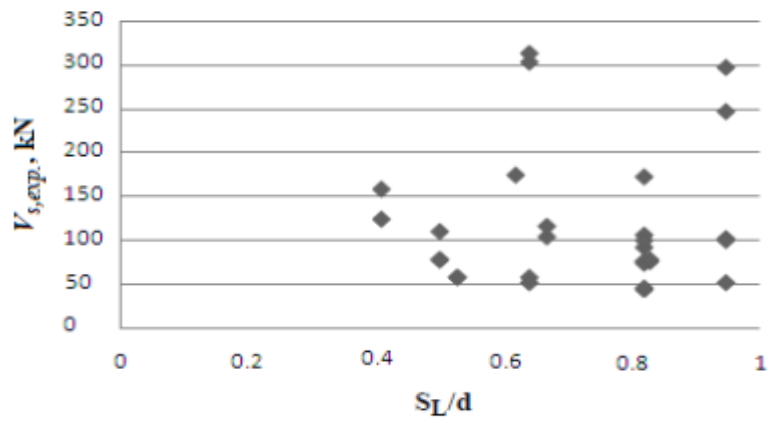


Figure 6.13:  $V_{s,exp.}$  versus  $S_L/d$ .

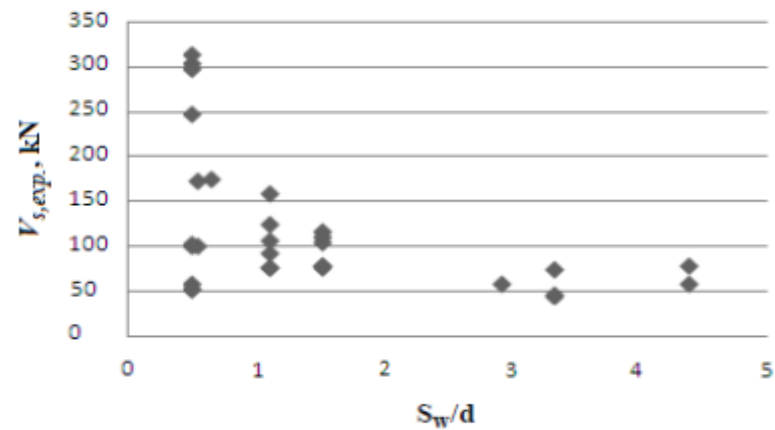
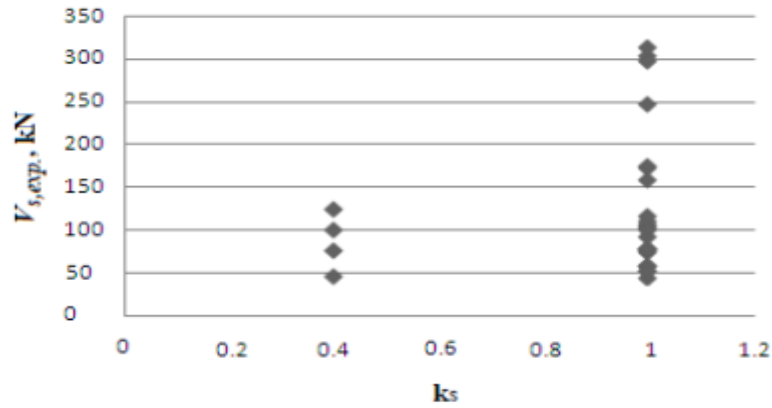


Figure 6.14:  $V_{s,exp.}$  versus  $S_W/d$ .



**Figure 6.15:**  $V_{s,exp.}$  versus  $k_s$ .

The new parameters obtained from Figures 6.3 to 6.15 to be proposed for developing a new prediction model were concluded in Table 6.2 and are summarised as follows:

1. Based on Figures 6.3 and 6.4 (for  $V_c$ ) and Figures 6.8 and 6.9 (for  $M_u$ ), the effect of the absolute value of  $\rho_s$  minus  $\rho_{s'}$  (i.e.  $|\rho_s - \rho_{s'}|$ ) on  $V_c$  and  $M_u$  strengths has been noted, taken into the consideration, and represented as shown in Figures 6.16 and 6.17, respectively. Referring to Figures 6.16 and 6.17,  $|\rho_s - \rho_{s'}|$  must be corrected by F-factor based on the values of  $|\rho_s - \rho_{s'}|$  and  $k_s$ .
2. Based on Figures 6.5, 6.6 and 6.7 (for  $V_c$ ) and Figures 6.10, 6.11 and 6.12 (for  $M_u$ ), the effect of the minimum ratio of the support- or load- width to the beam-width ( $k$ ) when is raised to the  $h/b_w$  power on  $V_c$  and  $M_u$  strengths has been noted, taken into the consideration, and represented as shown in Figures 6.18 and 6.19, respectively. Referring to Figures 6.18 and 6.19,  $k^{(h/b_w)}$  must be treated by the square-root.
3. Based on Figures 6.13 and 6.14, the effect of the ratio of longitudinal to transverse stirrup-legs spacing ( $S_L/S_w$ ) on  $V_s$  strength has been noted, taken into the consideration, and represented as shown in Figure 6.20. Referring to Figure 6.20,  $S_L/S_w$  must be treated by the square-root.
4. Based on Figure 6.15, the effect of the support-width to the beam-width ratio ( $k_s$ ) when is raised to the  $1-k_s$  power on  $V_s$  strength has been noted, taken into the consideration, and represented as shown in Figure 6.21. Referring to Figure 6.21,  $k_s^{(1-k_s)}$  must be treated by the square-root.

**Table 6.2:** Details and Summary of the Test Results of Wide RC Beams Previously Tested Based on New Parameters to the Proposed Prediction-Model.

Beams	$\rho_s$	$\rho_s'$	$ \rho_s - \rho_s' $	$S_L$	$S_W$	$S_L/S_W$	$k_p$	$k_s$	$k_s^{(1-k_s)}$	$k$	$k^{(b/b_w)}$	$F$	Test Strengths, kN - m				ACI318 & SBC304			EC2 Code		
	%	%	%	mm	mm	-	-	-	-	-	-	-	$V_{c,ex}$	$V_{s,ex}$	$V_{u,ex}$	$M_{u,ex}$	$V_c$	$V_s$	$M_u$	$V_c$	$V_s$	$M_u$
Reference: Serna-Ros et al (2002)																						
R0	2.20	0.94	1.26	-	-	-	1.00	1.00	1.00	1.00	1.00	100	244	-	244	-	139	-	-	173	-	-
R1	2.20	0.94	1.26	170	690	0.25	1.00	1.00	1.00	1.00	1.00	100	244	22	266	-	139	87	-	173	79	-
A0	2.20	0.94	1.26	-	-	-	1.00	1.00	1.00	1.00	1.00	100	187	-	187	-	128	-	-	147	-	-
A1	2.20	0.94	1.26	170	230	0.74	1.00	1.00	1.00	1.00	1.00	100	187	78	265	-	128	92	-	147	82	-
A2	2.20	0.94	1.26	170	690	0.25	1.00	1.00	1.00	1.00	1.00	100	187	47	234	-	128	97	-	147	88	-
A3	2.20	0.94	1.26	170	230	0.74	1.00	1.00	1.00	1.00	1.00	100	187	95	282	-	128	113	-	147	102	-
C0	2.20	0.94	1.26	-	-	-	1.00	1.00	1.00	1.00	1.00	100	182	-	182	-	130	-	-	151	-	-
C1	2.20	0.94	1.26	170	690	0.25	1.00	1.00	1.00	1.00	1.00	100	182	76	258	-	130	122	-	151	110	-
C2	2.20	0.94	1.26	170	230	0.74	1.00	1.00	1.00	1.00	1.00	100	182	109	291	-	130	109	-	151	98	-
C3	2.20	0.94	1.26	170	115	1.48	1.00	1.00	1.00	1.00	1.00	100	182	176	358	-	130	123	-	151	111	-
C4	2.20	0.94	1.26	127.5	138	0.92	1.00	1.00	1.00	1.00	1.00	100	182	178	360	-	130	164	-	151	147	-
C5	2.20	0.94	1.26	85	230	0.37	1.00	1.00	1.00	1.00	1.00	100	182	161	343	-	130	246	-	151	221	-
D0	2.20	0.94	1.26	-	-	-	1.00	0.40	0.58	0.40	0.74	120	218	-	218	-	148	-	-	171	-	-
D1	2.20	0.94	1.26	170	690	0.25	1.00	0.40	0.58	0.40	0.74	120	218	48	266	-	148	121	-	171	108	-
D2	2.20	0.94	1.26	170	230	0.74	1.00	0.40	0.58	0.40	0.74	120	218	78	296	-	148	105	-	171	94	-
D3	2.20	0.94	1.26	170	115	1.48	1.00	0.40	0.58	0.40	0.74	120	218	102	320	-	148	118	-	171	106	-
D5	2.20	0.94	1.26	85	230	0.37	1.00	0.40	0.58	0.40	0.74	120	218	127	345	-	148	237	-	171	213	-
Reference: Shuraim (2012)																						
S0	1.34	1.026	0.314	-	-	-	1.00	1.00	1.00	1.00	1.00	389	161	-	161	-	94	-	-	124	-	-
S1-80	1.34	1.026	0.314	80	660	0.12	1.00	1.00	1.00	1.00	1.00	389	161	60	221	-	94	142	-	124	128	-
S2-80	1.34	1.026	0.314	80	440	0.18	1.00	1.00	1.00	1.00	1.00	389	161	61	222	-	94	142	-	124	128	-
S3-80	1.34	1.026	0.314	80	230	0.35	1.00	1.00	1.00	1.00	1.00	389	161	71	232	-	94	142	-	124	128	-
S0-1	1.34	1.026	0.314	-	-	-	1.00	1.00	1.00	1.00	1.00	389	162	-	162	-	94	-	-	124	-	-
S1-75-1A	1.34	1.026	0.314	75	660	0.11	1.00	1.00	1.00	1.00	1.00	389	162	0	162	-	94	188	-	124	169	-
S3-75-1	1.34	1.026	0.314	75	230	0.33	1.00	1.00	1.00	1.00	1.00	389	162	58	220	-	94	144	-	124	130	-
S13-75-1A	1.34	1.026	0.314	75	230	0.33	1.00	1.00	1.00	1.00	1.00	389	162	112	274	-	94	188	-	124	169	-
S13-100-1	1.34	1.026	0.314	100	230	0.43	1.00	1.00	1.00	1.00	1.00	389	162	106	268	-	94	143	-	124	129	-
S13-125-1	1.34	1.026	0.314	125	230	0.54	1.00	1.00	1.00	1.00	1.00	389	162	79	241	-	94	110	-	124	99	-
S0-2	1.34	1.026	0.314	-	-	-	1.00	1.00	1.00	1.00	1.00	389	160	-	160	-	94	-	-	124	-	-
S1-75-2	1.34	1.026	0.314	75	660	0.11	1.00	1.00	1.00	1.00	1.00	389	160	81	241	-	94	188	-	124	169	-
S3-75-2	1.34	1.026	0.314	75	230	0.33	1.00	1.00	1.00	1.00	1.00	389	160	81	241	-	94	144	-	124	130	-

Beams	$\rho_s$	$\rho_s'$	$ \rho_s - \rho_s' $	$S_L$	$S_w$	$S_L/S_w$	$k_p$	$k_s$	$k_s^{(1-k_s)}$	$k$	$k^{(1/bw)}$	$F$	Test Strengths, kN - m				ACI318 & SBC304			EC2 Code		
	%	%	%	mm	mm	-	-	-	-	-	-	-	$V_{c,ex}$	$V_{s,ex}$	$V_{u,ex}$	$M_{u,ex}$	$V_c$	$V_s$	$M_u$	$V_c$	$V_s$	$M_u$
S13-75-2	1.34	1.026	0.314	75	230	0.33	1.00	1.00	1.00	1.00	1.00	389	160	146	306	-	94	188	-	124	169	-
S13-100-2	1.34	1.026	0.314	100	230	0.43	1.00	1.00	1.00	1.00	1.00	389	160	118	278	-	94	143	-	124	129	-
S13-125-2	1.34	1.026	0.314	125	230	0.54	1.00	1.00	1.00	1.00	1.00	389	160	81	241	-	94	110	-	124	99	-
Reference: Hanafy et al (2012)																						
NB1	4.61	0.65	3.96	-	-	-	1.00	1.00	1.00	1.00	1.00	60	245	-	245	-	110	-	-	191	-	-
NB2	4.61	0.65	3.96	200	110	1.82	1.00	1.00	1.00	1.00	1.00	60	245	105	350	-	110	67	-	191	60	-
NB3	4.61	0.65	3.96	200	110	1.82	1.00	1.00	1.00	1.00	1.00	60	245	55	300	-	110	40	-	191	36	-
NB4	4.61	0.65	3.96	135	110	1.23	1.00	1.00	1.00	1.00	1.00	60	245	61	306	-	110	49	-	191	44	-
NB5	4.61	0.65	3.96	200	110	1.82	1.00	1.00	1.00	1.00	1.00	60	245	250	495	-	110	201	-	191	181	-
NB6	4.61	0.65	3.96	135	110	1.23	1.00	1.00	1.00	1.00	1.00	60	245	305	550	-	110	230	-	191	207	-
HB1	4.61	0.65	3.96	-	-	-	1.00	1.00	1.00	1.00	1.00	60	295	-	295	-	165	-	-	250	-	-
HB2	4.61	0.65	3.96	200	110	1.82	1.00	1.00	1.00	1.00	1.00	60	295	103	398	-	165	67	-	250	60	-
HB3	4.61	0.65	3.96	200	110	1.82	1.00	1.00	1.00	1.00	1.00	60	295	45	340	-	165	40	-	250	36	-
HB4	4.61	0.65	3.96	135	110	1.23	1.00	1.00	1.00	1.00	1.00	60	295	55	350	-	165	49	-	250	44	-
HB5	4.61	0.65	3.96	200	110	1.82	1.00	1.00	1.00	1.00	1.00	60	295	300	595	-	165	201	-	250	181	-
HB6	4.61	0.65	3.96	135	110	1.23	1.00	1.00	1.00	1.00	1.00	60	295	315	610	-	165	230	-	250	207	-
Reference: Al.Dywany (2010)																						
A1	1.29	0.0	1.29	-	-	-	1.00	1.00	1.00	1.00	1.00	100	179	-	179	-	166	-	-	168	-	-
A1/2	1.29	0.0	1.29	-	-	-	1.00	0.50	0.71	0.50	0.79	120	188	-	188	-	166	-	-	168	-	-
A1/4	1.29	0.0	1.29	-	-	-	1.00	0.25	0.35	0.25	0.63	120	178	-	178	-	166	-	-	168	-	-
RA1/2	1.29	0.0	1.29	-	-	-	1.00	0.50	0.71	0.50	0.79	120	194	-	194	-	166	-	-	168	-	-
RA1/4	1.29	0.0	1.29	-	-	-	1.00	0.25	0.35	0.25	0.63	120	191	-	191	-	166	-	-	168	-	-
B1	1.29	0.036	1.254	110	160	0.69	1.00	1.00	1.00	1.00	1.00	100	-	-	241	-	166	67	-	168	61	-
B1/2	1.29	0.036	1.254	110	160	0.69	1.00	0.50	0.71	0.50	0.79	120	-	-	195	-	166	67	-	168	61	-
B1/4	1.29	0.036	1.254	110	130	0.85	1.00	0.25	0.35	0.25	0.63	120	-	-	198	-	166	67	-	168	61	-
RB1/2	1.29	0.036	1.254	110	135	0.81	1.00	0.50	0.71	0.50	0.79	120	-	-	251	-	166	67	-	168	61	-
RB1/4	1.29	0.036	1.254	110	135	0.81	1.00	0.25	0.35	0.25	0.63	120	-	-	237	-	166	67	-	168	61	-
Reference: Lubell et al (2008, 2009)																						
AX8	1.75	0.0	1.75	-	-	-	0.22	0.22	0.31	0.22	0.48	120	272	-	272	-	200	-	-	237	-	-
AX7	0.89	0.0	0.89	-	-	-	1.00	1.00	1.00	1.00	1.00	140	249	-	249	-	200	-	-	189	-	-
AX6	1.75	0.0	1.75	-	-	-	1.00	1.00	1.00	1.00	1.00	60	281	-	281	-	217	-	-	250	-	-
AX1	1.75	0.20	1.55	175	625	0.28	1.00	1.00	1.00	1.00	1.00	100	-	-	458	-	217	105	-	250	95	-
AX2	1.75	0.20	1.55	175	625	0.28	1.00	1.00	1.00	1.00	1.00	100	-	-	338	-	200	101	-	237	91	-

Beams	$\rho_s$	$\rho_s'$	$ \rho_s - \rho_s' $	$S_L$	$S_W$	$S_L/S_W$	$k_p$	$k_s$	$k_s^{(1-k_s)}$	$k$	$k^{(b/bw)}$	$F$	Test Strengths, kN - m				ACI318 & SBC304			EC2 Code		
	%	%	%	mm	mm	-	-	-	-	-	-	-	$V_{c,ex}$	$V_{s,ex}$	$V_{u,ex}$	$M_{u,ex}$	$V_c$	$V_s$	$M_u$	$V_c$	$V_s$	$M_u$
AX3	1.75	0.30	1.45	175	350	0.50	1.00	1.00	1.00	1.00	1.00	100	-	-	450	-	217	119	-	250	107	-
AX4	1.75	0.40	1.35	175	235	0.74	1.00	1.00	1.00	1.00	1.00	100	-	-	415	-	217	109	-	250	98	-
AX5	1.75	0.40	1.35	175	470	0.37	1.00	1.00	1.00	1.00	1.00	100	-	-	359	-	217	105	-	250	95	-
AW8	1.68	0.0	1.68	-	-	-	1.00	1.00	1.00	1.00	1.00	60	789	-	789	-	648	-	-	653	-	-
AW6	1.68	0.07	1.61	300	1080	0.28	1.00	1.00	1.00	1.00	1.00	60	-	-	826	-	648	301	-	653	271	-
AW7	1.68	0.14	1.54	300	370	0.81	1.00	1.00	1.00	1.00	1.00	100	-	-	1062	-	580	215	-	606	194	-
AW1	0.79	0.0	0.79	-	-	-	0.26	0.26	0.37	0.26	0.51	170	585	-	585	-	625	-	-	500	-	-
AW4	1.68	0.0	1.68	-	-	-	0.26	0.26	0.37	0.26	0.51	120	716	-	716	-	580	-	-	606	-	-
AW2	1.68	0.07	1.61	300	1080	0.28	0.26	0.26	0.37	0.26	0.51	120	-	-	809	-	580	301	-	606	271	-
AW3	1.68	0.07	1.61	300	800	0.38	0.26	0.26	0.37	0.26	0.51	120	-	-	828	-	580	301	-	606	271	-
AW5	1.68	0.14	1.54	300	375	0.80	0.26	0.26	0.37	0.26	0.51	120	-	-	953	-	580	215	-	606	194	-
Reference: McAllister (2011)																						
B1 (ACI)	0.76	0.075	0.685	134	600	0.22	1.00	1.00	1.00	1.00	1.00	140	-	-	285	-	171	173	-	163	156	-
B2 (EC2)	1.65	0.075	1.575	184	600	0.31	1.00	1.00	1.00	1.00	1.00	100	-	-	330	-	171	125	-	210	113	-
Reference: Author's Series (A) [Chapter 5]																						
ECC2	1.82	0.221	1.60	180	300	0.60	0.50	0.34	0.49	0.34	0.58	120	-	-	492	-	240	174	-	274	156	-
ECC3	1.82	0.221	1.60	180	122	1.47	0.50	0.34	0.49	0.34	0.58	120	-	-	-	700	-	-	505	-	-	483
Reference: Al-Harithy (2002)																						
B1-25	3.81	1.93	1.88	82	370	0.22	1.00	1.00	1.00	1.00	1.00	60	-	-	-	311	-	-	257.1	-	-	257.1
B1-65	3.81	1.93	1.88	82	370	0.22	1.00	1.00	1.00	1.00	1.00	60	-	-	-	351	-	-	277.5	-	-	261.5
B1-95	3.81	1.93	1.88	82	370	0.22	1.00	1.00	1.00	1.00	1.00	60	-	-	-	348	-	-	277.5	-	-	267.9
B2-25	2.62	1.35	1.27	82	370	0.22	1.00	1.00	1.00	1.00	1.00	100	-	-	-	215	-	-	176.8	-	-	176.8
B2-65	2.62	1.35	1.27	82	370	0.22	1.00	1.00	1.00	1.00	1.00	100	-	-	-	253	-	-	190.8	-	-	179.8
B2-95	2.62	1.35	1.27	82	370	0.22	1.00	1.00	1.00	1.00	1.00	100	-	-	-	263	-	-	190.8	-	-	184.2
B3-25	1.90	0.96	0.94	82	370	0.22	1.00	1.00	1.00	1.00	1.00	140	-	-	-	176	-	-	128.2	-	-	128.2
B3-65	1.90	0.96	0.94	82	370	0.22	1.00	1.00	1.00	1.00	1.00	140	-	-	-	195	-	-	138.4	-	-	130.4
B3-95	1.90	0.96	0.94	82	370	0.22	1.00	1.00	1.00	1.00	1.00	140	-	-	-	211	-	-	138.4	-	-	133.6
B4-25	0.70	0.35	0.35	82	370	0.22	1.00	1.00	1.00	1.00	1.00	400	-	-	-	64	-	-	47.2	-	-	47.2
B4-65	0.70	0.35	0.35	82	370	0.22	1.00	1.00	1.00	1.00	1.00	400	-	-	-	74	-	-	51.0	-	-	48.0
B4-95	0.70	0.35	0.35	82	370	0.22	1.00	1.00	1.00	1.00	1.00	400	-	-	-	73	-	-	51.0	-	-	49.2

1 mm = 0.0394 in, 1 kN = 1000 N = 0.225 kip, 1 MPa = 145 psi, 1 kN.m = 0.738 kip.ft = 8.858 kip.in.

$k_p$  = bp/bw,  $k_s$  = bs/bw, and  $k$  = the lesser of ( $k_p$  or  $k_s$ ).

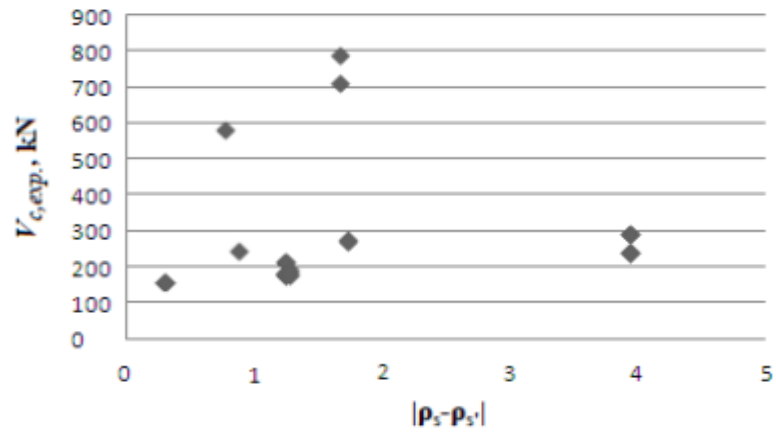


Figure 6.16:  $V_{c,exp.}$  versus  $|\rho_s - \rho_s'|$ .

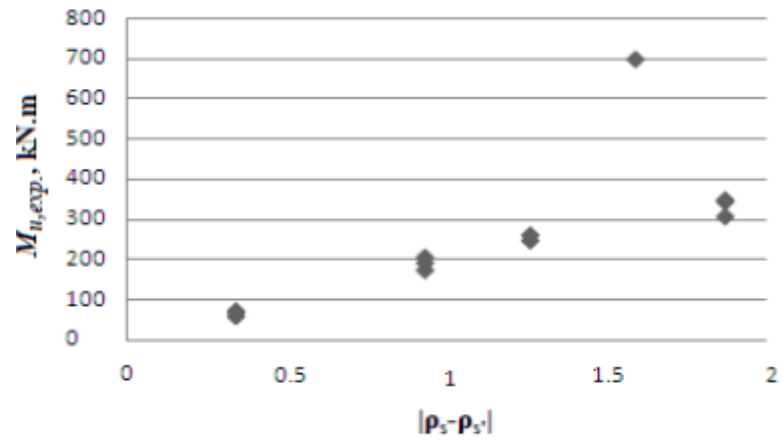


Figure 6.17:  $M_{u,exp.}$  versus  $|\rho_s - \rho_s'|$ .

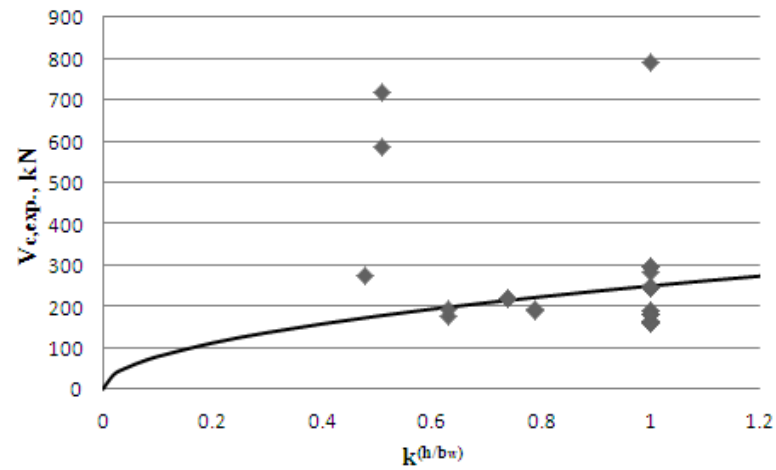


Figure 6.18:  $V_{c,exp.}$  versus  $k^{(h/b_w)}$ .

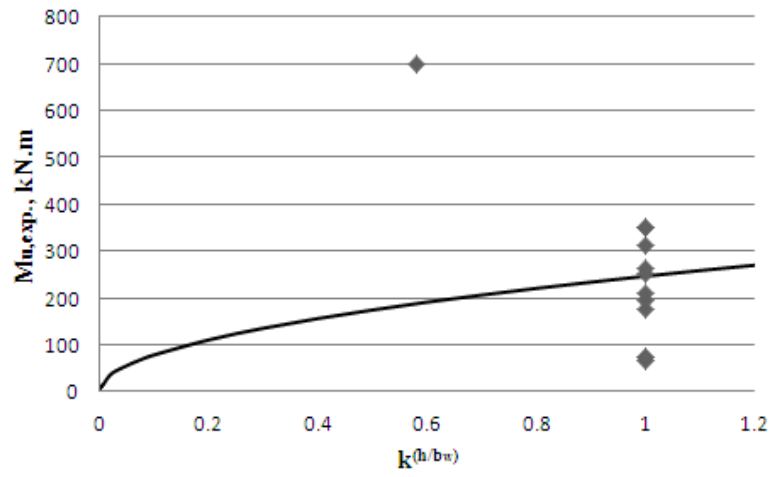


Figure 6.19:  $M_{u,exp.}$  versus  $k^{(h/b_w)}$ .

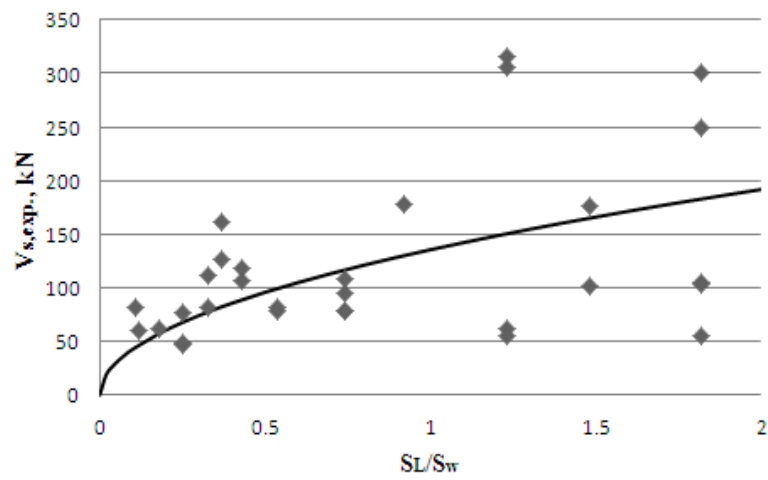


Figure 6.20:  $V_{s,exp.}$  versus  $S_L/S_w$ .

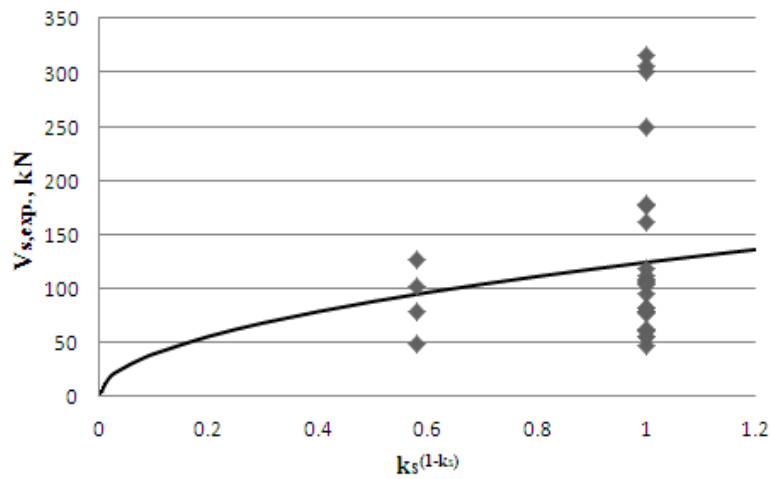


Figure 6.21:  $V_{s,exp.}$  versus  $k_s^{(1-k_s)}$ .



To develop a new prediction model, the general formulae used in the current Codes of Practice should be used, corrected and modified to be suitable for the wide RC members. To determine the shear strength, most current Codes of Practice predict the shear strength with a normalized formula, where the total ultimate shear strength is the summation of the shear strength resisted by concrete ( $V_c$ ) and the shear strength resisted by stirrups ( $V_s$ ), as shown in Equation (6.2).

$$V_u = V_c + V_s \quad (6.2)$$

Consequently, the term of " $V_c$ " should be corrected by a logical term to be illustrated by  $K_{cd}$  which includes two parts as shown in Equation (6.3) (Alluqmani, 2013a, 2013b). Part (1) must provide the influence of the longitudinal flexural reinforcement ratios for tensile reinforcement and compressive (or hanger) reinforcement, as illustrated by  $\mu_s$  in Equation (6.4). While Part (2) must provide the influence of the support- or load- width (or at best, the ratio of the support- or load- width to the beam-width, where the ratio which is less will be taken) and the cross-section geometry, as illustrated by  $\beta_g$  in Equation (6.5).

$$K_{cd} = \mu_s * \beta_g \quad (6.3)$$

$$\mu_s = F * (|\rho_s - \rho_s'|) \quad (6.4)$$

$$\beta_g = \sqrt{k \left(\frac{h}{b_w}\right)} \quad (6.5)$$

Where

$K_{cd}$  = design ratio of the concrete strength =  $\mu_s * \beta_g$ ,

$\mu_s$  = ratio of the longitudinal flexural reinforcement percentage =  $F * (|\rho_s - \rho_s'|)$ ,

For  $|\rho_s - \rho_s'| > 1.0\%$ :

$F = 100$  (but if  $|\rho_s - \rho_s'| > 1.60\%$ , use  $F = 60$ ) for  $k_s = 1.0$ ; while  $F = 120$  for  $k_s < 1.0$ .

For  $|\rho_s - \rho_s'| < 1.0\%$ :

$F = 140$  for  $k_s = 1.0$ ; while  $F = 170$  for  $k_s < 1.0$ . But if  $|\rho_s - \rho_s'| < 0.50\%$ , use  $F = (100 * b_w / h)$  whatever the support width.

$\rho_s$  = percentage of flexural-tensile reinforcement =  $A_s / b_w.d$ ,

$\rho_s'$  = percentage of flexural-compression reinforcement =  $A_s' / b_w.d$ ,

$A_s$  = total area of flexural-tensile reinforcement,

$A_s'$  = total area of flexural-compression reinforcement,

$\beta_g$  = ratio of the bearing plate size and cross-section geometry =  $\sqrt{k^{(h/bw)}}$ ,

$k$  = the lesser of ( $k_s = b_s/b_w$ , or  $k_p = b_p/b_w$ ),

$k_s$  = ratio of the support width to beam width =  $b_s/b_w$ ,

$k_p$  = ratio of the load width to beam width =  $b_p/b_w$ ,

$b_s$  = support width,  $b_p$  = load width,  $b_w$  = beam width, and  $h$  = beam height.

On the other hand, the term of " $V_s$ " should be corrected by a logical term to be illustrated by  $K_{sd}$  which includes two parts as shown in Equation (6.6) (Alluqmani, 2013a, 2013b). Part (1) must provide the influence of the transverse reinforcement (stirrup) legs spacing along the length and across the width, as illustrated by  $\mu_v$  in Equation (6.7). While Part (2) must provide the influence of the support-width (or at best, the ratio of support-width to beam-width), as illustrated by  $\beta_k$  in Equation (6.8).

$$K_{sd} = \mu_v * \beta_k \quad (6.6)$$

$$\mu_v = \sqrt{\frac{S_L}{S_w}} \quad (6.7)$$

$$\beta_k = \sqrt{k_s^{(1-k_s)}} \quad (6.8)$$

Where

$K_{sd}$  = design ratio of the stirrups strength =  $\mu_v * \beta_k$ ,

$\mu_v$  = ratio of the transverse reinforcement spacing =  $\sqrt{S_L/S_w}$ ,

$S_L$  = longitudinal spacing of the stirrup legs (along the length),

$S_w$  = transverse spacing of the stirrup legs (across the width),

$\beta_k$  = ratio of the bearing plate size =  $\sqrt{k_s^{(1-k_s)}}$ ,

$k_s$  = ratio of the support width to beam width =  $b_s/b_w$ ,

$b_s$  = support width, and  $b_w$  = beam width.

From Equations (6.2) to (6.8), the proposed prediction formula for **the one-way shear (beam-shear) capacity** of wide RC beams ( $V_{u,d}$ ) is illustrated in Equation (6.9) shown below (Alluqmani, 2013a, 2013b). The first term of the Equation " $V_{c,d}$ " demonstrates the shear strength resisted by concrete with taking into the account the effect of the longitudinal flexural reinforcement ratios as well as the support and load widths to beam width ratios and cross-section geometry which are illustrated in  $K_{cd}$ . The second term of the Equation " $V_{s,d}$ " demonstrates the shear strength resisted by stirrups with taking into the account the effect of

transverse reinforcement (stirrup legs) spacing in both longitudinal and transverse directions as well as support-width to beam-width ratio which are illustrated in  $K_{sd}$ .  $V_c$  and  $V_s$  are calculated according to the provisions of the applied Code. For the prediction purposes, it should be noted that no factors of safety are used neither in this prediction nor in calculation of  $V_c$  and  $V_s$ . In this proposed model,  $\theta$  is taken 45 degrees and  $\cot(\theta)$  is equal to 1.0 for calculating  $V_s$  (Alluqmani, 2013a, 2013b).

$$V_{u,d} = V_{c,d} + V_{s,d} = (K_{cd} * V_c) + (K_{sd} * V_s) \quad (6.9)$$

Where

$$V_{c,d} = K_{cd} * V_c = (\mu_s * \beta_g) * V_c = \left\{ [F * (|\rho_s - \rho_s'|)] * \left[ \sqrt{k \left( \frac{h}{b_w} \right)} \right] \right\} * V_c \quad (6.10)$$

$$V_{s,d} = K_{sd} * V_s = (\mu_v * \beta_k) * V_s = \left\{ \left[ \frac{S_L}{S_w} \right] * \left[ \sqrt{k_s^{(1-k_s)}} \right] \right\} * V_s \quad (6.11)$$

Equation (6.9) gives the general framework of the proposed prediction model for the one-way shear capacity. The shear strength of a beam without stirrups is equal to the  $V_{c,d}$  contribution of a beam with stirrups for the same characteristics.

There is a question for  $\mu_v$  in Equation (6.11),  $\mu_v = \sqrt{(S_L/S_w)}$ , where it seems that the proposed shear strength resisted by stirrups ( $V_{s,d}$ ) will increase as  $S_L$  increases (because  $\mu_v$  will increase); thus by logic and based on previous researches, this may be wrong. But the answer is that this is not wrong, it is right, because  $\mu_v$  will increase if  $S_L$  increases and then  $V_{s,d}$  will of course increase; however,  $\mu_v$  will be multiplied with  $\beta_k$  and by  $V_s$  (given by the Code), where  $V_s$  will be opposite of  $\mu_v$  - because  $V_s$  decreases as  $S_L$  increases. Finally,  $\mu_v$  and  $V_s$  will make balance for  $V_{s,d}$  as found by the proposed prediction model (Equation (6.11)) (Alluqmani, 2013a, 2013b). It should be emphasized that  $k_s$  in Equation (6.11), for  $\beta_k$ , was obtained from the previous research results, where  $k_s$  was in all cases the smaller amongst the values of  $k_p$  in all previous researches; therefore in some cases,  $k_s$  may be replaced by  $k$  which is the lesser of  $k_s$  or  $k_p$ .

The proposed prediction formula for **the two-way shear (punching-shear) capacity** of wide RC beams ( $v_{p,d}$ ) is illustrated in Equation (6.12) shown below (Alluqmani, 2013a, 2013b). The  $K_{cd}$  demonstrates the ratios of flexural-longitudinal reinforcement, the ratio of the bearing plate width to beam width and cross-section geometry, as shown in Equation (6.3) as  $K_{cd} = \mu_s * \beta_g$ , where  $\mu_s$  and  $\beta_g$  are given from Equations (6.4) and (6.5), respectively.  $v_p$  is the punching shear

stress which is determined according to the applied shear force (V), the member effective-depth (d) and the perimeter around the loaded area (u). For the prediction purposes, it should be noted that no factors of safety are used neither in this prediction nor in the calculation of  $v_p$ . Equation (6.12) gives the general framework of the proposed prediction model for the punching shear stress.

$$v_{p,d} = K_{cd} * v_p = (\mu_s * \beta_g) * v_p = \left\{ [F * (|\rho_s - \rho_s'|)] * \left[ \sqrt{k \left( \frac{h}{b_w} \right)} \right] \right\} * v_p \leq v_c \quad (6.12)$$

On the other hand, the proposed prediction formula for **the ultimate flexural capacity** (bending moment) of wide RC beams ( $M_{u,d}$ ) is illustrated in Equation (6.13) shown below (Alluqmani, 2013a, 2013b). The  $K_{cd}$  demonstrates the ratios of flexural-longitudinal reinforcement, the ratio of the bearing plate width to beam width and cross-section geometry, as shown in Equation (6.3) as  $K_{cd} = \mu_s * \beta_g$ , where  $\mu_s$  and  $\beta_g$  are given from Equations (6.4) and (6.5), respectively.  $M_{u,prop.}$  is the proposed ultimate bending moment (flexural capacity) in the section and is calculated as  $M_{u,prop.} = A_{s,prov.} * f_{y,act.} * jd$  (Equation 6.14), where  $jd$  is the lever arm and is proposed to be taken as  $(2/3) * h$  (Equation (6.15)) (Alluqmani, 2013a, 2013b). For the prediction purposes, it should be noted that no factors of safety are used neither in this prediction nor in the calculation of  $M_u$ . Equation (6.13) gives the general framework of the proposed prediction model for the flexural capacity.

$$M_{u,d} = K_{cd} * M_{u,prop.} = (\mu_s * \beta_g) * M_{u,prop.} = \left\{ [F * (|\rho_s - \rho_s'|)] * \left[ \sqrt{k \left( \frac{h}{b_w} \right)} \right] \right\} * M_{u,prop.} \quad (6.13)$$

Where

$$M_{u,prop.} = A_{s,prov.} * f_{y,act.} * jd \quad (6.14)$$

$$jd = \left( \frac{2}{3} \right) * h \quad (6.15)$$

#### 6.4 Validation of the Proposed Prediction-Model

To validate the proposed prediction model, Tables 6.3 to 6.11 and Figures 6.22 to 6.37 show the effect of  $k_s$ ,  $k_p$ ,  $k$ ,  $SL/d$ ,  $Sw/d$ , and  $SL/Sw$  on the ratios of  $V_{u,exp.}/V_{u,pred.}$ ,  $V_{c,exp.}/V_{c,pred.}$ ,  $V_{s,exp.}/V_{s,pred.}$ , and  $M_{u,exp.}/M_{u,pred.}$  of a) the proposed prediction-model, b) ACI Code, c) EC2 Code, d) Lubell model, e) Serna-Ros model, and f) Shuraim model. [See the Figure's title, each

Graph's title, and X- & Y- axes of each Graph] (Alluqmani, 2013a, 2013b). Table 6.2 shows the details of wide RC beams used in this validation. Note that the predictions which are obtained by the ACI318 Code are the same predictions given by SBC304 Code.

#### **6.4.1 The Ultimate Shear Capacity ( $V_u = V_c + V_s$ )**

From Figures 6.22, 6.26, 6.29, 6.32, 6.34 and 6.36, it is clear that the ratio of  $V_{u,exp.}/V_{u,pred.}$  for the proposed model lies in the range 0.91 to 1.23, which is the most close to 1.0, and has relatively lesser scatter with all values of  $k_s$ ,  $k_p$ ,  $k$ ,  $SL/d$ ,  $S_w/d$ , and  $SL/S_w$ , respectively; making it the most conservative method to predict the ultimate shear capacity ( $V_u = V_c + V_s$ ). The performance of the proposed model is better than the existing Codes and models. This shows that the predictions of the proposed model are very consistent and safe for all values of  $k_s$ ,  $k_p$ ,  $k$ ,  $SL/d$ ,  $S_w/d$ , and  $SL/S_w$ . Consequently, the proposed model can be safely used for prediction  $V_u$  with all values of  $k_s$ ,  $k_p$ ,  $k$ ,  $SL/d$ ,  $S_w/d$ , and  $SL/S_w$ .

#### **6.4.2 The Shear Capacity Resisted by Concrete ( $V_c$ )**

From Figures 6.23, 6.27, and 6.30, it is clear that the ratio of  $V_{c,exp.}/V_{c,pred.}$  for the proposed model lies in the range 0.94 to 1.16, which is the most close to 1.0, and has relatively lesser scatter with all values of  $k_s$ ,  $k_p$ , and  $k$ , respectively; making it the most conservative method to predict the shear capacity resisted by concrete ( $V_c$ ). The performance of the proposed model is better than the existing Codes and models. This shows that the predictions of the proposed model are very consistent and safe for all values of  $k_s$ ,  $k_p$ , and  $k$ . Consequently, the proposed model can be safely used for prediction  $V_c$  with all values of  $k_s$ ,  $k_p$ , and  $k$ .

#### **6.4.3 The Shear Capacity Resisted by Stirrups ( $V_s$ )**

From Figures 6.24, 6.33, 6.35 and 6.37, it is clear that the ratio of  $V_{s,exp.}/V_{s,pred.}$  for the proposed model lies in the range 0.93 to 1.24, which is the most close to 1.0, and has relatively lesser scatter with all values of  $k_s$ ,  $SL/d$ ,  $S_w/d$ , and  $SL/S_w$ , respectively; making it the most conservative method to predict the shear capacity resisted by stirrups ( $V_s$ ). The performance of the proposed model is better than the existing Codes and models. This shows that the predictions of the proposed model are very consistent and safe for all values of  $k_s$ ,  $SL/d$ ,  $S_w/d$ , and  $SL/S_w$ . Consequently, the proposed model can be safely used for prediction  $V_s$  with all values of  $k_s$ ,  $SL/d$ ,  $S_w/d$ , and  $SL/S_w$ .

#### 6.4.4 The Ultimate Flexural Capacity ( $M_u$ )

From Figures 6.25, 6.28 and 6.31, it is clear that the ratio of  $M_{u,exp.}/M_{u,pred.}$  for the proposed model lies in the range 0.90 to 1.16, which is the most close to 1.0, and has relatively lesser scatter with all values of  $k_s$ ,  $k_p$ ,  $k$ , respectively; making it the most conservative method to predict the ultimate flexural capacity ( $M_u$ ). The performance of the proposed model is better than the existing Codes. This shows that the predictions of the proposed model are very consistent and safe for all values of  $k_s$ ,  $k_p$ ,  $k$ . Consequently, the proposed model can be safely used for prediction  $M_u$  with all values of  $k_s$ ,  $k_p$ , and  $k$ .

#### 6.4.5 Validation on Series (A) Results

The two wide beams tested in Series (A), in Chapter 5, were used in this Chapter to validate Equations (6.9) and (6.13) as shown in Table 6.9. From Table 6.9, beam ECC3 had a predicted flexural capacity ( $M_{u,d}$ ) value of 706 kN.m, with a total predicted flexural failure load ( $P_{f,pred.} = P_{M,d}$ ) of 1008 kN, where the beam failed in flexure at a total failure load of 1000 kN ( $P_{f,exp.}/P_{f,pred.} = 1000/1008 = 0.99$ ) as obtained by both the test and the proposed prediction model of the flexural capacity (Equation (6.13)). On the other hand, beam ECC2 had a predicted shear capacity ( $V_{u,d}$ ) value of 485 kN, with a total predicted shear failure load ( $P_{f,pred.} = P_{V,d}$ ) of 970 kN, where the beam failed in shear at a total failure load of 985 kN ( $P_{f,exp.}/P_{f,pred.} = 985/970 = 1.01$ ) as obtained from both the test and the proposed prediction model of the one-way shear capacity (Equation (6.9)).

**Table 6.3a:** Validation of the Proposed Prediction Model on the Test Results obtained by Serna-Ros et al. (2002)  
Investigation on EC2 Code.

	Code Stren.,kN			Lubell Stren.,kN			Serna-Ros Stren.,kN			Shuraim Stren.,kN			Proposed Stren. (Model), kN					Test Stren., kN			$V_{c,ex}$	$V_{s,ex}$	$V_{u,ex}$																					
	$V_c$	$V_s$	$V_u$	$V_c$	$V_s$	$V_u$	$V_c$	$V_s$	$V_u$	$V_c$	$V_s$	$V_u$	K <sub>cd</sub>		$V_{c,d}$	K <sub>sd</sub>		$V_{s,d}$	$V_{u,d}$	$V_{c,ex}$	$V_{s,ex}$	$V_{u,ex}$	$V_{c,d}$	$V_{s,d}$	$V_{u,d}$																			
	EC2 Code												$\mu_s$	$\beta_g$		$\mu_v$	$\beta_k$																											
R0	173	-	173	173	-	173	173	-	173	173	-	173	1.26	1.0	218	-	-	-	218	244	-	244	1.12	-	1.12																			
R1	173	79	252	173	79	252	173	48	221	173	45	218	1.26	1.0	218	0.50	1.0	39	257	244	22	266	1.12	0.56	1.03																			
A0	147	-	147	147	-	147	147	-	147	147	-	147	1.26	1.0	185	-	-	-	185	187	-	187	1.01	-	1.01																			
A1	147	82	229	147	82	229	147	85	232	147	82	229	1.26	1.0	185	0.86	1.0	71	256	187	78	265	1.01	1.10	1.04																			
A2	147	88	235	147	88	235	147	53	200	147	50	197	1.26	1.0	185	0.50	1.0	44	229	187	47	234	1.01	1.07	1.02																			
A3	147	102	249	147	102	249	147	106	253	147	102	249	1.26	1.0	185	0.86	1.0	88	273	187	95	282	1.01	1.08	1.03																			
C0	151	-	151	151	-	151	151	-	151	151	-	151	1.26	1.0	190	-	-	-	190	182	-	182	0.96	-	0.96																			
C1	151	110	261	151	110	261	151	66	217	151	64	215	1.26	1.0	190	0.50	1.0	55	245	182	76	258	0.96	1.38	1.05																			
C2	151	98	249	151	98	249	151	102	253	151	98	249	1.26	1.0	190	0.86	1.0	84	274	182	109	291	0.96	1.30	1.06																			
C3	151	111	262	151	111	262	151	164	315	151	158	309	1.26	1.0	190	1.22	1.0	135	325	182	176	358	0.96	1.30	1.10																			
C4	151	147	298	151	147	298	151	228	379	151	177	328	1.26	1.0	190	0.96	1.0	141	331	182	178	360	0.96	1.26	1.09																			
C5	151	221	372	151	221	372	151	326	477	151	186	337	1.26	1.0	190	0.61	1.0	135	325	182	161	343	0.96	1.19	1.05																			
D0	171	-	171	140	-	140	171	-	171	171	-	171	1.51	0.86	222	-	-	-	222	218	-	218	0.98	-	0.98																			
D1	171	108	279	140	89	229	171	45	216	171	63	234	1.51	0.86	222	0.50	0.76	41	263	218	48	266	0.98	1.17	1.01																			
D2	171	94	265	140	77	217	171	67	238	171	95	266	1.51	0.86	222	0.86	0.76	62	284	218	78	296	0.98	1.26	1.04																			
D3	171	106	277	140	87	227	171	107	278	171	150	321	1.51	0.86	222	1.22	0.76	98	320	218	102	320	0.98	1.04	1.0																			
D5	171	213	384	140	175	315	171	216	387	171	180	351	1.51	0.86	222	0.61	0.76	99	321	218	127	345	0.98	1.28	1.07																			
Average																																										1.0	1.15	1.04

NOTE: bw = 750mm, h = 250mm, d = 206mm,  $\rho_c = 2.2\%$ ,  $\rho_s = 0.94\%$ ,  $\rho_w = 0.089\%$  (Beams R1, A1),  $\rho_w = 0.123\%$  (All other beams),  $f_c = 24.5-32.6$  MPa,  $f_{yv} = 512-670$  MPa,  $k_p = 1.0$  ( $b_p = bw = 750$ mm) for all Beams.  $k_s = 0.4$  ( $b_s = 300$ mm) for Beams in Series D,  $k_s = 1.0$  ( $b_s = bw = 750$ mm) for Beams in other Series.  $S_L = 85$ mm (Beams C5 and D5),  $S_L = 127.5$ mm (Beam C4),  $S_L = 170$ mm (all other Beams).  $S_w = 115$ mm (Beams C3 and D3),  $S_w = 135$ mm (Beam C4),  $S_w = 230$ mm (Beams A1, A3, C2, C5, D2, and D5),  $S_w = 690$ mm (Beams R1, A2, C1, and D1).  
1 mm = 0.0394 in, 1 kN = 1000 N = 0.225 kip, 1 MPa = 145 psi, 1 kN.m = 0.738 kip.ft = 8.858 kip.in.

**Table 6.3b:** Validation of the Proposed Prediction Model on the Test Results obtained by Serna-Ros et al. (2002)  
Investigation on ACI Code.

	Code Stren.,kN			Lubell Stren.,kN			Serna-Ros Stren.,kN			Shuraim Stren.,kN			Proposed Stren. (Model), kN					Test Stren., kN			$V_{c,ex}$	$V_{s,ex}$	$V_{u,ex}$																						
	$V_c$	$V_s$	$V_u$	$V_c$	$V_s$	$V_u$	$V_c$	$V_s$	$V_u$	$V_c$	$V_s$	$V_u$	K <sub>cd</sub>		$V_{c,d}$	K <sub>sd</sub>		$V_{s,d}$	$V_{u,d}$	$V_{c,ex}$	$V_{s,ex}$	$V_{u,ex}$	$V_{c,d}$	$V_{s,d}$	$V_{u,d}$																				
	ACI318 & SBC304												$\mu_s$	$\beta_g$		$\mu_v$	$\beta_k$																												
R0	139	-	139	139	-	139	139	-	139	139	-	139	1.26	1.0	175	-	-	-	175	244	-	244	1.39	-	1.39																				
R1	139	87	226	139	87	226	139	52	191	139	45	184	1.26	1.0	175	0.50	1.0	44	219	244	22	266	1.39	0.50	1.21																				
A0	128	-	128	128	-	128	128	-	128	128	-	128	1.26	1.0	161	-	-	-	161	187	-	187	1.16	-	1.16																				
A1	128	92	220	128	92	220	128	96	224	128	82	210	1.26	1.0	161	0.86	1.0	79	240	187	78	265	1.16	0.99	1.10																				
A2	128	97	225	128	97	225	128	58	186	128	50	178	1.26	1.0	161	0.50	1.0	48	209	187	47	234	1.16	0.98	1.12																				
A3	128	113	241	128	113	241	128	118	246	128	102	230	1.26	1.0	161	0.86	1.0	97	258	187	95	282	1.16	0.98	1.09																				
C0	130	-	130	130	-	130	130	-	130	130	-	130	1.26	1.0	164	-	-	-	164	182	-	182	1.11	-	1.11																				
C1	130	122	252	130	122	252	130	73	203	130	64	194	1.26	1.0	164	0.50	1.0	61	225	182	76	258	1.11	1.24	1.15																				
C2	130	109	239	130	109	239	130	114	244	130	98	228	1.26	1.0	164	0.86	1.0	94	258	182	109	291	1.11	1.16	1.13																				
C3	130	123	253	130	123	253	130	181	311	130	158	288	1.26	1.0	164	1.22	1.0	150	314	182	176	358	1.11	1.17	1.14																				
C4	130	164	294	130	164	294	130	255	385	130	177	307	1.26	1.0	164	0.96	1.0	157	321	182	178	360	1.11	1.13	1.12																				
C5	130	246	376	130	246	376	130	362	492	130	186	316	1.26	1.0	164	0.61	1.0	150	314	182	161	343	1.11	1.07	1.09																				
D0	148	-	148	121	-	121	148	-	148	148	-	148	1.51	0.86	192	-	-	-	192	218	-	218	1.13	-	1.13																				
D1	148	121	269	121	99	220	148	50	198	148	63	211	1.51	0.86	192	0.50	0.76	46	238	218	48	266	1.13	1.04	1.12																				
D2	148	105	253	121	86	207	148	75	223	148	95	243	1.51	0.86	192	0.86	0.76	69	261	218	78	296	1.13	1.13	1.13																				
D3	148	118	266	121	97	218	148	119	267	148	150	298	1.51	0.86	192	1.22	0.76	109	301	218	102	320	1.13	0.94	1.06																				
D5	148	237	385	121	194	315	148	240	388	148	180	328	1.51	0.86	192	0.61	0.76	110	302	218	127	345	1.13	1.15	1.14																				
Average																																											1.15	1.04	1.13

NOTE: bw = 750mm, h = 250mm, d = 206mm,  $\rho_c = 2.2\%$ ,  $\rho_s = 0.94\%$ ,  $\rho_w = 0.089\%$  (Beams R1, A1),  $\rho_w = 0.123\%$  (All other beams),  $f_c = 24.5-32.6$  MPa,  $f_{yv} = 512-670$  MPa,  $k_p = 1.0$  ( $b_p = bw = 750$ mm) for all Beams.  $k_s = 0.4$  ( $b_s = 300$ mm) for Beams in Series D,  $k_s = 1.0$  ( $b_s = bw = 750$ mm) for Beams in other Series.  $S_L = 85$ mm (Beams C5 and D5),  $S_L = 127.5$ mm (Beam C4),  $S_L = 170$ mm (all other Beams).  $S_w = 115$ mm (Beams C3 and D3),  $S_w = 135$ mm (Beam C4),  $S_w = 230$ mm (Beams A1, A3, C2, C5, D2, and D5),  $S_w = 690$ mm (Beams R1, A2, C1, and D1).  
1 mm = 0.0394 in, 1 kN = 1000 N = 0.225 kip, 1 MPa = 145 psi, 1 kN.m = 0.738 kip.ft = 8.858 kip.in.

**Table 6.4:** Validation of the Proposed Prediction Model on the Test Results obtained by Shuraim (2012) Investigation.

	Code Stren.,kN			Lubell Stren.,kN			Serna-Ros Stren.,kN			Shuraim Stren.,kN			Proposed Stren. (Model), kN						Test Stren., kN			$V_{c,ex}$	$V_{s,ex}$	$V_{u,ex}$	
	$V_c$	$V_s$	$V_u$	$V_c$	$V_s$	$V_u$	$V_c$	$V_s$	$V_u$	$V_c$	$V_s$	$V_u$	Kcd		$V_{c,d}$	Ksd		$V_{s,d}$	$V_{u,d}$	$V_{c,ex}$	$V_{s,ex}$	$V_{u,ex}$	$V_{c,d}$	$V_{s,d}$	$V_{u,d}$
	ACI318 & SBC304									$\mu_s$	$\beta_g$	$\mu_v$	$\beta_k$												
S0	140	-	140	140	-	140	140	-	140	140	-	140	1.22	1.0	170	-	-	-	170	161	-	161	0.95	-	0.95
S1-80	140	142	282	140	142	282	140	93	233	140	59	199	1.22	1.0	170	0.35	1.0	50	220	161	60	221	0.95	1.20	1.0
S2-80	140	142	282	140	142	282	140	114	254	140	71	211	1.22	1.0	170	0.43	1.0	61	231	161	61	222	0.95	1.0	0.96
S3-80	140	142	282	140	142	282	140	157	297	140	98	238	1.22	1.0	170	0.59	1.0	84	254	161	71	232	0.95	0.85	0.91
S0-1	140	-	140	140	-	140	140	-	140	140	-	140	1.22	1.0	170	-	-	-	170	162	-	162	0.95	-	0.95
S1-75-1A	140	188	328	140	188	328	140	127	267	140	74	214	1.22	1.0	170	0.34	1.0	64	234	162	0	162	0.95	-----	-----
S3-75-1	140	144	284	140	144	284	140	164	304	140	74	214	1.22	1.0	170	0.57	1.0	82	252	162	58	220	0.95	-----	0.87
S13-75-1A	140	188	328	140	188	328	140	215	355	140	126	266	1.22	1.0	170	0.57	1.0	107	277	162	112	274	0.95	1.05	0.99
S13-100-1	140	143	283	140	143	283	140	141	281	140	101	241	1.22	1.0	170	0.66	1.0	95	265	162	106	268	0.95	1.11	1.01
S13-125-1	140	110	250	140	110	250	140	97	237	140	86	226	1.22	1.0	170	0.74	1.0	81	251	162	79	241	0.95	0.98	0.96
S0-2	140	-	140	140	-	140	140	-	140	140	-	140	1.22	1.0	170	-	-	-	170	160	-	160	0.94	-	0.94
S1-75-2	140	188	328	140	188	328	140	127	267	140	74	214	1.22	1.0	170	0.34	1.0	64	234	160	81	241	0.94	1.26	1.03
S3-75-2	140	144	284	140	144	284	140	164	304	140	74	214	1.22	1.0	170	0.57	1.0	82	252	160	81	241	0.94	0.99	0.96
S13-75-2	140	188	328	140	188	328	140	215	355	140	126	266	1.22	1.0	170	0.57	1.0	107	277	160	146	306	0.94	1.36	1.10
S13-100-2	140	143	283	140	143	283	140	141	281	140	101	241	1.22	1.0	170	0.66	1.0	95	265	160	118	278	0.94	1.24	1.05
S13-125-2	140	110	250	140	110	250	140	97	237	140	86	226	1.22	1.0	170	0.74	1.0	81	251	160	81	241	0.94	1.0	0.96
Average																					0.95	1.09	0.98		

NOTE: bw = 700mm, h = 180mm, d = 150mm,  $\rho_s = 1.34\%$  and  $\rho_s = 1.026\%$  (for all beams),  $A_v = 157mm^2$  and  $201mm^2$ ,  $\rho_v = 0.28\%$ ,  $0.38\%$  and  $0.23\%$ ,  $f_{c,av} = 29$  MPa,  $f_{yv} = 483$  MPa and  $465$  MPa.  $S_L = 80, 75, 100$  and  $125mm$ .  $S_w = 660mm$  (for beams S1-80, S1-75-1A and S1-75-2),  $S_w = 440mm$  (for beam S2-80), and  $S_w = 230mm$  (for all other beams).  $k = 1.0$  ( $b_s = b_p = b_w = 700mm$ ) for all beams.

These Beams are continuous wide RC beams.

1 mm = 0.0394 in, 1 kN = 1000 N = 0.225 kip, 1 MPa = 145 psi, 1 kN.m = 0.738 kip.ft = 8.858 kip.in.

**Table 6.5:** Validation of the Proposed Prediction Model on the Test Results obtained by Hanafy et al. (2012) Investigation.

	Code Stren.,kN			Lubell Stren.,kN			Serna-Ros Stren.,kN			Shuraim Stren.,kN			Proposed Stren. (Model), kN						Test Stren., kN			$V_{c,ex}$	$V_{s,ex}$	$V_{u,ex}$	
	$V_c$	$V_s$	$V_u$	$V_c$	$V_s$	$V_u$	$V_c$	$V_s$	$V_u$	$V_c$	$V_s$	$V_u$	Kcd		$V_{c,d}$	Ksd		$V_{s,d}$	$V_{u,d}$	$V_{c,ex}$	$V_{s,ex}$	$V_{u,ex}$	$V_{c,d}$	$V_{s,d}$	$V_{u,d}$
	Av. Various Codes									$\mu_s$	$\beta_g$	$\mu_v$	$\beta_k$												
NB1	102	-	102	102	-	102	102	-	102	102	-	102	2.37	1.0	242	-	-	-	242	245	-	245	1.01	-	1.01
NB2	102	67	169	102	67	169	102	95	197	102	73	175	2.37	1.0	242	1.34	1.0	90	332	245	105	350	1.01	1.17	1.05
NB3	102	40	142	102	40	142	102	57	159	102	68	170	2.37	1.0	242	1.34	1.0	53	295	245	55	300	1.01	1.04	1.02
NB4	102	49	151	102	49	151	102	84	186	102	65	167	2.37	1.0	242	1.11	1.0	54	296	245	61	306	1.01	1.13	1.03
NB5	102	201	303	102	201	303	102	285	387	102	284	386	2.37	1.0	242	1.34	1.0	269	511	245	250	495	1.01	0.93	0.97
NB6	102	230	332	102	230	332	102	396	498	102	254	356	2.37	1.0	242	1.11	1.0	255	497	245	305	550	1.01	1.19	1.11
HB1	129	-	129	129	-	129	129	-	129	129	-	129	2.37	1.0	305	-	-	-	305	295	-	295	0.97	-	0.97
HB2	129	67	196	129	67	196	129	95	224	129	73	202	2.37	1.0	305	1.34	1.0	90	395	295	103	398	0.97	1.14	1.01
HB3	129	40	169	129	40	169	129	57	186	129	68	197	2.37	1.0	305	1.34	1.0	53	358	295	45	340	0.97	0.85	0.95
HB4	129	49	178	129	49	178	129	84	213	129	65	194	2.37	1.0	305	1.11	1.0	54	359	295	55	350	0.97	1.02	0.97
HB5	129	201	330	129	201	330	129	285	414	129	284	413	2.37	1.0	305	1.34	1.0	269	574	295	300	595	0.97	1.11	1.04
HB6	129	230	359	129	230	359	129	396	525	129	254	383	2.37	1.0	305	1.11	1.0	255	560	295	315	610	0.97	1.23	1.09
Average																					0.99	1.08	1.02		

NOTE: bw = 500mm, h = 250mm, d = 210mm,  $\rho_s = 4.61\%$ ,  $\rho_s = 0.65\%$ ,  $\rho_s = 0.16\%$ - $0.47\%$ ,  $f_{c,av} = 40$  MPa (for all beams in Series NB),  $f_{c,av} = 90$  MPa (for all beams in Series HB),  $f_y = 420$  MPa,  $f_{yv} = 300$  MPa (for beams NB2, NB3, NB4, HB2, HB3 and HB4),  $f_{yv} = 420$  MPa (for beams NB5, NB6, HB5 and HB6).  $S_L = 200mm$  (Beams NB2, NB3, NB5, HB2, HB3 and HB5),  $S_L = 135mm$  (Beams NB4, NB6, HB4 and HB6).  $S_w = 110mm$  (for all beams with stirrups).  $k = k_s = k_p = 1.0$  ( $b_s = b_p = b_w = 500mm$ ) for all beams.

These Beams may be considered beams with T-Sections.

1 mm = 0.0394 in, 1 kN = 1000 N = 0.225 kip, 1 MPa = 145 psi, 1 kN.m = 0.738 kip.ft = 8.858 kip.in.



**Table 6.6:** Validation of the Proposed Prediction Model on the Test Results obtained by Al.Dywany (2010) Investigation.

	Code Stren.,kN			Lubell Stren.,kN			Serna-Ros Stren.,kN			Shuraim Stren.,kN			Proposed Stren. (Model), kN					Test Stren., kN			$V_{c,ex}$	$V_{s,ex}$	$V_{u,ex}$		
	$V_c$	$V_s$	$V_u$	$V_c$	$V_s$	$V_u$	$V_c$	$V_s$	$V_u$	$V_c$	$V_s$	$V_u$	$K_{cd}$	$V_{c,d}$	$K_{sd}$	$V_{s,d}$	$V_{u,d}$	$V_{c,ex}$	$V_{s,ex}$	$V_{u,ex}$	$V_{c,d}$	$V_{s,d}$	$V_{u,d}$		
	BS8110 Code												$\mu_s$	$\beta_g$		$\mu_v$	$\beta_k$								
A1	137	-	137	137	-	137	137	-	137	137	-	137	1.29	1.0	177	-	-	-	177	179	-	179	-	-	1.01
A1/2	137	-	137	116	-	116	137	-	137	137	-	137	1.55	0.89	189	-	-	-	189	188	-	188	-	-	0.99
A1/4	137	-	137	106	-	106	137	-	137	137	-	137	1.55	0.79	168	-	-	-	168	178	-	178	-	-	1.06
RA1/2	137	-	137	116	-	116	137	-	137	137	-	137	1.55	0.89	189	-	-	-	189	194	-	194	-	-	1.03
RA1/4	137	-	137	106	-	106	137	-	137	137	-	137	1.55	0.79	168	-	-	-	168	191	-	191	-	-	1.14
B1	137	68	205	137	68	205	137	108	245	137	66	203	1.25	1.0	172	0.83	1.0	57	229	-	-	241	-	-	1.05
B1/2	137	68	205	116	58	174	137	81	218	137	66	203	1.50	0.89	183	0.83	0.84	48	231	-	-	195	-	-	0.84
B1/4	137	68	205	106	53	159	137	68	205	137	73	210	1.50	0.79	163	0.92	0.59	37	200	-	-	198	-	-	0.99
RB1/2	137	68	205	116	58	174	137	88	225	137	72	209	1.50	0.89	183	0.90	0.84	51	234	-	-	251	-	-	1.07
RB1/4	137	68	205	106	53	159	137	66	203	137	72	209	1.50	0.79	163	0.90	0.59	36	199	-	-	237	-	-	1.19
Average																						-	-	1.04	

NOTE: bw = 750mm, h = 250mm, d = 210mm,  $\rho_s = 1.29\%$ ,  $f_{c,av} = 28.5$  MPa,  $f_{yv} = 250$  MPa for all beams ( $\rho_s = 0.036\%$ ,  $\rho_s = 0.17\%$  for all beams in Series B).  $k_p = 1.0$  ( $b_p = bw = 750$ mm) for all Beams.  $k_s = 0.25$  ( $b_s = 190$ mm) for Beams A1/4, RA1/4, B1/4, and RB1/4.  $k_s = 0.50$  ( $b_s = 375$ mm) for Beams A1/2, RA1/2, B1/2, and RB1/2.  $k_s = 1.0$  ( $b_s = 750$ mm) for Beams A1 and B1.  $S_w = 110$ mm (for all Beams in Series B).  $S_w = 160$ mm (for Beams B1 and B1/2),  $S_w = 130$ mm (for Beam B1/4),  $S_w = 135$ mm (for Beams RB1/2 and RB1/4).

Beams without stirrups (in series A) are not references for beams with stirrups (in series B), because they did not have top flexural bars for  $\rho_s$  and ( $V_{c,ex}$ ) verifications. 1 mm = 0.0394 in, 1 kN = 1000 N = 0.225 kip, 1 MPa = 145 psi, 1 kN.m = 0.738 kip.ft = 8.858 kip.in.

**Table 6.7:** Validation of the Proposed Prediction Model on the Test Results obtained by Lubell et al. (2008, 2009) Investigation.

	Code Stren.,kN			Lubell Stren.,kN			Serna-Ros Stren.,kN			Shuraim Stren.,kN			Proposed Stren. (Model), kN					Test Stren., kN			$V_{c,ex}$	$V_{s,ex}$	$V_{u,ex}$		
	$V_c$	$V_s$	$V_u$	$V_c$	$V_s$	$V_u$	$V_c$	$V_s$	$V_u$	$V_c$	$V_s$	$V_u$	$K_{cd}$	$V_{c,d}$	$K_{sd}$	$V_{s,d}$	$V_{u,d}$	$V_{c,ex}$	$V_{s,ex}$	$V_{u,ex}$	$V_{c,d}$	$V_{s,d}$	$V_{u,d}$		
	ACI318 & SBC304												$\mu_s$	$\beta_g$		$\mu_v$	$\beta_k$								
AX8	200	-	200	153	-	153	200	-	200	200	-	200	2.10	0.69	290	-	-	-	290	272	-	272	-	-	0.94
AX7	200	-	200	200	-	200	200	-	200	200	-	200	1.25	1.0	250	-	-	-	250	249	-	249	-	-	1.0
AX6	217	-	200	200	-	200	200	-	200	200	-	200	1.05	1.0	228	-	-	-	228	281	-	281	-	-	1.23
AX1	217	105	322	217	105	322	217	91	308	217	63	280	1.55	1.0	336	0.53	1.0	56	392	-	-	458	-	-	1.17
AX2	200	101	301	200	101	301	200	87	287	200	60	260	1.55	1.0	310	0.53	1.0	53	363	-	-	338	-	-	0.93
AX3	217	119	336	217	119	336	217	138	355	217	95	312	1.45	1.0	315	0.71	1.0	84	399	-	-	450	-	-	1.13
AX4	217	109	326	217	109	326	217	154	371	217	106	323	1.35	1.0	293	0.86	1.0	94	387	-	-	415	-	-	1.07
AX5	217	105	322	217	105	322	217	105	322	217	72	289	1.35	1.0	293	0.61	1.0	64	357	-	-	359	-	-	1.01
AW8	648	-	621	621	-	621	621	-	621	621	-	621	1.01	1.0	654	-	-	-	654	789	-	789	-	-	1.20
AW6	648	301	922	621	301	922	621	269	890	621	181	802	0.97	1.0	629	0.53	1.0	160	789	-	-	826	-	-	1.04
AW7	580	215	795	580	215	795	580	328	908	580	221	801	1.54	1.0	893	0.90	1.0	194	1087	-	-	1062	-	-	0.98
AW1	625	-	625	486	-	486	625	-	625	625	-	625	1.34	0.71	594	-	-	-	594	585	-	585	-	-	0.98
AW4	580	-	580	451	-	451	580	-	580	580	-	580	2.02	0.71	832	-	-	-	832	716	-	716	-	-	0.86
AW2	580	301	881	451	234	685	580	155	735	580	181	761	1.93	0.71	795	0.53	0.61	97	892	-	-	809	-	-	0.91
AW3	580	301	881	451	234	685	580	180	760	580	210	790	1.93	0.71	795	0.61	0.61	112	907	-	-	828	-	-	0.91
AW5	580	215	795	451	167	618	580	188	768	580	219	799	1.85	0.71	762	0.89	0.61	117	879	-	-	953	-	-	1.08
Average																						-	-	1.03	

NOTE: For Beams in Series AX: bw = 700mm, h = 340mm, d = 286mm,  $\rho_s = 1.75\%$  ( $\rho_s = 0.89\%$  for beam AX7),  $\rho_s = 0.20\%$  (for beams AX1 & AX2),  $\rho_s = 0.30\%$  (for beam AX3),  $\rho_s = 0.40\%$  (for beams AX4 & AX5),  $\rho_s = 0.08\%$  - 0.11%. For Beams in Series AW: bw = 1170mm, h = 585mm, d = 509mm (d = 538mm for beam AW1),  $\rho_s = 1.68\%$  ( $\rho_s = 0.79\%$  for beam AW1),  $\rho_s = 0.07\%$  (for beams AW2, AW3 & AW6),  $\rho_s = 0.14\%$  (for beams AW5 & AW7),  $\rho_s = 0.08\%$  - 0.11%. For all:  $f_{c,av} = 36$ -43 MPa,  $f_{yv} = 458$ -625 MPa.  $S_L = 175$ mm (all Beams in Series AX),  $S_L = 300$ mm (all Beams in Series AW).  $S_w = 625, 625, 350, 235$  and 470mm (for Beams in Series AX),  $S_w = 1080, 800, 375, 1080$  and 370mm (for Beams in Series AW).  $k = k_s = k_p = 0.26$  ( $b_s = b_p = 305$ mm) for beams AW1, AW2, AW3, AW4 and AW5.  $k = k_s = k_p = 0.22$  ( $b_s = b_p = 152$ mm) for beam AX8.  $k_s = k_p = 1.0$  for all other Beams.

Beams without stirrups are not references for beams with stirrups, because they did not have top flexural bars for  $\rho_s$  and ( $V_{c,exp}$ ) verifications. 1 mm = 0.0394 in, 1 kN = 1000 N = 0.225 kip, 1 MPa = 145 psi, 1 kN.m = 0.738 kip.ft = 8.858 kip.in.

**Table 6.8:** Validation of the Proposed Prediction Model on the Test Results obtained by McAllister (2011) Investigation.

	Code Stren.,kN			Lubell Stren.,kN			Serna-Ros Stren.,kN			Shuraim Stren.,kN			Proposed Stren. (Model), kN						Test Stren., kN			$V_{c,ex}$	$V_{s,ex}$	$V_{u,ex}$	
	$V_c$	$V_s$	$V_u$	$V_c$	$V_s$	$V_u$	$V_c$	$V_s$	$V_u$	$V_c$	$V_s$	$V_u$	$K_{cd}$	$V_{c,d}$	$K_{sd}$	$V_{s,d}$	$V_{u,d}$	$V_{c,ex}$	$V_{s,ex}$	$V_{u,ex}$	$V_{c,d}$	$V_{s,d}$	$V_{u,d}$		
	Various Codes												$\mu_s$	$\beta_g$		$\mu_v$	$\beta_k$								
B1 (ACI & SBC)	172	173	345	172	173	345	172	180	352	172	99	271	0.96	1.0	165	0.47	1.0	81	246	-	-	285	-	-	1.16
B2 (EC2)	172	113	285	172	113	285	172	100	272	172	78	250	1.57	1.0	270	0.55	1.0	62	332	-	-	330	-	-	0.99
Average																							-	-	1.07

**NOTE:** bw = 703mm, h = 339mm, d = 295mm,  $f_{c,av.}$  = 24.8 MPa,  $f_{yv}$  = 500 MPa,  $k=1.0$  ( $b_s = b_p = b_w = 703mm$ ) for both Beams. Beam B1:  $\rho_s = 0.76\%$ ,  $\rho_s' = 0.075\%$ ,  $\rho_s'' = 0.167\%$ . Beam B2:  $\rho_s = 1.65\%$ ,  $\rho_s' = 0.075\%$ ,  $\rho_s'' = 0.121\%$ .  $S_T = 134mm$  (Beam B1) and  $S_T = 184mm$  (Beam B2).  $S_w = 600mm$  for both Beams.  
1 mm = 0.0394 in, 1 kN = 1000 N = 0.225 kip, 1 MPa = 145 psi, 1 kN.m = 0.738 kip.ft = 8.858 kip.in.

**Table 6.9:** Validation of the Proposed Prediction-Model on the Test Results obtained by Test-Series (A) Investigation in Chapter 5.

	Code Stren.,kN-m				Lubell Stren.,kN				Serna-Ros Stren.,kN				Shuraim Stren.,kN				Proposed Stren. (Model), kN-m										$P_{f,pred.}$ ,kN	Test Stren., kN			$P_{ft}$	
	$V_c$	$V_s$	$V_u$	$M_u$	$V_c$	$V_s$	$V_u$	$P_{V,f}$	$V_c$	$V_s$	$V_u$	$P_{V,f}$	$V_c$	$V_s$	$V_u$	$P_{V,f}$	$M_u$	$K_{cd}$	$V_{c,d}$	$K_{sd}$	$V_{s,d}$	$V_{u,d}$	$M_{u,d}$	$V_{d'}$	$P_{V,d}$	$P_{M,d}$	$V_{c,t}$	$V_{s,t}$	$P_{ft}$	$P_{f,pred}$		
	EC2 Code																$\mu_s$	$\beta_g$		$\mu_v$	$\beta_k$											
ECC3	274	235	509	483	220	188	408	816	274	310	584	1168	274	361	635	1270	484	1.92	0.76	400	1.21	0.70	200	600	706	350	1200	1008	-	-	1000	0.99
ECC2	274	156	430	483	220	125	345	690	274	131	405	810	274	153	427	854	484	1.92	0.76	400	0.77	0.70	85	485	706	282	970	1008	-	-	985	1.01
Average																													1.0			

**NOTE:** bw = 708mm, h = 353mm, d = 304mm, a = 1400mm, jd= 244.8mm (ACI-Model), jd= 234.3mm (EC2-Model), jd= 235mm (Proposed-Model),  $\epsilon_c = 0.0035$ ,  $E_c = 31000$  MPa,  $E_s = 200000$  MPa,  $\rho_s = 1.82\%$ ,  $\rho_s' = 0.221\%$ ,  $f_{c,y,d} = 45$  MPa,  $f_{y,d} = 525$  MPa,  $f_{y,v,d} = 512$  MPa.  $P_d = 600$  kN,  $V = 300$  kN, and  $M = 420$  kN.m.  $A_v = 201mm^2$  (4-Legs- $\Phi 8mm$ ) for Beam ECC2,  $A_v = 302mm^2$  (6-Legs- $\Phi 8mm$ ) for Beam ECC3.  $S_L = 180mm$  for Beams ECC2 and ECC3.  $S_w = 300mm$  for Beam ECC2,  $S_w = 122mm$  for Beam ECC3.  $k_p = 0.50$  ( $b_p = 350mm$ ) for both Beams,  $k_s = 0.34$  ( $b_s = 240mm$ ) for both Beams. Hence  $k = 0.34$ .  
Both beams were tested under a three point-loading system.  
 $P_{V,d}$  = Predicted shear failure load =  $2V_{u,d}$  and  $P_{M,d}$  = Predicted flexural failure load =  $2(M_{u,d}/a)$ .  $jd = (2/3)*h = 235mm$ .  
 $P_{f,pred.}$  = the smallest of ( $P_{V,d}$  or  $P_{M,d}$ ) and the predicted failure mode is the failure mode corresponding to  $P_{f,pred.}$ .  
Beam ECC3 failed in Flexure at 1000 kN. Beam ECC2 failed in Shear at 985 kN.  
1 mm = 0.0394 in, 1 kN = 1000 N = 0.225 kip, 1 MPa = 145 psi, 1 kN.m = 0.738 kip.ft = 8.858 kip.in.

**Table 6.10:** Validation of the Proposed Prediction Model on the Test Results obtained by Al-Harithy (2002) Investigation.

	Code Stren., kN.m	Proposed Stren., kN.m			Test Stren., kN.m	$M_{u,exp}$
	$M_u$	$M_u$	$K_{cd}$	$M_{u,d}$	$M_{u,exp}$	$M_{u,d}$
	ACI318 & SBC304	$\mu_s$	$\beta_g$			
B1-25	276	276	1.13	1.0	312	1.0
B1-65	276	276	1.13	1.0	312	1.12
B1-95	276	276	1.13	1.0	312	1.11
B2-25	190	190	1.27	1.0	241	0.89
B2-65	190	190	1.27	1.0	241	1.05
B2-95	190	190	1.27	1.0	241	1.09
B3-25	138	138	1.32	1.0	182	0.97
B3-65	138	138	1.32	1.0	182	1.07
B3-95	138	138	1.32	1.0	182	1.16
B4-25	51	51	1.40	1.0	71	0.90
B4-65	51	51	1.40	1.0	71	1.04
B4-95	51	51	1.40	1.0	71	1.03
Average						1.03

**NOTE:** bw = 800mm, h = 200mm, d = 165mm, jd= 123.5-133.3mm (ACI Code), jd= 123.5-125.6-128.7mm (EC2 Code), jd= 133mm (Proposed-Model) and  $\rho_v = 0.15\%$  (for all beams),  $\rho_s = 3.81\%$  and  $\rho_s' = 1.93\%$  (beam-type B1),  $\rho_s = 2.62\%$  and  $\rho_s' = 1.35\%$  (beam-type B2),  $\rho_s = 1.90\%$  and  $\rho_s' = 0.96\%$  (beam-type B3),  $\rho_s = 0.70\%$  and  $\rho_s' = 0.35\%$  (beam-type B4),  $f_{c,av.}$  = 25, 65 and 95 MPa,  $f_y = 414$  MPa.  $k = 1.0$  ( $b_s = b_p = b_w = 800mm$ ) for all Beams.  $S_T = 82mm$  and  $S_w = 370mm$  for all beams.  
1 mm = 0.0394 in, 1 kN = 1000 N = 0.225 kip, 1 MPa = 145 psi, 1 kN.m = 0.738 kip.ft = 8.858 kip.in.

**Table 6.11:** Average Strengths of all Wide RC Beams Validated by the Proposed Prediction-Model.

	No. of Beams	$(V_{c,exp./V_{c,d-prop.})_{av.}}$	$(V_{s,exp./V_{s,d-prop.})_{av.}}$	$(V_{u,exp./V_{u,d-prop.})_{av.}}$	$(M_{u,exp./M_{u,d-prop.})_{av.}}$
Beams in Table 6.3a	17	1.0	1.15	1.04	-
Beams in Table 6.3b	17	1.15	1.04	1.13	-
Beams in Table 6.4	16	0.95	1.09	0.98	-
Beams in Table 6.5	12	0.99	1.08	1.02	-
Beams in Table 6.6	10	-	-	1.04	-
Beams in Table 6.7	16	-	-	1.03	-
Beams in Table 6.8	2	-	-	1.07	-
Beams in Table 6.9	2	-	-	1.01	0.99
Beams in Table 6.10	12	-	-	-	1.03
<b>Average</b>		<b>1.03</b>	<b>1.09</b>	<b>1.04</b>	<b>1.02</b>

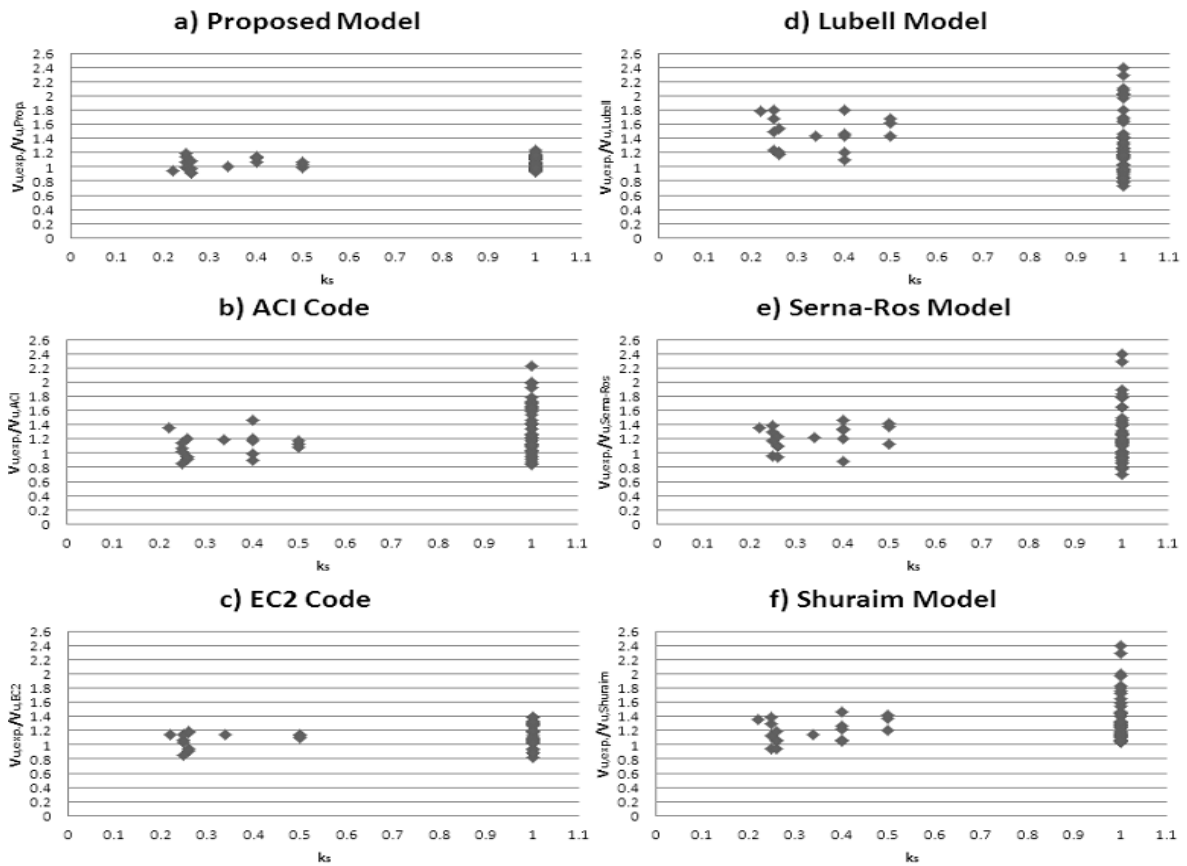


**Figure 6.22:**  $k_s$  versus  $V_{u,exp./V_{u,Pred.}}$ .

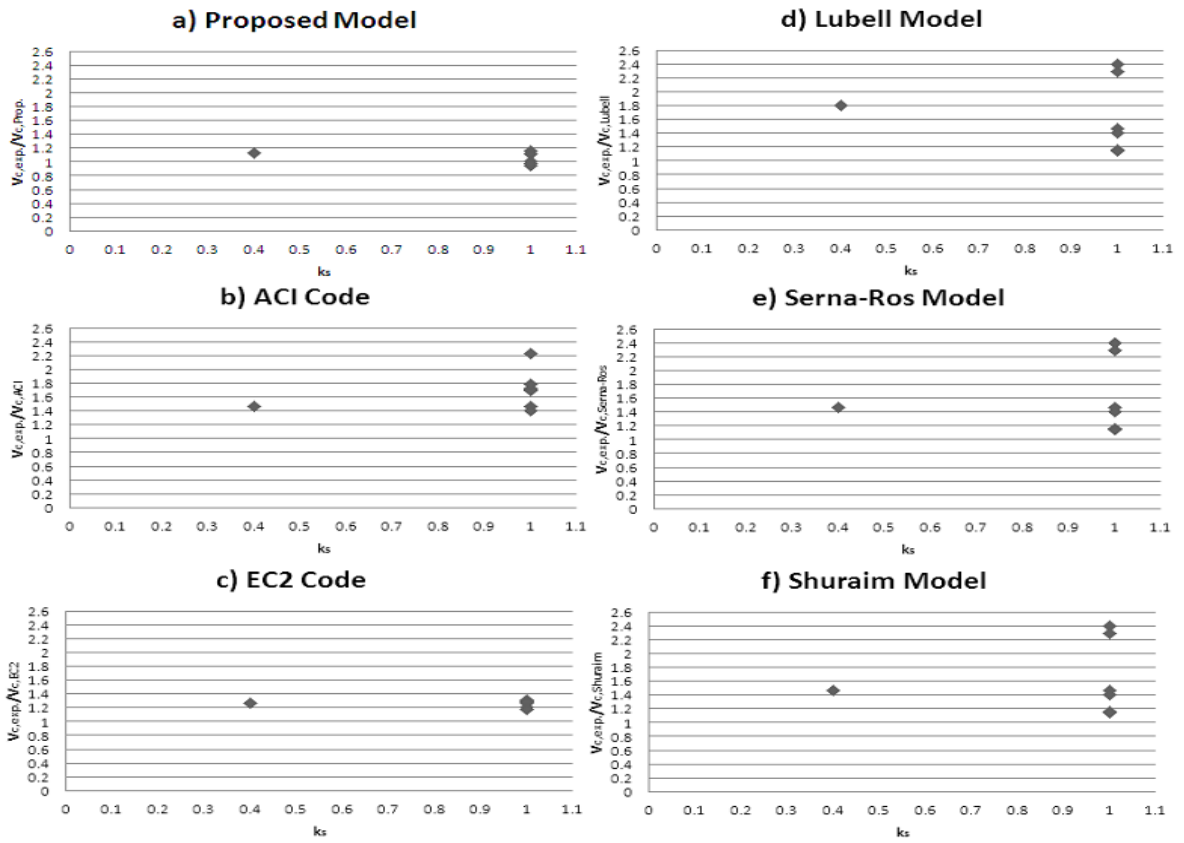


Figure 6.23:  $k_s$  versus  $V_{c,exp}/V_{c,Pred.}$ .

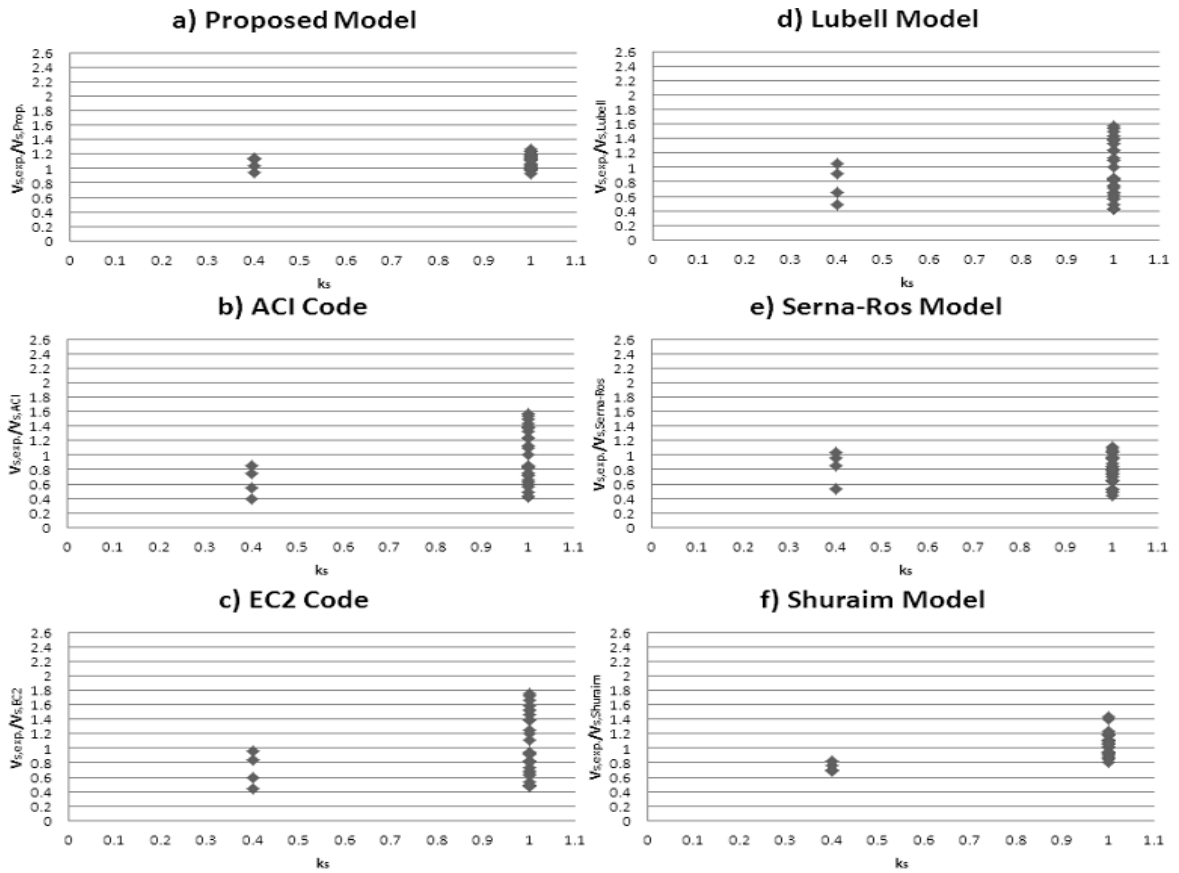


Figure 6.24:  $k_s$  versus  $V_{s,exp}/V_{s,Pred.}$ .

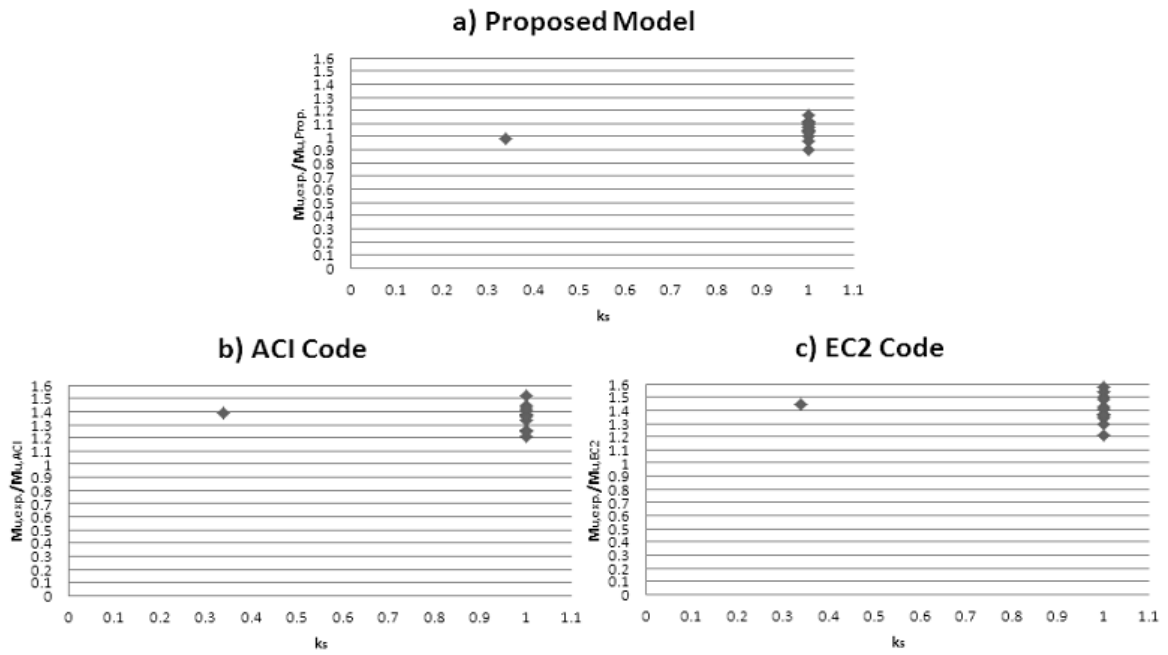


Figure 6.25:  $k_s$  versus  $M_{u,exp}/M_{u,Pred.}$ .

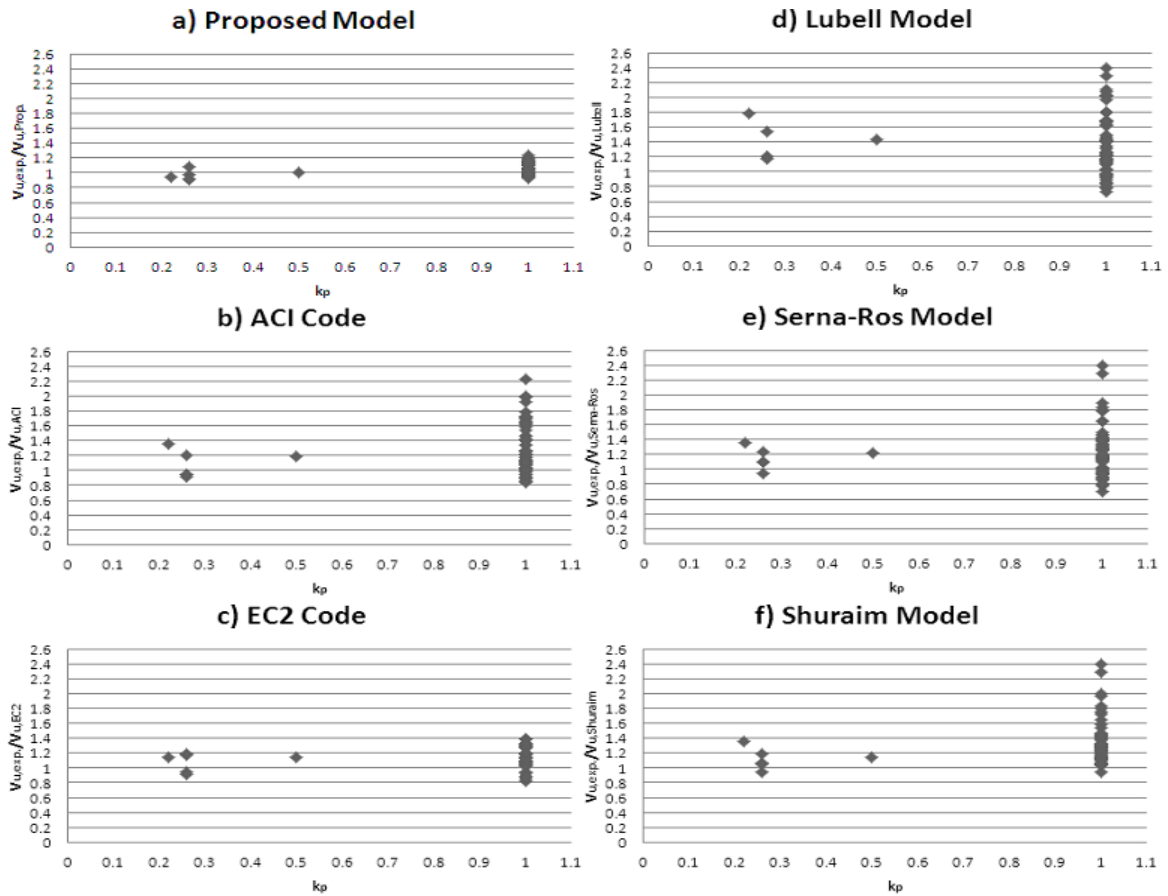


Figure 6.26:  $k_p$  versus  $V_{u,exp}/V_{u,Pred.}$ .

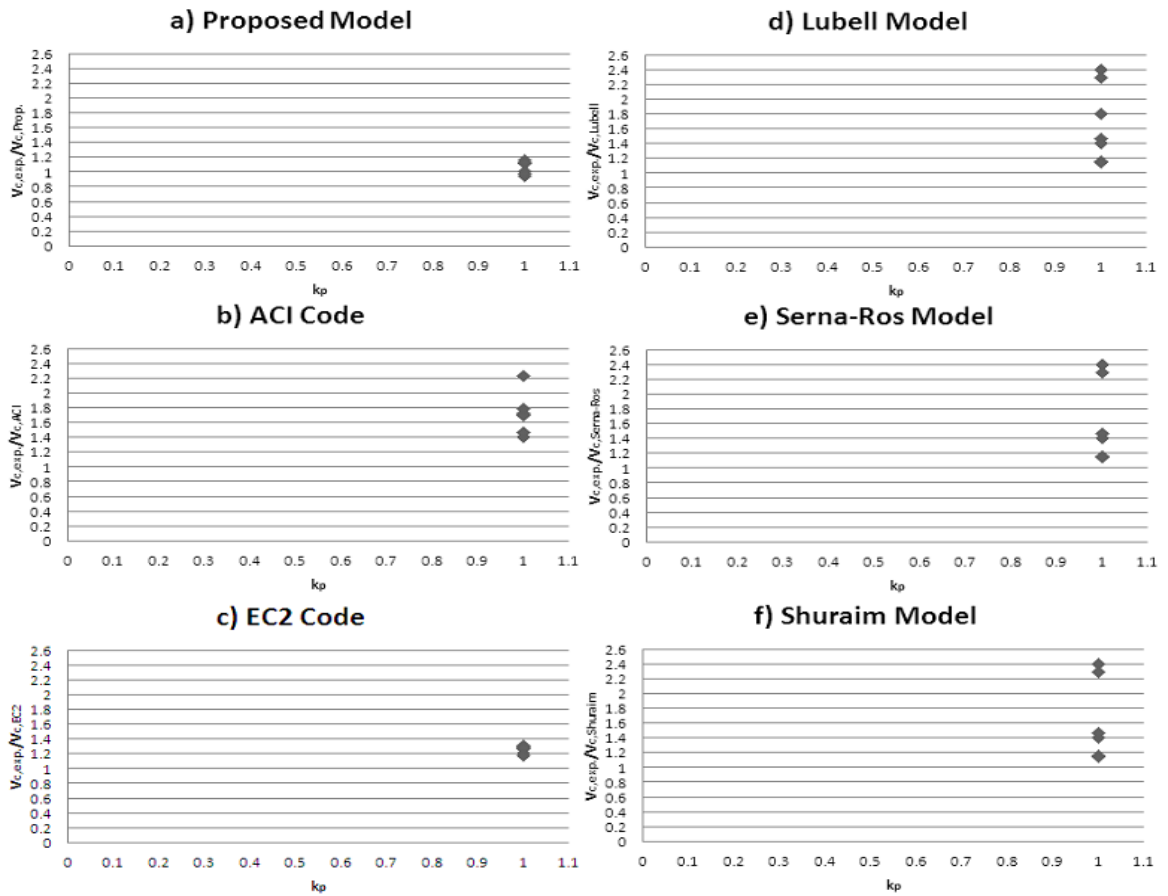


Figure 6.27:  $k_p$  versus  $V_{c,exp.}/V_{c,Pred.}$ .

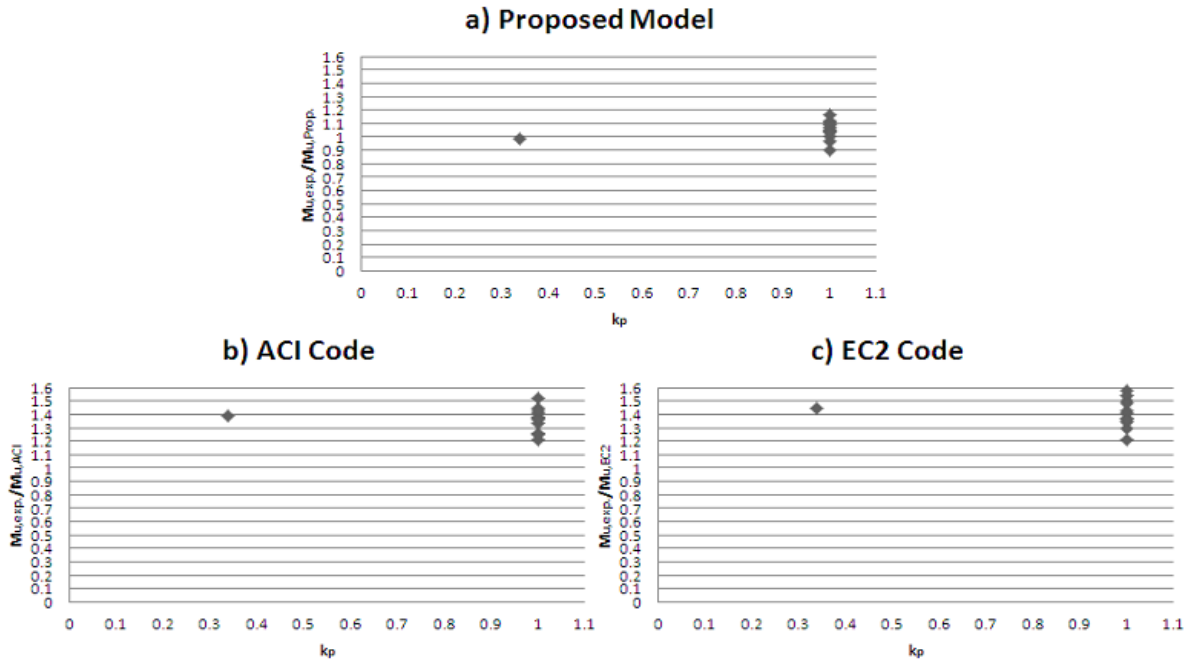


Figure 6.28:  $k_p$  versus  $\mu_{u,exp.}/\mu_{u,Pred.}$ .

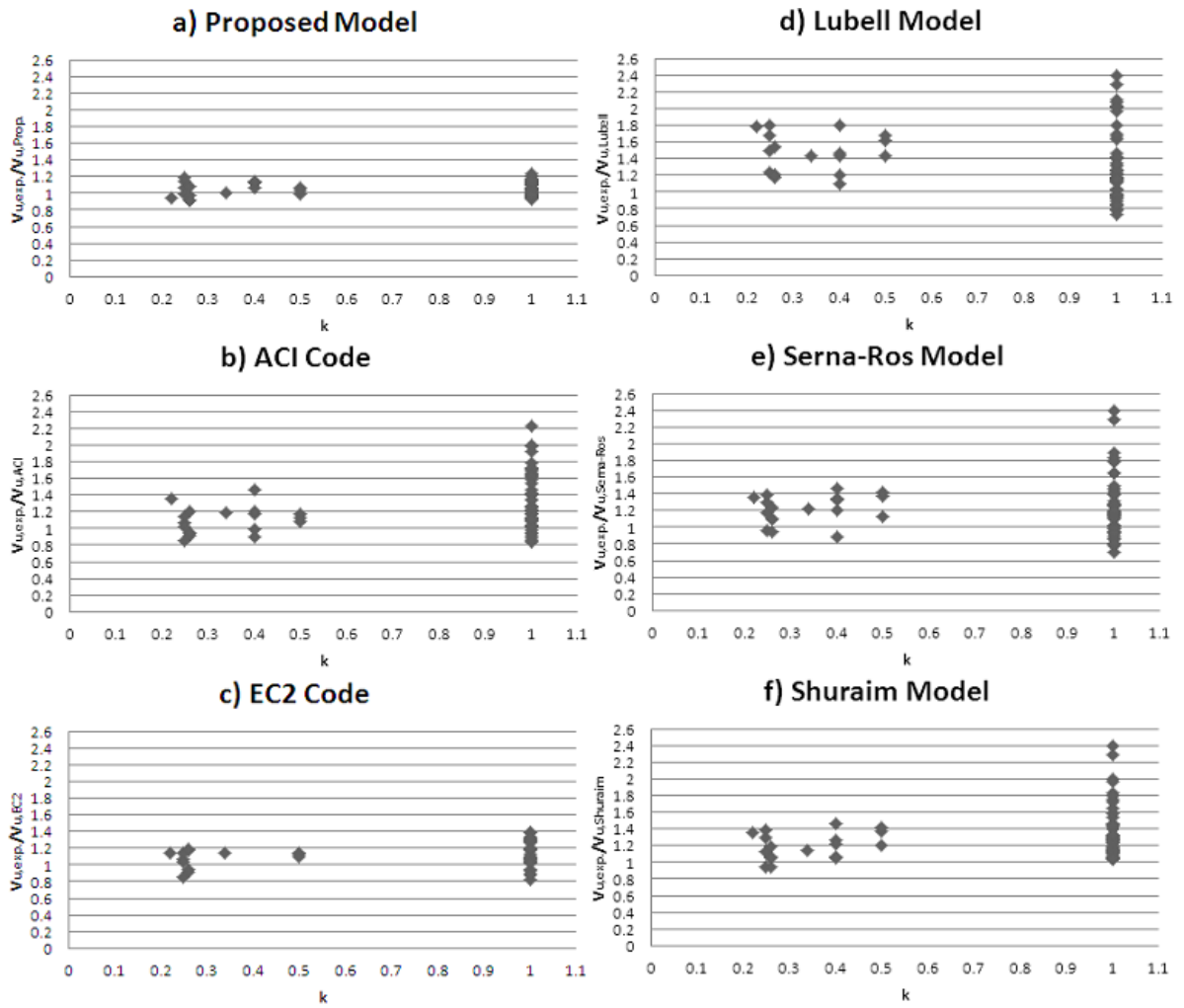


Figure 6.29:  $k$  versus  $V_{u,exp}/V_{u,Pred.}$ .

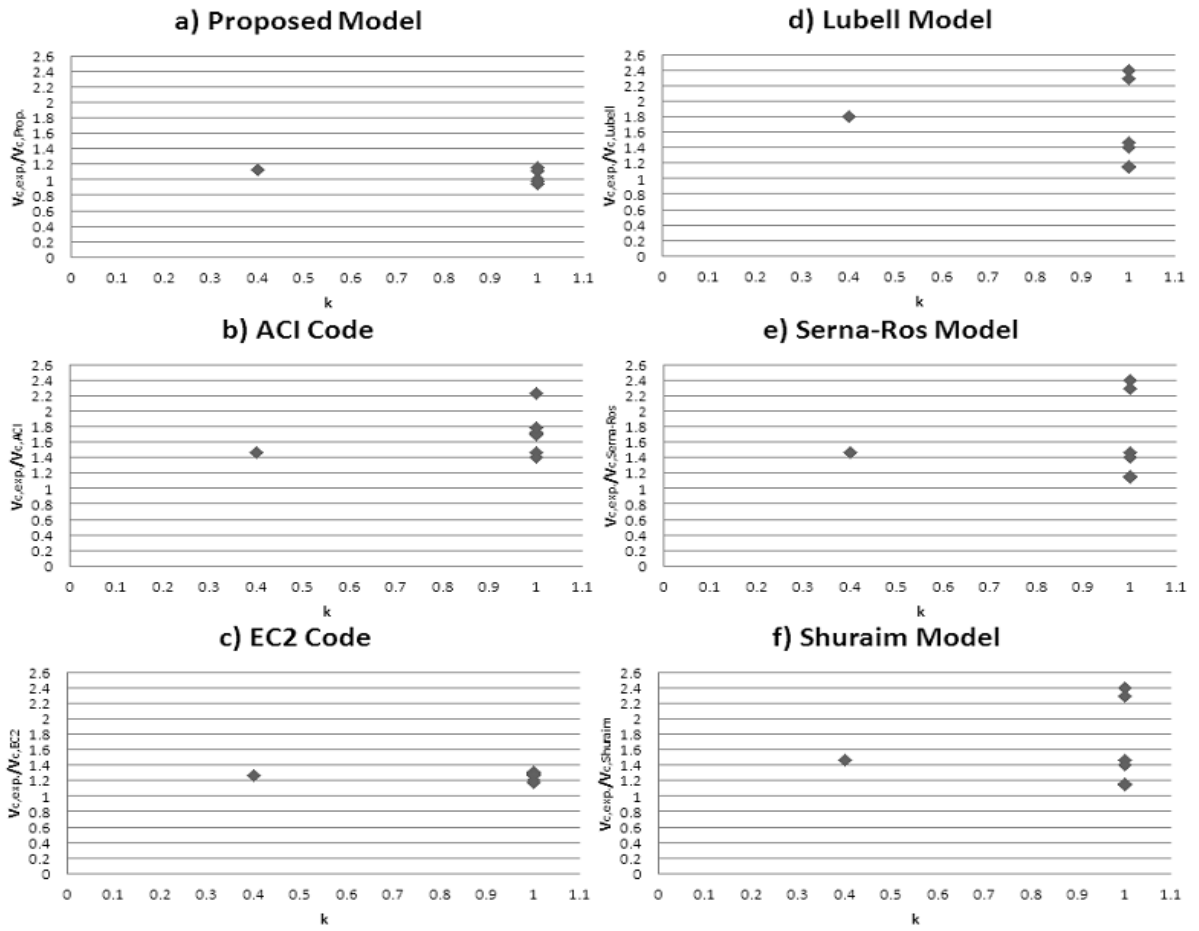


Figure 6.30:  $k$  versus  $V_{c,exp}/V_{c,Pred.}$ .

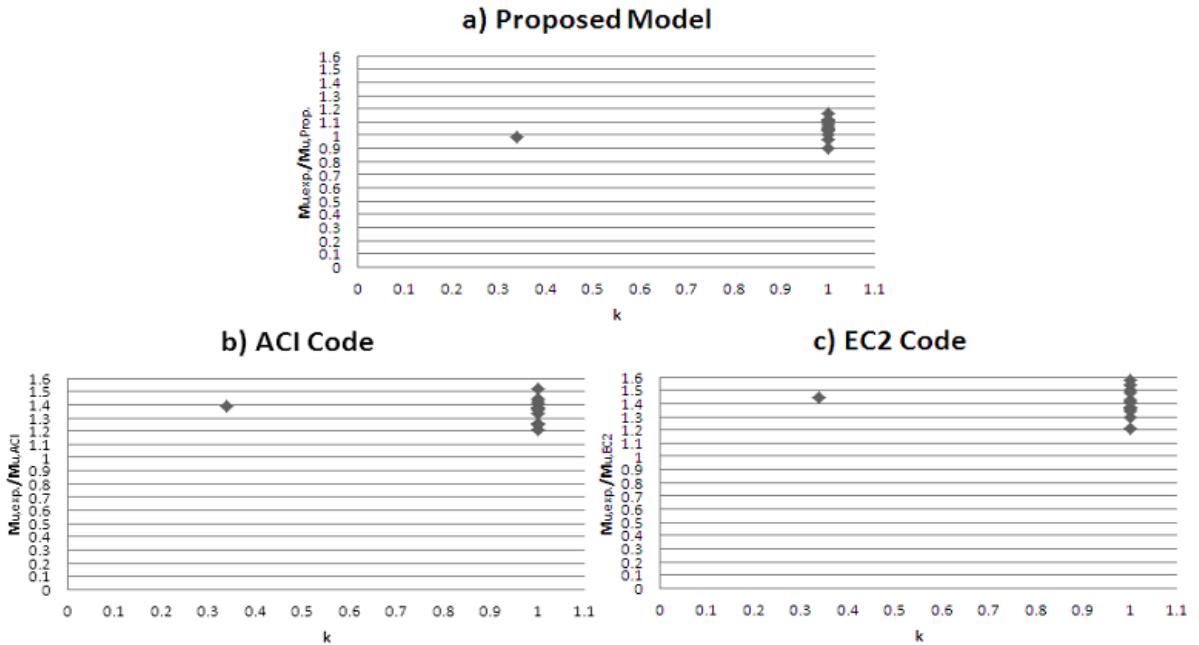


Figure 6.31:  $k$  versus  $\mu_{u,exp}/\mu_{u,Pred.}$ .



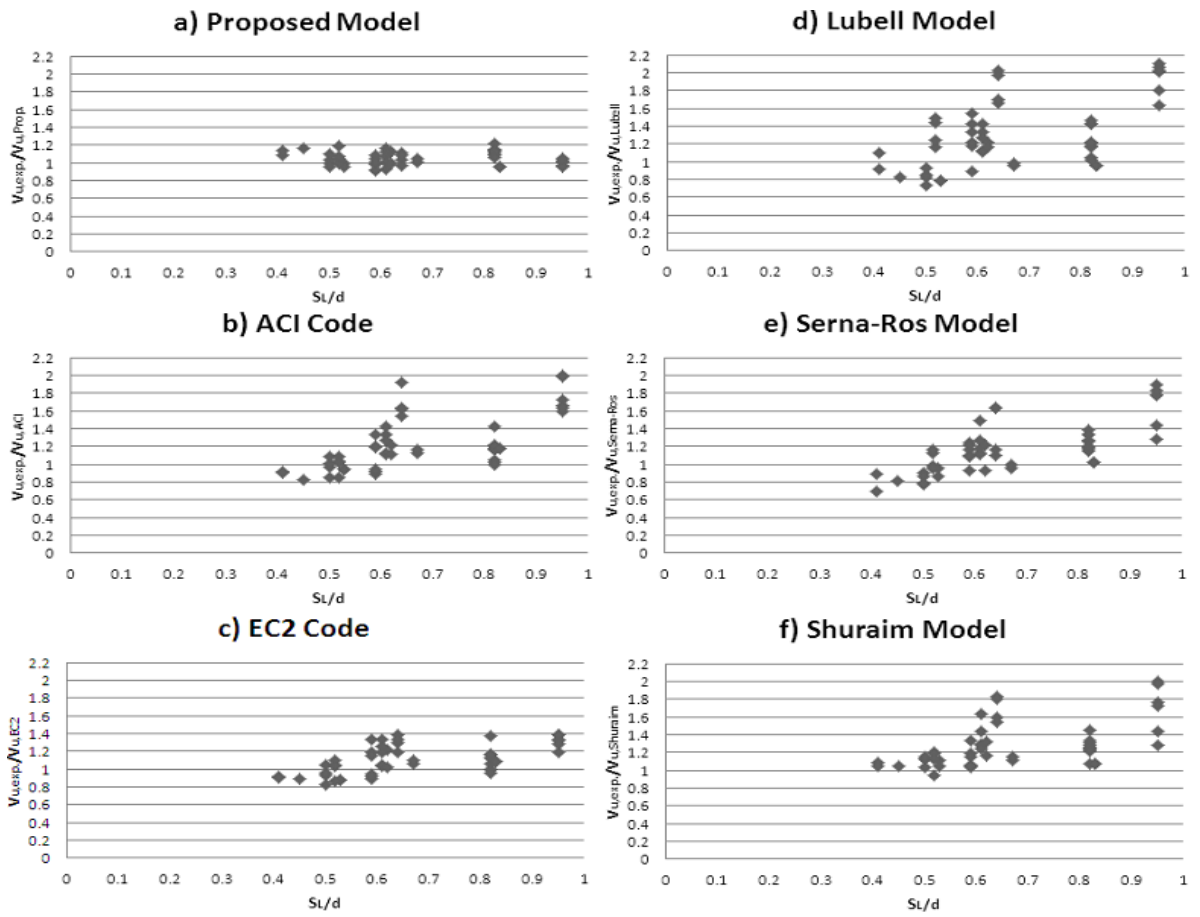


Figure 6.32:  $SL/d$  versus  $V_{u,exp}/V_{u,Pred}$ .

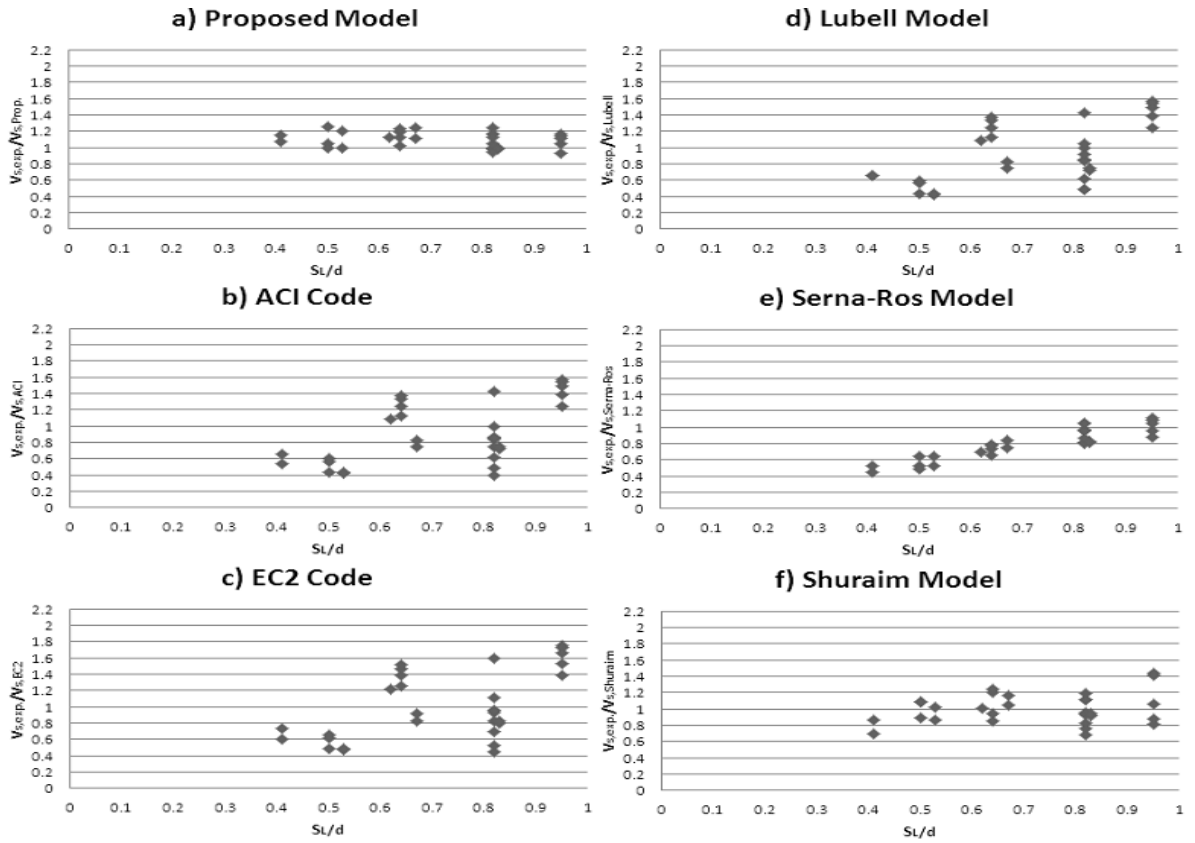


Figure 6.33:  $SL/d$  versus  $V_{s,exp}/V_{s,Pred.}$ .

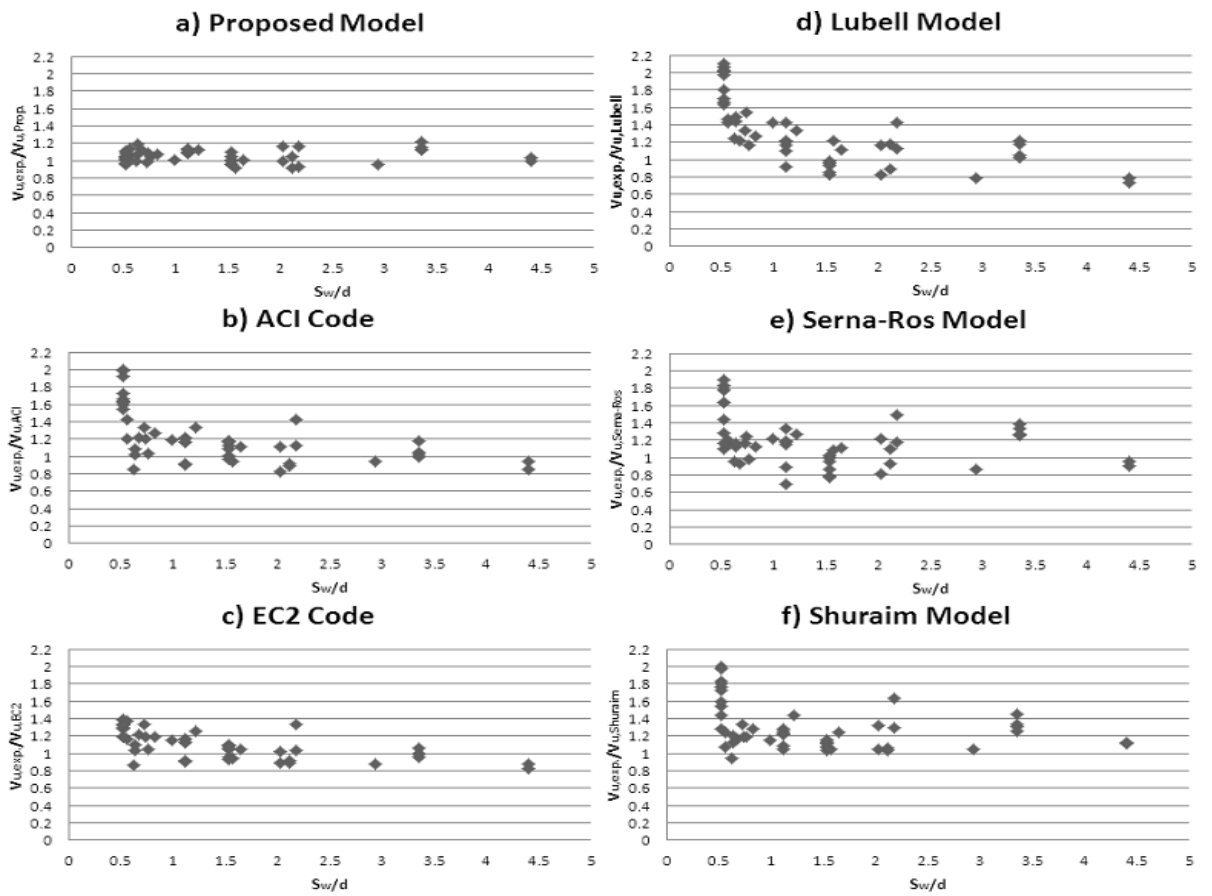


Figure 6.34:  $Sw/d$  versus  $V_{u,exp}/V_{u,Pred.}$ .

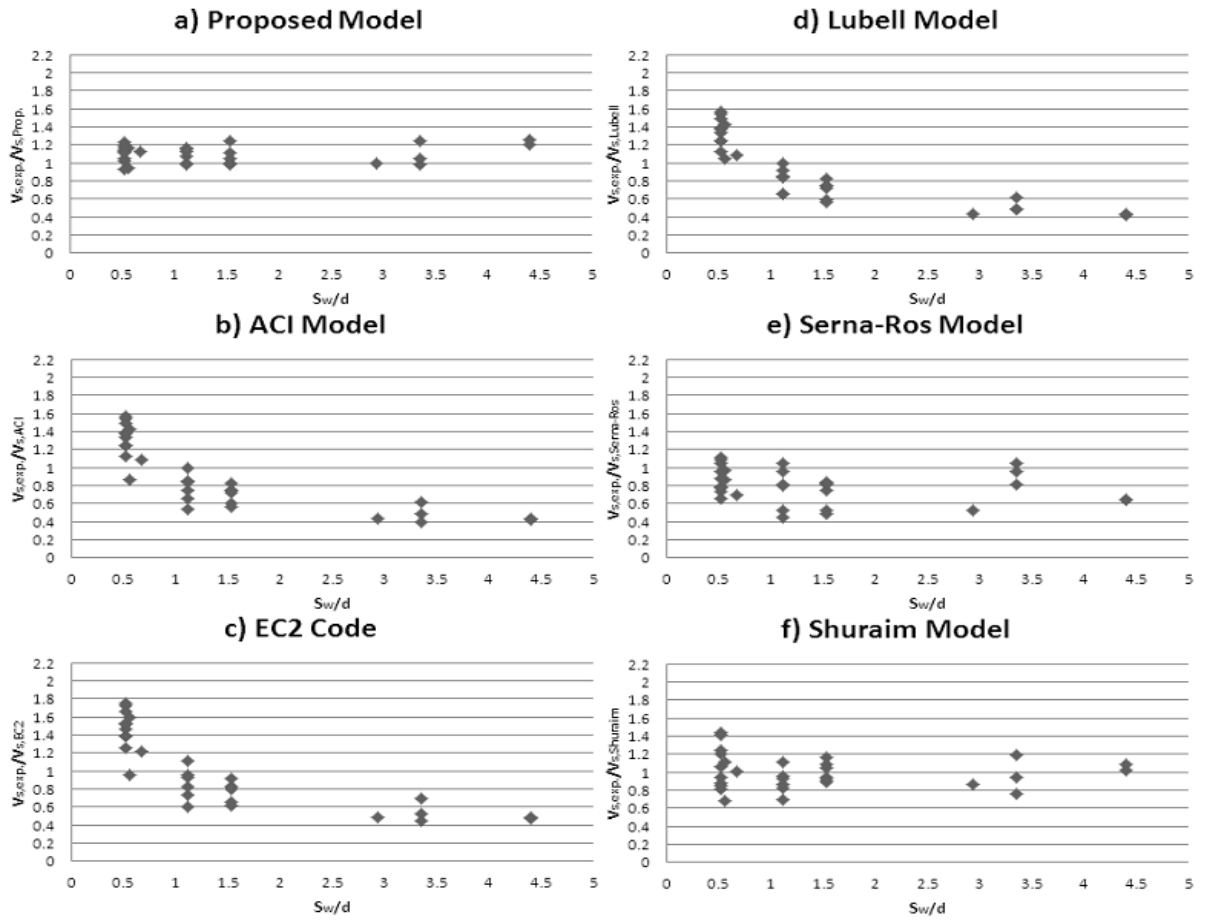


Figure 6.35:  $Sw/d$  versus  $V_{s,exp}/V_{s,Pred}$ .

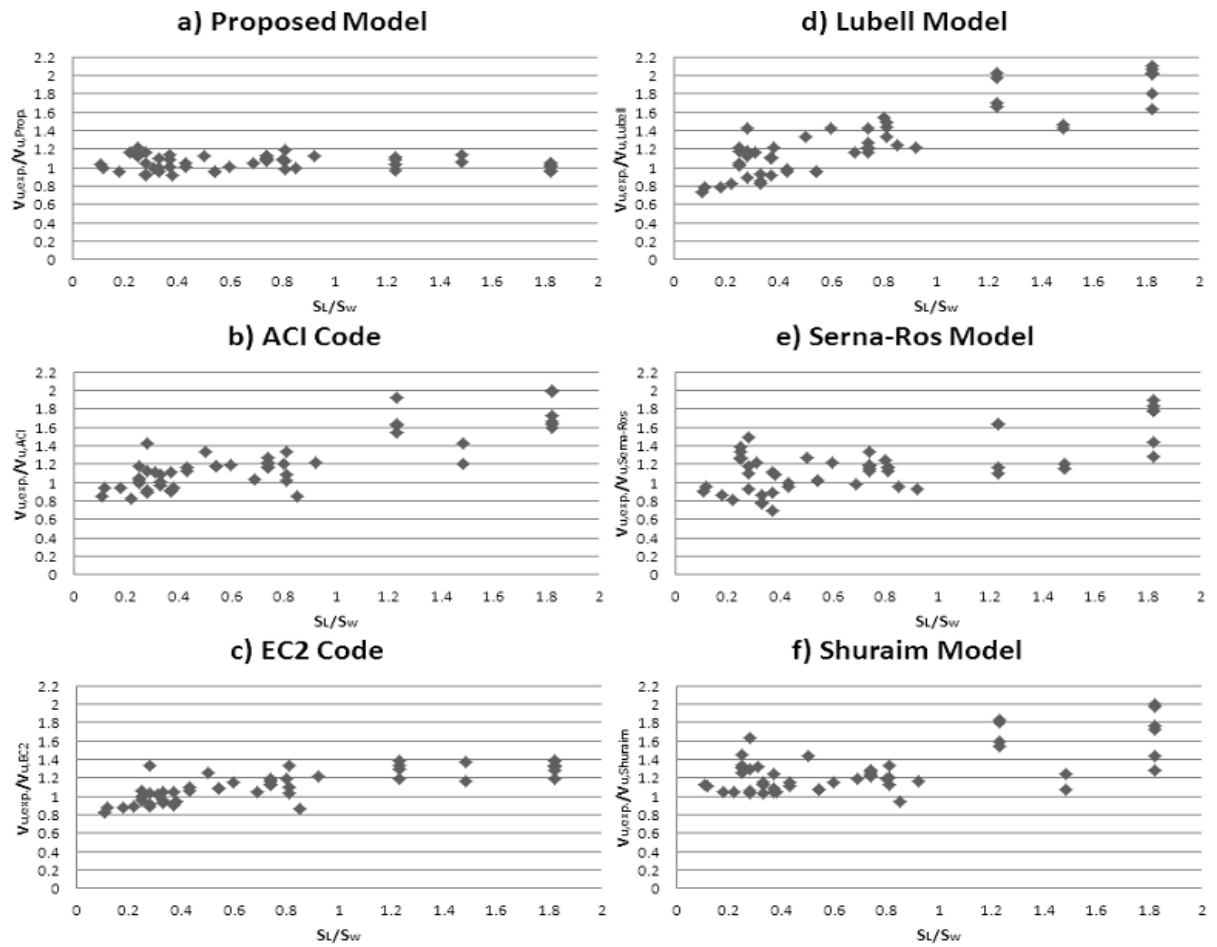


Figure 6.36:  $Sl/S_w$  versus  $V_{u,exp.}/V_{u,Pred.}$ .

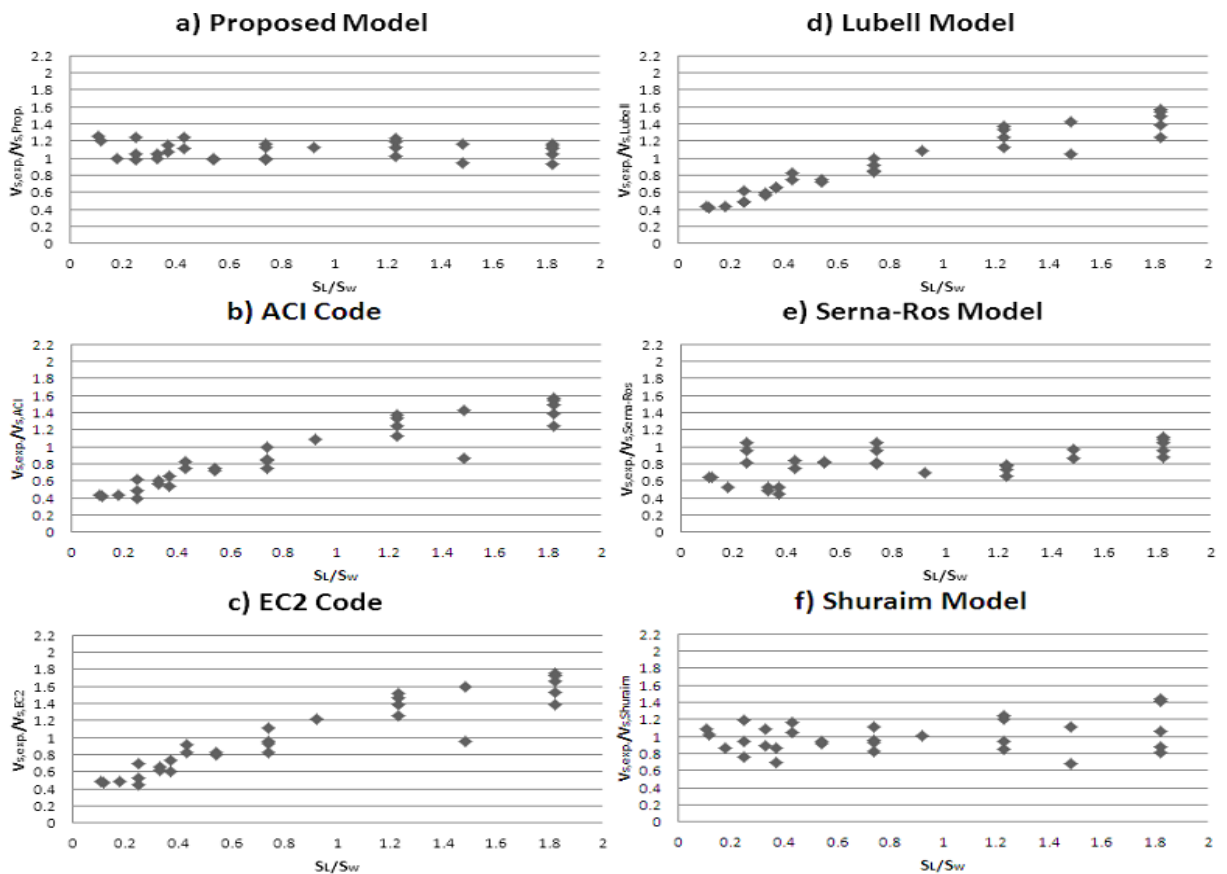


Figure 6.37:  $Sl/S_w$  versus  $V_{s,exp.}/V_{s,Pred.}$ .

## 6.5 The Suitable Load and Support Widths for Wide RC Beams

With various load and support widths, the ultimate design shear strength should be determined to check if the load and support widths are satisfied or not. Equation (6.16) is proposed to investigate the suitable load and support widths for wide RC beams, as shown below as a general framework (Alluqmani, 2013a).

$$V_{d'} = \left[ \left( (\sqrt{k}) * V_{c,d} \right) + \left( (\sqrt{k_s}) * V_{s,d} \right) \right] > V \quad (6.16)$$

If  $V_{d'} > V$ , hence the beam shear capacity as well as the load and support widths are satisfied. Where  $V_{c,d}$  and  $V_{s,d}$  are determined according to Equations (6.10) and (6.11) respectively, and  $V$  is the applied shear capacity on the designed section. The reduction in the concrete efficiency is taken as the value of  $\sqrt{k}$  (where,  $k$  is the lesser of  $k_p = b_p/b_w$  or  $k_s = b_s/b_w$ ), which is due the effect of the smallest narrow load or support. While the reduction in the stirrup efficiency is taken as the value of  $\sqrt{k_s}$  (where,  $k_s = b_s/b_w$ ), which is due the narrow support effect.

Because the proposed case, for the suitable width of loads and supports, shown in Equation (6.16) needs to be compared with the applied shear force ( $V$ ) that is determined from the applied design load and type of point-loading system, it is difficult, therefore, to find  $V$  for those beams validated in this study and then to get  $V_{d'}$  given by Equation (6.16). Nevertheless, Equation (6.16) was validated on the beams tested in Series (A) as shown in Table 6.9 (Alluqmani, 2013a, 2013b). From Table 6.9, beam ECC3 had a predicted  $V_{d'}$  value of 350 kN which was greater than  $V$  ( $V = P/2 = 300$  kN), this means, according to Equation (6.16), that both load and support widths as well as the beam shear capacity were satisfied for beam ECC3 where the beam failed in flexure as obtained from both the test and the proposed prediction model of flexural capacity (Equation (6.13)). On the other hand, beam ECC2 had a predicted  $V_{d'}$  value of 282 kN which was lesser than  $V$  (300 kN), this means, according to Equation (6.16), that both load and support widths (or at least the smallest bearing-plate width, which was the support-width ( $b_s = 240$ mm)) as well as the beam shear capacity were not satisfied for beam ECC2 where the beam failed in shear as obtained from both the test and the proposed prediction model of one-way shear capacity (Equation (6.9)). Therefore, both widths of load and supports (or at least the smallest bearing-plate width, which was the support width) of beam ECC2 should be changed to ensure that the beam shear capacity as well as the load and support widths will be satisfied.

## 6.6 Conclusion

The wide structural RC beams tested in the literature have highlighted the inadequacy of current design approaches to predict the shear and flexural strengths of wide beams (Alluqmani, 2013a, 2013b). These approaches do not treat under their design considerations the shear design of wide concrete members, especially in the transverse direction of these members when the stirrup legs are distributed across the width as well as when the bearing plates are narrower than, or equal to, the beam width. In addition, these approaches do not treat under their design considerations the flexural design of wide concrete members with full- or narrow- width loads and supports. A wide beam is firstly designed for flexure using the moment envelope and then it is designed for shear using the shear envelope (this is section design). In the design for shear, these models ignore the transverse stirrup-legs spacing as well as the widths of supports and loads of wide concrete beams, or at best, they deal with them as narrow beams for two stirrup legs across the width and full-width bearing plates (wide supports and loads). It is believed that in the design for shear, these models assume that part of the shear is carried by the concrete ( $V_c$ ) by beam and/or arch actions. The stirrups are assumed to carry the shear ( $V_s$ ) in excess of the concrete capacity through truss action. In addition,  $V_c$  is normally related to the strength of the cracked concrete below the level of the neutral axis through the so called aggregate interlock action which, if indeed it exists, is to be regarded as only a secondary mechanism (Bobrowski, 1982).

A new proposed Prediction-Model was developed based on main missed factors which show an actual influence on the flexural and shear strengths of both full- and narrow- width supported wide RC beams. It takes into the account the load- and support- widths to predict the flexural and shear strengths, as well as the transverse and longitudinal stirrup-legs spacing to predict the shear strength resisted by stirrups. The proposed prediction model was presented and validated in this Chapter. It predicts the wide RC beam strengths with improved accuracy with taking into the consideration logical influence parameters unconsidered in the design provisions of most of the current Codes of Practice which have real effect on the shear and flexural strengths. Comprehensive verification and evaluation of the proposed prediction model comparing with the existing design Codes (such as, EC2, ACI318, SBC304 and BS8110) and with other existing proposed models (such as, Lubell et al.'s model (2008), Serna-Ros et al.'s model (2002) and Shuraim's model (2012)) were conducted on more than 85 wide RC beams. It is shown that the proposed prediction model performs the best among the existing Codes and models. It shows that the flexural and shear strengths decrease as the ratios of the load- and support- width to beam width decrease, while the shear strength resisted by stirrups decreases as the transverse stirrup

legs spacing increases. These influences occur for members with and without shear reinforcement. In contrary with the existed design Codes and models mentioned above, they do not give accurate predictions for the wide RC beam strengths as the proposed prediction model developed in this study gave (Equations (6.9) and (6.13)), as shown in Tables 6.3 to 6.11 and Figures 6.22 to 6.37 (Alluqmani, 2013a, 2013b).

The two beams tested in Series (A), to investigate the shear and flexural behaviours of wide RC beams, were used together with those beams tested previously in the literature for developing the proposed Prediction-Model. The main feature of the proposed prediction model is that it can predict the failure load and failure mode of the wide RC beams. The main factors affecting the shear and flexural strengths of wide RC beams have been taken into the account when the proposed prediction model was being developed.

Because wide members subject to higher shear stresses have a greater proportion of their total shear strength from the stirrup contribution ( $V_s$ ), Lubell et al (2009a) recommended that it is essential that a high stirrup efficiency factor is achieved. Accordingly, this recommendation validates the proposed prediction model provided in Equations (6.9) where the factor is  $K_{sd}$  (Equation (6.6)), which consists of two terms, namely:  $\mu_v$  and  $\beta_k$  (Equations (6.7) and (6.8), respectively) explained in this Chapter.

Based on the results given by the proposed prediction model, it can be concluded that (Alluqmani, 2013a, 2013b):

1. The shear strength (shear force) of wide RC beams provided by concrete and stirrups ( $V_c$  and  $V_s$ , respectively) can be determined using the provisions of the current Codes of Practice if they are corrected by the factors of  $K_{cd}$  and  $K_{sd}$ , respectively, as given by the proposed prediction model. It should be noted that for this model the strut angle ( $\theta$ ) should be assumed 45 degrees.

2. The flexural strength (bending moment) of wide RC beams can be determined using the provisions of the current Codes of Practice if it is corrected by the factor of  $K_{cd}$ , as given by the proposed prediction model.

## CHAPTER 7

# BEHAVIOUR OF WIDE RC BEAMS DESIGNED TO THE EC2 CODE: SERIES (1)

### 7.1 Introduction

The main variables for investigating the behaviour of beam specimens in Test-Series (1) are to study the influence of the longitudinal and transverse spacing of stirrup-legs ( $S_L$  and  $S_w$ ) and the ratios of the load- and support- width to the beam-width ( $k_p$  and  $k_s$ ) on the capacities of wide RC beams with full- and narrow- width loads and supports, as well to verify the proposed Prediction-Model (Alluqmani, 2013a).

Test-Series (1) included 16 simply supported wide RC beams with concentrated load for a three point-loading system. The specimens in Test-Series (1) were detailed and designed according to the design provisions (requirements) of the current Codes of Practice, such as EC2 Code. The experimental test programme, the material properties, beam manufacture, test arrangements and procedures, and experimental methodology for Test-Series (1) specimens are described and discussed in this Chapter. Moreover, this Chapter discusses the experimental works in general for those wide RC beams tested and investigated in Test-Series (1).

### 7.2 Description of Test Specimens

Test-Series (1) included 16 wide RC beam specimens made with normal-strength concrete and high-strength reinforcement. The specimens were designed, constructed and examined at The University of Strathclyde, Glasgow-UK (Alluqmani, 2013a). All wide RC beam specimens to be experimentally investigated were simply supported beams using a three point-loading system. The specimens were detailed and designed for flexure and shear using the methods in current Codes of Practice, such as EC2 Code. The scope of this programme of research for the beams in Test-Series (1) focuses on the behaviours of wide concrete beams, with constant cross section and constant flexural (longitudinal) reinforcement along the beam length. The shear (transverse) reinforcement made up exclusively by closed vertical stirrups with 4-legs 8mm diameter distributed along the beam length and across the beam width. The main concern is to analyse the influence of the longitudinal stirrup-legs spacing ( $S_L$ ), transversal stirrup-legs spacing ( $S_w$ ),



support-width to beam-width ratio ( $k_s = b_s/b_w$ ) and load-width to beam-width ratio ( $k_p = b_p/b_w$ ) on the strengths of wide RC beams. Where  $b_s$  is support width,  $b_p$  is load width, and  $b_w$  is beam width.

The results to be analysed were obtained from the test to failure carried out on 16 wide beams (Table 7.1). The analysis will also focus on the comparison between the strengths actually reached in the tests and those values that would be obtained applying the calculation formulae included in the Codes, such as EC2, ACI318 and SBC304 Codes, and with those values obtained from the proposed prediction model and the existing shear models. Several improvements to the Codes are proposed in order to take such effects into account for use in practice. Some design recommendations about spacing of stirrups to optimise the vertical shear reinforcement effectiveness, and about distribution of longitudinal flexural bras to resist the high stresses within the effective-widths of supports and loads are included in this study to make the wide beam behaves in a ductile flexural manner and then to prevent premature shear failures.

**Table 7.1<sup>#</sup>:** Test Series "1" to study the Effect of **SL**, **Sw**, **ks** and **kp** on Wide Beam Strengths and to verify the Proposed Prediction Model<sup>^</sup>.

		Beam-Type (A)	Beam-Type (B)	Beam-Type (C)	Beam-Type (D)
		$k_p = 1.0, k_s = 1.0$	$k_p = 0.50, k_s = 0.50$	$k_p = 0.25, k_s = 0.50$	$k_p = 0.50, k_s = 0.25$
		$k = 1.0$	$k = 0.50$	$k = 0.25$	$k = 0.25$
<b>Test-Series (1):</b> bw/h = 2.0 Normal Design (SL = 0.65d = 166) <sup>*1</sup> (SL = 0.75d = 192) <sup>*2</sup> d = 257mm	<b>Beam Group</b>	<b>Effect of SL, Sw, ks and kp on Wide-Beam Strengths</b>			
	<b>Without Stirrups</b>	<b>Beam A1-0</b>	<b>Beam B1-0</b>	<b>Beam C1-0</b>	<b>Beam D1-0</b>
	SL = 0.65d = 166 Sw ≈ 0.75d ≈ 1.16*SL = 192 <sup>*3</sup>	<b>Beam A1-1a</b> (Sw = 0.75d = 1.16*SL)	<b>Beam B1-1a</b> (Sw = 0.75d = 1.16*SL)	<b>Beam C1-1a</b> (Sw = 0.75d = 1.16*SL)	<b>Beam D1-1a</b> (Sw = 0.75d = 1.16*SL)
	SL = 0.75d = 192 Sw ≈ 0.75d ≈ SL = 192 <sup>*3</sup>	<b>Beam A1-1b</b> (Sw = 0.75d = SL)	<b>Beam B1-1b</b> (Sw = 0.75d = SL)	<b>Beam C1-1b</b> (Sw = 0.75d = SL)	<b>Beam D1-1b</b> (Sw = 0.75d = SL)
SL = 0.75d = 192 Sw = d = 1.34*SL = 257 <sup>*4</sup>	<b>Beam A1-2</b> (Sw = d = 1.34SL)	<b>Beam B1-2</b> (Sw = d = 1.34SL)	<b>Beam C1-2</b> (Sw = d = 1.34SL)	<b>Beam D1-2</b> (Sw = d = 1.34SL)	

# This Test Series is aimed to 1. Validate the proposed prediction Model, 2. Study the influence of SL, Sw, ks and kp on Wide-Beam Strengths and then modifications may be added to the proposed prediction model, and 3. Develop a new detailing and design model to be used in a new Test Series.

<sup>^</sup> The Proposed Prediction Model:

a) The Shear Strength:

$$V_{u,d} = V_{c,d} + V_{s,d} = (K_{cd} * V_c) + (K_{sd} * V_s), \text{ where } K_{cd} = \mu_s * \beta_g = \{ [F * (\rho_s - \rho_s')] * [\sqrt{k^{(b/b_w)}}] \}, K_{sd} = \mu_v * \beta_k = \{ [\sqrt{SL/Sw}] * [\sqrt{k_s^{(1-k_s)}}] \}.$$

b) The Flexural Strength:

$$M_{u,d} = K_{cd} * M_u = (\mu_s * \beta_g) * M_u = \{ [F * (\rho_s - \rho_s')] * [\sqrt{k^{(b/b_w)}}] \} * M_u, \text{ where } M_u = A_{s,prov} * f_{y,act} * j * d, \text{ and } j * d = Z = (2/3) * h.$$

For  $|\rho_s - \rho_s'| > 1.0\%$ :  $F = 100$  (but if  $|\rho_s - \rho_s'| > 1.60\%$ , use  $F = 60$ ) for  $k_s = 1.0$ ; while  $F = 120$  for  $k_s < 1.0$ .

For  $|\rho_s - \rho_s'| < 1.0\%$ :  $F = 140$  for  $k_s = 1.0$ ; while  $F = 170$  for  $k_s < 1.0$ . But if  $|\rho_s - \rho_s'| < 0.50\%$ , use  $F = (100 * bw/h)$  whatever the support width.

\*1 SL is calculated according to the limits of the Code provisions. SL ≈ 0.65d = 166mm for Group (1a), and must be distributed along the beam length.

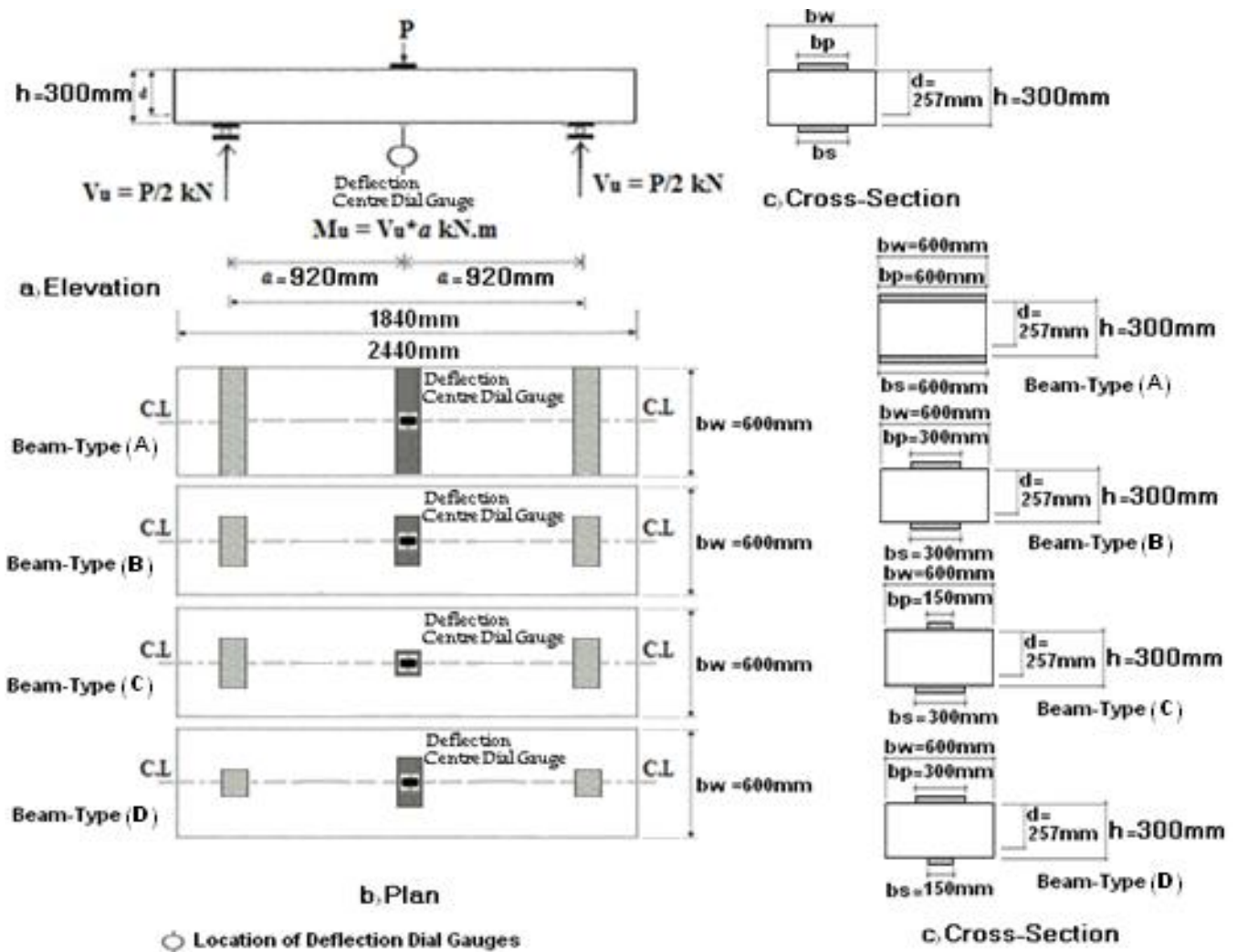
\*2 SL is calculated according to the Code provisions. SL ≈ 0.75d = 192mm for Groups (1b and 2), and must be distributed along the beam length.

\*3 Sw is taken as SL (≈ 0.75d = 192mm) for Groups (1a and 1b), and Sw is distributed within the beam width.

\*4 Sw is taken as d (≈ d = 257mm) for Group (2), and Sw is distributed within the beam width.

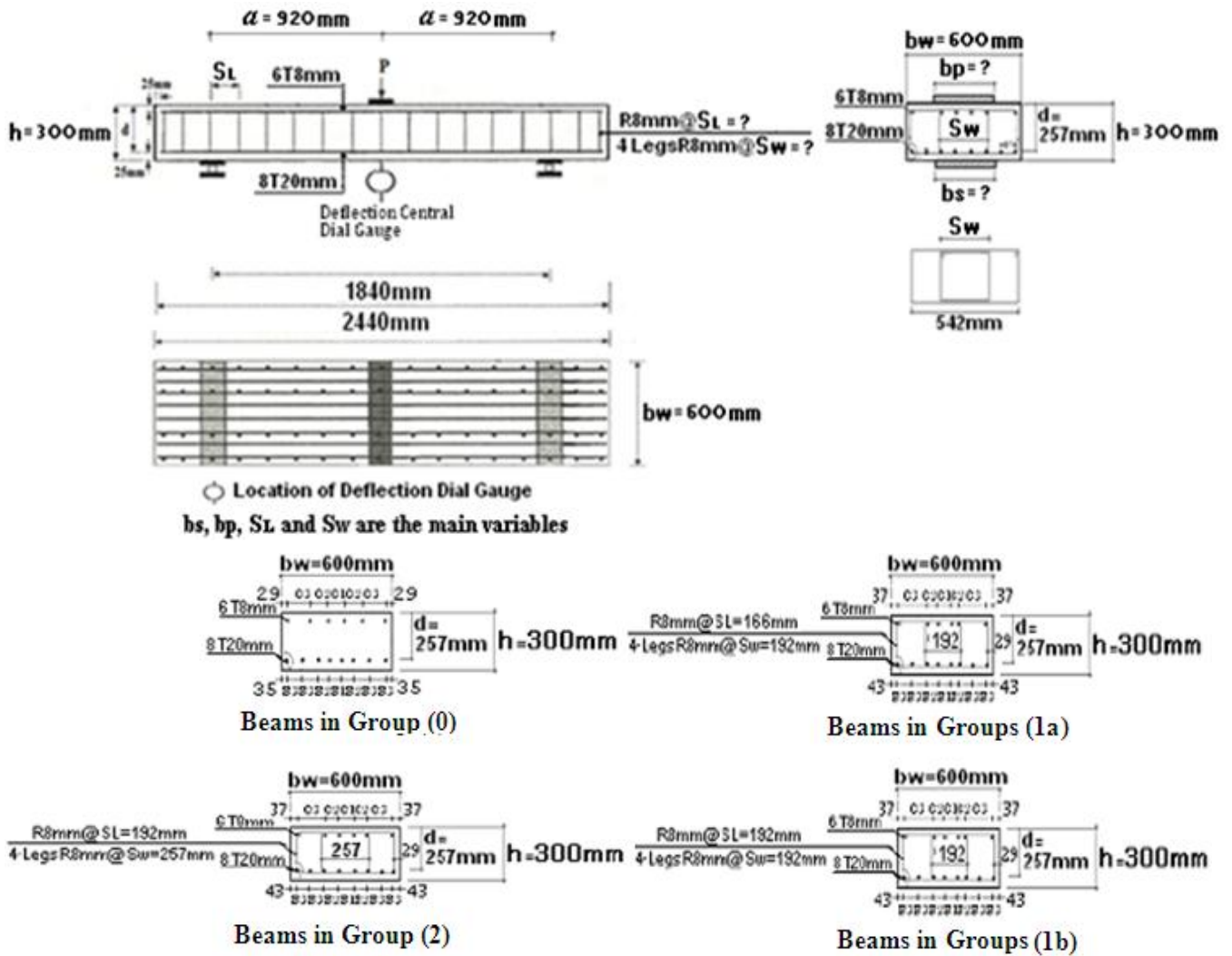
- All beams have the same bw/h ratio equal to 2.0 (bw = 600mm, h = 300mm, d = 257mm), the same  $\rho_s$  ratio greater than 1.0% (equal to 1.63%, 8Φ20mm), the same  $\rho_s'$  ratio less than 1.0% (equal to 0.196%, 6Φ8mm), and the same  $A_v$  equal to 201mm<sup>2</sup> (4-LegsΦ8mm).

Table 7.1 shows the types and groups of the beams in Test-Series (1) used to study the effect of  $S_L$ ,  $S_w$ ,  $k_s$  and  $k_p$  on the wide beam Strengths, and to verify the proposed prediction model. Figures 7.1 and 7.2 show typical description of the details and design of wide RC beam specimens, respectively, used in Test-Series (1).



Series (1)/ All Groups	No. of Beams	Beam Dimensions				Support Plate Dimensions			Loading Plate Dimensions		
		L	$b_w$	h	d	$b_s$	$C_s$	$T_s$	$b_p$	$C_p$	$t_p$
Beam-Type (A)	4	2440	600	300	257	600	150	25	600	150	25
Beam-Type (B)	4	2440	600	300	257	300	150	25	300	150	25
Beam-Type (C)	4	2440	600	300	257	300	150	25	150	150	25
Beam-Type (D)	4	2440	600	300	257	150	150	25	300	150	25

Figure 7.1: Details of Wide Beam Specimens in Test-Series "1".



Series (1)/ All Groups	No. of Beams	Beam Dimensions					Support Plate Dimensions			Loading Plate Dimensions			Stirrup Legs Spacing		Bottom (Tensile) Reinf. Spacing			Top (Comp.) Reinf. Spacing		
		L	bw	h	d	bs	C <sub>s</sub>	T <sub>s</sub>	bp	C <sub>p</sub>	tp	SL	Sw	S <sub>1</sub>	S <sub>2</sub>	S <sub>3</sub>	C <sub>1</sub>	C <sub>2</sub>	C <sub>3</sub>	
Beam-Type (A)	4	2440	600	300	257	600	150	25	600	150	25	-	-	70	70	80	94	94	130	
Beam-Type (B)	4	2440	600	300	257	300	150	25	300	150	25	166	192	55	54.5	87.5	59	58.5	175	
Beam-Type (C)	4	2440	600	300	257	300	150	25	150	150	25	192	192	55	54.5	87.5	59	58.5	175	
Beam-Type (D)	4	2440	600	300	257	150	150	25	300	150	25	192	257	77	76	71.25	81	80	142.5	

Figure 7.2: Design of Wide Beam Specimens in Test-Series "1".

### 7.3 Design and Configurations of Test Specimens

All beam specimens were designed for their reinforcements according to the current Codes of Practice, such as EC2 Code. The beams had 600mm wide, 300mm height, 2440mm overall length, 1840mm effective span, 20mm diameter of tension flexural bars, 8mm diameter of compression flexural (hanger) bars, 8mm diameter of stirrups, a longitudinal reinforcement ratio ( $\rho_s$ ) of 1.63%, a shear-span to effective-depth ratio ( $a/d$ ) of 3.58 (type II beams), a three point-loading arrangement, and full- and narrow- width load and support conditions ( $b_p = b_s$ ,  $b_p < b_s$  or  $b_p > b_s$ ). The stirrups legs spacing along the beam length and across the beam width, the support

width and the load width were the main variables in this investigation. The number of bars in the tension and compression zones was the same in all test specimens, where  $\rho_s = 1.63\%$  and  $\rho_s' = 0.196\%$ .

The specimens, which were described in Figures 7.1 and 7.2, and Table 7.2, were constructed to nominal dimensions of 600mm width, 300mm total height (257mm effective depth), and 2440mm total length (1840mm clear span). The specimens were analyzed, designed and tested under three-point loading with a central span of 1840mm and shear span of 920mm, giving a shear-span to effective-depth ratio ( $a/d$ ) of 3.58. They were designed to carry a concentrated design load ( $P_d$ ) in the mid-span point of 470 kN. The specimens were loaded and supported either with wide steel-plates by 25x150x600mm for full-width bearing-plates, or with narrow steel-plates by 25x150x300mm and/or 25x150x150mm for partial-width bearing-plates. The specimens in Group (0) were without shear-reinforcement. The specimens in Groups (1a, 1b and 2) were with shear- reinforcement.

Test-Series (1) includes beams with and without shear reinforcement. Series (1) was divided to four Types (Types A, B, C and D) which were based on the width of supports and loads, and each Beam-Type had four Groups (Groups 0, 1a, 1b and 2) which were based on the shear reinforcements and their spacing (Table 7.1). The beams in Type (A) had full-width loads and supports, where  $k_p = k_s = 1.0$ . The beams in Type (B) had narrow-width loads and supports, where  $k_p = k_s = 0.50$ . The beams in Type (C) had narrow-width loads and supports, but the loads were narrower than the supports, where  $k_p = 0.25$  and  $k_s = 0.50$ . The beams in Type (D) had narrow-width loads and supports, but the supports were narrower than the loads, where  $k_p = 0.50$  and  $k_s = 0.25$ . Each Beam-Type includes beams with and without shear reinforcement. The beams in Group (0) were without shear-reinforcement, and were used as references. The beams in Groups (1a, 1b and 2) were with shear-reinforcements and their longitudinal and transverse spacing ( $S_L$  and  $S_w$ ) were taken as a percentage of the effective-depth of the beam ( $d$ ). Web reinforcement patterns included four stirrup-legs across the width in all specimens, two legs near the specimen edges (external legs) and two legs concentrated between edge and central beam-width (internal legs), which are measured from the centre line of the beam width ( $b_w$ ). All specimens had the same main longitudinal reinforcement (8 $\varnothing$ 20mm), resulting in a  $\rho_s$  ratio of 1.63%. Top longitudinal (hanger) bars (6 $\varnothing$ 8mm) were used to anchor the stirrups, but would have minimal influence on overall member response.  $S_L$  should be distributed along the member length, and  $S_w$  should be arranged and distributed across the member width. The total number of the flexural -tensile and -compressive reinforcing bars was distributed within the beam width.

**Table 7.2:** Design Details of the Wide Beams in Test-Series "1".

Beam Type	Cross-Section Dimensions	Tensile Reinforcement	Compressive Reinforcement	Shear Reinforcement Along the Length, C/C	Shear Reinforcement Across the Width, C/C
Beam A1-0	600*300mm Ac =180000mm <sup>2</sup>	8T20mm As =2514mm <sup>2</sup>	6T8mm As' =302mm <sup>2</sup>	----	----
Beam A1-1a	600*300mm Ac =180000mm <sup>2</sup>	8T20mm As =2514mm <sup>2</sup>	6T8mm As' =302mm <sup>2</sup>	15 Stirrups R8mm@166mm	4 Stirrup Legs-R8mm @192-542mm
Beam A1-1b	600*300mm Ac =180000mm <sup>2</sup>	8T20mm As =2514mm <sup>2</sup>	6T8mm As' =302mm <sup>2</sup>	13 Stirrups R8mm@192mm	4 Stirrup Legs-R8mm @192-542mm
Beam A1-2	600*300mm Ac =180000mm <sup>2</sup>	8T20mm As =2514mm <sup>2</sup>	6T8mm As' =302mm <sup>2</sup>	13 Stirrups R8mm@192mm	4 Stirrup Legs-R8mm @257-542mm
Beam B1-0	600*300mm Ac =180000mm <sup>2</sup>	8T20mm As =2514mm <sup>2</sup>	6T8mm As' =302mm <sup>2</sup>	----	----
Beam B1-1a	600*300mm Ac =180000mm <sup>2</sup>	8T20mm As =2514mm <sup>2</sup>	6T8mm As' =302mm <sup>2</sup>	15 Stirrups R8mm@166mm	4 Stirrup Legs-R8mm @192-542mm
Beam B1-1b	600*300mm Ac =180000mm <sup>2</sup>	8T20mm As =2514mm <sup>2</sup>	6T8mm As' =302mm <sup>2</sup>	13 Stirrups R8mm@192mm	4 Stirrup Legs-R8mm @192-542mm
Beam B1-2	600*300mm Ac =180000mm <sup>2</sup>	8T20mm As =2514mm <sup>2</sup>	6T8mm As' =302mm <sup>2</sup>	13 Stirrups R8mm@192mm	4 Stirrup Legs-R8mm @257-542mm
Beam C1-0	600*300mm Ac =180000mm <sup>2</sup>	8T20mm As =2514mm <sup>2</sup>	6T8mm As' =302mm <sup>2</sup>	----	----
Beam C1-1a	600*300mm Ac =180000mm <sup>2</sup>	8T20mm As =2514mm <sup>2</sup>	6T8mm As' =302mm <sup>2</sup>	15 Stirrups R8mm@166mm	4 Stirrup Legs-R8mm @192-542mm
Beam C1-1b	600*300mm Ac =180000mm <sup>2</sup>	8T20mm As =2514mm <sup>2</sup>	6T8mm As' =302mm <sup>2</sup>	13 Stirrups R8mm@192mm	4 Stirrup Legs-R8mm @192-542mm
Beam C1-2	600*300mm Ac =180000mm <sup>2</sup>	8T20mm As =2514mm <sup>2</sup>	6T8mm As' =302mm <sup>2</sup>	13 Stirrups R8mm@192mm	4 Stirrup Legs-R8mm @257-542mm
Beam D1-0	600*300mm Ac =180000mm <sup>2</sup>	8T20mm As =2514mm <sup>2</sup>	6T8mm As' =302mm <sup>2</sup>	----	----
Beam D1-1a	600*300mm Ac =180000mm <sup>2</sup>	8T20mm As =2514mm <sup>2</sup>	6T8mm As' =302mm <sup>2</sup>	15 Stirrups R8mm@166mm	4 Stirrup Legs-R8mm @192-542mm
Beam D1-1b	600*300mm Ac =180000mm <sup>2</sup>	8T20mm As =2514mm <sup>2</sup>	6T8mm As' =302mm <sup>2</sup>	13 Stirrups R8mm@192mm	4 Stirrup Legs-R8mm @192-542mm
Beam D1-2	600*300mm Ac =180000mm <sup>2</sup>	8T20mm As =2514mm <sup>2</sup>	6T8mm As' =302mm <sup>2</sup>	13 Stirrups R8mm@192mm	4 Stirrup Legs-R8mm @257-542mm

The longitudinal stirrup-legs spacing (SL) was designed for each beam with stirrups to be either 166mm (= 0.65d) along the beam length for the beams in Group (1a), or 192mm ( $\approx$  0.75d) along the beam length for the beams in Groups (1b) and (2). The transverse stirrup-legs spacing ( $S_w$ ) for interior legs was designed for each beam with stirrups to be either 192mm (= 0.75d) across the beam width for the beams in Groups (1a) and (1b), or 257mm (= d) across the beam width for the beams in Group (2) where the spacing of d that equals to the beam effective-depth was chosen as an ultimate value for  $S_w$ .  $S_w$  for external legs was 542mm for all specimens with stirrups in Test-Series (1). Details of the reinforcements are shown in Figure 7.2.

The beams in Group (1a) had  $SL = 0.65d$  and  $S_w = 0.75d$ . The beams in Group (1b) had  $SL = 0.75d$  and  $S_w = 0.75d$ . Beams in Group (2) had  $SL = 0.75d$  and  $S_w = d$ .  $SL$  and  $S_w$  were

determined based on the provisions of the current Codes, such as EC2 Code, except  $S_w$  for the beams in Group (2) which was chosen as a maximum value equal to  $d$ , Tables 7.1, 7.2 and 7.3. Spacing, which was chosen to be approximately equal to  $0.65d$ ,  $0.75d$  or  $d$ , is because it seemed likely that members where the longitudinal spacing of the stirrups was close to the maximum permitted by EC2 Code would be more sensitive to any detrimental effects of wide spacing across the width of the member. The beams in Series (1) were also used to verify the proposed prediction-model for predicting the wide RC beam strengths. The design details of the test specimens in Test-Series (1) are shown in Table 7.2. The characteristics and properties of the test specimens are shown in Table 7.3. Figure 7.3 shows various steel plates used in different cases of load and support conditions.

**Table 7.3:** Properties of the Wide Beam Specimens in Test-Series "1".

Beams	bs mm	ks -	bp mm	kp -	k -	SL mm	S <sub>w</sub> mm	ρ <sub>v</sub> %	μ <sub>s</sub> -	β <sub>g</sub> -	μ <sub>v</sub> -	β <sub>k</sub> -
Beam A1-0	600	1.00	600	1.00	1.00	-	-	-	1.43	1.00	-	-
Beam A1-1a	600	1.00	600	1.00	1.00	166	192	0.20	1.43	1.00	0.93	1.00
Beam A1-1b	600	1.00	600	1.00	1.00	192	192	0.17	1.43	1.00	1.00	1.00
Beam A1-2	600	1.00	600	1.00	1.00	192	257	0.17	1.43	1.00	0.86	1.00
Beam B1-0	300	0.50	150	0.25	0.25	-	-	-	1.72	0.84	-	-
Beam B1-1a	300	0.50	150	0.25	0.25	166	192	0.20	1.72	0.84	0.93	0.84
Beam B1-1b	300	0.50	150	0.25	0.25	192	192	0.17	1.72	0.84	1.00	0.84
Beam B1-2	300	0.50	150	0.25	0.25	192	257	0.17	1.72	0.84	0.86	0.84
Beam C1-0	300	0.50	150	0.25	0.25	-	-	-	1.72	0.71	-	-
Beam C1-1a	300	0.50	150	0.25	0.25	166	192	0.20	1.72	0.71	0.93	0.84
Beam C1-1b	300	0.50	150	0.25	0.25	192	192	0.17	1.72	0.71	1.00	0.84
Beam C1-2	300	0.50	150	0.25	0.25	192	257	0.17	1.72	0.71	0.86	0.84
Beam D1-0	150	0.25	300	0.50	0.25	-	-	-	1.72	0.71	-	-
Beam D1-1a	150	0.25	300	0.50	0.25	166	192	0.20	1.72	0.71	0.93	0.59
Beam D1-1b	150	0.25	300	0.50	0.25	192	192	0.17	1.72	0.71	1.00	0.59
Beam D1-2	150	0.25	300	0.50	0.25	192	257	0.17	1.72	0.71	0.86	0.59

**NOTE:**  $b_w = 600\text{mm}$ ,  $h = 300\text{mm}$ ,  $d = 257\text{mm}$ ,  $\rho_s = 1.63\%$  ( $8\Phi 20\text{mm}$ ),  $\rho_{s'} = 0.196\%$  ( $6\Phi 8\text{mm}$ ),  $A_v = 201\text{mm}^2$  (4-Legs $\Phi 8\text{mm}$ ) for all beams.



**Figure 7.3:** Difference Sizes of Steel Plates Used for Load and Support Conditions in Series "1".

**The main features of the experimental programme of Series (1) are:**

- a) Cross section of beams: 600mm wide x 300mm height, and  $b_w/h$  ratio of 2.0.
- b) Support and load system: simple supported beams with a 2440mm total span and 1840mm free span. The load is applied at mid-span point (Figures 7.1 and 7.2) and the ratio of shear-span to effective-depth ( $a/d$ ) is equal to 3.58.
- c) The longitudinal reinforcement is kept constant along the beam and is eight 20mm diameter ( $\rho_s = 1.63\%$ ). Compression reinforcement is used as hanger bars and is six 8mm diameter ( $\rho_s = 0.196\%$ ). The effective depth ( $d$ ) is 257mm for all the beams.
- d) The reinforcement is designed according to the current Code specifications, such as EC2 Code.

**The variables analysed are:**

- a) Longitudinal spacing between stirrups ( $S_L$ ): 166 and 192mm, corresponding to stirrup-spacing/effective-depth ( $S_L/d$ ) ratios of 0.65 and 0.75, respectively.
- b) Shear reinforcement arrangement (NL): 4 stirrup legs in each beam.
- c) Transversal spacing of stirrup legs ( $S_w$ ): 192 and 257mm, corresponding to stirrup-spacing/effective-depth ( $S_w/d$ ) ratios of 0.75 and 1.0, respectively.
- d) Diameter of stirrups ( $\Phi_{str.}$ ): 8mm. The total area of shear reinforcement ( $A_v$ ) is  $201\text{mm}^2$ .
- e) Support width ( $b_s$ ): The beams in Type A are supported with wide bearing plates where  $b_s$  is equal to 600mm ( $k_s = b_s/b_w = 1.0$ ), whereas the beams in Types B, C and D are supported with narrow bearing plates placed at the centre of the beam width where  $b_s$  is equal to 300mm, 300mm and 150mm respectively (correspondingly to,  $k_s = b_s/b_w = 0.50, 0.50$  and  $0.25$  respectively).
- f) Load width ( $b_p$ ): The beams in Type A are loaded with wide bearing plates where  $b_p$  is equal to 600mm ( $k_p = b_p/b_w = 1.0$ ), whereas the beams in Types B, C and D are loaded with narrow bearing plates placed at the centre of the beam width where  $b_p$  is equal to 300mm, 150mm and 300mm respectively (correspondingly to,  $k_p = b_p/b_w = 0.50, 0.25$  and  $0.50$  respectively).

#### **7.4 Materials Information**

The performance and quality of concrete member depend to a large extent on the proportions and characteristics of its constituent materials (Ziara, 1993; Alluqmani, 2010; Alluqmani, 2014; Alluqmani and Haldane, 2011c). Therefore, it was important that the quality of the material

remained consistent during this programme of research. The information relating to the materials used to design the beam specimens and cast the concrete were the same as assumed in the design calculations, Tables 7.4.

**A brief detail and description of the materials used for test specimens are as follows:**

#### 7.4.1 Concrete

For all test specimens, a 40 MPa cylinder compressive strength (50 MPa cubic compressive strength) was used in the design calculations, which was used in this programme of research as it is being applied according to the design provisions of EC2 approach, as shown in Table 7.4.

All beam specimens with their own control samples (cubes and cylinders) were made simultaneously with concrete from the same mixture at the same time. Ready mixed concrete was used to cast the beam specimens and control samples, contained 10-20mm (3/8-3/4 in.) coarse aggregate, 4mm (3/16 in.) fine aggregate, 375 kg cement content per cubic metre of concrete, and 0.42 design water/cement (w/c) ratios to give a workability of 60-70mm slump. The aggregate was crushed limestone for all test specimens. The cube samples used in the laboratory tests had dimensions of 100x100x100 mm, where the cylinder samples had dimensions of 200mm height x 100mm diameter. The nominal specified strength of the concrete used to cast the specimens was as that used for the design purpose for class C40, which was 40 MPa for concrete cylinder strength or 50 MPa for concrete cubic strength (Table 7.4).

**Table 7.4:** Material Properties used to Design the Beam Specimens in Series "1".

	<b>Properties</b>	<b>Series (1)</b>
<b>Concrete</b>	<u>Cylinder</u> Compressive Strength ( $f_c$ ), MPa	40
	Cube Compressive Strength ( $f_{cu}$ ), MPa	50
	Young's Modulus ( $E_c$ ), MPa	28000
<b>Flexural Reinforcement</b>	Yield Strength for $\Phi 20$ mm ( $f_y$ ), MPa	500
	Yield Strength for $\Phi 8$ mm ( $f_y$ ), MPa	500
	Young's Modulus ( $E_s$ ), MPa	200000
<b>Shear Reinforcement</b>	Yield Strength for $\Phi 8$ mm ( $f_{yv}$ ), MPa	500
	Young's Modulus ( $E_s$ ), MPa	200000

Table 7.4 shows the material properties used to design the beam specimens. The mix proportions of concrete used to cast the beams are shown in Table 7.5. The concrete mixes used in the



experimental investigation were designed to give an average cubic compressive strength at 28 days ( $f_{cu}$ ) equal to the specified strength, this means, the target mean strength was taken to be equal to the characteristic strength.

**Table 7.5:** Mix Proportions of Concrete used to Cast the Beams in Series "1".

Properties	Test-Series (1)
Cement Type	Ordinary Portland Cement
Maximum Aggregate Size	10 to 20mm (3/8 to 3/4 in.)
Slump for Concrete	60-70mm
Coarse Aggregate Content	1025 kg/m <sup>3</sup>
Fine Aggregate Content	874 kg/m <sup>3</sup>
Cement Content	375 kg/m <sup>3</sup>
Water/Cement (w/c) Ratio	0.42
Free-Water Content	158 litre/m <sup>3</sup>

#### 7.4.2 Reinforcement

In all test specimens, high deformed yield steel bars were used in the design of the flexural (longitudinal) and shear (transverse) reinforcements. The sizes of steel bars used to fabricate the beam specimens are as follows:

**20mm** high strength deformed yield steel bars were used for tensile flexural (main) reinforcement for all test beams.

**8mm** high strength deformed yield steel bars were used for compressive flexural (hanger) reinforcement and transverse shear reinforcement (stirrups) for all test beams.

For all test specimens, a 500 MPa high yield steel strength was used in the design calculations for both flexural and shear reinforcements, which was used in this programme of research as it is being applied according to the design provisions of EC2 approach, as shown in Table 7.4.

The beams in Series (1) were made simultaneously with concrete from the same mixture. The actual average cube and cylinder concrete compressive strengths were  $f_{cu,act} = 52.80$  MPa and  $f_{cy,act} = 42.25$  MPa, respectively. Eight 20mm nominal diameter high-strength deformed steel bars were used for the longitudinal tensile reinforcement ( $A_s = 314.2$  mm<sup>2</sup> and  $f_y = 525$  MPa) for each beam. Six 8mm nominal diameter high-strength deformed steel bars were used for the longitudinal compressive (hanger) reinforcement ( $A_s = 50.3$  mm<sup>2</sup> and  $f_y = 510$  MPa) for each

beam in order to prevent accidental failure of the beam during the handling operations. It should be noted that these beams were designed for singly reinforcement only as required. The stirrups were fabricated from 8mm nominal diameter high-strength deformed steel bars ( $A_s = 50.3 \text{ mm}^2$  and  $f_y = 510 \text{ MPa}$ ) for each beam. Typical details of the test beams in Series (1) are shown in Figure 7.2.

## **7.5 Manufacture of Test Specimens**

### **7.5.1 Steel Cages**

The reinforcing steel bars were supplied as Take-Loose rebars, instead of the Prefab steel cages, from a local steel production company (BRC Steel Co Ltd, Block 14, Newhouse Industrial Estate, Lanarkshire, Glasgow-UK). All steel cages of beam specimens were made in the Concrete/Structures Laboratory at the University of Strathclyde.

To produce the steel cages of wide beam specimens, the main reinforcement bars were put straight through two Workbenches (Trestles); then the positions of the stirrups were marked out in the main bars according to the stirrups spacing along the beam length ( $S_L$ ) and across the beam width ( $S_w$ ). After that, the stirrups were tied to the main bars at each position. Also, the compression (hanger) reinforcement bars were put straight at the inside corners of the top face of the stirrups (in the compression concrete region), to prevent any movement during concrete pouring and compaction and also to assist in the assembly of the reinforcement cage and not to contribute to the flexural capacity of the beams (because these beams were designed for single reinforcement, as required). The steel bars were cleaned to remove any traces of oil, paint, or loose scale, i.e. surface rust, in order not to weaken the bond with the concrete.

The concrete covers were made using plastic spacers and were fixed on either the main bars or on the stirrups to ensure that the required cover distances were maintained and to avoid any movement of the reinforcement cages during compaction of the concrete, where 25mm thick spacers were attached to the stirrups (8mm diameter) and 33mm thick spacers were attached to the main bars (20mm diameter) for all test beam specimens. The steel cages and spacers were well fixed prior to the concrete pouring and compaction. In addition, two lifting points were placed in the ends of beams (one hanger at each end) for lifting purpose. Typical steel cages of test beam specimens investigated in this study are shown in Figure 7.4.



**Figure 7.4:** Typical Steel Cages for the Beams in Test-Series "1".

### **7.5.2 Shutters**

Structural steel channel sections were used in the manufacture of the shutters. The shutters were cleaned and coated with oil to prevent the concrete from adhering to the shutters during the concrete casting and curing; also, the steel cages were placed in the shutters and the plastic spacers were used to maintain the required cover distance.

For all beam specimens, the shutters had inside dimensions of 600\*300mm with overall length of 2440 mm. The steel shutters were manufactured and supplied by a local steel formwork (moulds) company (WM Services (Scotland) Ltd, Unit 2E, Greenhill Industrial Estate, Coatbridge, Glasgow-UK). The shutters were fixed firmly during the concrete pouring and compaction (or vibration) to prevent the shutters from moving. Typical steel shutters used for the casting purposes are shown in Figure 7.5.

### **7.5.3 Casting**

All beam specimens with their own control samples (cubes and cylinders) were made simultaneously with concrete from the same mixture at the same time to ensure the concrete's consistency. A total of sixteen beam specimens, six cubes and six cylinders were cast in steel shutters and moulds in the Concrete/Structures Laboratory at the University of Strathclyde. The volume of each beam, cube and cylinder was known, and then the total required volume of concrete was calculated. The concrete mixture was supplied from a local ready mixed concrete company (Robeslee Concrete Co Ltd, Southbank Rd, Kirkintilloch, Lanarkshire, Glasgow-UK). One lorry was brought to cast the beams and control specimens. All beams and control specimens were cast from the same mixture. The concrete workability depends on the water/cement (w/c) ratio to control the strength and consistency (slump) of the concrete; therefore, the w/c ratio was taken 0.42 to give a workability of 60-70mm slump for all specimens (Table 7.5).



Steel Channel Shutters

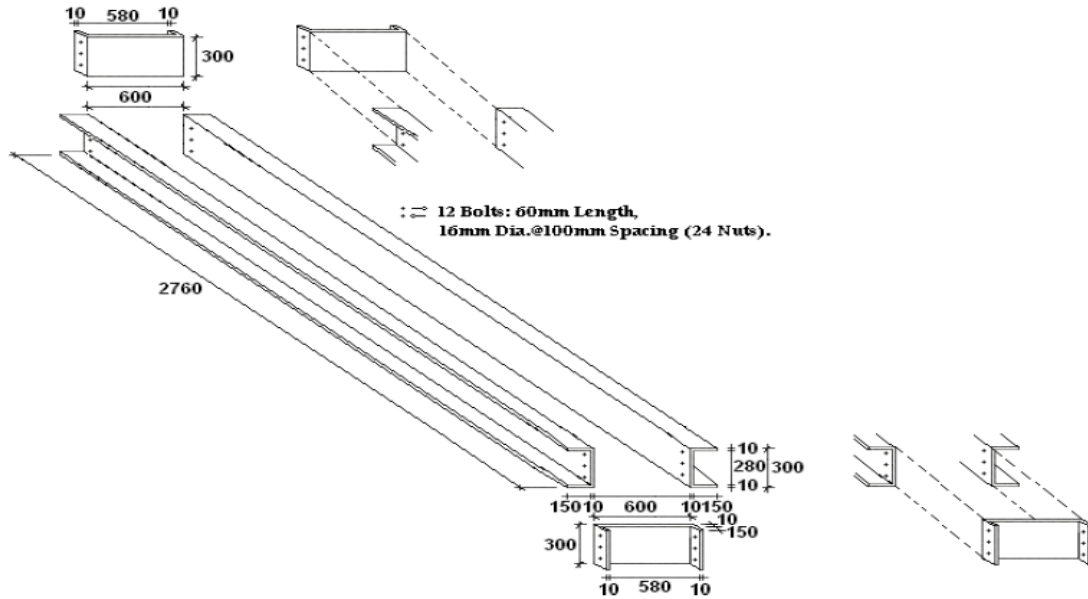


Figure 7.5: Typical Steel Shutters used for the Beam Specimens in Test-Series "1".

The casting process was initiated from the tension zone of the beam at the bottom surface of the shutter through two layers, and it was stopped at the outside face of the compression zone of the beam at the top surface of the shutter. This was to ensure that any bleeding of the concrete did not occur in the concrete compression region (Ziara, 1993). Also during the concrete casting of each layer, beam specimens were compacted using a poker vibrator and vibrated using a vibrator and rods to ensure quality, a strong consistent concrete mix, to increase concrete strength, and to reduce the air voids. The vibration was terminated when air bubbles stopped appearing at the top surface of the concrete (Ziara, 1993). The control specimens were compacted using a standard electrically operated vibrating table for a period of approximately 90 seconds. Figure 7.6 shows typical beams together with own set of control cube and cylinder samples after finishing the concrete casting and after the polishing.



**Figure 7.6:** Typical Beams for Series "1" together with own Control Samples after Concrete Casting.

#### **7.5.4 Curing**

After the concrete casting of all test specimens and control samples, they were stored in their moulds under ambient conditions inside the laboratory. To ensure that beams, cubes and cylinders were treated, damp sheets of hessian were placed over the beams and the control samples. In the following days after casting, beam specimens and control samples were treated by spraying water over all surfaces of beams, control samples and hessian. All beams and control specimens were cured, inside their moulds, under moist burlap and plastic for 7 days.

#### **7.5.5 Preparing the Test Specimens for Testing**

All beams and control specimens were removed from the moulds after about 12 days. Test beam specimens were whitewashed to enable the early identification of cracks development under loading. At this stage, test beam specimens and control samples were already prepared for the laboratory test programme. Figure 7.7 shows the curing process of typical beams after removing the shutters.

Specimens' age at the test was approximately between 40 and 50 days. The control specimens were made at the same time as the beams, were cured like the beams and were tested in crushing on the same day as the beams.



**Figure 7.7:** The Curing Process of Typical Beams in Series "1" after Removing the Shutters.

## 7.6 Testing Arrangements and Instrumentation

### 7.6.1 Testing Machine

Figure 7.8 shows the testing instrumentation and equipment that were used in the tests. All test beam specimens were loaded using a servo-controlled universal test machine (Figure 7.8a) which has a vertical load capacity of up to 890 kN (200,000 lb) with a resolution of 1 kN, where the applied force was controlled through manual operation of the hydraulic valve at the loading piston. The total load applied was displayed on a digital indicator on the control panel of the test machine. Each specimen was loaded in 50 kN (11,250 lb) load increments to failure.



a) Beams Testing Machine



b) Control Specimens Testing Machine



c) Test Instrumentation

**Test Instrumentation:** from left, Deflection Dial Gauge, and Crack Width Microscope.

**Figure 7.8:** Testing Instrumentation and Equipment used in the Tests of Series "1".

A Tonipact 3000 crushing machine (Figure 7.8b), which has a minimum vertical load capacity of 3000 kN with a resolution of 1 kN, was used to test the control samples (cubes and cylinders). The control specimens were tested in crushing on the same day as the beams. Continuous recordings of the applied load and deflections were provided throughout each test. The cracks were marked, photographed and measured with a microscope (Figure 7.8c). One electrically operated overhead crane was used to move the beams in the laboratory.

**The details of testing arrangements are discussed below:**

### **7.6.2 Loading Arrangement**

The test beams were loaded using a three-point loading arrangement. The load was concentrated from the hydraulic jack of testing machine to the loading plate of test beam specimens. According to the system of loading points for all test specimens, the beams were supported at three ends (for a three point-loading system) on an assembly consisting of roller or hinge bearing sandwiched between two steel plates. The length of the loading and support plates ( $C_p$  and  $C_s$ ), which was in contact with the beam parallel to its length, was 150mm in order to prevent bearing failures in the concrete. The thickness of the loading and support plates ( $t_p$  and  $t_s$ ) was 25mm. Moreover, according to the case of the load and support conditions, all loads and supports in Beam-Type (A) were applied with full-width plates (full-width load and support case) to the overall beam width ( $b_w$ ); while all loads and supports in Beam-Types (B, C and D) were applied with narrow-width plates (narrow-width load and support case) to the centreline of the overall beam width ( $b_w$ ). The width of the loading plate ( $b_p$ ), which was parallel to the beam width, was either equal to the support width ( $= b_s$ ) for Beam-Type (B), or half the support width ( $= 0.50*b_s$ ) for Beam-Type (C), or twice the support width ( $= 2*b_s$ ) for Beam-Type (D). The load-width to beam-width ( $k_p = b_p/b_w$ ) ratio was 1.0 for Beam-Type (A), 0.50 for Beam-Type (B), 0.25 for Beam-Type (C) and 0.50 for Beam-Type (D). While the support-width to beam-width ( $k_s = b_s/b_w$ ) ratio was 1.0 for Beam-Type (A), 0.50 for Beam-Type (B), 0.50 for Beam-Type (B) and 0.25 for Beam-Type (C). The loading arrangements and testing machine used to test the beams are shown in Figures 7.1 and Figure 7.8a, respectively.

### **7.6.3 Loading Procedures and Steps**

All beams were tested under loading control at a rate of 10 kN/minute. The data generated during each test (i.e. total applied loads, deflections, crack widths, etc.) were recorded after each 50 kN increments of loading. The loading steps for all test specimens were similar. The loading step started from zero and then increased incrementally of 50 kN until the collapse (failure) load of the beam reached.

The test sequences were continued until the beams failed. The time required to record a complete set of readings at each load stage varied between 10 to 15 minutes. The overall testing time of a beam varied from 3 to 4 hours.

#### **7.6.4 Instrumentation Arrangements**

Instrumentation for each specimen was designed to capture the load-deflection response and crack development. Vertical displacement measurements at the mid-span of the beam length were recorded from a Linear Variable Displacement Transformer (a LVDT). The deflection dial gauge was placed on each test beam specimen prior to testing at the intersection of the mid-span of the beam-span with the mid-point of the beam-width, corresponding to the center of loading plate. A crack width microscope was used to measure crack widths. Figure 7.1 shows a typical arrangement for the mid-span deflection dial gauge.

#### **7.6.5 Marking of Cracks**

The surfaces of all beam specimens were marked with different coloured Chalks to follow the development of the cracks. The crack width microscope was used for all test specimens to measure the crack widths during the test at each increment of the loading.

#### **7.7 Test Programme and Procedure**

The procedure of the experimental test programme used for testing the specimens is summarized as follows (Alluqmani, 2010):

Step.1: All beams were painted white to show of cracks.

Before testing, the sides of all beams were painted white, which has the benefit to show the cracks during the testing of the beams.

Step.2: Assembling of test arrangement.

The top surface of each beam, loading and support plates were coated with a layer of plaster to ensure the load is applied to a smooth level surface.

Step.3: Position the beam in the test arrangement and position loading and support plates at appropriate points.

Step.4: Concentration the center of hydraulic jack of testing machine on top of the center of loading plate. Some rubber sheets were placed at points between the beam and support plates, as well at loading points, to ensure load is applied on a level surface.

Step.5: First beam was tested; and some control samples were also tested.

Step.6: The remaining beams and control samples were also tested.



Before starting the test, all necessary Personal Protective Equipments (PPE), e.g. Overalls, safety Shoes, Gloves, Glasses and etc, were made available in the laboratory (Alluqmani, 2010). Figure 7.8 shows the instrumentation and testing equipments used in the tests.

The experimental work activities for manufacturing the steel cages, casting the concrete, and testing the specimens are included in Appendix B.

## **7.8 Measurements**

### **7.8.1 Total Applied Load**

The total load (P) applied to each test specimen was continuously displayed on the control unit of the test machine. The accuracy of the load readings was checked and found to be correct using a load cell which had been calibrated using a reference test machine.

### **7.8.2 Deflection**

A Linear Variable Differential Transducer (LVDT) was used to measure the deflections under the center point of loading plate (the intersection of mid-span with mid-width of each beam). The deflection dial gauge had a resolution of 0.01mm.

### **7.8.3 Cracking**

After each load increment, the beams were inspected for cracks. A crack width microscope was used to measure the crack widths with a resolution of 0.1mm.

The cracks were marked on each face of the test beam specimens with the corresponding applied load level at each load level. The crack patterns were photographed and hard copy sketches were also made.

### **7.8.4 Beam Testing Results**

At each load stage, the following recordings were made:

1. The total applied load (P) in kN.
2. The deflection dial gauge readings which were shown in millimetres on the display panel on the control unit of the test machine.
3. The flexural and the shear (diagonal) crack widths in millimetres.

#### 4. Comments on the physical state of each beam.

On completion of each increment of loading, the beams were inspected for cracks which were then measured using a crack micrometer. Cracks were marked on the beam surfaces. The magnitudes of the applied loads, deflections, and crack widths were also recorded at each stage. On the completion of each test, the beam was photographed to record the final deflected shape and the crack pattern developments.

All test results were finally recorded. The control samples (cubes and cylinders) were also tested, and the concrete compressive strengths were recorded at the time of the corresponding beam test.

### **7.9 Material Test-Results and Prediction of Beam-Results**

For the proposed prediction model, it is assumed that the ultimate flexural strength and the shear strength provided by concrete depend on the  $K_{cd}$  factor which in turn is related to the width of bearing plates and the percentage of flexural (tensile and compression) reinforcement; while the shear strength provided by stirrups depends on the  $K_{sd}$  factor which in turn is related to the width of bearing plates and the longitudinal and transversal spacing of the stirrup-legs. Based on the results of material strengths obtained by tests as shown in Tables 7.6 and 7.7, the both ultimate flexural and shear capacities ( $M_{u,d}$  and  $V_{u,d}$ ) of all specimens were predicted by the proposed prediction-model (Table 7.8). The proposed prediction model gave a reasonably prediction for the shear and flexural strengths as well for the proposed failure modes.

The concrete compressive strengths obtained from the control samples of cubes and cylinders are shown in Table 7.6. The actual average cube and cylinder concrete compressive strengths were  $f_{cu,act} = 52.80$  MPa and  $f_{cy,act} = 42.25$  MPa, respectively. The actual material strengths used to predict and analyze the test specimens for the compressive strength of concrete ( $f_c$ ), the yield tensile strength of the longitudinal reinforcing bars ( $f_y$ ), and the yield tensile strength of the stirrups ( $f_{yv}$ ) were determined and the results are given in Table 7.7. The value of  $f_c$  used for the analysis, reported in Table 7.7, represents the average strength of cylinders tested on the same day as the specimen, after having been cured under similar laboratory conditions. Table 7.8 shows the prediction of flexural and shear failure loads according to the proposed prediction model for the beams in Test-Series (1) based on the actual strengths of materials. It should be emphasised that no partial safety factors were included in the structural calculations for prediction the failure load.

**Table 7.6:** Actual Concrete Strengths for Test-Series "2".

Control Sample	Surface Area, mm <sup>2</sup>	Weight, gm	Load, lb	Load, kN	Strength, f <sub>c</sub> , N/mm <sup>2</sup>
<b>Actual Concrete Cube Compressive Strengths at 40 to 50 days, f<sub>cu</sub></b>					
1	10000	-	116430	517.50	51.75
2	10000	-	121245	539.0	53.90
<b>Average</b>	-	-	-	-	<b>52.80</b>
<b>Actual Concrete Cylinder Compressive Strengths at 40 to 50 days, f<sub>c</sub></b>					
1	7855	-	73325	326.0	41.50
2	7855	-	76000	337.80	43.0
<b>Average</b>	-	-	-	-	<b>42.25</b>
<b>Actual Concrete Cylinder Split Strengths, f<sub>ct</sub>, L = 300mm</b>					
1	102*199	-	22740	101.1	3.17
2	100*202	-	24480	108.8	3.43
<b>Average</b>	-	-	-	-	<b>3.30</b>

**Test-Series (1): Date of Casting:** 07 January 2013.

**Date of Testing:** 11 February 2013 to 28 February 2013.

$f_{ct} = 2P/(3.142*d*L) = 0.637*P/(d*L)$ . D is the cylinder diameter and L is the cylinder height.

**Table 7.7:** Material Properties used to Predict and Analyze the Tested Beams in Series "1".

	Properties	Series (1)
<b>Concrete</b>	Cylinder Compressive Strength (f <sub>c</sub> ), MPa	42.25
	Cube Compressive Strength (f <sub>cu</sub> ), MPa	52.80
	Cylinder Split Tensile Strength (f <sub>t</sub> ), MPa	3.30
	Young's Modulus (E <sub>c</sub> ), MPa	31500
<b>Flexural Reinforcement</b>	Yield Strength for Φ20mm (f <sub>y</sub> ), MPa	525
	Yield Strength for Φ8mm (f <sub>y</sub> ), MPa	510
	Young's Modulus (E <sub>s</sub> ), MPa	200000
<b>Shear Reinforcement</b>	Yield Strength for Φ8mm (f <sub>yv</sub> ), MPa	510
	Young's Modulus (E <sub>s</sub> ), MPa	200000

## 7.10 Test Results of Beams

In order to characterise the materials used in the beam manufacture, the compression strength of concrete is determined by cylindrical and cubic specimens. The actual reinforcement properties and strengths, the concrete strengths, and the actual beam dimensions were used to re-calculate the original design load, and to predict the failure load of each beam. Table 7.9 shows the re-calculation of the maximum design loads and the proposed predicted failure loads according to the actual results of material strengths, and also shows the experimental failure loads and capacities of the test specimens in Series (1).

The ultimate experimental shear strength ( $V_{u,exp.}$ ) of a test beam is half its shear failure load (=  $P_{fv,exp.}/2$ ); this is because the beams were tested under a three loading-point system at the mid-span of the beams. The experimental shear strength provided by concrete contribution ( $V_{c,exp.}$ ) of

a beam with stirrups is equal to the ultimate shear strength of the beam without stirrups ( $V_{u0,exp.}$ ) for the same characteristics (in the same Beam-Type). The experimental shear strength provided by stirrups contribution ( $V_{s,exp.}$ ) of a beam with stirrups is equal to its ultimate shear strength ( $V_{u,exp.}$ ) minus the ultimate shear strength of the beam without stirrups in the same Type ( $V_{u0,exp.}$ ), which is its shear strength provided by concrete contribution, for the same characteristics (in the same Beam-Type).

**Table 7.8:** Prediction of Flexural and Shear Failure Loads for Beams in Test-Series "1".

Series/Beams	Code Prediction, kN				Proposed-Model Prediction, kN												$P_{f,pred.}$	
	$V_c$	$V_s$	$V_u$	$M_u$	$M_u$	$\mu_s$	$\beta_g$	$K_{cd}$	$V_{c,d}$	$\mu_v$	$\beta_k$	$K_{sd}$	$V_{s,d}$	$V_{u,d}$	$M_{u,d}$	$V_d$	$P_{V,d}$	$P_{M,d}$
Beam A1-0	192	-	192	262	264	1.43	1.00	1.43	275	-	-	-	-	275	378	275	550	822
Beam A1-1a	192	143	335	262	264	1.43	1.00	1.43	275	0.93	1.00	0.93	133	408	378	408	816	822
Beam A1-1b	192	124	316	262	264	1.43	1.00	1.43	275	1.00	1.00	1.00	124	399	378	399	798	822
Beam A1-2	192	124	316	262	264	1.43	1.00	1.43	275	0.86	1.00	0.86	107	382	378	382	764	822
Beam B1-0	192	-	192	262	264	1.72	0.84	1.44	276	-	-	-	-	276	380	195	552	826
Beam B1-1a	192	143	335	262	264	1.72	0.84	1.44	276	0.93	0.84	0.78	112	388	380	274	776	826
Beam B1-1b	192	124	316	262	264	1.72	0.84	1.44	276	1.00	0.84	0.84	104	380	380	269	760	826
Beam B1-2	192	124	316	262	264	1.72	0.84	1.44	276	0.86	0.84	0.72	89	365	380	258	730	826
Beam C1-0	192	-	192	262	264	1.72	0.71	1.22	234	-	-	-	-	234	322	117	468	700
Beam C1-1a	192	143	335	262	264	1.72	0.71	1.22	234	0.93	0.84	0.78	112	346	322	196	692	700
Beam C1-1b	192	124	316	262	264	1.72	0.71	1.22	234	1.00	0.84	0.84	104	338	322	191	676	700
Beam C1-2	192	124	316	262	264	1.72	0.71	1.22	234	0.86	0.84	0.72	89	323	322	180	646	700
Beam D1-0	192	-	192	262	264	1.72	0.71	1.22	234	-	-	-	-	234	322	117	468	700
Beam D1-1a	192	143	335	262	264	1.72	0.71	1.22	234	0.93	0.59	0.55	79	313	322	157	626	700
Beam D1-1b	192	124	316	262	264	1.72	0.71	1.22	234	1.00	0.59	0.59	73	307	322	154	614	700
Beam D1-2	192	124	316	262	264	1.72	0.71	1.22	234	0.86	0.59	0.51	63	297	322	149	594	700

NOTE: For all beams:  $b_w = 600\text{mm}$ ,  $h = 300\text{mm}$ ,  $d = 257\text{mm}$ ,  $\rho_s = 1.63\%$  ( $8\Phi 20\text{mm}$ ),  $\rho_s' = 0.196\%$  ( $6\Phi 8\text{mm}$ ),  $A_v = 201\text{mm}^2$  (4-Legs $\Phi 8\text{mm}$ ),  $a = 920\text{mm}$ ,  $Z_{code} = 198.3\text{mm}$  (EC2),  $jd = Z_{code} = 205.6\text{mm}$  (ACI318-and-SBC304),  $\epsilon_c = 0.0035$  (EC2),  $\epsilon_c = 0.003$  (ACI318-and-SBC304),  $E_c = 31500\text{MPa}$ ,  $E_s = 200000\text{MPa}$ .

$P_d = 470\text{ kN}$ ,  $V = 235\text{ kN}$ , and  $M = 216\text{ kN.m}$ .  $A_v = 201\text{mm}^2$  (4-Legs $\Phi 8\text{mm}$ ).

$f_{y,d} = 525\text{ MPa}$ ,  $f_{v,d} = 510\text{ MPa}$ ,  $f_{c,d} = 42.25\text{ MPa}$  (for Beams in Series (1)).

$k_p$ ,  $k_s$ ,  $S_L$  and  $S_w$  values are taken from Table 7.3 for the beams in Test-Series (1).

$P = 470\text{ kN}$ ,  $V = 235\text{ kN}$ ,  $M = 216\text{ kN.m}$ ,  $a = 920\text{mm}$ ,  $A_{s,prov.} = 2514\text{ mm}^2$ ,  $f_{y,act.} = 525\text{ MPa}$ ,  $f_{c,act.} = 42.25\text{ MPa}$ .

$M_{u,prop.} = A_{s,prov.} * f_{y,act.} * jd$ , where,  $jd = (2/3) * h = 200\text{mm}$ .

$M_{u,code}$  (from Steel) =  $A_{s,prov.} * f_{y,act.} * Z = 262\text{ kN.m}$ . Where,  $Z = d - (s/2) = 198.3\text{ mm}$ .

$s = 0.8x = 117.50\text{mm}$ ,  $x = d * [\epsilon_c / (\epsilon_c + \epsilon_s)] = 146.86\text{mm}$ , where,  $\epsilon_s = f_{y,act.} / E_s = 0.002625$ ,  $\epsilon_c = 0.0035$ ,  $E_s = 200000\text{ MPa}$ .

$M_{u,code}$  (from Concrete) =  $(f_{c,act.} * b_w * d^2) * k = 334.9\text{ kN.m}$ . Where,  $k = -1.134 * (Z/d)^2 + 1.134 * (Z/d) = 0.20$  and  $Z = d - (s/2) = 198.3\text{ mm}$ .

No factors of safety are used neither in calculation of  $Z$  nor in calculation of  $M_{u,prop.}$  and  $M_{u,code}$ .

$P_{V,d}$  = Predicted shear failure load =  $2V_{u,d}$  and  $P_{M,d}$  = Predicted flexural failure load =  $2(M_{u,d}/a)$ .

$P_{f,pred.}$  = the smallest of ( $P_V$  or  $P_M$ ) and the predicted failure mode is the failure mode corresponding to  $P_{f,pred.}$ .

No factors of safety are used neither in this prediction  $V_c$  and  $V_s$  nor in calculation of  $P_{V,d}$  and  $P_{M,d}$ .

Table 7.10 shows validation of the proposed prediction model on the test results obtained from Test-Series (1), and also shows a comparison of the beam capacities predicted by the proposed prediction model with those values either obtained from the tests or predicted by the existing Codes and models, such as EC2, ACI318, SBC304, Lubell et al model (2008), Sernar-Ros et al model (2002) and Shuraim model (2012). The accuracy of the proposed prediction model to predict the capacity, failure load and failure mode of wide RC beams appears in Table 7.10. The deficiency of the current design models and Codes to predict the capacity of wide RC beams is

clear. Table 7.11 summarises the crack width measurements at different load levels for the beams in Test-Series (1).

Figure 7.9 shows critical failure modes and crack patterns for the beams in Test-Series (1). Figures 7.10a to 7.10d show the failure mode and crack patterns after failure for the beams in Types (A), (B), (C) and (D), respectively. The total applied load versus mid-span deflection curves obtained from the beams are shown in Figures 7.11 to 7.14. Tables 7.12 to 7.15 show the total applied load versus mid-span deflection for the beams in Types (A), (B), (C) and (D), respectively. Tables 7.16 to 7.19 show the total applied load versus crack widths for the beams in Types (A), (B), (C) and (D), respectively.

**Table 7.9:** Re-calculation of the Maximum Design Load and Prediction of the Failure Load based on the Proposed Prediction Model.

Beam Type	Max. Original Design Load, kN	Max. Original Flexural Capacity, kN.m	Max. Re-Calculated (Actual) Flexural Capacity, kN.m	Max. Re-Calculated (Actual) Design Load, kN	Predicted Failure Load, kN (F. Mode)	Actual Exp. Failure Load, kN (F. Mode)	$P_{f,exp}/P_d$	Test Strength, kN, m		
	$P_d$	$M_d$	$M_u = M_{d,act.}$	$P_{d,act.}$	$P_{f,pred.}$	$P_{f,exp.}$	-	$V_{c,exp}$	$V_{s,exp}$	$M_{u,exp.}$
AI-0	470	216	262	570	550 (Shear)	560 (Shear)	1.19	280	-	-
AI-1a	470	216	262	570	816 (Shear)	820 (Shear)	1.74	280	130	-
AI-1b	470	216	262	570	798 (Shear)	800 (Shear)	1.70	280	120	-
AI-2	470	216	262	570	764 (Shear)	790 (Shear)	1.68	280	115	-
B1-0	470	216	262	570	552 (Shear)	558 (Shear)	1.187	279	-	-
B1-1a	470	216	262	570	776 (Shear)	795 (Shear)	1.69	279	118	-
B1-1b	470	216	262	570	760 (Shear)	782 (Shear)	1.66	279	112	-
B1-2	470	216	262	570	730 (Shear)	745 (Shear)	1.58	279	93	-
C1-0	470	216	262	570	468 (Shear)	485 (Shear)	1.03	242	-	-
C1-1a	470	216	262	570	692 (Shear)	712 (Shear)	1.51	242	114	-
C1-1b	470	216	262	570	676 (Shear)	694 (Shear)	1.476	242	105	-
C1-2	470	216	262	570	646 (Shear)	654 (Shear)	1.39	242	85	-
D1-0	470	216	262	570	468 (Shear)	480 (Shear)	1.02	240	-	-
D1-1a	470	216	262	570	626 (Shear)	641 (Shear)	1.36	240	80	-
D1-1b	470	216	262	570	614 (Shear)	633 (Shear)	1.347	240	76	-
D1-2	470	216	262	570	594 (Shear)	602 (Shear)	1.28	240	61	-

$P_d = 470$  kN,  $V = 235$  kN,  $M = 216$  kN.m,  $a = 920$ mm,  $A_{s,prov.} = 2514$  mm<sup>2</sup>,  $f_{y,act.} = 525$  MPa,  $f_{c,act.} = 42.25$  MPa.

$P_{d,act.} = \text{Actual design load} = 2(M_{d,act.}/a) =$ , and  $M_{d,act.} = M_{u,code} = M_{small} = 262$  kN.m (from Steel).

$M_{u,code}$  (from Steel) =  $A_{s,prov.} * f_{y,act.} * Z = 262$  kN.m. Where,  $Z = d - (s/2) = 198.3$  mm.

$s = 0.8x = 117.50$ mm,  $x = d * [\epsilon_c / (\epsilon_c + \epsilon_s)] = 146.86$ mm, where,  $\epsilon_s = f_{y,act.} / E_s = 0.002625$ ,  $\epsilon_c = 0.0035$ ,  $E_s = 200000$  MPa.

$M_{u,code}$  (from Concrete) =  $(f_{c,act.} * b_w * d^2) * k = 334.9$  kN.m. Where,  $k = -1.134 * (Z/d)^2 + 1.134 * (Z/d) = 0.20$  and  $Z = d - (s/2) = 198.3$  mm.

No factors of safety are used neither in calculation of  $Z$  nor in calculation of  $M_{u,prop.}$  and  $M_{u,code}$ .

**Table 7.10:** Validation of the Proposed Prediction Model on the Test Results obtained from Test Series "1".

Beam Type	Code Strength, kN, m			Code Pred. Strength, kN		Lubell Pred. Strength, kN		Serna-Ros Pred. Strength, kN		Shuraim Pred. Strength, kN		Prop. Strength (Model), kN		Test Strength, kN		$\Delta u$ , mm	$P_{V,exp} / P_{V,pred}$	$P_{M,exp} / P_{M,pred}$
	Vc	Vs	Mu	$P_{V,d}$	$P_{M,d}$	$P_V$	$P_M$	$P_V$	$P_M$	$P_V$	$P_M$	$P_{V,pred}$	$P_{M,pred}$	$P_{V,exp}$	$P_{M,exp}$			
<b>According to EC2</b>																		
Al-0	192	-	262	<b>384</b>	570	<b>384</b>	570	<b>384</b>	570	<b>384</b>	570	550	822	560	-	9.98	1.02	-
Al-1a	192	143	262	670	570	670	570	796	570	702	570	816	822	820	-	13.82	1.0	-
Al-1b	192	124	262	632	570	632	570	716	570	658	570	798	822	800	-	13.64	1.0	-
Al-2	192	124	262	632	570	632	570	671	570	640	570	764	822	790	-	11.94	1.03	-
B1-0	192	-	262	<b>384</b>	570	<b>326</b>	570	<b>384</b>	570	<b>384</b>	570	552	826	558	-	10.11	1.01	-
B1-1a	192	143	262	670	570	570	570	694	570	702	570	776	826	795	-	13.72	1.02	-
B1-1b	192	124	262	632	570	537	570	634	570	658	570	760	826	782	-	12.05	1.03	-
B1-2	192	124	262	632	570	537	570	600	570	640	570	730	826	745	-	11.56	1.02	-
C1-0	192	-	262	<b>384</b>	570	298	570	<b>384</b>	570	<b>384</b>	570	468	700	485	-	8.70	1.04	-
C1-1a	192	143	262	670	570	519	570	694	570	702	570	692	700	712	-	11.47	1.03	-
C1-1b	192	124	262	632	570	490	570	634	570	658	570	676	700	694	-	11.23	1.03	-
C1-2	192	124	262	632	570	490	570	600	570	640	570	646	700	654	-	11.48	1.01	-
D1-0	192	-	262	<b>384</b>	570	298	570	<b>384</b>	570	<b>384</b>	570	468	700	480	-	8.84	1.03	-
D1-1a	192	143	262	670	570	519	570	617	570	702	570	626	700	641	-	11.81	1.02	-
D1-1b	192	124	262	632	570	490	570	572	570	658	570	614	700	633	-	11.68	1.03	-
D1-2	192	124	262	632	570	490	570	546	570	640	570	594	700	602	-	11.06	1.01	-
<b>According to ACI318 and SBC304</b>																		
Al-0	170	-	271	<b>340</b>	589	<b>340</b>	589	<b>340</b>	589	<b>340</b>	589	488	822	560	-	9.98	1.15	-
Al-1a	170	160	271	660	589	660	589	801	589	658	589	786	822	820	-	13.82	1.04	-
Al-1b	170	138	271	616	589	616	589	710	589	614	589	764	822	800	-	13.64	1.05	-
Al-2	170	138	271	616	589	616	589	659	589	596	589	726	822	790	-	11.94	1.09	-
B1-0	170	-	271	<b>340</b>	589	<b>289</b>	589	<b>340</b>	589	<b>340</b>	589	490	826	558	-	10.11	1.14	-
B1-1a	170	160	271	660	589	561	589	687	589	658	589	740	826	795	-	13.72	1.07	-
B1-1b	170	138	271	616	589	524	589	618	589	614	589	722	826	782	-	12.05	1.08	-
B1-2	170	138	271	616	589	524	589	580	589	596	589	690	826	745	-	11.56	1.08	-
C1-0	170	-	271	<b>340</b>	589	264	589	<b>340</b>	589	<b>340</b>	589	416	700	485	-	8.70	1.16	-
C1-1a	170	160	271	660	589	512	589	687	589	658	589	666	700	712	-	11.47	1.07	-
C1-1b	170	138	271	616	589	477	589	618	589	614	589	648	700	694	-	11.23	1.07	-
C1-2	170	138	271	616	589	477	589	580	589	596	589	616	700	654	-	11.48	1.06	-
D1-0	170	-	271	<b>340</b>	589	264	589	<b>340</b>	589	<b>340</b>	589	416	700	480	-	8.84	1.15	-
D1-1a	170	160	271	660	589	512	589	601	589	658	589	592	700	641	-	11.81	1.08	-
D1-1b	170	138	271	616	589	477	589	549	589	614	589	580	700	633	-	11.68	1.09	-
D1-2	170	138	271	616	589	477	589	521	589	596	589	558	700	602	-	11.06	1.08	-

**NOTE:** For all beams:  $b_w = 600\text{mm}$ ,  $h = 300\text{mm}$ ,  $d = 257\text{mm}$ ,  $\rho_s = 1.63\%$  ( $8\Phi 20\text{mm}$ ),  $\rho_s' = 0.196\%$  ( $6\Phi 8\text{mm}$ ),  $A_v = 201\text{mm}^2$  ( $4\text{-Legs}\Phi 8\text{mm}$ ),  $a = 920\text{mm}$ ,  $Z_{code} = 198.3\text{mm}$  (EC2),  $j_d = Z_{code} = 205.6\text{mm}$  (ACI318-and-SBC304),  $\epsilon_c = 0.0035$  (EC2),  $\epsilon_c = 0.003$  (ACI318-and-SBC304),  $E_c = 31500\text{MPa}$ ,  $E_s = 200000\text{MPa}$ .  
 $P_d = 470\text{ kN}$ ,  $V = 235\text{ kN}$ , and  $M = 216\text{ kN.m}$ .  $A_v = 201\text{mm}^2$  ( $4\text{-Legs}\Phi 8\text{mm}$ ).  
 $f_{y,d} = 525\text{MPa}$ ,  $f_{v,d} = 510\text{MPa}$ ,  $f_{c,y,d} = 42.25\text{MPa}$  (for Beams in Series (1)).  
 $k_p$ ,  $k_s$ ,  $SL$  and  $Sw$  values are taken from Table 7.3 for the beams in Test-Series (1).

$P_d = 470\text{ kN}$ ,  $V = 235\text{ kN}$ ,  $M = 216\text{ kN.m}$ ,  $a = 920\text{mm}$ ,  $A_{s,prov.} = 2514\text{mm}^2$ ,  $f_{y,act.} = 525\text{MPa}$ ,  $f_{c,act.} = 42.25\text{MPa}$ .

$P_{d,act.} = \text{Actual design load} = 2(M_{d,act.}/a)$ , and  $M_{d,act.} = M_{u,code} = M_{small}$ .

**Proposed Prediction-Model:**

$M_{u,prop.} = A_{s,prov.} * f_{y,act.} * j_d = 264\text{ kN.m}$ , where,  $j_d = (2/3) * h = 200\text{mm}$ .

**EC2:**

$M_{u,code, Flexure}$  (from Steel) =  $A_{s,prov.} * f_{y,act.} * Z = 262\text{ kN.m}$ . Where,  $Z = d - (s/2) = 198.3\text{mm}$ .

$s = 0.8x = 117.50\text{mm}$ ,  $x = d * [\epsilon_c / (\epsilon_c + \epsilon_s)] = 146.86\text{mm}$ , where,  $\epsilon_s = f_{y,act.} / E_s = 0.002625$ ,  $\epsilon_c = 0.0035$ ,  $E_s = 200000\text{MPa}$ .

$M_{u,code, Shear}$  (from Concrete) =  $(f_{c,act.} * b_w * d^2) * K = 334.9\text{ kN.m}$ . Where,  $K = -1.134 * (Z/d)^2 + 1.134 * (Z/d) = 0.20$  and  $Z = d - (s/2) = 198.3\text{mm}$ .

$M_{u,code}$  (EC2) =  $M_{small} = 262\text{ kN.m}$  (from Steel).

**ACI318-and-SBC304:**

$M_{u,code, Flexure}$  (from Steel) =  $A_{s,prov.} * f_{y,act.} * j_d = 271\text{ kN.m}$ . Where,  $j_d = Z = d - (a/2) = 205.6\text{mm}$ .

$a = \beta_1 * c = 102.8\text{mm}$ ,  $c = d * [\epsilon_c / (\epsilon_c + \epsilon_s)] = 137.1\text{mm}$ ,  $\beta_1 = 0.85$  for  $f_c' \leq 28\text{ N/mm}^2$ .  $\beta_1 = 0.85 - [0.05 * ((f_c' - 28) / 7)] \geq 0.65$  for  $f_c' > 28\text{ N/mm}^2$  (Hence:  $\beta_1 = 0.75$ ), where,  $\epsilon_s = f_{y,act.} / E_s = 0.002625$ ,  $\epsilon_c = 0.003$ ,  $E_s = 200000\text{MPa}$ .

$M_{u,code, Shear}$  (from Concrete) =  $(f_{c,act.} * b_w * d^2) * K = 299.7\text{ kN.m}$ . Where  $K = \omega * [1.0 - 0.59 * \omega] = 0.179$ , and  $\omega = \rho_{s,prov.} * (f_{y,act.} / f_{c,act.}) = 0.203$ , and  $j_d = Z = d - (a/2) = 205.6\text{mm}$ .

$M_{u,code}$  (ACI318-and-SBC304) =  $M_{small} = 271\text{ kN.m}$  (from Steel).

No factors of safety are used neither in calculation of  $Z$  nor in calculation of  $M_{u,prop.}$  and  $M_{u,code}$ .

$P_{V,d}$  = Predicted shear failure load =  $2V_{u,d}$  and  $P_{M,d}$  = Predicted flexural failure load =  $2(M_{u,d}/a)$ .

$P_{F,pred.}$  = the smallest of ( $P_V$  or  $P_M$ ) and the predicted failure mode is the failure mode corresponding to  $P_{F,pred.}$ .

No factors of safety are used neither in prediction of  $V_c$  and  $V_s$  nor in prediction of  $P_{V,pred.}$  and  $P_{M,pred.}$ .

**Table 7.11:** Summary of the Crack Widths at Different Load Levels for the Beams in Test-Series "1".

Beam Type	At 1 <sup>st</sup> Flexural Crack		At 1 <sup>st</sup> Shear Crack		Service (Working) Condition		Failure (Ultimate) Condition		
	Load, kN	Crack Width, mm	Load, kN	Crack Width, mm	Load, kN	Flex. Crack Width, mm	Load, kN	Flex. Crack Width, mm	Shear Crack Width, mm
A1-0	250	0.04	350	0.03	450	0.43	560	0.67	3.0
A1-1a	150	0.02	350	0.02	650	0.41	820	1.36	6.16
A1-1b	100	0.01	300	0.02	600	0.42	800	1.24	6.22
A1-2	200	0.02	350	0.03	550	0.43	790	1.44	6.40
B1-0	200	0.04	350	0.06	450	0.42	558	0.61	3.82
B1-1a	150	0.02	300	0.04	600	0.40	795	1.28	6.45
B1-1b	200	0.02	350	0.02	550	0.42	782	1.68	6.80
B1-2	200	0.04	350	0.04	550	0.41	745	1.32	6.25
C1-0	150	0.03	300	0.04	400	0.41	485	0.61	5.82
C1-1a	200	0.04	350	0.04	550	0.42	712	1.28	6.0
C1-1b	200	0.03	350	0.06	550	0.40	694	1.20	6.10
C1-2	100	0.02	300	0.07	500	0.41	654	1.26	6.25
D1-0	250	0.05	350	0.26	400	0.42	480	0.64	7.20
D1-1a	150	0.04	350	0.03	500	0.40	641	0.92	5.78
D1-1b	200	0.03	300	0.04	550	0.41	633	0.60	5.84
D1-2	150	0.04	250	0.05	500	0.42	602	0.63	6.20

\* Service (working) load is the total applied load when the maximum flexural crack width reaches to the limit per the applied Code of Practice, which is 0.40mm for EC2, ACI318 and SBC304.

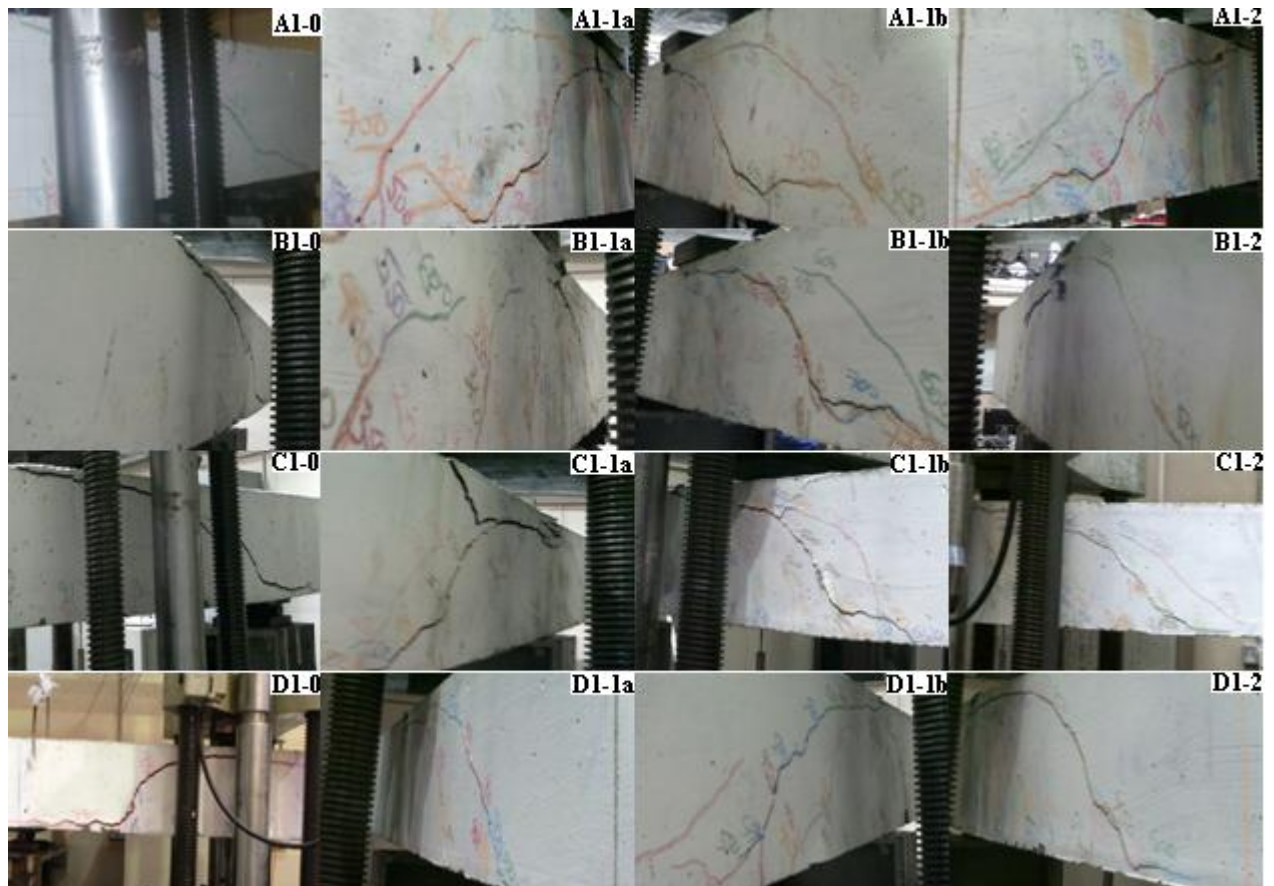
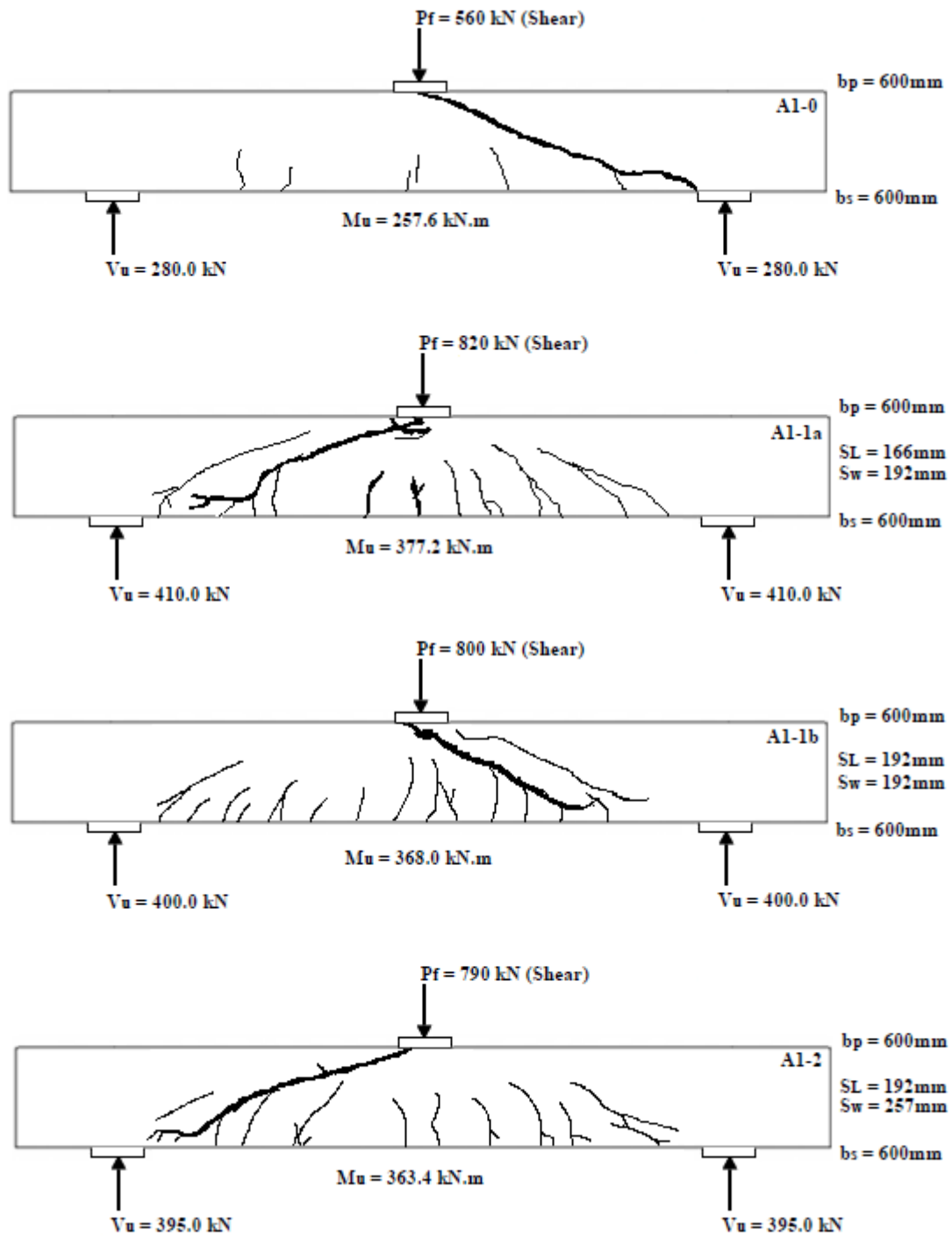
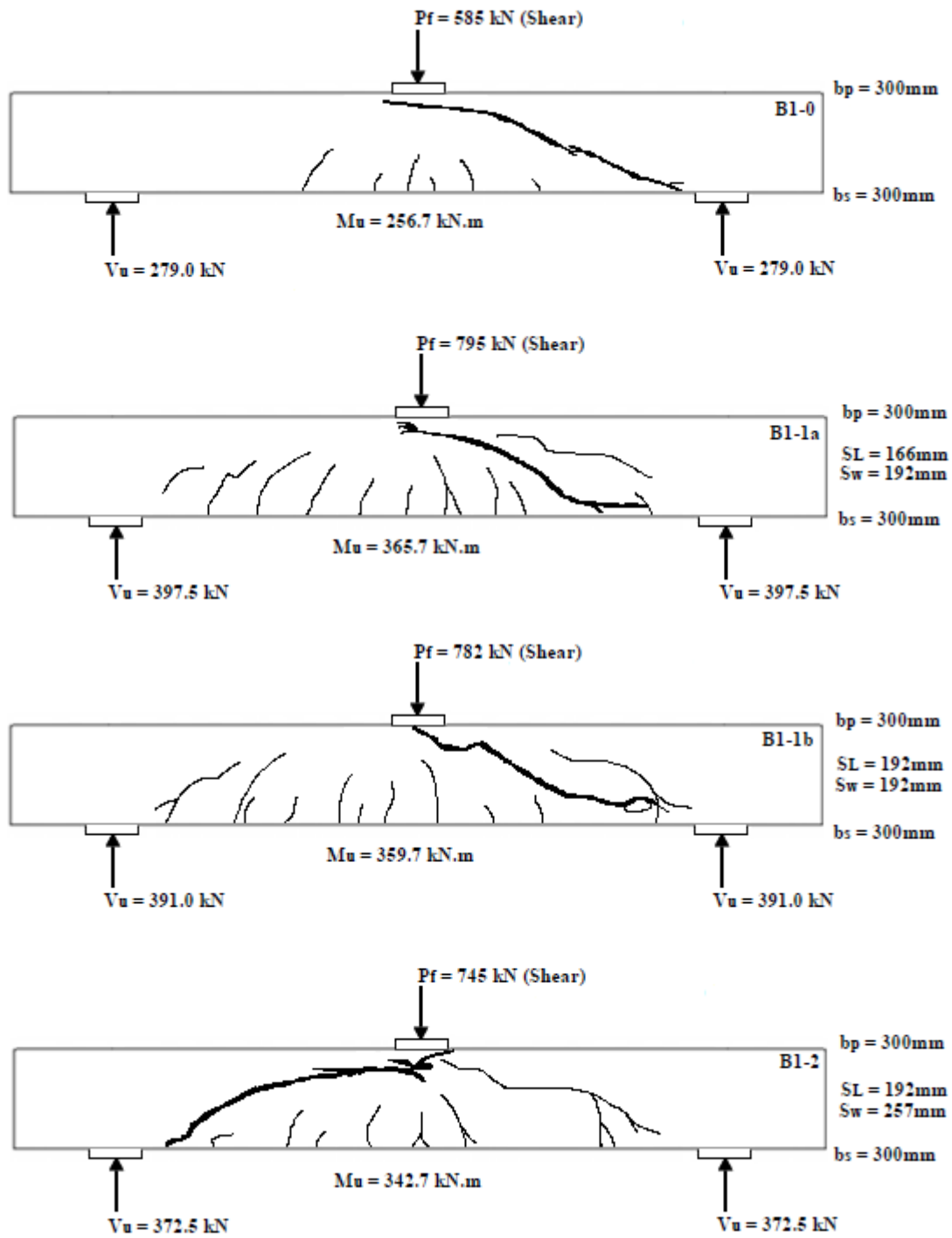


**Figure 7.9:** Critical Failure Modes and Crack Patterns for the Beams in Test-Series "1".

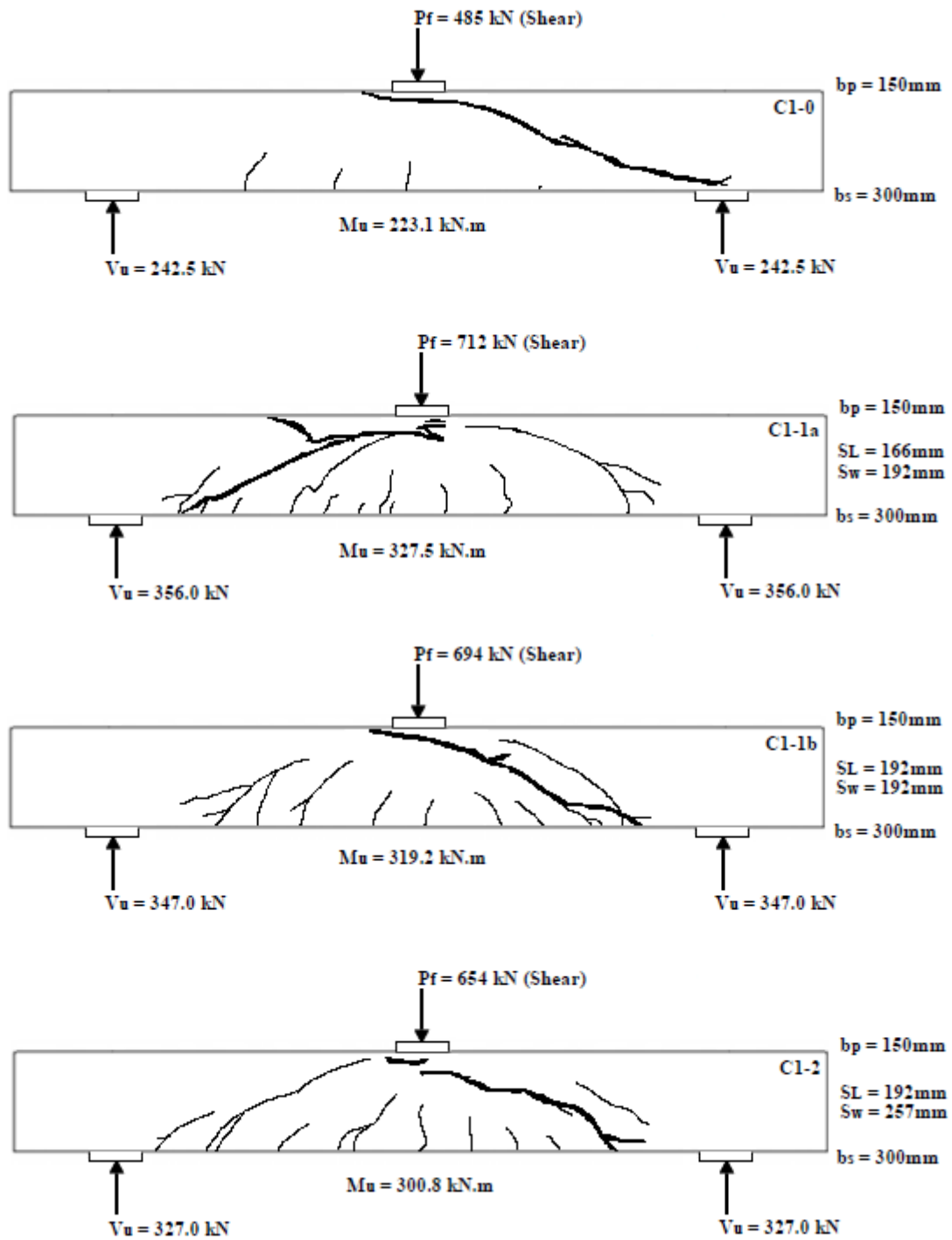


a) Beams in Type A

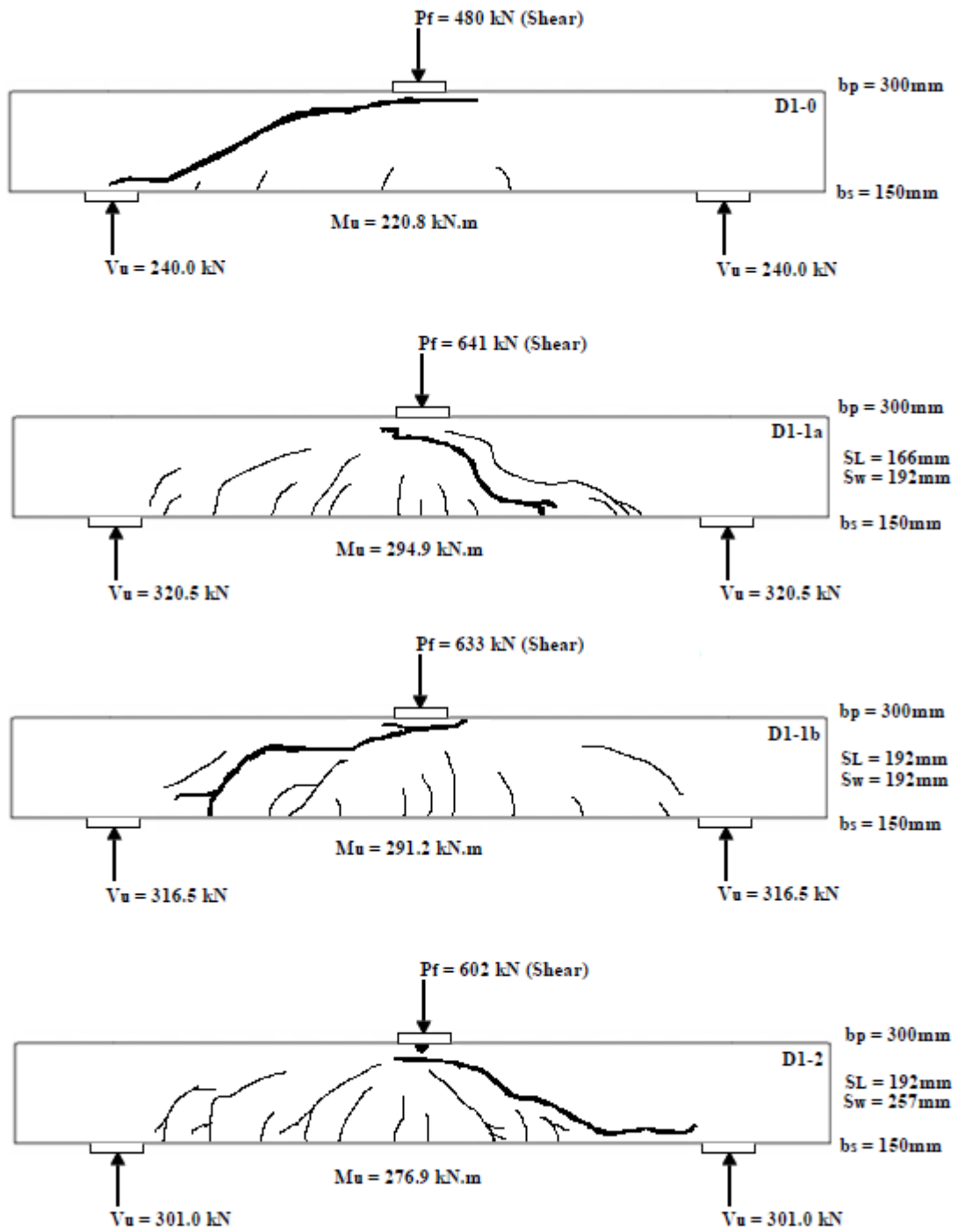




b) Beams in Type B



c) Beams in Type C



d) Beams in Type D

All beams had 4 stirrup-legs across their widths

**NOTE:** these Figures are enlarged to show Crack Patterns

**Figure 7.10:** Failure Modes and Crack Patterns after Failure for the Beams in Series "1".

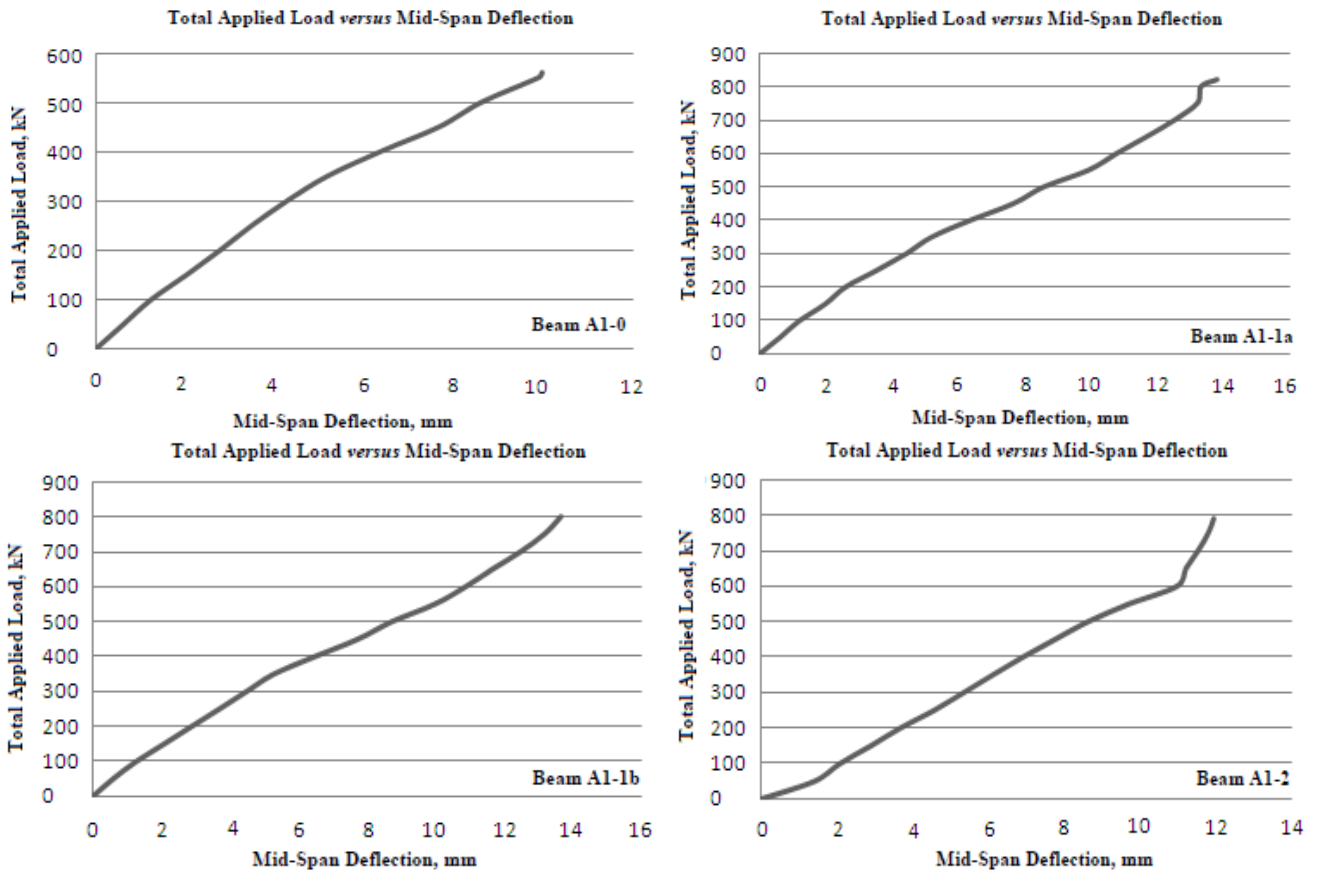


**Figure 7.11:** Total Applied Load versus Mid-Span Deflection for the Beams in Type (A) in Series "1".

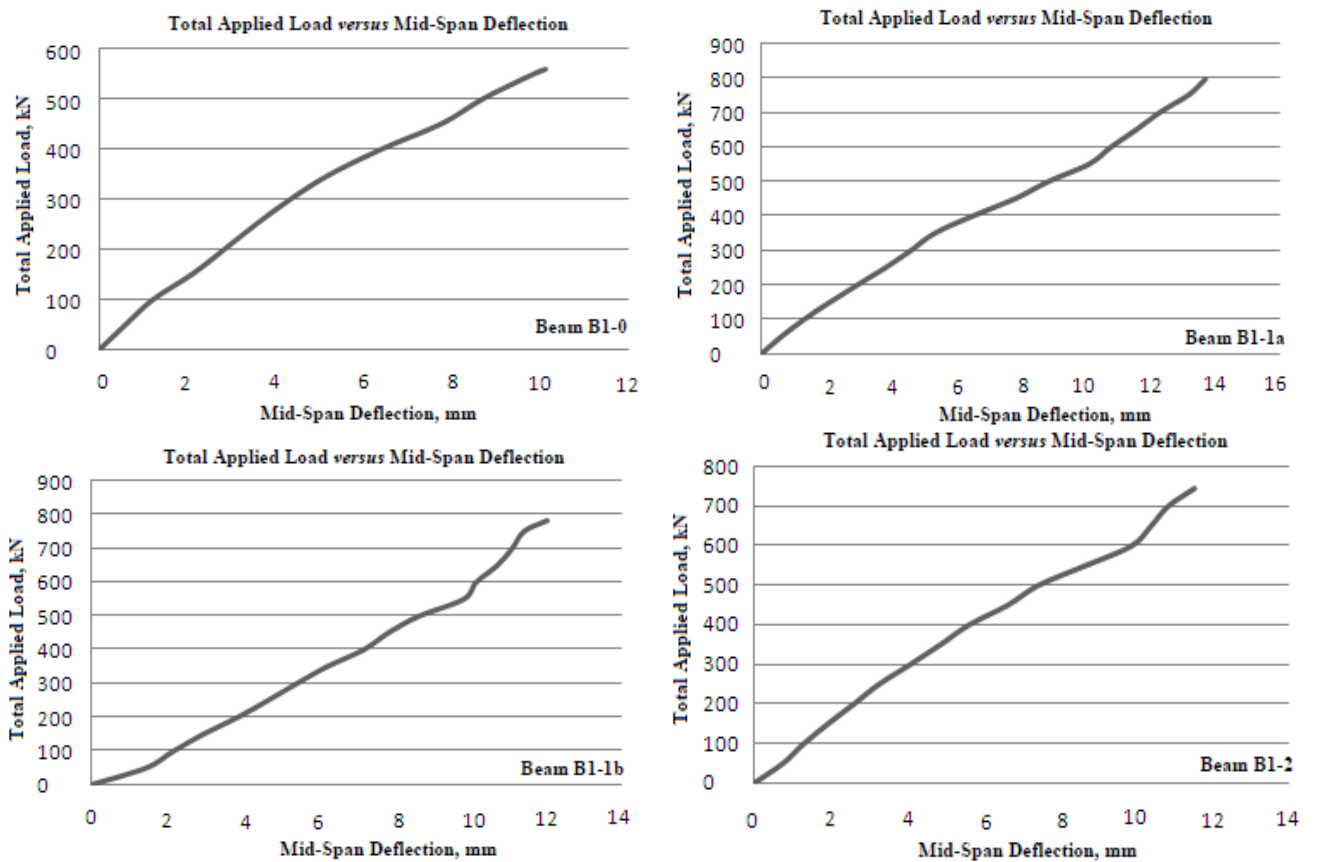


**Figure 7.12:** Total Applied Load versus Mid-Span Deflection for the Beams in Type (B) in Series "1".

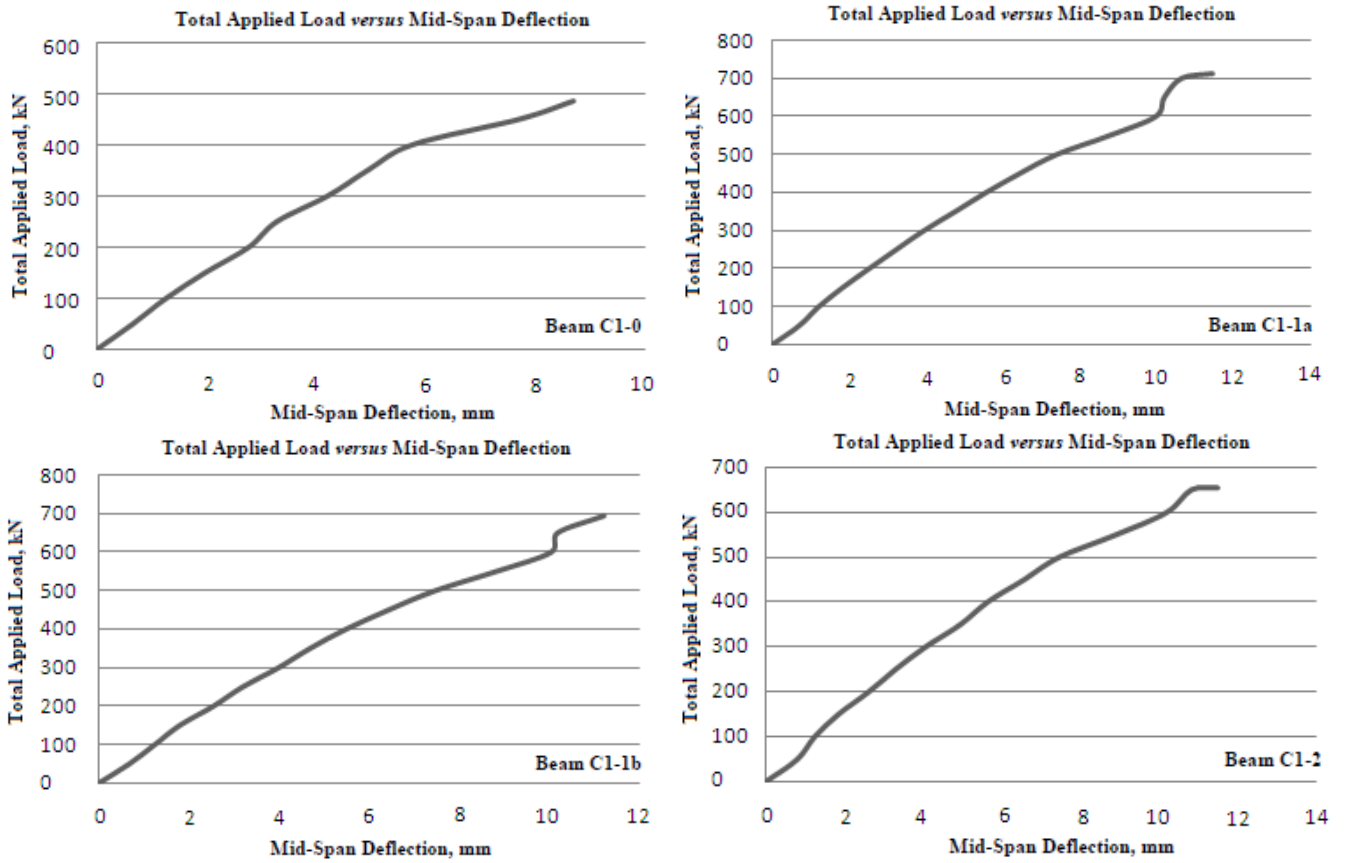


**Figure 7.13:** Total Applied Load versus Mid-Span Deflection for the Beams in Type (C) in Series "1".

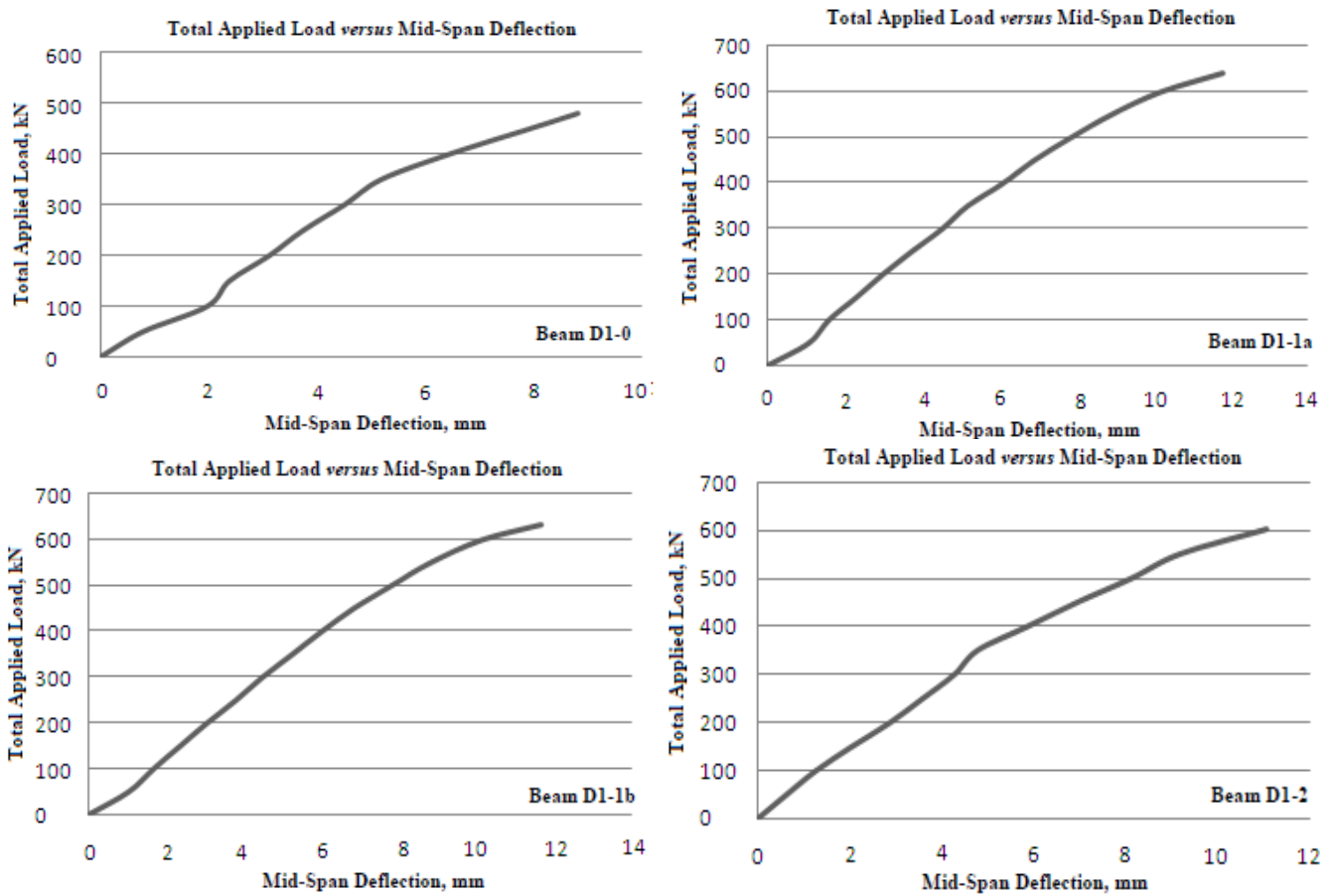


**Figure 7.14:** Total Applied Load versus Mid-Span Deflection for the Beams in Type (D) in Series "1".

**Table 7.12: Total Applied Load versus Mid-Span Deflections for Beams-Type (A) in Test-Series (1).**

Total Applied Load, kN	Beam (A1-0)		Beam (A1-1a)		Beam (A1-1b)		Beam (A1-2)	
	Centre Dial Reading, mm	Centre Dial Increment, $\Delta$ , mm	Centre Dial Reading, mm	Centre Dial Increment, $\Delta$ , mm	Centre Dial Reading, mm	Centre Dial Increment, $\Delta$ , mm	Centre Dial Reading, Mm	Centre Dial Increment, $\Delta$ , mm
0	14.09	0	29.75	0	29.81	0	29.02	0
50	14.71	0.62	30.38	0.63	30.40	0.59	30.43	1.41
100	15.33	1.24	30.97	1.22	31.08	1.27	31.11	2.09
150	16.12	2.03	31.75	2.0	31.89	2.08	31.92	2.90
200	16.87	2.78	32.35	2.60	32.69	2.88	32.70	3.68
250	17.58	3.49	33.29	3.54	33.50	3.69	33.59	4.57
300	18.37	4.28	34.19	4.44	34.29	4.48	34.37	5.35
350	19.27	5.18	34.96	5.21	35.09	5.28	35.14	6.12
400	20.46	6.37	36.13	6.38	36.28	6.47	35.93	6.91
450	21.77	7.68	37.43	7.68	37.54	7.73	36.78	7.76
500	22.72	8.63	38.35	8.60	38.53	8.72	37.65	8.63
550	24.00	9.91	39.70	9.95	39.78	9.97	38.73	9.71
600	$P_{f,exp.} = 560$ kN, $\Delta = 9.98$		40.55	10.80	40.68	10.87	40.00	10.98
650	Failure Mode = Shear		41.45	11.70	41.46	11.65	40.23	11.21
700			42.30	12.55	42.28	12.47	40.55	11.53
750			42.98	13.23	42.97	13.16	40.82	11.80
800			43.09	13.34	$P_{f,exp.} = 800$ kN, $\Delta = 13.64$		$P_{f,exp.} = 790$ kN, $\Delta = 11.94$	
			$P_{f,exp.} = 820$ kN, $\Delta = 13.82$		Failure Mode = Shear		Failure Mode = Shear	
			Failure Mode = Shear					

Locations of Deflection Dial Gauges refer to Figure 7.1.

**Table 7.13: Total Applied Load versus Mid-Span Deflections for Beams-Type (B) in Test-Series (1).**

Total Applied Load, kN	Beam (B1-0)		Beam (B1-1a)		Beam (B1-1b)		Beam (B1-2)	
	Centre Dial Reading, mm	Centre Dial Increment, $\Delta$ , mm	Centre Dial Reading, mm	Centre Dial Increment, $\Delta$ , mm	Centre Dial Reading, mm	Centre Dial Increment, $\Delta$ , mm	Centre Dial Reading, Mm	Centre Dial Increment, $\Delta$ , mm
0	14.12	0	29.80	0	29.0	0	20.75	0
50	14.72	0.60	30.42	0.62	30.46	1.46	21.51	0.76
100	15.34	1.22	31.12	1.32	31.18	2.18	22.06	1.31
150	16.22	2.10	31.92	2.12	31.97	2.97	22.69	1.94
200	16.96	2.84	32.77	2.97	32.88	3.88	23.37	2.62
250	17.68	3.56	33.64	3.84	33.68	4.68	24.03	3.28
300	18.46	4.34	34.43	4.63	34.44	5.44	24.85	4.10
350	19.37	5.25	35.17	5.37	35.24	6.24	25.64	4.89
400	20.54	6.42	36.35	6.55	36.21	7.21	26.39	5.64
450	21.88	7.76	37.66	7.86	36.86	7.86	27.41	6.66
500	22.83	8.71	38.69	8.89	37.68	8.68	28.21	7.46
550	23.99	9.87	39.94	10.14	38.86	9.86	29.45	8.70
600	$P_{f,exp.} = 558$ kN, $\Delta = 10.11$		40.62	10.82	39.18	10.18	30.66	9.91
650	Failure Mode = Shear		41.40	11.60	39.74	10.74	31.17	10.42
700			42.13	12.33	40.13	11.13	31.62	10.87
750			43.01	13.21	40.44	11.44	$P_{f,exp.} = 745$ kN, $\Delta = 11.56$	
			$P_{f,exp.} = 795$ kN, $\Delta = 13.72$		$P_{f,exp.} = 782$ kN, $\Delta = 12.05$		Failure Mode = Shear	
			Failure Mode = Shear		Failure Mode = Shear			

Locations of Deflection Dial Gauges refer to Figure 7.1.

**Table 7.14: Total Applied Load versus Mid-Span Deflections for Beams-Type (C) in Test-Series (1).**

Total Applied Load, kN	Beam (C1-0)		Beam (C1-1a)		Beam (C1-1b)		Beam (C1-2)	
	Centre Dial Reading, mm	Centre Dial Increment, $\Delta$ , mm	Centre Dial Reading, mm	Centre Dial Increment, $\Delta$ , mm	Centre Dial Reading, mm	Centre Dial Increment, $\Delta$ , mm	Centre Dial Reading, mm	Centre Dial Increment, $\Delta$ , mm
0	29.60	0	20.83	0	20.80	0	26.88	0
50	30.26	0.66	21.54	0.71	21.48	0.68	27.69	0.81
100	30.87	1.27	22.05	1.22	22.05	1.25	28.13	1.25
150	31.58	1.98	22.67	1.84	22.60	1.80	28.73	1.85
200	32.38	2.78	23.36	2.53	23.35	2.55	29.50	2.62
250	32.89	3.29	24.07	3.24	24.0	3.20	30.18	3.30
300	33.82	4.22	24.79	3.96	24.80	4.0	30.94	4.06
350	34.55	4.95	25.61	4.78	25.50	4.70	31.83	4.95
400	35.37	5.77	26.41	5.58	26.30	5.50	32.52	5.64
450	37.33	7.73	27.29	6.46	27.25	6.45	33.45	6.57
500	$P_{f,exp.} = 485 \text{ kN}, \Delta = 8.70$		28.25	7.42	28.28	7.48	34.34	7.46
550	Failure Mode = Shear		29.63	8.80	29.64	8.84	35.79	8.91
600			30.83	10.0	30.86	10.06	37.08	10.20
650			31.05	10.22	31.0	10.20	37.70	10.82
700			31.50	10.67	$P_{f,exp.} = 694 \text{ kN}, \Delta = 11.23$		$P_{f,exp.} = 654 \text{ kN}, \Delta = 11.48$	
			$P_{f,exp.} = 712 \text{ kN}, \Delta = 11.47$		Failure Mode = Shear		Failure Mode = Shear	
			Failure Mode = Shear					

Locations of Deflection Dial Gauges refer to Figure 7.1.

**Table 7.15: Total Applied Load versus Mid-Span Deflections for Beams-Type (D) in Test-Series (1).**

Total Applied Load, kN	Beam (D1-0)		Beam (D1-1a)		Beam (D1-1b)		Beam (D1-2)	
	Centre Dial Reading, mm	Centre Dial Increment, $\Delta$ , mm	Centre Dial Reading, mm	Centre Dial Increment, $\Delta$ , mm	Centre Dial Reading, mm	Centre Dial Increment, $\Delta$ , mm	Centre Dial Reading, mm	Centre Dial Increment, $\Delta$ , mm
0	1.38	0	29.50	0	29.58	0	14.088	0
50	2.17	0.79	30.59	1.09	30.62	1.04	14.72	0.63
100	3.36	1.98	31.10	1.60	31.26	1.68	15.36	1.27
150	3.77	2.39	31.82	2.32	31.95	2.37	16.14	2.05
200	4.51	3.13	32.50	3.0	32.64	3.06	16.97	2.88
250	5.14	3.76	33.25	3.75	33.39	3.81	17.68	3.59
300	5.90	4.52	34.04	4.54	34.07	4.49	18.37	4.28
350	6.58	5.20	34.70	5.20	34.84	5.26	18.87	4.78
400	7.85	6.47	35.62	6.12	35.60	6.02	19.96	5.87
450	9.34	7.96	36.42	6.92	36.42	6.84	21.04	6.95
500	$P_{f,exp.} = 480 \text{ kN}, \Delta = 8.84$		37.38	7.88	37.40	7.82	22.22	8.13
550	Failure Mode = Shear		38.42	8.92	38.40	8.82	23.26	9.17
600			39.71	10.21	39.74	10.16	25.08	10.99
			$P_{f,exp.} = 641 \text{ kN}, \Delta = 11.81$		$P_{f,exp.} = 633 \text{ kN}, \Delta = 11.68$		$P_{f,exp.} = 602 \text{ kN}, \Delta = 11.06$	
			Failure Mode = Shear		Failure Mode = Shear		Failure Mode = Shear	

Locations of Deflection Dial Gauges refer to Figure 7.1.

**Table 7.16: Total Applied Load versus Crack Widths for Beams-Type (A) in Test-Series (1).**

Load kN	Beam (A1-0) Crack Width, mm		Beam (A1-1a) Crack Width, mm		Beam (A1-1b) Crack Width, mm		Beam (A1-2) Crack Width, mm	
	Flexural	Shear	Flexural	Shear	Flexural	Shear	Flexural	Shear
0	-	-	-	-	-	-	-	-
50	-	-	-	-	-	-	-	-
100	-	-	-	-	0.01	-	-	-
150	-	-	0.02	-	-	-	-	-
200	-	-	0.03	-	0.02	-	0.02	-
250	0.04	-	0.06	-	0.03	-	0.04	-
300	0.16	-	0.10	-	0.14	0.02	0.18	-
350	0.27	0.03	0.18	0.02	0.21	0.04	0.26	0.03
400	0.35	0.18	0.22	0.18	0.24	0.22	0.30	0.24
450	0.43	0.36	0.24	0.30	0.29	0.32	0.32	0.38
500	0.49	0.60	0.28	0.48	0.30	0.55	0.34	0.66
550	0.56	1.88	0.34	1.22	0.38	1.46	0.43	1.64
600	P <sub>f,exp.</sub> = 560 kN, Δ = 9.98		0.39	1.74	0.42	1.86	0.56	1.99
650	Failure Mode = Shear		0.41	2.28	0.54	2.40	0.68	2.66
700	0.67	3.0	0.48	3.10	0.82	3.25	0.92	3.70
750			0.92	4.98	0.96	5.74	1.06	5.90
800			1.12	5.66	P <sub>f,exp.</sub> = 800 kN, Δ = 13.64		P <sub>f,exp.</sub> = 790 kN, Δ = 11.94	
			P <sub>f,exp.</sub> = 820 kN, Δ = 13.82		Failure Mode = Shear		Failure Mode = Shear	
			Failure Mode = Shear		1.24	6.22	1.44	6.40
			1.36	6.16				

**Table 7.17: Total Applied Load versus Crack Widths for Beams-Type (B) in Test-Series (1).**

Load kN	Beam (B1-0) Crack Width, mm		Beam (B1-1a) Crack Width, mm		Beam (B1-1b) Crack Width, mm		Beam (B1-2) Crack Width, mm	
	Flexural	Shear	Flexural	Shear	Flexural	Shear	Flexural	Shear
0	-	-	-	-	-	-	-	-
50	-	-	-	-	-	-	-	-
100	-	-	-	-	-	-	-	-
150	-	-	0.02	-	-	-	-	-
200	0.04	-	0.03	-	0.02	-	0.04	-
250	0.06	-	0.06	-	0.06	-	0.08	-
300	0.16	-	0.16	0.04	0.22	-	0.16	-
350	0.28	0.06	0.24	0.10	0.28	0.02	0.24	0.04
400	0.36	0.18	0.28	0.26	0.30	0.26	0.28	0.20
450	0.42	0.66	0.32	0.38	0.34	0.44	0.30	0.86
500	0.48	1.20	0.36	0.62	0.38	0.76	0.36	1.50
550	0.54	2.18	0.39	1.54	0.42	1.60	0.41	2.12
600	P <sub>f,exp.</sub> = 558 kN, Δ = 10.11		0.40	1.94	0.62	2.08	0.56	3.64
650	Failure Mode = Shear		0.56	2.56	0.72	2.80	0.72	4.38
700	0.61	3.82	0.88	3.34	0.96	3.74	0.92	5.52
750			1.0	5.82	1.12	4.66	P <sub>f,exp.</sub> = 745 kN, Δ = 11.56	
			P <sub>f,exp.</sub> = 795 kN, Δ = 13.72		P <sub>f,exp.</sub> = 782 kN, Δ = 12.05		Failure Mode = Shear	
			Failure Mode = Shear		Failure Mode = Shear		1.32	6.25
			1.28	6.45	1.68	6.80		



**Table 7.18: Total Applied Load versus Crack Widths for Beams-Type (C) in Test-Series (1).**

Load kN	Beam (C1-0) Crack Width, mm		Beam (C1-1a) Crack Width, mm		Beam (C1-1b) Crack Width, mm		Beam (C1-2) Crack Width, mm	
	Flexural	Shear	Flexural	Shear	Flexural	Shear	Flexural	Shear
0	-	-	-	-	-	-	-	-
50	-	-	-	-	-	-	-	-
100	-	-	-	-	-	-	0.02	-
150	0.03	-	-	-	-	-	-	-
200	0.05	-	0.04	-	0.03	-	0.04	-
250	0.07	-	0.08	-	0.06	-	0.09	-
300	0.18	0.04	0.12	-	0.10	-	0.15	0.07
350	0.30	0.22	0.22	0.04	0.20	0.06	0.21	0.36
400	0.41	0.76	0.26	0.24	0.24	0.32	0.26	0.80
450	0.56	2.50	0.28	0.98	0.28	1.23	0.32	1.10
500	P <sub>f,exp.</sub> = 485 kN, Δ = 8.70		0.34	1.62	0.33	1.80	0.41	1.44
550	Failure Mode = Shear		0.42	2.28	0.40	2.46	0.69	2.08
600	0.61	5.82	0.52	3.74	0.58	3.80	0.86	3.14
650			0.68	4.46	0.74	5.60	1.08	5.22
700			0.82	5.66	P <sub>f,exp.</sub> = 694 kN, Δ = 11.23		P <sub>f,exp.</sub> = 654 kN, Δ = 11.48	
			P <sub>f,exp.</sub> = 712 kN, Δ = 11.47		Failure Mode = Shear		Failure Mode = Shear	
			Failure Mode = Shear		1.20	6.10	1.26	6.25
			1.28	6.0				

**Table 7.19: Total Applied Load versus Crack Widths for Beams-Type (D) in Test-Series (1).**

Load kN	Beam (D1-0) Crack Width, mm		Beam (D1-1a) Crack Width, mm		Beam (D1-1b) Crack Width, mm		Beam (D1-2) Crack Width, mm	
	Flexural	Shear	Flexural	Shear	Flexural	Shear	Flexural	Shear
0	-	-	-	-	-	-	-	-
50	-	-	-	-	-	-	-	-
100	-	-	-	-	-	-	-	-
150	-	-	0.04	-	-	-	0.04	-
200	-	-	0.04	-	0.03	-	0.06	-
250	0.05	-	0.06	-	0.04	-	0.08	0.05
300	0.21	-	0.10	-	0.12	0.04	0.14	0.20
350	0.32	0.26	0.20	0.03	0.22	0.21	0.24	0.28
400	0.42	0.80	0.22	0.26	0.24	0.38	0.28	0.40
450	0.59	2.76	0.28	0.94	0.30	1.05	0.37	1.11
500	P <sub>f,exp.</sub> = 480 kN, Δ = 8.84		0.40	1.32	0.35	1.40	0.42	2.66
550	Failure Mode = Shear		0.48	2.26	0.41	2.17	0.50	4.39
600	0.64	7.20	0.64	3.42	0.54	3.24	0.62	5.98
			P <sub>f,exp.</sub> = 641 kN, Δ = 11.81		P <sub>f,exp.</sub> = 633 kN, Δ = 11.68		P <sub>f,exp.</sub> = 602 kN, Δ = 11.06	
			Failure Mode = Shear		Failure Mode = Shear		Failure Mode = Shear	
			0.92	5.78	0.60	5.84	0.63	6.20

## 7.11 Discussion of Test Results

All results, discussions, verifications and conclusions on the behaviour of the wide RC beams tested in Test-Series (1) are described in the following Sections (Alluqmani, 2013a):

The 16 wide RC beams tested in Series (1) were used to verify the proposed prediction model and to study the effect of  $k_s$ ,  $k_p$ ,  $SL$  and  $S_w$  on the beam capacities. All beams were predicted by the proposed prediction model to fail in shear according to EC2 and to ACI318 and SBC304 (and were also predicted by the existing Codes and Models). The beams without stirrups had a proposed predicted shear capacity ( $V_{u,d}$ ) between 234 kN and 276 kN with a total proposed predicted shear failure load ( $P_{f,pred.} = P_{V,d} = 2*V_{u,d}$ ) between 468 kN and 552 kN to EC2 and between 416 kN and 490 kN to ACI318 and SBC304 (and between 264 kN and 384 kN to the existing Codes and models), Tables 7.8 and 7.10. The beams without stirrups had a proposed predicted flexural capacity ( $M_{u,d}$ ) between 322 kN.m and 380 kN.m with a total proposed predicted flexural failure load ( $P_{f,pred.} = P_{M,d} = (M_{u,d}/a)*2$ ) between 700 kN and 826 kN (and between 570 kN and 589 kN to the existing Codes and models), Tables 7.8 and 7.10. The beams without stirrups failed experimentally in shear at a total failure load ( $P_{f,exp.} = P_{V,exp.} = 2*V_{u,exp.}$ ) between 480 kN and 560 kN as obtained from both the tests and the proposed prediction model of the one-way shear capacity (Equation (6.9)), Table 7.10. The beams with stirrups had a proposed predicted shear capacity ( $V_{u,d}$ ) between 297 kN and 408 kN with a total proposed predicted shear failure load ( $P_{f,pred.} = P_{V,d} = 2*V_{u,d}$ ) between 594 kN and 816 kN to EC2 and between 558 kN and 786 kN to ACI318 and SBC304 (and between 477 kN and 801 kN to the existing Codes and models), Tables 7.8 and 7.10. The beams with stirrups had a proposed predicted flexural capacity ( $M_{u,d}$ ) between 322 kN.m and 380 kN.m with a total proposed predicted flexural failure load ( $P_{f,pred.} = P_{M,d} = (M_{u,d}/a)*2$ ) between 700 kN and 826 kN (and between 570 kN and 589 kN to the existing Codes and models), Tables 7.8 and 7.10. The beams with stirrups failed experimentally in shear at a total failure load ( $P_{f,exp.} = P_{V,exp.} = 2*V_{u,exp.}$ ) between 602 kN and 820 kN as obtained from both the tests and the proposed prediction model of the one-way shear capacity (Equation (6.9)), Table 7.10.

All wide beams in Series (1) were designed and detailed by EC2 Code, and had a shear-span to effective-depth ( $a/d$ ) ratio of 3.58 where  $a = 920$ mm and  $d = 257$ mm. All beams without and with shear-reinforcement failed in shear as predicted by the proposed prediction model. All beams with stirrups in Beam-Group (1a), i.e. beams A1-1a, B1-1a, C1-1a and D1-1a, were designed with longitudinal and transverse stirrup legs spacing of  $SL = 0.65d = 166$ mm and  $S_w =$

$0.75d = 192\text{mm}$ , respectively, and failed in shear by diagonal cracking. All beams with stirrups in Beam-Group (1b), i.e. beams A1-1b, B1-1b, C1-1b and D1-1b were designed with longitudinal and transverse stirrup legs spacing of  $S_L = 0.75d = 192\text{mm}$  and  $S_w = 0.75d = 192\text{mm}$ , respectively, and failed in shear by diagonal cracking. While, all beams with stirrups in Beam-Group (2), i.e beams A1-2, B1-2, C1-2 and D1-2, were designed with longitudinal and transverse stirrup legs spacing of  $S_L = 192\text{mm}$  and  $S_w = d = 257\text{mm}$ , respectively, and also failed in shear by diagonal cracking.

### **7.11.1 Failure Modes**

The failure mode was the same for all the beams in Series (1). All beams without and with shear-reinforcement failed in shear by diagonal cracking in the shear-span regions. In all beams, hair-line flexural cracks developed in the lower part of the beams and extended vertically towards the neutral axis before the appearance of diagonal cracks. As loading continued, the flexural cracks proliferated and widened; and diagonal cracks appeared in the both shear spans.

### **7.11.2 Effect of $b_s$ and $b_p$**

As a comparison between each four beams in each Beam-Group with the other correspondingly beams [Beam-Group (0): beams A1-0, B1-0, C1-0 and D1-0; Beam-Group (1a): beams A1-1a, B1-1a, C1-1a and D1-1a; Beam-Group (1b): beams A1-1b, B1-1b, C1-1b and D1-1b; and Beam-Group (2): beams A1-2, B1-2, C1-2 and D1-2], the only difference between them is the width of support and loading plates. It can be seen that the width of loading and support plates ( $b_p$  and  $b_s$ ), or at best  $k_p$  and  $k_s$ , had influence on the strengths of wide RC beams, where the beam capacities decreased as the support width and/or the load width decreased, or at best, as  $k_s$  and  $k_p$  decreased. This happened for beams without and with shear-reinforcement. Accordingly, it can be concluded that the strengths of wide RC beams decrease as the load and/or support widths ( $b_p$  and/or  $b_s$ ) decrease, hence as  $k_p$  and/or  $k_s$  ratios decrease.

For each four beams in each Beam-Group, the beams with full-width bearing plates in Type (A) in regards to study the effect of  $b_p$  and  $b_s$ , or at best  $k_p$  and  $k_s$ , i.e beams A1-0, A1-1a, A1-1b and A1-2, had the best results and strengths comparing with the other correspondingly relevant beams in the same group. Thus, it can be said that proposed detailing approach and design model should be developed for this account in regards to study the effect of the full- and narrow- width supports and loads on the capacities of wide RC beams.

For all wide beams, loaded and supported via full-width bearing plates, without and with shear-reinforcement, all cracks stopped at the centreline of the load plate and stopped at the edge of the support plate. On the other hand, for wide beams without shear-reinforcement, loaded and supported via narrow-width bearing plates, all cracks passed the load plate and stopped at the centreline of the support plate. While for all wide beams with shear-reinforcement, loaded and supported via narrow-width bearing plates, all cracks passed the load plate and did not reach to the support plate.

To study the effect of the load width ( $b_p$ ), or at best  $k_p$ , on the capacity of wide beams, the beams in Type (B) are compared with those correspondingly relevant beams in Type (C) for the same group. When  $k_p$  was reduced from 0.50 for the beams in Type (B) to 0.25 for the beams in Type (C), the shear capacities and failure loads decreased by 13% for the beam without stirrups (beam C1-0) and decreased by 10.5%, 11.3% and 12.3% for the beams with stirrups (beams C1-1a, C1-1b and C1-2, respectively). This indicates that the load width affects on the shear strength of wide RC beams, where the shear strength decreased as the load width was reduced. This outcome is contrary with the conclusion made by Leonhardt and Walther (1964), where they concluded that the influence of load width was not much more than typical experimental scatter for the geometries studied.

To study the effect of the support width ( $b_s$ ), or at best  $k_s$ , on the capacity of wide beams, the beams in Type (B) are compared with those correspondingly relevant beams in Type (D) for the same group. When  $k_s$  was reduced from 0.50 for the beams in Type (B) to 0.25 for the beams in Type (D), the shear capacities and failure loads decreased by 14% for the beam without stirrups (beam D1-0) and decreased by 19.4%, 19.1% and 19.2% for the beams with stirrups (beams D1-1a, D1-1b and D1-2, respectively). This indicates that the support width affects on the shear strength of wide RC beams, where the shear strength decreased as the support width was reduced. This outcome is linked to the conclusions made by Lubell et al. (2008), Serna-Ros et al. (2002) and Al.Dywany (2010), where they concluded that the shear strength of wide RC beams decreases as the support width is reduced.

As result from the beams in Types B, C and D, it is clear that  $k_s$  has more influence than  $k_p$  on the shear capacity of wide beams without or with shear-reinforcement. Consequently, as the beams with stirrups in Type (D), beams D1-1a, D1-1b and D1-2, had decreasing in their shear capacities with percentages of 19.4%, 19.1% and 19.2%, respectively, when  $k_s$  was reduced from

0.50 to 0.25, the longitudinal stirrup-legs spacing ( $S_L$ ) should be strongly treated with  $k_s$ . This is because the change in the reduction percentage was 19.4% and 19.1% for the beams in Type (D), Groups (1a and 1b) respectively, where they were used for investigating  $S_L$  and the main variable for the beams was  $k_s$ . No change in the reduction percentage for the beams in Groups (1b and 2), where they had a percentage of 19.1% and 19.2%, respectively. Otherwise, as the beams with stirrups in Type (C), beams C1-1a, C1-1b and C1-2, had decreasing in their shear capacities with percentages of 10.5%, 11.3% and 12.3%, respectively, when  $k_p$  was reduced from 0.50 to 0.25, the transverse stirrup-legs spacing ( $S_w$ ) should be strongly treated with  $k_p$  and  $S_L$ . This is because the change in the reduction percentage was 11.3% and 12.3% for the beams in Type (C), Groups (1b and 2) respectively, where they were used for investigating  $S_w$  and the main variable for the beams was  $k_p$ . Furthermore, the lower reduction percentage was 10.5% for the beam in Group (1a), where it was specially detailed for  $S_L$  to be compared with the beam in Group (1b); thus, this therefore leads to that  $S_L$  has an influence on  $S_w$ .

### 7.11.3 Effect of $S_L$ and $S_w$

As a comparison between each four beams in each Beam-Type [Beam-Type (A): beams A1-0, A1-1a, A1-1b and A1-2; Beam-Type (B): beams B1-0, B1-1a, B1-1b and B1-2; Beam-Type (C): beams C1-0, C1-1a, C1-1b and C1-2; Beam-Type (D): beams D1-0, D1-1a, D1-1b and D1-2], the only difference between them is the shear reinforcement (stirrups). All beams were the same for their geometry and design, except  $S_L$  for the beams in groups (1a and 1b) and  $S_w$  for the beams in groups (1b and 2), where the beams in Group (0) did not contain stirrups. It can be seen that the longitudinal and transverse stirrup-legs spacing ( $S_L$  and  $S_w$ ) had influence on the strengths of wide RC beams, where the beam capacities decreased as  $S_L$  increased from 0.65d to 0.75d (beams in Groups (1a and 1b)), and/or as  $S_w$  increased from 0.75d to d (beams in Groups (1b and 2)), or as  $S_L$  and  $S_w$  were deleted (beams without stirrups in Group (0)). As a result, the beams in Type (A) had the best results, where the beams in Type (D) had the worst results; hence, as a comparison between beam A1-0 without stirrups and beam D1-2 with 4-leg stirrups (the worst beam with stirrups amongst the other beams with stirrups in the all types and groups of beams), beam D1-2 had a strength higher than that for beam A1-0 without stirrups. This indicates that the presence of the shear reinforcement in form of multi stirrup legs distributed across the wide beam width has increased the wide beam strengths even if they were loaded and supported with narrow-width bearing plates. Consequently, it can be suggested that, for wide RC beams, the shear-reinforcement (stirrups) should be included even if they are not required. This is hence that, for wide RC beams, at least four stirrups legs should be included in the beam as

shear reinforcement even if they are not required or the design requires a lesser quantity, and must be arranged and distributed across the beam width [Alluqmani, 2013a; Alluqmani and Saafi, 2014c]. Accordingly, it can be concluded, as a general case, that the strengths of wide RC beams decrease as the longitudinal and/or transverse stirrup-legs spacing ( $S_L$  and/or  $S_w$ ) increase.

For each four beams in each Beam-Type, the wide beams in Group (1a), designed for  $S_L = 0.65d$  and  $S_w = 0.75d$  in regards to study the effect of  $S_L$  and  $S_w$ , i.e beams A1-1a, B1-1a, C1-1a and D1-1a, had the best results and strengths comparing with the other correspondingly relevant beams in the same type (the other Beam-Groups in the same Beam-Type), as shown in Tables 7.9 and 7.10. Thus, it can be said that a proposed design model should be developed for this account with taking into the consideration the effect of the full- and narrow- width supports and loads on the longitudinal and transverse stirrup-legs spacing of wide RC beams. Beam A1-1a with full-width load and supports, designed for  $S_L = 0.65d$  and  $S_w = 0.75d$ , was the best and stronger beam amongst the other 15 beams in Series (1), but the beam failed in shear at 820 kN due to the effect of its  $S_w$ . For wide RC beams with full-width loads and supports, a value of  $0.65d$  for  $S_L$  and a value to be lesser than  $0.75d$  for  $S_w$  are strongly recommended. Thus, it can be said that the longitudinal and transverse spacing of the stirrup legs must be designed for wide RC beams as a percentage of  $d$  taking into the consideration ' $k_s$ ' for  $S_L$  and ' $k_p$  and  $S_L$ ' for  $S_w$  as mentioned above, where  $d$  is the effective-depth of the beam. A proposed design model should be developed for this account.

To study the effect of the longitudinal stirrup-legs spacing ( $S_L$ ) on the capacity of wide beams with full- and narrow- width loads and supports, each beam in Group (1a) in each Beam-Type is compared with the beam in Group (1b) in the same Beam-Type. For the beams with full-width loads and supports, i.e. Beam-Type (A), when  $S_L$  was increased from  $0.65d$  for beam A1-1a to  $0.75d$  for beam A1-1b, the shear capacity and failure load decreased by 2.5%. Beams A1-1a and A1-1b were used to investigate  $S_L$ , where beam A1-1a was designed with  $S_L = 0.65d$  and was the stronger and best beam in Series (1) but it failed in shear; therefore, it is strongly recommended that  $S_L$  for full-width loaded and supported wide beams must be taken  $0.65d$ . For the beams with narrow-width loads and supports, i.e. Beam-Types (B, C and D), when  $S_L$  was increased from  $0.65d$  for beams B1-1a, C1-1a and D1-1a to  $0.75d$  for beams B1-1b, C1-1b and D1-1b, the shear capacities and failure loads decreased by 1.6%, 2.5% and 1.25%, respectively. It is clear that the closer percentages of reduction was 1.6% and 1.25% for the beams in Types (B) and (D), respectively, where they followed to Groups (1a and 1b) for investigating  $S_L$  and the main variable for the beams was  $k_s$ ; therefore, it is strongly recommended that  $S_L$  for narrow-width

loaded and supported wide beams must be treated with  $k_s$ . These indicate that the longitudinal stirrup-legs spacing ( $S_L$ ) affects on the shear strength of wide RC beams, where the shear strength decreased as  $S_L$  increased. This outcome is linked to the conclusions made by Shuraim (2012), Serna-Ros et al (2002) and Anderson and Ramirez (1989), where they concluded that the shear strength of wide RC beams decreases as the longitudinal stirrup-legs spacing increases.

To study the effect of the transverse stirrup-legs spacing ( $S_w$ ) on the capacity of wide beams with full- and narrow- width loads and supports, each beam in Group (1b) in each Beam-Type is compared with the beam in Group (2) in the same Beam-Type. For the beams with full-width loads and supports, i.e. Beam-Type (A), when  $S_w$  was increased from  $0.75d$  for beam A1-1b to  $d$  for beam A1-2, the shear capacity and failure load decreased by 1.75%. Beams A1-1b and A1-2 were used to investigate  $S_w$ , where beam A1-1b was designed with  $S_w = 0.75d$  and failed in shear; therefore, it is strongly recommended that  $S_w$  for full-width loaded and supported wide beams must be lesser than  $0.75d$ . For the beams with narrow-width loads and supports, i.e. Beam-Types (B, C and D), when  $S_w$  was increased from  $0.75d$  for beams B1-1b, C1-1b and D1-1b to  $d$  for beams B1-2, C1-2 and D1-2, the shear capacities and failure loads decreased by 4.7%, 5.8% and 4.9%, respectively. It is clear that the difference in the reduction percentage (= 5.8%) was for beams C1-1b and C1-2 that followed to Groups (1b and 2) for investigating  $S_w$  and the main variable for the beams was  $k_p$ ; therefore, it is strongly recommended that  $S_w$  must be treated with  $k_p$ . These indicate that the transverse stirrup-legs spacing ( $S_w$ ) affects on the shear strength of wide RC beams, where the shear strength decreased as  $S_w$  increased. This outcome is linked to the conclusions made by Lubell et al (2009a), Serna-Ros et al (2002), Shuraim (2012), Hanafy et al (2012), Anderson and Ramirez (1989) and Zheng (1989), where they concluded that the shear strength of wide RC beams decreases as the transverse stirrup-legs spacing increases. On the other hand, this outcome is contrary with the conclusion of Hsiung and Frantz (1985), where they concluded based on their results that "the shear capacity of a large reinforced concrete beam is not affected by the transverse spacing of stirrups across the web width". This may due to that Hsiung and Frantz (1985)'s results are not considered for wide beams, where the width to height ( $b_w/h$ ) ratios of their specimens were  $1/3$ ,  $2/3$  and  $1.0$ , while the wide beams should have  $b_w/h$  ratio  $\geq 2.0$ .

As result from the beams in Types B, C and D, it is clear that  $k_s$  has more influence than  $k_p$  on the shear capacity of wide beams. Consequently, as the beams with stirrups in Type (D), beams D1-1a, D1-1b and D1-2, had decreasing in their shear capacities with percentages of 19.4%, 19.1% and 19.2%, respectively, when  $k_s$  was reduced from  $0.50$  to  $0.25$ , the longitudinal stirrup

legs spacing (SL) should be strongly treated with  $k_s$ . This is because the change in the reduction percentage was 19.4% and 19.1% for the beams in Type (D) in Groups (1a and 1b) respectively, where they were used for investigating SL and the main variable for the beams was  $k_s$ . No change in the reduction percentage for for the beams in Groups (1b and 2), where they had a percentage of 19.1% and 19.2%, respectively. Otherwise, as the beams with stirrups in Type (C), beams C1-1a, C1-1b and C1-2, had decreasing in their shear capacities with percentages of 10.5%, 11.3% and 12.3%, respectively, when  $k_p$  was reduced from 0.50 to 0.25, the transverse stirrup legs spacing ( $S_w$ ) should be strongly treated with  $k_p$  and SL. This is because the change in the reduction percentage was 11.3% and 12.3% for the beams in Type (C) in Groups (1b and 2) respectively, where they were used for investigating  $S_w$  and the main variable for the beams was  $k_p$ . Furthermore, the lower reduction percentage was 10.5% for the beam in Group (1a), where it was specially detailed for SL to be compared with the beam in Group (1b); thus, this therefore leads to that SL has an influence on  $S_w$ .

#### 7.11.4 Validation of $K_{cd,act.}$ and $K_{cd,act.,Prop.}$ On Series (1)

The ratio of the experimental-to-Code-predicted shear strength resisted by concrete ( $V_{c,exp.}/V_{c,Pred.-Code} = K_{cd,act.}$ ), which corresponds to  $K_{cd}$  given by the proposed prediction model ( $K_{cd,Prop.} = V_{c,Pred.-Prop.}/V_{c,Pred.-Code} = \mu_s * \beta_g$ ), was compared with that ratio to the proposed prediction ( $K_{cd,act.,Prop.} = V_{c,exp.}/V_{c,Pred.-Prop.} = K_{cd,act.}/K_{cd,Prop.}$ ). For full-width wide beams, the  $K_{cd,act.}$  was approximately 1.46 (correspondingly to  $K_{cd,Prop.} = \mu_s * \beta_g = 1.43$ ), while the the  $K_{cd,act.,Prop.}$  was approximately 1.02. Otherwise, for partial-width wide beams, the  $K_{cd,act.}$  was between 1.25 and 1.45 (correspondingly to  $K_{cd,Prop.} = \mu_s * \beta_g = 1.22$  and 1.44, respectively), while the  $K_{cd,act.,Prop.}$  was between 1.03 and 1.01, respectively. This seems that the  $K_{cd,act.,Prop.}$  obtained by the proposed prediction model gives more accuracy than that  $K_{cd,act.}$  obtained by the Codes of Practice, such EC2 Code. This has also shown the deficiency of the Code to predict the concrete contribution to the shear strength of wide RC beams. It should be noted that  $V_{c,Pred.-Prop.}$  is the  $V_{c,d}$  proposed in Equation (6.10),  $V_{c,Pred.-Code}$  is the  $V_c$  given by the Codes (Equations 4.23 and 4.26), and  $V_{c,exp.}$  is the  $V_c$  obtained by the test.

#### 7.11.5 Validation of $K_{sd,act.}$ and $K_{sd,act.,Prop.}$ On Series (1)

The ratio of the experimental-to-Code-predicted shear strength resisted by stirrups ( $V_{s,exp.}/V_{s,Pred.-Code} = K_{sd,act.}$ ), which corresponds to  $K_{sd}$  given by the proposed prediction model ( $K_{sd,Prop.} = V_{s,Pred.-Prop.}/V_{s,Pred.-Code} = \mu_v * \beta_k$ ), was compared with that ratio to the proposed prediction ( $K_{sd,act.,Prop.} = V_{s,exp.}/V_{s,Pred.-Prop.} = K_{sd,act.}/K_{sd,Prop.}$ ). For full-width wide beams, the  $K_{sd,act.}$  was 0.91,



0.97 and 0.93 (correspondingly to  $K_{sd,Prop.} = \mu_v * \beta_k = 0.93, 1.0$  and  $0.86$ , respectively), while the  $K_{sd,act.,Prop.}$  was between 0.98, 0.97 and 1.07, respectively. Otherwise, for partial-width wide beams, the  $K_{sd,act.}$  was 0.49 and 0.90 (correspondingly to  $K_{sd,Prop.} = \mu_v * \beta_k = 0.51, 1.0$  and  $0.84$ ), while the  $K_{sd,act.,Prop.}$  was between 0.97 and 1.08. This seems that the  $K_{sd,act.,Prop.}$  obtained by the proposed prediction model gives more accuracy than that  $K_{sd,act.}$  obtained by the Codes of Practice, such EC2 Code. This has also shown the deficiency of the Code to predict the stirrups contribution to the shear strength of wide RC beams. It should be noted that  $V_{s,Pred.-Prop.}$  is the  $V_{s,d}$  proposed in Equation (6.11),  $V_{s,Pred.-Code}$  is the  $V_s$  given by the Codes (Equations 4.24 and 4.27), and  $V_{s,exp.}$  is the  $V_s$  obtained by the test.

#### **7.11.6 Behaviour of the Beams in Series (1)**

The cracks development was similar on both elevation side faces (front and back faces) for each beam, and did not appear neither on both cross-section side faces (right and left faces) nor on both plan side faces (top and bottom faces) for all the beams. The flexural and diagonal cracks developed and widened under increasing loads. For all beams, the flexural cracks developed before the diagonal cracks.

Flexural cracks developed in the lower part of all the beams. First column in Table 7.11 shows the applied loads and flexural cracking widths at 1<sup>st</sup> formation of the flexural cracks. For full-width wide beam without stirrups (Beam A1-0), the flexural cracks developed at a load level approximately of 53.2% of the ultimate (design) load (470 kN). While for full-width wide beams with stirrups, the flexural cracks developed at a load level approximately between 21.3% to 42.5% of the ultimate (design) load (470 kN). Otherwise, for partial-width wide beams without stirrups, the flexural cracks developed at a load level approximately between 31.9% to 53.2% of the ultimate (design) load (470 kN). While for partial-width wide beams with stirrups, the flexural cracks developed at a load level approximately between 21.3% to 42.5% of the ultimate (design) load (470 kN).

Diagonal cracks appeared in the shear span regions of all the beams. Second column in Table 7.11 shows the applied loads and diagonal-shear cracking widths at 1<sup>st</sup> formation of the shear cracks. For full-width wide beam without stirrups (Beam A1-0), the diagonal cracks appeared at a load level approximately of 74.5% of the ultimate (design) load (470 kN). While for full-width wide beams with stirrups, the diagonal cracks appeared at a load level approximately between 63.8% to 74.5% of the ultimate (design) load (470 kN). Otherwise, for partial-width wide beams

without stirrups, the diagonal cracks appeared at a load level approximately between 63.8% to 74.5% of the ultimate (design) load (470 kN). While for partial-width wide beams with stirrups, the diagonal cracks appeared at a load level approximately between 53.2% to 74.5% of the ultimate (design) load (470 kN).

For full-width wide beam without stirrups (Beam A1-0), the flexural cracks were wider than the diagonal cracks up to a load level approximately of 95.7% of the ultimate (design) load (470 kN). While for full-width wide beams with stirrups, the flexural cracks were wider than the diagonal cracks up to a load levels approximately of 85.1% of the ultimate (design) load (470 kN). Otherwise, for partial-width wide beams without stirrups, the flexural cracks were wider than the diagonal cracks up to a load level approximately between 74.5% to 85.1% of the ultimate (design) load (470 kN). While for partial-width wide beams with stirrups, the flexural cracks were wider than the diagonal cracks up to a load level approximately between 63.8% to 85.1% of the ultimate (design) load (470 kN). In all beams, diagonal cracks developed in the shear spans as an extension of existing flexural cracks. The diagonal cracks extended towards the loading plate, passed the neutral axis of the beam, and reached to the concrete compression region.

Additional flexural and diagonal cracks appeared and widened under increasing loads. For full-width wide beam without stirrups (Beam A1-0), the maximum width of the critical flexural crack at a load level of 450 kN, which is one step prior to the design load (470 kN), was 0.43mm; the corresponding maximum width of the critical diagonal crack at the same load was 0.36mm. While for full-width wide beams with stirrups, the widths of the flexural cracks at a load level of 450 kN, which is one step prior to the design load (470 kN), were between 0.24mm and 0.32mm; the corresponding widths of the diagonal cracks at the same load were between 0.30mm to 0.38mm. Otherwise, for partial-width wide beams without stirrups, the widths of the flexural cracks at a load level of 450 kN, which is one step prior to the design load (470 kN), were between 0.42mm and 0.59mm; the corresponding widths of the diagonal cracks at the same load were between 0.66mm to 2.76mm. While for partial-width wide beams with stirrups, the widths of the flexural cracks at a load level of 450 kN, which is one step prior to the design load (470 kN), were between 0.28mm and 0.37mm; the corresponding widths of the diagonal cracks at the same load were between 0.38mm to 1.23mm.

Because all beams in Test-Series (1) failed in shear, the shear (diagonal) cracks were the critical and dominant on the beam behaviours. Wherefore, to analyze the behaviour of the beams under

the effect of loading- and support- widths and the longitudinal- and transverse- stirrup legs spacing, the widths of the diagonal cracks at the service (working) load levels and at the failure load levels should be discussed. As per the provisions of the EC2, ACI318 and SBC304 Codes, the service (working) load is the load level when the maximum width of the flexural crack exceeds 0.40mm.

For full-width wide beam without stirrups (Beam A1-0), the maximum width of the critical diagonal crack at the service (working) load level, which was approximately 95.7% of the design load (470 kN), was 0.36mm. While for full-width wide beams with stirrups, the widths of the diagonal cracks at the service (working) load levels, which were approximately between 117% to 138.3% of the design load (470 kN), were between 1.64mm and 2.28mm. Otherwise, for partial-width wide beams without stirrups, the widths of the diagonal cracks at the service (working) load levels, which were approximately between 85.1% to 95.7% of the design load (470 kN), were between 0.66mm and 0.80mm. While for partial-width wide beams with stirrups, the widths of the diagonal cracks at the service (working) load levels, which were between 106.4% to 127.7% of the design load (470 kN), were between 1.44mm and 2.66mm. Third column in Table 7.11 shows the applied loads and flexural cracking widths at the service (working) load levels.

Fourth column in Table 7.11 shows the applied loads and flexural- and shear- cracking widths at the failure load levels. For full-width wide beam without stirrups (Beam A1-0), the maximum width of the critical diagonal crack at the failure load level, which was 119.1% of the design load (470 kN), was 3.0mm. While for full-width wide beams with stirrups, the widths of the diagonal cracks at the failure load levels, which were between 168.1% to 174.5% of the design load (470 kN), were between 6.16mm and 6.40mm. Otherwise, for partial-width wide beams without stirrups, the widths of the diagonal cracks at the failure load levels, which were between 102.1% to 118.7% of the design load (470 kN), were between 3.82mm and 7.20mm. While for partial-width wide beams with stirrups, the widths of the diagonal cracks at the failure load levels, which were between 128.1% to 169.1% of the design load (470 kN), were between 5.78mm and 6.80mm.

The widths of flexural and diagonal-shear cracks increased as the ratios of support-width and/or load-width to beam-width ( $k_s$  and/or  $k_p$ ) reduced. The beams in Type (A) with full-width bearing plates, i.e. beams A1-0, A1-1a, A1-1b and A1-2, had the best results, cracks development and crack widths. The widths of flexural and diagonal-shear cracks increased as the longitudinal

spacing and/or the transverse spacing of stirrup-legs ( $S_L$  and/or  $S_w$ ) increased. The beams in Group (1a) with  $S_L = 0.65d$  and  $S_w = 0.75d$ , i.e. beams A1-1a, B1-1a, C1-1a and D1-1a, had the best results, cracks development and crack widths.

The widths of the diagonal cracks at the failure load levels for the beams with stirrups in Group (2) designed with  $S_w = d \approx 1.34*S_L$ , which are beams A1-2, B1-2, C1-2 and D1-2, were 6.40mm for full-width wide beams, and between 6.20mm and 6.25mm for partial-width wide beams. The widths of the diagonal cracks at the failure load levels for the beams with stirrups in Group (2) were larger than those widths obtained from the beams in Groups (1a) and (1b) at the nearest correspondingly load levels. It seems that the wide transverse spacing of stirrup legs for the beams in Group (2),  $S_w = 257\text{mm} = d \approx 1.34*S_L$ , arranged within the support widths ( $b_s = 600\text{mm}$  Type (A), 300mm Type (B), 300mm Type (C) and 150mm Type (D)) resulted in wider diagonal crack widths. This recommends that a proper design model for wide RC beams to account for  $S_w$  and  $S_L$  should be developed. The widths of the cracks in these beams, just at one step before the maximum load levels, support this conclusion.

The mid-span deflections were recorded at each step of the loading increments. For full-width wide beam without stirrups (Beam A1-0), the mid-span deflection at failure load level was 9.98mm. While for full-width wide beams with stirrups, the mid-span deflections at failure load levels were between 11.94mm and 13.82mm. Otherwise, for partial-width wide beams without stirrups, the mid-span deflections at failure load levels were between 8.70mm and 10.11mm. While for partial-width wide beams with stirrups, the mid-span deflections at failure load levels were between 11.06mm and 13.72mm.

As result, it is clear that  $k_s$  had more influence on the shear strength, flexural and shear crack widths, and mid-span deflection than  $k_p$ . This was based on the results and measurements obtained from the beams in Types (C and D) comparing with those correspondingly relevant beams in Types (A and B).

## 7.12 Conclusions

Sixteen wide beams were tested to study the effect of  $b_s$  and  $b_p$  (or,  $k_s$  and  $k_p$ ) &  $S_L$  and  $S_w$  on the behaviour and strength of wide RC beams, and to verify the proposed prediction model developed in this study. The observations described above explain the following conclusions (Alluqmani, 2013a).

As a result, the shear strengths of wide-beams decreased for those beams without and with shear-reinforcement tested in Test-Series (1) when the support-width and/or load load-width ( $b_s$  and  $b_p$ ) decreased, or at best, when the ratios of the support-width and/or load-width to the beam-width ( $k_s$  and  $k_p$ ) decreased. As a result also, the shear strengths of wide-beams decreased for those beams with full- and narrow- width supports and loads tested in Test-Series (1) when the longitudinal or transverse spacing of stirrup-legs ( $S_L$  and  $S_w$ ) increased, and when they were also ignored (beams without stirrups).

In general, the widths of flexural and diagonal-shear cracks and the mid-span deflections increased as the ratios of support-width and/or load-width to beam-width ( $k_s$  and/or  $k_p$ ) reduced. The beams in Type (A) with full-width bearing plates, i.e. beams A1-0, A1-1a, A1-1b and A1-2, had the best results and measurements (deflections and crack widths). Furthermore, in general, the widths of flexural and diagonal-shear cracks and the mid-span deflections increased as the longitudinal or transverse stirrup-legs spacing ( $S_L$  or  $S_w$ ) increased. The beams in Groups 1a (for  $S_L$ ) and 1b (for  $S_w$ ) had the best results and measurements (deflections and crack widths). It was clear that  $k_s$  had more influence on the shear strength, flexural and shear crack widths, and mid-span deflection than  $k_p$ . This was based on the results and measurements obtained from the beams in Types (C and D) comparing with those correspondingly relevant beams in Types (A and B).

A proposed detailing approach must be developed based on 1) the widths of supports and loads ( $b_s$  and  $b_p$ ), 2) the ratios of the support- and load- widths to beam-width ( $k_s$  and  $k_p$ ), 3) the effective-widths of supports and loads ( $w_s$  and  $w_p$ ), and 4) the concentrating flexural -tensile and -compression reinforcement to be distributed within the effective widths of -supports and -loads ( $N_{w_s}$  and  $N_{w_p}$ ), respectively. For the wide-beams with and without shear reinforcement, the proposed detailing approach to be developed must enhance the flexural reinforcements (tensile and compression reinforcing bars) when they are distributed according to their portions of concentrations on the effective widths of the bearing plates (support and load widths). It was clear that the concentrating flexural tensile reinforcement distributed within the effective support-width ( $N_{w_s}$ ) has a relation with  $\sqrt{k_s}$ , and the effective support-width ( $w_s$ ) has a relation with  $b_s$ . Moreover, it was clear that the concentrating flexural compression reinforcement distributed within the effective load-width ( $N_{w_p}$ ) has a relation with  $\sqrt{k_p}$ , and the effective load-width ( $w_p$ ) has a relation with  $b_p$ . These outcomes must be used to develop a proposed detailing approach to account for  $N_{w_s}$  &  $w_s$  and  $N_{w_p}$  &  $w_p$ , respectively, with taking into the consideration

$k_s$  &  $b_s$  and  $k_p$  &  $b_p$ , respectively. These must be taken into the consideration to detail the wide RC beams in flexure and shear in order to ensure that the high stresses concentrated within the support- and load- widths can be distributed and then to ensure that the beams behave in a ductile flexural manner, as well to develop a detailing approach.

The beams designed with  $S_w = 0.75d$  (Groups 1a and 1b) were the best comparing with the other beams in Groups (0) and (2). A design value of  $0.75d$  for  $S_w$  of the wide beams in Groups (1a and 1b) did not succeed to prevent the shear failure for such beams. Consequently, the transverse stirrup legs of wide RC beams should be designed to be spaced across the beam width for an internal  $S_w$  to be lesser than  $0.75d$ . This must be taken into the consideration to develop a design model for designing the wide RC beams in shear. On the other hand, the support and load widths ( $b_s$  and  $b_p$ ), or the ratios of the support and load widths to the beam width ( $k_s$  and  $k_p$  respectively), should be taken into the consideration to develop a design method for wide RC beams in regards to determine  $S_L$  and  $S_w$ .

A proposed design model must be developed based on 1) the effective-depth of the beam ( $d$ ), 2) the ratios of the support- and load- widths to beam-width ( $k_s$  and  $k_p$ ). For the wide-beams with full- and narrow- width supports and loads, the proposed design model to be developed must enhance the shear reinforcements (longitudinal and transversal stirrups) when they are distributed along the beam length and across the beam width, especially for the interior stirrup legs when they are arranged within the effective support width. It was clear that the longitudinal stirrup-legs spacing ( $S_L$ ) has a relation with  $k_s$  and  $d$ . Moreover, it was clear that the transversal stirrup-legs spacing ( $S_w$ ) has a relation with  $k_p$  and  $S_L$ . These outcomes must be used to develop a proposed design model to account for  $S_L$  and  $S_w$  with taking into the consideration  $d$ ,  $k_s$  and  $k_p$ . These must be taken into the consideration to design the wide RC beams in shear in order to ensure that the shear strength of wide RC beams can be enhanced and then to ensure that the beams behave in a ductile flexural manner, as well to develop a design model.

The proposed prediction model has been verified for the one-way shear strengths of wide RC beams based on the results obtained from the beams with and without shear-reinforcement in Series (1). The shear strengths of wide RC beams provided by concrete and stirrups ( $V_c$  and  $V_s$ , respectively) can be determined using the provisions of the current Codes of Practice if they are corrected by the factors of  $K_{cd}$  and  $K_{sd}$ , respectively, as given by the proposed prediction model.

## CHAPTER 8

# NEW DETAILING-APPROACH AND DESIGN-MODEL FOR WIDE RC BEAMS

### 8.1 Introduction

In Test Series (1), Chapter 7, two main objectives have been studied which were: 1) influence of  $b_s$  and  $b_p$  (or at best,  $k_s$  and  $k_p$ ) on the wide RC beams behaviour and 2) influence of  $S_L$  and  $S_w$  on the wide RC beams behaviour. Based on the influence of  $b_s$  and  $b_p$  (or,  $k_s$  and  $k_p$ ), a proposed detailing approach must be developed. Further, based on the influence of  $S_L$  and  $S_w$ , a proposed design model must be developed.

### 8.2 Series (1) Summary on the Effect of $k_s$ and $k_p$

Anderson and Ramirez (1989) and Leonhardt and Walther (1964) concluded that the stirrups spacing should be reduced within the regions of high shear stresses, where members subject to high shear stresses are expected to be more heavily cracked at failure. Accordingly, this conclusion insists that a proposed detailing approach should be developed and adopted for wide RC beams to be used for determining the concentrating flexural -tensile and -compressive reinforcing bars distributed within the effective-widths of supports and loads, respectively, where the ratios of support-width and load-width to beam-width ( $k_s$  and  $k_p$ ) should be taken into the consideration. Based on the conclusions made by Lubell et al. (2008), Serna-Ros et al. (2002) and based on the results obtained from Series (1) that the shear strength of wide beams decreases as the widths of supports and/or loads ( $b_s$  and  $b_p$ ), or at best, as the ratios of support-width and/or load-width to beam-width ( $k_s$  and  $k_p$ ) reduce, the concentrating flexural -tensile and -compressive reinforcing bars distributed within the effective-widths of supports and loads must be determined based on the ratios of  $k_s$  and  $k_p$ , respectively; while the effective-widths of supports and loads must be determined based on  $b_s$  and  $b_p$ , respectively.

A proposed detailing approach must be developed based on a well understanding of the flexural and shear behaviours of wide RC beams. The ratios of the support-width and load-width to beam-width should be taken into the consideration for estimating the concentrating flexural (tensile and compression) reinforcements within the effective-widths of the supports and loads

(Alluqmani, 2013a, 2013b; Alluqmani and Saafi, 2014c). As concluded from the tests in Series (1), the proposed detailing approach must take into the account: 1) the widths of supports and loads ( $b_s$  and  $b_p$ ), 2) the ratios of the support- and load- widths to beam-width ( $k_s$  and  $k_p$ ), 3) the effective-widths of supports and loads ( $w_s$  and  $w_p$ ), and 4) the concentrating flexural -tensile and -compression reinforcement to be distributed within the effective widths of supports and loads ( $N_{w_s}$  and  $N_{w_p}$ ), respectively. For the wide-beams with and without shear reinforcement, the proposed detailing approach to be developed must enhance the flexural reinforcements (tensile and compression reinforcing bars) when they are distributed according to their portions of concentrations within the effective widths of the bearing plates (support and load widths).

The only difference between each Beam-Type in Series (1) was the width of support and loading plates. It was concluded that the width of loading and support plates ( $b_p$  and  $b_s$ ) had influence on the strengths of wide RC beams, where the beam capacities decreased as the bearing plate width decreased, or at best, as  $k_s$  and  $k_p$  decreased (Alluqmani, 2013a; Alluqmani and Saafi, 2014c). This happened for beams without and with shear reinforcement. The beams with full-width bearing plates in Type (A) in regard to study the effect of  $b_p$  and  $b_s$ , or at best  $k_p$  and  $k_s$ , had the best results and strengths comparing with the other correspondingly relevant beams. Thus, it was concluded that proposed detailing approach and design model should be developed for this account in regard to study the effect of the full- and narrow- width supports and loads on the capacities of wide RC beams.

As result from the beams in Series (1) in general, the widths of flexural and diagonal-shear cracks and the mid-span deflections increased as the ratios of support-width and/or load-width to beam-width ( $k_s$  and/or  $k_p$ ) reduced (Alluqmani, 2013a). The beams in Type (A) with full-width bearing plates had the best results and measurements (deflections and crack widths). As result from the beams in Types B, C and D in Series (1), it was clear that  $k_s$  had more influence on the shear strength, flexural and shear crack widths, and mid-span deflection than  $k_p$ . This was based on the results and measurements obtained from the beams in Types (C and D) comparing with those correspondingly relevant beams in Types (A and B).

It was clear that the concentrating flexural tensile reinforcement distributed within the effective support-width ( $N_{w_s}$ ) has a relation with  $\sqrt{k_s}$ , and the effective support-width ( $w_s$ ) has a relation with  $b_s$ . Moreover, it was clear that the concentrating flexural compression reinforcement distributed within the effective load-width ( $N_{w_p}$ ) has a relation with  $\sqrt{k_p}$ , and the effective load-width ( $w_p$ ) has a relation with  $b_p$ . This outcome must be used to develop the proposed detailing



approach to account for  $N_{w_s}$  &  $w_s$  and  $N_{w_p}$  &  $w_p$  with taking into the consideration  $k_s$  &  $b_s$  and  $k_p$  &  $b_p$ , respectively. These must be taken into the consideration to detail the wide RC beams in flexure and shear in order to ensure that the high stresses concentrated within the support- and load- widths can be distributed and then to ensure that the beams behave in a ductile flexural manner, as well to develop a detailing approach.

### **8.3 A Proposed Detailing-Approach**

As the width of bearing plates in the location of loads and supports affects the strength and capacity of wide concrete members as resulted from the literature and from the beams in Series (1), portions of both longitudinal (flexural) and transverse (shear) reinforcing bars should be distributed within the effective widths of supports and loads to resist the regions which have higher transverse stresses. Moreover, the effective-widths of the bearing plates (supports and loads) should be firstly determined, and then the number of longitudinal (tensile and compression) reinforcing bars to be distributed within the effective-width of bearing plates (supports and loads) must be determined.

As a result from the beams in Series (1), the capacities of wide RC beams without and with shear reinforcement decreased as the bearing plate widths decreased, or at best, as  $k_s$  and/or  $k_p$  decreased.  $k_s$  and  $k_p$  had also influence on the development and formation of cracks for both full- and narrow- width wide beams. The beams with full-width bearing plates in Type (A), in regards to study the effect of  $b_p$  and/or  $b_s$ , or at best  $k_p$  and/or  $k_s$ , had the best results and strengths comparing with the other correspondingly relevant beams.

As a comparison between the beams in Type (B) with those beams in Types (C) and (D) in order to study the effect of  $k_p$  and/or  $k_s$ , respectively, on the capacity of wide beams, the beam capacity decreased as  $k_p$  or  $k_s$  was reduced. The results of the beams in Types B, C and D showed that  $k_s$  had more an influence than  $k_p$  on the wide-beam. All wide beams in Series (1) were designed for singly reinforcement, where the tensile reinforcement is the critical in the bottom zone which is the region of the support, where the compression reinforcement is concentrated in the top zone which is the region of the load. As resulted that  $S_L$  had more influence on the beam behaviour than  $S_w$ , and as concluded by Lubell et al. (2009a) and Al.Dywany (2010) that high stresses on the beam section are concentrated at the region of the interior stirrup legs, or the region of the support, or in the middle bars near the supports; therefore,  $b_s$  must be used to estimate the effective support-width ( $w_s$ ) and  $k_s$  must be used to estimate the concentrating flexural tensile

reinforcing bars ( $N_{w_s}$ ) to be distributed within  $w_s$ . On the other hand,  $b_p$  is used to estimate the effective load-width ( $w_p$ ) and  $k_p$  is used to estimate the concentrating flexural compression reinforcing bars ( $N_{w_p}$ ) to be distributed within  $w_p$ .

It is recognised that the total distance between the pair-legs of the external stirrups across the beam width ( $S_t$ ) is the beam width ( $b_w$ ) minus twice the side concrete cover ( $2C_c$ ) minus twice the stirrup leg diameter ( $2\Phi_{str.}$ ), as  $S_t = b_w - (2C_c + 2\Phi_{str.}) = b_w - 2C_c - 2\Phi_{str.}$  (Alluqmani, 2013a). The term  $b_w$  can be replaced for wide beams by  $b_s$  and  $b_p$  to account for  $w_s$  and  $w_p$ , respectively, where  $w_s$  is the effective-width of the support and  $w_p$  is the effective-width of the load. Consequently,  $w_s$  and  $w_p$  are to be as follows:

$$\begin{aligned} w_s &= b_s - 2C_c - 2\Phi_{str.} \\ w_p &= b_p - 2C_c - 2\Phi_{str.} \end{aligned}$$

Al.Dywany (2010) used the following Equation to account for the effective support width of wide beams:

$$w_s = \left\{ \frac{[(h - d) * (b_w - b_s)]}{h} \right\} + b_s$$

Based on Al.Dywany's results, this Equation should be developed to account for various cases of the supports and loads for both full- and narrow- width conditions of wide RC beams with various  $b_w/h$  ratios. Thus, the first term of the Equation  $\{[(h-d)*(b_w-b_s)]/h\}$  must be multiplied by  $b_w/h$  ratio, and the second term of the Equation ( $b_s$ ) must be treated by  $2C_c + 2\Phi_{str.}$  where  $2C_c + 2\Phi_{str.}$  must be subtracted from  $b_s$ . The final form of the effective-width of the support ( $w_s$ ) is as follows (Alluqmani, 2013a, 2013b; Alluqmani and Saafi, 2014c):

$$w_s = \left\{ \left( \frac{b_w}{h} \right) * \frac{[(h - d) * (b_w - b_s)]}{h} \right\} + b_s - 2C_c - 2\Phi_{str.}$$

It seems that this Equation is precise to account for  $w_s$  for all support cases of wide RC beams. For full-width supported wide beams,  $w_s$  will be equal to  $b_w - 2C_c - 2\Phi_{str.}$  because  $b_s = b_w$  and then the first term of the Equation will be ignored. Furthermore, the Equation can account for the effective-width of the load ( $w_p$ ) by replacing  $b_s$  to  $b_p$ , as shown below (Alluqmani, 2013a, 2013b; Alluqmani and Saafi, 2014c):

$$w_p = \left\{ \left( \frac{b_w}{h} \right) * \frac{[(h - d) * (b_w - b_p)]}{h} \right\} + b_p - 2C_c - 2\Phi_{str.}$$

It seems that this Equation is precise to account for  $w_p$  for all load cases of wide RC beams. For full-width loaded wide beams,  $w_p$  will be equal to  $b_w - 2C_c - 2\Phi_{str}$ . because  $b_p = b_w$  and then the first term of the Equation will be ignored.

Based on the final forms of the  $w_s$  and  $w_p$  Equations, the corresponding  $w_s$  values for the beams in Test-Series (1) are 550mm for beam without stirrups and 534mm for beams with stirrups (for Beam-Type A), 336mm for beam without stirrups and 320mm for beams with stirrups (for Beam-Type B), 336mm for beam without stirrups and 320mm for beams with stirrups (for Beam-Type B), and 229mm for beam without stirrups and 213mm for beams with stirrups (for Beam-Type D). The corresponding  $w_p$  values are 550mm for beam without stirrups and 534mm for beams with stirrups (for Beam-Type A), 336mm for beam without stirrups and 320mm for beams with stirrups (for Beam-Type B), 229mm for beam without stirrups and 213mm for beams with stirrups (for Beam-Type C), and 336mm for beam without stirrups and 320mm for beams with stirrups (for Beam-Type D).

To study the influence of the effective-widths of the supports and loads ( $w_s$  and  $w_p$ ), the percentage of the number of the concentrating longitudinal flexural -tensile and -compression reinforcing bars distributed and arranged within the effective-widths of the supports and loads ( $N_{w_s}$  and  $N_{w_p}$ , respectively) to the total longitudinal flexural -tensile and -compression reinforcing bars ( $N_s$  and  $N_{s'}$ , respectively) should be determined for all wide beams investigated in Test-Series (1). The total longitudinal flexural tensile- and compression- reinforcing bars ( $N_s$  and  $N_{s'}$ , respectively) were the same for all full- and narrow- width wide beams, and they were eight bars 20mm diameter ( $8\Phi 20\text{mm}$ ) for the tensile bars ( $N_s$ ) and six bars 8mm diameter ( $6\Phi 8\text{mm}$ ) for the compression bars ( $N_{s'}$ ). Accordingly, for full-width wide beams in Type (A) with  $b_s = b_p = b_w$  [ $k_s = k_p = 1.0$ ], the percentage of concentrating/total tensile bars ( $N_{w_s}/N_s$ ) was 1.0 while the percentage of concentrating/total compression bars ( $N_{w_p}/N_{s'}$ ) was also 1.0. Otherwise, for partial-width wide beams with stirrups in Type (B) with  $b_s = b_p = b_w/2$  [ $k_s = k_p = 0.50$ ], the percentage of concentrating/total tensile bars ( $N_{w_s}/N_s$ ) was 0.75 while the percentage of concentrating/total compression bars ( $N_{w_p}/N_{s'}$ ) was 0.67. Furthermore, for partial-width wide beams with stirrups in Type (C) with  $b_s < b_w$  [ $k_s < 1.0$ , where  $k_s = 0.50$ ] and with  $b_p < b_w$  [ $k_p < 1.0$ , where  $k_p = 0.25$ ], the percentage of concentrating/total tensile bars ( $N_{w_s}/N_s$ ) was 0.75 while the percentage of concentrating/total compression bars ( $N_{w_p}/N_{s'}$ ) was 0.67. Whereas, for partial-width wide beams with stirrups in Type (D) with  $b_s < b_w$  [ $k_s < 1.0$ , where  $k_s = 0.25$ ] and with  $b_p$

$< b_w$  [ $k_p < 1.0$ , where  $k_p = 0.50$ ], the percentage of concentrating/total tensile bars ( $N_{w_s}/N_s$ ) was 0.50 while the percentage of concentrating/total compression bars ( $N_{w_p}/N_{s'}$ ) was 0.67.

It seems that the percentage of concentrating/total tensile bars ( $N_{w_s}/N_s$ ) is equal, or approximately to be near, to  $\sqrt{k_s}$  where  $k_s$  is the ratio of the support-width to the beam-width; while the percentage of concentrating/total compression bars ( $N_{w_p}/N_{s'}$ ) is equal, or approximately to be near, to  $\sqrt{k_p}$  where  $k_p$  is the ratio of the load-width to the beam-width. The  $\sqrt{k_s}$  values for the beams in Test-Series (1) are 1.0 (for Beam-Type A), 0.71 (for Beam-Type B), 0.71 (for Beam-Type C) and 0.50 (for Beam-Type D); while the  $\sqrt{k_p}$  values are 1.0 (for Beam-Type A), 0.71 (for Beam-Type B), 0.50 (for Beam-Type C) and 0.71 (for Beam-Type D). This outcome (consequence) must be used for developing a detailing approach to be used for wide RC beams, where  $N_{w_s}$  and  $N_{w_p}$  are proposed to be as shown below, respectively, (Alluqmani, 2013a, 2013b; Alluqmani and Saafi, 2014c):

$$N_{w_s} = N_s * \sqrt{k_s}$$

$$N_{w_p} = N_{s'} * \sqrt{k_p}$$

$N_{w_s}$  and  $N_{w_p}$  should be arranged and distributed within  $w_s$  and  $w_p$ , respectively.

For the proposed detailing approach,  $N_s$  and  $N_{s'}$  must be taken as the provided areas of the total flexural tensile- and compression- reinforcements ( $A_s$  and  $A_{s'}$ ) instead of the numbers of the bars, respectively, as well the equality symbol of the both Equations must be changed to larger than or equal, but anyway it must not be less than that of equality.

**The final form of the proposed detailing approach is as follows** (Alluqmani, 2013a, 2013b; Alluqmani and Saafi, 2014c):

$$N_{w_s} \geq A_s * \sqrt{k_s} = A_s * \sqrt{\left(\frac{b_s}{b_w}\right)} \quad (8.1a)$$

$$N_{w_p} \geq A_{s'} * \sqrt{k_p} = A_{s'} * \sqrt{\left(\frac{b_p}{b_w}\right)} \quad (8.1b)$$

$$w_s = \left\{ \left(\frac{b_w}{h}\right) * \frac{[(h-d) * (b_w - b_s)]}{h} \right\} + b_s - 2C_c - 2\Phi_{str}. \quad (8.2a)$$

$$w_p = \left\{ \left(\frac{b_w}{h}\right) * \frac{[(h-d) * (b_w - b_p)]}{h} \right\} + b_p - 2C_c - 2\Phi_{str}. \quad (8.2b)$$

It should be noted that the unit of  $N_{w_s}$  and  $N_{w_p}$  is the same unit of  $A_s$  and  $A_s'$ ; where if  $A_s$  and  $A_s'$  are taken in  $mm^2$  the  $N_{w_s}$  and  $N_{w_p}$  must be taken in  $mm^2$ , but if they are taken in number of bars the  $N_{w_s}$  and  $N_{w_p}$  must be also taken in number of bars. The unit of  $w_s$  and  $w_p$  is the same unit of  $b_w$ ,  $h$ ,  $b_s$ ,  $b_p$ ,  $C_c$  and  $\Phi_{str.}$ , which is one dimensional unit, such as  $mm$ .

Equations (8.1a) and (8.2a) are used to determine the concentrating flexural-tensile reinforcing bars distributed within the effective support width ( $N_{w_s}$ ) and the effective-width of support ( $w_s$ ), respectively. As mentioned in Chapter 3, Al.Dywany (2010) investigated Equation (8.1a) and similar to Equation (8.2a). He concluded that the concentrating of flexural reinforcement within the effective support width,  $N_{w_s}$ , using the Equation (8.1a), has no significant effect in increasing the shear strength of wide RC beams without stirrups; while in wide RC beams with stirrups, the concentrating of flexural reinforcement within the effective support width,  $N_{w_s}$ , using the same Equation increases the efficiency of the shear stirrups to reach its full capacity. On the other hand, Equations (8.1b) and (8.2b) were established by the author and are used to determine the concentrating flexural-compressive reinforcing bars distributed within the effective load width ( $N_{w_p}$ ) and the effective-width of load ( $w_p$ ), respectively. It should be noted that Equations (8.1a&b) and (8.2a&b) will be investigated in the next Chapter.

The  $N_{w_s}$  from Equation (8.1a) represents the amount of flexural tensile-reinforcement to be distributed equally on the effective support width ( $w_s$ ) either in term of ratio or bars number, and the remaining reinforcement are equally distributed in the remaining sides across the beam width. In addition, to satisfy the spacing requirements between bars, Equation (8.2a) represents the effective support width ( $w_s$ ) in which the  $N_{w_s}$  from Equation (8.1a) to be distributed in. On the other hand, the  $N_{w_p}$  from Equation (8.1b) represents the amount of flexural compressive-reinforcement to be distributed equally on the effective load width ( $w_p$ ) either in term of ratio or bars number, and the remaining reinforcement are equally distributed in the remaining sides across the beam width. In addition, to satisfy the spacing requirements between bars, Equation (8.2b) represents the effective load width ( $w_p$ ) in which the  $N_{w_p}$  from Equation (8.1b) to be distributed in.

According to Equations (8.1a) and (8.2a), the flexural tensile-reinforcement concentrated within the effective support width ( $N_{w_s}$ ) is arranged and distributed within the effective support width ( $w_s$ ) in the narrow supported wide beams that require reinforcement arrangement, so that the minimum spacing between the bars kept within the limits, as shown in Figure 8.1a. While,

according to the Equations (8.1b) and (8.2b), the flexural compressive-reinforcement concentrated within the effective load width ( $N_{w_p}$ ) is arranged and distributed within the effective load width ( $w_p$ ) in the narrow loaded wide beams that require reinforcement arrangement, so that the minimum spacing between the bars kept within the limits, as shown in Figure 8.1b.

Furthermore, for narrow-supported wide beams, it was concluded that if the wide beam is loaded using a full-width loading along its width, the load will cause uniform shear stresses within the beam width, as shown in Figure 8.2a (Al.Dywany, 2010). While if the wide beam is loaded using a narrow-width loading along its width, the load will cause high transverse and shear stresses in the effective support width ( $w_s$ ) and low stresses in the both edges of the beam width, as shown in Figure 8.2b (Al.Dywany, 2010).

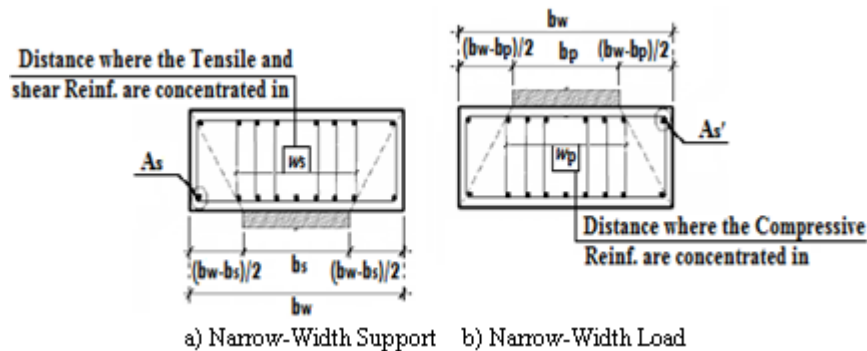


**Figure 8.1:** Application of Equations 8.1.a&b and 8.2.a&b on Wide Beams with Narrow-Width Load and Support Conditions.

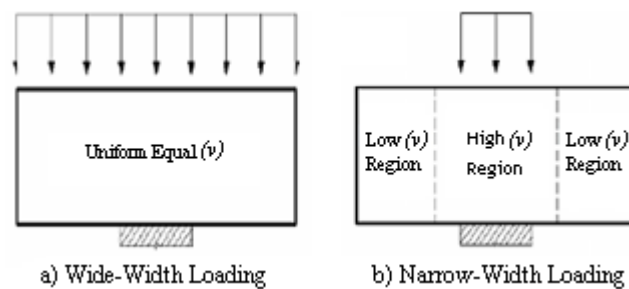


**Figure 8.2:** Effect of the Loading Width on Shear Stress Distributions of a Narrow Supported Wide Beam.

### Definitions of Parameters:

$N_{w_s}$  = Flexural tensile reinforcing bars to be distributed within the effective support width ( $w_s$ ),

$N_{w_p}$  = Flexural compressive reinforcing bars to be distributed within the effective load width ( $w_p$ ),

$w_s$  = Effective support width,  $w_p$  = Effective load width,

$A_s$  = Flexural tensile bars provided within the overall width of the tension zone of the beam,

$A_{s'}$  = Flexural compressive bars provided within the overall width of the compression zone of the beam,

$k_s$  = The ratio of support-width to beam-width =  $b_s/b_w$ ,

$k_p$  = The ratio of load-width to beam-width =  $b_p/b_w$ ,

$b_s$  = support width,  $b_p$  = load width,  $b_w$  = beam width,  $h$  = Overall depth of the beam,  $d$  = Effective depth of the beam, and  $C_c$  = Concrete Cover.

#### **8.4 Series (1) Summary on the Effect of $S_L$ and $S_w$**

Lubell et al. (2009a) concluded that the efficiency of shear reinforcement (stirrups) increases when the stirrup-legs spacing remains smaller than approximately  $d$  (effective depth), and they also recommended that the transverse spacing of the stirrup legs ( $S_w$ ) should be reduced in the higher shear stress regions. Where for wide RC beams with narrow-width loads and supports, the high shear stress regions are the regions of load- and support- widths, or at best, are the regions of the effective-widths of loads and supports in accordance with the proposed detailing approach. Furthermore, Anderson and Ramirez (1989) and Leonhardt and Walther (1964) concluded that the stirrup-legs spacing should be reduced within the regions of high shear stresses, where members subject to high shear stresses are expected to be more heavily cracked at failure. Accordingly, these conclusions insist that a proposed design model should be developed and adopted to be used for designing  $S_L$  and  $S_w$  of wide RC beams, where the effective depth ( $d$ ) and ratios of bearing plate width to beam width ( $k_s$  and  $k_p$ ) have effect on the stirrup legs spacing. Based on the conclusions made by Lubell et al. (2009a), Serna-Ros et al. (2002), Shuraim (2012), Hanafy et al. (2012) and Zheng (1989) and based on the results obtained from Series (1) that the shear strength of wide beams decreases as the transverse spacing of the stirrup legs ( $S_w$ ) increases, the design values of  $S_L$  and  $S_w$  must be reduced from  $0.75d$  with taking into the consideration the ratios of  $k_s$  and  $k_p$ .

The only difference between each Beam-Group in Series (1) was the shear reinforcement (stirrups). It was concluded that the longitudinal and transverse stirrup-legs spacing ( $S_L$  and  $S_w$ ) had influence on the strengths of wide RC beams, where the beam capacities decreased as  $S_L$  increased from  $0.65d$  to  $0.75d$  (beams in Groups (1a and 1b)) and as  $S_w$  increased from  $0.75d$  to  $d$  (beams in Groups (1b and 2)), or as  $S_L$  and  $S_w$  were deleted (beams without stirrups in Group (0)). As a comparison between beam A1-0 without stirrups and with full-width bearing plates (Type (A) had the best results) and beam D1-2 with wide-4-leg stirrups and with narrow-width bearing plates (the worst beam with stirrups amongst the other beams with stirrups in all Beam-Types), beam D1-2 had a strength higher than that for beam A1-0 without stirrups. Consequently, it was suggested that, for wide RC beams, the shear reinforcement (stirrups)

should be included even if they are not required. This, therefore, led to that, for wide RC beams, at least four stirrups legs should be included in the beam as shear reinforcement even if they are not required or the design requires a lesser quantity, and must be arranged and distributed across the beam width (Alluqmani, 2013a; Alluqmani and Saafi, 2014c). Accordingly, wide RC beams must be designed with shear reinforcement (stirrups); thus their longitudinal and transverse spacing of stirrup-legs must be designed based on a rational design model.

The beams in Series (1) that were designed with  $S_w = 0.75d$  (Groups 1a and 1b) were the best comparing with the other beams in Group (2) with  $S_w = d$ . A design value of  $0.75d$  for  $S_w$  of the wide beams in Groups (1a and 1b) did not succeed in prevention the shear failure for such beams. Consequently, it was suggested that the transverse stirrup legs of wide RC beams should be designed to be spaced across the beam width for an internal  $S_w$  to be lesser than  $0.75d$  (Alluqmani, 2013a). This must be taken into the consideration in order to design the wide RC beams in shear, as well to develop a design method. On the other hand, the support and load widths ( $b_s$  and  $b_p$ ), or the ratios of the support- and load- widths to the beam-width ( $k_s$  and  $k_p$ , respectively), should be taken into the consideration for developing a design method for wide RC beams in regards to determine SL and  $S_w$ .

A proposed design model must be developed based on a well understanding of the flexural and shear behaviours of wide RC beams. The ratios of the load-width and support-width to beam-width should be taken into the consideration for estimating the longitudinal and transverse spacing of stirrup legs (Alluqmani, 2013a, 2013b; Alluqmani and Saafi, 2014c). As concluded from the tests in Series (1), the proposed design model must take into the account: 1) the effective-depth of the beam ( $d$ ), 2) the ratios of the support- and load- widths to beam-width ( $k_s$  and  $k_p$ ), and 3) the longitudinal and transverse spacing of stirrup legs (SL and  $S_w$ ), respectively. For the wide-beams with full- and narrow- width supports and loads, the proposed design model to be developed must enhance the shear reinforcements (longitudinal and transversal stirrups) when they are distributed along the beam length and across the beam width (respectively), especially for the interior stirrup legs when they are arranged within the effective support width.

The only difference between the beams with shear reinforcement in Groups (1a, 1b and 2) in Series (1) was either the longitudinal spacing or the transverse spacing of stirrups-legs. It was concluded that the longitudinal and transverse spacing of stirrups-legs (SL and  $S_w$ ) had influence on the strengths of wide RC beams, where the beam capacities decreased as SL and/or  $S_w$  increased (Alluqmani, 2013a; Alluqmani and Saafi, 2014c). The beams in Group (1a), with SL =



0.65d and  $S_w = 0.75d$ , in regard to study the effect of  $S_L$  and  $S_w$ , had the best results and strengths comparing with the other correspondingly relevant beams in the other groups. However, the presence of the narrow -supports and -loads in Group (1a) for Types (B, C and D) reduced the shear strengths of those beams as a comparison with beam A1-1a with full-width support and load condition. Thus, it was concluded that a proposed design model should be developed for this account with taking into the consideration the effect of the full- and narrow-width supports and loads on  $S_L$  and  $S_w$  for the capacities of wide RC beams.

As result from the beams in Series (1) in general, the widths of flexural and diagonal-shear cracks and the mid-span deflections increased as the longitudinal and/or transverse stirrup-legs spacing ( $S_L$  or  $S_w$ ) increased (Alluqmani, 2013a). The beams in Groups (1a, for  $S_L$ ) and (1b, for  $S_w$ ) had the best results and measurements (deflections and crack widths). Beam A1-1a with full-width load and supports, designed for  $S_L = 0.65d$  and  $S_w = 0.75d$ , was the best and stronger beam amongst the other beams in Series (1), but the beam failed in shear at 820 kN due to the effect of its  $S_w$ . For wide RC beams with full-width loads and supports, a value of 0.65d for  $S_L$  and a value to be lesser than 0.75d for  $S_w$  were strongly recommended (Alluqmani, 2013a). Thus, it was suggested that the longitudinal and transverse spacing of the stirrup legs must be designed for wide RC beams as a percentage of  $d$  (the effective-depth) taking into the consideration ' $k_s$ ' for  $S_L$  and ' $k_p$  and  $S_L$ ' for  $S_w$ , where a proposed design model should be developed for this account. As result from the beams in Types B, C and D in Series (1), it was clear that  $k_s$  had more influence on the shear strength, flexural and shear crack widths, and mid-span deflection than  $k_p$ . This was based on the results and measurements obtained from the beams in Types (C and D) comparing with those correspondingly relevant beams in Types (A and B).

As result from the beams in Groups 1a, 1b and 2 in Series (1), it was clear that  $k_s$  had more influence on the shear strength, flexural and shear crack widths, and mid-span deflection than  $k_p$ . This was based on the results and measurements obtained from the beams in Types (C and D) comparing with those correspondingly relevant beams in Types (A and B). Referring to Test-Series (1), it was clear that the longitudinal stirrup-legs spacing ( $S_L$ ) had a relation with  $k_s$  and  $d$ ; and that the transversal stirrup-legs spacing ( $S_w$ ) had a relation with  $k_p$  and  $S_L$  (Alluqmani, 2013a). It was strongly recommended that  $S_L$  for full-width loaded and supported wide beams must be taken 0.65d. Moreover, it was strongly recommended that  $S_L$  for narrow-width loaded and supported wide beams must be trated with  $k_s$ . Furthermore, it was strongly recommended that  $S_w$  must be trated with  $k_p$ . While for full-width loaded and supported wide beams, it was

strongly recommended that  $S_w$  must be lesser than  $0.75d$ . This outcome must be used for developing the proposed design model to account for  $S_L$  and  $S_w$  with taking into the consideration  $d$ ,  $k_s$  and  $k_p$ , respectively. These must be taken into the account to design the wide RC beams in shear in order to enhance the shear strength of wide RC beams and then to ensure that the beams behave in a ductile flexural manner, as well to develop a design model.

It was recommended that the longitudinal stirrup-legs spacing ( $S_L$ ) should be strongly treated with  $k_s$  (Alluqmani, 2013a). This was because the change in the reduction percentage was for those beams in Type (D) in Groups (1a and 1b) where they were used for investigating  $S_L$  and the main variable for the beams was  $k_s$ . No change in the reduction percentage for the beams in Groups (1b and 2). On the other hand, it was also recommended that the transverse stirrup-legs spacing ( $S_w$ ) should be strongly treated with  $k_p$  and  $S_L$  (Alluqmani, 2013a). This was because the change in the reduction percentage was for those beams in Type (C) in Groups (1b and 2) where they were used for investigating  $S_w$  and the main variable for the beams was  $k_p$ . Furthermore, the lower reduction percentage was for the beam in Group (1a), where it was specially detailed for  $S_L$  to be compared with the beam in Group (1b); thus, this led to that  $S_L$  has an influence on  $S_w$ .

### 8.5 A Proposed Design-Model

The main objective of the design of wide structural concrete beams is to achieve full flexural capacity and to prevent a brittle diagonal shear failure. This is normally achieved by providing transverse reinforcement spaced along the beam length and across the beam width. In the case of wide RC beams which normally have large cross-sections, a proposed design model must be developed to account for both longitudinal and transverse spacing of stirrup legs for all cases of wide RC beams either with full- or narrow- width load and support conditions.

Shuraim (2012) developed a proposed Equation to estimate the transverse stirrup-legs spacing ( $S_w$ ) by equating  $S_{eq}$  to  $S_L$  in Equation (4.32) illustrated in Chapter 4 and solving for the transverse spacing,  $S_w$ , as shown in Equation (8.3). Equation (8.3) ignores the influence of the load and support widths (or at least the ratios of the load and support widths to the beam width) for determining the transverse stirrup-legs spacing. Therefore, Equation (8.3) gives the same  $S_w$  for all cases of wide beams with full- and narrow- width load and support conditions at the same characteristics.

$$S_w = \left( \frac{S_L}{d} \right)^{0.5} * d \tag{8.3}$$

Since the proposed design model, which is being developed in this study, concerns in studying the effect of narrow bearing plates on the behaviour of wide RC beams, the support width ( $b_s$ ) and load width ( $b_p$ ) are considered important variables to estimate the both longitudinal and transversal stirrup-legs spacing (Alluqmani, 2013a, 2013b; Alluqmani and Saafi, 2014c). The support and load symbols are assigned based on the ratios between the support-width to beam-width ( $k_s = b_s/b_w$ ) and the load-width to beam-width ( $k_p = b_p/b_w$ ), respectively.

As a result from the beams in Series (1), the capacities of wide RC beams without and with shear reinforcement decreased as the bearing plate width decreased, or at best, as  $k_s$  and  $k_p$  decreased (Alluqmani, 2013a; Alluqmani and Saafi, 2014c).  $k_s$  and  $k_p$  had also influence on the crack development and formation for both full- and narrow- width wide beams. The beams with full-width bearing plates in Type (A) in regard to study the effect of  $b_p$  and/or  $b_s$ , or at best  $k_p$  and/or  $k_s$ , had the best results and strengths comparing with the other correspondingly relevant beams.

As a comparison between the beams in Type (B) with those beams in Types (C) and (D) to study the effect of  $k_p$  and/or  $k_s$ , respectively, on the capacity of wide beams, the beam capacity decreased as  $k_p$  and/or  $k_s$  reduced. The results of the beams in Types B, C and D showed that  $k_s$  had more an influence than  $k_p$  on the wide-beam. Based on the results of the beams in Type (D) as mentioned in Chapter (7), the change in the reduction percentage was for the beams in Groups (1a and 1b) where they were used for investigating SL and the main variable for the beams was  $k_s$ ; therefore, the longitudinal stirrup-legs spacing (SL) should be strongly treated with  $k_s$  (Alluqmani, 2013a). No change was in the reduction percentage for the beams in Groups (1b and 2). Moreover, based on the results of the beams in Type (C) as mentioned in Chapter (7), the transverse stirrup-legs spacing ( $S_w$ ) should be strongly treated with  $k_p$  and SL (Alluqmani, 2013a). This is because for studying the effect of  $k_p$  on  $S_w$ , the change in the reduction percentage was for the beams in Groups (1b and 2) where they were used for investigating  $S_w$  and the main variable for the beams was  $k_p$ . This is also because for studying the effect of SL on  $S_w$ , the lower reduction percentage was for the beam in Group (1a), beam C1-1a, where it was specially detailed for SL to be compared with the beam in Group (1b), beam C1-1b; thus, this has led to that SL has an influence on  $S_w$ .

As resulted also from the beams in Series (1), the longitudinal and transverse stirrup-legs spacing (SL and  $S_w$ ) had effect on the strengths of wide RC beams, where the capacities of wide-beams decreased as SL or  $S_w$  increased, or as SL and  $S_w$  were deleted (i.e. beams in Group (0)) (Alluqmani, 2013a; Alluqmani and Saafi, 2014c). This has led to that, for wide RC beams, the

shear reinforcement (stirrups) should be included even if they are not required; where at least four stirrups legs should be included in the beam as a shear reinforcement even if the design requires a lesser quantity, and the stirrups must be arranged and distributed along the beam length and across the beam width (Alluqmani, 2013a; Alluqmani and Saafi, 2014c).

The wide-beams in Group (1a) had the best results and strengths comparing with the other correspondingly relevant beams (the other beam Groups in the same Beam-Type). Beam A1-1a with full-width load and supports, designed for  $S_L = 0.65d$  and  $S_w = 0.75d$ , was the best and strongest beam amongst the other 15 beams, but the beam failed in shear at 820 kN due to the effect of its  $S_w$ . This has led to that, for wide RC beams with full-width loads and supports, a value of  $0.65d$  for  $S_L$  and a value to be lesser than  $0.75d$  for  $S_w$  were strongly recommended (Alluqmani, 2013a). Based on the results, it has been concluded that the longitudinal and transverse spacing of the stirrup legs must be designed for wide RC beams as a percentage of  $d$  taking into consideration  $k_s$  for  $S_L$ , and  $k_p$  and  $S_L$  for  $S_w$  (Alluqmani, 2013a).

As a comparison between the beams in Groups (1a and 1b) and the beams in Groups (1b and 2) in the same Beam-Type to study the effect of  $S_L$  and  $S_w$ , respectively, on the capacity of wide beams with full- and narrow- width loads and supports, the beam capacity decreased as  $S_L$  or  $S_w$  increased. Based on the results of the beams in Groups 1a with 1b, and 1b with 2 as mentioned in Chapter (7), a proposed understanding of the influence of  $k_s$  and  $k_p$  on  $S_L$  and  $S_w$ , respectively, was concluded. For the beams with full-width loads and supports, beams A1-1a and A1-1b were used to investigate  $S_L$ , where beam A1-1a was designed with  $S_L = 0.65d$  and was the strongest and best beam in Series (1) but it failed in shear; therefore, it was strongly recommended that  $S_L$  for full-width loaded and supported wide beams must be taken  $0.65d$ . While beams A1-1b and A1-2 were used to investigate  $S_w$ , where beam A1-1b was designed with  $S_w = 0.75d$  and failed in shear; therefore, it was strongly recommended that  $S_w$  for full-width loaded and supported wide beams must be lesser than  $0.75d$ . Moreover for the beams with narrow-width loads and supports, Beam-Types (B, C and D), it was clear that the closer percentages of reduction was for the beams in Types (B) and (D) where they followed to Groups (1a and 1b) for investigating  $S_L$  and the main variable for the beams was  $k_s$ ; therefore, it was strongly recommended that  $S_L$  for narrow-width loaded and supported wide beams must be trated with  $k_s$ . While for Beam-Types (B and C), it was clear that the reduction percentage was for beams C1-1b and C1-2 where they followed to Groups (1b and 2) for investigating  $S_w$  and the main variable for the beams was  $k_p$ ; therefore, it was strongly recommended that  $S_w$  must be trated with  $k_p$  and with  $S_L$  also.

It is recognized that the Codes of Practice deal with  $S_L$  as a percentage of  $d$ , e.g. ACI318 (2008) and SBC304 (2007) take  $S_L$  to be equal to  $0.5d$  and EC2 (2004) takes  $S_L$  to be equal to  $0.75d$ . On the other hand, EC2 Code deals with  $S_w$  to be equal to  $S_L$ , i.e.  $S_w = S_L = 0.75d$ .

Based on the results, the beams with stirrups in Groups (1a and 1b), designed for  $S_w = 0.75d$ , were the best comparing with the other beams in Group (0) without stirrups and in Group (2) with stirrups designed for  $S_w = d$ . However, an attempt to choose a design value for  $S_w$  to be  $0.75d$  for the wide beams in Groups (1a and 1b) did not succeed to prevent the shear failure for such beams. Consequently, it was suggested that the transverse stirrup legs should be designed to be spaced across the beam width for an internal  $S_w$  lesser than  $0.75d$  (Alluqmani, 2013a). This must be taken into the consideration to design the wide RC beams in shear, as well as for developing a design method. On the other hand, the support and load widths ( $b_s$  and  $b_p$ ), or at best the ratios of the support- and load- widths to the beam-width ( $k_s = b_s/b_w$  and  $k_p = b_p/b_w$ ), should be taken into the consideration to develop a design method for wide RC beams in regards to determine  $S_L$  and  $S_w$  (Alluqmani, 2013a).

Based on the results obtained from Series (1) where all wide-beams failed in shear, a proposed design model to account for  $S_L$  and  $S_w$  must be developed.  $S_L$  and  $S_w$  must be reduced from those values used in Series (1). As concluded from the wide-beams in Groups (1a and 1b) and Groups (1b and 2) in Series (1), the shear strength of wide concrete beams decreases as  $k_s$  and/or  $k_p$  decrease. Accordingly, reducing  $S_L$  and  $S_w$  with decreasing  $k_s$  and  $k_p$  is required to enhance the shear strength of wide RC beams, with keeping  $S_L = 0.65d$  for full-width supported wide beams (Alluqmani, 2013a). It must be emphasized that the both full- and narrow- width supports and loads must be taken into the consideration to estimate proposed design values for  $S_L$  and  $S_w$ .

For wide RC beams with full-width supports (full-width supported wide beams), a proposed value of  $S_L$  is suggested to be as follows (Alluqmani, 2013a):

$$S_L = 0.65d$$

A "0.65d", given by the above Equation, was recommended based on beam A1-1a result and may enhance the shear strength of those wide RC beams with full-width supports as a comparison with the beams in Type (A) in Series (1) but after deriving  $S_w$ .

Based on the above Equation of  $S_L$  for full-width supported wide beams, an Equation to account for  $S_L$  of narrow-width supported wide beams must be developed with taking into consideration

the  $k_s$  ratio as concluded from Series (1). Based on the conclusions obtained from Series (1) as mentioned in Chapter (7) and above, and corresponding to the proposed detailing approach as  $k_s$  affects on the  $N_{Ws}$  and as  $k_p$  affects on  $N_{Wp}$ ,  $k_s$  must have an influence on  $S_L$ , and  $k_p$  and  $S_L$  must have influence on  $S_w$ . Consequently, the above Equation of  $S_L$  for full-width supported wide beams must be treated for narrow-width supported wide beams with taking  $\sqrt{k_s}$  into the consideration as suggested in Chapter (7) and as applied by the proposed detailing approach, which is used to estimate  $N_{Ws}$ . It should be emphasized that  $0.65d$ , given by the above Equation, must be increased to be  $0.70d$  for narrow-width supported wide beams. This is because decreasing  $k_s$  makes  $S_L$  for narrow-supported wide beams to be too small, and to be maybe lesser than  $0.5d$  which is given by ACI318 and SBC304 Codes. Accordingly, for wide RC beams with narrow-width supports (narrow-width supported wide beams), a proposed value of  $S_w$  is suggested to be as follows (Alluqmani, 2013a):

$$S_L = 0.70d * \sqrt{k_s}$$

Where,  $k_s$  is the ratio of support-width to beam-width ( $b_s/b_w$ ). A " $0.70d*\sqrt{k_s}$ ", given by the above Equation, gives a closely logical understanding and may enhance the shear strength of those wide RC beams with narrow-width supports as a comparison with the beams in Types (B), (C) and (D) in Series (1) but after deriving  $S_w$ .

According to EC2 Code,  $S_w$  is taken to be equal to  $S_L$  for all cases of wide RC beams, where both  $S_L$  and  $S_w$  are assumed to be equal to  $0.75d$ . As concluded from the beams in Types (B, C and D) and as mentioned above,  $k_p$  and  $S_L$  have influence on  $S_w$ . Moreover, based on the requirement of EC2 Code for assuming  $S_w$  to be equal to  $S_L$  and as obtained from the beams in Group (1b) in Series (1) with  $S_w = 0.75d$  which had best results and behaviours comparing with the other correspondingly relevant beams in Group (2) with  $S_w = d$ ,  $S_w$  must be equal to  $S_L$  after it is corrected by a factor depends on the coefficient of geometry ( $\beta_g$ ) given by the proposed prediction model to be based on  $k_p$  and  $h/b_w$  (Alluqmani, 2013a). To find a proposed design value for  $S_w$  to be used for all cases of loads and supports,  $\beta_g (= \sqrt{k^{(h/b_w)}}$ ), given by the proposed prediction model (see Chapter 6), must be treated by replacing  $k$  to  $k_p$  (as recommended) and corrected by multiplying  $k_p^{(h/b_w)}$  with  $\phi_s$ , and  $S_L$  from both above Equations must be reformulated with using a turning point for  $k_s$  value to be as a reference point for classifying the wide RC beams to be considered as full-width or narrow-width supported wide beams (Alluqmani, 2013a). Thus,  $S_w$  is proposed to be " $S_L*\beta_{g,correct.}$ ", where  $\beta_{g,correct.} = \sqrt{[\phi_s*k_p^{(h/b_w)}]}$ . As suggested based on the results of Series (1), Chapter 7,  $S_w$  must be assumed to be lesser than  $0.75d$ ; where as a suggestion and based on the proposed prediction model (Beam A1-1/PB, Table 8.1),  $S_w$  is

taken to be equal to "0.70d" for wide RC beams with full-width loads and supports (Alluqmani, 2013a). This is because based on the proposed design model, the proposed beam, beam A1-1/PB (Table 8.1), with full-width loads and supports designed with  $S_w = 0.70d$  will fail in flexure. Based on this assumption and outcome, for wide RC beams with full-width supports and loads,  $S_L$  is taken 0.65d and  $S_w$  is taken 0.70d; hence,  $\phi_s$  can be determined to be 1.16 as shown below:

$$S_w = S_L * \beta_{g,correct.} = S_L * \sqrt{\left[ \phi_s * k_p \left( \frac{h}{b_w} \right) \right]}$$

$$\text{Hence, } S_w = 0.70d = 0.65d * \beta_{g,correct.} = 0.65d * \sqrt{\left[ \phi_s * k_p \left( \frac{h}{b_w} \right) \right]}$$

For full – width load condition,  $k_p = 1.0$ , hence:  $k_p \left( \frac{h}{b_w} \right) = 1.0$

Hence,  $0.70d = 0.65d * \sqrt{\phi_s}$ , then,  $\sqrt{\phi_s} = 1.077$ , **Hence:  $\phi_s = 1.16$**

As  $S_L$  must be reformulated with using a turning point for  $k_s$  to be as a reference point for classifying the wide RC beams as full-width or narrow-width supported wide beams. A value of  $k_s$  to be "0.85" is taken as a reference point to estimate  $S_L$  for classifying the wide beam, to be either a full-width or a narrow-width supported wide beam (Alluqmani, 2013a). As an assumption, all wide RC beams which have  $k_s > 0.85$  are considered full-width supported wide beams; otherwise, all wide RC beams which have  $k_s \leq 0.85$  are considered narrow-width supported wide beams. Consequently, both Equations mentioned above for  $S_L$  must be reformulated as follows (Alluqmani, 2013a; Alluqmani and Saafi, 2014c):

$$S_L = 0.65d, \text{ for } k_s > 0.85$$

$$S_L = 0.70d * \sqrt{k_s}, \text{ for } k_s \leq 0.85$$

Where,  $k_s = b_s/b_w$ . Based on the above both Equations of  $S_L$  for full-width and narrow-width supported wide beams, respectively,  $S_w$  must be formulated to be used for both cases of full- and narrow- width supported and loaded wide RC beams (wide beams with full and narrow supports and loads). The proposed design value of  $S_w$  to be used for all cases of wide RC beams, with taking into consideration the affecting factors mentioned above, is suggested to be as follows (Alluqmani, 2013a; Alluqmani and Saafi, 2014c):

$$S_w = S_L * \sqrt{\left[ 1.16 * k_p \left( \frac{h}{b_w} \right) \right]}$$

Where,  $k_p$  is the ratio of load-width to beam-width ( $b_p/b_w$ ). The  $S_w$  Equation is used for all cases of loads and supports, where  $S_L$  must be determined from the two Equations above based on  $k_s$  if it is greater than 0.85 or, if it is less than or equal to 0.85.

**The final form of the proposed design model is as follows** (Alluqmani, 2013a, 2013b; Alluqmani and Saafi, 2014c):

$$S_L = 0.65d, \text{ for } k_s > 0.85 \quad (8.4a)$$

$$S_L = 0.70d * \sqrt{k_s}, \text{ for } k_s \leq 0.85 \quad (8.4b)$$

$$S_w = S_L * \sqrt{\left[ 1.16 * k_p \left( \frac{h}{b_w} \right) \right]} \quad (8.5)$$

It should be noted that the unit of  $S_L$  and  $S_w$  is the same unit of  $d$ ,  $b_s$ ,  $b_p$ ,  $b_w$  and  $h$ , which is one dimensional unit, such as *mm*, where  $k_s = b_s/b_w$  and  $k_p = b_p/b_w$ .

#### **Definitions of Parameters:**

$d$  = effective depth of the beam,

$k_s$  = ratio of the support width to beam width =  $b_s/b_w$ ,

$k_p$  = ratio of the load width to beam width =  $b_p/b_w$ ,

$b_s$  = support width,  $b_p$  = load width,  $b_w$  = beam width,

$S_L$  = longitudinal spacing of stirrup legs (along the length), and

$S_w$  = transverse spacing of stirrup legs (across the width).

In order to determine the stirrup legs spacing along the member length (longitudinal stirrup-legs spacing), Equations (8.4a and 8.4b) were established by the author.  $S_L$  should be distributed along the member length. On the other hand, in order to determine the stirrup legs spacing across the member width (transverse stirrup-legs spacing), Equation (8.5) was established by the author.  $S_w$  should be arranged within the effective support width ( $w_s$ ). It should be noted that Equations (8.4a&b) and (8.5) will be investigated in the next Chapter.

It should be emphasized that the transverse stirrup-legs spacing obtained from Equation (8.5) is the design spacing between the interior legs of a four-stirrup legs wide RC beam; while the spacing between the external legs is determined as  $S_{w,t} = b_w - 2C_c - 2\Phi_{str.}/2$ , where  $b_w$  is the beam width,  $C_c$  is the concrete cover and  $\Phi_{str.}$  is the diameter of the stirrup leg (Alluqmani, 2013a,



2013b). For wide RC beams with multi-stirrup legs, the transverse stirrup-legs spacing between the interior stirrups and external stirrups are taken as those legs spacing correspondingly for 4-stirrup legs wide RC beams, as mentioned above; but the transverse spacing between the middle stirrups, which are between the interior and external stirrups, are determined based on the requirements of the shear design for stirrup legs and based on the requirements of the structural design of these beams. The transverse spacing of the middle stirrup legs for multi-stirrup legs wide RC beams should be taken as percentage of  $d$  (the member effective depth), and should be arranged between  $\{[1.25]*S_w\}$  to  $\{[(b_w/h) - 0.15]*d\}$  according to the total number of stirrup legs distributed between the interior and external stirrup legs, where  $S_w$  is the design transverse stirrup-legs spacing obtained from Equation (8.5),  $b_w$  is the beam width and  $h$  is the overall height of the beam [Alluqmani, 2013a, 2013b]. On the other hand, if needed as per the design situation, additional stirrup legs may be arranged inside the interior stirrup legs, where their transverse spacing are taken as percentage of the design transverse spacing for the interior stirrup legs ( $S_w$ ) given by Equation (8.5) to be arranged between  $\{0.60*S_w\}$  to  $\{0.90*S_w\}$  (Alluqmani, 2013a, 2013b).

It is necessary to clarify that the transverse spacing is a centered distance between one-unit of a two-legs stirrup located symmetrically to the middle axis of the beam width; this means, the central axis of the beam width is the symetrical axis which halves the spacing of these two legs for one-unit of a stirrup (Alluqmani, 2013a, 2013b). Figures 8.3a and 8.3b show the effect of the loading and the narrow support on a wide beam without and with shear reinforcement, respectively; where the tension region of the beam is subject to compressive stresses while the compression region is subject to tensile stresses (Al.Dywany, 2010). For wide RC beam with open shear (stirrups) reinforcement (Figure 8.3b), the compression region should include top legs along the beam width to resist the tensile stresses and the crack width propagation (Al.Dywany, 2010). Consequently, closed stirrups are always required for wide RC beams.

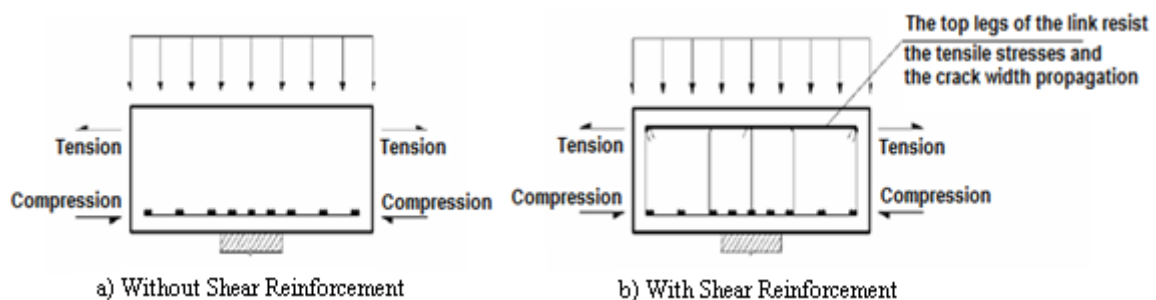


**Figure 8.3:** The Effect of Narrow Support on a Wide RC Beam.

Table 8.1 shows an example for a comparison of the predicted strengths and failure loads given by the proposed prediction model for those wide RC beams tested in Group (1b) in Series (1) for all Types (A, B, C and D, Chapter 7) when they are designed according to the design Code (Traditional Beams (TB),  $S_L = S_w = 0.75d$  to EC2 Code) and to the proposed design model (Proposed Beams (PB)), and when they are loaded and supported with wide and narrow bearing plates. Both groups of beams (TB and PB) have the same properties. The difference is only for the bearing plate width (different  $k$ ), and then  $S_L$  and  $S_w$  will be different for the both beams.  $S_L$  and  $S_w$  for the beams in Group TB are designed according to EC2 Code, while they are designed according to the proposed design model (Equations 8.4 and 8.5, respectively) for the beams in Group PB. Beams TB and PB in Type (A) have wide support and load widths where  $k_s = k_p = 1.0$ . Beams TB and PB in Type (B) have narrow support and load widths where  $k_s = k_p = 0.50$ . Beams TB and PB in Type (C) have narrow support and load widths where  $k_s = 0.50$  and  $k_p = 0.25$ . Beams TB and PB in Type (D) have narrow support and load widths where  $k_s = 0.25$  and  $k_p = 0.50$ .

**Table 8.1:** Prediction of Flexural & Shear Failure Loads for Traditional and Proposed Wide Beams (TB & PB) with Wide and Narrow Bearing Plates Compared with EC2; i.e. the Beams in Group (1b) in Series (1).

Beams	Code Prediction				Proposed-Model Prediction											$P_{f,pred.}$		
	$V_c$	$V_s$	$V_u$	$M_u$	$\mu_s$	$\beta_g$	$K_{cd}$	$V_{c,d}$	$\mu_v$	$\beta_k$	$K_{sd}$	$V_{s,d}$	$V_{u,d}$	$M_{u,d}$	$V_d'$	$P_V$	$P_M$	F. Mode
<b>Type (A): Wide Bearing Plates (<math>k_p = 1.0, k_s = 1.0, k = 1.0</math>)</b>																		
A1-1/TB	192	123	315	262	1.43	1.0	1.43	275	1.0	1.0	1.0	123	398	375	398	796	815	Shear
A1-1/PB	192	143	335	262	1.43	1.0	1.43	275	0.97	1.0	0.97	139	414	375	414	828	815	Flexure
<b>Type (B): Narrow Bearing Plates (<math>k_p = 0.50, k_s = 0.50, k = 0.50</math>)</b>																		
B1-1/TB	192	123	315	262	1.72	0.84	1.44	276	1.0	0.84	0.84	103	379	377	268	758	820	Shear
B1-1/PB	192	187	379	262	1.72	0.84	1.44	276	1.06	0.84	0.89	166	442	377	312	884	820	Flexure
<b>Type (C): Narrow Bearing Plates (<math>k_p = 0.25, k_s = 0.50, k = 0.25</math>)</b>																		
C1-1/TB	192	123	315	262	1.72	0.71	1.22	234	1.0	0.84	0.84	103	337	320	190	674	696	Shear
C1-1/PB	192	187	379	262	1.72	0.71	1.22	234	1.14	0.84	0.96	180	414	320	244	828	696	Flexure
<b>Type (D): Narrow Bearing Plates (<math>k_p = 0.50, k_s = 0.25, k = 0.25</math>)</b>																		
D1-1/TB	192	123	315	262	1.72	0.71	1.22	234	1.0	0.59	0.59	73	307	320	154	614	696	Shear
D1-1/PB	192	263	455	262	1.72	0.71	1.22	234	1.05	0.59	0.62	163	397	320	199	794	696	Flexure

**NOTE:**  $b_w = 600\text{mm}$ ,  $h = 300\text{mm}$ ,  $d = 257\text{mm}$ ,  $a = 920\text{mm}$ ,  $jd = (2/3)*h = 200\text{mm}$ ,  $\epsilon_c = 0.0035$ ,  $E_c = 31000\text{ MPa}$ ,  $E_s = 200000\text{ MPa}$ ,  $A_{s,prov.} = 8\Phi 20\text{mm} = 2514\text{ mm}^2$ ,  $\rho_s = 1.63\%$ ,  $\rho_s' = 0.196\%$  ( $6\Phi 8\text{mm}$ ),  $f_{c,y,d} = 42.25\text{ MPa}$ ,  $f_{y,d} = 525\text{ MPa}$ ,  $f_{y,v,d} = 510\text{ MPa}$ .  $A_v = 201\text{mm}^2$  (4-Legs  $\Phi 8\text{mm}$ ) for all beams.

$P_d = 470\text{ kN}$ ,  $V = 235\text{ kN}$ , and  $M = 216\text{ kN.m}$ .

Traditional Beams to EC2:  $S_L = 0.75d = 192\text{mm}$  and  $S_w = 0.75d = 192\text{mm}$  for Beam-Type TB (A1-1/TB, B1-1/TB, C1-1/TB and D1-1/TB). NOTE, these beams are same the beams in Group (1b) in Series (1), Chapter 7.

Proposed Beam A1-1/PB to Eq. (8.4a) & (8.5):  $S_L = 0.65d = 166\text{mm}$  and  $S_w = 0.70d = 177\text{mm}$ .

Proposed Beam B1-1/PB to Eq. (8.4b) & (8.5):  $S_L = 0.50d = 127\text{mm}$  and  $S_w = 0.44d = 114\text{mm}$ .

Proposed Beam C1-1/PB to Eq. (8.4b) & (8.5):  $S_L = 0.50d = 127\text{mm}$  and  $S_w = 0.38d = 97\text{mm}$ .

Proposed Beam D1-1/PB to Eq. (8.4b) & (8.5):  $S_L = 0.35d = 90\text{mm}$  and  $S_w = 0.32d = 82\text{mm}$ .

$k_p = k_s = 1.0$  ( $b_p = b_s = b_w = 600\text{mm}$ ) for both Beams in Type (A). Hence  $k = 1.0$ .

$k_p = k_s = 0.50$  ( $b_p = b_s = 300\text{mm}$ ) for both Beams in Type (B). Hence  $k = 0.50$ .

$k_p = 0.25$  ( $b_p = 150\text{mm}$ ) and  $k_s = 0.50$  ( $b_s = 300\text{mm}$ ) for both Beams in Type (C). Hence  $k = 0.25$ .

$k_p = 0.50$  ( $b_p = 300\text{mm}$ ) and  $k_s = 0.25$  ( $b_s = 150\text{mm}$ ) for both Beams in Type (D). Hence  $k = 0.25$ .

$P_{V,d}$  = Predicted shear failure load =  $2V_{u,d}$  and  $P_{M,d}$  = Predicted flexural failure load =  $2(M_{u,d}/a)$ .  $P_d = 470\text{ kN}$ ,  $V = 235\text{ kN}$ ,  $M = 216\text{ kN.m}$ .

$P_{f,pred.}$  is the predicted failure load = the smallest of ( $P_{V,d}$  or  $P_{M,d}$ ), and the predicted failure mode (F. Mode) is the failure mode corresponding to  $P_{f,pred.}$ .

1 mm = 0.0394 in, 1 kN = 1000 N = 0.225 kip, 1 MPa = 145 psi, 1 kN.m = 0.738 kip.ft = 8.858 kip.in.

From Table 8.1 and based on the proposed prediction model for shear and flexural strengths (Chapter 6), it can be concluded that all the beams in Group TB, which are designed according to EC2 design Code, will fail in shear when they are loaded and supported with either wide or narrow bearing plates. These beams in Group TB, which are beams A1-1/TB, B1-1/TB, C1-1/TB and D1-1/TB, correspond to the beams in Group (1b) in Series (1) which are beams A1-1b, B1-1b, C1-1b and D1-1b. This is because EC2 Code is the only approach which deals with the transverse spacing of wide RC beams stirrup legs. Otherwise, it can be concluded that all the beams in Group PB, which are designed according to the proposed design model and proposed to be investigated in the next Chapter after they are detailed by the proposed detailing approach, will fail in flexure when they are loaded and supported with either wide or narrow bearing plates. It is also shown that beam A1-1/PB, which is a wide beam with full-width load and support conditions and proposed to be designed with  $S_L = 0.65d$  and  $S_w = 0.75d$  as given by the proposed design model, will fail in flexure at 815 kN as predicted by the proposed prediction model. An experimental investigation for this beam is required (beam A2-1 in Chapter 9).

Table 8.2 shows an example for a comparison of the predicted strengths and failure loads given by the proposed prediction model for a wide RC beam when is designed according to the design Code (Type TB) and the proposed design model (Type PB), and when is loaded and supported with wide and narrow bearing plates. Beam-Type TB is a traditional beam, while Beam-Type PB is a proposed beam. Both beams have the same properties. The difference is only for the bearing plate width (different  $k$ ), and then  $S_L$  and  $S_w$  will be different for the both Beams.  $S_L$  and  $S_w$  for beam-Type TB are designed according to EC2 Code, while they are designed according to the proposed design model (Equations 8.4 and 8.5, respectively) for beam-Type PB. Beams TB and PB in group (A) have wide support and load widths where  $k_s = k_p = 1.0$ . Beams TB and PB in group (B) have narrow support and load widths where  $k_s = k_p = 0.50$ . Beams TB and PB in group (C) have narrow support and load widths where  $k_s = k_p = 0.25$ . From Table 8.2 and based on the proposed prediction model for shear and flexural strengths (Chapter 6), it can be concluded that Beam-Type TB, which is designed according to EC2 design Code, will fail in shear when it is loaded and supported with either wide or narrow bearing plates; while Beam-Type PB, which is designed according to the proposed design model, will fail in flexure when it is loaded and supported with either wide or narrow bearing plates.

Table 8.2 also shows an example for a comparison of the predicted strengths and failure loads given by the proposed prediction model for that wide RC beam with four-leg stirrups tested in

Series (A) and failed in shear (beam ECC2, Chapter 5) when it was designed according to the design Code (beam ECC2-TB,  $S_L \approx 0.6d = 180\text{mm}$  and  $S_w \approx d = 300\text{mm}$ ) and when it is designed according to the proposed design model (beam ECC2-PB,  $S_L \approx 0.41d = 124\text{mm}$  and  $S_w \approx 0.37d = 112\text{mm}$ ), and when it is loaded and supported with narrow bearing plates according to the actual test made for beam ECC2 in Series (A). Both beams (ECC2-TB and ECC2-PB) have the same properties. The difference is only for  $S_L$  and  $S_w$ .  $S_L$  and  $S_w$  for beam ECC2-TB are same those values used for beam ECC2 in Series (A), Chapter 5; while they are designed according to the proposed design model (Equations 8.4b and 8.5, respectively) for beam ECC2-PB. Both beams have the same bearing plates used for beam ECC2 in Series (A) which had narrow support and load widths where  $k_p = 0.50$  and  $k_s = 0.34$ . From Table 8.2 and based on the proposed prediction model for shear and flexural strengths (Chapter 6), it can be concluded that beam ECC2-TB, which is same beam ECC2 in Series (A) and designed according to the Code, will fail in shear at 968 kN; while beam ECC2-PB, which is designed according to the proposed design model, will fail in flexure at 1001 kN. Beam ECC2 in Series (A) failed in shear at 985 kN, where the correspondingly relevant beam (beam ECC2-TB) designed to the Code is proposed to fail in shear at 968 kN ( $P_{f,\text{exp.}}/P_{f,\text{pred.}} = 985/968 = 1.02$ ) when it is predicted by the proposed prediction model as shown in Table 8.2. Furthermore, beam ECC2-PB is the correspondingly relevant beam to beam ECC2 tested in Series (A) (or beam ECC2-TB shown in Table 8.2). Beam ECC2-PB designed to the proposed design model is proposed to fail in flexure at 1001 kN when it is predicted by the proposed prediction model as shown in Table 8.2. It is clear that the proposed Design-Model performs better than EC2 Code as given by the proposed Prediction-Model.

It should be noted that the required area of shear reinforcement ( $A_{v,\text{req.}}$ ) for beam ECC2 in Series (A) was equal to  $279 \text{ mm}^2$ , where the beam was designed for a provided area of shear reinforcement ( $A_{v,\text{prov.}}$ ) of  $201 \text{ mm}^2$  to fail in shear, and the beam failed in shear as predicted. Accordingly, beam ECC2-PB, which is proposed to be instead of beam ECC2 (or ECC2-TB), will fail in flexure where the provided area of shear reinforcement will be the same area used for beam ECC2 ( $A_{v,\text{prov.}} = 201 \text{ mm}^2$ , lesser than the required area,  $A_{v,\text{req.}} = 279 \text{ mm}^2$ ) as shown in Table 8.2. This means that designing and distribution the stirrup legs along the wide beam length and across its width, as given by the proposed design model, will enhance the shear strengths of the beam and will make the beam behave in a ductile flexural manner even if the beam is designed for a provided amount of shear reinforcement to be lesser than the required amount (Alluqmani, 2013a, 2013b).

**Table 8.2:** Prediction of Flexural & Shear Failure Loads for Traditional and Proposed Wide Beams (TB & PB) with Wide and Narrow Bearing Plates Compared with Beam ECC2 in Series (A).

Beams	Code Prediction				Proposed-Model Prediction											P <sub>f,pred.</sub>		
	V <sub>c</sub>	V <sub>s</sub>	V <sub>u</sub>	M <sub>u</sub>	μ <sub>s</sub>	β <sub>g</sub>	K <sub>cd</sub>	V <sub>c,d</sub>	μ <sub>v</sub>	β <sub>k</sub>	K <sub>sd</sub>	V <sub>s,d</sub>	V <sub>u,d</sub>	M <sub>u,d</sub>	V <sub>d</sub>	P <sub>V</sub>	P <sub>M</sub>	F. Mode
<b>Group (A): Wide Bearing Plates (k<sub>p</sub> = 1.0, k<sub>s</sub> = 1.0, k = 1.0)</b>																		
Beam TB-A	274	123	397	480	1.60	1.0	1.60	416	1.0	1.0	1.0	123	539	768	539	<b>1078</b>	<b>1097</b>	Shear
Beam PB-A	274	143	417	480	1.60	1.0	1.60	416	0.97	1.0	0.97	139	555	768	555	<b>1110</b>	<b>1097</b>	Flexure
<b>Group (B): Narrow Bearing Plates (k<sub>p</sub> = 0.50, k<sub>s</sub> = 0.50, k = 0.50)</b>																		
Beam TB-B	274	123	397	480	1.92	0.84	1.61	419	1.0	0.84	0.84	103	522	773	369	<b>1044</b>	<b>1104</b>	Shear
Beam PB-B	274	188	462	480	1.92	0.84	1.61	419	1.05	0.84	0.88	165	584	773	413	<b>1168</b>	<b>1104</b>	Flexure
<b>Group (C): Narrow Bearing Plates (k<sub>p</sub> = 0.25, k<sub>s</sub> = 0.25, k = 0.25)</b>																		
Beam TB-C	274	123	397	480	1.92	0.71	1.36	354	1.0	0.59	0.59	73	427	653	214	<b>854</b>	<b>933</b>	Shear
Beam PB-C	274	266	540	480	1.92	0.71	1.36	354	1.14	0.59	0.67	178	532	653	266	<b>1064</b>	<b>933</b>	Flexure
<b>Beam (ECC2) in Series (A): Narrow Bearing Plates (k<sub>p</sub> = 0.50, k<sub>s</sub> = 0.34, k = 0.34)</b>																		
ECC2-TB	274	156	430	480	1.92	0.76	1.46	400	0.77	0.70	0.54	84	484	701	292	<b>968</b>	<b>1001</b>	Shear
ECC2-PB	274	227	501	480	1.92	0.76	1.46	400	1.05	0.70	0.74	168	568	701	352	<b>1136</b>	<b>1001</b>	Flexure

NOTE: bw =708mm, h =353mm, d =304mm, a =1400mm, jd =233mm, ε<sub>c</sub> = 0.0035, E<sub>c</sub> = 31000 MPa, E<sub>s</sub> = 200000 MPa, A<sub>s,prov.</sub> =8Φ25mm =3927 mm<sup>2</sup>, ρ<sub>s</sub> =1.82%, ρ<sub>s'</sub> =0.221% (6Φ10mm), f<sub>cy,d</sub> = 40 MPa, f<sub>y,d</sub> = 525 MPa, f<sub>yv,d</sub> = 512 MPa. A<sub>v</sub> =201mm<sup>2</sup> (4-LegsΦ8mm) for all beams.  
P<sub>d</sub> = 600 kN, V = 300 kN, and M = 420 kN.m.  
Traditional Beams to EC2: SL = 0.75d = 228mm and Sw = 0.75d = 228mm for Beam-Type TB (TB-A, TB-B and TB-C).  
Proposed Beam PB-A to Eq. (8.4a) & (8.5): SL = 0.65d = 197mm and Sw = 0.70d = 210mm for Beam PB -A.  
Proposed Beam PB-B to Eq. (8.4b) & (8.5): SL = 0.49d = 150mm and Sw = 0.45d = 135mm for Beam PB -B.  
Proposed Beam PB-C to Eq. (8.4b) & (8.5): SL = 0.35d = 106mm and Sw = 0.27d = 81mm for Beam PB -C.  
k<sub>p</sub> = k<sub>s</sub> = 1.0 (b<sub>p</sub> = b<sub>s</sub> = bw = 708mm) for both Beams in Group (A). Hence k = 1.0.  
k<sub>p</sub> = k<sub>s</sub> = 0.50 (b<sub>p</sub> = b<sub>s</sub> = 350mm) for both Beams in Group (B). Hence k = 0.50.  
k<sub>p</sub> = k<sub>s</sub> = 0.25 (b<sub>p</sub> = b<sub>s</sub> = 175mm) for both Beams in Group (C). Hence k = 0.25.  
Traditional Beam (Beam ECC2-TB): SL ≈ 0.6d = **180mm** and Sw ≈ d = **300mm**.  
Proposed Beam (Beam ECC2-PB) to Eq. (8.4b) & (8.5): SL = 0.41d = **124mm** and Sw = 0.37d = **112mm**.  
For beams ECC2-TB & ECC2-PB, k<sub>p</sub> = 0.50 (b<sub>p</sub> = 354mm) and k<sub>s</sub> = 0.34 (b<sub>s</sub> = 241mm). Hence k = 0.34.

**NOTES:**  
1. Beam ECC2-TB is same beam ECC2 in Series (A), Chapter 5.  
2. Beam ECC2-PB is suggested by the proposed design model.  
3. Beam ECC2 in series (A) failed in shear at 985 kN, where the correspondingly relevant beam (beam ECC2-TB) designed to the Code is predicted to fail in shear at 968 kN as shown in the Table.  
4. Beam ECC2-PB is the correspondingly relevant beam to beam ECC2 tested in series (A) (or beam ECC2-TB shown in the Table). Beam ECC2-PB designed to the proposed design model is predicted to fail in flexure at 1001 kN as shown in the Table.

P<sub>V,d</sub> = Predicted shear failure load = 2V<sub>u,d</sub> and P<sub>M,d</sub> = Predicted flexural failure load = 2(M<sub>u,d</sub>/a). P<sub>d</sub>=600 kN, V=300 kN, M=420 kN.m.

P<sub>f,pred.</sub> is the predicted failure load = the smallest of (P<sub>V,d</sub> or P<sub>M,d</sub>), and the predicted failure mode (F. Mode) is the failure mode corresponding to P<sub>f,pred.</sub>.

1 mm = 0.0394 in, 1 kN = 1000 N= 0.225 kip, 1 MPa = 145 psi, 1 kN.m = 0.738 kip.ft = 8.858 kip.in.

## 8.6 Conclusion

Proposed Detailing-Approach and Design-Model have been developed based on a well understanding of the flexural and shear behaviours of wide RC beams to enhance the shear stresses and strengths of wide RC beams, and then to ensure that the wide RC beams behave in a ductile flexural manner (Alluqmani, 2013a; Alluqmani and Saafi, 2014c).

The effects of b<sub>s</sub>, b<sub>p</sub>, k<sub>s</sub>, k<sub>p</sub> and d have been taken into the account when the detailing approach and design model have been developed. The proposed detailing approach was developed to

account for the effective-widths of supports and loads ( $w_s$  and  $w_p$ ), and the concentrating flexural -tensile and -compression reinforcing bars distributed within the effective widths of -supports and -loads ( $N_{w_s}$  and  $N_{w_p}$ ), respectively. A portion of the flexural -tensile and -compression reinforcements should be distributed within the effective-widths of supports and loads, respectively, as given by the proposed detailing approach. The proposed design model was developed to account for the longitudinal and transverse spacing of stirrup legs ( $S_L$  and  $S_w$ ).  $S_L$  should be distributed along the beam length, while  $S_w$  should be arranged across the beam width to be measured from the centreline of the beam width, as given by the proposed design model.

The proposed design model shows that the longitudinal and transversal stirrup-legs spacing decrease as the ratios of the support-width and load-width to beam-width decrease, and then, this will enhance in increasing the shear strength; therefore, the failure mode will change from brittle to ductile manner. This influence occurs for members with shear reinforcement. Moreover, for the members with and without shear reinforcement, the proposed detailing approach will enhance the flexural reinforcements (tensile and compressive bars) when they are distributed according to their portions of concentrations on the effective widths of the bearing plates (support and load widths). An experimental verification on the proposed detailing approach and design model comparing with the existing design Codes and models is required in order to validate the proposed models developed in this study, as presented in Table 8.1; where from Table 8.1, it is shown that the proposed design model performs better than EC2 Code.

## CHAPTER 9

# BEHAVIOUR OF WIDE RC BEAMS DESIGNED TO THE PROPOSED MODELS: SERIES (2)

### 9.1 Introduction

The main variables for investigating the behaviour of beam specimens in Test-Series (2) are to validate the proposed Detailing-Approach and Design-Model (Alluqmani, 2013a; Alluqmani and Saafi, 2014c), to verify the proposed Prediction-Model for the both flexural and shear strengths, and to find a new guideline and design provisions for flexure and shear to be used in Practice for wide RC beams with full- and narrow- width loads and supports (Alluqmani, 2013a).

Test-Series (2) included 8 simply supported wide RC beams with concentrated load for a three point-loading system. The specimens in Test-Series (2) were designed for flexure using the current Codes of Practice, such as EC2 Code, detailed for flexural and shear reinforcements according to the proposed Detailing-Approach, and designed for shear according to the proposed Design-Model in order to determine the longitudinal and transversal stirrup-legs spacing ( $S_L$  and  $S_w$ ). The experimental test programme, the material properties, beam manufacture, test arrangements and procedures, and experimental methodology for Test-Series (2) specimens are described and discussed in this Chapter. Moreover, this Chapter discusses the experimental works in general for those wide RC beams tested and investigated in Test-Series (2).

### 9.2 Description of Test Specimens

Test-Series (2) included 8 wide RC beam specimens made with normal-strength concrete and high-strength reinforcement. The specimens were designed, constructed and examined at The University of Strathclyde, Glasgow-UK (Alluqmani, 2013a). All wide RC beam specimens to be experimentally investigated were simply supported beams using a three point-loading system. The specimens were detailed and designed for flexure and shear using the proposed Detailing-Approach and Design-Model. All beams (with and without stirrups) were detailed according to the proposed detailing approach. The beams with stirrups were designed for the longitudinal and transverse stirrup-legs spacing according to the proposed design model. All beams were tested to validate the proposed detailing approach and design model, to verify the proposed prediction

model, and to investigate the behaviour of the beams with full- and narrow- bearing plates. The scope of this programme of research for the beams in Test-Series (2) focuses on the flexural and shear behaviours of wide concrete beams, with constant cross section and constant flexural (longitudinal) reinforcement along the beam length. The shear (transverse) reinforcement made up exclusively by closed vertical stirrups with 4-legs 8mm diameter distributed along the beam length and across the beam width.

**Table 9.1#:** Test-Series "2" to Validate of the Proposed Detailing/Design Models and to Verify the Proposed Prediction Model<sup>^</sup>.

		Beam-Type (A)	Beam-Type (B)	Beam-Type (C)	Beam-Type (D)
		$k_p = 1.0, k_s = 1.0$	$k_p = 0.50, k_s = 0.50$	$k_p = 0.25, k_s = 0.50$	$k_p = 0.50, k_s = 0.25$
		$k = 1.0$	$k = 0.50$	$k = 0.25$	$k = 0.25$
<b>Test-Series (2)<sup>*/*</sup>:</b>	<b>Beam Group</b>	<b>Validation of the Proposed Detailing &amp; Design Model<sup>^^</sup></b>			
$b_w/h = 2.0$ <u>Detailing &amp; Design</u> <u>Model Validation</u> (SL = 0.65d) <sup>*1</sup> (SL = 0.7d* $\sqrt{k_s}$ ) <sup>**1</sup> d = 257mm	<b>Without Stirrups</b>	<b>Beam A2-0</b>	<b>Beam B2-0</b>	<b>Beam C2-0</b>	<b>Beam D2-0</b>
	$S_w = f(SL)$ <sup>*2</sup>	<b>Beam A2-1</b> (SL = 0.65d = 166) ( $S_w \approx 0.70d =$ 1.07SL = 177)	<b>Beam B2-1</b> (SL $\approx 0.49d = 127$ ) ( $S_w \approx 0.44d =$ 0.90SL = 114)	<b>Beam C2-1</b> (SL $\approx 0.49d = 127$ ) ( $S_w \approx 0.38d = 0.77SL =$ 97)	<b>Beam D2-1</b> (SL $\approx 0.35d = 90$ ) ( $S_w \approx 0.32d = 0.91SL$ = 82)

# This Test Series is aimed to 1. Validate the proposed prediction Model, 2. Validate the proposed detailing and design Model and then modifications may be added to the proposed detailing and design model, and 3. Find a new guide and design provisions to be used in Practice for Wide RC Beams.

<sup>^</sup> The Proposed Prediction Model:

a) The Shear Strength:

$$V_{u,d} = V_{c,d} + V_{s,d} = (K_{cd} * V_c) + (K_{sd} * V_s), \text{ where } K_{cd} = \mu_s * \beta_g = \{ [F * (\rho_s - \rho_s)] * [\sqrt{k}^{(h/bw)}] \}, K_{sd} = \mu_v * \beta_k = \{ [\sqrt{SL/S_w}] * [\sqrt{k_s^{(1-k_s)}}] \}.$$

b) The Flexural Strength:

$$M_{u,d} = K_{cd} * M_u = (\mu_s * \beta_g) * M_u = \{ [F * (\rho_s - \rho_s)] * [\sqrt{k}^{(h/bw)}] \} * M_u, \text{ where } M_u = A_{s,prov} * f_{y,act} * j_d, \text{ and } j_d = Z = (2/3) * h.$$

For  $|\rho_s - \rho_s| > 1.0\%$ :  $F = 100$  (but if  $|\rho_s - \rho_s| > 1.60\%$ , use  $F = 60$ ) for  $k_s = 1.0$ ; while  $F = 120$  for  $k_s < 1.0$ .

For  $|\rho_s - \rho_s| < 1.0\%$ :  $F = 140$  for  $k_s = 1.0$ ; while  $F = 170$  for  $k_s < 1.0$ . But if  $|\rho_s - \rho_s| < 0.50\%$ , use  $F = (100 * b_w/h)$  whatever the support width.

<sup>^^</sup> The Proposed Detailing & Design Model:

a) The Proposed Detailing Model:

$$N_{w_s} = A_s * \sqrt{k_s} = A_s * \sqrt{(b_s/b_w)}$$

$$N_{w_p} = A_s * \sqrt{k_p} = A_s * \sqrt{(b_p/b_w)}$$

$$w_s = \{ (b_w/h) * [(h-d) * (b_w - b_s)] / h \} + b_s - 2C_c - 2\Phi_{str}.$$

$$w_p = \{ (b_w/h) * [(h-d) * (b_w - b_p)] / h \} + b_p - 2C_c - 2\Phi_{str}.$$

b) The Proposed Design Model:

$$SL = 0.65d \text{ for } k_s > 0.85$$

$$SL = 0.70d * \sqrt{k_s} \text{ for } k_s \leq 0.85$$

$$S_w = SL * \sqrt{1.16 * k_p^{(h/bw)}}$$

\*1 SL = 0.65d for  $k_s > 0.85$ . SL must be distributed along the beam length.

\*\*1 SL = 0.70d \*  $\sqrt{k_s}$  for  $k_s \leq 0.85$ . SL must be distributed along the beam length.

\*2  $S_w = SL * \sqrt{1.16 * k_p^{(h/bw)}}$ , and  $S_w$  should be distributed within the effective width of the bearing plates.

\*/\* The  $N_{w_s}$  bars are arranged within the  $w_s$  width, and the  $N_{w_p}$  bars are arranged within the  $w_p$  width.

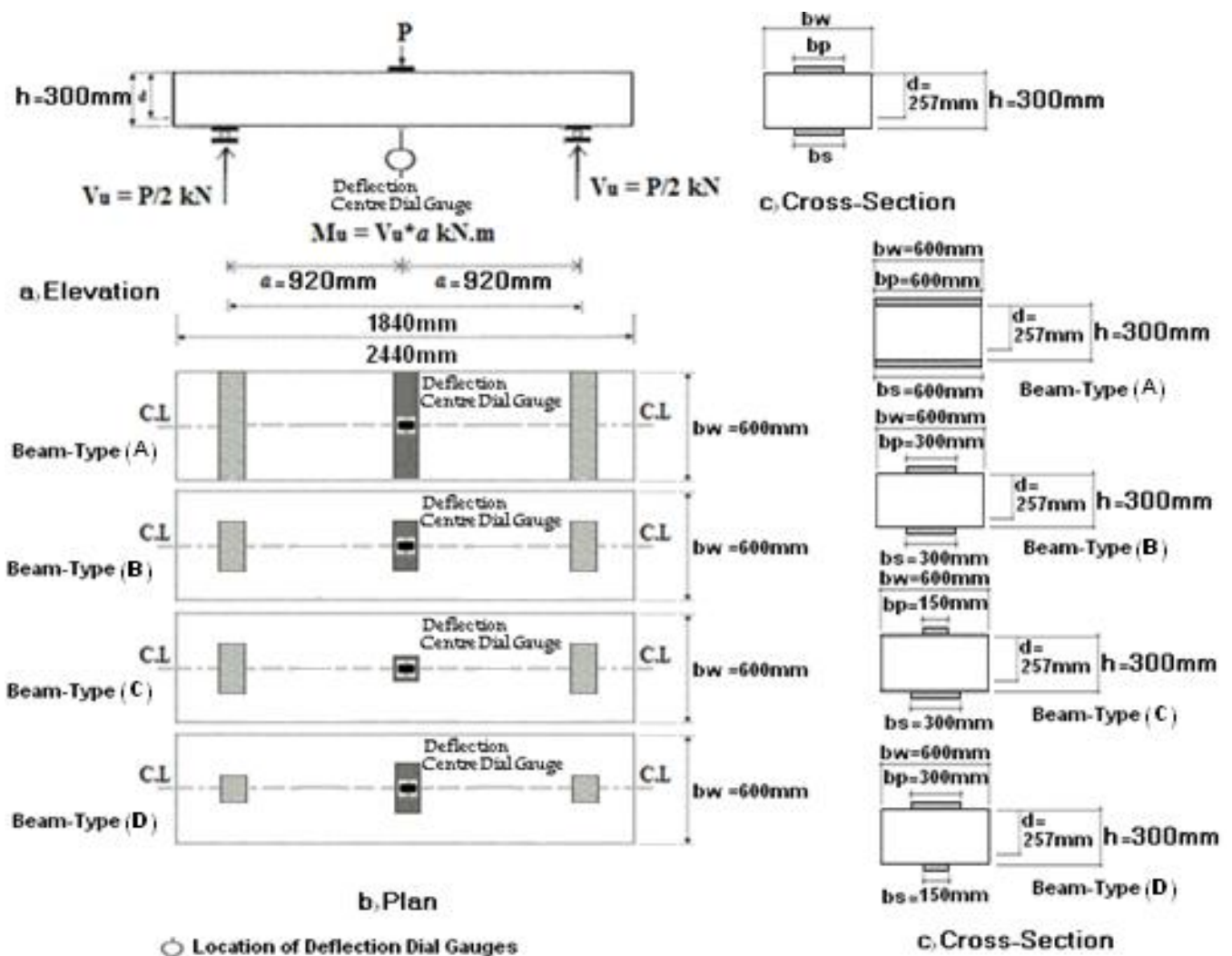
- All beams have the same  $b_w/h$  ratio equal to 2.0 ( $b_w = 600\text{mm}$ ,  $h = 300\text{mm}$ ,  $d = 257\text{mm}$ ), the same  $\rho_s$  ratio greater than 1.0% (equal to 1.63%,  $8\Phi 20\text{mm}$ ), the same  $\rho_s'$  ratio less than 1.0% (equal to 0.196%,  $6\Phi 8\text{mm}$ ), and the same  $A_v$  equal to  $201\text{mm}^2$  (4-Legs  $\Phi 8\text{mm}$ ).

The results to be analysed were obtained from the test to failure carried out on 8 wide beams (Table 9.1). The analysis will focus on the comparison between the flexural and shear capacities actually reached in the tests and those values that would be obtained applying the calculation formulae included in the EC2, ACI318 and SBC304 Codes, and with those values obtained from



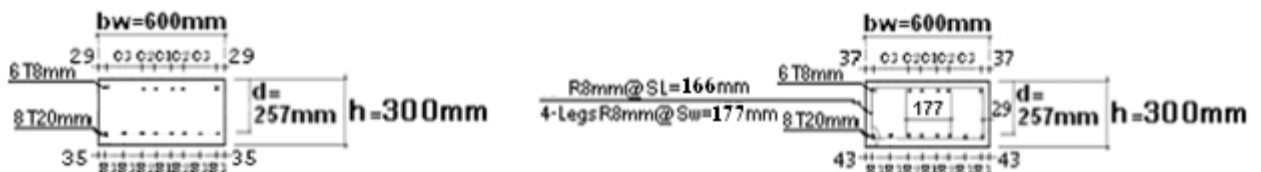
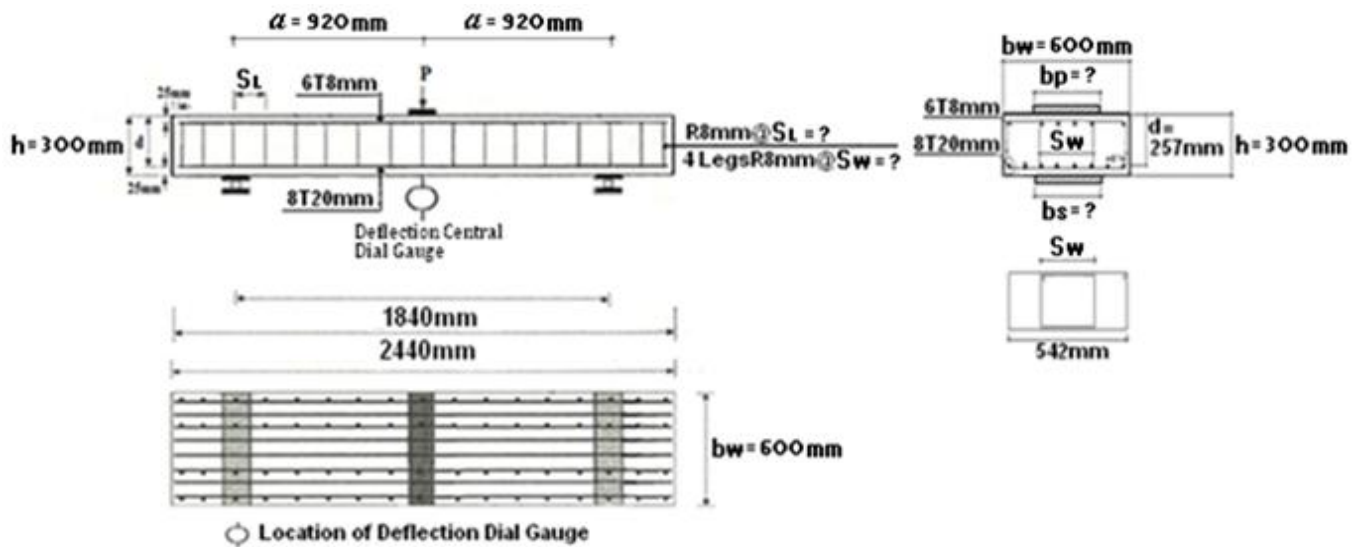
the proposed prediction model and the existing shear models. Moreover, the analysis will include a comparison between the flexural and shear capacities obtained from the results of this Series with those results obtained from Test-Series (1). Final conclusions are included in order to take such effects into account for use in practice.

Table 9.1 shows the types and groups of the beams in Test-Series (2) used to validate of the proposed detailing and design models, and to verify the proposed prediction model. Figures 9.1 and 9.2 show typical description of the details and design of wide RC beam specimens, respectively, used in Test-Series (2).



Series (2)/ All Groups	No. of Beams	Beam Dimensions				Support Plate Dimensions			Loading Plate Dimensions		
		L	bw	h	d	bs	Cs	Is	bp	Cp	tp
Beam-Type (A)	2	2440	600	300	257	600	150	25	600	150	25
Beam-Type (B)	2	2440	600	300	257	300	150	25	300	150	25
Beam-Type (C)	2	2440	600	300	257	300	150	25	150	150	25
Beam-Type (D)	2	2440	600	300	257	150	150	25	300	150	25

Figure 9.1: Details of Wide Beam Specimens in Test-Series "2".



Beams in Type (A)



Beams in Type (B)



Beams in Type (C)



Beams in Type (D)

Series (2)/ Group (0)	No. of Beams	Beam Dimensions				Stirrup Legs Spacing		Support Plate Dimensions			Bottom (Tensile) Reinforcement Spacing					Loading Plate Dimensions			Top (Compression) Reinforcement Spacing				
		L	bw	h	d	SL	Sw	bs	Cs	ts	S1	S2	S3	ws	Nws	bp	Cp	tp	C1	C2	C3	wp	Nwp
Beam A2-0	1	2440	600	300	257	-	-	600	150	25	51	52.5	93.5	550	8φ20	600	150	25	59	56.5	185	550	6φ8
Beam B2-0	1	2440	600	300	257	-	-	300	150	25	86	56	110	336	6φ20	300	150	25	102	110	110	336	4φ8
Beam C2-0	1	2440	600	300	257	-	-	300	150	25	70	60	110	336	6φ20	150	150	25	82	65	165	229	4φ8
Beam D2-0	1	2440	600	300	257	-	-	150	150	25	58	72	82	229	4φ20	300	150	25	72	125	110	336	4φ8

Series (2)/ Group (1)	No. of Beams	Beam Dimensions				Stirrup Legs Spacing		Support Plate Dimensions			Bottom (Tensile) Reinforcement Spacing					Loading Plate Dimensions			Top (Compression) Reinforcement Spacing				
		L	bw	h	d	SL	Sw	bs	Cs	ts	S1	S2	S3	ws	Nws	bp	Cp	tp	C1	C2	C3	wp	Nwp
Beam A2-1	1	2440	600	300	257	166	177	600	150	25	49	50	91.25	534	8φ20	600	150	25	53	54	182.5	534	6φ8
Beam B2-1	1	2440	600	300	257	127	114	300	150	25	86	53.5	107	320	6φ20	300	150	25	98	107	107	320	4φ8
Beam C2-1	1	2440	600	300	257	127	97	300	150	25	69	57.75	107	320	6φ20	150	150	25	81	62	160.5	213	4φ8
Beam D2-1	1	2440	600	300	257	90	82	150	150	25	54	69.5	80.25	213	4φ20	300	150	25	66	123	107	320	4φ8

**For Wide Beams with Narrow-width Loads and Supports:**

$$s_1 = S_w - (2\Phi_{str./2}) - (2\Phi_s/2), \text{ and } s_2 = [w_s - (2\Phi_s/2) - s_1] / (Nw_s - 2), \text{ and } s_3 = [bw - 2C_c - (2\Phi_{str.}) - w_s] / (N_s - Nw_s).$$

$$c_1 = S_w - (2\Phi_{str./2}) - (2\Phi_s/2), \text{ and } c_2 = [w_p - (2\Phi_s/2) - s_1] / (Nw_p - 2), \text{ and } c_3 = [bw - 2C_c - (2\Phi_{str.}) - w_p] / (N_s' - Nw_p).$$

$s_1$  and  $s_2$  are located within the effective support-width ( $w_s$ ).  $c_1$  and  $c_2$  are located within the effective support-width ( $w_p$ ).

**Figure 9.2:** Design of Wide Beam Specimens in Test-Series "2".

### 9.3 Design and Configurations of Test Specimens

All beam specimens were designed for their flexural reinforcements according to the current Codes of Practice, such as EC2 Code. The beams had 600mm wide, 300mm height, 2440mm overall length, 1840mm effective span, 20mm diameter of tension flexural bars, 8mm diameter of compression flexural (hanger) bars, 8mm diameter of stirrups, a longitudinal reinforcement ratio ( $\rho_s$ ) of 1.63%, a shear-span to effective-depth ratio ( $a/d$ ) of 3.58 (type II beams), a three point-loading arrangement, and full- and narrow- width load and support conditions ( $b_p = b_s$ ,  $b_p < b_s$  or  $b_p > b_s$ ). The stirrups legs spacing along the beam length and across the beam width, the support width and the load width were the main variables in this investigation. The number of bars in the tension and compression zones was the same in all test specimens, where  $\rho_s = 1.63\%$  and  $\rho_s' = 0.196\%$ .

The specimens, which were described in Figures 9.1 and 9.2, and Table 9.2, were constructed to nominal dimensions of 600mm width, 300mm total height (257mm effective depth), and 2440mm total length (1840mm clear span). The specimens were analyzed, designed and tested under three-point loading with a central span of 1840mm and shear span of 920mm, giving a shear-span to effective-depth ratio ( $a/d$ ) of 3.58. They were designed to carry a concentrated design load ( $P_d$ ) in the mid-span point of 470 kN. The specimens were loaded and supported either with wide steel-plates by 25x150x600mm for full-width bearing-plates, or with narrow

steel-plates by 25x150x300mm and/or 25x150x150mm for partial-width bearing-plates. The specimens in Group (0) were without shear-reinforcement. The specimens in Group (1) were with shear-reinforcement.

**Table 9.2:** Design Details of the Wide Beams in Test-Series "2".

Beam Type	Cross-Section Dimensions	Tensile Reinforcement	Compressive Reinforcement	Shear Reinforcement Along the Length, C/C	Shear Reinforcement Across the Width, C/C
Beam A2-0	600*300mm Ac =180000mm <sup>2</sup>	8T20mm As =2514mm <sup>2</sup>	6T8mm As' =301mm <sup>2</sup>	----	----
Beam A2-1	600*300mm Ac =180000mm <sup>2</sup>	8T20mm As =2514mm <sup>2</sup>	6T8mm As' =301mm <sup>2</sup>	15 Stirrups R8mm@166mm	4 Stirrup Legs-R8mm @177-542mm
Beam B2-0	600*300mm Ac =180000mm <sup>2</sup>	8T20mm As =2514mm <sup>2</sup>	6T8mm As' =301mm <sup>2</sup>	----	----
Beam B2-1	600*300mm Ac =180000mm <sup>2</sup>	8T20mm As =2514mm <sup>2</sup>	6T8mm As' =301mm <sup>2</sup>	20 Stirrups R8mm@127mm	4 Stirrup Legs-R8mm @114-542mm
Beam C2-0	600*300mm Ac =180000mm <sup>2</sup>	8T20mm As =2514mm <sup>2</sup>	6T8mm As' =301mm <sup>2</sup>	----	----
Beam C2-1	600*300mm Ac =180000mm <sup>2</sup>	8T20mm As =2514mm <sup>2</sup>	6T8mm As' =301mm <sup>2</sup>	20 Stirrups R8mm@127mm	4 Stirrup Legs-R8mm @97-542mm
Beam D2-0	600*300mm Ac =180000mm <sup>2</sup>	8T20mm As =2514mm <sup>2</sup>	6T8mm As' =301mm <sup>2</sup>	----	----
Beam D2-1	600*300mm Ac =180000mm <sup>2</sup>	8T20mm As =2514mm <sup>2</sup>	6T8mm As' =301mm <sup>2</sup>	27 Stirrups R8mm@90mm	4 Stirrup Legs-R8mm @82-542mm

Test-Series (2) includes beams with and without shear reinforcement. Series (2) was divided to four Types (Types A, B, C and D) which were based on the width of supports and loads and were similar to the beams in Test-Series (1); where each Beam-Type had two Groups (Groups 0 and 1) which were based on the detail and arrangement of flexural reinforcement and the design of shear reinforcements spacing (Table 9.1). The beams in Type (A) had full-width loads and supports, where  $k_p = k_s = 1.0$ . The beams in Type (B) had narrow-width loads and supports, where  $k_p = k_s = 0.50$ . The beams in Type (C) had narrow-width loads and supports, but the loads were narrower than the supports, where  $k_p = 0.25$  and  $k_s = 0.50$ . The beams in Type (D) had narrow-width loads and supports, but the supports were narrower than the loads, where  $k_p = 0.50$  and  $k_s = 0.25$ . Each Beam-Type includes a beam without shear reinforcement and a beam with shear reinforcement. The beams in Group (0) were without shear-reinforcement, and were used as references. The beams in Groups (1) were with shear-reinforcements and their longitudinal and transverse spacing (SL and  $S_w$ ) were determined in accordance with the proposed Design-Model based on the effective depth of the beam and the ratios of the support- and load- width to beam-width. Web reinforcement patterns included four stirrup-legs across the width in all specimens, two legs near the specimen edges (external legs), and two legs concentrated between edge and central beam-width (internal legs), which are measured from the centre line of the beam width ( $b_w$ ). SL was given as  $SL = 0.65d$  for  $k_s > 0.85$ , and as  $SL = 0.70d \cdot \sqrt{k_s}$  for  $k_s \leq 0.85$ , and SL

was distributed along the member length.  $S_w$  was taken as  $S_w = S_L \cdot \sqrt{[1.16 \cdot k_p^{(h/b_w)}]}$ , and  $S_w$  was arranged and distributed across the member width and within the effective support width ( $w_s$ ) for the interior legs. All specimens had the same main longitudinal reinforcement (8Ø20mm), resulting in a  $\rho_s$  ratio of 1.63%. Top longitudinal (hanger) bars (6Ø8mm) were used to anchor the stirrups, but would have minimal influence on overall member response. Portions of the flexural -tensile and -compressive reinforcing bars were arranged and distributed within the effective-widths of supports and loads, respectively, in accordance with the proposed Detailing-Approach based on the widths of support and loads and the ratios of the support- and load- width to beam-width. The remaining flexural -tensile and -compressive reinforcing bars were equally arranged and distributed within the both edges of the beam width in the regions which are outside the effective-widths of supports and loads.

All beams were detailed in accordance with the proposed Detailing-Approach in order to determine the concentrating flexural-tensile reinforcing bars within the effective support width ( $N_{w_s}$ ), the effective support width ( $w_s$ ), the concentrating flexural-compressive reinforcing bars within the effective load width ( $N_{w_p}$ ) and the effective load width ( $w_p$ ). Moreover, all beams were designed in accordance with the proposed Design-Model in order to determine the longitudinal and transversal spacing of stirrup legs ( $S_L$  and  $S_w$ ), Tables 9.1, 9.2 and 9.3. The longitudinal legs spacing ( $S_L$ ) was designed for each beam with stirrups to be distributed for the whole beam span with values of 166mm ( $\approx 0.65 \cdot d$ ) for beam A2-1, 127mm ( $\approx 0.49 \cdot d$ ) for beam B2-1, 127mm ( $\approx 0.49 \cdot d$ ) for beam C2-1, and 90mm ( $\approx 0.35 \cdot d$ ) for beam D2-1. The transversal legs spacing ( $S_w$ ) was designed for four 8mm stirrup legs diameter for each beam with stirrups to be distributed across the beam width with spacing of the interior legs of 177mm ( $\approx 0.69 \cdot d \approx 1.07 \cdot S_L \approx 0.33 \cdot w_s$ ) for beam A2-1, 114mm ( $\approx 0.44 \cdot d \approx 0.90 \cdot S_L \approx 0.36 \cdot w_s$ ) for beam B2-1, 97mm ( $\approx 0.38 \cdot d \approx 0.76 \cdot S_L \approx 0.30 \cdot w_s$ ) for beam C2-1, and 82mm ( $\approx 0.32 \cdot d \approx 0.91 \cdot S_L \approx 0.38 \cdot w_s$ ) for beam D2-1. The transversal spacing of stirrup legs was  $S_w$  as mentioned above for the interior legs, which was determined by the proposed design model, and was 542mm for external legs for all specimens with stirrups in Test-Series (2). Details of the reinforcements are shown in Figure 9.2. The beams in Series (2) were also used to verify the proposed Prediction-Model for predicting the shear and flexural strengths of wide RC beams.

The design details of the test specimens in Test-Series (2) are shown in Table 9.2. The characteristics and properties of the test specimens are shown in Table 9.3. Figure 9.3 shows various steel plates used in different cases of load and support conditions.



**Figure 9.3:** Difference Sizes of Steel Plates Used for Load and Support Conditions in Series "2".

**Table 9.3:** Properties of the Wide Beam Specimens in Test-Series "2".

Beams	$b_s$ mm	$k_s$ -	$N_{ws}$ -	$w_s$ mm	$b_p$ mm	$k_p$ -	$N_{wp}$ -	$w_p$ mm	$k$ -	SL mm	$S_w$ mm	$\rho_v$ %	$\mu_s$ -	$\beta_g$ -	$\mu_v$ -	$\beta_k$ -
Beam A2-0	600	1.00	8 $\Phi$ 20	550	600	1.00	6 $\Phi$ 8	550	1.00	-	-	-	1.43	1.00	-	-
Beam A2-1	600	1.00	8 $\Phi$ 20	534	600	1.00	6 $\Phi$ 8	534	1.00	166	177	0.20	1.43	1.00	0.97	1.00
Beam B2-0	300	0.50	6 $\Phi$ 20	336	300	0.25	4 $\Phi$ 8	336	0.25	-	-	-	1.72	0.84	-	-
Beam B2-1	300	0.50	6 $\Phi$ 20	320	300	0.25	4 $\Phi$ 8	320	0.25	127	114	0.26	1.72	0.84	1.06	0.84
Beam C2-0	300	0.50	6 $\Phi$ 20	336	150	0.25	4 $\Phi$ 8	229	0.25	-	-	-	1.72	0.71	-	-
Beam C2-1	300	0.50	6 $\Phi$ 20	320	150	0.25	4 $\Phi$ 8	213	0.25	127	97	0.26	1.72	0.71	1.14	0.84
Beam D2-0	150	0.25	4 $\Phi$ 20	229	300	0.50	4 $\Phi$ 8	336	0.25	-	-	-	1.72	0.71	-	-
Beam D2-1	150	0.25	4 $\Phi$ 20	213	300	0.50	4 $\Phi$ 8	320	0.25	90	82	0.37	1.72	0.71	1.05	0.59

**NOTE:**  $b_w = 600\text{mm}$ ,  $h = 300\text{mm}$ ,  $d = 257\text{mm}$ ,  $\rho_s = 1.63\%$  (8 $\Phi$ 20mm),  $\rho_{s'} = 0.196\%$  (6 $\Phi$ 8mm),  $A_v = 201\text{mm}^2$  (4-Legs $\Phi$ 8mm) for all beams.

**The main features of the experimental programme of Series (2) are:**

- Cross section of beams: 600mm wide x 300mm height, and  $b_w/h$  ratio of 2.0.
- Support and load system: simple supported beams with a 2440mm total span and 1840mm free span. The load is applied at mid-span point (Figures 9.1 and 9.2) and the ratio of shear-span to effective-depth ( $a/d$ ) is equal to 3.58.
- The longitudinal reinforcement is kept constant along the beam and is eight 20mm diameter ( $\rho_s = 1.63\%$ ). Compression reinforcement is used as hanger bars and is six 8mm diameter ( $\rho_{s'} = 0.196\%$ ). The effective depth ( $d$ ) is 257mm for all the beams.
- The reinforcement is designed according to the current Code specifications, such as EC2 Code, except for the shear reinforcement spacing, which is considered as one of the variables in this investigation.

**The variables analysed are:**

- Longitudinal spacing of stirrup legs (SL): 166, 127 and 90mm, corresponding to stirrup-spacing/effective-depth (SL/d) ratios of 0.65, 0.49 and 0.35, respectively.
- Shear reinforcement arrangement (NL): 4 stirrup legs in each beam.

- c) Transversal spacing of stirrup legs ( $S_w$ ): 177, 114, 97 and 82mm, corresponding to stirrup-spacing/effective-depth ( $S_w/d$ ) ratios of 0.69, 0.44, 0.38 and 0.32, respectively.
- d) Diameter of stirrups ( $\Phi_{str.}$ ): 8mm. The total area of shear reinforcement ( $A_v$ ) is  $201\text{mm}^2$ .
- e) Support width ( $b_s$ ): The beams in Type A are supported with wide bearing plates where  $b_s$  is equal to 600mm ( $k_s = b_s/b_w = 1.0$ ), whereas the beams in Types B, C and D are supported with narrow bearing plates placed at the centre of the beam width where  $b_s$  is equal to 300mm, 300mm and 150mm respectively (correspondingly to,  $k_s = b_s/b_w = 0.50, 0.50$  and  $0.25$  respectively).
- f) Load width ( $b_p$ ): The beams in Type A are loaded with wide bearing plates where  $b_p$  is equal to 600mm ( $k_p = b_p/b_w = 1.0$ ), whereas the beams in Types B, C and D are loaded with narrow bearing plates placed at the centre of the beam width where  $b_p$  is equal to 300mm, 150mm and 300mm respectively (correspondingly to,  $k_p = b_p/b_w = 0.50, 0.25$  and  $0.50$  respectively).

## 9.4 Materials Information

The performance and quality of concrete member depend to a large extent on the proportions and characteristics of its constituent materials (Ziara, 1993; Alluqmani, 2010; Alluqmani, 2014; Alluqmani and Haldane, 2011c). Therefore, it was important that the quality of the material remained consistent during this programme of research. The information relating to the materials used to design the beam specimens and cast the concrete were the same as assumed in the design calculations, Tables 9.4.

**A brief detail and description of the materials used for test specimens are as follows:**

### 9.4.1 Concrete

For all test specimens, a 40 MPa cylinder compressive strength (50 MPa cubic compressive strength) was used in the design calculations, which was used in this programme of research as it is being applied according to the design provisions of EC2 approach, as shown in Table 9.4.

All beam specimens with their own control samples (cubes and cylinders) were made simultaneously with concrete from the same mixture at the same time. Ready mixed concrete was used to cast the beam specimens and control samples, contained 10-20mm (3/8-3/4 in.) coarse aggregate, 4mm (3/16 in.) fine aggregate, 375 kg cement content per cubic metre of concrete, and 0.42 design water/cement (w/c) ratios to give a workability of 60-70mm slump. The aggregate was crushed limestone for all test specimens. The cube samples used in the

laboratory tests had dimensions of 100x100x100 mm, where the cylinder samples had dimensions of 200mm height x 100mm diameter. The nominal specified strength of the concrete used to cast the specimens was as that used for the design purpose for class C40, which was 40 MPa for concrete cylinder strength or 50 MPa for concrete cubic strength (Table 9.4).

Table 9.4 shows the material properties used to design the beam specimens. The mix proportions of concrete used to cast the beams are shown in Table 9.5. The concrete mixes used in the experimental investigation were designed to give an average cubic compressive strength at 28 days ( $f_{cu}$ ) equal to the specified strength, this means, the target mean strength was taken to be equal to the characteristic strength.

**Table 9.4:** Material Properties used to Design the Beam Specimens in Series "2".

	Properties	Series (2)
<b>Concrete</b>	Cylinder Compressive Strength ( $f_c$ ), MPa	40
	Cube Compressive Strength ( $f_{cu}$ ), MPa	50
	Young's Modulus ( $E_c$ ), MPa	28000
<b>Flexural Reinforcement</b>	Yield Strength for $\Phi 20$ mm ( $f_y$ ), MPa	500
	Yield Strength for $\Phi 8$ mm ( $f_y$ ), MPa	500
	Young's Modulus ( $E_s$ ), MPa	200000
<b>Shear Reinforcement</b>	Yield Strength for $\Phi 8$ mm ( $f_{yv}$ ), MPa	500
	Young's Modulus ( $E_s$ ), MPa	200000

**Table 9.5:** Mix Proportions of Concrete Used to Cast the Beams in Series "2".

Properties	Test-Series (2)
Cement Type	Ordinary Portland Cement
Maximum Aggregate Size	10 to 20mm (3/8 to 3/4 in.)
Slump for Concrete	60-70mm
Coarse Aggregate Content	1025 kg/m <sup>3</sup>
Fine Aggregate Content	874 kg/m <sup>3</sup>
Cement Content	375 kg/m <sup>3</sup>
Water/Cement (w/c) Ratio	0.42
Free-Water Content	158 litre/m <sup>3</sup>

#### 9.4.2 Reinforcement

In all test specimens, high deformed yield steel bars were used in the design of the flexural (longitudinal) and shear (transverse) reinforcements. The sizes of steel bars used to fabricate the beam specimens are as follows:

20mm high strength deformed yield steel bars were used for tensile flexural (main) reinforcement for all test beams.



8mm high strength deformed yield steel bars were used for compressive flexural (hanger) reinforcement and transverse shear reinforcement (stirrups) for all test beams.

For all test specimens, a 500 MPa high yield steel strength was used in the design calculations for both flexural and shear reinforcements, which was used in this programme of research as it is being applied according to the design provisions of EC2 approach, as shown in Table 9.4.

The beams in Series (2) were made simultaneously with concrete from the same mixture. The actual average cube and cylinder concrete compressive strengths were  $f_{cu,act} = 55.60$  MPa and  $f_{cy,act} = 44.50$  MPa, respectively. Eight 20mm nominal diameter high-strength deformed steel bars were used for the longitudinal tensile reinforcement ( $A_s = 314.2$  mm<sup>2</sup> and  $f_y = 525$  MPa) for each beam. According to the proposed detailing approach, eight of eight, six of eight, six of eight, and four of eight tensile reinforcing bars were arranged and distributed within the effective support widths for the beams in Types (A), (B), (C) and (D), respectively. Six 8mm nominal diameter high-strength deformed steel bars were used for the longitudinal compressive (hanger) reinforcement ( $A_s = 50.3$  mm<sup>2</sup> and  $f_y = 510$  MPa) for each beam in order to prevent accidental failure of the beam during the handling operations. According to the proposed detailing approach, six of six, four of six, four of six, and four of six compressive reinforcing bars were arranged and distributed within the effective load widths for the beams in Types (A), (B), (C) and (D), respectively. It should be noted that these beams were designed for singly reinforcement only as required. The stirrups were fabricated from 8mm nominal diameter high-strength deformed steel bars ( $A_s = 50.3$  mm<sup>2</sup> and  $f_y = 510$  MPa) for each beam. The inner stirrup legs were arranged and designed within the effective support width in accordance with the proposed detailing approach and design model. Typical details of the test beams in Series (2) are shown in Figure 9.2.

## **9.5 Manufacture of Test Specimens**

### **9.5.1 Steel Cages**

The reinforcing steel bars were supplied as Take-Loose rebars, instead of the Prefab steel cages, from a local steel production company (BRC Steel Co Ltd, Block 14, Newhouse Industrial Estate, Lanarkshire, Glasgow-UK). All steel cages of beam specimens were made in the Concrete/Structures Laboratory at the University of Strathclyde.

To produce the steel cages of wide beam specimens, the main reinforcement bars were put straight through two Workbenches (Trestles); then the positions of the stirrups were marked out in the main bars according to the stirrups spacing along the beam length (SL) and across the beam width (S<sub>w</sub>). After that, the stirrups were tied to the main bars at each position. Also, the compression (hanger) reinforcement bars were put straight at the inside corners of the top face of the stirrups (in the compression concrete region), to prevent any movement during concrete pouring and compaction and also to assist in the assembly of the reinforcement cage and not to contribute to the flexural capacity of the beams (because these beams were designed for single reinforcement, as required). The steel bars were cleaned to remove any traces of oil, paint, or loose scale, i.e. surface rust, in order not to weaken the bond with the concrete.

The concrete covers were made using plastic spacers and were fixed on either the main bars or on the stirrups to ensure that the required cover distances were maintained and to avoid any movement of the reinforcement cages during compaction of the concrete, where 25mm thick spacers were attached to the stirrups (8mm diameter) and 33mm thick spacers were attached to the main bars (20mm diameter) for all test beam specimens. The steel cages and spacers were well fixed prior to the concrete pouring and compaction. In addition, two lifting points were placed in the ends of beams (one hanger at each end) for lifting purpose. Typical steel cages of test beam specimens investigated in this study are shown in Figure 9.4.



**Figure 9.4:** Typical Steel Cages for the Beams in Test-Series "2".

### 9.5.2 Shutters

Structural steel channel sections were used in the manufacture of the shutters. The shutters were cleaned and coated with oil to prevent the concrete from adhering to the shutters during the concrete casting and curing; also, the steel cages were placed in the shutters and the plastic spacers were used to maintain the required cover distance.

For all beam specimens, the shutters had inside dimensions of 600\*300mm with overall length of 2440 mm. The steel shutters were manufactured and supplied by a local steel formwork (moulds) company (WM Services (Scotland) Ltd, Unit 2E, Greenhill Industrial Estate, Coatbridge, Glasgow-UK). The shutters were fixed firmly during the concrete pouring and compaction (or vibration) to prevent the shutters from moving. Typical steel shutters used for the casting purposes are shown in Figure 9.5.

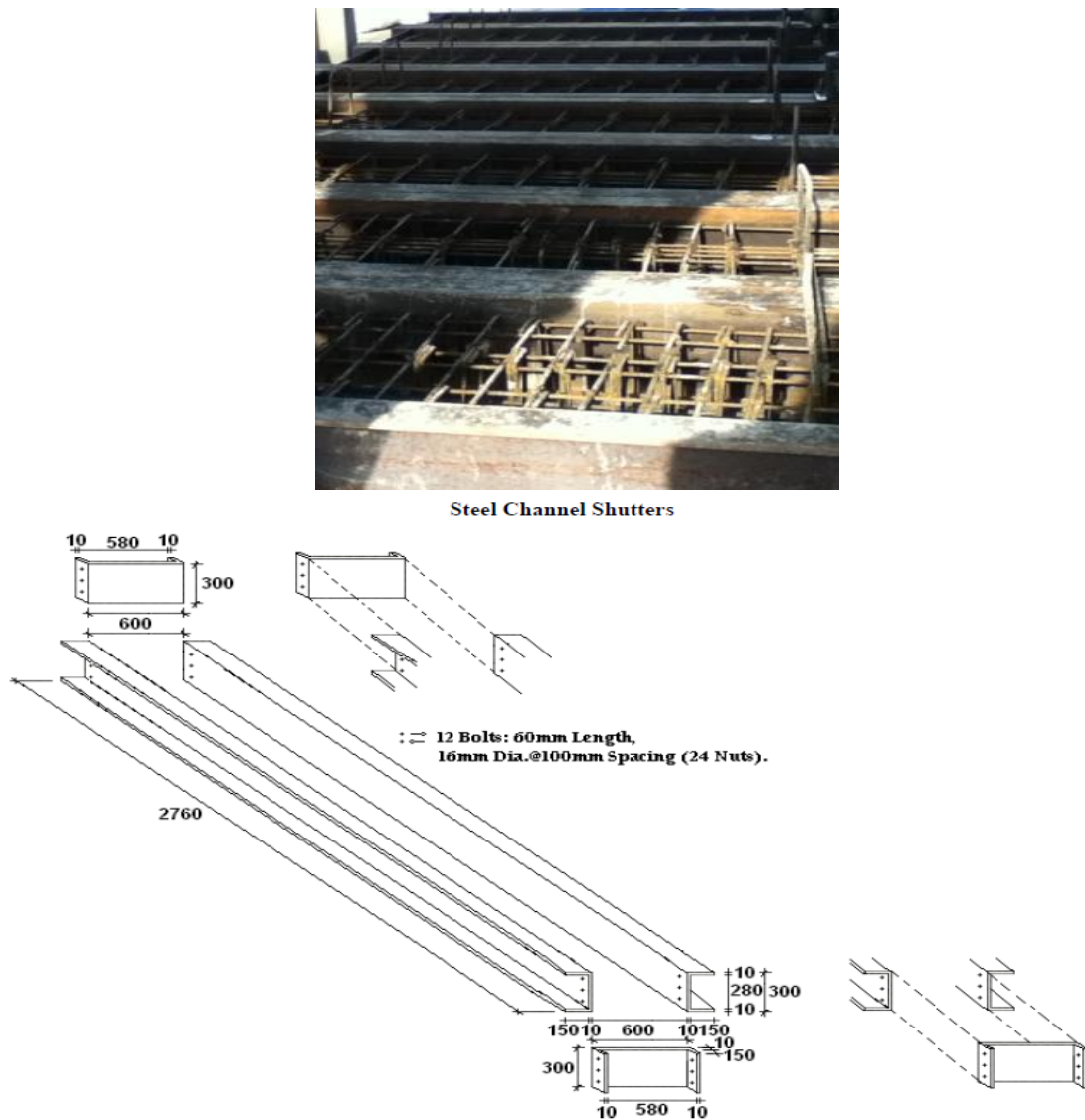


**Figure 9.5:** Typical Steel Shutters used for the Beam Specimens in Test-Series "2".

### 9.5.3 Casting

All beam specimens with their own control samples (cubes and cylinders) were made simultaneously with concrete from the same mixture at the same time to ensure the concrete's consistency. A total of eight beam specimens, six cubes and six cylinders were cast in steel shutters and moulds in the Concrete/Structures Laboratory at the University of Strathclyde. The

volume of each beam, cube and cylinder was known, and then the total required volume of concrete was calculated. The concrete mixture was supplied from a local ready mixed concrete company (Robeslee Concrete Co Ltd, Southbank Rd, Kirkintilloch, Lanarkshire, Glasgow-UK). One lorry was brought to cast the beams and control specimens. All beams and control specimens were cast from the same mixture. The concrete workability depends on the water/cement (w/c) ratio to control the strength and consistency (slump) of the concrete; therefore, the w/c ratio was taken 0.42 to give a workability of 60-70mm slump for all specimens (Table 9.5).

The casting process was initiated from the tension zone of the beam at the bottom surface of the shutter through two layers, and it was stopped at the outside face of the compression zone of the beam at the top surface of the shutter. This was to ensure that any bleeding of the concrete did not occur in the concrete compression region (Ziara, 1993). Also during the concrete casting of each layer, the beam specimens were compacted using a poker vibrator and vibrated using a vibrator and rods to ensure quality, a strong consistent concrete mix, to increase concrete strength, and to reduce the air voids. The vibration was terminated when air bubbles stopped appearing at the top surface of the concrete (Ziara, 1993). The control specimens were compacted using a standard electrically operated vibrating table for a period of approximately 90 seconds. Figure 9.6 shows typical beams together with own set of control cube and cylinder samples after finishing the concrete casting and after the polishing.



**Figure 9.6:** Typical Beams for Series "2" together with own Control Samples after Concrete Casting.

#### **9.5.4 Curing**

After the concrete casting of all test specimens and control samples, they were stored in their moulds under ambient conditions inside the laboratory. To ensure that beams, cubes and cylinders were treated, damp sheets of hessian were placed over the beams and the control samples. In the following days after casting, beam specimens and control samples were treated by spraying water over all surfaces of beams, control samples and hessian. All beams and control specimens were cured, inside their moulds, under moist burlap and plastic for 5 days.

### 9.5.5 Preparing the Test Specimens for Testing

All beams and control specimens were removed from the moulds after about 10 days. Test beam specimens were whitewashed to enable the early identification of cracks development under loading. At this stage, test beam specimens and control samples were already prepared for the laboratory test programme. Figure 9.7 shows the curing process of typical beams after removing the shutters.

Specimens' age at the test was approximately between 33 and 42 days. The control specimens were made at the same time as the beams, were cured like the beams and were tested in crushing on the same day as the beams.

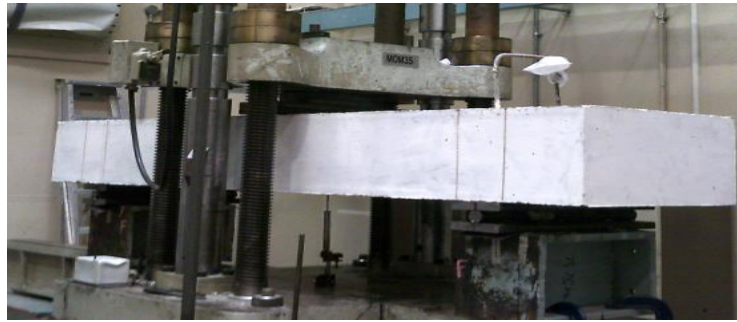


Figure 9.7: The Curing Process of Typical Beams in Series "2" after Removing the Shutters.

## 9.6 Testing Arrangements and Instrumentation

### 9.6.1 Testing Machine

Figure 9.8 shows the testing instrumentation and equipment that were used in the tests. All test beam specimens were loaded using a servo-controlled universal test machine (Figure 9.8a) which has a vertical load capacity of up to 890 kN (200,000 lb) with a resolution of 1 kN, where the applied force was controlled through manual operation of the hydraulic valve at the loading piston. The total load applied was displayed on a digital indicator on the control panel of the test machine. Each specimen was loaded in 50 kN (11,250 lb) load increments to failure. A Tonipact 3000 crushing machine (Figure 9.8b), which has a minimum vertical load capacity of 3000 kN with a resolution of 1 kN, was used to test the control samples (cubes and cylinders). The control specimens were tested in crushing on the same day as the beams. Continuous recordings of the applied load and deflections were provided throughout each test. The cracks were marked, photographed and measured with a microscope (Figure 9.8c). One electrically operated overhead crane was used to move the beams in the laboratory.



a) Beams Testing Machine



b) Control Specimens Testing Machine



c) Test Instrumentation

**Test Instrumentation:** from left, Deflection Dial Gauge, and Crack Width Microscope.

**Figure 9.8:** Testing Instrumentation and Equipment used in the Tests of Series "2".

**The details of testing arrangements are discussed below:**

### 9.6.2 Loading Arrangement

The test beams were loaded using a three-point loading arrangement. The load was concentrated from the hydraulic jack of testing machine to the loading plate of test beam specimens. According to the system of loading points for all test specimens, the beams were supported at three ends (for a three point-loading system) on an assembly consisting of roller or hinge bearing sandwiched between two steel plates. The length of the loading and support plates ( $C_p$  and  $C_s$ ), which was in contact with the beam parallel to its length, was 150mm in order to prevent bearing failures in the concrete. The thickness of the loading and support plates ( $t_p$  and  $t_s$ ) was 25mm. Moreover, according to the case of the load and support conditions, all loads and supports in Beam-Type (A) were applied with full-width plates (full-width load and support case) to the overall beam width ( $b_w$ ); while all loads and supports in Beam-Types (B, C and D) were applied with narrow-width plates (narrow-width load and support case) to the centreline of the overall beam width ( $b_w$ ). The width of the loading plate ( $b_p$ ), which was parallel to the beam width, was either equal to the support width ( $= b_s$ ) for Beam-Type (B), or half the support width ( $= 0.50*b_s$ ) for Beam-Type (C), or twice the support width ( $= 2*b_s$ ) for Beam-Type (D). The load-width to beam-width ( $k_p = b_p/b_w$ ) ratio was 1.0 for Beam-Type (A), 0.50 for Beam-Type (B), 0.25 for Beam-Type (C) and 0.50 for Beam-Type (D). While the support-width to beam-width ( $k_s =$

$b_s/b_w$ ) ratio was 1.0 for Beam-Type (A), 0.50 for Beam-Type (B), 0.50 for Beam-Type (B) and 0.25 for Beam-Type (C). The loading arrangements and testing machine used to test the beams are shown in Figures 9.1 and Figure 9.8a, respectively.

### **9.6.3 Loading Procedures and Steps**

All beams were tested under loading control at a rate of 10 kN/minute. The data generated during each test (i.e. total applied loads, deflections, crack widths, etc.) were recorded after each 50 kN increments of loading. The loading steps for all test specimens were similar. The loading step started from zero and then increased incrementally of 50 kN until the collapse (failure) load of the beam reached.

The test sequences were continued until the beams failed. The time required to record a complete set of readings at each load stage varied between 10 to 15 minutes. The overall testing time of a beam varied from 3 to 4 hours.

### **9.6.4 Instrumentation Arrangements**

Instrumentation for each specimen was designed to capture the load-deflection response and crack development. Vertical displacement measurements at the mid-span of the beam length were recorded from a Linear Variable Displacement Transformer (a LVDT). The deflection dial gauge was placed on each test beam specimen prior to testing at the intersection of the mid-span of the beam-span with the mid-point of the beam-width, corresponding to the center of loading plate. A crack width microscope was used to measure crack widths. Figure 9.1 shows a typical arrangement for the mid-span deflection dial gauge.

### **9.6.5 Marking of Cracks**

The surfaces of all beam specimens were marked with different coloured Chalks to follow the development of the cracks. The crack width microscope was used for all test specimens to measure the crack widths during the test at each increment of the loading.

## **9.7 Test Programme and Procedure**

The procedure of the experimental test programme used for testing the specimens is summarized as follows (Alluqmani, 2010):

Step.1: All beams were painted white to show of cracks.

Before testing, the sides of all beams were painted white, which has the benefit to show the cracks during the testing of the beams.

Step.2: Assembling of test arrangement.

The top surface of each beam, loading and support plates were coated with a layer of plaster to ensure the load is applied to a smooth level surface.

Step.3: Position the beam in the test arrangement and position loading and support plates at appropriate points.

Step.4: Concentration the center of hydraulic jack of testing machine on top of the center of loading plate. Some rubber sheets were placed at points between the beam and support plates, as well at loading points, to ensure load is applied on a level surface.

Step.5: First beam was tested; and some control samples were also tested.

Step.6: The remaining beams and control samples were also tested.

Before starting the test, all necessary Personal Protective Equipments (PPE), e.g. Overalls, safety Shoes, Gloves, Glasses and etc, were made available in the laboratory (Alluqmani, 2010). Figure 9.8 shows the instrumentation and testing equipments used in the tests.

The experimental work activities for manufacturing the steel cages, casting the concrete, and testing the specimens are included in Appendix B.

## **9.8 Measurements**

### **9.8.1 Total Applied Load**

The total load (P) applied to each test specimen was continuously displayed on the control unit of the test machine. The accuracy of the load readings was checked and found to be correct using a load cell which had been calibrated using a reference test machine.

### **9.8.2 Deflection**

A Linear Variable Differential Transducer (LVDT) was used to measure the deflections under the center point of loading plate (the intersection of mid-span with mid-width of each beam). The deflection dial gauge had a resolution of 0.01mm.



### 9.8.3 Cracking

After each load increment, the beams were inspected for cracks. A crack width microscope was used to measure the crack widths with a resolution of 0.1mm.

The cracks were marked on each face of the test beam specimens with the corresponding applied load level at each load level. The crack patterns were photographed and hard copy sketches were also made.

### 9.8.4 Beam Testing Results

At each load stage, the following recordings were made:

1. The total applied load (P) in kN.
2. The deflection dial gauge readings which were shown in millimetres on the display panel on the control unit of the test machine.
3. The flexural and the shear (diagonal) crack widths in millimetres.
4. Comments on the physical state of each beam.

On completion of each increment of loading, the beams were inspected for cracks which were then measured using a crack micrometer. Cracks were marked on the beam surfaces. The magnitudes of the applied loads, deflections, and crack widths were also recorded at each stage. On the completion of each test, the beam was photographed to record the final deflected shape and the crack pattern developments.

All test results were finally recorded. The control samples (cubes and cylinders) were also tested, and the concrete compressive strengths were recorded at the time of the corresponding beam test.

### 9.9 Material Test-Results and Prediction of Beam-Results

1. For the proposed design model, both longitudinal and transversal stirrup-legs spacing ( $S_L$  and  $S_w$ ) were determined based on the ratios of the support- and load- width to the beam-width ( $k_s$  and  $k_p$ ), Table 9.3.

2. For the proposed detailing approach, all beams were detailed to follow the detailing approach in regards to arrange the flexural (tensile and compression) and shear reinforcements. Both effective-widths of supports and loads ( $w_s$  and  $w_p$ ) were determined based on the support and

load widths ( $b_s$  and  $b_p$ ), Table 9.3. Furthermore, both concentrating flexural -tensile and -compressive reinforcing bars distributed within the effective-width of supports and loads ( $N_{ws}$  and  $N_{wp}$ ), respectively, were determined based on the ratios of the support- and load- width to the beam-width ( $k_s$  and  $k_p$ ), Table 9.3.

3. For the proposed prediction model, it is assumed that the ultimate flexural strength and the shear strength provided by concrete depend on the  $K_{cd}$  factor which in turn is related to the width of bearing plates and the percentage of flexural (tensile and compression) reinforcement; while the shear strength provided by stirrups depends on the  $K_{sd}$  factor which in turn is related to the width of bearing plates and the longitudinal and transversal spacing of the stirrup-legs. Based on the results of material strengths obtained by tests as shown in Tables 9.6 and 9.7, the both ultimate flexural and shear capacities ( $M_{u,d}$  and  $V_{u,d}$ ) of all specimens were predicted by the proposed prediction-model (Table 9.8). The proposed prediction model gave a reasonably prediction for the shear and flexural strengths as well for the proposed failure modes.

**Table 9.6:** Actual Concrete Strengths for Test-Series "2".

Control Sample	Surface Area, mm <sup>2</sup>	Weight, gm	Load, lb	Load, kN	Strength, $f_c$ , N/mm <sup>2</sup>
<b>Actual Concrete Cube Compressive Strengths at 33 to 42 days, <math>f_{cu}</math></b>					
1	10000	-	123180	547.50	54.75
2	10000	-	127100	565.0	56.50
<b>Average</b>	-	-	-	-	<b>55.60</b>
<b>Actual Concrete Cylinder Compressive Strengths at 33 to 42 days, <math>f_c</math></b>					
1	7855	-	78325	348.0	44.30
2	7855	-	79075	351.50	44.75
<b>Average</b>	-	-	-	-	<b>44.50</b>
<b>Actual Concrete Cylinder Split Strengths, <math>f_{ct}</math>, <math>L = 300</math>mm</b>					
1	99*202	-	<b>25150</b>	111.8	3.56
2	101*201	-	<b>23825</b>	105.9	3.32
<b>Average</b>	- -	-	-	-	<b>3.44</b>

**Test-Series (2): Date of Casting:** 13 May 2013.

**Date of Testing:** 17 June 2013 to 04 July 2013.

$f_{ct} = 2P/(3.142*d*L) = 0.637*P/(d*L)$ . D is the cylinder diameter and L is the cylinder height.

The concrete compressive strengths obtained from the control cubes and cylinders are shown in Table 9.6. The actual average cube and cylinder concrete compressive strengths were  $f_{cu,act} = 55.60$  MPa and  $f_{cy,act} = 44.50$  MPa, respectively. The actual material strengths used to predict and analyze the test specimens for the compressive strength of concrete ( $f_c$ ), the yield tensile strength of the longitudinal reinforcing bars ( $f_y$ ), and the yield tensile strength of the stirrups ( $f_{yv}$ ) were determined and the results are given in Table 9.7. The value of  $f_c$  used for the analysis, reported in Table 9.7, represents the average strength of cylinders tested on the same day as the

specimen, after having been cured under similar laboratory conditions. Table 9.8 shows the prediction of flexural and shear failure loads according to the proposed prediction model for the beams in Test-Series (2) based on the actual strengths of materials. It should be emphasised that no partial safety factors were included in the structural calculations for prediction the failure load.

**Table 9.7:** Material Properties used to Predict and Analyze the Tested Beams in Series "2".

	Properties	Series (1)
<b>Concrete</b>	Cylinder Compressive Strength ( $f_c$ ), MPa	<u>44.50</u>
	Cube Compressive Strength ( $f_{cu}$ ), MPa	55.60
	Cylinder Split Tensile Strength ( $f_t$ ), MPa	3.44
	Young's Modulus ( $E_c$ ), MPa	31500
<b>Flexural Reinforcement</b>	Yield Strength for $\Phi 20$ mm ( $f_y$ ), MPa	525
	Yield Strength for $\Phi 8$ mm ( $f_y$ ), MPa	510
	Young's Modulus ( $E_s$ ), MPa	200000
<b>Shear Reinforcement</b>	Yield Strength for $\Phi 8$ mm ( $f_{yv}$ ), MPa	510
	Young's Modulus ( $E_s$ ), MPa	200000

**Table 9.8:** Prediction of Flexural and Shear Failure Loads for Beams in Test-Series "2".

Series/Beams	Code Prediction, kN				Proposed-Model Prediction, kN												$P_{f,pred}$	
	$V_c$	$V_s$	$V_u$	$M_u$	$M_u$	$\mu_s$	$\beta_g$	$K_{cd}$	$V_{c,d}$	$\mu_v$	$\beta_k$	$K_{sd}$	$V_{s,d}$	$V_{u,d}$	$M_{u,d}$	$V_{d'}$	$P_{V,d}$	$P_{M,d}$
Beam A2-0	196	-	196	262	264	1.43	1.00	1.43	280	-	-	-	-	280	378	280	560	822
Beam A2-1	196	143	339	262	264	1.43	1.00	1.43	280	0.97	1.00	0.97	139	419	378	419	838	822
Beam B2-0	196	-	196	262	264	1.72	0.84	1.44	282	-	-	-	-	282	380	200	564	826
Beam B2-1	196	187	383	262	264	1.72	0.84	1.44	282	1.06	0.84	0.89	166	448	380	317	896	826
Beam C2-0	196	-	196	262	264	1.72	0.71	1.22	239	-	-	-	-	239	322	120	478	700
Beam C2-1	196	187	383	262	264	1.72	0.71	1.22	239	1.14	0.84	0.96	180	419	322	247	838	700
Beam D2-0	196	-	196	262	264	1.72	0.71	1.22	239	-	-	-	-	239	322	120	478	700
Beam D2-1	196	264	460	262	264	1.72	0.71	1.22	239	1.05	0.59	0.62	164	403	322	202	806	700

NOTE: For all beams:  $b_w = 600$ mm,  $h = 300$ mm,  $d = 257$ mm,  $\rho_s = 1.63\%$  ( $8\Phi 20$ mm),  $\rho_s' = 0.196\%$  ( $6\Phi 8$ mm),  $A_v = 201$ mm<sup>2</sup> (4-Legs $\Phi 8$ mm),  $a = 920$ mm,  $Z_{code} = 198.3$ mm (EC2),  $j_d = Z_{code} = 206.9$ mm (ACI318-and-SBC304),  $\epsilon_c = 0.0035$  (EC2),  $\epsilon_c = 0.003$  (ACI318-and-SBC304),  $E_c = 31500$  MPa,  $E_s = 200000$  MPa.

$P_d = 470$  kN,  $V = 235$  kN, and  $M = 216$  kN.m.  $A_v = 201$ mm<sup>2</sup> (4-Legs $\Phi 8$ mm).

$f_{y,d} = 525$  MPa,  $f_{yv,d} = 510$  MPa,  $f_{c,y,d} = 44.50$  MPa (for Beams in Series (2)).

$k_p$ ,  $k_s$ ,  $S_L$  and  $S_w$  values are taken from Table 9.3 for the beams in Test-Series (2).

$P = 470$  kN,  $V = 235$  kN,  $M = 216$  kN.m,  $a = 920$ mm,  $A_{s,prov} = 2514$  mm<sup>2</sup>,  $f_{y,act} = 525$  MPa,  $f_{c,act} = 44.50$  MPa.

$M_{u,prop} = A_{s,prov} \cdot f_{y,act} \cdot j_d$ , where,  $j_d = (2/3) \cdot h = 200$ mm.

$M_{u,code}$  (from Steel) =  $A_{s,prov} \cdot f_{y,act} \cdot Z = 262$  kN.m. Where,  $Z = d - (s/2) = 198.3$  mm.

$s = 0.8x = 117.50$ mm,  $x = d \cdot [\epsilon_c / (\epsilon_c + \epsilon_s)] = 146.86$ mm, where,  $\epsilon_s = f_{y,act} / E_s = 0.002625$ ,  $\epsilon_c = 0.0035$ ,  $E_s = 200000$  MPa.

$M_{u,code}$  (from Concrete) =  $(f_{c,act} \cdot b_w \cdot d^2) \cdot k = 352.7$  kN.m. Where,  $k = -1.134 \cdot (Z/d)^2 + 1.134 \cdot (Z/d) = 0.20$  and  $Z = d - (s/2) = 198.3$  mm.

No factors of safety are used neither in calculation of  $Z$  nor in calculation of  $M_{u,prop}$  and  $M_{u,code}$ .

$P_{V,d}$  = Predicted shear failure load =  $2V_{u,d}$  and  $P_{M,d}$  = Predicted flexural failure load =  $2(M_{u,d}/a)$ .

$P_{f,pred}$  = the smallest of ( $P_V$  or  $P_M$ ) and the predicted failure mode is the failure mode corresponding to  $P_{f,pred}$ .

No factors of safety are used neither in this prediction  $V_c$  and  $V_s$  nor in calculation of  $P_{V,d}$  and  $P_{M,d}$ .

## 9.10 Test Results of Beams

In order to characterise the materials used in the beam manufacture, the compression strength of concrete is determined by cylindrical and cubic specimens. The actual reinforcement properties and strengths, the concrete strengths, and the actual beam dimensions were used to re-calculate the original design load, and to predict the failure load of each beam. Table 9.9 shows the re-calculation of the maximum design loads and the proposed predicted failure loads according to the actual results of material strengths, and also shows the experimental failure loads and capacities of the test specimens in Series (2).

The ultimate experimental flexural strength ( $M_{u,exp.}$ ) of a test beam is half its flexural failure load times its shear-span length ( $= (P_{fM,exp.}/2)*a$ ), and the ultimate experimental shear strength ( $V_{u,exp.}$ ) of a test beam is half its shear failure load ( $= P_{fV,exp.}/2$ ); this is because the beams were tested under a three loading-point system at the mid-span of the beams, where  $a$  = shear span = 920mm.

Table 9.10 shows validation of the proposed prediction model on the test results obtained from Test-Series (2), and also shows a comparison of the beam capacities predicted by the proposed prediction model with those values either obtained from the tests or predicted by the existing Codes and models, such as EC2, ACI318, SBC304, Lubell et al model (2008), Sernar-Ros et al model (2002) and Shuraim model (2012). The accuracy of the proposed prediction model to predict the capacity, failure load and failure mode of wide RC beams appears in Table 9.10. The deficiency of the current design models and Codes to predict the capacity of wide RC beams is clear. Table 9.11 summarises the crack width measurements at different load levels for the beams in Test-Series (2).

Figure 9.9 shows critical failure modes and crack patterns for the beams in Test-Series (2). Figures 9.10a to 9.10d show the failure mode and crack patterns after failure for the beams in Types (A), (B), (C) and (D), respectively. The total applied load versus mid-span deflection curves obtained from the beams are shown in Figures 9.11 to 9.14.

Tables 9.12 to 9.15 show the total applied load versus mid-span deflection for the beams in Types (A), (B), (C) and (D), respectively. Tables 9.16 to 9.19 show the total applied load versus crack widths for the beams in Types (A), (B), (C) and (D), respectively.

**Table 9.9:** Re-calculation of the Maximum Design Load and Prediction of the Failure Load based on the Proposed Prediction Model.

Beam Type	Max. Original Design Load, kN	Max. Original Flexural Capacity, kN.m	Max. Re-Calculated (Actual) Flexural Capacity, kN.m	Max. Re-Calculated (Actual) Design Load, kN	Predicted Failure Load, kN (F. Mode)	Actual Exp. Failure Load, kN (F. Mode)	$P_{f,exp}/P_d$	Test Strength, kN, m		
	$P_d$	$M_d$	$M_u = M_{d,act.}$	$P_{d,act.}$	$P_{f,pred.}$	$P_{f,exp.}$		-	$V_{c,exp}$	$V_{s,exp}$
A2-0	470	216	262	570	560 (Shear)	569 (Shear)	1.21	284	-	-
A2-1	470	216	262	570	822 (Flexure)	835 (Flexure)	1.78	-	-	384
B2-0	470	216	262	570	564 (Shear)	565 (Shear)	1.20	282	-	-
B2-1	470	216	262	570	826 (Flexure)	830 (Flexure)	1.76	-	-	382
C2-0	470	216	262	570	478 (Shear)	491 (Shear)	1.04	245	-	-
C2-1	470	216	262	570	700 (Flexure)	740 (Flexure)	1.57	-	-	340
D2-0	470	216	262	570	478 (Shear)	483 (Shear)	1.03	241	-	-
D2-1	470	216	262	570	700 (Flexure)	725 (Flexure)	1.54	-	-	333

$P_d = 470$  kN,  $V = 235$  kN,  $M = 216$  kN.m,  $a = 920$ mm,  $A_{s,prov.} = 2514$  mm<sup>2</sup>,  $f_{y,act.} = 525$  MPa,  $f_{c,act.} = 44.50$  MPa.

$P_{d,act.} = \text{Actual design load} = 2(M_{d,act.}/a) =$ , and  $M_{d,act.} = M_{u,code} = M_{small} = 262$  kN.m (from Steel).

$M_{u,code}$  (from Steel) =  $A_{s,prov.} * f_{y,act.} * Z = 262$  kN.m. Where,  $Z = d - (s/2) = 198.3$  mm.

$s = 0.8x = 117.50$ mm,  $x = d * [\epsilon_c / (\epsilon_c + \epsilon_s)] = 146.86$ mm, where,  $\epsilon_s = f_{y,act.}/E_s = 0.002625$ ,  $\epsilon_c = 0.0035$ ,  $E_s = 200000$  MPa.

$M_{u,code}$  (from Concrete) =  $(f_{c,act.} * b_w * d^2) * k = 352.7$  kN.m. Where,  $k = -1.134 * (Z/d)^2 + 1.134 * (Z/d) = 0.20$  and  $Z = d - (s/2) = 198.3$  mm.

No factors of safety are used neither in calculation of  $Z$  nor in calculation of  $M_{u,prop.}$  and  $M_{u,code}$ .

**Table 9.10:** Validation of the Proposed Prediction Model on the Test Results obtained from Test Series "2".

Beam Type	Code Strength, kN, m			Code Pred. Strength, kN		Lubell Pred. Strength, kN		Serna-Ros Pred. Strength, kN		Shuraim Pred. Strength, kN		Prop. Strength (Model), kN		Test Strength, kN		$\Delta u$ , mm	$P_{V,exp}/P_{V,pred.}$	$P_{M,exp}/P_{M,pred.}$
	$V_c$	$V_s$	$M_u$	$P_{V,d}$	$P_{M,d}$	$P_V$	$P_M$	$P_V$	$P_M$	$P_V$	$P_M$	$P_{V,pred.}$	$P_{M,pred.}$	$P_{V,exp.}$	$P_{M,exp.}$			
<b>According to EC2</b>																		
A2-0	196	-	262	392	570	392	570	392	570	392	570	560	822	569	-	22.78	1.02	-
A2-1	196	143	262	678	570	678	570	821	570	710	570	838	822	-	835	10.01	-	1.02
B2-0	196	-	262	392	570	333	570	392	570	392	570	564	826	565	-	20.52	1.002	-
B2-1	196	187	262	766	570	651	570	993	570	806	570	896	826	-	830	8.02	-	1.005
C2-0	196	-	262	392	570	304	570	392	570	392	570	478	700	491	-	16.20	1.03	-
C2-1	196	187	262	766	570	594	570	1044	570	806	570	838	700	-	740	6.74	-	1.06
D2-0	196	-	262	392	570	304	570	392	570	392	570	478	700	483	-	16.28	1.01	-
D2-1	196	264	262	920	570	713	570	1286	570	978	570	806	700	-	725	22.78	-	1.04
<b>According to ACI318 and SBC304</b>																		
A2-0	175	-	273	350	593	350	593	350	593	350	593	501	822	569	-	22.78	1.13	-
A2-1	175	160	273	670	593	670	593	830	593	668	593	814	822	-	835	10.01	-	1.02
B2-0	175	-	273	350	593	298	593	350	593	350	593	504	826	565	-	20.52	1.12	-
B2-1	175	207	273	764	593	649	593	1016	593	764	593	872	826	-	830	8.02	-	1.005
C2-0	175	-	273	350	593	271	593	350	593	350	593	427	700	491	-	16.20	1.15	-
C2-1	175	207	273	764	593	592	593	1071	593	764	593	826	700	-	740	6.74	-	1.06
D2-0	175	-	273	350	593	271	593	350	593	350	593	427	700	483	-	16.28	1.13	-
D2-1	175	293	273	936	593	725	593	1342	593	936	593	792	700	-	725	22.78	-	1.04

**NOTE:** For all beams:  $b_w = 600$ mm,  $h = 300$ mm,  $d = 257$ mm,  $\rho_s = 1.63\%$  ( $8\Phi 20$ mm),  $\rho_s' = 0.196\%$  ( $6\Phi 8$ mm),  $A_v = 201$ mm<sup>2</sup> ( $4\text{-Legs}\Phi 8$ mm),  $a = 920$ mm,  $Z_{code} = 198.3$ mm (EC2),  $j_d = Z_{code} = 206.9$ mm (ACI318-and-SBC304),  $\epsilon_c = 0.0035$  (EC2),  $\epsilon_c = 0.003$  (ACI318-and-SBC304),  $E_c = 31500$  MPa,  $E_s = 200000$  MPa.  
 $P_d = 470$  kN,  $V = 235$  kN, and  $M = 216$  kN.m.  $A_v = 201$ mm<sup>2</sup> ( $4\text{-Legs}\Phi 8$ mm).  
 $f_{y,d} = 525$  MPa,  $f_{y,v,d} = 510$  MPa,  $f_{c,y,d} = 44.50$  MPa (for Beams in Series (2)).  
 $k_p$ ,  $k_s$ ,  $SL$  and  $Sw$  values are taken from Table 9.3 for the beams in Test-Series (2).

$P_d = 470 \text{ kN}$ ,  $V = 235 \text{ kN}$ ,  $M = 216 \text{ kN.m}$ ,  $a = 920 \text{ mm}$ ,  $A_{s,prov.} = 2514 \text{ mm}^2$ ,  $f_{y,act.} = 525 \text{ MPa}$ ,  $f_{c,act.} = 44.50 \text{ MPa}$ .

$P_{d,act.} = \text{Actual design load} = 2(M_{d,act.}/a)$ , and  $M_{d,act.} = M_{u,code} = M_{small}$ .

**Proposed Prediction-Model:**

$M_{u,prop.} = A_{s,prov.} * f_{y,act.} * j * d = \underline{264 \text{ kN.m}}$  where,  $j * d = (2/3) * h = \underline{200 \text{ mm}}$ .

**EC2:**

$M_{u,code, Flexure} \text{ (from Steel)} = A_{s,prov.} * f_{y,act.} * Z = \underline{262 \text{ kN.m}}$  Where,  $Z = d - (s/2) = \underline{198.3 \text{ mm}}$ .

$s = 0.8x = 117.50 \text{ mm}$ ,  $x = d * [\epsilon_c / (\epsilon_c + \epsilon_s)] = 146.86 \text{ mm}$ , where,  $\epsilon_s = f_{y,act.} / E_s = 0.002625$ ,  $\epsilon_c = 0.0035$ ,  $E_s = 200000 \text{ MPa}$ .

$M_{u,code, Shear} \text{ (from Concrete)} = (f_{c,act.} * b_w * d^2) * K = \underline{352.7 \text{ kN.m}}$  Where,  $K = -1.134 * (Z/d)^2 + 1.134 * (Z/d) = 0.20$  and  $Z = d - (s/2) = \underline{198.3 \text{ mm}}$ .

$M_{u,code} \text{ (EC2)} = M_{small} = \underline{262 \text{ kN.m (from Steel)}}$ .

**ACI318-and-SBC304:**

$M_{u,code, Flexure} \text{ (from Steel)} = A_{s,prov.} * f_{y,act.} * j * d = \underline{273 \text{ kN.m}}$  Where,  $j * d = Z = d - (a/2) = \underline{206.9 \text{ mm}}$ .

$a = \beta_1 * c = 100.1 \text{ mm}$ ,  $c = d * [\epsilon_c / (\epsilon_c + \epsilon_s)] = 137.1 \text{ mm}$ ,  $\beta_1 = 0.85$  for  $f_c' \leq 28 \text{ N/mm}^2$ .  $\beta_1 = 0.85 - [0.05 * ((f_c' - 28) / 7)] \geq 0.65$  for  $f_c' > 28 \text{ N/mm}^2$  (Hence:  $\beta_1 = 0.73$ ), where,  $\epsilon_s = f_{y,act.} / E_s = 0.002625$ ,  $\epsilon_c = 0.003$ ,  $E_s = 200000 \text{ MPa}$ .

$M_{u,code, Shear} \text{ (from Concrete)} = (f_{c,act.} * b_w * d^2) * K = \underline{299.8 \text{ kN.m}}$  Where  $K = \omega * [1.0 - 0.59 * \omega] = 0.170$ , and  $\omega = \rho_{s,prov.} * (f_{y,act.} / f_{c,act.}) = 0.192$ , and  $j * d = Z = d - (a/2) = \underline{206.9 \text{ mm}}$ .

$M_{u,code} \text{ (ACI318-and-SBC304)} = M_{small} = \underline{273 \text{ kN.m (from Steel)}}$ .

No factors of safety are used neither in calculation of Z nor in calculation of  $M_{u,prop.}$  and  $M_{u,code}$ .

$P_{V,d} = \text{Predicted shear failure load} = 2V_{u,d}$  and  $P_{M,d} = \text{Predicted flexural failure load} = 2(M_{u,d}/a)$ .

$P_{f,pred.} = \text{the smallest of } (P_V \text{ or } P_M) \text{ and the predicted failure mode is the failure mode corresponding to } P_{f,pred.}$

No factors of safety are used neither in prediction of  $V_c$  and  $V_s$  nor in prediction of  $P_{V,pred.}$  and  $P_{M,pred.}$

**Table 9.11:** Summary of the Crack Widths at Different Load Levels for the Beams in Test-Series "2".

Beam Type	At 1 <sup>st</sup> Flexural Crack		At 1 <sup>st</sup> Shear Crack		Service (Working) Condition		Failure (Ultimate) Condition		
	Load, kN	Crack Width, mm	Load, kN	Crack Width, mm	Load, kN	Flex. Crack Width, mm	Load, kN	Flex. Crack Width, mm	Shear Crack Width, mm
A2-0	250	0.03	350	0.02	450	0.41	569	0.72	2.90
A2-1	200	0.02	450	0.04	650	0.42	835	2.0	1.20
B2-0	200	0.02	350	0.025	450	0.42	565	0.65	3.55
B2-1	150	0.04	450	0.06	650	0.43	830	2.20	1.34
C2-0	150	0.02	300	0.03	400	0.40	491	0.64	5.14
C2-1	200	0.04	450	0.05	600	0.41	740	3.22	1.28
D2-0	250	0.04	350	0.24	400	0.41	483	0.68	6.60
D2-1	200	0.05	450	0.06	600	0.40	725	3.64	1.46

\* Service (working) load is the total applied load when the maximum flexural crack width reaches to the limit per the applied Code of Practice, which is 0.40mm for EC2, ACI318 and SBC304.

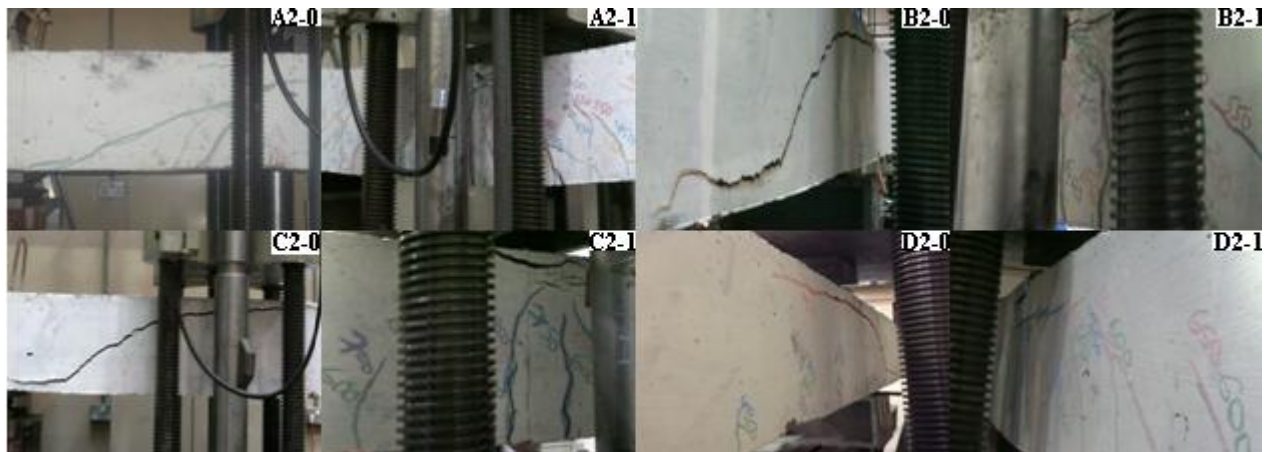
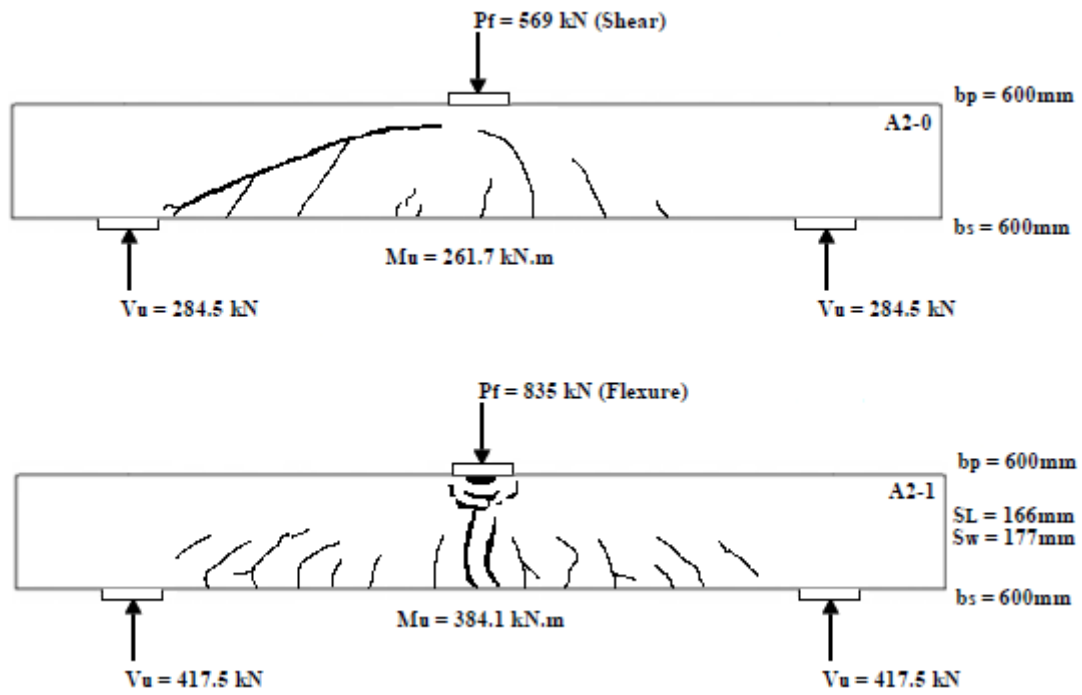
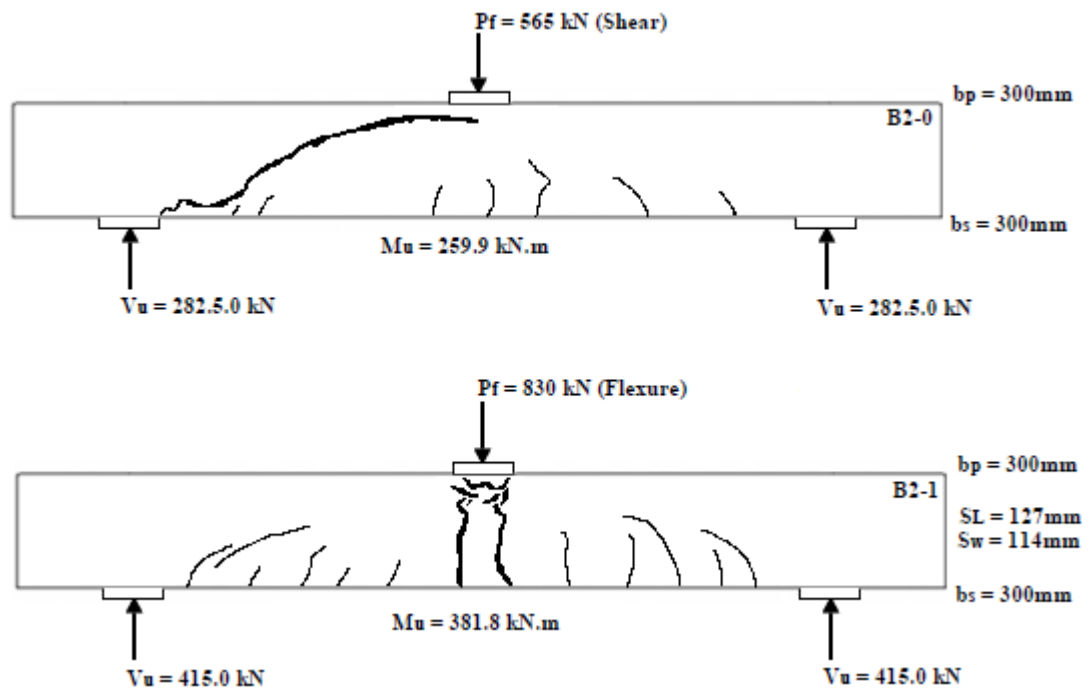


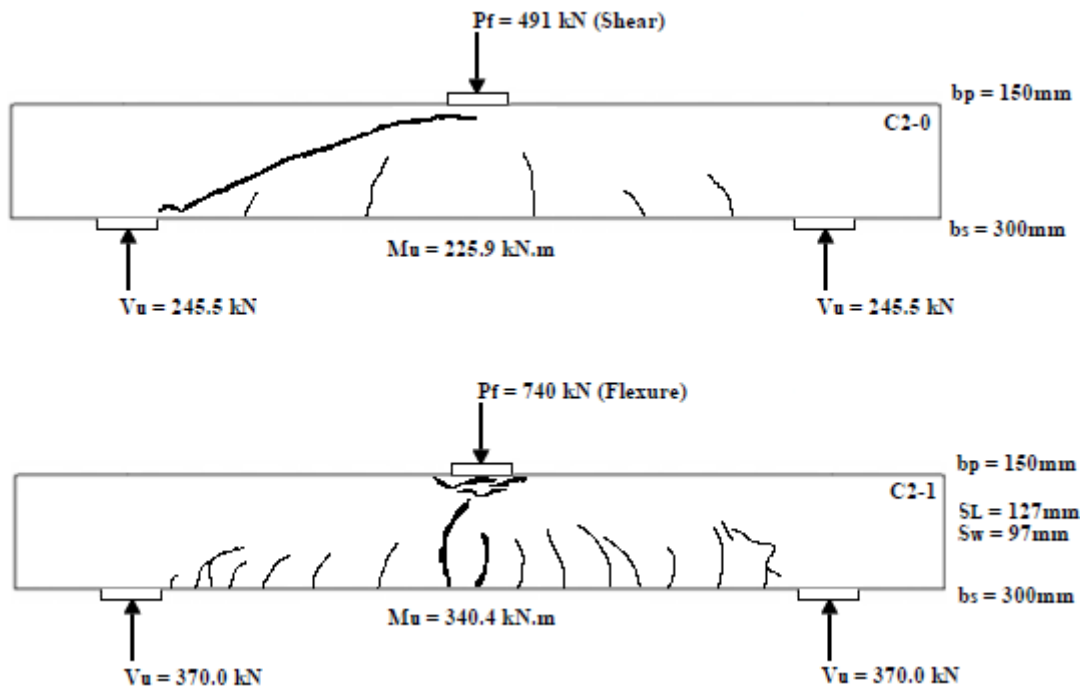
**Figure 9.9:** Critical Failure Modes and Crack Patterns for the Beams in Test-Series "2".



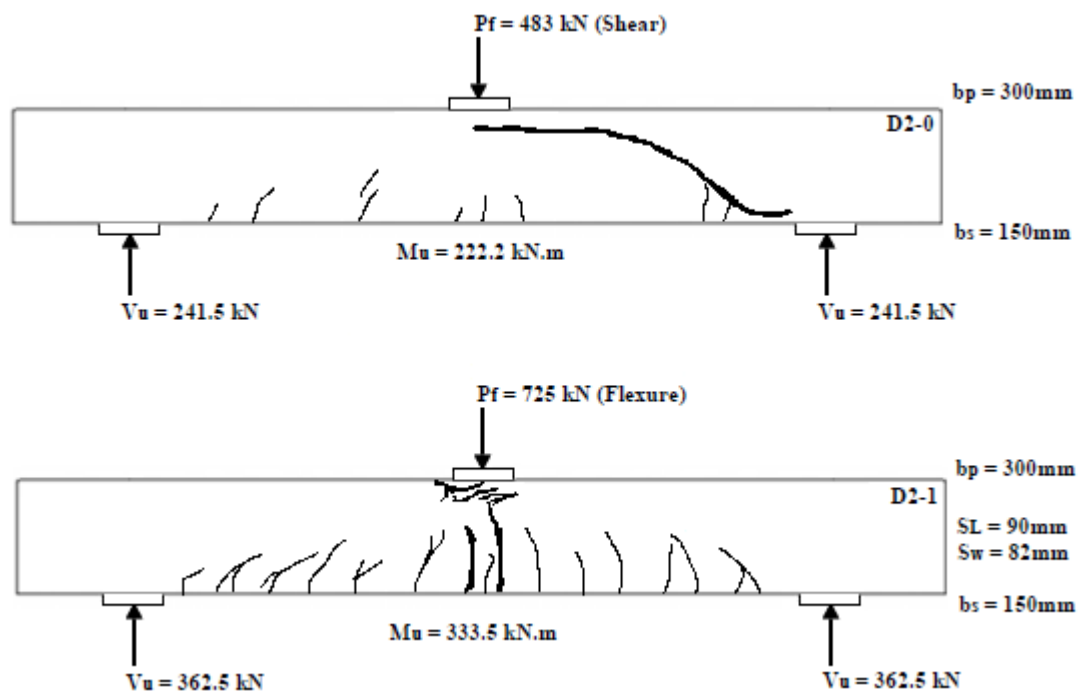
a) Beams A2-0 and A2-1 (Type A)



b) Beams B2-0 and B2-1 (Type B)



c) Beams C2-0 and C2-1 (Type C)



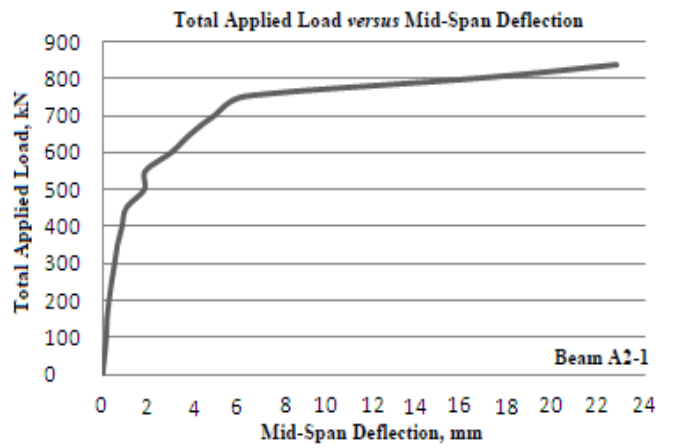
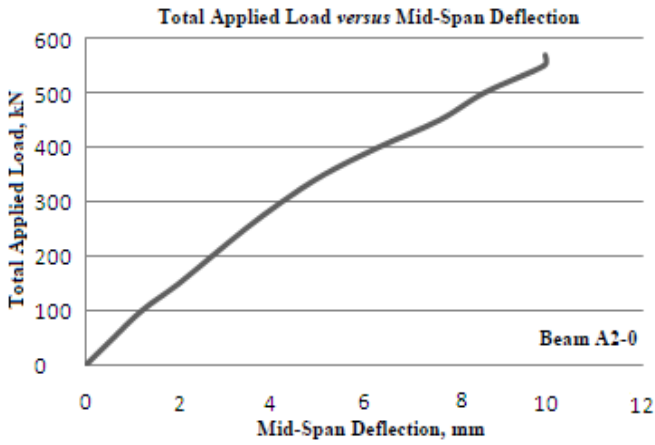
d) Beams D2-0 and D2-1 (Type D)

All beams had 4 stirrup-legs across their widths

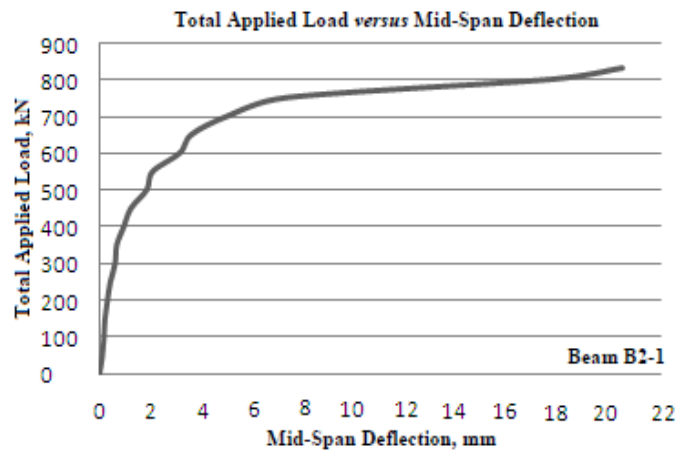
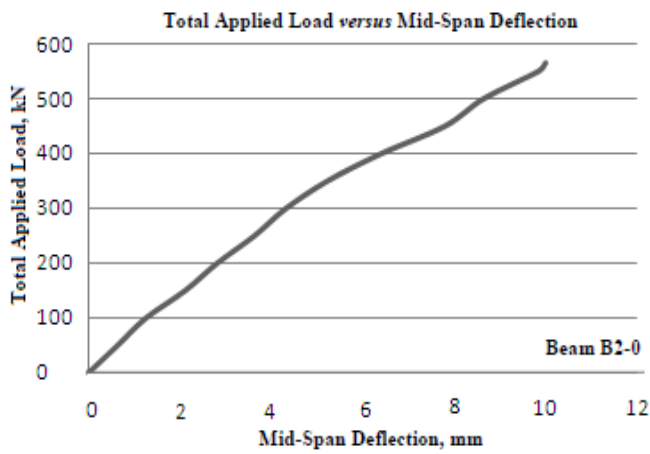
NOTE: these Figures are enlarged to show Crack Patterns

Figure 9.10: Failure Modes and Crack Patterns after Failure for the Beams in Series "2".





**Figure 9.11:** Total Applied Load versus Mid-Span Deflection for the Beams in Type (A) in Series "2".



**Figure 9.12:** Total Applied Load versus Mid-Span Deflection for the Beams in Type (B) in Series "2".

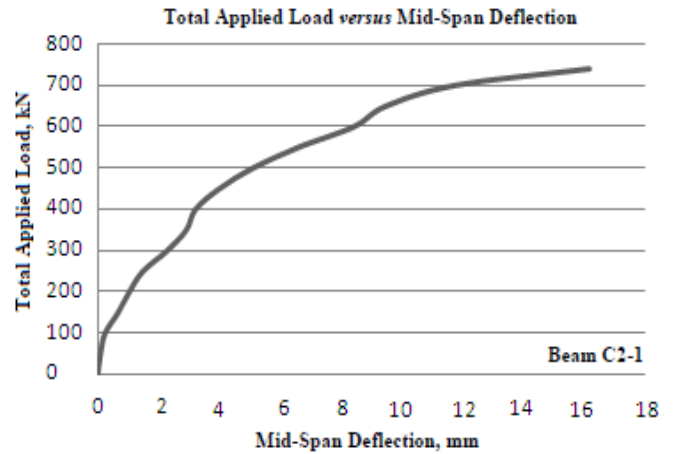
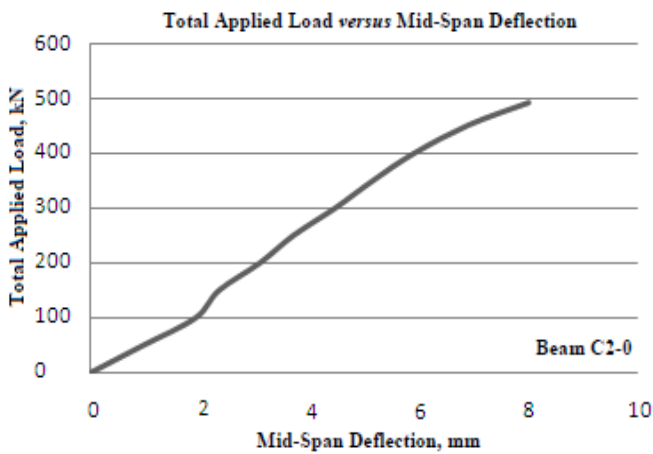


**Figure 9.13:** Total Applied Load versus Mid-Span Deflection for the Beams in Type (C) in Series "2".

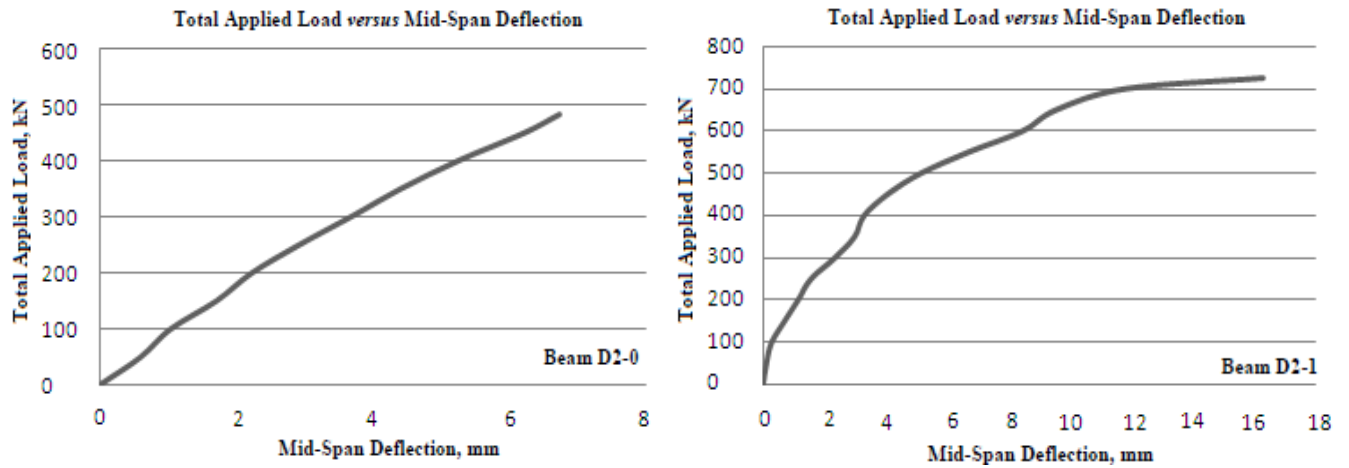


Figure 9.14: Total Applied Load versus Mid-Span Deflection for the Beams in Type (C) in Series "2".

Table 9.12: Total Applied Load versus Mid-Span Deflections for Beams-Type (A) in Test-Series (2).

Total Applied Load, kN	Beam (A2-0)		Beam (A2-1)	
	Centre Dial Reading, mm	Centre Dial Increment, $\Delta$ , mm	Centre Dial Reading, mm	Centre Dial Increment, $\Delta$ , mm
0	14.098	0	29.81	0
50	14.70	0.60	29.89	0.08
100	15.31	1.21	29.97	0.16
150	16.11	2.01	30.00	0.19
200	16.82	2.72	30.09	0.28
250	17.54	3.44	30.20	0.39
300	18.33	4.23	30.34	0.53
350	19.24	5.14	30.46	0.65
400	20.41	6.31	30.67	0.86
450	21.73	7.63	30.85	1.04
500	22.69	8.59	31.66	1.85
550	23.98	9.88	31.71	1.90
600	$P_{f,exp.} = 569 \text{ kN}, \Delta = 9.90$		32.87	3.06
650	Failure Mode = Shear		33.73	3.92
700			34.79	4.98
750			36.12	6.31
800			46.70	16.89
			$P_{f,exp.} = 835 \text{ kN}, \Delta = 22.78$	
			Failure Mode = Flexure	

Locations of Deflection Dial Gauges refer to Figure 9.1.

**Table 9.13:** Total Applied Load versus Mid-Span Deflections for **Beams-Type (B)** in Test-Series (2).

Total Applied Load, kN	Beam (B2-0)		Beam (B2-1)	
	Centre Dial Reading, mm	Centre Dial Increment, $\Delta$ , mm	Centre Dial Reading, mm	Centre Dial Increment, $\Delta$ , mm
0	14.10	0	29.78	0
50	14.74	0.64	29.90	0.12
100	15.36	1.26	29.96	0.18
150	16.22	2.12	30.00	0.22
200	16.92	2.82	30.10	0.32
250	17.74	3.64	30.21	0.43
300	18.43	4.33	30.40	0.62
350	19.34	5.24	30.46	0.68
400	20.52	6.42	30.74	0.96
450	21.91	7.81	31.02	1.24
500	22.76	8.66	31.64	1.86
550	23.96	9.86	31.88	2.10
600	$P_{f,exp.} = 565 \text{ kN}, \Delta = 10.01$		32.94	3.16
650	Failure Mode = Shear		33.40	3.62
700			34.82	5.04
750			37.13	7.35
800			47.58	17.80
			$P_{f,exp.} = 830 \text{ kN}, \Delta = 20.52$	
			Failure Mode = Flexure	

Locations of Deflection Dial Gauges refer to Figure 9.1.

**Table 9.14:** Total Applied Load versus Mid-Span Deflections for **Beams-Type (C)** in Test-Series (2).

Total Applied Load, kN	Beam (C2-0)		Beam (C2-1)	
	Centre Dial Reading, mm	Centre Dial Increment, $\Delta$ , mm	Centre Dial Reading, mm	Centre Dial Increment, $\Delta$ , mm
0	29.60	0	29.019	0
50	30.57	0.97	29.11	0.09
100	31.53	1.93	29.26	0.24
150	31.96	2.36	29.69	0.67
200	32.71	3.11	30.06	1.04
250	33.32	3.72	30.51	1.49
300	34.09	4.49	31.31	2.29
350	34.78	5.18	31.94	2.92
400	35.54	5.94	32.24	3.22
450	36.51	6.91	33.03	4.01
500	$P_{f,exp.} = 491 \text{ kN}, \Delta = 8.02$		34.14	5.12
550	Failure Mode = Shear		35.63	6.61
600			37.46	8.44
650			38.52	9.50
700			40.80	11.78
			$P_{f,exp.} = 740 \text{ kN}, \Delta = 16.20$	
			Failure Mode = Flexure	

Locations of Deflection Dial Gauges refer to Figure 9.1.

**Table 9.15:** Total Applied Load versus Mid-Span Deflections for **Beams-Type (D)** in Test-Series (2).

Total Applied Load, kN	Beam (D2-0)		Beam (D2-1)	
	Centre Dial Reading, mm	Centre Dial Increment, $\Delta$ , mm	Centre Dial Reading, mm	Centre Dial Increment, $\Delta$ , mm
0	1.378	0	29.02	0
50	1.98	0.60	29.13	0.11
100	2.42	1.04	29.30	0.28
150	3.09	1.71	29.72	0.70
200	3.61	2.23	30.16	1.14
250	4.30	2.92	30.58	1.56
300	5.06	3.68	31.36	2.34
350	5.79	4.41	32.00	2.98
400	6.63	5.25	32.31	3.29
450	7.60	6.22	33.7	4.05
500	$P_{f,exp.} = 483 \text{ kN}, \Delta = 6.74$		34.16	5.14
550	Failure Mode = Shear		35.71	6.69
600			37.48	8.46
650			38.57	9.55
700			40.84	11.82
			$P_{f,exp.} = 725 \text{ kN}, \Delta = 16.28$	
			Failure Mode = Flexure	

Locations of Deflection Dial Gauges refer to Figure 9.1.

**Table 9.16:** Total Applied Load versus Crack Widths for **Beams-Type (A)** in Test-Series (2).

Load kN	Beam (A2-0) Crack Width, mm		Beam (A2-1) Crack Width, mm	
	Flexural	Shear	Flexural	Shear
0	-	-	-	-
50	-	-	-	-
100	-	-	-	-
150	-	-	-	-
200	-	-	0.02	-
250	0.03	-	0.08	-
300	0.14	-	0.09	-
350	0.22	0.02	0.14	-
400	0.36	0.16	0.19	-
450	0.41	0.33	0.20	0.04
500	0.50	0.60	0.27	0.12
550	0.58	1.84	0.30	0.32
600	$P_{f,exp.} = 569 \text{ kN}, \Delta = 9.90$		0.34	0.46
650	Failure Mode = Shear		0.42	0.64
700	0.72	2.90	0.86	0.72
750			1.24	0.88
800			1.82	1.0
			$P_{f,exp.} = 835 \text{ kN}, \Delta = 22.78$	
			Failure Mode = Flexure	
			2.0	1.20

**Table 9.17:** Total Applied Load versus Crack Widths for **Beams-Type (B)** in Test-Series (2).

Load kN	Beam (B2-0) Crack Width, mm		Beam (B2-1) Crack Width, mm	
	Flexural	Shear	Flexural	Shear
0	-	-	-	-
50	-	-	-	-
100	-	-	-	-
150	-	-	0.04	-
200	0.02	-	0.06	-
250	0.08	-	0.14	-
300	0.14	-	0.18	-
350	0.22	0.025	0.22	-
400	0.38	0.20	0.23	-
450	0.42	0.44	0.26	0.06
500	0.52	0.82	0.28	0.16
550	0.61	2.14	0.31	0.36
600	$P_{f,exp.} = 565 \text{ kN}, \Delta = 10.01$		0.34	0.52
650	Failure Mode = Shear		0.43	0.76
700	0.65	3.55	0.92	0.84
750			1.46	1.08
800			2.02	1.22
			$P_{f,exp.} = 830 \text{ kN}, \Delta = 20.52$	
			Failure Mode = Flexure	
			2.20	1.34

**Table 9.18:** Total Applied Load versus Crack Widths for **Beams-Type (C)** in Test-Series (2).

Load kN	Beam (C2-0) Crack Width, mm		Beam (C2-1) Crack Width, mm	
	Flexural	Shear	Flexural	Shear
0	-	-	-	-
50	-	-	-	-
100	-	-	-	-
150	0.02	-	-	-
200	0.04	-	0.04	-
250	0.07	-	0.10	-
300	0.17	0.03	0.13	-
350	0.28	0.22	0.19	-
400	0.40	0.70	0.21	-
450	0.54	2.44	0.25	0.05
500	$P_{f,exp.} = 491 \text{ kN}, \Delta = 8.02$		0.29	0.16
550	Failure Mode = Shear		0.35	0.36
600	0.64	5.14	0.41	0.50
650			1.18	0.71
700			2.08	0.94
			$P_{f,exp.} = 740 \text{ kN}, \Delta = 16.20$	
			Failure Mode = Flexure	
			3.22	1.28

**Table 9.19:** Total Applied Load versus Crack Widths for **Beams-Type (D) in Test-Series (2)**.

Load kN	Beam (D2-0) Crack Width, mm		Beam (D2-1) Crack Width, mm	
	Flexural	Shear	Flexural	Shear
0	-	-	-	-
50	-	-	-	-
100	-	-	-	-
150	-	-	-	-
200	-	-	0.05	-
250	0.04	-	0.12	-
300	0.20	-	0.14	-
350	0.31	0.24	0.20	-
400	0.41	0.76	0.24	-
450	0.58	2.72	0.28	0.06
500	$P_{f,exp.} = 483 \text{ kN}, \Delta = 6.74$		0.31	0.18
550	Failure Mode = Shear		0.36	0.38
600	0.68	6.60	0.40	0.52
650			1.24	0.74
700			2.52	1.02
			$P_{f,exp.} = 725 \text{ kN}, \Delta = 16.28$	
			Failure Mode = Flexure	
			3.64	1.46

### 9.11 Discussion of Test Results

All results, discussions, validations, verifications and conclusions on the behaviour of the wide RC beams tested in Test-Series (2) are described in the following Sections (Alluqmani, 2013a):

The 8 wide RC beams tested in Series (2) were used to validate the proposed detailing approach and design model, as well to verify the proposed prediction model on the flexural and shear strengths of wide RC beams. All beams were predicted by the proposed prediction model to fail either in shear for the beams without stirrups or in flexure for the beams with stirrups according to EC2 and to ACI318 and SBC304 (and were also predicted by the existing Codes and Models). The beams without stirrups had a proposed predicted shear capacity ( $V_{u,d}$ ) between 239 kN and 282 kN with a total proposed predicted shear failure load ( $P_{f,pred.} = P_{V,d} = 2*V_{u,d}$ ) between 478 kN and 564 kN to EC2 and between 427 kN and 504 kN to ACI318 and SBC304 (and between 271 kN and 392 kN to the existing Codes and models), Tables 9.8 and 9.10. The beams without stirrups had a proposed predicted flexural capacity ( $M_{u,d}$ ) between 322 kN.m and 380 kN.m with a total proposed predicted flexural failure load ( $P_{f,pred.} = P_{M,d} = (M_{u,d}/a)*2$ ) between 700 kN and 826 kN (and between 570 kN and 593 kN to the existing Codes and models), Tables 9.8 and 9.10. The beams without stirrups failed experimentally in shear at a total failure load ( $P_{f,exp.} =$

$P_{v,exp.} = 2*V_{u,exp.}$ ) between 483 kN and 569 kN as obtained from both the tests and the proposed prediction model of the one-way shear capacity (Equation (6.9)), Table 9.10. The beams with stirrups had a proposed predicted shear capacity ( $V_{u,d}$ ) between 403 kN and 448 kN with a total proposed predicted shear failure load ( $P_{f,pred.} = P_{v,d} = 2*V_{u,d}$ ) between 806 kN and 896 kN to EC2 and between 792 kN and 872 kN to ACI318 and SBC304 (and between 592 kN and 1342 kN to the existing Codes and models), Tables 9.8 and 9.10. The beams with stirrups had a proposed predicted flexural capacity ( $M_{u,d}$ ) between 322 kN.m and 380 kN.m with a total proposed predicted flexural failure load ( $P_{f,pred.} = P_{M,d} = (M_{u,d}/a)*2$ ) between 700 kN and 826 kN (and between 570 kN and 593 kN to the existing Codes and models), Tables 9.8 and 9.10. The beams with stirrups failed experimentally in flexure at a total failure load ( $P_{f,pred.} = P_{M,d} = (M_{u,d}/a)*2$ ) between 725 kN and 835 kN as obtained from both the tests and the proposed prediction model of the ultimate flexural capacity (Equation (6.13)), Table 9.10.

All wide beams without and with stirrups in Series (2) were detailed by the proposed detailing approach. The wide beams with shear-reinforcement were designed by the proposed design model, and had a shear-span to effective-depth ( $a/d$ ) ratio of 3.58 where  $a = 920\text{mm}$  and  $d = 257\text{mm}$ . As predicted by the proposed prediction model, the beams without shear-reinforcement failed in shear, while the beams with shear-reinforcement failed in flexure. All beams with stirrups in Beam-Group (1), i.e. beams A2-1, B2-1, C2-1 and D2-1, were designed with longitudinal and transverse stirrup-legs spacing in accordance with the proposed design model, and failed in flexure by flexural deformation and cracking. The longitudinal and transverse stirrup-legs spacing designed to the proposed design model were  $S_L = 0.65d = 166\text{mm}$  and  $S_w = 0.69d \approx 1.07*S_L = 177\text{mm}$  for Beam-Type A (beam A2-1),  $S_L = 0.50d = 127\text{mm}$  and  $S_w = 0.44d \approx 0.90*S_L = 114\text{mm}$  for Beam-Type B (beam B2-1),  $S_L = 0.50d = 127\text{mm}$  and  $S_w = 0.38d \approx 0.77*S_L = 97\text{mm}$  for Beam-Type C (beam C2-1), and  $S_L = 0.35d = 90\text{mm}$  and  $S_w = 0.32d \approx 0.92*S_L = 82\text{mm}$  for Beam-Type D (beam D2-1).

### 9.11.1 Failure Modes

For each Group of beams in Series (2), the failure mode was the same. All Types of beams without stirrups in Group 0 (Types A, B, C and D), which are beams A2-0, B2-0, C2-0 and D2-0, had the same failure mode where the beams failed in shear by diagonal cracking in the shear-span regions. All Types of beams with stirrups in Group 1 (Types A, B, C and D), which are beams A2-1, B2-1, C2-1 and D2-1, had the same failure mode where the beams failed in flexure by flexural deformation and cracking. In all beams, hair-line flexural cracks developed in the

lower part of the beams and extended vertically towards the neutral axis before the appearance of diagonal cracks. As loading continued, the flexural cracks proliferated and widened; and some diagonal cracks appeared in the both shear spans. In general, the beams with stirrups were behaving in flexure as loading was being increased.

### **9.11.2 Effect of $b_s$ and $b_p$ on the flexural and shear Strengths**

As a comparison between the four beams in Group (1) for Series (2), which are beams A2-1, B2-1, C2-1 and D2-1, with those the correspondingly relevant four beams in Group (1a) for Series (1), which are beams A1-1a, B1-1a, C1-1a and D1-1a, respectively, the differences between them were 1) the design of the longitudinal and transverse spacing of stirrup legs ( $S_L$  and  $S_w$ ), and 2) the detail of the longitudinal flexural -tensile and -compression reinforcing bars concentrated within the effective-widths of the support and load ( $N_{W_s}$  and  $N_{W_p}$ ), respectively.  $S_L$  and  $S_w$ , and  $N_{W_s}$  and  $N_{W_p}$  for the beams in Group (1) in Series (1) were designed and detailed according to the EC2 Code; while they were designed and detailed according to the proposed design model and detailing approach, respectively, for the beams in Group (1) in Series (2). All beams, whether in Series (1) or in Series (2), were the same for their geometry and design, except  $S_L$  and  $S_w$  for each Beam-Group (Groups 0, 1a, 1b and 2) and  $b_s$  and  $b_p$  (or at best,  $k_s$  and  $k_p$ ) for each Beam-Type (Types A, B, C and D). It can be seen that the width of loading and support plates ( $b_p$  and  $b_s$ ), or at best  $k_p$  and  $k_s$ , had influence on the both flexural and shear strengths of wide RC beams, where the flexural and shear capacities of wide RC beams decreased as the support width and/or the load width decreased, or at best, as  $k_s$  and  $k_p$  decreased. This happened for beams without and with shear-reinforcement. Accordingly, it can be concluded that the strengths of wide RC beams decrease as the load and/or support widths ( $b_p$  and/or  $b_s$ ) decrease, hence as  $k_p$  and/or  $k_s$  ratios decrease.

For each four beams in each Beam-Group, the beams with full-width bearing plates in Type (A) in regards to study the effect of  $b_s$  and  $b_p$ , or at best  $k_p$  and  $k_s$ , i.e beams A2-0 and A2-1, had the best results and strengths comparing with the other correspondingly relevant beams in the same group (i.e. beams B2-0, C2-0 and D2-0, and beams B2-1, C2-1 and D2-1). The proposed detailing approach and design model have succeeded to prevent the shear failure for those full- and narrow- width wide beams with shear-reinforcement in Group (1) for Series (2).

For all wide beams without shear-reinforcement detailed by the proposed detailing approach, loaded and supported via either full- or narrow- width bearing plates, all cracks stopped at the



edge of the support plate and did not reach to the compression zones. For the wide beams without shear-reinforcement loaded and supported via narrow- width bearing plates, the critical cracks passed the loading plate but did not reach to the compression zones. On the other hand, for all wide beams with shear-reinforcement detailed by the proposed detailing approach and designed by the proposed design model, loaded and supported via either full- or narrow- width bearing plates, all beams failed in flexure by flexural bending, deflection and critical flexural cracks; therefore, all cracks were in the flexural regions and reached to the compression zones but without spalling of concrete. For the wide beams with shear-reinforcement loaded and supported via narrow- width bearing plates (beams B2-1, C2-1 and D2-1), the beams failed in flexure at load levels are lower than that load of the wide beam with shear-reinforcement loaded and supported via full- width bearing plates (beam A2-1).

To study the effect of the load width ( $b_p$ ), or at best  $k_p$ , on the shear and flexural strengths of wide RC beams, the beams in Type (B) are compared with those correspondingly relevant beams in Type (C) for the same group. For the beams without shear-reinforcement failed in shear, the shear capacity and failure load decreased by 13.1% for the beam without stirrups (beam C2-0) when  $k_p$  was reduced from 0.50 for Type (B) to 0.25 for Type (C). For the beams with shear-reinforcement failed in flexure, the flexural capacity and failure load decreased by 10.8% for the beam with stirrups (beam C2-1) when  $k_p$  was reduced from 0.50 for Type (B) to 0.25 for Type (C). This indicates that the load width affects on the shear and flexural strengths of wide RC beams, where both shear and flexural strengths decreased as the load width, or at best as  $k_p$ , was reduced. This outcome is contrary with the conclusion made by Leonhardt and Walther (1964), where they concluded that the influence of load width was not much more than typical experimental scatter for the geometries studied.

To study the effect of the support width ( $b_s$ ), or at best  $k_s$ , on the shear and flexural strengths of wide RC beams, the beams in Type (B) are compared with those correspondingly relevant beams in Type (D) for the same group. For the beams without shear-reinforcement failed in shear, the shear capacity and failure load decreased by 14.5% for the beam without stirrups (beam D2-0) when  $k_s$  was reduced from 0.50 for Type (B) to 0.25 for Type (D). For the beams with shear-reinforcement failed in flexure, the flexural capacity and failure load decreased by 12.7% for the beam with stirrups (beam D2-1) when  $k_s$  was reduced from 0.50 for Type (B) to 0.25 for Type (D). This indicates that the support width affects on the shear and flexural strengths of wide RC beams, where both shear and flexural strengths decreased as the support width, or at best as  $k_s$ , was reduced. This outcome is linked to the conclusions made by Lubell et al. (2008), Serna-Ros

et al. (2002) and Al.Dywany (2010) regarding to the shear strength, where they concluded that the shear strength of wide RC beams decreases as the support width is reduced. As result from the beams in Types B, C and D, it is clear that  $k_s$  has more influence than  $k_p$  on the both shear and flexural strengths of wide beams without or with shear-reinforcement.

### **9.11.3 Effect of $S_L$ and $S_w$ on the Beam Behaviours**

As a comparison between each two beams in each Beam-Type [Beam-Type (A): beams A2-0 and A2-1; Beam-Type (B): beams B2-0 and B2-1; Beam-Type (C): beams C2-0 and C2-1; Beam-Type (D): beams D2-0 and D2-1], the only difference between them is the shear reinforcement (stirrups). All beams were the same for their geometry and design, except  $S_L$  and  $S_w$  for the beams with stirrups in Group (1), where the beams in Group (0) did not contain stirrups. It can be seen that the beam with stirrups behaved in a ductile flexural manner when they were designed and detailed to the proposed design model and detailing approach, respectively. Based on the results obtained from Test-Series (1) and as previously concluded, it is suggested that, for wide RC beams, at least four stirrups legs should be included in the beam as shear reinforcement even if they are not required or the design requires a lesser quantity, and must be arranged and distributed across the beam width.

As a comparison between the four beams in Group (1) for Series (2), which are beams A2-1, B2-1, C2-1 and D2-1, with those the correspondingly relevant four beams in Group (1a) for Series (1), which are beams A1-1a, B1-1a, C1-1a and D1-1a, respectively, in regards to study the effect of  $S_L$  and  $S_w$ , the beams in Series (2) had the best results and strengths compared with the other correspondingly relevant beams in Series (1) (the other beam Groups in the same relevant Beam-Type in Series (1)), as shown in Tables 9.9 and 9.10 (Chapter 7, Tables 7.9 and 7.10). The comparison was made with those beams in Group (1a) in Series (1) because those beams were the best and strongest beams in Series (1) amongst the other Beam-Groups in the same Series. Accordingly, it can be concluded that the flexural and shear strengths of wide RC beams decrease as the longitudinal and/or transversal stirrup-legs spacing ( $S_L$  and/or  $S_w$ ) increase. Thus, it can be said that the proposed detailing approach and design model have succeeded to prevent the shear failure for those full- and narrow- width wide beams with shear-reinforcement in Series (2) as compared with Series (1).

### 9.11.4 Validation of $K_{cd,Vc,act.}$ and $K_{cd,Mu,act.}$ on Series (2)

The ratio of the experimental-to-Code-predicted shear strength resisted by concrete ( $V_{c,exp.}/V_{c,Pred.-Code} = K_{cd,Vc,act.}$ ) for wide concrete beams without stirrups in Group (0) in Series (2) failed in shear, which corresponds to  $K_{cd,Vc}$  given by the proposed prediction model ( $K_{cd,Vc,Prop.} = V_{c,Pred.-Prop.}/V_{c,Pred.-Code} = \mu_s * \beta_g$ ), was compared with that ratio to the proposed prediction ( $K_{cd,Vc,act.,Prop.} = V_{c,exp.}/V_{c,Pred.-Prop.} = K_{cd,Vc,act.}/K_{cd,Vc,Prop.}$ ). For full-width wide beams, the  $K_{cd,Vc,act.}$  was approximately 1.45 (correspondingly to  $K_{cd,Vc,Prop.} = \mu_s * \beta_g = 1.43$ ), while the the  $K_{cd,Vc,act.,Prop.}$  was approximately 1.01. Otherwise, for partial-width wide beams, the  $K_{cd,Vc,act.}$  was between 1.44, 1.25 and 1.23 (correspondingly to  $K_{cd,Vc,Prop.} = \mu_s * \beta_g = 1.44, 1.22$  and  $1.22$ , respectively), while the  $K_{cd,Vc,act.,Prop.}$  was between 1.0, 1.03 and 1.01, respectively. This seems that the  $K_{cd,Vc,act.,Prop.}$  obtained by the proposed prediction model gives more accuracy than that  $K_{cd,Vc,act.}$  obtained by the Codes of Practice, such EC2 Code. This has also shown the deficiency of the Code to predict the concrete contribution to the shear strength of wide RC beams. It should be noted that  $V_{c,Pred.-Prop.}$  is the  $V_{c,d}$  proposed in Equation (6.10),  $V_{c,Pred.-Code}$  is the  $V_c$  given by the Codes (Equations 4.23 and 4.26), and  $V_{c,exp.}$  is the  $V_c$  obtained by the test.

The ratio of the experimental-to-Code-predicted flexural strength ( $M_{u,exp.}/M_{u,Pred.-Code} = K_{cd,Mu,act.}$ ) for wide RC beams with stirrups in Group (1) in Series (2) failed in flexure, which corresponds to  $K_{cd,Mu}$  given by the proposed prediction model ( $K_{cd,Mu,Prop.} = M_{u,Pred.-Prop.}/M_{u,Pred.-Code} = \mu_s * \beta_g$ ), was compared with that ratio to the proposed prediction ( $K_{cd,Mu,act.,Prop.} = M_{u,exp.}/M_{u,Pred.-Prop.} = K_{cd,Mu,act.}/K_{cd,Mu,Prop.}$ ). For full-width wide beams, the  $K_{cd,Mu,act.}$  was approximately 1.47 (correspondingly to  $K_{cd,Mu,Prop.} = \mu_s * \beta_g = 1.43$ ), while the the  $K_{cd,Mu,act.,Prop.}$  was approximately 1.02. Otherwise, for partial-width wide beams, the  $K_{cd,Mu,act.}$  was between 1.46, 1.30 and 1.27 (correspondingly to  $K_{cd,Mu,Prop.} = \mu_s * \beta_g = 1.44, 1.22$  and  $1.22$ , respectively), while the  $K_{cd,Mu,act.,Prop.}$  was between 1.01, 1.06 and 1.03, respectively. This seems that the  $K_{cd,Mu,act.,Prop.}$  obtained by the proposed prediction model gives more accuracy than that  $K_{cd,Mu,act.}$  obtained by the Codes of Practice, such EC2 Code. This has also shown the deficiency of the Code to predict the ultimate flexural strength of wide RC beams. It should be noted that  $M_{u,Pred.-Prop.}$  is the  $M_{u,d}$  proposed in Equation (6.13),  $M_{u,Pred.-Code}$  is the  $M_u$  given by the Codes (Equations 4.21 and 4.22), and  $M_{u,exp.}$  is the  $M_u$  obtained by the test.

### 9.11.5 Behaviour of the Beams in Series (2)

The cracks development was similar on both elevation side faces (front and back faces) for each beam, and did not appear neither on both cross-section side faces (right and left faces) nor on both plan side faces (top and bottom faces) for all the beams. The flexural and diagonal cracks developed and widened under increasing loads. For all beams, the flexural cracks developed before the diagonal cracks.

Flexural cracks developed in the lower part of the all beams. First column in Table 9.11 shows the applied loads and flexural cracking widths at 1<sup>st</sup> formation of the flexural cracks. For full-width wide beam without stirrups (Beam A2-0), the flexural cracks developed at a load level approximately of 53.2% ( $(250/470)*100$ ) of the ultimate (design) load (470 kN). While for full-width wide beam with stirrups (Beam A2-1), the flexural cracks developed at a load level approximately of 42.5% ( $(200/470)*100$ ) of the ultimate (design) load (470 kN). Otherwise, for partial-width wide beams without stirrups, the flexural cracks developed at a load level approximately between 31.9% to 53.2% of the ultimate (design) load (470 kN). While for partial-width wide beams with stirrups, the flexural cracks developed at a load level approximately between 31.9% to 42.5% of the ultimate (design) load (470 kN).

Diagonal cracks appeared in the shear span regions of the all beams. Second column in Table 9.11 shows the applied loads and diagonal-shear cracking widths at 1<sup>st</sup> formation of the shear cracks. For full-width wide beam without stirrups (Beam A2-0), the diagonal cracks appeared at a load level approximately of 74.5% ( $(350/470)*100$ ) of the ultimate (design) load (470 kN). While for full-width wide beam with stirrups (Beam A2-1), the diagonal cracks appeared at a load level approximately of 95.7% ( $(450/470)*100$ ) of the ultimate (design) load (470 kN). Otherwise, for partial-width wide beams without stirrups, the diagonal cracks appeared at a load level approximately between 63.8% to 74.5% of the ultimate (design) load (470 kN). While for partial-width wide beams with stirrups, the diagonal cracks appeared at a load level approximately between 95.7% of the ultimate (design) load (470 kN).

For full-width wide beam without stirrups (Beam A2-0), the flexural cracks were wider than the diagonal cracks up to a load level approximately of 95.7% ( $(450/470)*100$ ) of the ultimate (design) load (470 kN). While for full-width wide beam with stirrups (Beam A2-1), the flexural cracks were wider than the diagonal cracks up to a load level approximately of 106.4% ( $(500/470)*100$ ) of the ultimate (design) load (470 kN). For the same beam (beam A2-1), the

flexural cracks were again wider than the diagonal cracks from a load level approximately of 148.9%  $((700/470)*100)$  of the ultimate (design) load (470 kN) up to failure. Otherwise, for partial-width wide beams without stirrups, the flexural cracks were wider than the diagonal cracks up to a load level approximately between 74.5% to 85.1% of the ultimate (design) load (470 kN). While for partial-width wide beams with stirrups, the flexural cracks were wider than the diagonal cracks up to a load level approximately of 106.4% of the ultimate (design) load (470 kN). For the same beams, the flexural cracks were again wider than the diagonal cracks from a load level approximately between 138.3% to 148.9% of the ultimate (design) load (470 kN) up to failure. In all beams, diagonal cracks developed in the shear spans as an extension of existing flexure cracks. The diagonal cracks extended towards the loading plate and reached to the concrete compression region.

Additional flexural and diagonal cracks appeared and widened under increasing loads. For full-width wide beam without stirrups failed in shear (Beam A2-0), the maximum width of the critical flexural crack at a load level of 450 kN, which is one step prior to the design load (470 kN), was 0.41mm; the corresponding maximum width of the critical diagonal crack at the same load was 0.33mm. While for full-width wide beam with stirrups failed in flexure (Beam A2-1), the widths of the flexural cracks at a load level of 450 kN, which is one step prior to the design load (470 kN), was 0.20mm; the corresponding widths of the diagonal cracks at the same load was 0.04mm. Otherwise, for partial-width wide beams without stirrups failed in shear, the widths of the flexural cracks at a load level of 450 kN, which is one step prior to the design load (470 kN), were between 0.42mm and 0.58mm; the corresponding widths of the diagonal cracks at the same load were between 0.44mm to 2.72mm. While for partial-width wide beams with stirrups failed in flexure, the widths of the flexural cracks at a load level of 450 kN, which is one step prior to the design load (470 kN), were between 0.25mm and 0.28mm; the corresponding widths of the diagonal cracks at the same load were between 0.05mm to 0.06mm.

It can be concluded that, based on the test results and comparison with the correspondingly relevant beams in Series (1), for all beams without stirrups in Series (2) detailed in accordance with the proposed detailing approach, the concentrating flexural and shear reinforcements distributed within the effective widths of bearing plates (supports and loads) enhanced the shear stresses for the beams in those regions (regions of bearing plate widths) which have high shear stresses; and hence made the beams resisted higher shear loads than those beams in Series (1). It should be noted that the presence of portions of the flexural and shear reinforcements arranged and distributed within the effective widths of the bearing plates, which were detailed based on

the proposed detailing approach, has succeeded in prevention the propagation of the diagonal cracks into the compression zone in those regions, thus resulting in an increase in the load carrying capacity of the beams without stirrups comparing with Series (1).

Furthermore, It can be concluded that, based on the test results and comparison with the correspondingly relevant beams in Series (1), for all beams with stirrups in Series (2) detailed and designed in accordance with the proposed detailing approach and design model, respectively, the concentrating flexural and shear reinforcements distributed within the effective widths of bearing plates (supports and loads) and the proposed longitudinal and transversal stirrup-legs designed to be spaced along the length and across the width have enhanced the shear stresses for the beams in those regions (regions of bearing plate widths) which have high shear stresses, and succeeded in prevention the appearance of shear failure for the beams; hence, made the beams behaved in a ductile flexural manner. It should be noted that the presence of portions of the flexural and shear reinforcements arranged and distributed within the effective widths of the bearing plates, which were detailed and designed based on the proposed detailing and design models, respectively, has succeeded in prevention the propagation of the diagonal cracks into the compression zone in those regions, thus resulting in an increase in the load carrying capacity of shear for the beams with stirrups comparing with Series (1); therefore, the beams failed in flexure.

Because all beams without stirrups in Test-Series (2) failed in shear, the shear (diagonal) cracks were the critical and dominant on the beam behaviours. Wherefore, to analyze the behaviour of the beams under the effect of loading and support widths and the longitudinal and transversal stirrup-legs spacing, the widths of the diagonal cracks at the service (working) load levels and at the failure load levels should be discussed. Moreover, because all beams with stirrups in Test-Series (2) failed in flexure, the flexural cracks are the critical and dominant on the beam behaviours. Wherefore, to analyze the behaviour of the beams under the effect of loading and support widths and the longitudinal and transversal stirrup-legs spacing, the widths of the flexural cracks at the service (working) load levels and at the failure load levels should be discussed. As per the provisions of the EC2, ACI318 and SBC304 Codes, the service (working) load is the load level when the maximum width of the flexural crack exceeds 0.40mm.

For full-width wide beam without stirrups failed in shear (Beam A2-0), the maximum width of the critical diagonal crack at the service (working) load level, which was 95.7%  $((450/470)*100)$  of the design load (470 kN), was 0.33mm. While for full-width wide beam with stirrups failed in

flexure (Beam A2-1), the width of the flexural crack at the service (working) load level, which was 138.3%  $((650/470)*100)$  of the design load (470 kN), was 0.42mm. Otherwise, for partial-width wide beams without stirrups failed in shear, the widths of the diagonal cracks at the service (working) load levels, which were between 85.1% to 95.7% of the design load (470 kN), were between 0.44mm and 0.76mm. While for partial-width wide beams with stirrups failed in flexure, the widths of the flexural cracks at the service (working) load levels, which were between 127.7% to 138.3% of the design load (470 kN), were between 0.40mm and 0.43mm. Third column in Table 9.11 shows the applied loads and flexural cracking widths at the service (working) load levels.

For full-width wide beam without stirrups failed in shear (Beam A2-0), the maximum width of the critical diagonal crack at the failure load level, which was 121.1%  $((569/470)*100)$  of the design load (470 kN), was 2.90mm. While for full-width wide beams with stirrups failed in flexure (Beam A2-1), the width of the flexural crack at the failure load level, which was 177.7%  $((835/470)*100)$  of the design load (470 kN), was 2.0mm. Otherwise, for partial-width wide beams without stirrups failed in shear, the widths of the diagonal cracks at the failure load levels, which were between 102.8% to 120.2% of the design load (470 kN), were between 3.55mm and 6.60mm. While for partial-width wide beams with stirrups failed in flexure, the widths of the flexural cracks at the failure load levels, which were between 154.3% to 176.6% of the design load (470 kN), were between 2.20mm and 3.64mm. Fourth column in Table 9.11 shows the applied loads and flexural- and shear- cracking widths at the failure load levels.

The widths of flexural and diagonal-shear cracks increased as the ratios of support-width and/or load-width to beam-width ( $k_s$  and/or  $k_p$ ) reduced. The beams in Type (A) with full-width bearing plates, i.e. beams A2-0 and A2-1, had the best results, cracks development and crack widths.

The mid-span deflections were recorded at each step of the loading increments. For full-width wide beam without stirrups failed in shear (Beam A2-0), the mid-span deflection at failure load level was 9.90mm. While for full-width wide beam with stirrups failed in flexure (Beam A2-1), the mid-span deflection at failure load level was 22.78mm. Otherwise, for partial-width wide beams without stirrups failed in shear, the mid-span deflections at failure load levels were between 6.74mm and 10.01mm. While for partial-width wide beams with stirrups failed in flexure, the mid-span deflections at failure load levels were between 16.20mm and 20.52mm.

As result, it is clear that  $k_s$  had more influence on the shear strength, flexural strength, flexural and shear crack widths, and mid-span deflection than  $k_p$ . This was based on the results and measurements, mentioned above, obtained from the beams in Types (C and D) comparing with those correspondingly relevant beams in Types (A and B).

## 9.12 Conclusions

Eight wide beams were tested to validate the proposed detailing approach and design model developed in this study, and also to verify the proposed prediction model for the both flexural and shear strengths of wide RC beams. The observations described above explain the following conclusions (Alluqmani, 2013a).

As a result, for those wide beams without shear-reinforcement failed in shear (Group (0)), the shear strengths of wide-beams decreased for those beams tested in Test-Series (2) when the support-width and/or load-width ( $b_s$  and/or  $b_p$ ) decreased, or at best, when the ratios of the support-width and/or load-width to the beam-width ( $k_s$  and/or  $k_p$ ) decreased. As a result also, for those wide beams with shear-reinforcement failed in flexure (Group (1)), the flexural strengths of wide-beams decreased for those beams tested in Test-Series (2) when the support-width and/or load-width ( $b_s$  and/or  $b_p$ ) decreased, or at best, when the ratios of the support-width and/or load-width to the beam-width ( $k_s$  and/or  $k_p$ ) decreased.

In this regard, the beams without shear-reinforcement in Series (2) can be compared for their deflection and cracking behaviours. In general, the widths of flexural and diagonal-shear cracks and the mid-span deflections increased as the ratios of support-width and/or load-width to beam-width ( $k_s$  and/or  $k_p$ ) reduced. The beam in Type (A) with full-width bearing plates had the best results and measurements (deflections and crack widths). It was clear that  $k_s$  had more influence on the shear strength, flexural strength, flexural and shear crack widths, and mid-span deflection than  $k_p$ . This was based on the results and measurements obtained from the beams in Types (C and D) comparing with those correspondingly relevant beams in Types (A and B).

The beams without shear-reinforcement, detailed in accordance with the proposed detailing approach, had higher shear load and best results comparing with those correspondingly relevant beams without shear-reinforcement in Series (1).



For all beams with shear-reinforcement (stirrups) in Series (2) designed and detailed to the proposed Design-Model and Detailing-Approach, respectively, the stirrups, and the concentrating flexural -tensile and -compressive reinforcing bars arranged within the effective-widths of supports and loads, have succeeded in preventing the shear failures for such beams (Alluqmani, 2013a; Alluqmani and Saafi, 2014c), as well as succeeded in preventing further extension of the diagonal cracks into the neutral axis zone and across the beam widths. The beams behaved in ductile flexural manners and failed in flexure. The proposed spacing of stirrup legs in the longitudinal and transverse directions enhanced the shear strengths and load carrying capacities of those beams; this led to make the beams failed in flexure.

The proposed prediction model has been verified for the one-way shear strengths of wide RC beams based on the results obtained from the beams with and without shear-reinforcement in Series (1) and also based on the results obtained from the beams without shear-reinforcement in Series (2). The shear strengths of wide RC beams provided by concrete and stirrups ( $V_c$  and  $V_s$ , respectively) can be determined using the provisions of the current Codes of Practice if they are corrected by the factors of  $K_{cd}$  and  $K_{sd}$ , respectively, as given by the proposed prediction model (Alluqmani, 2013a). It should be noted that for this model the strut angle ( $\theta$ ) should be assumed 45 degrees.

The proposed prediction model has been also verified for the ultimate flexural strengths of wide RC beams with shear-reinforcement based on the results obtained from Series (2). The ultimate flexural strength of wide RC beams ( $M_u$ ) can be determined using the provisions of the current Codes of Practice if it is corrected by the factor of  $K_{cd}$ , as given by the proposed prediction model (Alluqmani, 2013a).

## CHAPTER 10

### CONCLUSIONS AND RECCOMENDATIONS

#### 10.1 Conclusions

In reinforced concrete structures, wide RC beams are commonly used as primary structural members to support floor loads and also to transfer forces from the floor to the vertical elements which are below them, e.g. columns and walls. In these cases, wide beams may be loaded and supported by wide columns or walls (full-width loads and supports) and/or by narrow columns (partial-width loads and supports). In the both cases of support and load conditions, the one-way (beam) and two-way (punching) shear capacities should be checked for wide RC members. For both the wide and narrow load/support configurations, the provisions of current design Codes require that one-way shear capacity is assessed for a cross-section involving the full width of the beam, and the contribution of shear strength resisted by stirrups is assessed according to the longitudinal stirrup legs spacing where the transverse stirrup legs spacing is neglected. Moreover, the current design Codes neglect the load and support widths to predict the flexural and shear strengths of these wide beams. Design of wide RC members should follow to a logical approach. None of the current design approaches take into their design considerations the design provisions of shear and flexure for wide RC beams, where these approaches are widely admitted as being inadequate to design the RC beams in general.

The main concern of the current research conducted in this study was whether the requirements of current design Codes and existing models may lead to poor prediction, detailing and design of wide concrete beams in flexure and shear, especially for narrow-width loaded/supported wide beams. The principal aim of this programme of research has been directed towards the development of simple analytical models for the detailing, designing and prediction of the structural wide concrete beams under static loadings either with full-width or narrow-width load and support conditions. Accordingly, a proposed Prediction-Model was developed to predict the strengths of both wide- and narrow- supported wide RC beams. The proposed prediction model takes into the consideration the load- and support- widths to predict the flexural and shear strengths, and the transverse stirrup legs spacing to predict the shear strength resisted by stirrups. Moreover, proposed Detailing-Approach and Design-Model were developed to estimate the

flexural reinforcing bars that should be concentrated and distributed within the effective widths of supports and loads, and to estimate the longitudinal and transversal stirrup-legs spacing, respectively. All models developed in this study performed the best amongst the compared Codes and models.

### **10.1.1 Wide RC Beams**

The investigations conducted on wide RC beams previously tested and the discussions concluded in the literature (Chapter 3) have showed the effect of support width, load width, longitudinal and transverse spacing of stirrup legs, and flexural -tensile and -compression reinforcement ratios on the strengths of wide RC beams. The influence of both support and load widths on the ultimate flexural and shear strengths of wide RC beams was highlighted. Furthermore, the influence of both longitudinal and transverse spacing of stirrup legs on the ultimate shear strength of wide RC beams was clear, especially on the shear strength resisted by stirrup contribution. In addition, the influence of flexural -tensile and -compression reinforcement ratios on the ultimate flexural strength of wide RC beams, as well on the ultimate shear strength, or at best, on the shear strength resisted by concrete contribution of wide RC beams, was also clear. These factors have been taken into the consideration in the present study for developing rational models to predict, detail and design the wide RC beams. The support width, load width, longitudinal and transverse spacing of stirrup legs were the main variables that were studied in this research to investigate the flexural and shear strengths and behaviours of wide RC beams.

### **10.1.2 Current Provisions of Design and Prediction**

The current provisions of design and prediction the flexural and shear strengths in accordance with the EC2, ACI318 and SBC304 Codes were discussed. The existing shear models developed by previous researches for wide RC beams were also studied and discussed. The experimental results of shear and flexural strengths of wide RC beams obtained from the current available data based on the investigations carried on wide RC beams were compared with the existing Codes and models. The discussions showed the effect of support width, load width, longitudinal and transverse spacing of stirrup legs on the strengths of wide RC beams. These factors have been taken into the consideration to develop Prediction-Model, Detailing-Approach and Design-Model to be used in Practice for wide RC beams. When these models were being developed, the general formulae used by the current Codes of Practice were taken into consideration.

The inadequacy of current design approaches to design and predict the strengths of wide structural concrete beams subjected to the actions of shear force or bending moment was clear. The design approaches do not treat under their design considerations the flexural and shear design of wide concrete members, especially in the transverse direction which is parallel to the width of these members, i.e. the effect of support width, load width and transverse spacing of stirrup legs. In the design for shear, the current design models ignore the stirrup-legs spacing in the transverse direction of wide concrete beams, or at best deal them as narrow beams for two stirrup legs across the width and for full-width load and support conditions. The design methods adopted by the different Codes of Practice do not relate the failure of beams to the actual state of stress which exists in the transverse direction where shear stresses are distributed across the beam width.

The discussions showed the influence of the support and load widths, or at best the ratios of support and load widths to wide beam width, and the longitudinal and transverse spacing of stirrup legs on the ultimate flexural and shear strengths of wide RC beams. The deficiency of the current Codes of Practice and the existing shear strength models to predict the strengths of wide RC beams was concluded. Current Codes of Practice ignore these factors in their design provisions. However, even if there were attempts to develop shear strength models by Lubell et al. (2008), Serna-Ros et al. (2002) and Shuraim (2012), these existing shear strength models are confined for some factors and do not cover all requirements.

### **10.1.3 The Initial Stage of This Study**

Two wide RC beams were tested as an initial stage of this programme of research to investigate the shear and flexural behaviours of wide RC beams and to be used with those beams tested in the literature (Chapter 3) for developing a proposed Prediction-Model (see Chapters 5 and 6). The observations obtained from these beams explained that 1) the shear strength of wide beams decreases as the transverse spacing of their stirrup legs ( $S_w$ ) increases, 2) the shear and flexural strengths of wide RC beams cannot be determined using the provisions of the current Codes and models; however, the general formulae for the design and prediction methods should be used as guideline to develop a new Prediction-Model and should also be corrected by factors depending on the real variables which affect the wide concrete beam strengths (i.e.  $k_s$ ,  $k_p$ ,  $S_L$  and  $S_w$ ), and 3) the presence of portions of the flexural -tensile and -compressive reinforcing bars within the support- and load- widths, respectively, has succeeded to prevent the punching shear (two-way) failure; therefore, it was recommended that a detailing approach to account for detailing,

arranging and distribution of the reinforcements of wide RC beams within the support and load widths should be developed.

#### **10.1.4 The Current Programme of Research**

The evaluation of both full- and narrow- width support and load conditions, among other variables such as the longitudinal and transverse spacing of stirrup legs, on both ultimate flexural strength ( $M_u$ ) and ultimate shear strength ( $V_u$ ) was investigated, discussed and concluded in the present study (see Chapters 6 to 9) in order to develop and validate the proposed models developed and adopted in this study (i.e. the proposed Prediction-Model, Detailing-Approach and Design-Model).

##### **10.1.4.1 The Proposed Models**

The wide structural RC beams tested in the literature (Chapter 3) have highlighted the inadequacy of current design approaches to predict the shear and flexural strengths of wide beams. These approaches do not treat under their design considerations the shear design of wide concrete members, especially in the transverse direction of these members when the stirrup legs are distributed across the width as well as when the bearing plates are narrower than, or equal to, the beam width. In addition, these approaches do not treat under their design considerations the flexural design of wide concrete members with full- or narrow- width loads and supports (see Chapter 4). A wide beam is firstly designed for flexure using the moment envelope and then it is designed for shear using the shear envelope (this is section design). In the design for shear, these models ignore the transverse stirrup legs spacing as well as the widths of supports and loads of wide concrete beams, or at best, they deal with them as narrow beams for two stirrup legs across the width and full-width bearing plates (wide supports and loads).

A proposed prediction model was developed in this study in order to predict the shear and flexural strengths of wide RC beams as illustrated in Chapter 6. Based on the results given by the proposed prediction model, it can be concluded that 1) the shear strengths of wide RC beams provided by concrete and stirrups ( $V_c$  and  $V_s$ , respectively) can be determined using the provisions of the current Codes of Practice if they are corrected by the factors of  $K_{cd}$  and  $K_{sd}$ , respectively, as given by the proposed prediction model for the one-way shear strength, where it should be noted that for this model the strut angle ( $\theta$ ) should be assumed 45 degrees; and 2) the ultimate flexural strength of wide beams can be determined using the provisions of the current

Codes of Practice if it is corrected by the factor of  $K_{cd}$ , as given by the proposed prediction model for the ultimate flexural strength. Sixteen wide RC beams were tested in Test-Series (1) to study the effect of SL,  $S_w$ ,  $b_s$  and  $b_p$ , as well to verify the proposed prediction-model (see Chapter 7).

Furthermore, proposed detailing-approach and design-model were developed based on a thorough well understanding of the flexural and shear behaviours of wide RC beams to enhance the shear stresses and strengths of wide RC beams, and then to ensure that the wide RC beams behave in a ductile flexural manner (see Chapter 8). The effects of  $b_s$ ,  $b_p$ ,  $k_s$ ,  $k_p$  and  $d$  have been taken into the considerations when the detailing approach and design model were being developed. The proposed detailing-approach was developed to account for the effective-widths of supports and loads ( $w_s$  and  $w_p$ ), and the concentrating flexural -tensile and -compression reinforcing bars distributed within the effective widths of -supports and -loads ( $N_{w_s}$  and  $N_{w_p}$ ), respectively. Portions of the flexural -tensile and -compression reinforcements should be distributed within the effective-widths of supports and loads, respectively, as given by the proposed detailing approach. The proposed design-model was developed to account for the longitudinal and transverse spacings of stirrup legs (SL and  $S_w$ ). SL should be distributed along the beam length, while  $S_w$  should be arranged and distributed across the beam width to be measured from the centreline, as given by the proposed design model. Eight wide beams were tested in Test-Series (2) to validate the proposed detailing-approach and design-model, as well to verify the proposed prediction-model for the both flexural and shear strengths of wide RC beams (see Chapter 9).

#### **10.1.4.2 Summary of This Study**

The principal objectives of this programme of research were achieved. New Prediction, Detailing and Design Models for wide RC beams were developed to be used in Practice. The results of 26 tests on wide RC beam specimens were discussed in this study. The proposed models reported in this study have shown the deficiency of the current Codes and models to predict, detail and design the wide RC beams.

The proposed Prediction, Detailing and Design models were developed based on the main missed parameters which show an actual influence on the flexural and shear strengths of wide RC beams with full- and narrow- width load and support conditions (wide- and narrow-supported wide RC beams). The load- and support- widths (or at best, the ratios of load- and

support- width to beam-width) and the transverse and longitudinal stirrup-legs spacing have been taken into the consideration. Comprehensive verification, evaluation and validation comparing with the existing design Codes and other proposed models were conducted.

The proposed prediction-model has been validated on more than 85 wide RC beams tested previously, as well using 26 wide RC beams tested in this programme of research (Test-Series “A”, “1” and “2”). It predicts both shear and flexural strengths with improved accuracy taking into the consideration logical influencing factors not considered in the design provisions of most of the current Codes of Practice which have real effect on both strengths. It is shown that the proposed prediction model performs the best among the compared Codes and models. It shows that the flexural and shear strengths decrease as the ratios of the support- and/or load- width to beam-width decrease, while the shear strength resisted by stirrups contribution decreases as the longitudinal and/or transverse stirrup-legs spacings increase. These influences occur for members with and without shear reinforcement. Consequently, proposed detailing-approach and design-model have been developed based on the results obtained from 16 wide RC beams (Test-Series “1”), and validated based on the results obtained from 8 wide RC beams (Test-Series “2”).

The proposed detailing-approach and design-model have been validated on the wide RC beams tested in Series (2). It is shown that the proposed detailing approach and design model perform the best among the compared Codes and models.

The proposed design-model shows that the longitudinal and transversal stirrup-legs spacings decrease as the ratios of the support-width and/or load-width to beam-width reduce. This has enhanced the shear strengths of the beams with shear reinforcement in Series (2), prevented the brittle shear failures for those beams, and made the beams to fail in a ductile flexural manner.

The proposed detailing-approach shows that the effective-widths of supports and loads decrease as the support and load widths decrease, and that the concentrating flexural -tensile and -compressive reinforcing bars distributed within the effective-widths of supports and loads are to be more concentrated in the regions of supports and loads as the ratios of the support-width and load-width to the beam-width reduce. This has enhanced the shear strengths of the beams with shear reinforcement in Series (2), prevented the brittle shear failures for those beams, and made the beams to fail in a ductile flexural manner. These enhanced the flexural reinforcements (tensile and compressive bars) of the beams without shear reinforcement in Series (2) when they were distributed according to their portions of concentrations within the effective-widths of

supports and loads, enhanced the shear strengths of the beams, and increased the load carrying capacities of the beams comparing with those correspondingly relevant beams in Series (1).

For wide RC beams without and with shear-reinforcement tested in Series “1” and “2”, tests results showed that the shear strength decreased as the support-width and/or load-width was reduced. In addition, for wide RC beams with shear-reinforcement tested in Series “1” and “2”, tests results showed that the shear strength decreased as the longitudinal and/or transverse spacing of stirrup-legs increased. The tests results also showed that the flexural strength of wide RC beams with shear-reinforcement tested in Series “2” decreased as the support-width and/or load-width was reduced.

Finally, it is hoped that the new simplified models proposed in this Study can help others improve their understanding of the structural behaviour of wide RC beams as easily as it has for the author. In addition, it is hoped that it can help in the development of new Codes of Practice that could one day become internationally accepted for shear and flexural design of structural RC wide beams.

## **10.2 Recommendations**

This research has resulted in a significant simplification of the prediction, detailing and design of wide RC members. It is shown that these simplified proposed models are capable of predicting and designing the flexural and shear strengths of wide RC members with various load and support conditions (various bearing plate widths). The expressions developed in this Thesis can form the basis of simple, general, and accurate flexural and shear design methods for wide RC members. The author believes that this detailed study, described in this Thesis, is carried out for the first time and will be very useful to concrete technology. However, the following recommendations are suggested for further investigations on wide RC beams:

1. The proposed prediction model needs to be validated on the other bearing plate widths mentioned in Chapter 3 (Section 3.8: Cases 3 and 4); this means for example, at narrow-width load plates and full-width support plates, or at full-width load plates and narrow-width support plates.
2. The proposed prediction model must be validated on wide concrete beams with various  $b_w/h$  ratios under both three and four point-loading systems.



3. The proposed prediction model must be validated on wide RC beams with various  $\rho_s$  and  $\rho_s'$  ratios.
4. The proposed prediction model need to be developed for the torsion (torque) capacity of wide RC beams with various load and support width conditions.
5. The proposed detailing approach must be validated on wide RC beams with shear reinforcement at detailing of  $N_{w_s}$  and  $N_{w_p}$  within  $w_s$  and  $w_p$ , respectively, and with keeping all other parameters are constant.
6. A Flexural-Shear Interaction Prediction Model for wide RC beams should be developed. The longitudinal and transverse stirrup-legs spacing of wide-beams shear reinforcement must be accounted for the flexural strength of wide beams. This means that factor  $\mu_v$  (where,  $\mu_v = \sqrt{S_L/S_w}$ ) must be taken into the consideration to determine the flexural strength of wide RC beams. This effect needs to be investigated.
7. A Flexural-Shear Interaction Design Model should be developed for wide RC beams with various bearing-plates widths and stirrup-legs spacings.
8. The proposed models developed in this study need to be investigated for wide RC beams under the effect of narrow-width bearing plates on punching shear action and/or under the effect of full- and narrow- width bearing plates on torsion action of edge (marginal) wide beams.
9. The proposed models developed in this study should also be investigated for wide RC beams on the strain measurements in concrete, flexural (tensile and compression) reinforcing bars and shear (stirrups) reinforcing bars.
10. New models for predicting the deflection and crack widths of wide RC beams need to be developed with taking into account the load and/or support widths and the longitudinal and transverse spacing of stirrup legs.

# APPENDICES

## APPENDIX (A): Design and Prediction Calculations

### A.1: Design Procedure of Wide Beams

The design process used in EC2 Code is shown as following for a proposed wide beam as an example:

$f_c = f_{ck} = f_{cy} =$  Characteristic cylinder compressive strength of concrete  $= 0.8f_{cu}$

$f_{cu} =$  Characteristic cube compressive strength of concrete  $= f_{cy}/0.80$

$f_y = f_{yk} =$  Characteristic tensile strength of flexural reinforcement

$f_{yv} = f_{yw} =$  Characteristic tensile strength of shear reinforcement (stirrups)

$b_w =$  Beam width

$h =$  Beam height

$C_c =$  Concrete cover to reinforcement

$\Phi_s = d_b =$  Diameter of main flexural-tensile reinforcing bar

$\Phi_{s'}$  = Diameter of flexural-compression reinforcing bar

$\emptyset_{str.} =$  Diameter of shear reinforcing bar (stirrups)

$\gamma_m =$  Material partial factor of safety,  $\gamma_c = 1.50$ , For flexure and shear concrete

$\gamma_s = 1.15$ , For reinforcement steel

$\alpha_{cc} = 0.85$  for flexural and axial loading, ( $\alpha_{cc} = 1.0$  for other loading)

$\eta = 1.0$ , for  $f_{ck} \leq 50\text{MPa}$

$\eta = 1.0 - \left[ \frac{(f_{ck} - 50)}{200} \right]$ , for  $50\text{MPa} < f_{ck} \leq 90\text{MPa}$

$\lambda = 0.8$ , for  $f_{ck} \leq 50\text{MPa}$

$\lambda = 0.8 - \left[ \frac{(f_{ck} - 50)}{400} \right]$ , for  $50\text{MPa} < f_{ck} \leq 90\text{MPa}$

Design Strength ( $R_d$ ) = Characteristic Strength ( $R_k$ ) / Partial factor of safety ( $\gamma_m$ )

$f_c' = f_c =$  Specified compressive strength of concrete  $= f_{ck}/\gamma_c = 0.67f_{ck}$

$f_{cd} =$  design compressive strength of concrete  $= \alpha_{cc} * f_c = \alpha_{cc} * (f_{ck}/\gamma_c) = 0.85 * 0.67f_{ck} = 0.567f_{ck}$

$f_{yd} = f_y =$  Specified tensile strength of tensile steel  $= f_{yk}/\gamma_s = 0.87f_{yk}$

$f_{yvd} = f_{yw} =$  Specified tensile strength of shear steel  $= f_{yw}/\gamma_s = 0.87f_{yk}$

$E_s =$  Modulus of Elasticity of steel  $= 200,000 \text{ N/mm}^2$

$E_c =$  Modulus of Elasticity of concrete

$f_{ctm} = 0.30 * (f_{ck})^{\frac{2}{3}}$ , for  $f_{ck} \leq 50\text{MPa}$

$$f_{ctm} = 20.12 * \ln \left[ 1 + \left( \frac{f_{cm}}{10} \right) \right], \text{ for } f_{ck} > 50 \text{ MPa}$$

$$f_{cm} = f_{ck} + 8.0 \text{ MPa}$$

L = Total length of beam

$L_o$  = Effective Span of beam

a = Shear span

P =  $P_d$  = Applied load

V =  $V_{Ed}$  = Maximum shear force (shear strength)

M =  $M_b$  = Maximum bending moment (flexural strength)

$N_s$  = Total number of flexural-tensile bars

$N_s'$  = Total number of flexural-tensile bars

$N_L$  = Total number of stirrup-legs across the member-width

d = Effective depth of beam = h -  $C_c$  -  $\emptyset_{str.}$  -  $\Phi_s/2$

a/d = shear-span to effective-depth ratio

$$K = \frac{M}{f_{ck} * b_w * d^2} < K' = 0.167$$

$$jd = Z = \text{Lever arm} = d - \left( \frac{s}{2} \right) = d * I_a = d * \left\{ 0.5 + \sqrt{\left[ 0.25 - \left( \frac{K}{1.134} \right) \right]} \right\} < 0.95d$$

Where,  $s = \lambda * x = 0.8x$ ;  $x = [\epsilon_c / (\epsilon_c + \epsilon_s)] * d$ ;  $\epsilon_{cu} = \epsilon_c = 0.0035$ ;  $\epsilon_s = f_y / E_s = (f_{yk} / \gamma_s) / E_s < \epsilon_{max.} = 0.005$ .

## 1. Flexural Reinforcement

$$K = \frac{M}{f_{ck} * b_w * d^2} \leq K' = 0.167$$

If  $K \leq K' = 0.167$ , hence: the compression reinforcement is not required

$$jd = Z = \text{Lever arm} = d - (s/2) = d * I_a = d * \{ 0.5 + \sqrt{[0.25 - (K/1.134)]} \} < 0.95d$$

Where,  $s = \lambda * x = 0.8x$ ;  $x = [\epsilon_c / (\epsilon_c + \epsilon_s)] * d$ ;  $\epsilon_{cu} = \epsilon_c = 0.0035$ ;  $\epsilon_s = f_y / E_s = (f_{yk} / \gamma_s) / E_s < \epsilon_{max.} = 0.005$ .

If  $\epsilon_s < \epsilon_{max.}$ , this means that the tension steel has yielded

$$\frac{x}{\epsilon_c} = \frac{d}{(\epsilon_c + \epsilon_s)}$$

x = Distance from extreme compression fibre to Neutral Axis. (N.A.) =  $[\epsilon_c / (\epsilon_c + \epsilon_s)] * d$

s = Depth of equivalent rectangular stresses block of concrete stress ( $0.85f_c$ ) =  $\lambda * x$

$$\text{Area of Tensile reinforcement required} = A_{s,req.} = \frac{M}{\left(\frac{f_{yk}}{\gamma_s}\right) * jd}$$

$$F_c = (0.85f_c) * s * b_w = \left[0.85 \left(\frac{f_{ck}}{\gamma_c}\right)\right] * (0.8x) * b_w$$

$$F_s = f_y * A_s = \left(\frac{f_{yk}}{\gamma_s}\right) * A_s$$

$$M_u = F_c * Z = F_s * Z.$$

If  $K > K' = 0.167$ , hence: the compression reinforcement is required

$$Z = \text{Lever arm} = I_a.d = d * \{0.5 + \sqrt{[0.25 - (K'/1.134)]}\}$$

$$d' = C + \emptyset_{str.} + \frac{\Phi_s'}{2}$$

### A. Single Flexural Reinforcement

$d$  = Effective depth of beam =  $h - C_c - \emptyset_{str.} - \Phi_s/2$

$a/d$  = shear span to effective depth ratio

$$K = \frac{M}{f_{ck} * b_w * d^2}$$

If  $K \leq K' = 0.167$ , hence: the compression reinforcement is not required

$$Z = jd = \text{Lever arm} = d - (s/2) = d * I_a = d * \{0.5 + \sqrt{[0.25 - (K/1.134)]}\} < 0.95d$$

Where,  $s = \lambda * x = 0.8x$ ;  $x = [\epsilon_c / (\epsilon_c + \epsilon_s)] * d$ ;  $\epsilon_{cu} = \epsilon_c = 0.0035$ ;  $\epsilon_s = f_y / E_s = (f_{yk} / \gamma_s) / E_s < \epsilon_{max.} = 0.005$ .

If  $\epsilon_s < \epsilon_{max.}$ , this means that the tension steel has yielded

$$\frac{x}{\epsilon_c} = \frac{d}{(\epsilon_c + \epsilon_s)}$$

$x$  = Distance from extreme compression fibre to Neutral Axis. (N.A.) =  $[\epsilon_c / (\epsilon_c + \epsilon_s)] * d$

$s$  = Depth of equivalent rectangular stresses block of concrete stress  $(0.85f_c) = \lambda * x$

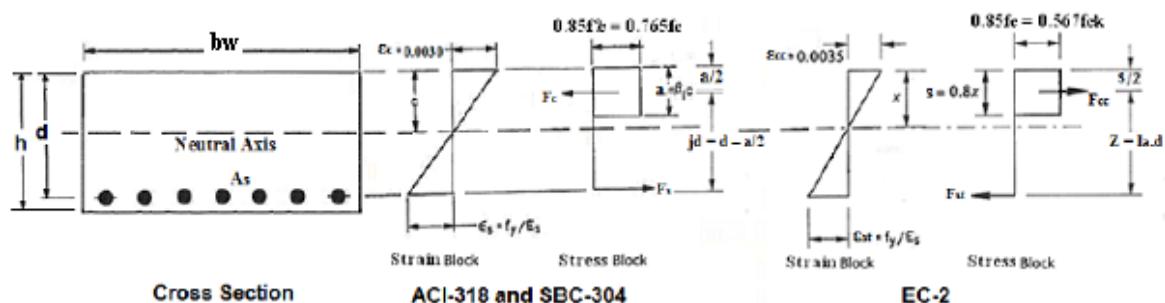


Figure A.1: Equivalent Stresses and Strains Distributions on a Section for Single Flexural Reinforcement.

## 1) Tensile Reinforcement:

$$A_{s,req.} = \text{Area of Tensile reinforcement required} = \frac{M}{f_{yd} * Z} = \frac{M}{\left(\frac{f_{yk}}{\gamma_s}\right) * Z}$$

USE:  $N_s \Phi Y_{mm}$ ,  $A_{s,prov.} = A_{s,prov.}(N_s \Phi Y_{mm}) = N_s * A_{s(1)}$

$\rho_s = \text{Reinforcement ratio} = (A_{s,prov.}/b_w * d)\%$

Maximum allowable % at U.L.S. =  $\rho_{s,max.(ULS)} = 4\%$ ,

$A_{s,max.} = 0.04 * A_c = 0.04 * (b_w * h) > A_{s,prov.}$

Maximum allowable % at S.L.S. =  $\rho_{s,max.(SLS)} = 0.13\%$

$\rho_{s,act} = (A_{s,prov.}/A_c) * 100 = 100 * (A_{s,prov.} / b_w * h) < \rho_{s,max.(ULS)} = 4\%$

$A_{s,min.} = \rho_{s,max.(SLS)} * b_w * h / 100 = 0.0013 * b_w * h < A_{s,prov.}$

Or,  $A_{s,min.} = [(0.26 * f_{ctm})/f_{yk}] * b_w * d < A_{s,prov.}$

$S_{bar} = S_{bar,t}/(N_s - 1) = [b_w - 2C_c - 2(\Phi_s/2)] / (N_s - 1)$

$N_s = \text{Total number of flexural-tensile bars, and } N_s' = \text{Total number of flexural-tensile bars}$

$S_{bar,min.} > 20\text{mm} > d_{agg.} + 5\text{mm}$

## 2) Compression Reinforcement:

**Assume:**  $A_s' = 12\% * A_{s,prov.}$

### B. Double Flexural Reinforcement

$d = \text{Effective depth of beam} = h - C_c - \Phi_{str.} - \Phi_s/2$

$K = M / f_{ck} * b_w * d^2$

If  $K > K' = 0.167$ , hence: the compression reinforcement is required

$Z = \text{Lever arm} = I_a.d = d' * \{0.5 + \sqrt{[0.25 - (K'/1.134)]}\}$ , where:  $d' = C + \Phi_{str.} + \Phi_s/2$

$\epsilon_c = \epsilon_{cu} = \epsilon_{cc} = 0.0035$ ,  $\epsilon_{max.} = 0.0050$ ,  $\epsilon_s = f_y/E_s = (1/\gamma_s) * f_{yk}/E_s < \epsilon_{s,max.} = 0.005$ ,

$\epsilon_y = [(d-x)/x] * \epsilon_{cu} < \epsilon_{max.}$

If  $\epsilon_s < \epsilon_{max.}$ , i.e. the tension steel has yielded

If  $\epsilon_s < \epsilon_y$ , hence:  $f_y = f_{yk}$ , i.e. the tension steel has yielded

$x = \text{Distance from extreme compression fibre to Neutral Axis. (N.A.)} = [\epsilon_c/(\epsilon_c + \epsilon_s)] * d$

$s = \text{Depth of equivalent rectangular stresses block of concrete stress } (0.85f_c) = \lambda.x$

If  $d'/x < 0.38$ , hence:  $f_{sc} = f_{yd} = 0.87f_{yk}$

$\epsilon_{sc} = [(x-d')/x] * \epsilon_{cu} < \epsilon_{max.}$ , if O.K., hence:  $f_{sc} = E_s * \epsilon_{sc}$ ,

Also,  $f_{sc} = 700 * (\epsilon_{sc}/\epsilon_{cu}) = 700 * [(x-d')/x] \leq f_{yd} = (1/\gamma_s) * f_{yk}$ .

Hence,  $f_{sc}$  is known.  $Z = jd = \text{Lever arm} = d - (s/2)$

Where,  $s = \lambda * x$ ,  $x = [\epsilon_c / (\epsilon_c + \epsilon_s)] * d$ ,  $\epsilon_c = 0.0035$ ,  $\epsilon_{max.} = 0.0050$ ,  $\epsilon_s = f_y / E_s = (1/\gamma_s) * f_{yk} / E_s$ ,

$\epsilon_y = [(d-x)/x] * \epsilon_{cu}$ .

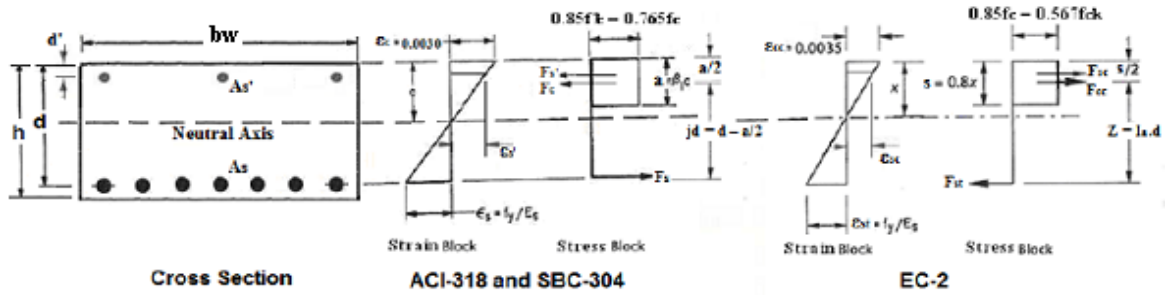


Figure A.2: Equivalent Stresses and Strains Distributions on a Section for Double Flexural Reinforcement.

### 1) Compression Reinforcement:

$$A_{s,req.} = \text{Area of Compression reinforcement required} = \left\{ \frac{[(K - K') * (f_{ck} * b_w * d^2)]}{f_{sc} * (d - d')} \right\}$$

USE:  $N_s \Phi Y_{mm}$ ,  $A_{s',prov.} = A_{s',prov.}(N_s \Phi Y_{mm}) = N_s' * A_{s'}(1)$

### 2) Tensile Reinforcement:

$$A_{s1} = \left[ \frac{(K' * f_{ck} * b_w * d^2)}{0.87 * f_{yk} * Z} \right]$$

$$A_{s2} = \left[ A_s * \left( \frac{f_{sc}}{0.87 * f_{yk}} \right) \right]$$

$A_{s,req.} = \text{Area of Tensile reinforcement required} = A_{s1} + A_{s2}$

Hence:

$$A_{s,req.} = \left[ \frac{(K' * f_{ck} * b_w * d^2)}{0.87 * f_{yk} * Z} \right] + \left[ A_s * \left( \frac{f_{sc}}{0.87 * f_{yk}} \right) \right] \leq 0.04 A_c$$

USE:  $N_s \Phi Y_{mm}$ ,  $A_{s,prov.} = A_{s,prov.}(N_s \Phi Y_{mm}) = N_s * A_s(1)$

$\rho_s = \text{Reinforcement ratio} = (A_{s,prov.} / b_w * d) \%$

Maximum allowable % at U.L.S. =  $\rho_{s,max.(ULS)} = 4\%$ ,

$A_{s,max.} = 0.04 * A_c = 0.04 * (b_w * h) > A_{s,prov.}$

Maximum allowable % at S.L.S. =  $\rho_{s,max.(SLS)} = 0.13\%$

$\rho_{s,act} = (A_{s,prov.} / A_c) * 100 = 100 * (A_{s,prov.} / b_w * h) < \rho_{s,max.(ULS)} = 4\%$

$A_{s,min.} = \rho_{s,max.(SLS)} * b_w * h / 100 = 0.0013 * b_w * h < A_{s,prov.}$

$$\text{Or, } A_{s,\text{min.}} = [(0.26 \cdot f_{ctm}) / f_{yk}] \cdot b_w \cdot d < A_{s,\text{prov.}}$$

$$S_{\text{bar}} = S_{s,1} = S_{\text{bar},t} / (N_s - 1) = [b_w - 2C_c - 2(\Phi_s/2)] / (N_s - 1)$$

$$S_{\text{bar},\text{min.}} > 20\text{mm} > d_{\text{agg.}} + 5\text{mm}$$

**Check:**

$P_d$ ,  $M$  and  $V$  are known.

$$M_u = A_{s,\text{prov.}} \cdot (1/\gamma_s) \cdot f_{yk} \cdot Z$$

$V_u = M_u/a$ , and  $P_u = 2 \cdot V_u$ . If  $P_u > P_d$ , hence O.K.

**2. Shear Reinforcement**

**A. One-Way Shear (Beam-Shear)**

The general formula used to estimate the ultimate one-way shear strength is illustrated in Figures A.3 and A.4, and is as follows:

**ACI318-and-SBC304:**

$$V_u = V_c + V_s \geq V$$

**EC2:**

$$V_u = V_{Rd,d} = V_{Rd,c} + V_{Rd,s} = V_c + V_s \geq V$$

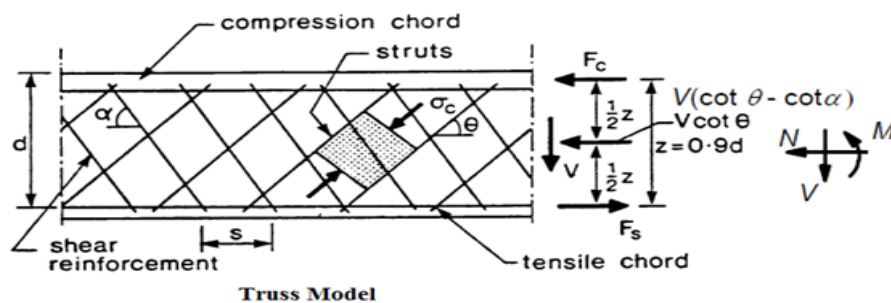


Figure A.3: Truss Model

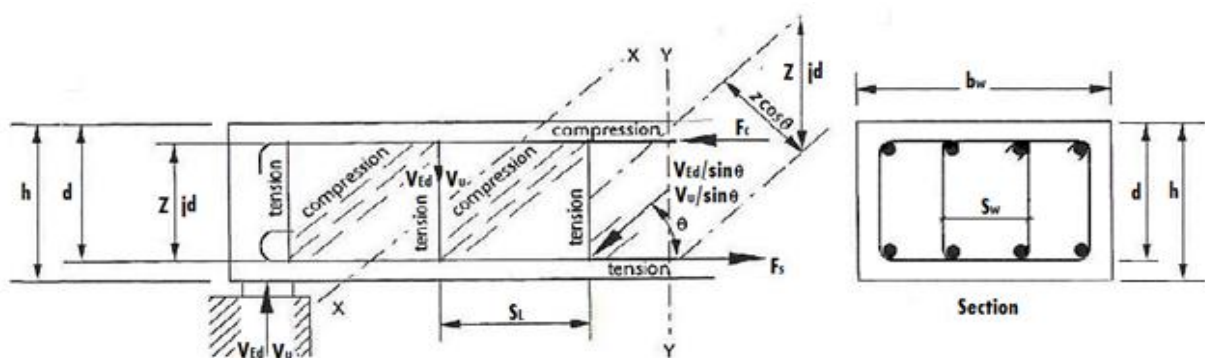


Figure A.4: Longitudinal and Shear Reinforcements in a Beam to EC2, ACI318 and SBC304 Codes.

Where:

$V = V_{Ed}$  = design shear force,

$V_c = V_{Rd,c}$  = shear strength resisted by concrete,

$V_s = V_{Rd,s}$  = shear strength resisted by stirrups, and

$V_u = V_{Rd,d}$  = ultimate shear strength resisted,

**For ACI318-and-SBC304:**

$$v = \frac{V}{(b_w * d)} = \text{design Shear stress,}$$

$$v_c = \frac{V_c}{(b_w * d)} = 0.166 * \sqrt{f_c'} = \text{shear stress resisted by concrete,}$$

$$v_s = \frac{V_s}{(b_w * d)} = \frac{A_v * f_{yv}}{(S_t * b_w)} = \rho_v * f_{yv} = \text{shear stress resisted by stirrups,}$$

$$\rho_v = \frac{A_v}{(S_t * b_w)}$$

**For EC2:**

$$v = \frac{V}{b_w * d} = \text{design shear stress,}$$

$v_c = v_{Rd,c}$  = shear stress resisted by concrete,

$$v_c = v_{Rd,c} = \frac{V_{Rd,c}}{(b_w * 0.9d)} = \left[ \left( C_{Rd,c} * k * (100\rho_1 * f_{ck})^{\frac{1}{3}} \right) + (k_1 * \sigma_{cp}) \right]$$

$v_s = v_{Rd,s}$  = shear stress resisted by stirrups,

$$v_s = v_{Rd,s} = \frac{V_{Rd,s}}{(b_w * 0.9d)} = \frac{A_v * f_{yv}}{(S_t * b_w)} = \rho_v * f_{yv}$$

$$\rho_v = \frac{A_v}{(S_t * b_w)}$$

**1) Concrete Shear Capacity:**

The shear strength resisted by concrete ( $V_c = V_{Rd,c}$ ) is as follows:

**ACI318-and-SBC304:**

$$V_c = [0.166 * (\sqrt{f_c'})] * b_w * d$$

$$v_c = \frac{V_c}{(b_w * d)} = 0.166 * \sqrt{f_c'}$$

**EC2:**

$$V_c = V_{Rd,c} = \left[ \left( C_{Rd,c} * k * (100\rho_1 * f_{ck})^{\frac{1}{3}} \right) + (k_1 * \sigma_{cp}) \right] * b_w \geq [v_{min.} + (k_1 * \sigma_{cp})] * b_w * Z$$



$$v_c = v_{Rd,c} = \frac{V_{Rd,c}}{(b_w * Z)} = \left[ \left( C_{Rd,c} * k * (100\rho_1 * f_{ck})^{\frac{1}{3}} \right) + (k_1 * \sigma_{cp}) \right]$$

**Where:**

$$C_{Rd,c} = 0.18/\gamma_c = 0.18/1.50 = 0.12$$

$$k = 1.0 + \sqrt{\left(\frac{200}{d}\right)} = 1.81 < 2.0, \text{ where } d \text{ in mm}$$

$$k_1 = 0.15, Z = 0.9d, \rho_1 = \rho_s = A_{s,prov.}/(b_w*d) = 0.0184 \leq 0.02$$

$$\sigma_{cp} = \frac{N_{Ed}}{A_c} < 0.2 * f_{cd} = 0.2 * \left[ \alpha_{cc} * \left(\frac{f_{ck}}{\gamma_c}\right) \right], \text{ where } \sigma_{cp} \text{ in MPa}$$

$$v_{min.} = 0.035 * k^{\frac{3}{2}} * f_{ck}^{\frac{1}{2}}$$

**Hence for EC2:**

$$V_c = V_{Rd,c} = \left[ \left(\frac{0.18}{\gamma_c}\right) * \left(1 + \sqrt{\frac{200}{d}}\right) * (100\rho_1 * f_{ck})^{\frac{1}{3}} + 0.15\sigma_{cp} \right] * b_w * 0.9d, \text{ OR}$$

$$V_c = V_{Rd,c} = \left\{ \left[ 0.25 * \left(0.21 * (f_{ck} - 8)^{\frac{2}{3}}\right) \right] * \left(1.6 - \left(\frac{d}{1000}\right)\right) * (1.2 + 40\rho_s) + 0.15\sigma_{cp} \right\} * b_w * d$$

$$V_c = V_{Rd,c} \geq \left[ \left(0.035 * \left(1 + \sqrt{\frac{200}{d}}\right)^{\frac{3}{2}} * f_{ck}^{\frac{1}{2}}\right) + 0.15\sigma_{cp} \right] * b_w * 0.9d$$

$$v_c = v_{Rd,c} = \frac{V_{Rd,c}}{(b_w * 0.9d)} = \left[ \left(\frac{0.18}{\gamma_c}\right) * \left(1 + \sqrt{\frac{200}{d}}\right) * (100\rho_s * f_{ck})^{\frac{1}{3}} + 0.15\sigma_{cp} \right]$$

## 2) Shear Strut Capacity:

To determine the shear reinforcement (stirrups), ACI318 and SBC304 deal with the **Strut-and-Tie** method while EC2 deals with the **Variable Strut-Inclination** method. Both methods are represented by tensile reinforcement at the bottom of the member section for tensile members, and represented by vertical stirrups at the top of the section for compression member, Figure A.5.

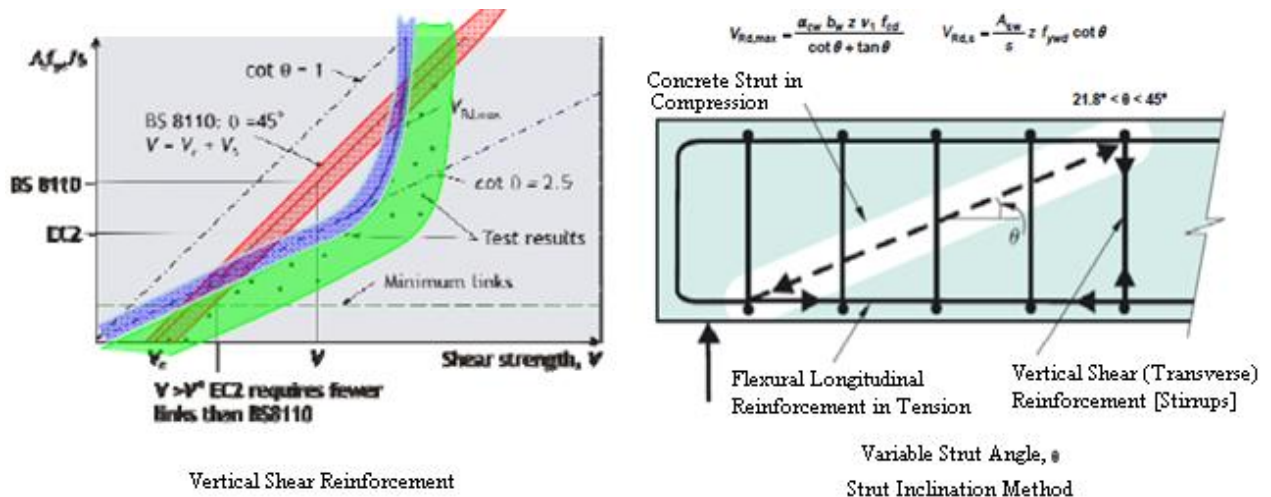


**Figure A.5: Strut Inclination Method**

## 1. Strut-and-Tie Method (ACI318 and SBC304 Codes)

$\alpha$  = angle of shear links =  $90^\circ$  for vertical stirrups (links), hence:  $\sin\alpha = 1.0$ .

$\theta$  = angle of Struts =  $45^\circ$ , hence:  $\cot(\theta) = 1.0$ .

$$V_s = \frac{[A_v * f_{yv} * d * \cot(\theta)]}{S_t} = \frac{[A_v * f_{yv} * d]}{S_t}$$

$$v_s = \frac{V_s}{(b_w * d)} = \frac{A_v * f_{yv}}{(S_t * b_w)} = \rho_v * f_{yv} = \text{shear stress resisted by stirrups, and}$$

$$\rho_v = \frac{A_v}{(S_t * b_w)}$$

## 2. Variable Strut-Inclination Method (EC2 Code)

### a) Vertical Shear Links:

$\alpha$  = angle of shear links =  $90^\circ$  for vertical stirrups (links), hence:  $\sin\alpha = 1.0$ .

$$V_{Rd,max} = \frac{[\alpha_{cw} * v_1 * f_{cd}]}{[\cot(\theta) + \tan(\theta)]} * b_w * Z \geq V_{Ed}$$

$$V_s = V_{Rd,s} = \left(\frac{A_{sw}}{S_t}\right) * f_{yv} * Z * \cot(\theta) = \frac{[A_v * f_{yv} * Z * \cot(\theta)]}{S_t} \leq V_{Ed}$$

$$v_s = v_{Rd,s} = \frac{V_{Rd,s}}{(b_w * Z)} = \frac{[A_v * f_{yv} * Z * \cot(\theta)]}{S_t * b_w} = \rho_v * f_{yv}$$

$v_s$  = shear stress resisted by stirrups,

$$\rho_v = \frac{A_v}{(S_t * b_w)}$$

### b) Inclined Shear Links:

$$V_{Rd,max} = \left\{ \frac{[\alpha_{cw} * v_1 * f_{cd}] * (\cot(\theta) + \tan(\alpha))}{[1.0 + \cot^2(\theta)]} \right\} * b_w * Z \geq V_{Ed}$$

$$V_s = V_{Rd,s} = \left[ \left(\frac{A_{sw}}{S_t}\right) * f_{yv} * Z * (\cot(\theta) + \cot(\alpha)) * \sin(\alpha) \right] \geq V_{Ed}$$

$v_s = v_{Rd,s}$  = shear stress resisted by stirrups

$$v_s = v_{Rd,s} = \frac{V_{Rd,s}}{(b_w * Z)} = \frac{A_v * f_{yv} * (\cot(\theta) + \cot(\alpha)) * \sin(\alpha)}{S_t * b_w} = \rho_v * f_{yv}$$

$$\rho_v = \frac{A_v}{(S_t * b_w)}$$

**Where:** $\alpha$  = angle of shear links (stirrups) $\theta$  = angle of Struts $\alpha_{cw} = 1.0$  $Z = 0.9d$ 

$$v_1 = 0.6 * \left[ 1 - \left( \frac{f_{ck}}{250} \right) \right]$$

$$f_{cd} = \alpha_{cc} * f_c = 1.0 * \left( \frac{f_{ck}}{\gamma_c} \right) = 0.67f_{ck}$$

 $f_{yd}$  = Specified tensile strength of tensile steel =  $f_{yk}/\gamma_s = 0.87f_{yk}$ 
 $f_{ywd}$  = Specified tensile strength of shear steel =  $f_{ywk}/\gamma_s = 0.87f_{ywk}$ 
**Hence for Vertical Shear Links to EC2:**

$$V_{Rd,max} = \left[ \frac{\left( 0.6 \left[ 1 - \left( \frac{f_{ck}}{250} \right) \right] * \left( \frac{f_{ck}}{\gamma_c} \right) \right)}{(\cot(\theta) + \tan(\theta))} \right] * b_w * 0.9d \geq V$$

$$V_s = V_{Rd,s} = \frac{\left[ A_v * \left( \frac{f_{ywk}}{\gamma_s} \right) * 0.9d * \cot(\theta) \right]}{S_L} \leq V$$

$$v_s = v_{Rd,s} = \frac{V_{Rd,s}}{(b_w * Z)} = \frac{A_v * f_{ywd} * \cot(\theta)}{S_L * b_w} = \rho_v * f_{ywd}, \text{ and}$$

$$\rho_v = \frac{A_v}{(S_L * b_w)}$$

**Hence for Inclined Shear Links to EC2:**

$$V_{Rd,max} = \left[ \frac{\left( 0.6 \left[ 1 - \left( \frac{f_{ck}}{250} \right) \right] * \left( \frac{f_{ck}}{\gamma_c} \right) \right) * (\cot(\theta) + \tan(\alpha))}{[1.0 + \cot^2(\theta)]} \right] * b_w * 0.9d \geq V$$

$$V_s = V_{Rd,s} = \frac{\left[ A_v * \left( \frac{f_{ywk}}{\gamma_s} \right) * 0.9d * (\cot(\theta) + \cot(\alpha)) * \sin(\alpha) \right]}{S_L} \geq V$$

$$v_s = v_{Rd,s} = \frac{V_{Rd,s}}{(b_w * 0.9d)} = \frac{A_v * f_{ywd} * (\cot(\theta) + \cot(\alpha)) * \sin(\alpha)}{S_L * b_w} = \rho_v * f_{ywd}, \text{ and}$$

$$\rho_v = \frac{A_v}{(S_L * b_w)}$$

**Where at  $\theta = 21.8^\circ$ ,  $\cot(\theta) = 2.5$ :**

$$V_{Rd,max.} = \left\{ 0.138 * f_{ck} * \left[ 1 - \left( \frac{f_{ck}}{250} \right) \right] \right\} * b_w * 0.9d$$

$$v_{Rd,max.} = \frac{V_{Rd,max.}}{(b_w * 0.9d)} = 0.138 * f_{ck} * \left[ 1 - \left( \frac{f_{ck}}{250} \right) \right]$$

**Where at  $\theta = 45^\circ$ ,  $\cot(\theta) = 1.0$ :**

$$V_{Rd,max.} = \left\{ 0.20 * f_{ck} * \left[ 1 - \left( \frac{f_{ck}}{250} \right) \right] \right\} * b_w * 0.9d$$

$$v_{Rd,max.} = \frac{V_{Rd,max.}}{(b_w * 0.9d)} = 0.20 * f_{ck} * \left[ 1 - \left( \frac{f_{ck}}{250} \right) \right]$$

If  $v_{Rd,c} < v_{Ed}$ , hence: shear reinforcement is required

If  $v_{Rd,c} \geq v_{Ed}$ , hence:  $A_{sw}/S_L = A_{sw,min.}/S_L$

If  $v_{Rd,c} < v_{Ed} \leq v_{Rd,max.}$ , hence:  $\theta = 21.8^\circ$ , and

$$\frac{A_{sw}}{S_L} = \frac{V_{Ed}}{Z * f_{ywd} * \cot(\theta)} \geq \frac{A_{sw,min.}}{S_L}$$

If  $v_{Rd,max.} < v_{Ed}$ , hence: a failure condition is declared, and  $\theta$  should be changed

$$A_{sw}/S_L = V_{Ed}/(Z * f_{ywd} * \cot(\theta)) \geq A_{sw,min.}/S_L$$

$$\theta = 0.5 * \sin^{-1} \left[ \frac{v_{Ed}}{0.20 * f_{ck} * \left( 1 - \left( \frac{f_{ck}}{250} \right) \right)} \right]$$

$$S_{L,max.} = 0.75 * d < 600 \text{mm}$$

$$\frac{A_{sw}}{S_L} = \frac{v_{Ed} * b_w}{\left( \frac{f_{yv}}{\gamma_s} \right) * \cot(\theta)} = \frac{V_{Ed}}{\left( \frac{f_{yv}}{\gamma_s} \right) * Z * \cot(\theta)}$$

$$A_{sw} = S_L * \left( \frac{A_{sw}}{S_L} \right)$$

$$\frac{A_{sw,min.}}{S_L} = \frac{[(0.8 * (\sqrt{f_{ck}}) * b_w) * \sin(\alpha)]}{f_{yv}} < \frac{A_{sw}}{S_L}$$

$$\frac{A_{sw,min.}}{S_L} = \frac{A_v}{S_L} = \frac{(N_L * A_{stir.}(\varnothing 8 \text{mm}))}{S_L}$$

For  $N_L$  (number of legs) is known, hence:  $(A_{sw,min.}/S_L)$  is known.

$$V_{Rd,s,min.} = \left( \frac{A_{sw,min.}}{S_L} \right) * Z * \left( \frac{f_{yv}}{\gamma_s} \right) * \cot(\theta) > V_{Ed}$$

If  $V_{Rd,s,min.} > V_{Ed}$ , this means that  $N_L$  is sufficient for this beam design.

Where,  $Z = 0.9d$  (for EC2), and  $v_{Ed} = V_{Ed}/(b_w * Z)$ .

## B. Two-Way Shear (Punching-Shear)

The footing (or the wide member) may act essentially as a wide beam and shear failure may occur across the entire width of the member, as shown in Figure A.6a. This is beam-type shear (or, one-way shear) and the shear strength of the critical section is calculated as for a beam. The critical section for this type of shear failure is usually assumed to be located at a distance  $d$  (according to ACI318 and SBC304) or  $1.5d$  (according to EC2) from the face of the column (the support) or concentrated load (Figure A.6a). Beam-type shear (or, one-way shear) is often critical for footings and wide structural members but will rarely cause concern in the design of floor slabs. The design one-way (wide-beam) shear stresses at the critical wide-beam shear ( $v$ ) are calculated as follows:

ACI318-and-SBC304:

$$v = \frac{V}{l * d}$$

EC2:

$$v = \frac{V}{l * 1.5d}$$

Where  $V$  is the corresponding shear force at the critical shear section; and  $l$  is equal to the smaller of  $l_1$  or  $l_2$  (usually it is taken equal to the member width,  $b_w$ ) and  $d$  is the effective-depth of the member.

An alternative type of shear failure may occur in the vicinity of a concentrated load or column, and is shown in Figure A.6b. Failure may occur on a surface that forms a truncated cone or pyramid around the loaded area (Figure A.6b). This is known as punching-shear failure (or two-way shear failure) and usually is more critical than one-way shear in wide members or slab systems supported directly on columns. Punching shear (or, two-way shear) is often a critical consideration when determining the thickness of pad footings and flat slabs at the slab-column intersection. The critical section for failure cone of punching shear is approximated as a prism with vertical sides and is usually taken to be geometrically similar to the loaded area and located at a distance  $d/2$  (according to ACI318 and SBC304) or  $2d$  (according to EC2) from the face of the loaded area to the four edges or corners of columns; concentrated loads; reaction areas for narrow-width columns and loads or to the two long edges for full-width columns and loads; and

changes in member thickness, such as edges of columns capitals (column head) or drop panels in flat slabs.

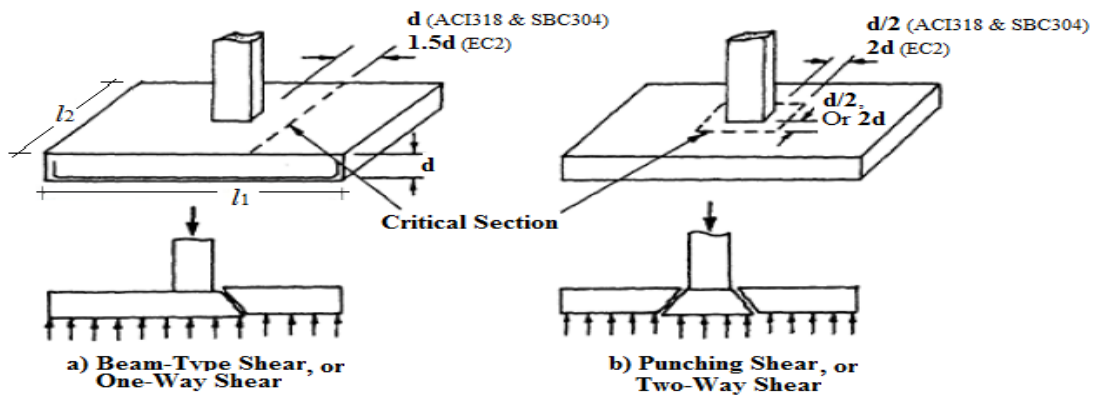


Figure A.6: Type of Shear Failure Surfaces in a Wide Member.

### Punching Shear Stresses

The critical section (or surface) of the punching shear is assumed to be perpendicular to the plane of the footing, slab, or wide beam, Figure A.6b. As an example for calculating the punching-shear stresses for a reinforced concrete wide member, a beam with design data of  $b_w = 700\text{mm}$ ,  $h = 350\text{mm}$ ,  $d = 304\text{mm}$ ,  $L = 3500\text{mm}$ ,  $A_{s,prov.} = 3927\text{mm}^2$ , load (or support) dimensions ( $x = C_p$  and  $y = b_p$ ) of  $150\text{mm}$  and  $350\text{mm}$ , respectively, and  $f_c = 40\text{ MPa}$ , is assumed in this section. For reinforced concrete (non-prestressed) wide members, footings, or flat slabs of normal-weight concrete, the design two-way (punching) shear stresses at the critical punching shear section ( $v_p$ ) are calculated as follows:

#### 1) According to ACI318 and SBC304:

$$v_p = \frac{V}{(u * d)} \leq \Phi * v_c$$

$$u = \text{Critical perimeter} = 2(x+d) + 2(y+d) = 2216\text{mm}.$$

Where  $x = C_p = 150\text{mm}$  and  $y = b_p = 350\text{mm}$  are the plan dimensions of a rectangular load (support) area. The sides of the critical section for failure cone of punching shear are taken to be geometrically similar to the loaded area and located at a distance  $d/2$ .

$v_c$  = the smallest of:

$$1. v_c \leq \Phi * 0.166 * \left[ 1.0 + \left( \frac{2.0}{\beta_c} \right) \right] * \sqrt{f_c'} = 1.05\text{ MPa}$$

$$2. v_c \leq \Phi * 0.083 * \left[ 2.0 + \left( \alpha_s * \left( \frac{d}{u} \right) \right) \right] * \sqrt{f_c'} = 2.80 \text{ MPa}$$

$$3. v_c \leq \Phi * (0.33) * \sqrt{f_c'} = 1.49 \text{ MPa}$$

If  $v_p \leq \Phi v_c$ : hence the punching shear reinforcement is not required

If  $v_p > \Phi v_n$ : hence the member section should be changed

If  $\Phi v_n > v_p \leq \Phi v_c$ : hence the punching shear reinforcement is required

$$\text{For stirrups, } \Phi v_n = \Phi * 0.50 * \sqrt{f_c'}$$

$$\text{For Studs, } \Phi v_n = \Phi * 0.66 * \sqrt{f_c'}$$

$$A_v = \frac{[(v_p - \Phi v_c) * u * S]}{\Phi * f_{yv} * \sin(\alpha)} \geq A_{v,\min.} = \frac{(2.0 * \sqrt{f_c'} * u * S)}{f_{yv}}$$

**Hence:**

$v_c = 1.05 \text{ MPa}$ , and  $\Phi * v_c = 0.79 \text{ MPa}$ . Where  $\alpha_s$  is taken as 40.

$v_p = V/(u*d) = 0.44 \text{ MPa} \leq \Phi * v_c = 0.79 \text{ MPa}$ , hence: the punching shear reinforcement is not required.

Where  $v_p$  is the design factored punching shear stress at the critical punching shear section (it will usually be the support reaction at the ultimate strength state),  $v_c = 0.166 * \sqrt{f_c'}$  for stirrup and  $v_c = 0.25 * \sqrt{f_c'}$  for studs,  $\beta_c = l_1/l_2$  ( $l_1$  is greater than  $l_2$ , where  $l_1 = L = 3500\text{mm}$  and  $l_2 = b_w = 700\text{mm}$ ),  $\alpha_s$  is equal 40 for interior column case; 30 for edge column case; and 20 for corner column case,  $\alpha$  is angle of shear reinforcement (take as  $\theta$ ),  $S$  is shear reinforcement spacing (taken as  $d/2$  according to ACI318 and SBC304 Codes),  $\Phi_F = 0.90$ ,  $\Phi_S = 0.75$ ,  $f_c' = \Phi_F * f_c$ , and all other variables are defined in Section A for one-way shear.

**2) According to EC2:**

$$v_p = \frac{\beta * V}{u * d} \geq v_{Rd,c}$$

$u = \text{Critical Perimeter} = (2dx) + (2dy) = 2(x+4d) + 2(y+4d) = 5864\text{mm}$ .

Where  $x = C_p = 150\text{mm}$  and  $y = b_p = 350\text{mm}$  are the plan dimensions of a rectangular load (support) area. The sides of the critical section for failure cone of punching shear are taken to be geometrically similar to the loaded area and located at a distance  $2d$ .

$$1. v_{Rd} = 0.30 * \left(\frac{f_{ck}}{\gamma_c}\right) * \left[1.0 - \left(\frac{f_{ck}}{250}\right)\right] = 7.15 \text{ MPa}$$

$$2. v_{Rd,c} = C_{Rd,c} * k * (100\rho_1 * f_{ck})^{\frac{1}{3}} = 0.54 \text{ MPa}$$

If  $v_p \leq v_{Rd,c}$ : hence the punching shear reinforcement is not required

If  $v_p > v_{Rd}$ : hence the member section should be changed

If  $v_p > v_{Rd,c}$ : hence the punching shear reinforcement is required

$$C_{Rd,c} = 0.18/\gamma_c = 0.18/1.50 = 0.12.$$

$$k = 1.0 + \sqrt{\left(\frac{200}{d}\right)} = 1.81 < 2.0, \text{ O.K.}$$

$$\rho_1 = \sqrt{\left[\left(\frac{A_{sx}}{(b_w * dx)}\right) * \left(\frac{A_{sy}}{(b_w * dy)}\right)\right]}$$

Where  $A_{sx} \approx A_{sy}$ ,  $dx = x+4d$ , and  $dy = y+4d$

$\rho_1 = 0.00384 = 0.384\%$ ,  $A_{sx} \approx A_{sy} = A_{s,prov.} = 3927 \text{ mm}^2$ ;  $dx = x+4d = 1366\text{mm}$ , and  $dy = y+4d = 1566\text{mm}$ .

$$f_{ywd,ef.} = 250 + 0.25d \leq f_{ywd} = f_{yk}/\gamma_s = 0.87f_{yk}$$

$$A_v = \frac{[(v_p - 0.75 * v_{Rd,c}) * u * S]}{[1.5 * f_{ywd,eff.} * n]}$$

**Hence:**

$$v_{Rd,c} = 0.54 \text{ MPa.}$$

$v_p = \beta * V_{Ed}/(u*d) = 0.19 \text{ MPa} \leq v_{Rd,c} = 0.54 \text{ MPa}$ , hence: the punching shear reinforcement is not required. Where  $\beta$  is taken as 1.15.

Where  $v_p$  is the design punching shear stress at the critical punching shear section (it will usually be the support reaction at the ultimate limit state),  $S$  is shear reinforcement spacing (taken as  $2d$  according to EC2 Code),  $\beta$  is equal 1.15 for interior column case; 1.40 for edge column case; and 1.50 for corner column case, and all other variables are defined in Section A for one-way shear.



### 3. Serviceability Check

#### A. Deflection

The maximum mid-span deflection is calculated as follows:

ACI318-and-SBC304:

For concentrated load case:

$$\delta = \frac{P \cdot (L_0)^3}{48 \cdot E_c \cdot I} < \frac{L}{360}$$

For uniform distributed load case:

$$\delta = \frac{5w \cdot (L_0)^4}{384 \cdot E_c \cdot I} < \frac{L}{360}$$

Where, P = applied concentrated load, w = applied uniform distributed load, L<sub>0</sub> = clear span length of the beam, L = overall span length of the beam, E<sub>c</sub> = concrete modulus of elasticity = 4700\*√f<sub>c</sub>, and I = section moment of inertia = [(b<sub>w</sub>\*h<sup>3</sup>)/12] for a rectangular section.

EC2:

For all cases of load:

$$a = k \cdot (L_0)^2 \cdot \left(\frac{1}{r_b}\right) < \frac{L}{d} \text{ or } \frac{L}{250}$$

Where

$$k = 0.125 - \left[\frac{a^2}{6}\right], \text{ where } a = 0.025, \left(\frac{1}{r_b}\right) = \frac{M}{E_c \cdot I}, \text{ and } I = \frac{b_w \cdot h^3}{12}$$

Where, L<sub>0</sub> = clear span length of the beam, L = overall span length of the beam, M = section bending moment, E<sub>c</sub> = concrete modulus of elasticity = 5500\*√f<sub>c</sub>, and I = section moment of inertia = [(b<sub>w</sub>\*h<sup>3</sup>)/12] for a rectangular section.

## B. Crack Width

The maximum flexural crack width is calculated as follows:

ACI318-and-SBC304:

$$z = \frac{\left[0.03f_s * (d_c * A)^{\frac{1}{3}}\right]}{1000} < 0.40\text{mm}$$

Where

$$f_s = 0.6f_y,$$

$$A = \frac{b_w * 2d_c}{N_s}$$

$$d_c = C_c + \emptyset_{\text{stir.}} + \frac{\emptyset_s}{2}$$

Where,  $z$  = flexural crack width,  $f_s$  = specified flexural reinforcing steel strength,  $f_y$  = characteristic flexural reinforcing steel strength,  $N_s$  = total numbers of flexural tensile reinforcing bars,  $C_c$  = concrete cover,  $\emptyset_s$  = diameter of the main tensile reinforcing bar,  $\emptyset_{\text{stir.}}$  = diameter of the stirrups leg, and  $b_w$  = member web-width.

EC2:

$$w_{,k} = S_{r,\text{max.}} * (\varepsilon_{sm} - \varepsilon_{cm}) < 0.40\text{mm}$$

Where

$$S_{r,\text{max.}} = 3.4C + \left[ \frac{(0.42 * k_1 * k_2 * \emptyset_s)}{\rho_{p,\text{eff.}}} \right]$$

$$\varepsilon_{sm} - \varepsilon_{cm} = 0.6 * \varepsilon_s = 0.6 * \left( \frac{f_y}{E_s} \right)$$

$$\rho_{p,\text{eff.}} = \frac{A_s}{b_w * d}$$

Where,  $w_{,k}$  = flexural crack width,  $S_{r,\text{max.}}$  = maximum spacing of cracks,  $(\varepsilon_{sm}-\varepsilon_{cm})$  = change in the flexural steel and concrete strains,  $k_1 = 0.70$ ,  $k_2 = 0.40$ ,  $C$  = concrete cover,  $\emptyset_s$  = diameter of the main tensile reinforcing bar,  $f_y$  = specified flexural reinforcing steel strength =  $0.87 * f_{yk}$ ,  $f_{yk}$  = characteristic flexural reinforcing steel strength,  $\varepsilon_s$  = flexural steel bar strain,  $E_s$  = modulus of elasticity of flexural steel,  $\rho_{p,\text{eff.}}$  = effective flexural tensile reinforcement ratio,  $A_s$  = total area of flexural tensile reinforcing bars,  $b_w$  = member web-width, and  $d$  = member effective-depth.

## A.2: Prediction Procedure of Wide Beams

### 1) Design Strengths:

$P_d$ ,  $M$ , and  $V$  are known.

### 2) Unity of all Factors of Safety:

All factors of safety ( $1/\gamma_m$  and  $\Phi$ ) = 1.0, for flexure and shear.

### 3) Actual Beam Dimensions:

$b_w$ ,  $h$ ,  $d$ ,  $L$ ,  $L_o$ , and  $a$  are known.

### 4) Actual Material Strengths:

$f_{c,act.}$ ,  $f_{y,act.}$ ,  $f_{yv,act.}$ , and  $E_s$  are known.

### 5) Reinforcement Details as Built:

#### Tensile Reinforcement:

$A_{s,prov.}$ , and  $\rho_{s,prov.} = (A_{s,prov.}/b_w.d)$  are known.

#### Compression Reinforcement:

$A_{s',prov.}$ , and  $\rho_{s',prov.} = (A_{s',prov.}/b_w.d)$  are known.

#### Shear Reinforcement:

Shear reinforcement along the member length:

$S_L$  at centre spacing (C/C) is known.

Shear reinforcement across the member width:

$A_{v,prov.}$ , and  $S_w$  at centre spacing (C/C) is known.

## 1. Predicted Flexural Failure Load

$A_{s,prov.}$  = Total area of flexural reinforcement provided =  $A_{s,prov.}(8\Phi 25mm) = N_s * A_{s1}$

$Z = jd$  = Lever arm =  $d - (s/2)$

Where,  $s$  = Depth of equivalent rectangular stress block of concrete stress ( $0.85f_c$ ) =  $\lambda * x$

$\lambda = 0.8$  for  $f_{c,act.} \leq 50 \text{ N/mm}^2$ .  $\lambda = 0.8 - [(f_{c,act.} - 50)/400]$  for  $50 \text{ N/mm}^2 < f_{c,act.} \leq 90 \text{ N/mm}^2$ .

$x$  = Distance from extreme compression fibre to Neutral Axis. (N.A.) =  $[\epsilon_c / (\epsilon_c + \epsilon_s)] * d$

Where,  $\epsilon_{cu} = \epsilon_c = 0.0035$ ,  $\epsilon_{max.} = 0.0050$ , and  $\epsilon_s = f_{y,act.}/E_s = 0.002625 < \epsilon_{max.}$ ,  $\epsilon_y = [(d-x)/x] * \epsilon_{cu} < \epsilon_{max.}$ .

**Hence:**  $x$ ,  $\epsilon_y$ ,  $s$ , and  $Z$  are known.

Hence:  $M_u = A_{s,prov.} * f_{y,act.} * Z$

Hence:  $M_u$  = known,  $V_u = M_u / a$  = known,  $P_u = 2 * V_u$  = known.

**Hence: Predicted Failure Load =  $P_{f,pred.} = P_u > P_d$**

### Or Another Method as:

$F_c = \text{Total compressive force in Concrete} = (0.85 \cdot f_{c,act}) \cdot s \cdot b_w = \text{known}$

$F_s = \text{Total tensile force in Reinforcement} = f_{y,act} \cdot A_{s,prov.} = \text{known}$

$M = F_c \cdot Z = F_s \cdot Z$ , **hence:**  $M = \text{known}$  (for concrete), and  $M = \text{known}$  (for steel).

**Hence:**  $M_u = M_{small}$  (either for concrete or for steel) = known,  $V_u = M_u / a = \text{known}$ ,  $P_u = 2 \cdot V_u = \text{known}$ .

**Hence: Predicted Failure Load =  $P_{f,pred.} = P_u > P_d$**

## 2. Predicted One-Way Shear Failure Load

$\alpha = 90^\circ$  for vertical stirrups (links), hence:  $\sin \alpha = 1.0$ . Assume:  $\theta = 45^\circ$ , hence:  $\cot(\theta) = 1.0$ .

### ACI318-and-SBC304:

$$V_c = [0.166 \cdot \sqrt{f_{c,act}}] \cdot b_w \cdot d$$

$$V_s = \frac{[A_{v,prov.} \cdot f_{yv,act} \cdot d]}{S_t}$$

$$V_u = V_c + V_s$$

### EC2:

$$V_c = \left[ (0.18) \cdot \left( 1 + \sqrt{\frac{200}{d}} \right) \cdot (100 \rho_{s,prov.} \cdot f_{c,act})^{\frac{1}{3}} + 0.15 \sigma_{cp} \right] \cdot b_w \cdot 0.9d$$

Where,  $\sigma_{cp}$  is taken zero for no axial load.

$$V_s = \frac{[A_{v,prov.} \cdot f_{yv,act} \cdot 0.9d]}{S_t}$$

$$V_u = V_c + V_s$$

**Hence:**  $V_c$  and  $V_s$  are known.

Hence:  $V_u = V_c + V_s$

Hence:  $V_u = \text{known}$ ,  $P_u = 2 \cdot V_u = \text{known}$ .

**Hence: Predicted Failure Load =  $P_{f,pred.} = P_u > P_d$**

## 3. Check of Two-Way Shear (Punching-Shear) Stress

$$v_p = \frac{\beta \cdot V}{u \cdot d} \leq v_{Rd,c}$$

$x = C_p = \text{length of loading plate} = \text{known}$ , and  $y = b_p = \text{width of loading plate} = \text{known}$ .

The sides of the critical section for failure cone of punching shear are taken to be geometrically similar to the loaded area and located at a distance  $2d$  to EC2 Code.

$$u = \text{Critical Perimeter} = (2 * dx) + (2 * dy) = 2(x+4d) + 2(y+4d) = \text{known.}$$

If  $v_p \leq v_{Rd,c} = C_{Rd,c} * k * (100\rho_1 * f_{ck})^{\frac{1}{3}}$ : Hence, punching shear reinforcement is not required.

If  $v_p > v_{Rd} = 0.30 * \left(\frac{f_{ck}}{\gamma_c}\right) * \left[1.0 - \left(\frac{f_{ck}}{250}\right)\right]$ : Hence, the member section should be changed.

If  $v_p > v_{Rd,c} = C_{Rd,c} * k * (100\rho_1 * f_{ck})^{\frac{1}{3}}$ : Hence, punching shear reinforcement is required.

$$v_{Rd} = 0.30 * (f_{c,act}) * \left[1.0 - \left(\frac{f_{c,act}}{250}\right)\right]$$

$$v_{Rd,c} = C_{Rd,c} * k * (100\rho_1 * f_{c,act})^{\frac{1}{3}}$$

$$C_{Rd,c} = \frac{0.18}{\gamma_c} = 0.18$$

$$k = 1.0 + \sqrt{\left(\frac{200}{d}\right)}$$

$$\rho_1 = \sqrt{\left[\left(\frac{A_{sx}}{(b_w * dx)}\right) * \left(\frac{A_{sy}}{(b_w * dy)}\right)\right]}$$

Where  $A_{sx} \approx A_{sy} = A_{s,prov.} = \text{known}$ ;  $dx = x+4d = \text{known}$ , and  $dy = y+4d = \text{known}$ .

$$A_v = \frac{[(v_{Ed} - 0.75 * v_{Rd,c}) * u * S]}{[1.5 * f_{ywd,eff.} * n]}$$

$$v_{Rd} = 0.30 * (f_{c,act}) * [1.0 - (f_{c,act}/250)]$$

$$v_{Rd,c} = C_{Rd,c} * k * (100\rho_1 * f_{c,act})^{\frac{1}{3}}$$

$$C_{Rd,c} = 0.18/\gamma_c = 0.18$$

$$k = 1.0 + \sqrt{(200/d)}$$

$$\rho_1 = \sqrt{[(A_{sx}/(b_w * dx)) * (A_{sy}/(b_w * dy))],}$$

Where  $A_{sx} \approx A_{sy} = A_{s,prov.} = \text{known}$ ;  $dx = x+4d = \text{known}$ , and  $dy = y+4d = \text{known}$ .

$$A_v = [(v_{Ed} - (0.75 * v_{Rd,c})) * u * S] / [1.5 * f_{ywd,eff.} * n]$$

$$f_{ywd,eff.} = 250 + 0.25d \leq f_{yv} = f_{yk}/\gamma_s = 0.87f_{yk}$$

**Hence:**  $V$ ,  $u$ ,  $d$ ,  $\beta$ , and  $v_{Rd,c}$  known.

Where  $\beta$  is taken as 1.0.

Hence:  $v_p = \beta * V / (u * d) = \text{known} \leq v_{Rd,c} = \text{known}$ .

**Hence:** the punching shear reinforcement is not required; therefore, no prediction for punching shear.

Where  $v_p$  is the design punching shear stress at the critical punching shear section (it will usually be the support reaction at the ultimate limit state),  $S$  is shear reinforcement spacing,  $2d$  to EC2,  $\beta$  is equal 1.15 for interior column case; 1.40 for edge column case; and 1.50 for corner column case, and all other variables are defined in Chapter 4 and Appendix A.1.

#### 4. Final Predicted Failure Load and Mode

The final predicted failure load is the lesser load obtained from flexural and shear strengths, and the predicted failure mode is the mode which is corresponding to the lesser predicted load.

#### A.3: Analysis and Design of Wide Beams [Beam ECC2 and ECC3]

The design process used in EC2 Code is shown as following:

$f_c = f_{ck} = f_{cy} =$  Characteristic cylinder compressive strength of concrete =  $0.8f_{cu} = 40 \text{ N/mm}^2$

$f_{cu} =$  Characteristic cube compressive strength of concrete =  $f_{cy}/0.80 = 50 \text{ N/mm}^2$

$f_y = f_{yk} =$  Characteristic tensile strength of flexural reinforcement =  $500 \text{ N/mm}^2$

$f_{yv} = f_{yw} =$  Characteristic tensile strength of shear reinforcement (stirrups) =  $500 \text{ N/mm}^2$

$b_w =$  Beam width =  $700 \text{ mm}$

$h =$  Beam height =  $350 \text{ mm}$

$C_c =$  Concrete cover to reinforcement =  $25 \text{ mm}$

$\Phi_s = d_b =$  Diameter of main flexural-tensile reinforcing bar =  $25 \text{ mm}$

$\Phi_{s'} =$  Diameter of flexural-compression reinforcing bar

$\emptyset_{str.} =$  Diameter of shear reinforcing bar (stirrups) =  $8 \text{ mm}$

$\gamma_m =$  Material partial factor of safety,  $\gamma_c = 1.50$ , For flexure and shear concrete

$\gamma_s = 1.15$ , For reinforcement steel

$\alpha_{cc} = 0.85$  for flexural and axial loading, ( $\alpha_{cc} = 1.0$  for other loading)

$\eta = 1.0$  for  $f_{ck} \leq 50 \text{ MPa}$

$\eta = 1.0 - [(f_{ck}-50)/200]$  for  $50 \text{ MPa} < f_{ck} \leq 90 \text{ MPa}$

$\lambda = 0.8$  for  $f_{ck} \leq 50 \text{ MPa}$

$\lambda = 0.8 - [(f_{ck}-50)/400]$  for  $50 \text{ MPa} < f_{ck} \leq 90 \text{ MPa}$

Design Strength ( $R_d$ ) = Characteristic Strength ( $R_k$ ) / Partial factor of safety ( $\gamma_m$ )

$f_{c'} = f_c =$  Specified compressive strength of concrete =  $f_{ck}/\gamma_c = 0.67f_{ck} = 26.7 \text{ N/mm}^2$

$f_{cd}$  = design compressive strength of concrete =  $\alpha_{cc} * f_c = \alpha_{cc} * (f_{ck} / \gamma_c) = 0.85 * 0.67 f_{ck} = 0.567 f_{ck}$   
 $f_{yd} = f_y$  = Specified tensile strength of tensile steel =  $f_{yk} / \gamma_s = 0.87 f_{yk} = 0.87 * 500 = 435 \text{ N/mm}^2$   
 $f_{yvd} = f_{ywd}$  = Specified tensile strength of shear steel =  $f_{ywk} / \gamma_s = 0.87 f_{yk} = 0.87 * 500 = 435 \text{ N/mm}^2$   
 $E_s$  = Modulus of Elasticity of steel =  $200,000 \text{ N/mm}^2$   
 $E_c$  = Modulus of Elasticity of concrete =  $5500 * \sqrt{f_c} = 5500 * \sqrt{f_{ck} / \gamma_c} = 28,000 \text{ N/mm}^2$   
 $f_{ctm} = 0.30 * f_{ck}^{(2/3)}$ , for  $f_{ck} \leq 50 \text{ MPa}$   
 $f_{ctm} = 20.12 * \ln [1 + (f_{cm} / 10)]$ , for  $f_{ck} > 50 \text{ MPa}$   
 $f_{cm} = f_{ck} + 8.0 \text{ MPa}$   
 $L$  = Total length of beam =  $3500 \text{ mm}$   
 $L_o$  = Effective Span of beam =  $2800 \text{ mm}$   
 $a$  = Shear span =  $1400 \text{ mm}$   
 $P = P_d$  = Applied load =  $600 \text{ kN}$  to EC2 ( $550 \text{ kN}$  to ACI318 and SBC304)  
 $V = V_{Ed}$  = Maximum shear force (shear strength) =  $300 \text{ kN}$  to EC2 ( $275 \text{ kN}$  to ACI318 and SBC304)  
 $M = M_b$  = Maximum bending moment (flexural strength) =  $420 \text{ kN.m}$  to EC2 ( $385 \text{ kN.m}$  to ACI318 and SBC304)  
 $N_s$  = Total number of flexural-tensile bars =  $8\Phi 25 \text{ mm}$   
 $N_{s'}$  = Total number of flexural-tensile bars =  $6\Phi 10 \text{ mm}$   
 $N_L$  = Total number of stirrup-legs across the width =  $4\Phi 8 \text{ mm}$  (ECC2) and  $6\Phi 8 \text{ mm}$  (ECC3)  
 $d$  = Effective depth of beam =  $h - C_c - \Phi_{str.} - \Phi_s / 2 = 304 \text{ mm}$   
 $a/d$  = shear-span to effective-depth ratio =  $4.6$   
 $K = M / f_{ck} * b * d^2 = 0.162 < K' = 0.167$   
 $jd = Z = \text{Lever arm} = d - (s/2) = d * I_a = d * \{0.5 + \sqrt{[0.25 - (K/1.134)]}\} = 253 \text{ mm} < 0.95d \approx 290 \text{ mm}$   
 Where,  $s = \lambda * x = 0.8x$ , and  $x = [\epsilon_c / (\epsilon_c + \epsilon_s)] * d$ ,  $\epsilon_{cu} = \epsilon_c = 0.0035$ ,  $\epsilon_s = f_y / E_s = (f_{yk} / \gamma_s) / E_s < \epsilon_{max.} = 0.005$ .

## 1. Beam Analysis

The two beams tested in Series "A", which need to be analysed, were simply supported beams. They carried a concentrated load ( $P$ ) in the mid-span point of  $600 \text{ kN}$ . The total length of the beam ( $L$ ) is  $3500 \text{ mm}$  with a clear-span ( $L_o$ ) of  $2800 \text{ mm}$  and shear-span ( $a$ ) is  $1400 \text{ mm}$ . The beams had dimensions of  $700 \text{ mm}$  width ( $b_w$ ) and  $350 \text{ mm}$  height ( $h$ ).

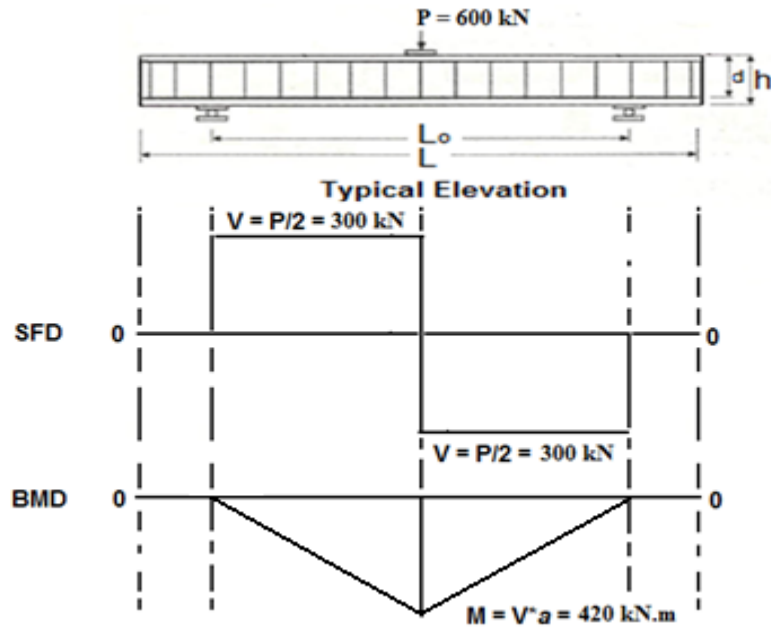


**Figure A.7:** SFD and BMD Diagrams for the Beams in Test-Series "A".

$$\sum M_{\text{Left Support}} = 0, \text{ Anti-Clockwise}$$

$$V_R (2.8) - P (1.4) = 0, \text{ Hence: } V_R = P/2 = 300 \text{ kN}$$

$$\sum F_y = 0, \text{ Upward}$$

$$V_L + V_R - P = 0, \text{ Hence: } V_L = V_R = V = P/2 = 300 \text{ kN}$$

$$\sum M_{\text{at P}} = 0, \text{ Anti-Clockwise or On-Clockwise}$$

$$M - V_R(a) = 0, \text{ Hence: } M = V * a = 420 \text{ kN.m.}$$

### **Take:**

$$V_{\text{max.}} = 300 \text{ kN}$$

$$\sum M_{\text{at P}} = 0, \text{ Anti-Clockwise}$$

$$M_{\text{max.}} - V_{\text{max.}}(a) = 0, \text{ hence: } M_{\text{max.}} = 420 \text{ kN.m.}$$

## **2. Beam Design**

The design procedure used in the the EC2 Code was applied for the two beams in Series "A". The beam had dimensions of 3500mm length (L), 700mm width ( $b_w$ ), and 350mm height (h). The design details and check are summarized in Tables A.1 to A.5. Moreover, a brief outline of the design details is concluded in Sections A and B below.



**Table A.1:** Flexural Reinforcement for the Beams in Series "A".

Beam	M	As,req.	T. Reinf.	As,prov.	$\rho_s$	As,max.	$\rho_{s,act.}$	As,min.	x	s	As'	C. Reinf.	$\rho_{s'}$
	kN.m	mm <sup>2</sup>		mm <sup>2</sup>	%	mm <sup>2</sup>	%	mm <sup>2</sup>	mm	mm	mm <sup>2</sup>		%
ECC2	420	3816	<b>8Φ25mm</b>	3928	<b>1.82</b>	9800	1.60	319	177	142	471	<b>6Φ10mm</b>	<b>0.221</b>
ECC3	420	3816	<b>8Φ25mm</b>	3928	<b>1.82</b>	9800	1.60	319	177	142	471	<b>6Φ10mm</b>	<b>0.221</b>

**Table A.2:** Beam-Shear (One-Way) Reinforcement & Spacing for the Beams in Series "A".

Beam	V <sub>Ed</sub>	V <sub>Rd,max.</sub>	V <sub>Rd,c</sub>	V <sub>Rd,s</sub>	V <sub>Rd,d</sub>	Shear Reinf.	A <sub>v</sub>	SL	S <sub>w</sub>	$\rho_v$	$\nu$
	kN	kN	kN	kN	kN		mm <sup>2</sup>	mm	mm	%	N/mm <sup>2</sup>
ECC2	300	1293	194	133	<b>327</b>	<b>4-LegsΦ8mm</b>	201	<b>180</b>	<b>300</b>	0.16	0.80
ECC3	300	1293	194	200	<b>394</b>	<b>6-LegsΦ8mm</b>	302	<b>180</b>	<b>122</b>	0.24	1.20

**Table A.3:** Punching-Shear (Two-Way) Check for the Beams in Series "A".

Beam	V <sub>Ed</sub>	x = C <sub>p</sub>	y = b <sub>p</sub>	u	v <sub>Rd</sub>	v <sub>Rd,c</sub>	v <sub>Ed,p</sub>
	kN	mm	mm	mm	N/mm <sup>2</sup>	N/mm <sup>2</sup>	N/mm <sup>2</sup>
ECC2	300	150	350	5864	6.72	0.54	<b>0.19</b>
ECC3	300	150	350	5864	6.72	0.54	<b>0.19</b>

**Table A.4:** Calculations of Deflections for the Beams in Series "A" at P<sub>d</sub> = 600 kN.

Beam	k	I	1/r <sub>b</sub>	a	a (Test)
		mm <sup>4</sup>		mm	mm
ECC2	0.125	2501*10 <sup>6</sup>	5.99*10 <sup>-6</sup>	<b>5.9</b>	<b>3.14</b>
ECC3	0.125	2501*10 <sup>6</sup>	5.99*10 <sup>-6</sup>	<b>5.9</b>	<b>9.44</b>

**Table A.5:** Calculations of Crack Widths for the Beams in Series "A" at P<sub>d</sub> = 600 kN.

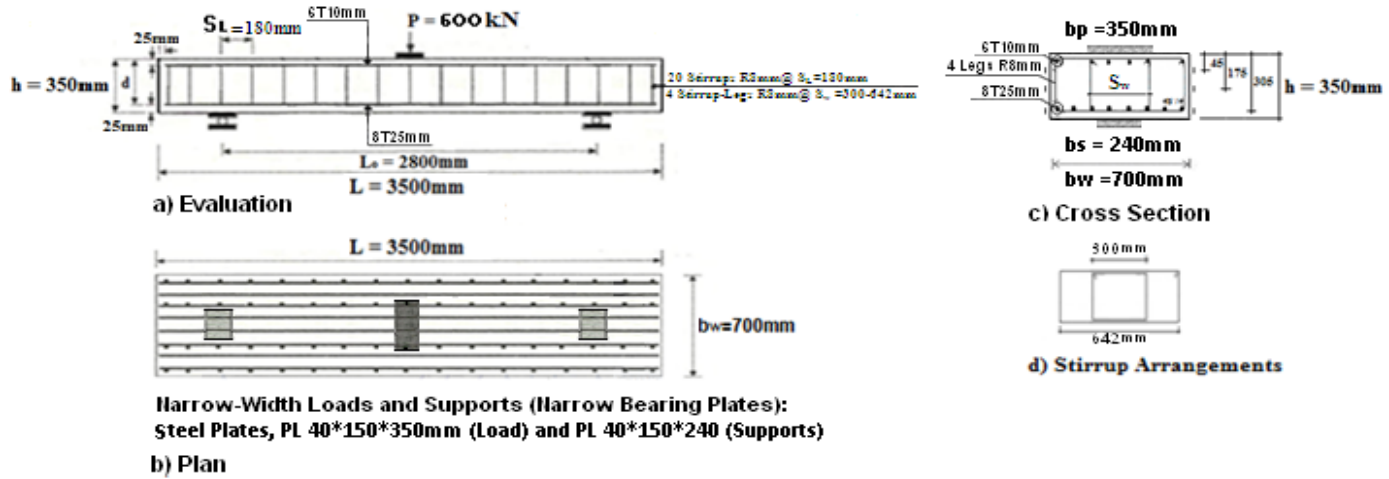
Beam	S <sub>r,max.</sub>	$\epsilon_{sm} - \epsilon_{cm}$	w <sub>k</sub>	w <sub>k</sub> (Test)
			mm	mm
ECC2	244	1.3*10 <sup>-3</sup>	<b>0.318</b>	<b>0.50</b>
ECC3	244	1.3*10 <sup>-3</sup>	<b>0.318</b>	<b>0.27</b>

## NOTES:

- 1) The mid-span deflections and flexural crack-widths, which are shown in Tables A.4 and A.5, were measured during the tests at a load level equals to the design load of 600 kN.
- 2) Beam ECC2 failed in shear at 985 kN, while beam ECC3 failed in flexure at 1000 kN.

**A. Design Calculations of Beam ECC2**

<p><b>Summary of the design of EC2 wide beam (Beam ECC2)</b>  USE: b<sub>w</sub> = 700mm, h = 350mm  <b>Tensile Reinforcement:</b> 8T25mm  <b>Compression Reinforcement:</b> 6T10mm  <b>Shear Reinforcement</b>  Maximum Spacing of Stirrups along the member length:  USE: 20 stirrupsR8mm@S<sub>L,max.</sub>=180mm, at centre spacing (C/C)  Maximum Spacing of Stirrups across the member width:  USE: 4 stirrup LegsR8mm@S<sub>w,max.</sub>=300mm, and 642mm, at centre spacing (C/C)</p>
---



**Details of Beam ECC2**

Various scales are used to show the sections and details

**Figure A.8:** Design Details and Reinforcement Drawing of Beam ECC2 in Series "A".

**Table A.6:** Bar Bending Schedule for Beam ECC2 in Series "A".

Beam Type	Reinf. Type	Reinf. Size	No. of Units	No. in Each	Total No.	Length mm	Shape Code	A – C mm	B – D mm
Beam ECC2	T.R	T25	8	1	8	3450	_____	3450 – 0	---
	C.R	T10	6	1	6	3450	_____	3450 – 0	---
	S.R	R8	1	20	20	1960 1264	[_____] [_____]	650-30 302-30	300-30 300-30

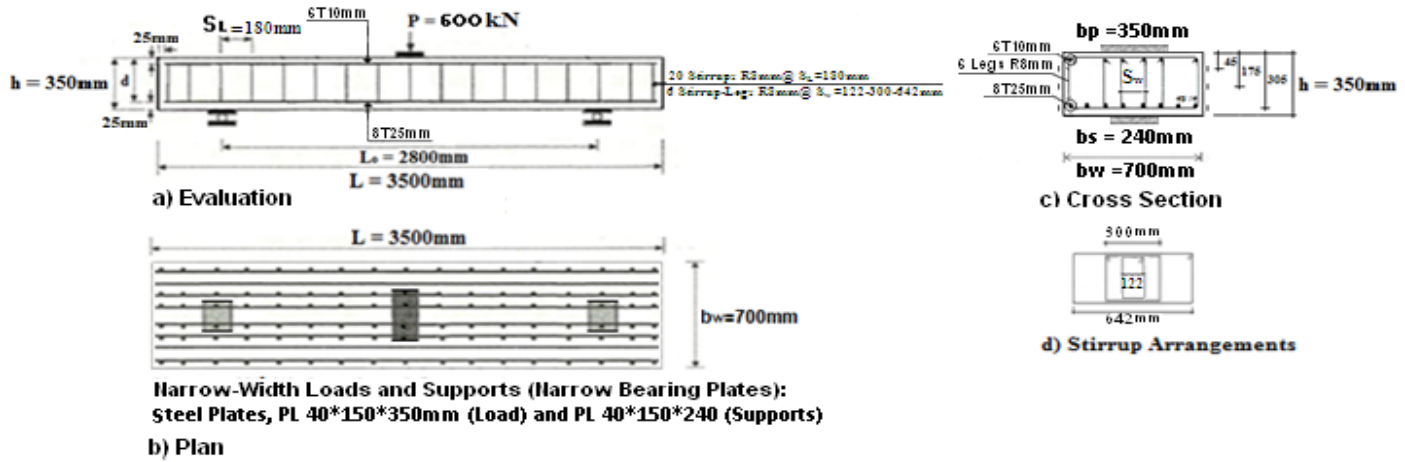
**T.R** = Tensile Reinforcement, **C.R**= Compressive Reinforcement, and **S.R**= Shear Reinforcement

**NOTES:**

- Cover to Stirrups (links) is 25mm for beam ECC2.
- Cover to main Reinforcement is 33mm for beam ECC2.
- Stirrups along the member length, 20 links R8mm@ SL=180mm for beam ECC2.
- Stirrups across the member width, 4 stirrup-legs R8mm@ Sw=300-642mm for beam ECC2.

**B. Design Calculation of Beam ECC3**

<p><b>Summary of the design of EC2 wide beam (Beam ECC3)</b>          USE: <math>b_w = 700\text{mm}</math>, <math>h = 350\text{mm}</math>  <b>Tensile Reinforcement:</b> 8T25mm  <b>Compression Reinforcement:</b> 6T10mm  <b>Shear Reinforcement</b>          Maximum Spacing of Stirrups along the member length:          USE: 20 stirrups R8mm@<math>S_{L,max.}=180\text{mm}</math>, at centre spacing (C/C)          Maximum Spacing of Stirrups across the member width:          USE: 6 stirrup Legs R8mm@<math>S_{w,max.} = 122\text{mm}</math>, 300mm, and 642mm, at centre spacing (C/C)</p>
--



**Details of Beam ECC3**

Various scales are used to show the sections and details

**Figure A.9:** Design Details and Reinforcement Drawing of Beam ECC3 in Series "A".

**Table A.7:** Bar Bending Schedule for Beam ECC3 in Series "A".

Beam Type	Reinf. Type	Reinf. Size	No. of Units	No. in Each	Total No.	Length mm	Shape Code	A – C mm	B – D mm
Beam ECC3	T.R	T25	8	1	8	3450	—————	3450 – 0	---
	C.R	T10	6	1	6	3450	—————	3450 – 0	---
	S.R	R8	1	20	20	1960	[—————]	650-30	300-30
						1264	[———]	302-30	300-30
					916	[—]	128-30	300-30	

**T.R** = Tensile Reinforcement, **C.R**= Compressive Reinforcement, and **S.R**= Shear Reinforcement

**NOTES:**

- Cover to Stirrups (links) is 25mm for beam ECC3.
- Cover to main Reinforcement is 33mm for beam ECC3.
- Stirrups along the member length, 20 links R8mm@ SL=180mm for beam ECC3.
- Stirrups across the member width, 6 stirrup-legs R8mm@ Sw=122-300-642mm for beam ECC3.

Figure A.10 shows an example of the shape Code and the notations (A, B, C and B) for flexural and shear reinforcements.

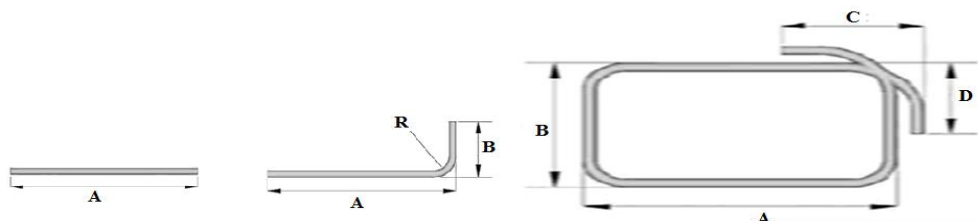


**Figure A.10:** Shape Codes of the Reinforcing Steel Bars.

### 3. Material Quantities

The concrete quantities used in the cast were calculated. Each beam had dimensions of 700\*350\*3500 mm, while each cube had dimensions of 100x100x100mm and each cylinder had dimensions of 150mm diameter x 300mm height. Table A.8 shows the volumes for the concrete used in the laboratory study for the beams, cubes and cylinders.

**Table A.8:** Concrete Quantities of the Beams in Test-Series "A".

Specimens	Width, m	Depth, m	Length, m	Volume, m <sup>3</sup>	No. of Specimens	Total Volume, m <sup>3</sup>
<b>Beam</b>	0.700	0.350	3.500	0.86	2	<b>1.72</b>
<b>Cube</b>	0.100	0.100	0.100	0.001	6	<b>0.006</b>
<b>Cylinder</b>	0.150	-	0.300	0.005	6	<b>0.03</b>
<b>Total Volume, m<sup>3</sup></b>						<b>1.76</b>

Note: The total concrete volume for the beams, cubes and cylinders used in Test Series "A" is approximately 1.8 m<sup>3</sup>. The concrete quantity was increased from 0.50 to 1 m<sup>3</sup> before the ordering of the concrete.

The steel quantities for the tensile, compression and shear reinforcements of both beams were calculated. Table A.9 shows the quantities of the steels for both flexural and shear reinforcements used in the experimental study for the beams. Moreover, the steel density was 7850 kg/m<sup>3</sup>, whereas the weight of the steel per unit length (W) is expressed as (kg/m). It is calculated as the density of steel times the cross-section area of the bar, to get:

$$W \text{ (Kg/m)} = D * A_{s1} = D * (\pi * \Phi^2 / 4) * 10^{-6} = [0.006166 * \Phi^2].$$

Where, D = Density of steel, kg/m<sup>3</sup>, A<sub>s1</sub> = Cross section area of the steel bar,  $\Phi$  = Diameter of steel bar, mm.

**The steel weight per unit length (W) is taken as:**

W = 3.854 kg/m for steel diameter,  $\Phi$  = 25mm [tensile reinforcement].

W = 0.617 kg/m for steel diameter,  $\Phi$  = 10mm [compression reinforcement].

W = 0.395 kg/m for steel diameter,  $\Phi$  = 8mm [shear reinforcement].

**The total weight of each steel bar size is summed as following:**

212.80 kg for steel diameter,  $\Phi$  = 25mm [tensile reinforcement].

25.60 kg for steel diameter,  $\Phi$  = 10mm [compression reinforcement].

58.20 kg for steel diameter,  $\Phi$  = 8mm [shear reinforcement].

**Table A.9:** Flexural and Shear Reinforcement Quantities of the Beams in Test-Series "A".

Beam	Tensile Reinforce.	Compressive Reinforce.	Shear Reinforce. Along the Length	Shear Reinforce. Across The Width	Length, m Width, m Height, m	Total Weight of Steel, kg		
						T. R.	C. R.	S. R.
Beam ECC2	8T25mm	6T10mm	20LinksR8mm @180mm	4 LegsR8mm @300-642mm	3.500 0.700 0.350	106.4	12.8	10.0+15.5 = 25.5
Beam ECC3	8T25mm	6T10mm	20LinksR8mm @180mm	6 LegsR8mm @122-300-642mm	3.500 0.700 0.350	106.4	12.8	7.2+10.0 +15.5 = 32.7
<b>Total Weight, kg</b>						<b>212.80</b>	<b>25.60</b>	<b>58.20</b>

T.R. = Flexural Tensile Reinforcement, C.R. = Flexural Compressive Reinforcement, and S.R. = Shear Reinforcement

#### 4. Compression and Tensile Tests of Concrete

**Table A.10:** Actual Concrete Strengths for Series "A".

Control Sample	Dimensions, mm*mm*mm	Weight, kg	Density, kg/m <sup>3</sup>	Load, kN	Correct. Load, kN	Strength, fc, N/mm <sup>2</sup>
<b>Actual Concrete Cube Compressive Strengths at 140 days, fcu</b>						
1	101*100*102	2.46	2388	590.4	560.7	56.07
2	99*103*101	2.39	2320	582.3	552.9	54.22
3	100*101*100	2.43	2406	581.1	551.8	54.63
4	100*102*99	2.42	2396	577.2	548.1	53.74
5	100*100*102	2.39	2343	615.1	584.2	58.42
6	101*99*101	2.39	2366	621.4	590.6	59.06
Average	--	--	<b>2371</b>	--	--	<b>56.0</b>
<b>Actual Concrete Cylinder Compressive Strengths at 140 days, fc</b>						
1	150*301	12.77	2400	727.2	799.92	45.27
2	152*303	13.28	2414	740.8	814.88	44.91
Average	--	--	<b>2407</b>	--	--	<b>45.0</b>
<b>Actual Concrete Cylinder Split Strengths, fet, L = 300mm</b>						
1	151*302	13.26	2451	201.6	221.75	3.10
2	150*300	12.71	2397	237.4	261.15	3.70
Average	--	--	<b>2424</b>	--	--	<b>3.40</b>

Test-Series (A): Date of Casting: 24 November 2011, Date of Testing: 11 April 2012.

$f_{ct} = 2P/(3.142*d*L) = 0.637*P/(d*L)$ . D is the cylinder diameter and L is the cylinder height.

**Table A.11:** Material Properties used to Predict and Analyze the Beams in Series "A".

	Properties	Series (A)
Concrete	Cylinder Compressive Strength (fc), MPa	45
	Cube Compressive Strength (fcu), MPa	56
	Cylinder Split Tensile Strength (ft), MPa	3.40
	Young's Modulus (Ec), MPa	31000
Flexural Reinforcement	Yield Strength for Φ25mm (fy), MPa	525
	Yield Strength for Φ10mm (fy), MPa	517
	Young's Modulus (Es), MPa	200000
Shear Reinforcement	Yield Strength for Φ8mm (fyv), MPa	512
	Young's Modulus (Es), MPa	200000

## 5. Tensile Tests of Steel

**Table A.12:** Results of Indirect Tensile Stress Test For Reinforcing Steel Bars in Series "A".

Test	Maximum Load (P), KN		Stress ( $\sigma=P/A$ ), N/mm <sup>2</sup>		Extension ( $\Delta$ ), mm	Ultimate Strain ( $\epsilon_u = \Delta/L$ ), mm/mm	Ultimate Elastic Modulus ( $E_s$ ), N/mm <sup>2</sup>
	Yield	Ultimate	Yield	Ultimate			
<b>For <math>\Phi 25</math>mm bars (<math>A = 483.1\text{mm}^2</math>, <math>L = 500\text{mm}</math>)</b>							
1	256.7	303.3	531.4	627.8	60	0.12	<b>200000</b>
2	250.5	312.4	518.5	646.6	55	0.11	
<b>Average</b>	--	--	<b>524.95</b>	<b>637.2</b>	--	<b>0.115</b>	
<b>For <math>\Phi 10</math>mm bars (<math>A = 73.9\text{mm}^2</math>, <math>L = 500\text{mm}</math>)</b>							
1	37.7	45.5	510.1	615.7	47	0.09	<b>200000</b>
2	38.7	48.1	523.9	650.8	50	0.10	
<b>Average</b>	--	--	<b>517.0</b>	<b>633.2</b>	--	<b>0.095</b>	
<b>For <math>\Phi 8</math>mm bars (<math>A = 49.1\text{mm}^2</math>, <math>L = 500\text{mm}</math>)</b>							
1	24.2	29.4	492.9	598.8	31	0.06	<b>200000</b>
2	26.1	31.2	531.5	635.4	35	0.07	
<b>Average</b>	--	--	<b>512.2</b>	<b>617.1</b>	--	<b>0.065</b>	

Date of Testing: January/2012.

**Table A.13:** Tensile Strength and Strain of Reinforcing Steel Bars in Series "A".

Bar Type	Nominal Diameter, (mm)	Measured Diameter, (mm)	Measured Area, (mm <sup>2</sup> )	Strength, (N/mm <sup>2</sup> )		Young's Modulus, (N/mm <sup>2</sup> )	Strain, (mm/mm)	
				Yield ( $f_y$ )	Ultimate		Yield ( $\epsilon_s$ )	Ultim.
$\Phi 25$	25	24.8	483.1	<u>525</u>	637	200000	0.002625	0.003185
$\Phi 10$	10	9.7	73.9	<u>517</u>	633	200000	0.002585	0.003165
$\Phi 8$	8	7.9	49.1	<u>512</u>	617	200000	0.00256	0.003085

Date of Testing: January/2012.

$$x = [\epsilon_c / (\epsilon_c + \epsilon_s)] * d, s = \lambda * x = 0.8x, \text{ and } Z = d - (s/2).$$

$$\epsilon_{cu} = \epsilon_c = 0.0035, \epsilon_{max} = 0.0050, \epsilon_s = f_y / E_s = (1/\gamma_s) * f_{yk} / E_s < \epsilon_{max}, \epsilon_y = [(d-x)/x] * \epsilon_{cu} < \epsilon_{max}.$$

$$\epsilon_s < \epsilon_{max} = 0.0050, \text{ O.K., i.e. the tension steel has yielded}$$

$$\epsilon_s < \epsilon_y = ??, \text{ O.K., } (f_y = f_{yk} = ? \text{ N/mm}^2), \text{ i.e. the tension steel has yielded}$$

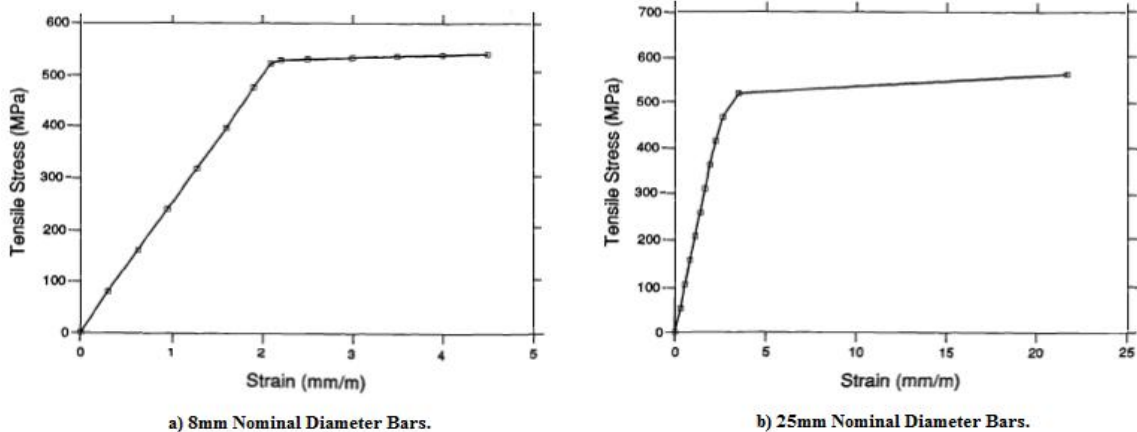


**Figure A.11:** Typical Stress-Strain Curves for Steel Reinforcement Bars in Series "A": a) 8mm Nominal Diameter Bars, and b) 25mm Nominal Diameter Bars.

#### A.4: Prediction of Wide Beams [Beam ECC2 and ECC3]

The prediction procedure used in the the EC2 Code was applied for the two beams in Series "A".  
The prediction methods and check are shown as following:

##### 1. Beam ECC2

###### 1) Design Strengths:

$P_d = 600 \text{ kN}$ ,  $M = 420 \text{ kN.m}$ , and  $V = 300 \text{ kN}$ .

###### 2) Unity of all Factors of Safety:

$1/\gamma_m = 1.0$ , for flexure and shear.

###### 3) Actual Beam Dimensions:

$b_w = 708 \text{ mm}$ ,  $h = 353 \text{ mm}$ ,  $d = 304 \text{ mm}$ ,  $L = 3500 \text{ mm}$ ,  $L_o = 2800 \text{ mm}$ , and  $a = 1400 \text{ mm}$ .

###### 4) Actual Materral Strengths:

$f_{c,act.} = 45 \text{ N/mm}^2$ ,  $f_{y,act.} = 525 \text{ N/mm}^2$ ,  $f_{yv,act.} = 512 \text{ N/mm}^2$ , and  $E_s = 200,000 \text{ N/mm}^2$ .

###### 5) Reinforcement Details as Built:

###### Tensile Reinforcement:

8T25mm,  $A_{s,prov.} = A_{s,prov.}(8\Phi 25 \text{ mm}) = N_s * A_{s1} = 3927 \text{ mm}^2$ .  $\rho_{s,prov.} = (A_{s,prov.}/b_w.d) = (3927/708*304) = 1.82\%$ .

###### Compression Reinforcement:

6T10mm,  $A_{s',prov.} = 472 \text{ mm}^2$ .  $\rho_{s',prov.} = (A_{s',prov.}/b_w.d) = (472/708*304) = 0.221\%$ .

###### Shear Reinforcement:

Shear reinforcement along the member length:

20 stirrups R8mm@ $S_{L,max.} = 180 \text{ mm}$ , at centre spacing (C/C)

Shear reinforcement across the member width:

$A_{v,prov.} = 201 \text{ mm}^2$ , 4 stirrup Legs-R8mm@ $S_{w,max.} = 300 \text{ mm}$  and  $642 \text{ mm}$ , at centre spacing (C/C).

#### A. Predicted Flxural Failure Load

$A_{s,prov.} = \text{Total area of flexural reinforcement provided} = A_{s,prov.}(8\Phi 25 \text{ mm}) = N_s * A_{s(1)} = 3927 \text{ mm}^2$

$jd = Z = \text{Lever arm} = d - (s/2)$

Where,  $s = \text{Depth of equivalent rectangular stresses block of concrete stress } (0.85f_c) = \lambda * x$

$\lambda = 0.8$  for  $f_{c,act.} \leq 50 \text{ N/mm}^2$ .  $\lambda = 0.8 - [(f_c - 50)/400]$  for  $50 \text{ N/mm}^2 < f_{c,act.} \leq 90 \text{ N/mm}^2$ .

$x = \text{Distance from extreme compression fibre to Neutral Axis. (N.A.)} = [\epsilon_c / (\epsilon_c + \epsilon_s)] * d$

Where,  $\epsilon_{cu} = \epsilon_c = 0.0035$ ,  $\epsilon_{max.} = 0.0050$ , and  $\epsilon_s = f_{y,act.}/E_s = 0.002625 < \epsilon_{max.}$ .

**Hence:**  $x = 173.7\text{mm}$ ,  $\epsilon_y = [(d-x)/x] * \epsilon_{cu} = 0.263 < \epsilon_{max.}$ ,  $s = \lambda * x = 0.8 * 173.7 = 139\text{mm}$ ,  $Z = 234.5\text{mm}$ .

Hence:  $M_u = A_{s,prov.} * f_{y,act.} * Z = 483 \text{ kN.m}$

Hence:  $M_u = 483 \text{ kN}$ ,  $V_u = M_u / a = 483 / 1.4 = 345 \text{ kN}$ ,  $P_u = 2 * V_u = 690 \text{ kN}$

**Hence: Predicted Failure Load =  $P_{f,pred.} \approx 690 \text{ kN} > P_d = 600 \text{ kN}$**

### Or Another Method as:

$F_c = \text{Total compressive force in Concrete} = (0.85 * f_{c,act.}) * s * b_w = 3764 \text{ kN}$

$F_s = \text{Total tensile force in Reinforcement} = f_{y,act.} * A_{s,prov.} = 2062 \text{ kN}$

$M = F_c * Z = F_s * Z$ , **hence:**  $M = 883 \text{ kN.m}$  (for concrete), or  $M = 483 \text{ kN.m}$  (for steel).

**Hence:**  $M_u = M_{small}$  (which is for steel)  $= 483 \text{ kN}$ ,  $V_u = M_u / a = 483 / 1.4 = 345 \text{ kN}$ ,  $P_u = 2 * V_u = 690 \text{ kN}$

**Hence: Predicted Failure Load =  $P_{f,pred.} \approx 690 \text{ kN} > P_d = 600 \text{ kN}$**

## B. Predicted One-Way Shear Failure Load

### Strut Inclination Method (SIM)

$\alpha = 90^\circ$  for vertical stirrups (links), hence:  $\sin \alpha = 1.0$ . Assume:  $\theta = 45^\circ$ , hence:  $\cot(\theta) = 1.0$ .

$V_c = V_{Rd,c} = [(0.18) * (1 + \sqrt{200/d}) * (100 \rho_s * f_{c,act.})^{1/3} + 0.15 \sigma_{cp}] * b_w * 0.9d = 274 \text{ kN}$ .

OR  $V_c = V_{Rd,c} = \{ [0.25 * (0.21 * (f_{c,act.} - 8)^{2/3})] * (1.6 - (d/1000)) * (1.2 + 40 \rho_{s,prov.}) + 0.15 \sigma_{cp} \} * b_w * d = 313 \text{ kN}$ .

$V_{Rd,c} \geq [(0.035 * (1 + \sqrt{200/d})^{3/2} * f_{c,act.}^{1/2}) + 0.15 \sigma_{cp}] * b_w * 0.9d = 111 \text{ kN}$ .

$V_{Rd,max.} = [(0.6 [1 - (f_{c,act.}/250)] * f_{c,act.}) / (\cot(\theta) + \tan(\theta))] * b_w * 0.9d = 2144 \text{ kN} \geq V = 300 \text{ kN}$

$V_s = V_{Rd,s} = [A_{v,prov.} * f_{yv,act.} * 0.9d * \cot(\theta)] / S_L = 156 \text{ kN}$ .

$V_u = V_{Rd,d} = V_{Rd,c} + V_{Rd,s} = V_c + V_s = 274 + 156 = 430 \text{ kN} \geq V = 300 \text{ kN}$ .

Hence:  $V_u = 430 \text{ kN}$ ,  $P_u = 2 * V_u = 860 \text{ kN}$

**Hence: Predicted Failure Load =  $P_{f,pred.} \approx 860 \text{ kN} > P_d = 600 \text{ kN}$**

## C. Final Predicted Failure Load and Mode for Beam ECC2

The final predicted failure load for beam ECC2 is the lesser load obtained from flexural and shear strengths, and the predicted failure mode is the mode which is corresponding to the lesser predicted load. Accordingly, the predicted failure load and mode for beam ECC2 are as follows:

**Predicted Failure Load ( $P_{f,pred.}$ ) = 690 kN.**

**Predicted Failure Mode = Flexural Failure-Mode.**



## 2. Beam ECC3

### 1) Design Strengths:

$P_d = 600 \text{ kN}$ ,  $M = 420 \text{ kN.m}$ , and  $V = 300 \text{ kN}$ .

### 2) Unity of all Factors of Safety:

$1/\gamma_m = 1.0$ , for flexure and shear.

### 3) Actual Beam Dimensions:

$b_w = 708 \text{ mm}$ ,  $h = 353 \text{ mm}$ ,  $d = 304 \text{ mm}$ ,  $L = 3500 \text{ mm}$ ,  $L_o = 2800 \text{ mm}$ , and  $a = 1400 \text{ mm}$ .

### 4) Actual Material Strengths:

$f_{c,act.} = 45 \text{ N/mm}^2$ ,  $f_{y,act.} = 525 \text{ N/mm}^2$ ,  $f_{yv,act.} = 512 \text{ N/mm}^2$ , and  $E_s = 200,000 \text{ N/mm}^2$ .

### 5) Reinforcement Details as Built:

#### Tensile Reinforcement:

8T25mm,  $A_{s,prov.} = A_{s,prov.}(8\Phi 25 \text{ mm}) = N_s * A_{s1} = 3927 \text{ mm}^2$ .  $\rho_{s,prov.} = (A_{s,prov.}/b_w.d) = (3927/708*304) = 1.82\%$ .

#### Compression Reinforcement:

6T10mm,  $A_{s',prov.} = 472 \text{ mm}^2$ .  $\rho_{s',prov.} = (A_{s',prov.}/b_w.d) = (472/708*304) = 0.221\%$ .

#### Shear Reinforcement:

Shear reinforcement along the member length:

20 stirrups R8mm @  $S_{L,max.} = 180 \text{ mm}$ , at centre spacing (C/C)

Shear reinforcement across the member width:

$A_{v,prov.} = 302 \text{ mm}^2$ , 6 stirrup Legs R8mm @  $S_{w,max.} = 122 \text{ mm}$ , 300mm, 642mm, at centre spacing (C/C)

## A. Predicted Flexural Failure Load

$A_{s,prov.} = \text{Total area of flexural reinforcement provided} = A_{s,prov.}(8\Phi 25 \text{ mm}) = N_s * A_{s(1)} = 3927 \text{ mm}^2$

$j d = Z = \text{Lever arm} = d - (s/2)$

Where,  $s = \text{Depth of equivalent rectangular stresses block of concrete stress } (0.85f_c) = \lambda * x$

$\lambda = 0.8$  for  $f_{c,act.} \leq 50 \text{ N/mm}^2$ .  $\lambda = 0.8 - [(f_c - 50)/400]$  for  $50 \text{ N/mm}^2 < f_{c,act.} \leq 90 \text{ N/mm}^2$ .

$x = \text{Distance from extreme compression fibre to Neutral Axis. (N.A.)} = [\epsilon_c / (\epsilon_c + \epsilon_s)] * d$

Where,  $\epsilon_{cu} = \epsilon_c = 0.0035$ ,  $\epsilon_{max.} = 0.0050$ , and  $\epsilon_s = f_{y,act.}/E_s = 0.002625 < \epsilon_{max.}$ .

**Hence:**  $x = 173.7 \text{ mm}$ ,  $\epsilon_y = [(d-x)/x] * \epsilon_{cu} = 0.263 < \epsilon_{max.}$ ,  $s = \lambda * x = 0.8 * 173.7 = 139 \text{ mm}$ ,  $Z = 234.5 \text{ mm}$ .

Hence:  $M_u = A_{s,prov.} * f_{y,act.} * Z = 483 \text{ kN.m}$

Hence:  $M_u = 483 \text{ kN}$ ,  $V_u = M_u / a = 483 / 1.4 = 345 \text{ kN}$ ,  $P_u = 2 * V_u = 690 \text{ kN}$

**Hence: Predicted Failure Load =  $P_{f,pred.} \approx 690 \text{ kN} > P_d = 600 \text{ kN}$**

**Or Another Method as:**

$F_c = \text{Total compressive force in Concrete} = (0.85 \cdot f_{c,act.}) \cdot s \cdot b_w = 3764 \text{ kN}$

$F_s = \text{Total tensile force in Reinforcement} = f_{y,act.} \cdot A_{s,prov.} = \mathbf{2062 \text{ kN}}$

$M = F_c \cdot Z = F_s \cdot Z$ , **hence:**  $M = 883 \text{ kN.m}$  (for concrete), or  $M = 483 \text{ kN.m}$  (for steel).

**Hence:  $M_u = M_{small}$**  (which is for steel)  $= 483 \text{ kN}$ ,  $V_u = M_u / a = 483 / 1.4 = 345 \text{ kN}$ ,  $P_u = 2 \cdot V_u = 690 \text{ kN}$

**Hence: Predicted Failure Load =  $P_{f,pred.} \approx 690 \text{ kN} > P_d = 600 \text{ kN}$**

## **B. Predicted Shear Failure Load**

### **Strut Inclination Method (SIM)**

$\alpha = 90^\circ$  for vertical stirrups (links), hence:  $\sin \alpha = 1.0$ . Assume:  $\theta = 45^\circ$ , hence:  $\cot(\theta) = 1.0$ .

$V_c = V_{Rd,c} = [(0.18) \cdot (1 + \sqrt{200/d}) \cdot (100 \rho_s \cdot f_{c,act.})^{1/3} + 0.15 \sigma_{cp}] \cdot b_w \cdot 0.9d = \mathbf{274 \text{ kN}}$ .

OR  $V_c = V_{Rd,c} = \{ [0.25 \cdot (0.21 \cdot (f_{c,act.} - 8)^{2/3})] \cdot (1.6 - (d/1000)) \cdot (1.2 + 40 \rho_{s,prov.}) + 0.15 \sigma_{cp} \} \cdot b_w \cdot d = 313 \text{ kN}$ .

$V_{Rd,c} \geq [(0.035 \cdot (1 + \sqrt{200/d})^{3/2} \cdot f_{c,act.}^{1/2}) + 0.15 \sigma_{cp}] \cdot b_w \cdot 0.9d = 111 \text{ kN}$ .

$V_{Rd,max.} = [(0.6 [1 - (f_{c,act.}/250)] \cdot f_{c,act.}) / (\cot(\theta) + \tan(\theta))] \cdot b_w \cdot 0.9d = 2144 \text{ kN} \geq V = 300 \text{ kN}$

$V_s = V_{Rd,s} = [A_{v,prov.} \cdot f_{yv,act.} \cdot 0.9d \cdot \cot(\theta)] / S_L = \mathbf{235 \text{ kN}}$ .

$V_u = V_{Rd,d} = V_{Rd,c} + V_{Rd,s} = V_c + V_s = 274 + 235 = \mathbf{509 \text{ kN}} \geq V = 300 \text{ kN}$ .

**Hence:  $V_u = 509 \text{ kN}$ ,  $P_u = 2 \cdot V_u = 1018 \text{ kN}$**

**Hence: Predicted Failure Load =  $P_{f,pred.} \approx 1018 \text{ kN} > P_d = 600 \text{ kN}$**

## **C. Final Predicted Failure Load and Mode for Beam ECC2**

The final predicted failure load for beam ECC3 is the lesser load obtained from flexural and shear strengths, and the predicted failure mode is the mode which is corresponding to the lesser predicted load. Accordingly, the predicted failure load and mode for beam ECC3 are as follows:

**Predicted Failure Load ( $P_{f,pred.}$ ) = 690 kN.**

**Predicted Failure Mode = Flexural Failure-Mode.**

### 3. Check of Two-Way Shear (Punching-Shear) Stress

$$v_p = \beta * V_{Ed} / (u * d) \leq v_{Rd,c}$$

$$u = \text{Critical Perimeter} = (2 * dx) + (2 * dy) = 2(x + 4d) + 2(y + 4d) = 2732 + 3132 = 5864 \text{ mm.}$$

Where  $x = C_p = 150 \text{ mm}$  and  $y = b_p = 350 \text{ mm}$  are the plan dimensions of a rectangular load (support) area. The sides of the critical section for failure cone of punching shear are taken to be geometrically similar to the loaded area and located at a distance  $2d$ .

If  $v_p \leq v_{Rd,c} = C_{Rd,c} * k * (100\rho_1 * f_{ck})^{1/3} = 0.84 \text{ MPa}$ : hence the punching shear reinforcement is not required

If  $v_p > v_{Rd} = 0.30 * (f_{ck} / \gamma_c) * [1.0 - (f_{ck} / 250)] = 11.07 \text{ MPa}$ : hence the member section should be changed

If  $v_p > v_{Rd,c} = C_{Rd,c} * k * (100\rho_1 * f_{ck})^{1/3} = 0.84 \text{ MPa}$ : hence the punching shear reinforcement is required.

$$v_{Rd} = 0.30 * (f_{c,act.}) * [1.0 - (f_{c,act.} / 250)] = 11.07 \text{ MPa}$$

$$v_{Rd,c} = C_{Rd,c} * k * (100\rho_1 * f_{c,act.})^{1/3} = 0.84 \text{ MPa}$$

$$C_{Rd,c} = 0.18 / \gamma_c = 0.18$$

$$k = 1.0 + \sqrt{(200/d)} = 1.81.$$

$$\rho_1 = \sqrt{[(A_{sx} / (b_w * dx)) * (A_{sy} / (b_w * dy))]} = 0.00384 = 0.384\%,$$

Where  $A_{sx} \approx A_{sy} = A_{s,prov.} = 3927 \text{ mm}^2$ ;  $dx = x + 4d = 1366 \text{ mm}$ , and  $dy = y + 4d = 1566 \text{ mm}$

$$A_v = [(v_{Ed} - 0.75 * v_{Rd,c}) * u * S] / [1.5 * f_{ywd,eff.} * n]$$

$$f_{ywd,eff.} = 250 + 0.25d \leq f_{ywd} = f_{yv,k} / \gamma_s = 0.87 f_{yv,k}$$

**Hence:**

$$v_p = 300 * 10^3 / (5864 * 304) = 0.168 \text{ N/mm}^2 \leq v_{Rd,c} = 0.18 * 1.81 * (0.384 * 45)^{1/3} = 0.84 \text{ N/mm}^2.$$

Where  $\beta$  is taken as 1.0.

**Hence:** the punching shear reinforcement is not required; therefore, no prediction for punching shear.

Where  $v_p$  is the design punching shear stress at the critical punching shear section (it will usually be the support reaction at the ultimate limit state),  $S$  is shear reinforcement spacing,  $2d$  to EC2,  $\beta$  is equal 1.15 for interior column case; 1.40 for edge column case; and 1.50 for corner column case, and all other variables are defined in Chapter 4 and in Appendix A.1.

## **APPENDIX (B): Experimental Work Activities**

### **B.1: Activities to Manufacture the Steel Cages**

1. Prepare working area, and placing of 2 Trestles at correct spacing.
2. Place 2 Trestles opposite each other and placing of two main support links between Trestles.
3. Lift ends of support bars, and slide on all links and space out.
4. Tie links to the bottom reinforcement bars (main tensile bars) on the tension zone.
5. Rotate the cage 180 degrees, and tie on the top reinforcement bars (secondary compression (hanger) bars) on the compression zone.
6. Once cage is complete, turn the cage back to original position and tie on lifting hanger-hooks at both ends.
7. Lift cage using slings tied onto the lifting hanger-hooks and move the cage using Forklift to required position.

#### **Equipments:**

Trestles; sweeping brush; bucket; chalk; measuring tape; wire snips; tying wire; pre bent lifting hooks; 2-lifting slings; forklift; another person.

### **B.2: Activities to Cast the Concrete**

1. Prepare (clear) area for casting, assemble the steel shutters on polythene sheeting using overhead crane.
2. Assemble cube/cylinder moulds, and coat the shutters and cube/cylinder moulds with release oil.
3. Attach concrete cover spacers to the assembled cages, carefully lift and lower the reinforcement cages into shutters.
4. Gather and check all tools needed for cast.

5. On arrival of concrete truck, carefully direct the driver to position vehicle where the chute can distribute the concrete in a controlled manner into the moulds.
6. After moulds have been cast and vibrated, request the driver to dump any excess concrete in designated area.
7. Float off top surface of beams and when the concrete has cured for a few hours, cover with wet hessian and polythene and leave for a minimum of 24 hours before stripping the beam shutters and cube/cylinder moulds.
8. Using overhead crane to lift beams and shutters, and to place into storage area. Shutters and casting site are cleaned.

**Equipments:**

Hand tools (not powered); sweeping brush; overhead crane; lifting chains; polythene sheeting; steel shutters; release oil; cube/cylinder moulds; reinforcement cages; concrete spacers; vibrating poker (110v); transformer; shovels; trowels; floats; ready mix concrete truck; wet concrete; hessian; polythene; water.

**B.3: Activities to Test the Beams**

1. Clear test rig and any obstacles between beam and machine.
2. Place load frame into rig and allow jaws of machine to grip and raise to a safe height.
3. Distribute 4 chains onto lifting hanger-hooks cast into beam and lift the complete test piece over to the rig; placing one end on a roller on the machine surface and other end on top of a tressil sat on the floor.
4. Raise outside end of beam with overhead crane and in a reverse movement let the sample move into the rig with the roller until the lifting hanger-hooks can be used at the other side of the machine.
5. Locate both overhead cranes either side of machine and place chains onto lifting hanger-hooks and lift at the same time onto the billets that will hold the lower load points.

6. Have steel plates and rollers ready to put under beam and mix a cement mortar that will connect with the specimen on the top plates.
7. Lower both ends onto the plates and rollers at the marked points and remove cranes.
8. Place a cement mortar mix onto the above centre point of beam and place a plate and roller on top.
9. The beam should be marked out in a manner which it requires.
10. Deflection dial gauges will then be positioned under the specimen to be as required.
11. A fully trained operator will then start to lower the load frame in a controlled manner on top of the middle roller (loading plate).
12. The test shall now begin with the machine operator loading the beam in the required increments.
13. Once requested increment has been reached (for each incrementally stage), the deflections, concrete strains, main steel strains, stirrup strains, any loading movement by the beam and crack widths will be measured and recorded. This will continue until the predicted failure load has nearly been achieved.
14. Once the beam has failed, the machine operator will raise the crosshead and the clear up operation will begin.

**Equipments:**

Brushes; shovels; overhead crane; test machine; tressil; steel billets; steel plates; rollers; cement; water; bucket; trowel; aroldite glue; demec buttons; pencil; demec spacer bar; deflection dial gauges; forklift.

## APPENDIX (C): Author's Contributions

**The author's contributions shown below have been undertaken in reviews, debates, corrections and revisions:**

### C.1: Technical and Published Works

1. Alluqmani, A. E. 2013a. "Flexural and Shear Behaviour of Wide RC Beams". The Civil Engineering PhD Conference, University of Strathclyde, Glasgow, Scotland-UK. 30 October 2013. This Paper summarizes all Thesis Chapters, with focusing on Chapters (1, 3, 6, 7, 8, 9).
2. Alluqmani, A. E. 2013b. "Development of Detailing and Design Models for Wide Concrete Beams". The Engineering RPD Conference, University of Strathclyde, Glasgow, Scotland-UK. 27 June 2013. 13 pp. This Paper summarizes Chapters (3, 6, 8).
3. Alluqmani, A. E.; and Saafi, M. B. 2014a. "Structural Reinforced Concrete Beams in Shear". The 2014 SSC-07 Conference, University of Edinburgh, Edinburgh, Scotland-UK. ISBN: 9780956904522, Session 11: Engineering, Paper No. ENG 506. 1-2 February 2014. 6 pp. This Paper quotes some of Chapters (1, 2).
4. Alluqmani, A. E.; and Saafi, M. B. 2014b. "The Effect of Bearing Plate Widths on Wide Concrete Member Capacities". The 2014 SSC-07 Conference, University of Edinburgh, Edinburgh, Scotland-UK. ISBN: 9780956904522, Session 12: Engineering, Paper No. ENG 507. 1-2 February 2014. 6 pp. This Paper quotes some of Chapters (1, 3, 6). *This Paper got a Prize of 1000 Sterling Pound and a travel grant.*
5. Alluqmani, A. E.; and Saafi, M. B. 2014c. "New Detailing-Approach and Design-Model for Wide RC Beams". The 16<sup>th</sup> Young Structural Researchers' Conference 2014 (YRC), the Institution of Structural Engineers, London, England-UK. 5 March 2014. This Paper summarizes Chapters (8, 9). *This Paper got a travel grant.*
6. Alluqmani, A. E. 2014. "Design and Behaviour of R.C. Beams to ACI318-and-SBC304; and EC2 Codes When Subjected To Asymmetric Loading". Journal of Engineering, Design and Technology (JEDT), ISSN: 1726-0531, Vol. 12, Issue 2, April-May 2014. pp.158 - 176. This Paper outlines Chapters (2, 3, 4) and quotes some of Chapters (5, 7, 9).

7. Alluqmani, A. E.; and Haldane, D. 2011a. "Design of Reinforced Concrete Beams to ACI318-and-SBC304; and EC2 Codes". COBRA-2011 (RICS) Conference, University of Salford, Manchester, England-UK, ISBN: 978-1-907842-19-1, Section Six, Session 1: Building Technology, Paper No.2150. 12-13 September 2011. pp 459-468. This Paper outlines Chapters (3, 4).

8. Alluqmani, A. E.; and Haldane, D. 2011b. "Structural Design of Reinforced Concrete Beams: Comparison In Accordance With ACI318-and-SBC304; and EC2 Codes". The 5<sup>th</sup> SSIC-2011 Conference, University of Warwick, Coventry, England-UK. ISBN: 978-0-9569045-0-8, Section 5, Session 21: Construction and Architecture, Paper No.21. 23-26 June 2011. 8pp. This Paper outlines Chapters (3, 4, 5). *This Paper was awarded the second best paper in Engineering, and got an iPad and a Prize of 945 Sterling Pound.*

9. Alluqmani, A. E.; and Haldane, D. 2011c. "Structural Behaviour of Reinforced Concrete Beams: Comparison In Accordance With ACI318-and-SBC304; and EC2 Codes". The 5<sup>th</sup> SSIC-2011 Conference, University of Warwick, Coventry, England-UK. ISBN: 978-0-9569045-0-8, Section 5, Session 21: Construction and Architecture, Paper No.22. 23-26 June 2011. 9pp. This Paper quotes some of Chapters (5, 7, 9).

10. Alluqmani, A. E. 2010. "Reinforced Concrete Beams Design: Comparison In Accordance With Saudi Building Code (SBC304) and Eurocode (EC2) Subjected To Asymmetric Loading". MSc Dissertation, Heriot-Watt University. UK. 23 August 2010. 111pp.

## **C.2: Oral Presentations in Conferences**

Presentation 1: "Structural Reinforced Concrete Beams in Shear". The 2014 SSC-07 Conference, University of Edinburgh, Edinburgh, Scotland-UK. 1-2 February 2014.

Presentation 2: "The Effect of Bearing Plate Widths on Wide Concrete Member Capacities". The 2014 SSC-07 Conference, University of Edinburgh, Edinburgh, Scotland-UK. 1-2 February 2014.

Presentation 3: "Flexural and Shear Behaviour of Wide RC Beams". The Civil Engineering PhD Conference, University of Strathclyde, Glasgow, Scotland-UK. 30 October 2013.



Presentation 4: "Development of Detailing and Design Models for Wide Concrete Beams". The Engineering RPD Conference, University of Strathclyde, Glasgow, Scotland-UK. 27 June 2013.

Presentation 5: "Design of Reinforced Concrete Beams to ACI318-and-SBC304; and EC2 Codes". COBRA-2011 (RICS) Conference, University of Salford, Manchester, England-UK. 12-13 September 2011.

Presentation 6: "Structural Design of Reinforced Concrete Beams: Comparison In Accordance With ACI318-and-SBC304; and EC2 Codes". The 5<sup>th</sup> SSIC-2011 Conference, University of Warwick, Coventry, England-UK. 23-26 June 2011.

Presentation 7: "Structural Behaviour of Reinforced Concrete Beams: Comparison In Accordance With ACI318-and-SBC304; and EC2 Codes". The 5<sup>th</sup> SSIC-2011 Conference, University of Warwick, Coventry, England-UK. 23-26 June 2011.

### **C.3: Posters in Conferences**

1. Alluqmani, A. E. 2014. "A New Prediction-Model for Wide Concrete Members". The University Research Day (URD) Conference, University of Strathclyde, Glasgow-UK, 19 June 2014.

2. Alluqmani, A. E. 2011. "Structural Design and Behaviour of R.C. Beams Accordance With the Combined of American and Saudi Building Codes (ACI318-and-SBC304) and EuroCode (EC2)". The Joint Research Institute of Civil & Environmental Engineering Review Visit Conference (JRI-CEE REVIEW VISIT), Heriot-Watt University, Edinburgh-UK, 27-29 June 2011.

### **C.4: Technical Reports on PhD Research Area**

**The following technical reports have been undertaken in reviews, debates, corrections and revisions:**

1. Alluqmani, A. E. "New Models for Design and Prediction the Wide Concrete Beams with Various Loads and Supports". Annual Research Report (3<sup>rd</sup> PhD-Year Report), University of Strathclyde, Glasgow-UK, November 2013, 214 pp.

2. Alluqmani, A. E. "Structural Design and Behaviour of Wide RC Beams". Annual Research Report (2<sup>nd</sup> PhD-Year Report), University of Strathclyde, Glasgow-UK, March 2013, 77 pp.
3. Alluqmani, A. E. "Structural Design and Behaviour of Wide Structural Concrete Members". Annual Research Report (1<sup>st</sup> PhD-Year Report), University of Strathclyde, Glasgow-UK, June 2012, 109 pp.
4. Alluqmani, A. E. "Structural Wide Reinforced Concrete Members". Research Report, Heriot-Watt University, UK, December 2011, 75 pp.

### **C.5: Attendance and Participation in Conferences, Workshops, and Training Courses**

1. The Young Structural Researchers' Conference 2014 (YRC), the Institution of Structural Engineers, London, UK. 5/March/2014.
2. The 2014 SSC-07 Conference at University of Edinburgh, Edinburgh, UK. 12/February/2014.
3. The Civil Engineering PhD Conference at the University of Strathclyde, Glasgow, U.K. 30/October/2013.
4. The Engineering RPD Conference at University of Strathclyde, Glasgow, U.K. 27/June/2013.
5. The University Research Day (URD) Conference at University of Strathclyde, Glasgow, U.K. 6/June/2013.
6. International Development Conference for Scotland and North East England (EWB) at University of Strathclyde, Glasgow, U.K. 1-3/March/2013.
7. The University Research Day (URD) Conference at University of Strathclyde, Glasgow, U.K. 19/June/2014.
8. Engage! Mini-Conference on Becoming an Engaging Researcher (BECE17) at the University of Strathclyde, Glasgow, U.K. 1/May/2014.
9. COBRA-2011 (RICS) Conference at University of Salford, Manchester, U.K. 12-13/September/2011.

10. The Joint Research Institute of Civil & Environmental Engineering Review Visit Conference (JRI-CEE REVIEW VISIT) at Heriot-Watt University, Edinburgh, U.K. 27-29/JUNE/2011.
11. The 6<sup>th</sup> Annual Heriot-Watt Research Conference, SUSTAINABILITY & SURVIVAL: Emerging Technologies and Innovative Ideas for a Promising Future in PG Researcher at Heriot-Watt University, Edinburgh, U.K. 9/June/2011.
12. The 5<sup>th</sup> SSIC-2011 Conference at Warwick University, Coventry, U.K. 23-26/June/2011.
13. Training Session (Parts 1 and 2) on How to write and get published in scientific journals in 2014 SSC-07 Conference at University of Edinburgh, Edinburgh, UK. 12/February/2014.
14. URD Poster Presentation Training Session 1 at the University of Strathclyde, Glasgow, U.K. 22/April/2014.
15. URD Poster Presentation Training Session 2 at the University of Strathclyde, Glasgow, U.K. 13/May/2014.
16. A Session/Course on Writing Winning Research Proposals (BBSR07) at the University of Strathclyde, Glasgow, U.K. 23/April/2014.
17. A Research Seminar: Important Developments in Structural Engineering 1850-1920. The Royal College, University of Strathclyde, Glasgow, U.K. 12/March/2014.
18. A Seminar on Britain's Energy Future: A Geologist View at the University of Strathclyde, Glasgow, UK. 4 March 2013.
19. The Design Workshop at the University of Strathclyde, Glasgow, UK. 13 March 2013.
20. The Department Research Seminar at the University of Strathclyde, Glasgow, UK. 20 March 2013.
21. A Session on Health and Safety induction at the University of Strathclyde, Glasgow, UK. 21 November 2012.
22. Workshop on Geographic Information Systems (GIS) in the 5<sup>th</sup> SSIC-2011 Conference at Warwick University. 23-26/June/2011.

23. Workshop on Mind Mapping in the 5<sup>th</sup> SSIC-2011 Conference at Warwick University. 23-26/June/2011.
24. Workshop on Research Design in the 5<sup>th</sup> SSIC-2011 Conference at Warwick University. 23-26/June/2011.
25. Four Workshops on Getting Started on PhD at Heriot-Watt University, Edinburgh, U.K:  
Getting Started 3: Good Writing Practice: Tuesday 26 October 2010.  
Getting Started 4: Effective Use of Library (Literature Searching): Science and Engineering: Tuesday 2 November 2010.  
Getting Started 5: Critical Thinking: Tuesday 9 November 2010.  
Getting Started 6: Working with your Supervisor: Tuesday 23 November 2010.
26. Three Workshops on Communication Skills at Heriot-Watt University, Edinburgh, U.K:  
Communication Skills 1: Thursday 10 November 2010.  
Communication Skills 2: Thursday 18 November 2010.  
Communication Skills 3: Thursday 25 November 2010.

## BIBLIOGRAPHY

AASHTO. AASHTO-LRFD Bridge Design Specifications and Commentary, 3<sup>rd</sup> Edition. American Association of State Highway Transportation Officials, Washington, DC, 2004. 1264pp.

Abbas, A.; Kotsovos, D. M.; and Pullen, A. D. Wide Beam Stirrup Configurations. *Concrete International*, March 2010.

ACI, American Concrete Institute (ACI-318). Building Code Requirements for Structural Concrete and Commentary. United State of America. 2008. 465 pp. (and versions of 2011 and 2014).

ACI, American Concrete Institute (ACI-318). Building Code Requirements for Structural Concrete, ACI 318-02, American Concrete Institute, Farmington Hills, Michigan. Detroit. 2002.

ACI, American Concrete Institute, Detroit. Building Code Requirements for Reinforced Concrete and Commentary, (ACI 318-89 / ACI 318R-89), 1989. 353 pp.

ACI, American Concrete Institute (ACI-318). Commentary on Building Code Requirements for Reinforced Concrete (ACI318-84), ACI Committee 318, Standard Building Code, Second Printing, 1985.

ACI-318-08 Code Requirements for Design of Concrete Floor Systems. Technical Note, Your Partner in Structural Concrete Design, TN331, ACI Floor Design, 040509, ACI-318-08, Section 10.2.6, ADAPT Corporation, Redwood City, California, USA. 2009.

Adebar, P. Diagonal Cracking and Diagonal Crack Control in Structural Concrete. Design and Construction Practices to Mitigate Cracking. ACI; SP204, 2001. pp 85-116.

Ahmed, S. H.; and Lue, D. M. Flexure-Shear Interaction of Reinforced High-Strength Concrete Beams. *ACI Structural Journal*, Vol. 84 (4), July-August 1987. pp 330–341.

Aitken, M. W. Investigation of Long Reinforced Concrete Beams Designed to the Unified Design Approach, B.Eng Dissertation, Heriot-Watt University, Edinburgh, UK. 2009.

Al.Dywany, H. R. Behaviour of Wide Reinforced Concrete Beam in Shear. MSc Thesis, University Technology Malaysia (UTM), Malaysia. December 2010.

Alexander, S.D.B. and Simmonds, S.H. (1987), Ultimate strength of slab-column connections, *ACI Structural Journal*, Vol.84 (3), pp.255-261.

Al-Harithy, K. A. Effects of Tension-Reinforcement Ratio and Concrete Strength on Deflection of Wide-Beams, MSc Thesis, King AbdulAziz University, Jeddah, KSA, February 2002, 126pp.

Alluqmani, A. E. 2013a. Flexural and Shear Behaviour of Wide RC Beams. The Civil Engineering PhD Conference, University of Strathclyde, Glasgow, Scotland-UK. October 2013.

Alluqmani, A. E. 2013b. Development of Detailing and Design Models for Wide Concrete Beams. The Engineering RPD Conference, University of Strathclyde, Glasgow, Scotland-UK. June 2013. 13 pp.

Alluqmani, A. E.; and Saafi, M. B. 2014a. Structural Reinforced Concrete Beams in Shear. The 2014 SSC-07 Conference, ISBN-14: 9780956904522, University of Edinburgh, Edinburgh, Scotland-UK. Paper No.506. February 2014. 12pp.

Alluqmani, A. E.; and Saafi, M. B. 2014b. The Effect of Bearing Plate Widths on Wide Concrete Member Capacities. The 2014 SSC-07 Conference, ISBN-14: 9780956904522, University of Edinburgh, Edinburgh, Scotland-UK. Paper No.507. February 2014. 8pp.

Alluqmani, A. E.; and Saafi, M. B. 2014c. New Detailing-Approach and Design-Model for Wide RC Beams. Young Structural Researchers' Conference 2014 (YRC), the Institution of Structural Engineers, London, England-UK. March 2014.

Alluqmani, A. E. 2014. Design and Behaviour of R.C. Beams to ACI318-and-SBC304; and EC2 Codes When Subjected To Asymmetric Loading. JEDT Journal, Emerald Group Publishing Ltd, ISSN: 1726-0531. Vol. 12 (2), April-May 2014. pp.158 - 176.

Alluqmani, A. E.; and Haldane, D. 2011a. Design of Reinforced Concrete Beams to ACI318-and-SBC304; and EC2 Codes. COBRA-2011 (RICS) Conference, University of Salford, Manchester, England-UK, ISBN: 978-1-907842-19-1, Section Six, Session 1: Building Technology, Paper No.2150. September 2011. pp 459-468.

Alluqmani, A. E.; and Haldane, D. 2011b. Structural Design of Reinforced Concrete Beams: Comparison In Accordance With ACI318-and-SBC304; and EC2 Codes. The 5<sup>th</sup> SSIC-2011 Conference, ISBN: 978-0-9569045-0-8, University of Warwick, Coventry, England-UK, ISBN 978-0-9569045-0-8, Section Five, Session 21: Construction and Architecture, Paper No.21. June 2011. 8pp.

Alluqmani, A. E.; and Haldane, D. 2011c. Structural Behaviour of Reinforced Concrete Beams: Comparison In Accordance With ACI318-and-SBC304; and EC2 Codes. The 5<sup>th</sup> SSIC-2011 Conference, ISBN: 978-0-9569045-0-8, University of Warwick, Coventry, England-UK, ISBN 978-0-9569045-0-8, Section Five, Session 21: Construction and Architecture, Paper No.22. June 2011. 9pp.

Alluqmani, A. E. 2010. Reinforced Concrete Beams Design: Comparison In Accordance With Saudi Building Code (SBC304) and Eurocode (EC2) Subjected To Asymmetric Loading. MSc Dissertation, Heriot-Watt University, UK. August 2010, 111pp.

- Al-Nahlawi, K. A.; and Wight, J. K. Beam Analysis Using Concrete Tensile Strength in Truss Models, *ACI Structural Journal*, Vol. 89 (3), May-June 1992, pp. 284-289.
- Anderson, N. S.; and Ramirez, A. J. Detailing of Stirrup Reinforcement. *ACI Structural Journal*, Vol. 86 (5), October 1989. pp 507-515.
- Angelakos, D.; Bentz, E. C.; and Collins, M. P. Effect of Concrete Strength and Minimum Stirrups on Shear Strength of Large Members, *ACI Structural Journal*, Vol. 98 (3), May-June 2001, pp. 290-300.
- ASCE-ACI Committee 326, American Concrete Institute. Shear Strength and Diagonal Tension, January, February, and March 1962. (ACI Proceedings, pp. 1-30, 277-334, and 353-396).
- ASCE-ACI Committee 426, American Concrete Institute. The Shear Strength of Reinforced Concrete Members. *Journal of the Structural Division, Proceedings of ASCE*, Vol. 99, No. ST6, June 1973. pp 1091-1187 (ACI 426-74) (Re-approved 1980), Detroit, 1974. pp. 111.
- ASCE-ACI Committee 426, American Concrete Institute. Shear in Reinforced Concrete, *ACI Special Publication SP-42*, Detroit, 1974, Vol. 1, pp. 1-424, and Vol. 2, pp. 425-949.
- ASCE-ACI Committee 445, American Concrete Institute. Recent Approaches to Shear Design of Structural Concrete, *Journal of Structural Engineering, ASCE*, Vol. 124 (12), 1998, pp. 1375-1417. (and version of 2000).
- Base, G. D.; and Read, J. B. Effectiveness of helical binding in the compression zone of concrete beams. *ACI Journal*, Vol. 62 (No. 4), July 1965. pp. 763-781.
- Bass, R. A.; Carrasquillo, R. L.; and Jirsa, J. O. Shear transfer across new and existing concrete interfaces. *ACI Structural Journal*, Vol. 86 (4), July-August 1989. pp. 383-393.
- Batchelor, B. Shear in R.C. Beams without Web Reinforcement. *Journal of Structural Division*, 107 (ST 5), 1981. pp 907-919.
- Baumann, T. Tests to Study the Dowel Action of the Bending Tension Reinforcement of Reinforced Concrete Beams. Bericht Nr. 77, Munich Technischen Hochschule, (English Translation by PCA), 1968.
- Bazant, Z. P. Crack Band Model for Fracture of Geomaterials. In *Proceedings, 4th International Conference on Numerical Methods in Geomechanics*, Vol. 3, pages 1137-1152, Edmonton, 1982. University of Alberta.
- Bazant, Z. P.; and Oh, B. H. Crack band theory for fracture of concrete. *Materials and Structures, Research and Testing (RILEM, Paris)*, Vol. 16 (93), May-June 1983. pp. 155-177.

- Bazant, Z.P. Size effect in blunt fracture: concrete, rock, metal, *J. Eng. Mech.* Vol. 110 (4), pp.518-35. 1984.
- Bazant, Z. P.; and Cao, Z. Size effect in punching shear failure of slabs, *ACI Structural Journal*, Vol. 84 (1), pp.44-51. 1987.
- Belarbi, A.; and Hsu, T. C. Stirrup stresses in reinforced concrete beams. *ACI Structural Journal*, Vol. 87 (5), September-October 1990. pp. 530-538.
- Bentz, E. C.; Vecchio, F. J.; and Collins, M. P. Simplified Modified Compression Field Theory for Calculating Shear Strength of Reinforced Concrete Elements. *ACI Structural Journal*, Vol. 103 (2), 2006. pp 614-24.
- Berg, F. J. Shear Strength of Reinforced Concrete Beams Without Web Reinforcement. *ACI Structural Journal*, Vol. 59 (11), 1962. pp. 1587–1599.
- Bobrowski, J. Origins of Safety in Concrete Structures. PhD Thesis, Department of Civil Engineering, University of Surrey, June 1982.
- Bond, A. J.; Harrison, T.; and et al. How to Design Concrete Structures Using Eurocode2, A Cement and Concrete Industry Publication, BCA, The Concrete Centre, U.K., Surrey. 2006.
- Bresler, B.; and MacGregor, J. G. Review of concrete beams falling in shear. *Journal of Structural Division, ASCE*, Vol. 93 (2), February 1967. pp. 343-372.
- Bresler, B.; and Scordelis, A. C. Shear strength of reinforced concrete beams. *ACI Journal, Proceedings*, Vol. 60 (1), January 1963. pp. 51-72.
- British Standards Institution. BS8110, British Standard, Structural Use of Concrete, Part I, Code of Practice for Design and Construction, 1985. 145pp.
- British Standards Institution. BS8110, British Standard, Structural Use of Concrete, Part I, Code of Practice for Design and Construction, 1997.
- Bukhari, I. A.; and Ahmed, S. Evaluation of Shear Strength of High-Strength Concrete Beams without Stirrups. *The Arabian Journal for Science and Engineering*, Vol. 33, No. 2B, October 2007. pp 321-336.
- Campbell, P. Aims of Structural Design, *Journal of the Institution of Structural Engineers*, Vol. 61A (1), January 1983.
- Campbell, T. I.; Batchelor, B. deV.; and Chitnuyanondh, L. Web Crushing in Concrete Girders with Prestressing Ducts in the Web. *Journal of Prestressed Concrete Institute*, Vol. 24 (5), September-October 1979. pp. 70-88.



Campbell, T. I.; Chitnuyanondh, L.; and Batchelor, B. deV. Rigid Plastic Theory v. Truss Analogy Method for Calculating the Shear Strength of Reinforced Concrete Beams. Magazine of Concrete Research (London), Vol. 32 (110), March 1980. pp. 39-44.

CEB-FIP. Comite Euro-International du Beton/Federation Internationale de La Precontrainte, Paris. CEB-FIP Model Code for Concrete Structures, Paris, 3rd edition, 1990. (English Edition, Cement and Concrete Association, Wexham Springs).

CEB-FIP. State-of-the-art report on high-strength concrete. 901111, Bulletin d'Information No. 197, 1990.

Chana, P. S. Investigation of the Mechanism of Shear Failure of Reinforced Concrete Beams. Magazine of Concrete Research (London), Vol. 39 (141), December 1987. pp. 196-204.

Chana, P. S. Punching Shear in Concrete Slabs. The Structural Engineer, Vol. 69 (15), 1991. pp.282-285.

Collins, M. P. Towards a Rational Theory for RC Members in Shear. Journal of Structural Division, ASCE, Vol. 104 (4), April 1978. pp. 649-666.

Collins, M. P.; Bentz, E. C.; and Sherwood, E. G. Where is Shear Reinforcement Required? Review of Research Results and Design Procedures, ACI Structural Journal. 2008.

Collins, M. P.; Bentz, E. C.; Sherwood, E. G; and Xie, L. An Adequate Theory for the Shear Strength of Reinforced Concrete Structures. University of Cambridge. 2007.

Collins, M. P.; and Kuchma, D. How Safe Are Our Large, Lightly Reinforced, Concrete Beams, Slabs and Footings?. ACI Structural Journal, Vol. 96 (4), August 1999. pp 482-490.

Collins, M. P.; Mitchell, D.; Adebar, P.; and Vecchio, F. J. A General Shear Design Method. ACI Structural Journal, Vol. 93 (1), 1996. pp 36-45.

Concrete Society TR49. Design Guidance for High Strength Concrete. Technical Report, Concrete Society, Camberley, UK. 1998.

Crist, R. A. Static and Dynamic Shear Behaviour of Uniformly Reinforced Concrete Deep Beams. Technical Report AFWL-TR-71-74, University of New Mexico at Albuquerque, New Mexico, November 1975.

CSA-A23.3. Canadian Standards Association, "Design of Concrete Structures" (CAN/CSA-A23.3-04). Mississauga, Canada, 2004.

De Silva, S.; Mutsuyoshi, H.; Witchukreangkrai, E.; and Uramatsu, T. Analysis of Shear Cracking Behavior in Partially Prestressed Concrete Beams. Proceedings of JCI, 27 (2), 2005. pp 865-870.

De Silva, S.; Mutsuyoshi, H.; Witchukreangkrai, E. Evaluation of Shear Crack Width in I-Shaped Prestressed Reinforced Concrete Beams. *Journal of Advanced Concrete Technology*, Vol. 6 (3), 2008. pp 443-458.

Diaz de Cossio, R. Discussion of ACI-ASCE Committee 326, "Shear and Diagonal Tension". *ACI Structural Journal, Proceedings*, Vol. 59 (9), September 1962. pp 1323-1332.

Drucker, D. C. On Structural Concrete and the Theorems of Limit Analysis. Publications, International Association for Bridge and Structural Engineering, V. 21, Zürich, Switzerland, 1961, pp 49-59.

Engineering Investigation. Final Report MRR2 Forensic Engineering Investigation Group. University Technology Malaysia (UTM), 2005. pp 50-59.

Etebar, K. The Influence of Aggregate Interlock on the Shear Capacity of Rectangular Reinforced Concrete. PhD Thesis, University of Sussex, Sussex, September 1987.

Eurocode2 (EC2). Design of Concrete Structures-Part 1-1: General Rules and Rules for Buildings (EN1992-1-1). European Committee for Standardization. Brussels, Belgium, December 2004. 225pp. (and version of 2008).

Eurocode (0), EC2, Structural Eurocodes. Basis of Structural Design, Second Edition, BSI, London, 2007.

Falamaki, M. (1990), Punching shear strength of reinforced concrete flat plates with spandrel beams, PhD Thesis, University of Wollongong.

Fenwick, R. C.; and Paulay, T. Discussion of Kani (1964), *Journal of the American Concrete Institute, Proceedings* Vol. 61 (12), 1964. pp 1590-1595.

Fenwick, R. C. The Shear Strength of Reinforced Concrete beams. PhD Thesis, University of Canterbury, Christchurch, New Zealand, December 1966.

Fenwick, R. C.; and Paulay, T. Mechanisms of Shear Resistance of Concrete Beams. *Journal of the Structural Division, ASCE*, Vol. 94, No. ST10, October 1968. pp 2325-2350.

Ferguson, P. M. Some Implications of recent Diagonal Tension Tests. *Journal of ACI*, Vol. 28 (2), 1956, pp 157-172.

Fernandez Ruiz, M.; and Muttoni, A. Applications of the Critical Shear Crack Theory to Punching of R/C Slabs with Transverse Reinforcement. *ACI Structural Journal*, Vol. 106 (4), Farmington Hills, USA, 2010, pp. 485-494.

Fernandez Ruiz, M.; Muttoni, A.; and Kunz, J. Strengthening of Flat Slabs Against Punching Shear Using Post-Installed Shear Reinforcement. *ACI Structural Journal*, Vol. 107 (4), USA, 2010, pp. 434–442.

Gergely, P. Splitting Cracks Along the Main Reinforcement in Concrete Members. Report to Bureau of Public Roads, U.S. Department of Transportation, Cornell University, Ithaca, New York, April 1969.

Gerstle et al. Strength of Concrete under Multiaxial Stress State. Special Publication No. S.P. 55-5, American Concrete Institute, Detroit, 1976. pp. 103-131 pp.

Grant, J. F. Strengthening of Reinforced Concrete Beams in Shear Using External Unbonded Reinforcement, Ph.D Thesis, Heriot-Watt University, Edinburgh, UK, 2003.

Guan, H. Cracking and Punching Shear Failure Analysis of Reinforced Concrete Flat Plates by Layered Finite Element Method. Ph.D. Thesis, Griffith University. 1996.

Gunneswara Rao, T. D.; and et.al. An Appraisal of The Shear Resistance Of Ferrocement Elements. *Asian Journal of Civil Engineering (Building & Housing)* Vol.7 (6), 2006. pp 591-602.

Haddadin, M.; Hong, S. T.; and Mattock, A. H. Stirrup effectiveness in reinforced concrete beams with axial force. *Proceedings, ASCE*, Vol. 97 (9), September 1971. pp. 2277-2297.

Hamadi, Y. D.; and Regan, P. E. Behaviour in shear of beams with flexural cracks. *Magazine of Concrete Research (London)*, Vol. 32 (111), June 1980. pp. 67-78.

Hanafy, M. M.; Mohamed, H. M.; and Yehia, N. A. B. On the Contribution of Shear Reinforcement in Shear Strength of Shallow Wide Beams, *Life Science Journal*, Vol. 9 (3), June 2012, pp. 484-498.

Hasan, G. A. Design of Reinforced Concrete Beams, PhD Thesis, Heriot-Watt University, Edinburgh, UK, 2008.

Hassan, H. M.; and Ueda, T. Relative Displacement Along Shear Crack of Reinforced Concrete Beam. *Proceedings of JCI*, Vol. 9 (2), 1987. pp 699-704.

Hillerborg, A. The Application of Fracture Mechanics to Concrete. In *Conference on Contemporary European Concrete Research*, Stockholm, 9-11 June 1981.

Hognestad, E. What do we know about diagonal tension and web reinforcement? *Historical Study. University of Illinois, Bulletin*, Vol. 49 (50), June 1951. 56pp.

Hsiung, W.; and Frantz, G. C. Transverse Stirrup Spacing in Reinforced Concrete Beams, *ASCE Journal of Structural Engineering*, Vol. 111 (2), February 1985, pp 353-362.

Hsu, T. T. Unified Approach to Shear Analysis and Design. University of Houston, Houston, TX 77204, USA, Cement and Concrete Composites, Elsevier Science Ltd. 1998, pp 419-435.

Jeng, C. H.; and Hsu, T. T. A Softened Membrane Model for Torsion in Reinforced Concrete Members. Journal of Engineering Structures, Vol. 31 (6), 2009. pp 1944-54.

Jensen, U. G.; and Hoang, L. C. Shear strength prediction of circular RC members by the crack sliding model, Magazine of Concrete Research Vol. 61. 2009

Kani, G. N. J. The Riddle of Shear and its Solution. ACI Structural Journal, Proceedings, Vol. 61 (4), April 1964. pp. 441-469.

Kani, G. N. J. Basic Facts Concerning Shear Failure. ACI Structural Journal, Proceedings, Vol. 63 (6), June 1966. pp. 675-692.

Kani, G. N. J. How Safe are Our Large Concrete Beams?. ACI Structural Journal, Proceedings, Vol. 64 (3), March 1967. pp 128-142.

Kani, G. N. J. A Rational Theory for the Function of Web Reinforcement. ACI Journal, Proceedings, Vol. 66 (3), March 1969. pp. 185-197.

Kani, G. N. J.; Huggins, M. W.; and Wittkopp, R. R. Kani on Shear in Reinforced Concrete. Department of Civil Engineering, University of Toronto, Toronto, Canada, 1979.

Kaufmann, W. Strength and Deformations of Structural Concrete Subjected to In-Plane Shear and Normal Forces. PhD Thesis, Swiss Federal Institute of Technology Zurich, July 1998. 155pp.

Kotsovos, M. D. Fracture Processes of Concrete under Generalized Stress State. Materials and Structures, Research and Testing, RILEM, Paris, Vol. 12 (72), November-December 1979. pp. 431-437.

Kotsovos, M. D. A Fundamental Explanation of the Behavior of Reinforced Concrete Beam in Flexure Based on the Properties of Concrete under Multiaxial Stress. Materials and Structures, Vol. 15, 1982. pp. 529-537.

Kotsovos, M. D. Mechanisms of 'Shear' Failure. Magazine of Concrete Research, London, Vol. 35 (123), June 1983. pp. 99-105.

Kotsovos, M. D. Deformation and Failure of Concrete in a Structure. In International Conference of Concrete under Multiaxial Conditions, Toulouse, 1984.

Kotsovos, M. D. Consideration of Triaxial Stress Condition in Design: A Necessity. ACI Structural Journal, Vol. 84 (3), May-June 1987. pp. 263-273.

- Kotsovos, M. D. Compressive Force Path Concept: Basis for Ultimate Limit State Reinforced Concrete Design. *ACI Structural Journal*, Vol. 85 (1), January-February 1988. pp. 68-85.
- Kotsovos, M. D. Design of Reinforced Deep Beams. *The Structural Engineer*, Vol. 66, 1988. pp. 28-32.
- Kotsovos, M. D.; and Pavlovic', M. N. *Ultimate Limit-State Design of Concrete Structures - A New Approach*. Thomas Telford Ltd., London. 1999.
- Kotsovos, M. D.; and Cheong, H. K. Applicability of Test Specimen Results for the Description of the Behaviour of Concrete in a Structure. *ACI Journal*, 81 (4), July-August 1984. pp. 358-363.
- Kotsovos, M. D.; and Newman, J. B. Fracture Mechanics and Concrete Behaviour. *Magazine of Concrete Research (London)*, Vol. 33 (115), June 1981. pp. 103-112.
- Kotsovos, M. D.; and Newman, J. B. Behaviour of Concrete under Multiaxial Stress. *ACI Journal*, Vol. 74 (9), September 1977. pp. 443-446.
- Krefeld, W. J.; and Thurston, C. W. Studies of the Shear and Diagonal Tension Strength of Simply-Supported Reinforced Concrete Beams. *Journal of the American Concrete Institute, Proceedings*, Vol. 63 (4), April 1966. pp 451-476.
- Kumar, D.; and Tech, P. G. Shear Strength of R.C.C. Beams without web reinforcement. Palakkad, N.D. 7pp.
- Kuo, W. W.; Cheng, T. J.; and Hwang, S. J. Force Transfer Mechanism and Shear Strength of Reinforced Concrete Beams. *Journal of Engineering Structures*, 32: 1537-1546, Elsevier Ltd., 2010. pp 1538-1544.
- Lantsoght, E.; Veen, C. der; and Walraven, J. Experimental Study of Shear in Reinforced Concrete One-Way Slabs Subjected to Concentrated Loads, *FIB Symposium PRAGUE*, 2011.
- Laupa, A.; Siess, C. P.; and Newmark, N. M. Strength in Shear of Reinforced Concrete Beams. Bulletin no. 428, Engineering Experiment Station, University of Illinois, Urbana, Illinois. 1955.
- Lee, J., and Kim, U. Effects of longitudinal tensile reinforcement ratio and shear span-depth ratio on minimum shear reinforcement in beams, *ACI Structural Journal* Vol. 105 (2), pp 134-144. 2008.
- Lee, J. Y.; Mansour, M. Y. New Algorithm for Fixed-Angle Softened-Truss Model. *Structural Build*, 159 (SB6), 2006. pp 349-59.

Leonhardt, F.; and Walther, R. The Stuttgart Shear Tests. Translation of articles from *Beton und Stahlbetonbau*, V.56, No. 12, 1961 and V.57, No. 2, 3, 6, 7 and 8, 1962, Cement and Concrete Association Library Translation No. 111, Wexham Springs, UK, December 1964, 134 pp.

Leonhardt, F.; and Walther, R. Shear Tests on Beams With and Without Shear Reinforcement. *Deutscher Ausschuss für Stahlbeton*, No. 151, 1962. 83 pp.

Li, B., and Kulkarni, S. A. Seismic Behavior of Reinforced Concrete Exterior Wide Beam-Column Joints, *Journal of Structural Engineering*, ASCE, Vol. 136 (1), January 2010, pp. 26-36.

Linhua, J.; Dahai, H.; and Nianxiang, X. Behaviour of Concrete under Triaxial Compressive-Compressive Tensile Stresses. *ACI Material Journal*, Vol. 88 (2), March-April 1991. pp.181-185.

Lubell, A. S.; Sherwood, E. G.; Bentz, E. C.; and Collins, M. P. Safe Shear Design of Large, Wide Beams. *Concrete International*, American Concrete Institute, Vol. 26, No. 1, January 2004, pp. 66-78 and discussion Vol. 28 (8), pp.14-17.

Lubell, A. S. Shear in Wide Reinforced Concrete Members. PhD Thesis, University of Toronto, Toronto, Canada, May 2006, 455pp.

Lubell, A. S.; Bentz, E. C.; and Collins, M. P. One-Way Shear in Wide Concrete Beams with Narrow Supports. *ASCE Journal of Structural Engineering*, 2008.

Lubell, A. S.; Bentz, E. C.; and Collins, M. P. Shear Reinforcement Spacing in Wide Members. *ACI Structural Journal*, Vol. 106 (2), Mar-Apr 2009a, pp.205-214.

Lubell, A. S.; Bentz, E. C.; and Collins, M. P. Influence of Longitudinal Reinforcement on One-way Shear in Slabs and Wide Beams. *ASCE Journal of Structural Engineering*, Vol. 135 (1), Jan 2009b, pp.78-87.

MacGregor, J. G. Discussion of Kani. *Journal of the American Concrete Institute*, Proceedings Vol. 61 (12), 1964. pp 1598-1604.

MacGregor, J. G. Discussion of Kani (1967): "How Safe are our Large Reinforced Concrete Beams?". *ACI Journal*, Proceedings, Vol. 64 (9), September 1967. pp. 603-604.

MacGregor, J. G.; and Walters, J. R. Analysis of Inclined Cracking Shear in Slender Reinforced Concrete Beams. *ACI Journal*, Proceedings, Vol. 64 (10), October 1967. pp 644- 653.

MacGregor J. G.; Barlett, F. Reinforced Concrete, Mechanisms and Design. 1<sup>st</sup> Canadian ed. Toronto, Canada: Prentice Hall; 2000.

MacGregor, J. G.; and Wight, J. K., Reinforced Concrete: Mechanics and Design, 4th Edition, Pearson Prentice Hall, Upper Saddle River, N.J., 2005, 1314 pp.

- Manual, R. F. Failure of Deep Beams. Shear in Reinforced Concrete Vol. 2 (SP- 42), American Concrete Institute, Detroit, 1974. pp. 425-440.
- Marti, P. Dimensioning and Detailing. In the Proceedings of the IABSE Colloquium, Structural Concrete, Stuttgart, 1991, pp. 411-443.
- Mathey, R.; and Watstein, D. Shear Strength of Beams without Web Reinforcement Containing Deformed Bars of Different Yield Strengths. ACI Structural Journal, Vol. 60 (2), February 1963.
- Mattock, A. H.; and Hawkins, N. M. Research on Shear Transfer in Reinforced Concrete. PCI Journal, Vol. 17 (2), March-April 1972. pp. 55-75.
- Mau, S. T.; and Hsu, T. T. C. Shear Strength Prediction for Deep Beams with Web Reinforcement. ACI Structural Journal, Vol. 84 (6), November- December 1987. pp. 513-523.
- Mau, S. T.; and Hsu, T. T. C. Formula for the Shear Strength of Deep Beams. ACI Structural Journal, Vol. 86 (5), September-October 1989. pp. 516-521.
- May, I. Recent and Future Innovations in The Concrete Construction Industry. CBM-CI International Workshop, Karachi, Pakistan, 2008. 6pp.
- McAllister, D. D. Reinforced Concrete Wide Members. BSc Dissertation, Heriot-Watt University, UK, 2011.
- McCormac, J. C. Design of Reinforced Concrete, Fifth Edition, John Wiley & Sons. INC., New York, 2001.
- McLay, S. Strengthening of Reinforced Concrete Beams. BSc Dissertation, Heriot-Watt University (HWU), Edinburgh, UK, March 2008.
- Menetrey, P., Walther, R., Zirnermann, T., William, K.J. and Regan, P.E. Simulation of Punching Failure in Reinforced-Concrete Structures", Journal of Structural Engineering, ASCE, Vol. 123 (5), 1997. pp.652-658.
- Menetrey, P. Synthesis of Punching Failure in Reinforced Concrete, Cement & Concrete Composites, Vol.24, 2002. pp.497-507.
- Millard, S. G.; and Johnson, R. P. Shear Transfer in Cracked Reinforced Concrete. Magazine of Concrete Research (London), Vol. 37 (130), March 1985. pp. 3-15.
- Moe, J. Shearing Strength of Reinforced Concrete Slabs and Footings under Concentrated Loads, Bulletin 047, Portland Cement Association. 1961.
- Moe, J. Discussion of ACI-ASCE Committee 326. ACI Journal, Proceedings, Vol. 59 (9), 1962. pp 1334-1339.

Monteleone, V. Headed Shear Reinforcement in Shell Elements Under Reversed Cyclic Loading. MSc Thesis, Department of Civil Engineering, University of Toronto, Toronto, Canada, 1993. 245pp.

Mosley B., Bungey J. and Hulse R. Reinforced Concrete Design to Eurocode 2, Edition (2), Basingstoke, Hampshire: Palgrave MacMillan, 2007. (and version of 2008).

Mörsch, E. Concrete-Steel Construction. Technical report, Engineering News Publishing Goodrich Co., English Translation of the third German Edition of Der Eisenbetonbau (1st edition 1902). Goodrich, McGraw-Hill, New York, 1909. pp368.

Mörsch, E. Der Eisenbetonbau-Seine Theorie und Anwendung (Reinforced Concrete Construction – Theory and Application), 5<sup>th</sup> Edition, Verlag von Konrad Wittwer, Stuttgart, Germany, Volume 1 – Part 1, 1920.

Mörsch, E. Der Eisenbetonbau-Seine Theorie und Anwendung (Reinforced Concrete Construction – Theory and Application), 5<sup>th</sup> Edition, Verlag von Konrad Wittwer, Stuttgart, Germany, Volume 1 – Part 2, 1922, 460 pp.

Mphonde, A. G.; and Frants, G. C. Shear Tests of High- and Low-Strength Concrete Beams with Stirrups. Technical report, American Concrete Institute, Detroit, 1985. pp. 179-196.

Mphonde, A. G. Use of Stirrup Effectiveness in Shear Design of Concrete. ACI Structural Journal, Vol. 86 (5), September-October 1989. pp. 541-89.

Muttoni; and Ruiz, M. F. Shear Strength of Members without Transverse Reinforcement as Function of Critical Shear Crack Width. ACI Journal, Vol.105 (2), April 2008. pp 163-172.

Ngo, D. Punching Shear Resistance of High-Strength Concrete Slabs", Electr. Journal of Structural Engineering, Vol. I (1), 2001. pp.2-14.

Nielsen, M. P. Limit Analysis and Concrete Plasticity. 2<sup>nd</sup> edition, CRC Press, 1998.

Nielsen, M. P.; Braestrup, M. W.; and Bach, F. Rational Analysis of Shear in Reinforced Concrete Beams. IABSE Proceedings, P-15/78, Zurich, Switzerland. 1978.

Nielsen, M. P.; Braestrup, M. W.; Jensen, B. C.; and Bach, F. Concrete Plasticity, Beam Shear – Shear in Joints - Punching Shear. Danish Society for Structural Science and Engineering. Denmark Technical University, Lyngby. 1978. 129 pp.

Nielsen, M. P.; and Braestrup, M. W. Concrete Plasticity. Technical Report, Danish Society for Structural Science and Engineering, December 1976. (Extract CEB Bulletin 126).

Nilson, H.; and G. Winter. Design of Concrete Structures. McGraw-Hill, 11<sup>th</sup> edition, 1991.



- Palaskas, M. N.; Attiogbe, E. K.; and Darwin, D. Shear strength of lightly reinforced T-beams. *ACI Journal, Proceedings*, Vol. 78 (6), November- December 1981. pp. 447-455.
- Pandor, D. A. Behavior of High Strength Fiber Reinforced Concrete Beams in Shear. Imperial College, University of London, February 1994.
- Pang, X. B.; and Hsu, T. T. Fixed Angle Softened Truss Model for Reinforced Concrete. *ACI Structural Journal*, Vol. 93 (2), 1996. pp 197-207.
- Park, R.; and Paulay, T. Reinforced Concrete Structures. John Wiley and Sons, 1975. 769 pp.
- Parmalee, R. A. A Study of the Ultimate Strength of Reinforced Concrete Beams. Structural Engineering and Structural Mechanics Report #61-11, University of California, Berkely, California, January 1961. 66pp.
- Paulay, T.; and Priestley, M. J. Seismic Design of Reinforced Concrete and Masonry Buildings. John Wiley and Sons Inc., New York, 1992.
- Rao, A. K.; and Reddy, K. N. Rotational Capacity of Partially Prestressed Concrete Sections with Stirrup Confinement. Institution of Engineers (India), 1981. pp 551-59.
- Regan, P. E. Research on Shear: A Benefit to Humanity or a Waste of Time?. *Structural Engineer*, Vol. 71 (19), 1993, pp. 337-347.
- Regan, P. E.; and et al. Behaviour of High Strength Concrete Slabs. Proceedings of Concrete 2000, Dundee University, September 1993, pp. 761-773.
- Regan, P. E. Punching Shear in Prestressed Concrete Slab Bridge, Technical Report, Engineering Structures Research Group, Polytechnic of Central London. 1983.
- Regan, P. E. Shear in Reinforced Concrete Beams. *Magazine of Concrete Research (London)*, Vol. 21 (66), March 1969. pp. 31-42.
- Regan, P. E.; and Rezai-Jorabi, H.. Shear Resistance of One-Way Slabs Under Concentrated Loads. *ACI Structural Journal*, Vol. 85 (2), April 1989. pp 150-157.
- Regan, P. E.; and Placas, A. Limit-State Design for Shear in Rectangular and T Beams. *Magazine of Concrete Research (London)*, Vol. 22 (73), December 1970. pp. 197-208.
- Reineck, K. Model for Structural Concrete Members without Transverse Reinforcement. In the Proceedings of the IABSE Colloquium, Structural Concrete, Stuttgart, 1991a. pp. 643-648.

Reineck, K. Ultimate Shear Force of Structural Concrete Members without Transverse Reinforcement Derived from a Mechanical Model. *ACI structural Journal*, Vol. 88 (5), September-October 1991b. pp. 592-602.

Ritter, W. Die Bauweise Hennebique (Construction Techniques of Hennebique), *Schweizerische Bauzeitung*, Zürich, Vol. 33 (7), February 1899, pp. 59-61.

Russo, G.; Zingone, G.; and Puleri, G. Flexural-Shear Interaction Model for Longitudinally Reinforced Beams. *ACI Structural Journal*, Vol. 88 (1), January-February 1991. pp. 60-68.

Sagaseta, J.; and Vollum, R. L. Influence of Beam Cross-Section, Loading Arrangement, and Aggregate Type on Shear Strength. *Magazine of Concrete Research*, Vol. 63 (2), Thomas Telford Ltd., 2011. pp 139-155.

SBC304, Structural Saudi Building Code. Building Requirements for Concrete Structures, First Edition, SBCNC, Riyadh. 2007.

Schlaich, J.; and Schäfer, K. Design and Detailing of Structural Concrete Using Strut-and-Tie Models. *The Structural Engineer*, Vol. 69 (6), March 1991. pp. 74-150.

Schlaich, J.; Schäfer, K.; and Jennewein, M. Toward a Consistent Design of Structural Concrete. *PCI Journal*, Vol. 32 (3), May-June 1987, pp. 75-150 (and November-December 1988, pp. 171-179).

Serna-Ros, P.; Fernandez-Prada, M. A.; Miguel-Sosa, P.; and Debb. O. A. Influence of Stirrup Distribution and Support Width on the Shear Strength of Reinforced Concrete Wide Beams. *Magazine of Concrete Research*, Vol. 54 (3), June 2002. pp 181-191.

Sherwood, E. G.; Lubell, A. S.; Bentz, E. C.; and Collins, M. P. One-Way Shear Strength of Thick Slabs, *ACI Structural Journal*, Vol. 103 (6), Nov-Dec, 2006, pp. 794-802.

Sherwood, E. G.; Lubell, A. S.; Bentz, E. C.; and Collins, M. P. One-Way Shear Strength of Thick Slabs and Wide Beams, *ACI Structural Journal*, Vol. 103, No. 6, Nov-Dec 2006, pp. 180-190, pp. 794-802 and discussion Vol. 104 (5), 2007, pp.640-641.

Sherwood, E. G.; Bentz, E. C.; and Collins, M. P. Effects of Aggregate Size on Beam Shear Strength of Thick Slabs, *ACI Structural Journal*, Vol. 104 (2), March-April, 2007, pp. 180-190

Sherwood, E. G. One-Way Shear Behavior of Large, Lightly-Reinforced Concrete Beams and Slabs. PhD Dissertation. University of Toronto, Canada; 2008.

Sherwood, E. G.; Bentz, E.; and Collins, M. P. Effective Shear Design of Large, Lightly-Reinforced Concrete Slabs Employing High-Strength Steel. 2nd Canadian Conference on Effective Design of Structures, McMaster University, Hamilton, Ontario, May 20-23, 2008, 10pp.

Shioya, T. Shear Properties of Large Reinforced Concrete Member. Special Report of Institute of Technology, Shimizu Corporation, No. 25, February 1989. 198 pp.

Shuraim, A. B. Transverse Stirrup Configurations in RC Wide Shallow Beams Supported on Narrow Columns, ASCE Journal of Structural Engineering, Vol. 138 (3), March 2012, pp. 416-424.

Sozen, M. A.; and Hawkins, N. M. Discussion of: 'Shear and Diagonal Tension' by ACI-ASCE Committee 326. ACI Proceedings, Vol. 59 (9), September 1962. pp. 1341-1347.

Standard Association of New Zealand, Wellington. Code of Practice For The Design of Concrete Structures (NZS 310 : 1982), 1982.

Stratford, T. J.; and Burgoyne, C. J. Crack-Based Analysis of Shear in Concrete with Brittle Reinforcement. Magazine of Concrete Research, Vol. 54 (5), 2002.

Stratford, T. J.; and Burgoyne, C. J. Shear Analysis of Concrete with Brittle Reinforcement. Journal of Composites for Construction, ASCE, Vol. 7 (4), November 2003. pp. 323-330.

Sudhakat, M.; Seshu, D.; and Rao, A. A Study of Confined Steel Fiber Reinforced Concrete in The Plastic Hinging Regions of R. C. Beams. Asian Journal of Civil Engineering (Building and Housing), Vol. 10 (2), 2009.

Sudheer, R. L.; Ramana Rao, N. V.; and Gunneswara Rao, T. D. Shear Resistance of High Strength Concrete Beams without Shear Reinforcement. International Journal of Civil and Structural Engineering, Vol. 1 (1), 2010. pp 101-113.

Taylor, R. Some Shear Tests on Reinforced Concrete Beams without Shear Reinforcement. Magazine of Concrete Research, Vol. 12 (36), 1960. pp 145–154.

Taylor, H. P. J. Shear Stresses in Reinforced Concrete Beams without Shear Reinforcement. Technical Report TRA 407, Cement and Concrete Association, London. February 1968. 23 pp.

Taylor, H. P. Investigation of the Forces Carried Across Cracks in Reinforced Concrete Beams in Shear by Interlock of Aggregate. Cement and Concrete Association, London, 1970, technical report 42.447.

Taylor, H. P. J. Shear Strength of Large Beams. Journal of the Structural Division, ASCE, Vol. 98 (11), November 1972. pp. 2473-2490.

Taylor, H. P. The Fundamental Behaviour of Reinforced Concrete Beams in Bending and Shear. ACI Special Report SP 42, pp. 43-77. 1974.

- Teck FU, D. L. The Behaviour of Wide Beam with Different Arrangement of Shear Link. BEng Dissertation, University Technology Malaysia (UTM), Malaysia. 2009.
- Thfilimann, B. Plastic Analysis of Reinforced Concrete Beams. In the Proceedings of the IABSE Colloquium on Plasticity in Reinforced Concrete, Copenhagen, 1979. pp. 71-90.
- Vecchio, F. J.; and Collins, M. P. The Response of Reinforced Concrete to In-Plane Shear and Normal Stresses. Technical Report Publication No. 82-03, Department of Civil Engineering, University of Toronto, March 1982. 332 pp.
- Vecchio, F. J.; and Collins, M. P. The Modified Compression Field Theory for Reinforced Concrete Elements Subjected to Shear. ACI Journal, Vol. 83 (2), 1986. pp 219-31.
- Vecchio, F. J.; and Collins, M. P. Predicting the Response of Reinforced Concrete Beams Subjected to Shear Using the Modified Compression Field Theory. ACI Structural Journal, Vol. 85 (3), 1988. pp 258-68.
- Wagner, H. Ebene Blechwandträger mit sehr dünnem Stegblech (Metal Girders with Very Thin Web). Zeitschrift für Flugtechnik und Motorluftschiffahrt, Vol. 20 (8), pp. 200-207, No. 9, pp. 227-233, No. 10, pp. 256-262, No. 11, pp. 279-284, and No. 12, pp. 306-314, Berlin, 1929.
- Wange, Chu-Kia; and Salmon, C. G. Reinforced Concrete Design. Harper & Row, 3rd edition, 1979. 918 pp.
- White, R. N.; Gergely, P.; and Robert, G. Structural Engineering, Volume3, Behaviour of Members and Systems, Published by John Wiley & Sons, INC., USA. 1974.
- Zakaria, M.; Ueda, T.; Wu, Z.; and Meng, L. Experimental Investigation on Shear Cracking Behavior in Reinforced Concrete Beams with Shear Reinforcement. Journal of Advanced Concrete Technology, Vol. 7 (1), 79-96, Japan Concrete Institute, February 2009. pp 81-94.
- Zararis, P. D. Shear Strength and Minimum Shear Reinforcement of Reinforced Concrete Slender Beams. ACI Structural Journal, 2003. pp 203-214.
- Zhang, X. Punching Shear Failure Analysis of Reinforced Concrete Flat Plates Using Simplified UST Failure Criterion, MPhil Dissertation, Griffith University, Australia. 2002.
- Zheng, L. Shear Tests to Investigate Stirrup Spacing Limits. MSc Thesis, Department of Civil Engineering, University of Toronto, Toronto, Canada, 1989. 161pp.
- Ziara, M. M. The Influence of Confining the Compression Zone in the Design of Structural Concrete Beams. PhD Thesis, Heriot-Watt University, Edinburgh, UK, 1993.